GEORGIA INSTITUTE OF TECHNOLOGY

ENGINEERING EXPERIMENT STATION

ATLANTA, GEORGIA

April 8, 1958

Division of Highway Planning
State Highway Department of Georgia
Atlanta, Georgia

Attention: Mr. Roy A. Flynt
State Highway Planning Engineer

Subject: Quarterly Progress Report No. 1 - Project B-133
Contract No. HPS-1(53)
"The Study of the Stresses Produced in a Flexible Pavement System"

Gentlemen:

Because of a lack of personnel to conduct the work, little progress was made until late March. The director made a brief survey of similar studies by the Road Research Laboratory in Great Britain and The CAA Technical Development Laboratory of Indianapolis. The purpose was to find the best method of instrumentation.

Preliminary tests were made of a new type of resistance-pressure load cell. It is promising enough to warrant future study.

Mr. Charles Hedges, graduate student was hired, beginning March 24 to work fifteen hours per week on the project. Plans for the testing pit are nearing completion and will be submitted to the Highway Department for approval before commencing construction.

George F. Sowers
Project Director

APPROVED: _____

Thomas W. Jackson, Chief
Mechanical Sciences Division

GEORGIA INSTITUTE OF TECHNOLOGY
ENGINEERING EXPERIMENT STATION
ATLANTA, GEORGIA

July 16, 1958

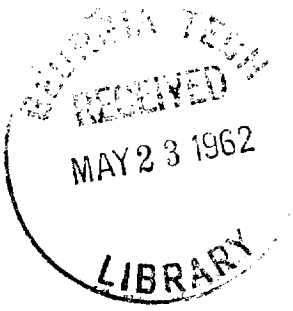

Division of Highway Planning
State Highway Department of Georgia
Atlanta, Georgia

Attention: Mr. Roy A. Flynt
State Highway Planning Engineer

Subject: Quarterly Progress Report No. 2, Project B-133
Contract No. HPS-1(53)
"The Study of the Stresses Produced in a Flexible Pavement System"

Gentlemen:

Good progress has been made since March in constructing equipment and instruments for the testing program. This is a major undertaking since no commercial apparatus is available for the types of measurements to be made in this project.

A reinforced concrete test pit 8 feet deep, 13 feet long and 9 feet wide was constructed in an open area outside the Soil Engineering Laboratory in the Joint Highway Research Building. Controlled fill, subgrade, base course, and pavement will be constructed in this pit for the testing work. The purpose of the pit is to isolate the test soils from the surrounding ground and thereby achieve better control over moisture changes and stress propagation.

A structural steel loading frame 10 feet high spanning the 12 foot length of the pit has been fabricated, but not installed. This will provide the reaction for placing loads on the pavement in the pit.

A loading assembly consisting of a calibrated hydraulic jack, a carriage, and a supporting system for a standard 20-inch truck axle has been fabricated. Mounts are under construction for both dual and dual-tandem 20-inch truck wheels. When completed the assembly will consist of single, dual, and dual-tandem 9.00 x 20 truck wheels which are the same as are being used in the heavier tractor-trailer trucks now in use on the Georgia Highways. Even larger tire assemblies can be mounted in the loading arms which are provided with quick-change connectors.

Thirty pressure cells for measuring stresses in the subgrade and base course are under construction. They will be capable of measuring pressures of from 10 psi to 50 psi, depending on their size. They are of a simplified design, utilizing SR-4 electric strain gages, which was developed previously in the Georgia Tech Soil Engineering Laboratory. The waterproofing of these cells is a serious problem which is under study at the present time.

A new type of pressure cell is being developed to measure the pressures immediately beneath the tire. This utilizes a material whose electrical resistance varies with pressure. Preliminary tests indicate that a cell one inch in diameter and 0.03 inches thick is feasible. Such a cell will be a marked improvement over other devices previously used to measure tire pressures.

Still to be constructed are the fill, subgrade, base and surface in the test pit. These are scheduled for late July depending on weather. Actual tests should commence early in August.

The project still suffers from a lack of personnel. Mr. Hedges, graduate assistant, worked less than half time from April to June. In mid-June he went on full time. A full-time research associate who has been under contract with the School of Civil Engineering since spring has been delayed because of passport difficulties (he is coming from Belgium). He will arrive early in September and will be able to contribute one-fourth time for the remainder of the year.

George F. Sowers
Project Director

Approved: _____

Thomas W. Jackson, Chief
Mechanical Sciences Division

GEORGIA INSTITUTE OF TECHNOLOGY
ENGINEERING EXPERIMENT STATION
ATLANTA, GEORGIA

October 15, 1958

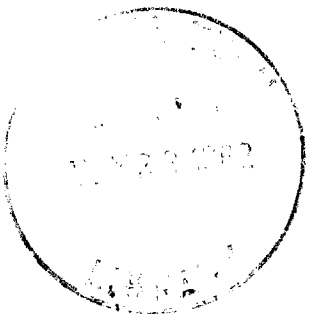

Division of Highway Planning
State Highway Department of Georgia
Atlanta, Georgia

Attention: Mr. Roy A. Flynt
State Highway Planning Engineer

Subject: Quarterly Progress Report No. 3, Project No. B-133
Contract No. HPS-1(53)
"The Study of the Stresses Produced in a Flexible Pavement System"

Gentlemen:

The work on the subject project progressed on schedule during the past three months. The construction of the equipment and instruments for testing is nearly complete and the study of past research on pavement stresses is about one-third complete. Preliminary subgrade tests should commence in November.

The personnel problem has been solved. Dr. Aleksandar Vesic arrived from Belgium late in August and joined the project staff immediately. He began the detailed study of past research on stresses in layered system and has made excellent progress. He will continue one-fourth time for the remainder of the project.

Mr. Charles Hedges, who has served full time since June, will leave October 20 for military service. His work will be continued by Mr. Tom Stapler, Graduate Assistant and Mr. R. Earl Housworth, Undergraduate Assistant.

In September Dr. Vesic and Professor Sowers inspected the pavement stress research facilities of the U. S. Waterways Experiment Station at Vicksburg, Mississippi. Mr. Richard Ahlvin, the project director, spent five hours discussing the detailed procedures followed in the research carried out by the Corps of Engineers. Mr. M. J. Hvorslev, Research Consultant, spent one hour describing the instrumentation. It is significant that their pressure cells cost $600 each, which severely limited the number of cells used. According to Mr. Ahlvin, large numbers of simple, cheap cells, would be preferable. Test data from the Corps of Engineers work were obtained to serve as guides to this project. Unfortunately the Corps of Engineers research was stopped before it could be completed, due to lack of funds which were supplied by the Air Force.

The loading system for the test pit has been completed. This includes the mounts for single, dual and dual tandem truck tires. Others can be mounted and tested to loads up to 35,000 pounds per axle.

Thirty pressure cells have been completed. A new waterproofing of vinyl plastic has been employed which protected a test cell for six weeks under water. All the cells have been calibrated under full pressure. Corrections for actual soil pressure have been found by experiments on typical cells. It is interesting that the cost per cell is $15 to $20, which is in agreement with the suggestions of Mr. Ahlvin. In view of the difficulties experienced by the Corps of Engineers, thirty additional cells are now under construction to increase the pattern of stress measurement.

The test pit has been partially backfilled with micaceous sandy silt, a poor subgrade or embankment material, compacted to 90-95% of the maximum AASHO density. The first layer of cells has been installed and their function checked. The remainder will be installed shortly, and testing will begin in November.

Respectfully submitted,

George F. Sowers
Project Director GFS

Approved:

Thomas W. Jackson, Chief
Mechanical Sciences Division

B-133

GEORGIA INSTITUTE OF TECHNOLOGY

ENGINEERING EXPERIMENT STATION

ATLANTA, GEORGIA

October 2, 1959

Division of Highway Planning
State Highway Department of Georgia
Atlanta, Georgia

Attention: Mr. Roy A. Flynt
State Highway Planning Engineer

Subject: Quarterly Progress Report
Project No. B-133
Contract No. HPS-1(53)
"The Study of the Stresses Produced in a Flexible Pavement System"

Gentlemen:

Progress during the past three months has been good. Three distinct phases of work have been completed since the annual report of June 30.

First, all the pressure cells have been removed and then calibrations re-checked. Some were found to have changed. These were recalibrated. Others were found to have admitted moisture. These were completely rebuilt and recalibrated. All the cells were completely re-waterproofed before installation. Additional cells were made to replace a few which had been permanently damaged. All were re-installed in the subgrade, using a slightly different arrangement so as to secure more accurate results. The new installation gives much more consistent results than the original.

Second, a new large diameter triaxial cell for 4 in, 6 in, and 8 in. diameter samples was designed. This was constructed with Civil Engineering Department Funds. It is being used for tests of the base course materials which contain large particles.

Third, a new series of tests has been conducted using a soil-aggregate base, and both single and dual wheels. The preliminary results indicate considerably better load spreading ability than for the topsoil used in the first tests.

Tests will be commenced shortly on a soil-cement stabilized base. Meanwhile the physical property tests of the soil aggregate base will be determined through laboratory tests.

Respectfully submitted.

George F. Sowers
Project Director

Approved:

Thomas W. Jackson, Chief
Mechanical Sciences Division

GEORGIA INSTITUTE OF TECHNOLOGY
ENGINEERING EXPERIMENT STATION
ATLANTA, GEORGIA

October 2, 1959

Division of Highway Planning
State Highway Department of Georgia
Atlanta, Georgia

Attention: Mr. Roy A. Flynt
State Highway Planning Engineer

Subject: Quarterly Progress Report
Project No. B-133
Contract No. HPS-1(53)
"The Study of the Stresses Produced in a Flexible Pavement System"

Gentlemen:

Progress during the past three months has been good. Three distinct phases of work have been completed since the annual report of June 30.

First, all the pressure cells have been removed and then calibrations re-checked. Some were found to have changed. These were recalibrated. Others were found to have admitted moisture. These were completely rebuilt and recalibrated. All the cells were completely re-waterproofed before installation. Additional cells were made to replace a few which had been permanently damaged. All were re-installed in the subgrade, using a slightly different arrangement so as to secure more accurate results. The new installation gives much more consistent results than the original.

Second, a new large diameter triaxial cell for 4 in, 6 in, and 8 in. diameter samples was designed. This was constructed with Civil Engineering Department Funds. It is being used for tests of the base course materials which contain large particles.

Third, a new series of tests has been conducted using a soil-aggregate base, and both single and dual wheels. The preliminary results indicate considerably better load spreading ability than for the topsoil used in the first tests.

Tests will be commenced shortly on a soil-cement stabilized base. Meanwhile the physical property tests of the soil aggregate base will be determined through laboratory tests.

Respectfully submitted.

George F. Sowers
Project Director

Approved:

Thomas W. Jackson, Chief
Mechanical Sciences Division

GEORGIA INSTITUTE OF TECHNOLOGY
ENGINEERING EXPERIMENT STATION
ATLANTA, GEORGIA

February 2, 1960

Division of Highway Planning
State Highway Department of Georgia
Atlanta, Georgia

Attention: Mr. Roy A. Flynt
State Highway Planning Engineer

Subject: Quarterly Progress Report
Project No. B-133
Contract No. HPS-1(53)
"The Study of the Stresses Produced in a Flexible Pavement System"

Gentlemen:

During the fall months work on the project continued on schedule. A soil cement subgrade using a topsoil coarse aggregate mix was constructed using the present highway department standards and a thickness of 8 inches. Testing was completed on this base by Christmas, and it has been removed for installation of the sand asphalt base.

The analysis of the load test data is keeping pace with the tests. The results of the soil-aggregate bare tests indicate that it does not spread the load better than does the topsoil by itself. The soil cement base shows a much greater ability to spread the load than does the other two tested.

The laboratory testing is somewhat behind schedule due to limitations of equipment. Compaction molds for samples 4 in. in diameter by 8 in. high, 6 by 12 and 8 by 16 have been designed, and built by the Civil Engineering Department shop. These will permit testing of the aggregate mixes.

Mr. Francois Chabrol, who has contributed much to the load testing program, has left to return to his native France. No other changes in personnel have been made.

Respectfully submitted,

George F. Sowers
Project Director

Approved:

Thomas W. Jackson, Chief
Mechanical Sciences Division

GEORGIA INSTITUTE OF TECHNOLOGY
ENGINEERING EXPERIMENT STATION
ATLANTA 13, GEORGIA

October 17, 1960

Division of Highway Planning
State Highway Department of Georgia
2 Capitol Square, S. W.
Atlanta, Georgia

Attention: Mr. Roy A. Flynt
State Highway Planning Engineer

Subject: Quarterly Progress Report
Project No. B-133
Contract No. HPS-1(53)
"The Study of Stresses Produced in a Flexible Pavement System"

Gentlemen:

From July 1 through September 30 work continued on the extension of the project: evaluation of the effect of an asphaltic concrete overlay on stresses. Two full-scale systems were tested with a 4 inch thick overlay: (1) a sand asphalt base with an initial 4 inch thick pavement, and (2) a "topsoil" with a 4 inch thick initial pavement.

A new device was developed to measure the maximum deflection of the pavement immediately beneath the wheel. It consists of a vertical reference bar, driven to the bottom of the test pit, and a moveable hollow piston mounted in the pavement. The deflection is indicated on a removable telescoping sleeve.

The project was visited and the testing observed in detail during August by Mr. J. A. Kelly of the Bureau of Public Roads in Washington. He was accompanied by Mr. C. A. Bergey of the Regional Office, Mr. Danielson of the Division Office BPR, and Mr. Abercrombie of the Georgia State Highway Department.

As suggested by Mr. Bergey and Mr. Abercrombie, cores have been cut from the asphaltic concrete pavement. Tests will be run to determine the density of this material, and the properties will be correlated with the properties being measured in Project B-135 (Asphaltic Pavement Design).

Mr. Charles Snepp, Graduate Research Assistant, resigned after completing his formal classroom work and accepting full-time employment elsewhere. Mr. J. M. Duncan was hired to replace him, working part-time as needed.

Respectfully submitted,

George F. Sowers
Project Director

Approved:

Thomas W. Jackson, Chief

GEORGIA INSTITUTE OF TECHNOLOGY
ENGINEERING EXPERIMENT STATION
ATLANTA 13, GEORGIA

April 12, 1961

Division of Highway Planning
State Highway Department of Georgia
2 Capitol Square, S. W.
Atlanta, Georgia

Attention: Mr. Roy A. Flynt
State Highway Planning Engineer

Subject: Quarterly Progress Report
Project No. B-133
Contract No. HPS-1(53)
"The Study of Stresses Produced in a Flexible Pavement System"

Gentlemen:

During the winter months progress was slow because of the construction of facilities for pile testing adjacent to the test pit employed for the pavements. As a result the tests of pavement overlays, which had been scheduled for completion in November were not finished until February.

All tests involving the effectiveness of asphaltic concrete overlays, the work authorized for performance between 1 July 1960 and 31 December, 1960, have been completed. In addition two series of tests were conducted that were not a part of the contract: the effects of repeated loading of the pavement system employing a soil cement base, and the effects of inundating the subgrade. Both were suggested in conferences with technical personnel of the Highway Department and the Bureau of Public Roads, particularly Mr. Shadburn, Mr. Abercrombie, and Mr. Bergey.

The data from the last authorized tests and the two added test series are being processed. Because of the construction delay and the advisability of including the results of the extra tests in the final report on stresses, the publication has been delayed from the authorized date of March 1 to some time in June.

Mr. Wesley Johnson and Mr. Walter Boyd, who have contributed much to the testing and the processing of the data have left to accept permanent employment with the U. S. Bureau of Reclamation. Fortunately, Mr. Charles Hedges, who served in the same capacity at the commencement of the project, returned from military duty and was able to fill the gap while finishing his degree. Mr. D. Wheeless and Mr. Harold Estes, senior students in Civil Engineering, have now replaced Mr. Johnson and Mr. Boyd in conducting the tests and processing the results.

Respectfully submitted,

George F. Sowers
Project Director

Approved:

Thomas W. Jackson, Chief

GEORGIA INSTITUTE OF TECHNOLOGY
ENGINEERING EXPERIMENT STATION
ATLANTA 13, GEORGIA

November 3, 1961

Division of Highway Planning
State Highway Department of Georgia
2 Capitol Square, S. W.
Atlanta, Georgia

Attention: Mr. Roy A. Flynt
State Highway Planning Engineer

Subject: Quarterly Progress Report
Project No. B-133
Contract No. HPS-1(53)
"The Study of Stresses Produced in a Flexible Pavement System"

Gentlemen:

From June 15th to September 15th work continued on the extension of the project: (1) stresses beneath a flexible pavement using a sand subgrade; and (2), investigation of pavement failure and correlation with subgrade stresses.

The last of a series of tests of full scale pavement models was conducted using a sand subgrade, a 8 inch-thick sand-asphalt base, and a 3 inch thick pavement. In addition to pressure measurements in the subgrade, the surface deformation under wheel load was observed. The asphalt concrete surface was cored and the physical properties of the surface determined by the Georgia Highway Department.

The initial phase of the study of pavement failures was an analysis of the data from the AASHO Test Road. However, this information has not been released, necessitating a delay of this phase of the work.

Studies of pavement failures on the South Expressway (U.S. 41) and the Northeast Expressway (Ga. 403) were conducted jointly by project personnel and the Highway Department. The investigation included a description of the failed area and of the environs. The Highway Department conducted the sampling of the pavement surface and subgrade. These investigations were also used as a pilot study for procedures to use when sampling pavements and subgrades throughout the state.

A survey of pavement failures was conducted throughout the state with the exception of the Cartersville Division (#6) in northwest Georgia; which will be done at a later date. The study projects were selected on the basis of recommendations from the Division Engineers. After touring these

locations a number of failures were selected for further study. The sampling of these sites will be done by the Highway Department beginning in December 1961.

Mr. Richard Barksdale was hired on part time as needed to evaluate test data and assist in conducting the triaxial shear tests on the subgrade samples taken from the study projects.

Respectfully submitted,

George F. Sowers
Project Director

Approved:

Thomas W. Jackson, Chief
Mechanical Sciences Division

GEORGIA INSTITUTE OF TECHNOLOGY
ENGINEERING EXPERIMENT STATION
ATLANTA 13, GEORGIA

February 8, 1962

Division of Highway Planning
State Highway Department of Georgia
2 Capitol Square, S. W.
Atlanta, Georgia

Attention: Mr. Roy A. Flynt
State Highway Planning Engineer

Subject: Quarterly Progress Report
Project No. B-133
Contract No. HPS-1(53)
"The Study of Stresses Produced in a Flexible Pavement System"

Gentlemen:

From September 15 to December 31 work continued on the following phases of the project: (1) stresses beneath a flexible pavement on a sand subgrade; and (2) investigation of failures of Georgia highway pavements.

The model tests of the sand subgrade were completed in the early fall. The plotted test results, however, were inconsistent with the data obtained in the earlier tests. Detailed experiments were made on the pressure cells which showed that their performance in clean sand was different than in the micaceous silt subgrade employed in previous tests. Extensive calibration tests showed that the difference was caused by arching of the sand over the cell diaphrams, a condition that was not of importance in the other soil. As a result it was necessary to re-test the cells and develop calibration corrections for the arching. The corrected stresses have been found consistent with the previous results.

The survey of pavement failures was extended to the Cartersville Division (No. 6) and sites selected for further study. Sampling of the sites in South Georgia was begun by Highway Department personnel in December and is continuing. The field work is expected to be completed during February 1962.

A comprehensive paper on the pavement stress measurements was prepared for presentation to the Annual Meeting of the Highway Research Board in January 1962.

Respectfully submitted,

Approved:

George F. Sowers
Project Director

Thomas W. Jackson, Chief
Mechanical Sciences Division

GEORGIA INSTITUTE OF TECHNOLOGY
ENGINEERING EXPERIMENT STATION
ATLANTA 13, GEORGIA

April 20, 1962

Division of Highway Planning
State Highway Department of Georgia
2 Capitol Square
Atlanta, Georgia

Attention: Mr. Roy A. Flynt
State Highway Planning Engineer

Subject: Quarterly Progress Report No. 14
Project No. B-133
Contract No. HPS-1(53)
"The Study of Stresses Produced in a Flexible Pavement System"

Gentlemen:

From December 31 to March 31 work continued on the model test with a sand subgrade and on failure studies of Georgia pavements.

Recalibration of the pressure cells employed in the pavement tests with the sand subgrade were finally completed. The final results are being drafted and the report is in preparation. The data confirm the higher pressures in the subgrade immediately beneath the tire that were found in the earlier tests with the sand-asphalt base course.

Laboratory tests continued slowly on the subgrade and base course samples secured by the Highway Department personnel in December.

Preliminary copies of the final report on the AASHO Test Road were received from Mr. Abercrombie. They will form the basis for evaluating the AASHO tests in terms of the Georgia pavement materials.

The paper on pavement stresses presented at the Highway Research Board Annual meeting provoked considerable discussion. Over 250 requests have been received for copies of this paper from all over the United States.

Respectfully submitted

George F. Sowers
Project Director

Approved:

Thomas W. Jackson, Chief
Mechanical Sciences Division

REVIEW
PATENT 4-24 19 62 BY
FORMAT ✓ 19 BY

GEORGIA INSTITUTE OF TECHNOLOGY
ENGINEERING EXPERIMENT STATION
ATLANTA 13, GEORGIA

August 31, 1962

Division of Highway Planning
State Highway Department of Georgia
2 Capitol Square
Atlanta, Georgia

Attention: Mr. Roy A. Flynt
State Highway Planning Engineer

Subject: Quarterly Progress Report No. 15
Project No. B-133
Contract No. HPS-1 (53)
"The Study of Stresses Produced in a Flexible Pavement System"

Gentlemen:

From April 1st through June 30th report, No. 4, on pavement models with sand was prepared and issued. This report showed that stresses in the sand subgrade were substantially higher than those in the compressible silt subgrade previously tested.

Laboratory experiments continued on the subgrade and base course samples secured by the Highway Department in December.

Discussions were held with Mr. Abercrombie and his staff regarding the evaluation of the "AASHO Test Road" data in terms of Georgia Highways.

Respectfully submitted

George F. Sowers
Project Director

Approved:

Thomas W. Jackson, Chief
Mechanical Sciences Division

REVIEW
PATENT 9-10 19.62 BY

GEORGIA INSTITUTE OF TECHNOLOGY
ENGINEERING EXPERIMENT STATION
ATLANTA 13, GEORGIA

December 15, 1962

Division of Highway Planning
State Highway Department of Georgia
2 Capitol Square
Atlanta, Georgia

Attention: Mr. Roy A. Flynt
State Highway Planning Engineer

Subject: Quarterly Progress Report No. 16
Project No. B-133
Contract No. HPS-1(53)
"The Study of Stresses Produced in a Flexible Pavement System"

Gentlemen:

Laboratory testing continued on soil samples obtained from Georgia Highways as of December 15th were over 60 per cent completed.

Work commenced in preparing the test pit for another series of stress measurements in subgrades produced by wheel loads. All the pressure cells previously used were in disrepair and all had to be rebuilt. The design was modified slightly to obtain better stability: foil gages replace the wire strain gages and the cells were sealed with epoxy resin rather than by bolting.

Considerable difficulty was experienced in duplicating the micaceous silt subgrade used for the previous tests. Finally, a mixture of 3 parts micaceous sandy silt from the Chemical Engineering Building excavation to 1 part micaceous silt from the State Archieves Building excavation was found to produce nearly identical properties.

Mr. D. Wheeless, graduate assistant, resigned to enter the armed services. His place was taken by Mr. T. Wallace. Mr. R. Barksdale transferred to another research project. He was temporarily replaced by Mr. S. P. Clemence, graduate research assistant, and Mr. Eugene Parker, undergraduate research assistant.

Respectfully submitted,

George F. Sowers
Project Director

GEORGIA INSTITUTE OF TECHNOLOGY
ENGINEERING EXPERIMENT STATION
ATLANTA 13, GEORGIA

March 15, 1963

Division of Highway Planning
State Highway Department of Georgia
2 Capitol Square
Atlanta, Georgia

Attention: Mr. Roy A. Flynt
State Highway Planning Engineer

Subject: Quarterly Progress Report No. 17
Project No. B-133
Contract No. HPS-1(53)
"The Study of Stresses Produced in a Flexible Pavement System"

Gentlemen:

Laboratory testing continued of samples obtained from Georgia Highways. Work also continued in preparing the test pit for stress measurements in subgrades. The program calls for testing a 3 inch asphaltic concrete surface laid directly on a compacted subgrade, without any base course other than the soil itself. The model was prepared and ready for testing by March 15th.

Mr. Keith Brasher, graduate research assistant, was hired to speed up the testing program and assist in the pavement stress measurements.

Respectfully submitted,

G. F. Sowers
Project Director

GEORGIA INSTITUTE OF TECHNOLOGY
ENGINEERING EXPERIMENT STATION
ATLANTA 13, GEORGIA

March 15, 1963

Division of Highway Planning
State Highway Department of Georgia
2 Capitol Square
Atlanta, Georgia

Attention: Mr. Roy A. Flynt
State Highway Planning Engineer

Subject: Quarterly Progress Report No. 17
Project No. B-133
Contract No. HPS-1(53)
"The Study of Stresses Produced in a Flexible Pavement System"

Gentlemen:

Laboratory testing continued of samples obtained from Georgia Highways. Work also continued in preparing the test pit for stress measurements in subgrades. The program calls for testing a 3 inch asphaltic concrete surface laid directly on a compacted subgrade, without any base course other than the soil itself. The model was prepared and ready for testing by March 15th.

Mr. Keith Brasher, graduate research assistant, was hired to speed up the testing program and assist in the pavement stress measurements.

Respectfully submitted,

G. F. Sowers
Project Director

GEORGIA INSTITUTE OF TECHNOLOGY
ENGINEERING EXPERIMENT STATION
ATLANTA 13, GEORGIA

July 1, 1963

Division of Highway Planning
State Highway Department of Georgia
2 Capitol Square
Atlanta, Georgia

Attention: Mr. Roy A. Flynt
State Highway Planning Engineer

Subject: Quarterly Progress Report No. 18 (Quarter Ending July 1, 1963)
Project No. B-133
Contract No. HPS-1(53)
"The Study of Stresses Produced in a Flexible Pavement System"

Gentlemen:

Work continued on both phases of the project, the experimental study of stresses in subgrades and the evaluation of Georgia subgrades.

The tests of the subgrade received a severe setback when it was discovered that nearly all of the re-designed pressure cells ceased to function after a short time. These new cells employed foil strain gages instead of wire, so as to reduce deterioration at the points of electrical contact with the strain-sensing element and were cemented together with epoxy resin to insure more positive rim rigidity. The pilot models proved to be far superior to the original design. The epoxy cement of the production models, however, broke, probably due to repeated flexing and fatigue cracking. As a result, all of the new cells had to be rebuilt and the entire test program repeated. It is probable that an extension of the project time will be required as a consequence.

The testing of soil samples from Georgia Highways is nearly complete and the analysis of the results is under way.

Respectfully submitted,

George F. Sowers
Project Director

GFS/c

REVIEW
PATENT 11-6 1963 BY
FORMAT 11-8 1963 BY

GEORGIA INSTITUTE OF TECHNOLOGY
ENGINEERING EXPERIMENT STATION
ATLANTA, GEORGIA 30332
November 18, 1963

Division of Highway Planning
State Highway Department of Georgia
2 Capitol Square
Atlanta, Georgia

Attention: Mr. Roy A. Flynt
State Highway Planning Engineer

Subject: Quarterly Progress Report No. 19 (Quarter Ending October 1, 1963)
Project No. B-133
Contract No. HPS-1(53)
"The Study of Stresses Produced in a Flexible Pavement System"

Gentlemen:

The earth pressure cells, which failed structurally in the subgrade stress tests, were rebuilt and recalibrated. The cells were fabricated by both bolting (as in earlier models) and by a semi-rigid epoxy cement and then sealed as before with a polyvinyl chloride-solvent resin. These new cells proved to be the best so far with no failures in two series of subgrade tests.

The experimental tests of stresses in soil subgrades were nearly complete by October 1. The series employing an asphaltic concrete resting directly on a soil subgrade were finished, after which the 3 in. pavement was replaced with an equal thickness of compacted soil. The later tests were about half complete by October 1. The results of both tests indicated that the stresses in the subgrade produced by wheel loads are within about 10 per cent of the stresses computed by the Boussinesq equation.

The testing of soil samples from Georgia Highway subgrades and from the Ottawa Test Road subgrade is complete and the analyses are in progress.

Mr. T. Wallace resigned to resume employment in California following completion of his M. S. degree.

Respectfully submitted,

George F. Sowers
Project Director

GFS/c

GEORGIA INSTITUTE OF TECHNOLOGY
ENGINEERING EXPERIMENT STATION
ATLANTA, GEORGIA 30332
December 5, 1963

Division of Highway Planning
State Highway Department of Georgia
2 Capitol Square
Atlanta, Georgia

Attention: Mr. Roy A. Flynt
State Highway Planning Engineer

Subject: Monthly Progress Report, November 1963, No. 1
Project No. B-133
Contract No. HPS-1(53)
"The Study of Stresses Produced in a Flexible Pavement System"

Gentlemen:

All experimental work on stress measurements in the subgrade beneath a simple asphaltic surface (without base) and in a homogeneous subgrade without a surface were completed and the results analyzed. Tests of the subgrade properties were commenced. Analyses were continued on the results of soil tests of Georgia pavements.

Very truly yours,

George F. Sowers
Project Director

GFS/c

REVIEW
PATENT 1-17 1964 BY
FORMAT 1-20 1964 BY

GEORGIA INSTITUTE OF TECHNOLOGY
ENGINEERING EXPERIMENT STATION
ATLANTA, GEORGIA 30332

January 30, 1964

Division of Highway Planning
State Highway Department of Georgia
2 Capitol Square
Atlanta, Georgia

Attention: Mr. H. H. Huckeba
State Highway Planning Engineer

Subject: Monthly Progress Report, December 1963, No. 2
Project No. R-133
Contract No. HPS-1(53)
"The Study of Stresses Produced in a Flexible Pavement System"

Gentlemen:

Tests of the subgrade properties for the tests of a simple asphaltic pavement on a homogeneous elastic silt subgrade were completed. The test results are being plotted in final form and the report of this work is in preparation.

Analyses continues on the results of soil tests of Georgia Pavements.

Very truly yours,

George F. Sowers
Project Director

GFS/c

REVIEW
PATENT 2-13 1964 BY
FORMAT 2-14 1964 BY

REPORT NO. 4

PROJECT NO. B-133
HPS-1(53)

THE STUDY OF STRESSES IN A FLEXIBLE PAVEMENT SYSTEM

By

GEORGE F. SOWERS and ALEKSANDAR B. VESIĆ

Contract with
THE STATE HIGHWAY DEPARTMENT OF GEORGIA
in Cooperation with
THE BUREAU OF PUBLIC ROADS

DECEMBER 31, 1960 through DECEMBER 31, 1961

Engineering Experiment Station
Georgia Institute of Technology
Atlanta, Georgia

ENGINEERING EXPERIMENT STATION
of the Georgia Institute of Technology
Atlanta, Georgia

REPORT NO. 4

PROJECT NO. B-133
HPS-1(53)

THE STUDY OF STRESSES IN A FLEXIBLE PAVEMENT SYSTEM

By

GEORGIA F. SOWERS and ALEKSANDAR B. VESIĆ

Contract with
THE STATE HIGHWAY DEPARTMENT OF GEORGIA
in Cooperation with
THE BUREAU OF PUBLIC ROADS

DECEMBER 31, 1960 through DECEMBER 31, 1961

TABLE OF CONTENTS

This report contains 31 pages.

LIST OF FIGURES

LIST OF FIGURES (Continued)

CHAPTER I

INTRODUCTION

1. Scope of Project

It has been the purpose of the entire investigation to determine the stresses produced in the soil subgrade beneath a flexible pavement by wheel loads on the surface. A review of theoretical methods for analyzing stresses in elastic masses was followed by a full scale static load tests of pavement-base subgrade systems in which the stresses were measured. The results of tests of topsoil, soil bound macadam, sand asphalt, and soil cement bases with different base and asphaltic concrete surface thicknesses but all with the same elastic silt subgrade, were presented in the previous project reports, Annual Report 1, Annual Report 2, and Final Report.

2. Summary of Present Phase

It was pointed out in the review of Annual Report 2 and the Final Report that the test data for the sand asphalt base supported by the elastic silt subgrade might not be a valid representation of the sand asphalt base as used in highway construction in Georgia. Such bases are invariably built on sand subgrades whose elastic properties may be significantly different from those of the silt subgrade used in the pavement stress measurements in the previous phases of the project.

A new test subgrade was constructed of compacted sand, with pressure cells embedded at different levels. The same sand as previously employed for the sand asphalt was again used for the sand asphalt base, and a 3 in. asphaltic concrete surface was formed as for the previous tests. This report presents the results of the stress measurements in the sand subgrade as well as the

pertinent physical properties of the base and subgrade materials.

The results indicate that the sand asphalt base distributes the wheel load to the sand subgrade in about the same manner as it does to the elastic silt. The maximum stresses measured in the subgrade are somewhat higher than those determined by the Boussinesq theory for a homogeneous, isotropic, semi-infinite elastic solid.

CHAPTER II

MATERIALS AND THEIR PROPERTIES

1. Material Classification

The asphaltic surface was the same hot mix secured from an asphalt plant in Atlanta. No tests were made of this material; however, it was purchased under the same specifications from the same source as before and it was compacted in the same way.

The soil for the base course was the remainder of the natural Coastal Plain sand secured from a borrow pit on a current State Highway Project in South Georgia. It is a clean uniform, medium size subangular quartz sand classifying as A-3 by the Revised Public Roads System. It is typical of the ancient shore and beach terrace deposits of the Coastal Plain. The grain size test results on this material are given in Fig. 1. This soil was mixed with 5 per cent by weight of RC-3 cutback asphalt and compacted to approximately 100 per cent of the maximum density as given by ASTM D698-58T, method A.

The subgrade was a subangular uniform medium size quartz sand slightly stained with iron oxide and with a trace of mica. It was obtained by washing of the creek bottom deposits of a tributary of the Chattahoochee River just south of Atlanta. The grain size curve, Fig. 1 shows its gradation is almost identical to that of the base course sand. It also falls in the A-3 classification.

A standard compaction test, ASTM D698-58T was made. The results are given on Fig. 2.

2. Triaxial Tests

Triaxial shear tests were made of samples of both the sand asphalt and the subgrade sand, the former compacted to 100 per cent and the latter to 95 or more

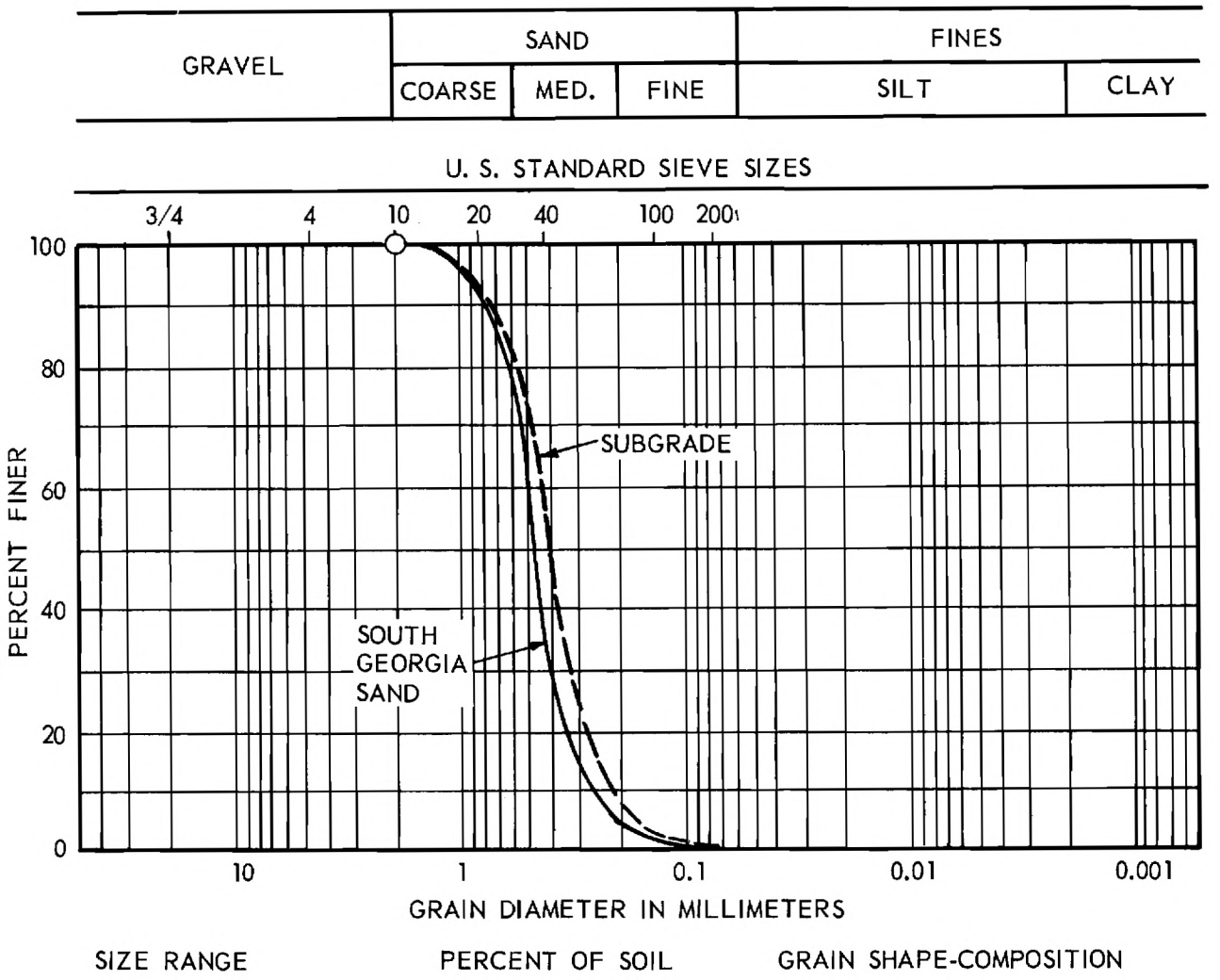

SOIL DESCRIPTION:

———— South Georgia Sand for Sand-Asphalt Base – 600 Test Series.

— — — — — Subgrade Sand 600 Test Series.

Figure 1. Grain Size Curves: Base and Subgrade Sands.

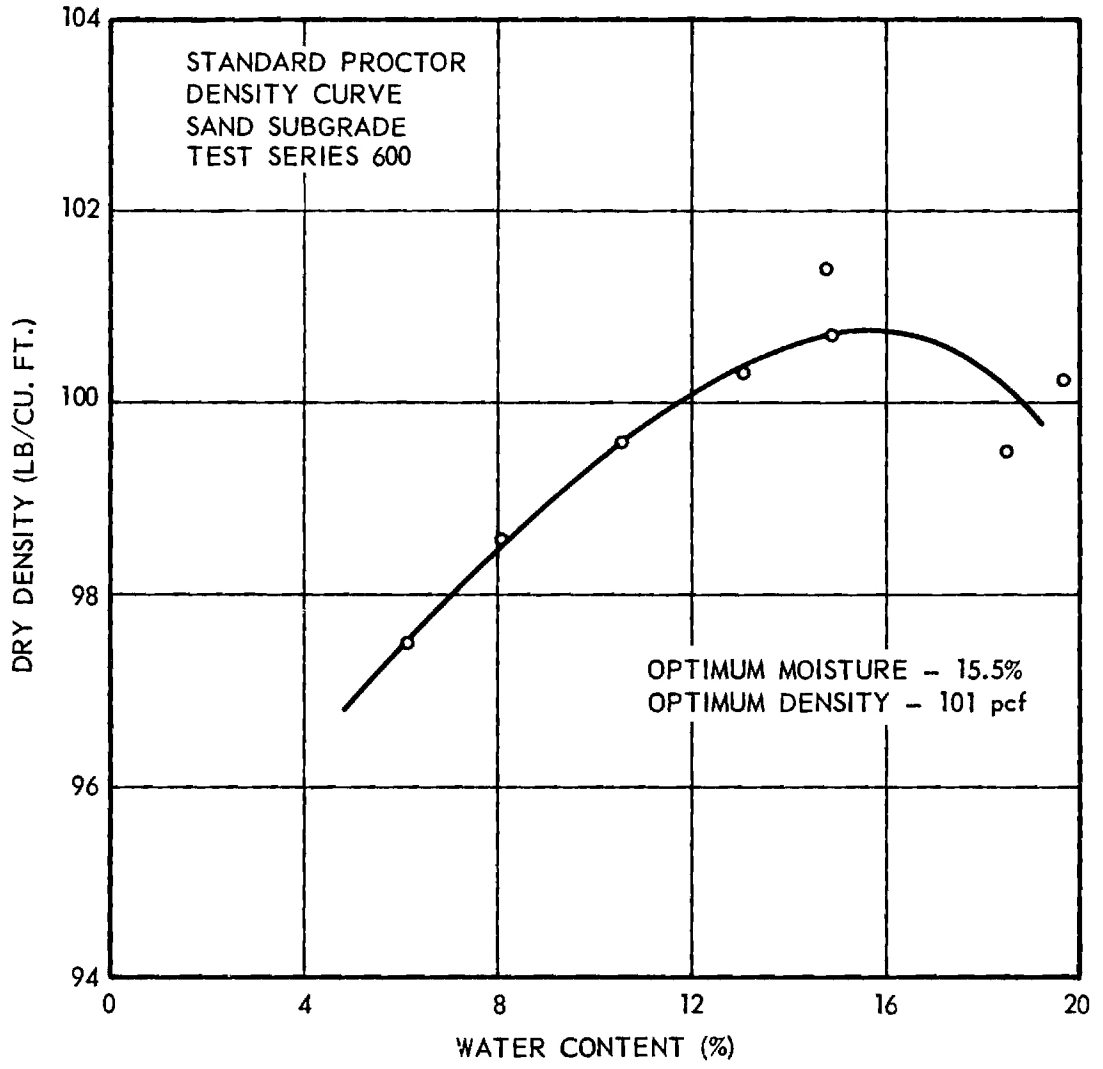

Figure 2. Compaction Test: Subgrade Sand.

per cent of the maximum as given by ASTM Standard D698-58T.

The data for the sand asphalt samples are given in the form of stress-strain curves, Fig. 3a and a Mohr Envelope, Fig. 3b. It is significant that the results are almost identical to those found for the sand asphalt base prepared by different personnel two years ago: the new "cohesion" is 3 psi compared with the earlier 2 psi and the new ϕ is 31 deg compared with the earlier 33 deg. (Both tested at 80° F and at a deformation rate of 0.02 in. per min.) The tangent modulus of elasticity from the triaxial compression is given on Fig. 4. It shows that E increases approximately in proportion to the confining pressure.

Similar data for the subgrade sand are given in Fig. 5 and 6. The sand has an angle of internal friction, ϕ of 35 deg but no cohesion. The modulus of elasticity, Fig. 6, was found to be approximately proportional to the confining pressure similar to that of the base. A comparison between E values for the base and subgrade soils at equal confining pressures, Fig. 7, shows that the base is three-fourths as rigid as the subgrade. This might be expected because the asphalt interferes with true particle-to-particle contact, interposing asphalt between the more rigid quartz grains of the sand.

3. In-Place Tests

In-place load tests were made on both the base and on the subgrade. Only the smallest plate, 8 in. in diameter, was used on the base because of the limited sand asphalt thickness (8 in.). Tests of the sand subgrade employed both 8 in. diameter and 30 in. diameter plates.

All the plate load tests employed a similar loading: two cycles of load to approximately half the computed failure pressure followed by unloading and

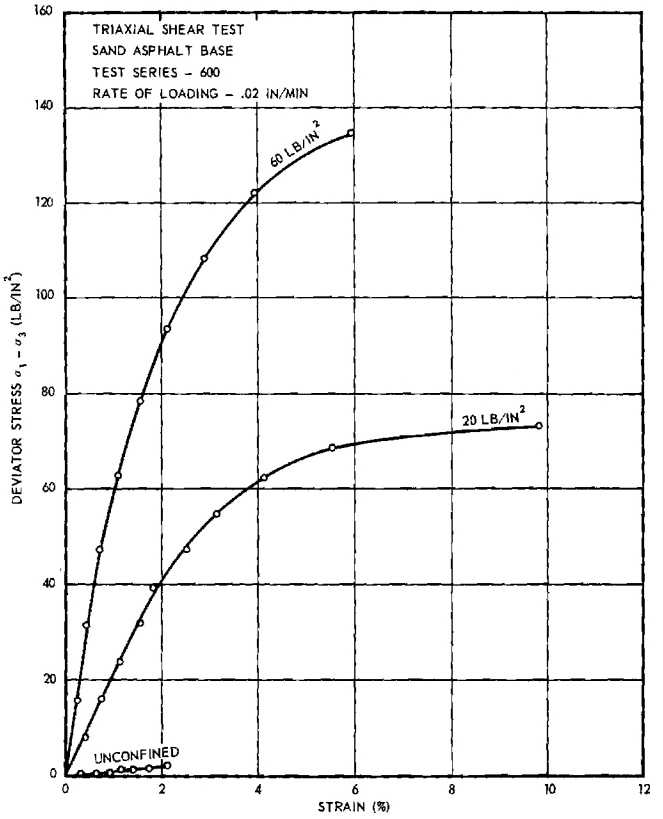

Figure 3a. Triaxial Test Results: Stress Strain of Sand Asphalt Base.

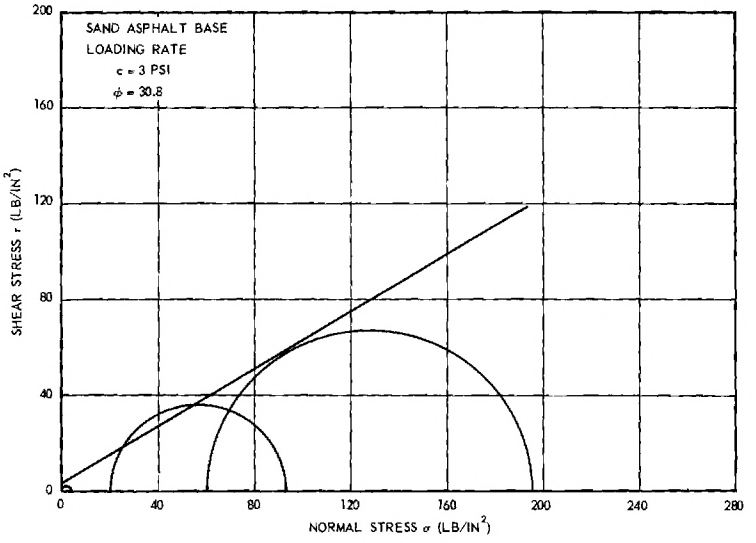

Figure 3b. Triaxial Test Results: Mohr Envelope of Sand Asphalt Base.

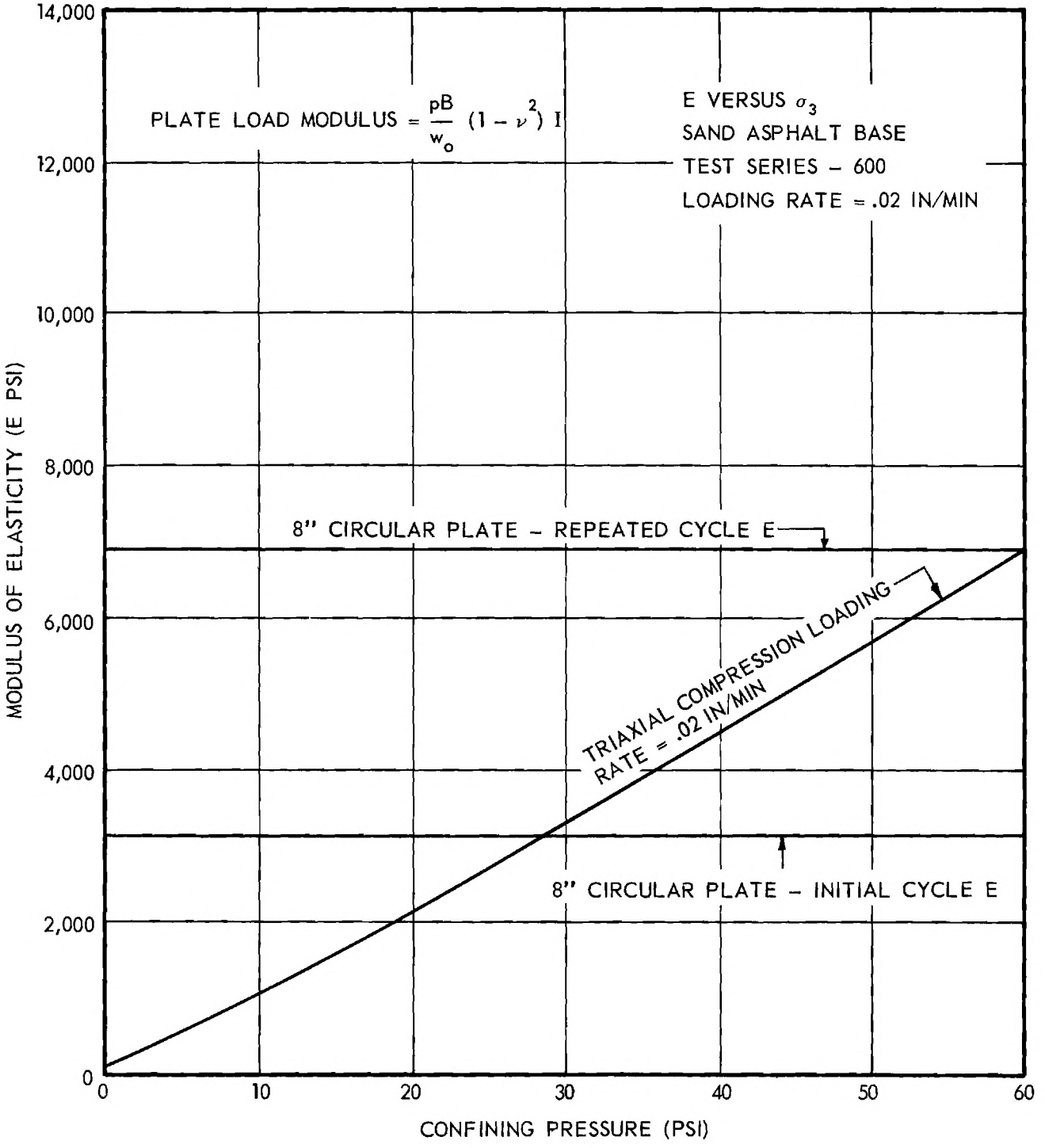

Figure 4. Modulus of Elasticity of Sand Asphalt Base from Triaxial Tests at Different Confining Pressures and Computed from Plate Load Tests

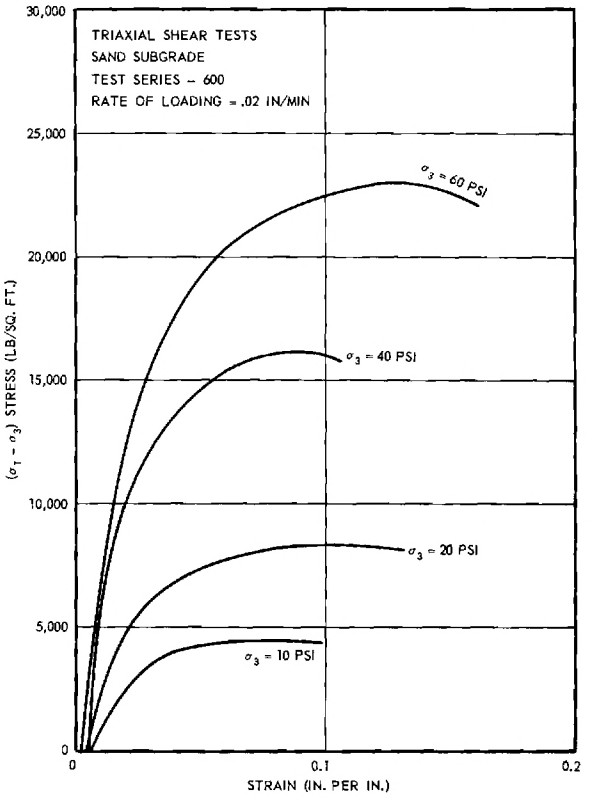

Figure 5a. Triaxial Test Results: Stress Strain of Sand Subgrade.

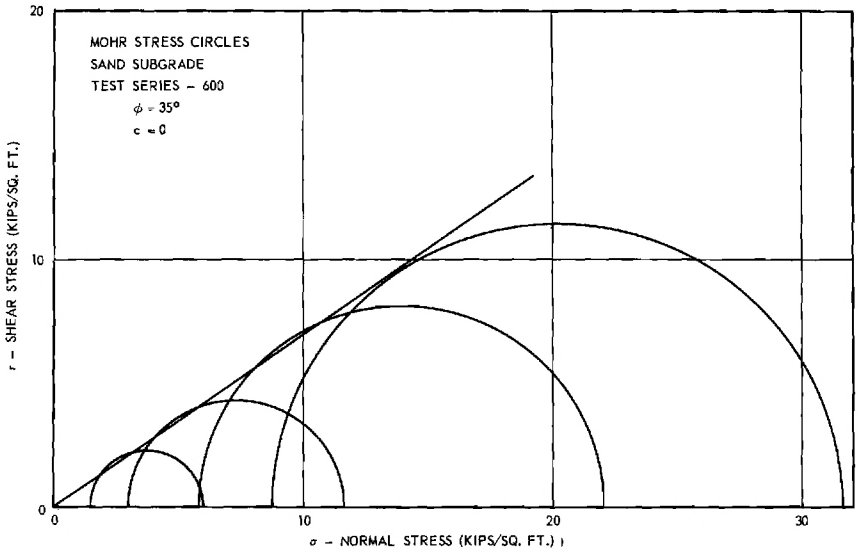

Figure 5b. Triaxial Test Results: Mohr Envelope of Sand Subgrade.

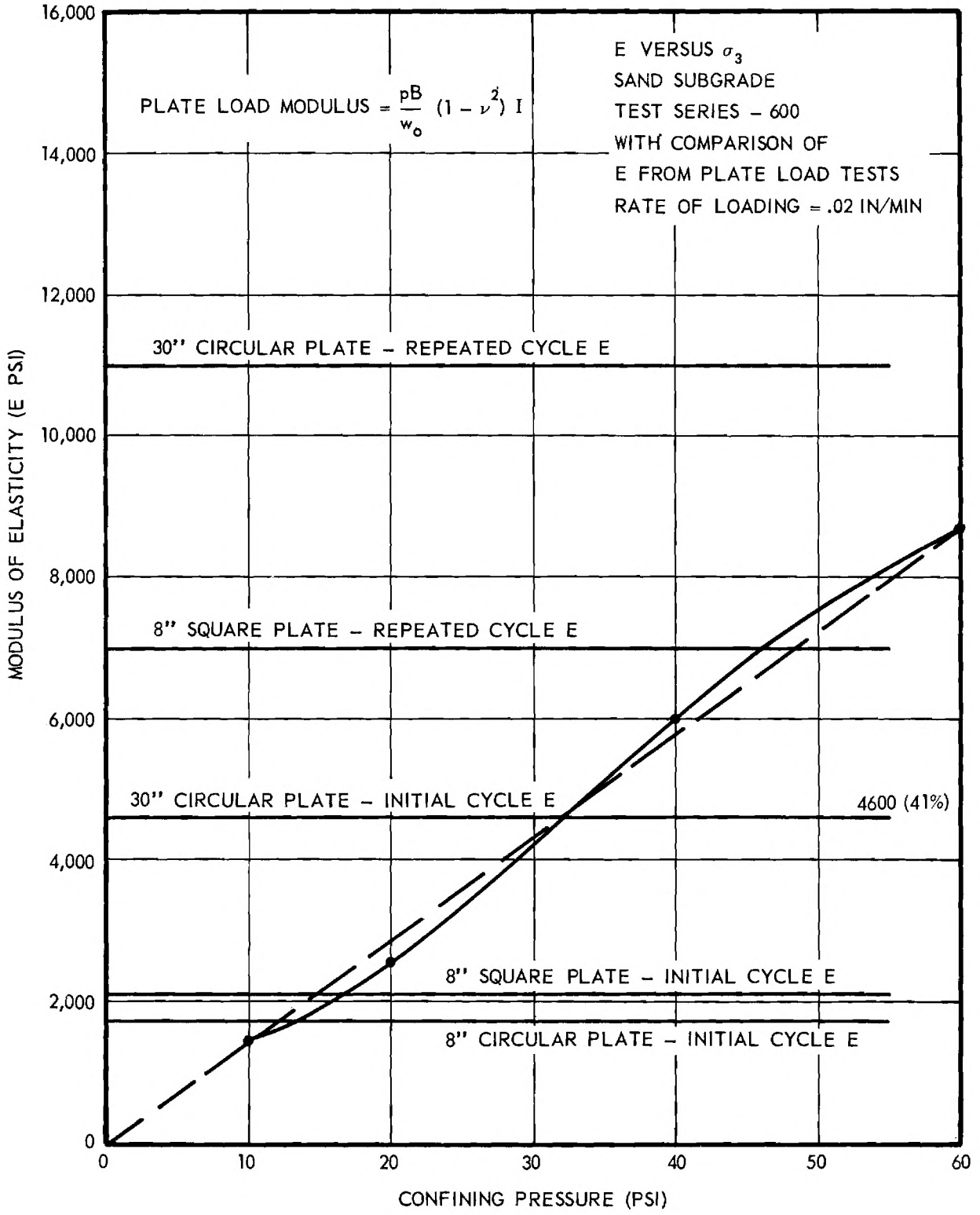

Figure 6. Modulus of Elasticity of Sand Subgrade from Triaxial Tests at Different Confining Pressures and Computed from Plate Load Tests.

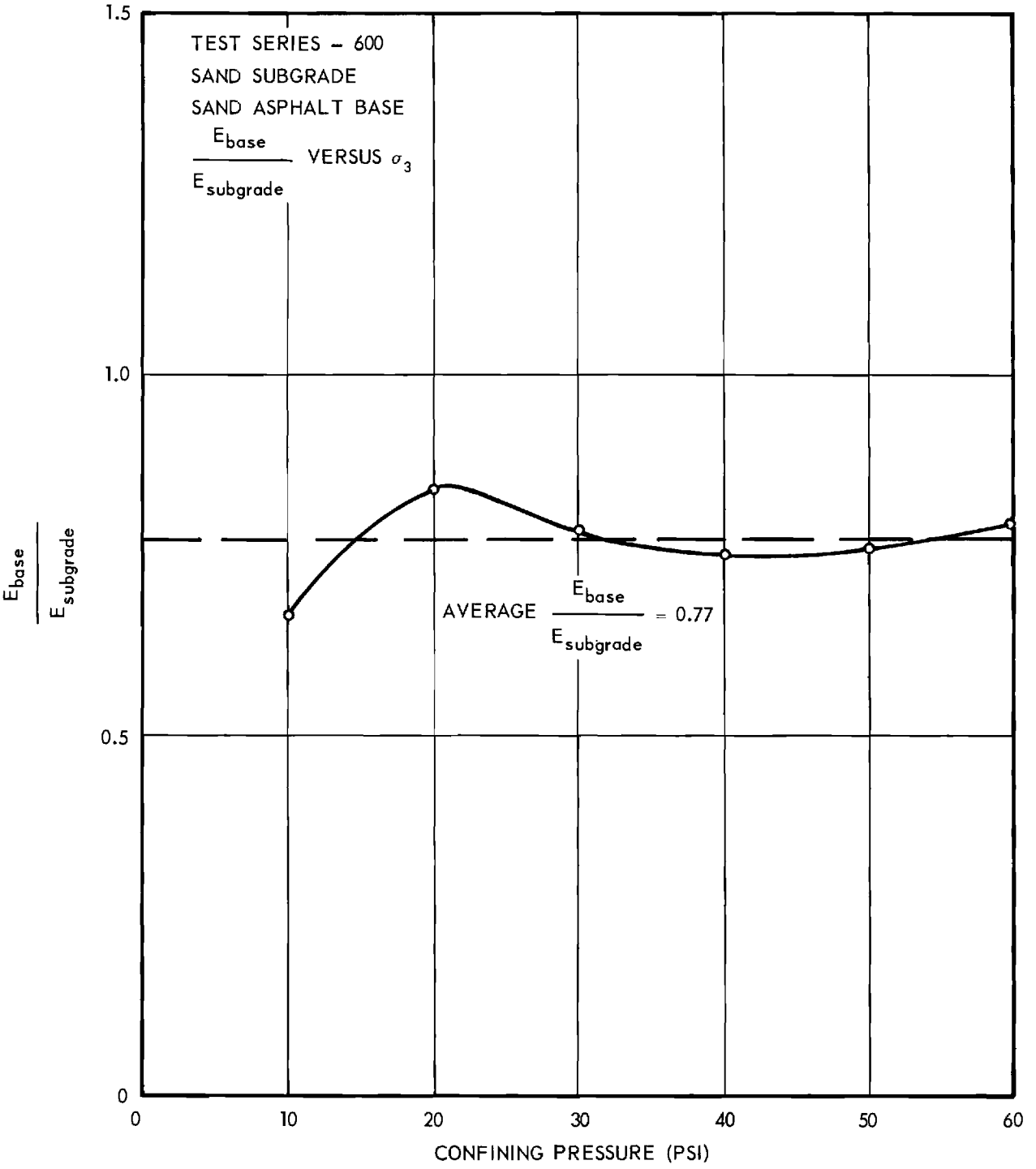

Figure 7. Ratio of Moduli of Elasticity: Sand Asphalt Base to Sand Subgrade at Different Lateral Confining Pressures.

then a third loading to twice the repeated load. The results for the 30 in. diameter plate on the sand subgrade are given in Fig. 8; the results of the other tests are similar. The rate of deformation with respect to pressure is more rapid on the first loading than for the others. The second and third loadings exhibit identical rates of deformation with respect to pressure that are 37 to 45 per cent of the initial loading rates. The "effective" modulus of elasticity of the soil immediately below the test plate was computed from the rate of deformation with respect to pressure using the theory of a homogeneous isotropic semi-infinite elastic solid. The results are shown by horizontal lines on the modulus of elasticity data charts, Figs. 4 and 6.

A field California Bearing ratio test was made on the sand asphalt to define its strength in terms of that widely used design index. The results, Fig. 9, indicate a CBR of 14.

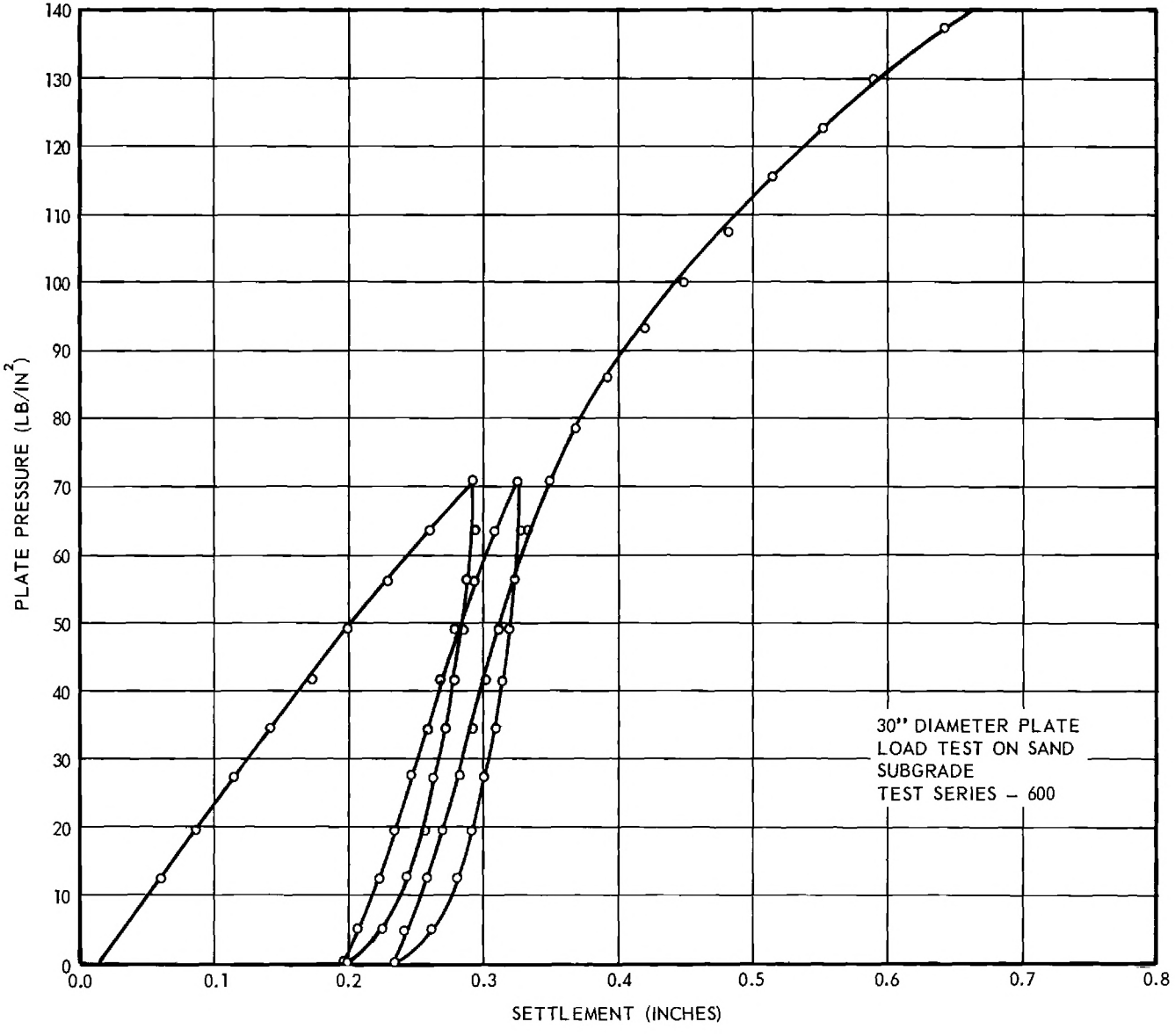

Figure 8. Plate Load Test Results: 30 in. Circular Plate on the Sand Subgrade.

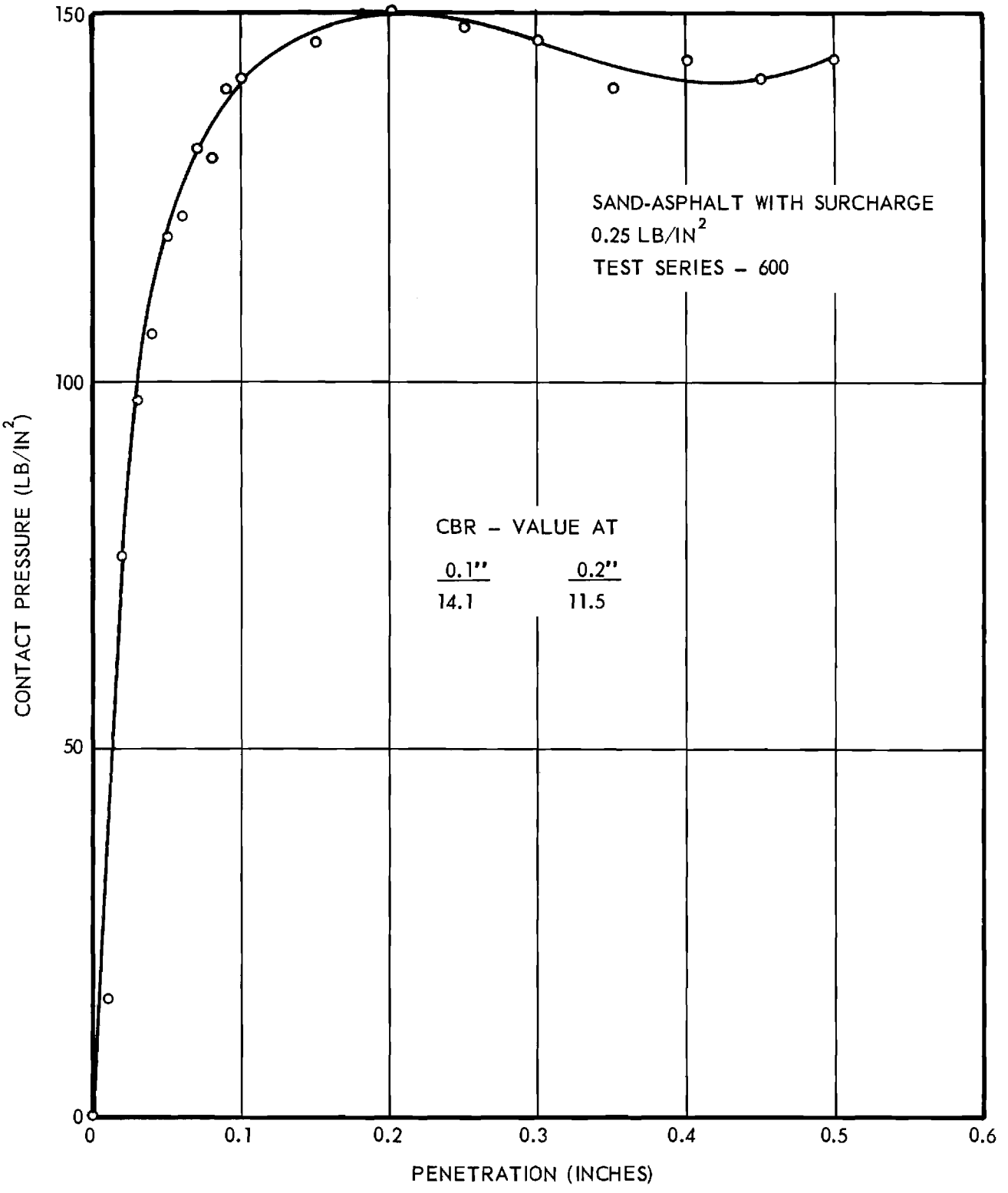

Figure 9. California Bearing Ratio: Sand Asphalt Base.

CHAPTER III

PAVEMENT TESTS

1. Pavement Construction

The subgrade and pavement were constructed in the same 8 ft. wide, 12 ft. long and 7 ft. deep test pit as employed for the previous tests. The bottom 3 ft. of subgrade was compacted to 95 per cent of the maximum as specified by ASTM D698-58T and the remaining 3 ft. to 100 per cent of the maximum by a vibrating tamper, the Jay-Tamp. The 8 in. sand asphalt base was compacted to 100 per cent of the same maximum in 1 in. thick layers. The 3 in. asphaltic concrete surface was compacted in 2 layers until no further densification was observed.

2. Pressure Cell Installation

The same 4 in., 5 in. and 6 in. diameter pressure cells employed for the previous tests were installed in the subgrade at 3 different levels. A slightly different placement pattern was used to secure a better coverage of the more highly stressed zone.

The cells had all previously been calibrated in the elastic silt. Calibration studies had shown that arching over the cells' flexible diaphrams was negligible and that the pressure indicated by each cell in the silt was the same as that indicated when the cell diaphram was subjected to a uniform fluid pressure.

When the calibration was checked in the subgrade sand an appreciable error developed. The cells indicated less than half of the pressure actually exerted on the sand in the calibration chamber. When the chamber was subjected to shock or vibration the cells indicated the correct pressure. It was obvious from these tests that the sand was arching across the cells. As might be expected the

arching error was greater for the wider cells and the more flexible diaphrams than for the smaller cells. It was therefore necessary to recalibrate all the cells and find an arching correction factor for the sand. Reasonably consistent factors were found for the 4 in. and 5 in. cells employed in the upper two layers of cells. The corrections for the 6 in. cells were erratic.

3. Wheel Load Tests

Tests loads were applied to the pavement surface using single tires with loads of 9000 lb and 13,500 lb and to dual tires with total loads of 9000 lb, 13,500 lb and 18,000 lb. The loads were statically applied to 9 in. by 20 in. truck tires and the stresses in the subgrade were measured by pressure cells, using essentially the same equipment and procedures as employed in the previous tests. The test results are given in Figs. 10 through 19. These show the measured increase in vertical normal stress on a horizontal plane as a function of the horizontal distance from the center of the load. Two or three graphs are given on each figure, each representing a different depth below the pavement surface. Two types of plots are shown: the basic data, Figs. 10, 12, 14, 16, and 18, show all the pressure cell measurements. These are the same form of data representation that were included in all the previous reports and show the extent of the scatter or variation in the individual readings obtained in successive tests or by different cells at the same distance from the load center. The second form of plot, Figs. 11, 13, 15, 17, and 19, shows only the average of all the measured stresses at any one distance from the load center. In this plot the effect of the scatter between individual readings is minimized and the stress trend is more easily seen.

The theoretical stress distribution for each depth is shown by the solid or solid and dashed curves on each graph. These were computed by the Boussinesq

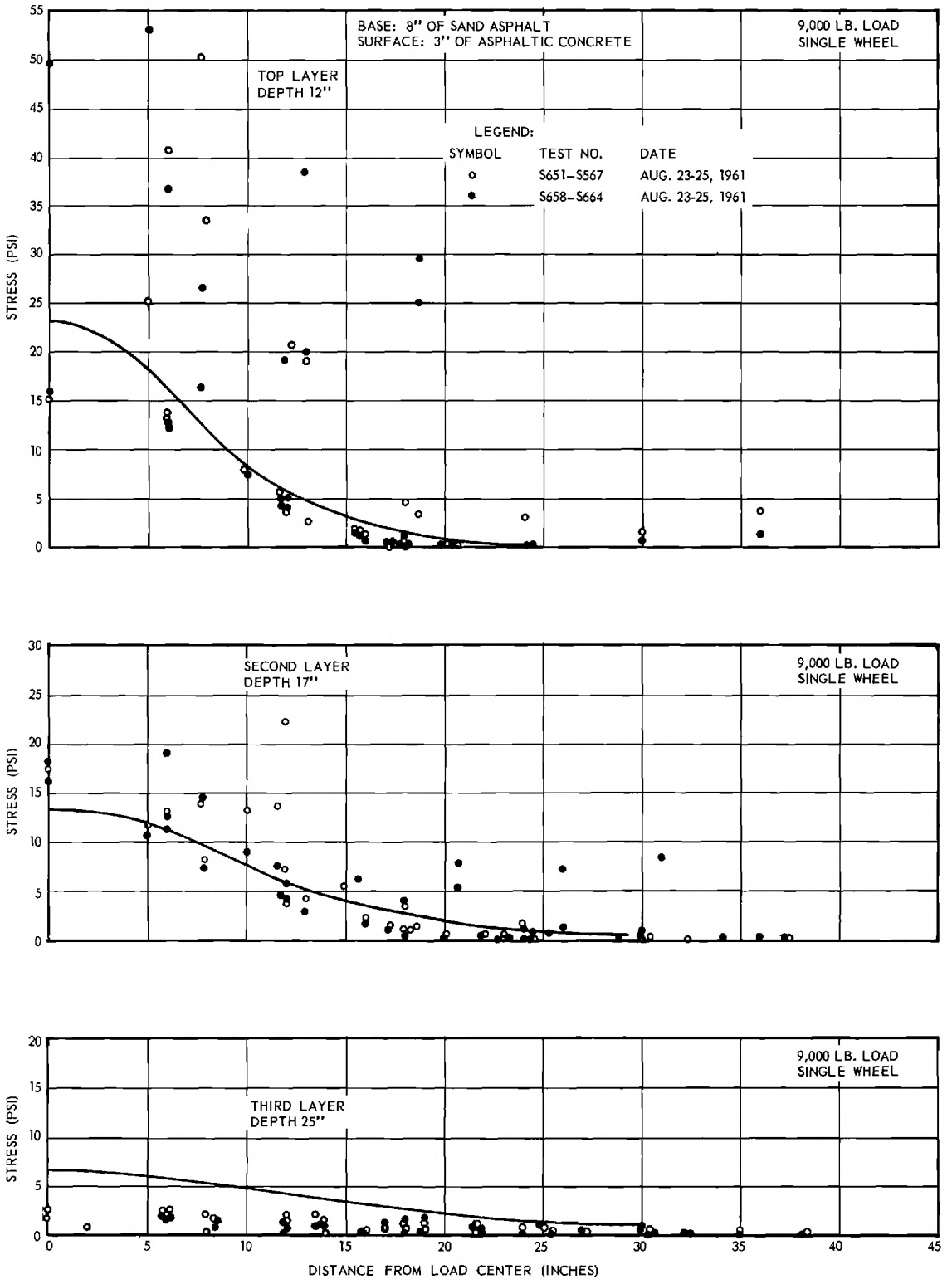

Figure 10. Measured Stresses in Sand Subgrade: 9000 lb Single Wheel, Sand Asphalt Base.

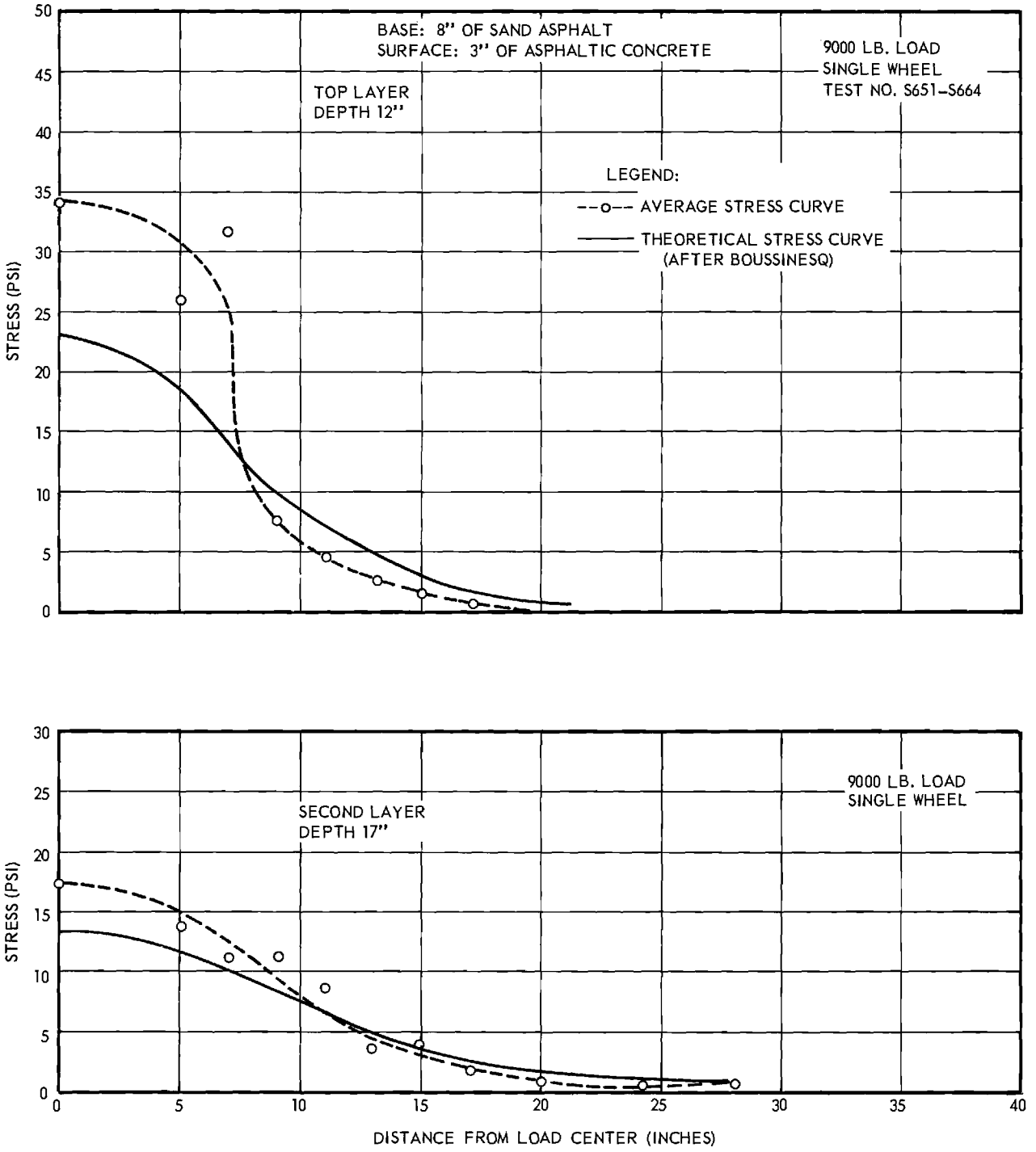

Figure 11. Average Measured Stresses in Sand Subgrade: 9000 lb Single Wheel, Sand Asphalt Base.

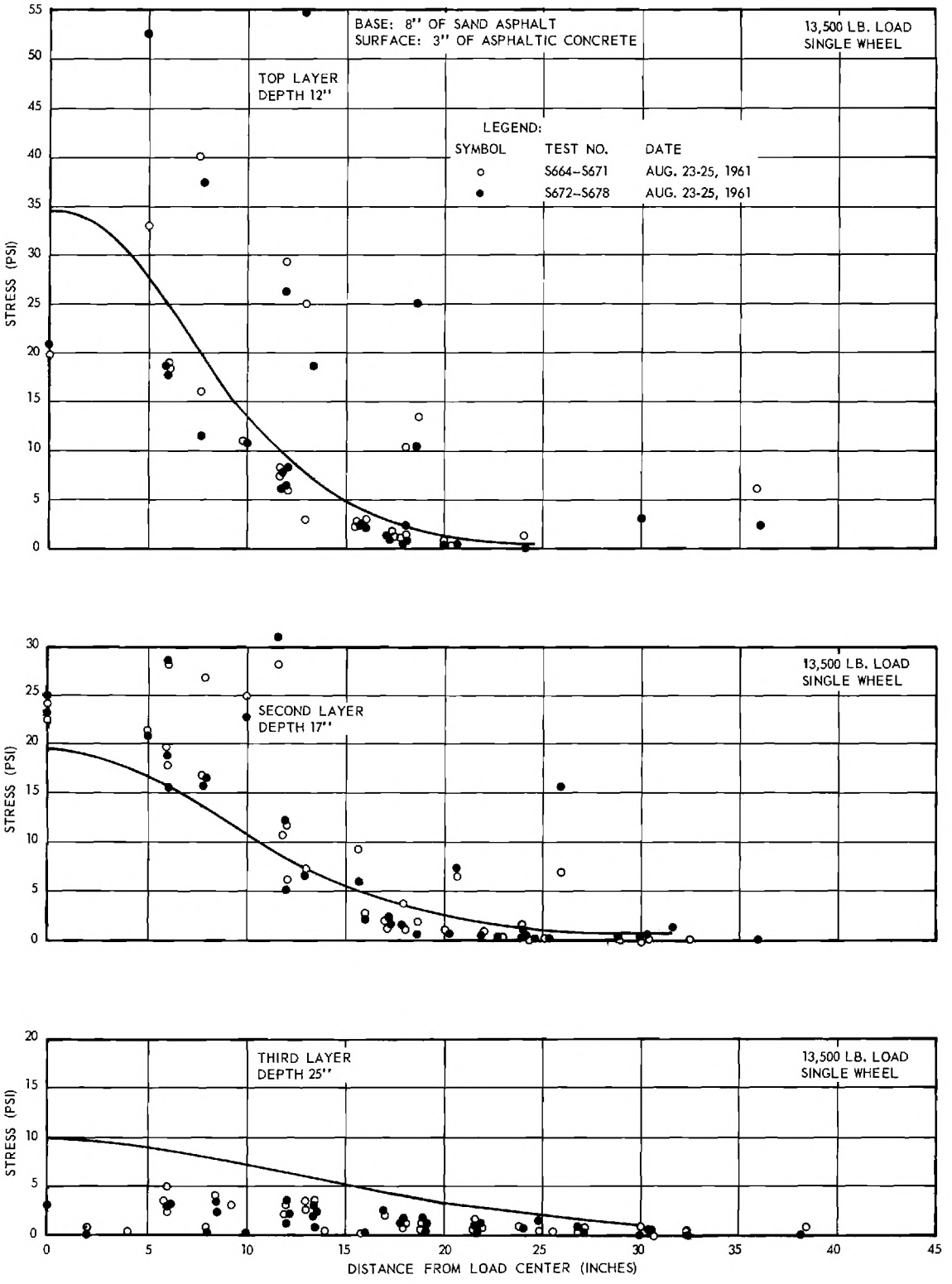

Figure 12. Measured Stresses in Sand Subgrade: 13,500 lb Single Wheel and Sand Asphalt Base.

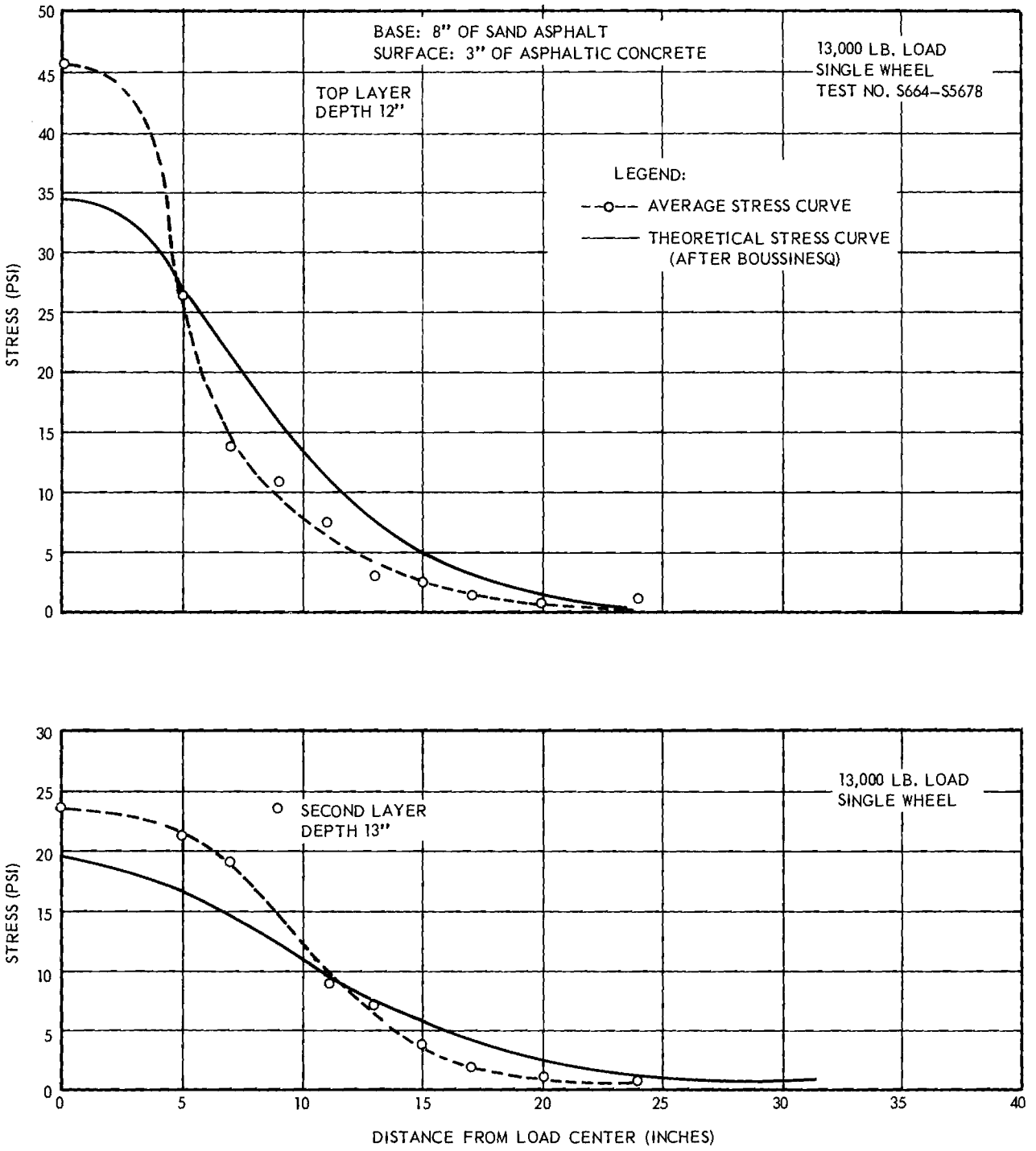

Figure 13. Average Measured Stresses in Sand Subgrade: 13,500 lb Single Wheel, Sand Asphalt Base.

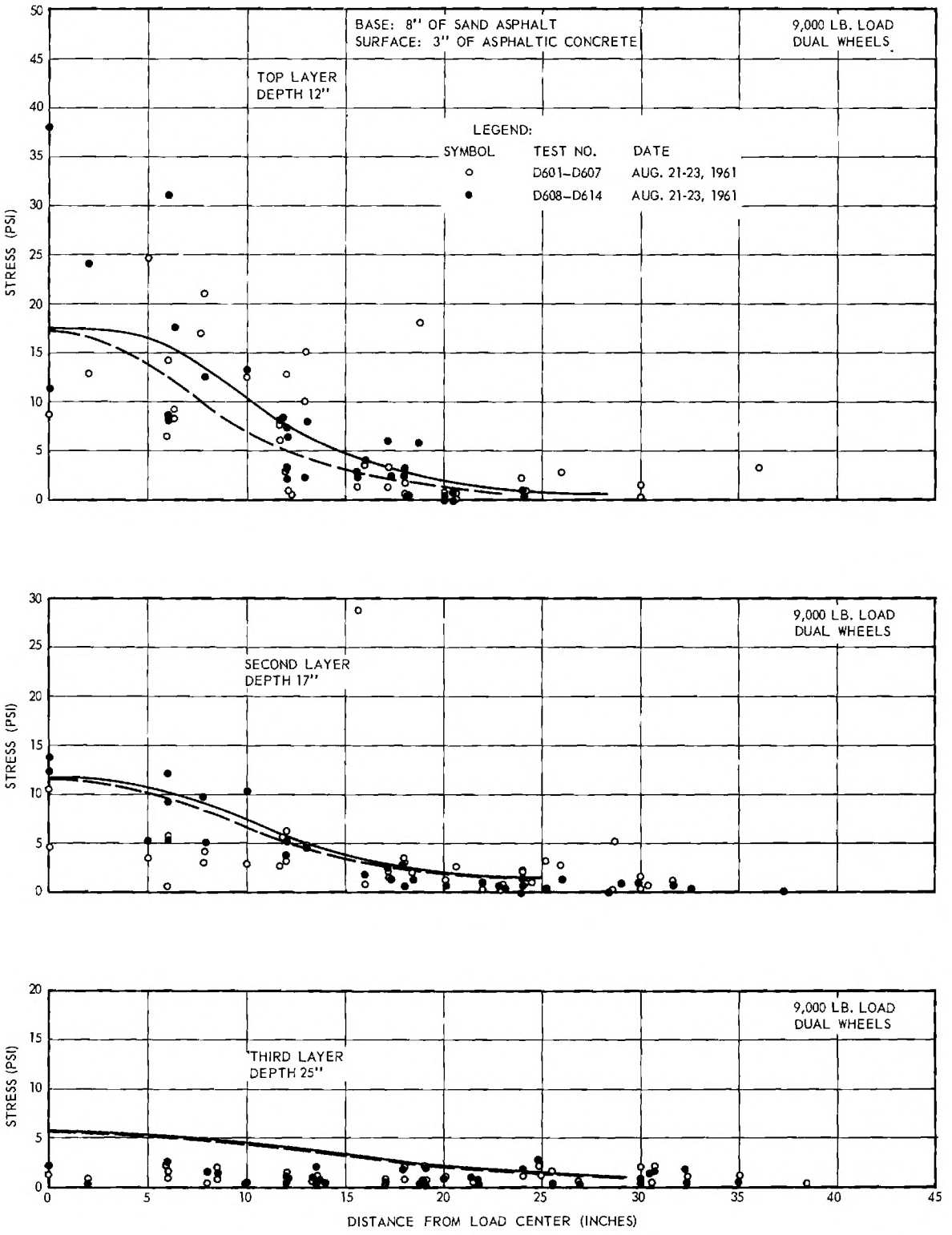

Figure 14. Measured Stresses in Sand Subgrade: 9000 lb Dual Wheels, Sand Asphalt Base.

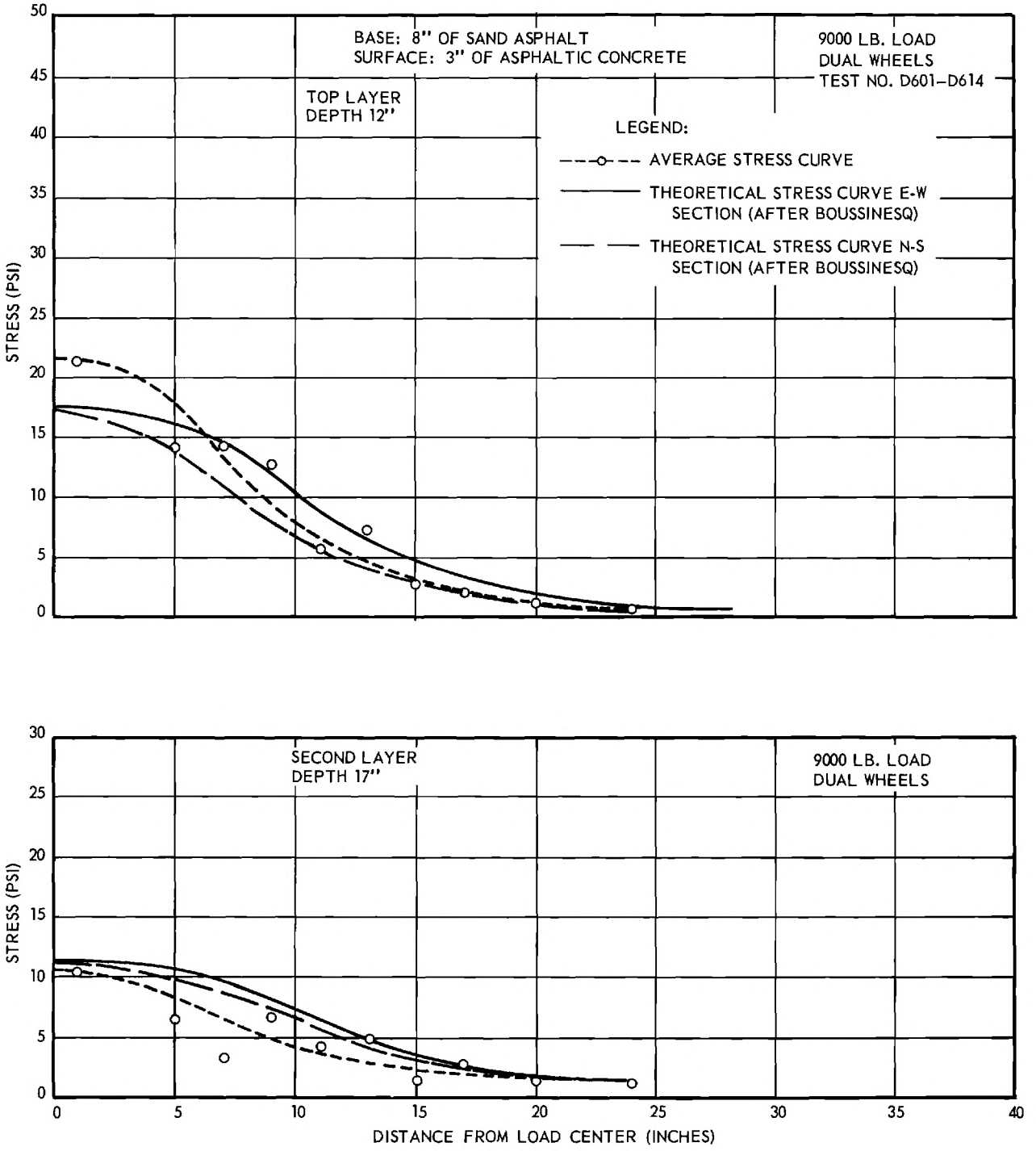

Figure 15. Average Measured Stresses in Sand Subgrade: 9000 lb Dual Wheels, Sand Asphalt Base.

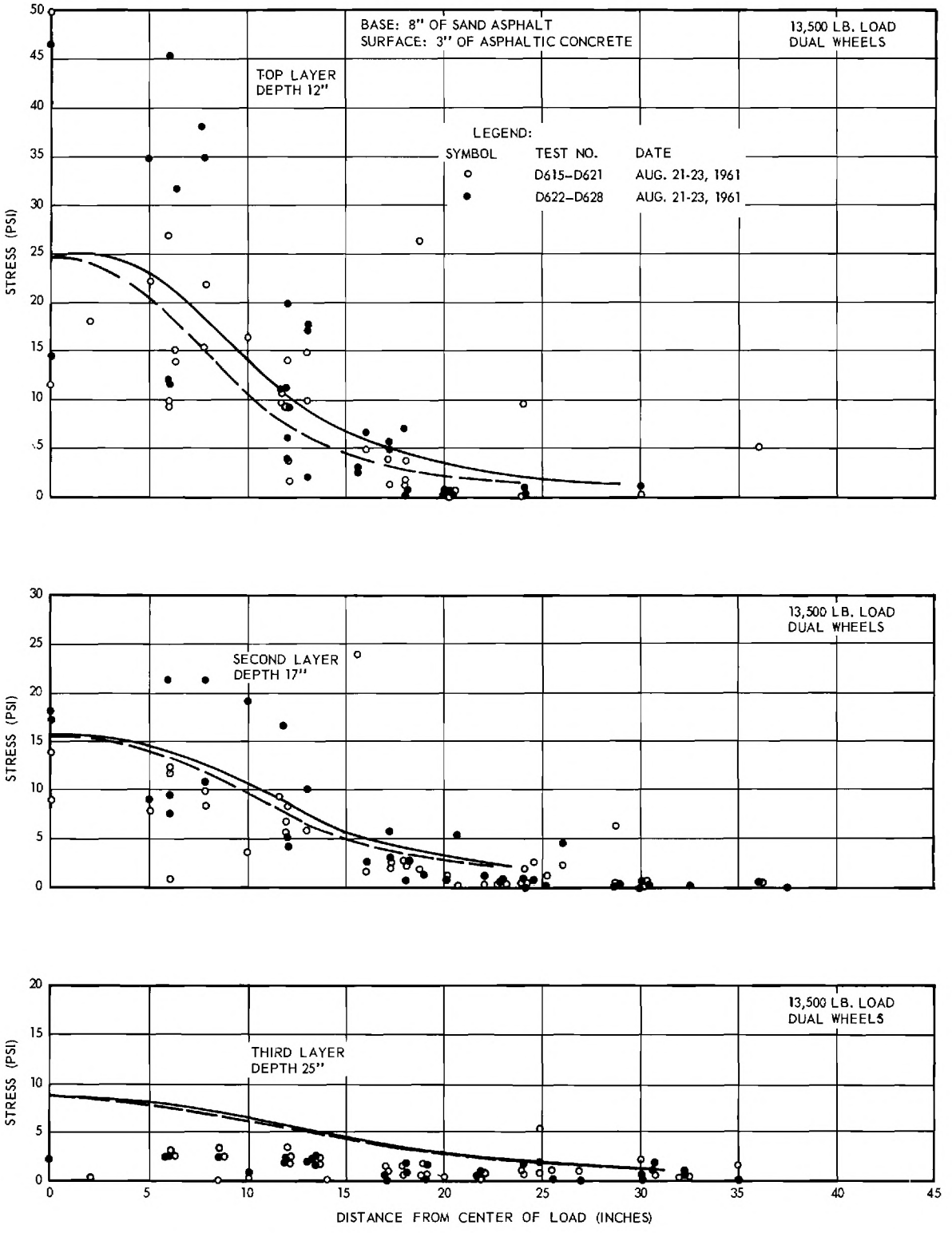

Figure 16. Measured Stresses in Sand Subgrade: 13,500 lb Dual Wheels, Sand Asphalt Base.

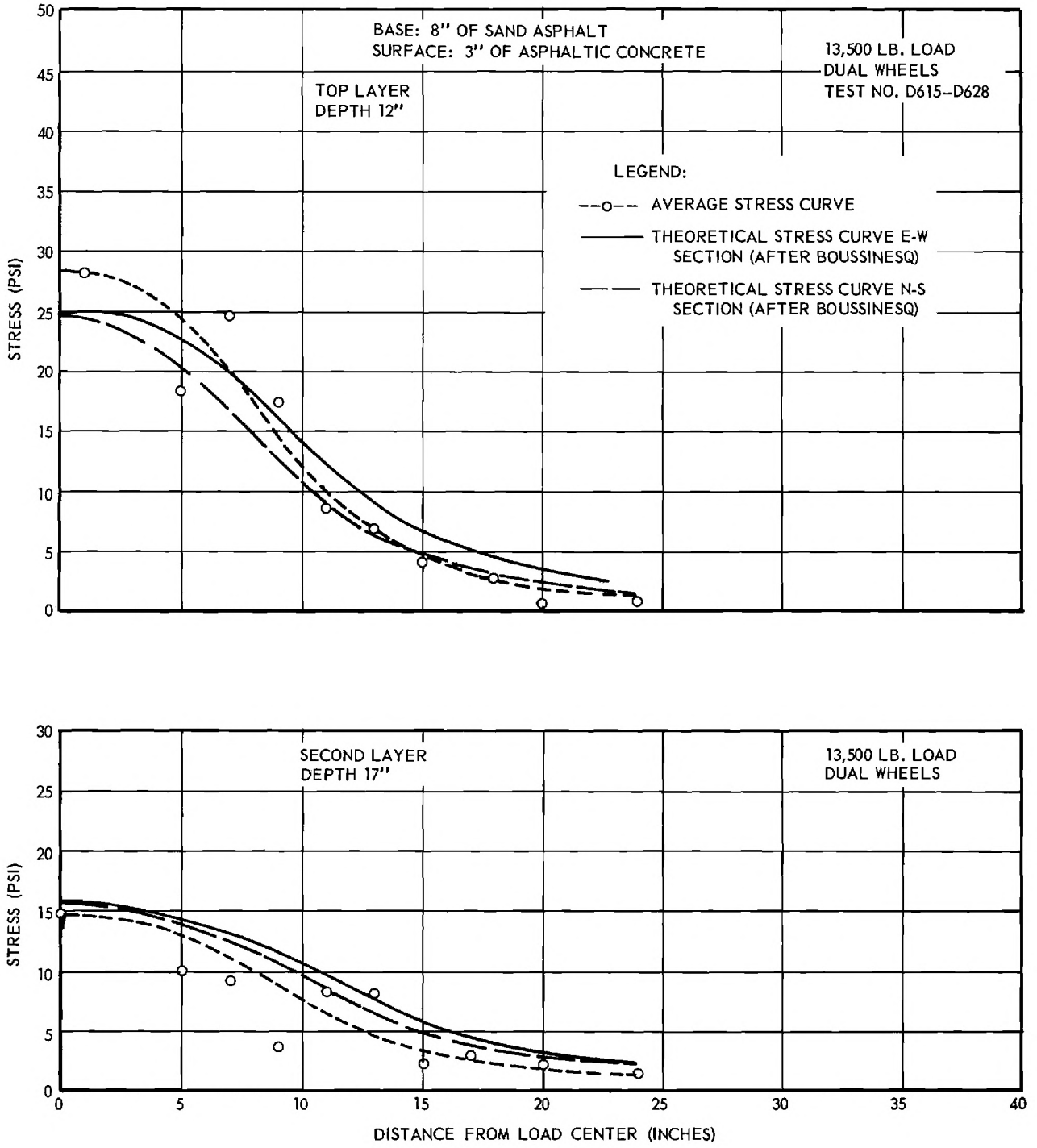

Figure 17. Average Measured Stresses in Sand Subgrade: 13,500 lb Dual Wheels, Sand Asphalt Base.

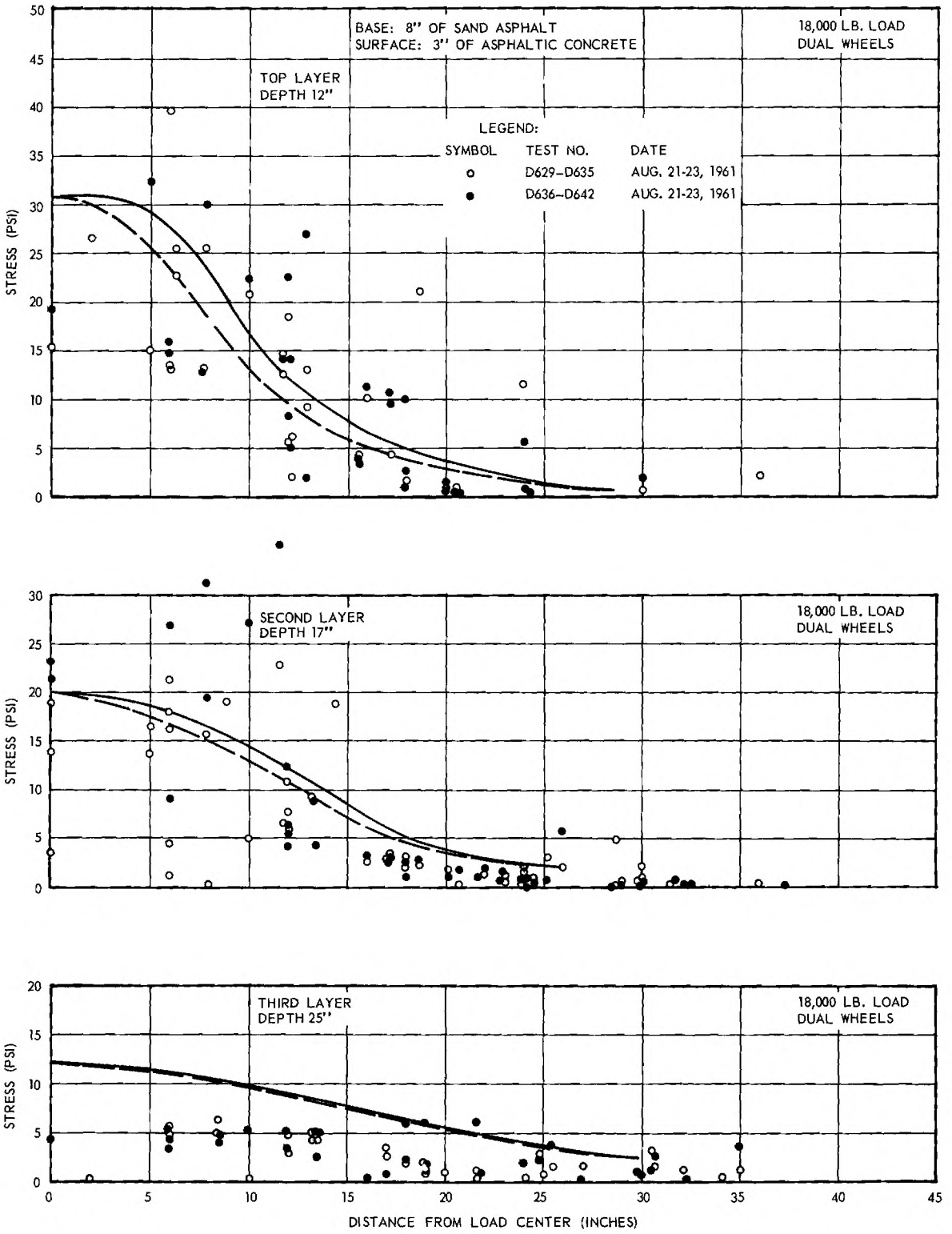

Figure 18. Measured Stresses in Sand Subgrade: 18,000 lb Dual Wheels, Sand Asphalt Base.

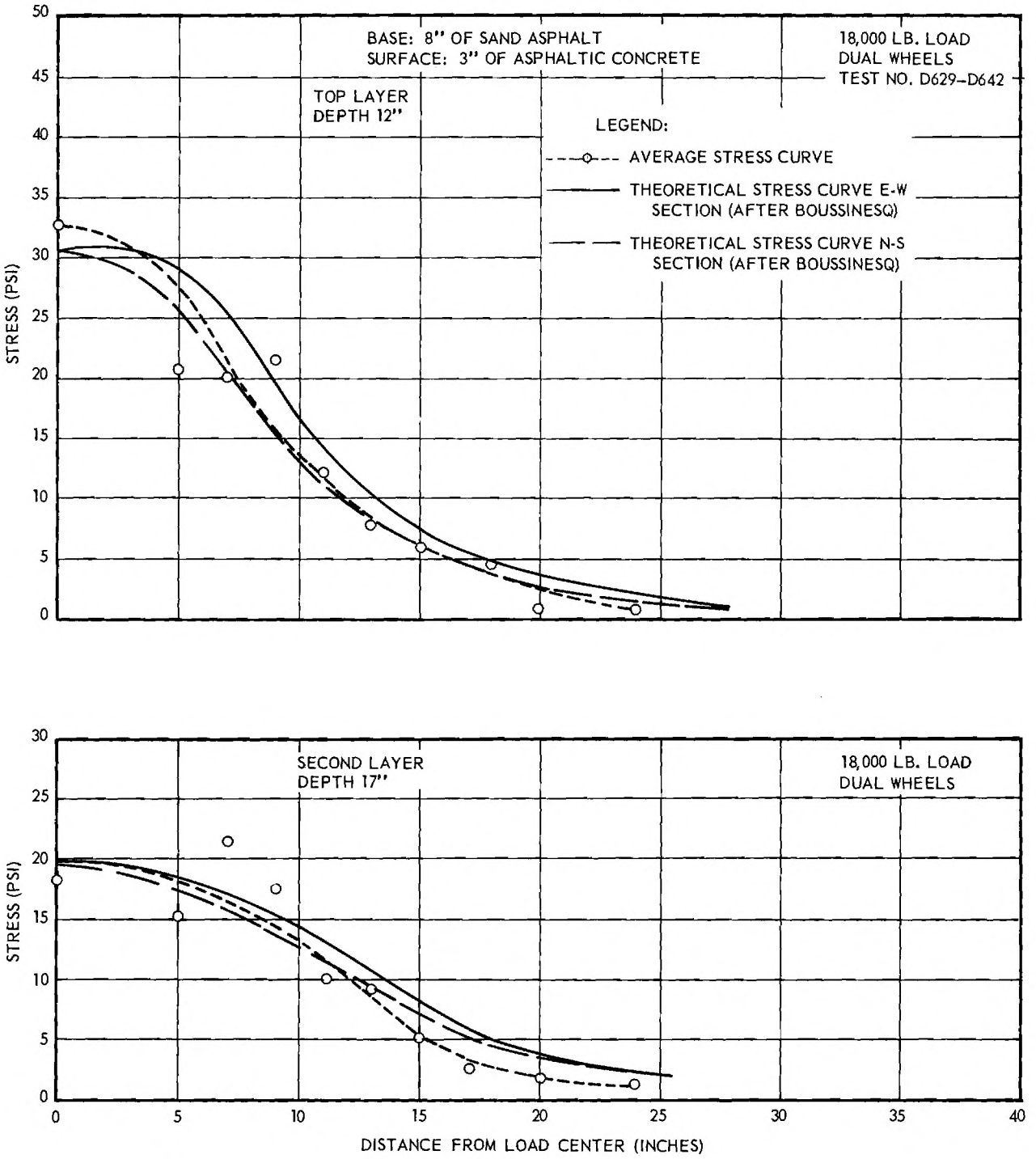

Figure 19. Average Measured Stresses in Sand Subgrade: 18,000 lb Dual Wheels, Sand Asphalt Base.

theory for a semi-infinite homogeneous, isotropic, elastic solid. They are based on a circular or rectangular approximation of the actual loaded area (p. 16, Annual Report 1) and a uniform tire pressure computed from the contact area. Two curves are shown for the dual tires: the solid curve represents the stresses on a cross section parallel to and directly below the axle while the dash line represents stresses on a cross section perpendicular to the axle and midway between the two tires. A dotted curve appears on Figs. 11, 13, 15, 17, and 19; it represents the observed average stresses.

4. Discussion of Test Results

As in all the previous tests there was considerable scatter among the individual readings. In general the scatter was more pronounced in this test series than in any of the previous ones although the testing techniques had improved. The reason appeared to be variations in the degree of arching across the individual cells, from one test to the next which affected the cell zero readings. This should be expected because arching is intimately related to minute variations in soil structure and to details of stress history. The averages of the measurements, however, indicate a well-defined variation of stress with depth and distance in spite of the scatter.

The test data all indicate that the stress in the sand subgrade decreases with increasing depth and with increasing horizontal distance from the load center. The stresses indicated by the third layer of cells (a depth of 25 in.) were very low. They are inconsistent with the indicated stresses in the upper two layers of cells and are far lower than can be computed by any of the theories of soil stress distribution. Since consistent calibrations could not be obtained for these cells, it is the author's opinion that these data are invalid. They

are presented only for completeness and are not discussed further in this report.

The average stress curves exhibit a similarity to the theoretical Boussinesq stress distribution. The maximum stress, however, is generally greater than the Boussinesq as shown by the following table.

Ratio of Maximum Average Measured Stress to Boussinesq Maximum Stress

Depth	Single Wheel	Dual Wheel
12 in.	1.42	1.14
17 in.	1.28	.95

Similar but greater excesses of the measured stresses over the Boussinesq were found in the upper part of the elastic silt subgrade beneath a sand asphalt base. For the single tires and loads of 9000 and 13,000 psf the average ratio at a depth of 11.3 in. was 1.5 and for the dual tires, 1.3. Deeper in the subgrade the stresses were essentially the Boussinesq. The excess was explained by the Griffith-Fröhlich Theory (1) which demonstrates that in a material whose modulus of elasticity increases with confining pressure there is a concentration of stresses immediately beneath the load. The disappearance of the difference deeper in the silt subgrade was explained by the fact that the elastic properties of the silt are more nearly like those assumed in the Boussinesq analysis.

In the present tests, the modulus of elasticity data, Figs. 4, 6, and 7 show that both the sand asphalt base and the sand subgrade E's increase in proportion to the confining pressure. Although the Griffith-Fröhlich theory has not been extended to a two layer system it would be reasonable to presume that a similar stress concentration would exist if both layers had an increasing E. In fact, if the upper layer (base) had a smaller E than the lower (subgrade), we would expect a greater concentration of stress close to the interface between the

layers than deeper within the second layer. Such was the case in the present test results.

The observed degree of stress concentration for the single tire is comparable to a Griffith-Frölich concentration factor of 4. This is the concentration factor found by others for cohesionless sands such as the subgrade employed in the current tests.

The smaller degree of stress concentration for the dual tires can be explained by wider distribution of the load. This tends to counteract the stress concentration.

The plate load test data show that both the sand asphalt base and the sand subgrade increase in rigidity after the first application of load. The effect of the elasticity increase, if any, on the stresses beneath the loaded wheel could not be detected. Little change in the stress distributing capabilities would be expected because both increased in comparable proportions.

CHAPTER IV

FUTURE WORK

The previous tests all refer to the Boussinesq theory as a standard for comparison. Tests by the U. S. Waterways Experiment Station (2) on a homogeneous elastic clay soil with a uniform circular load have verified the validity of the Boussinesq theory for that soil. Similar tests on the elastic silt employed in these studies would fill in a gap in the knowledge gained in these tests.

Deflection data have been obtained in all the tests. These will be analyzed as a part of the current pavement evaluation study.

Respectfully submitted:

George F. Sowers
Project Director

Approved by:

Thomas W. Jackson, Chief
Mechanical Sciences Division

REFERENCES

1. Griffith, J. H., "The Pressures Under Substructures," Engineering and Contracting, Vol. 1, 1929, p. 113.

   Frŏhlich, O. K., Drukverteilung im Baugrunde, J. Springer, Berlin, 1934.

2. Turnbull, W., A. A. Maxwell and R. G. Ahlvin, "Stress Distribution in Homogeneous Soil Masses," Proceedings Fifth International Conference on Soil Mechanics and Foundation Engineering, Paris, 1961, Vol. II, p. 337.

   Foster, H. A. and R. G. Ahlvin, "Stresses and Deflections Induced by a Uniform Circular Load," Proceedings Highway Research Board, Vol. 33, 1954, p. 467.

B-133

REPORT 5

PROJECT B-133 HPS-1(53)

THE STUDY OF STRESSES IN A FLEXIBLE PAVEMENT SYSTEM

GEORGE F. SOWERS

December 31, 1961 through December 31, 1963

Contract with
The State Highway Department of Georgia
in cooperation with
The Bureau of Public Roads

1963

Engineering Experiment Station
GEORGIA INSTITUTE OF TECHNOLOGY
Atlanta, Georgia

REVIEW
PATENT 3-25 1964 BY RAM SC
FORMAT 3-25 1964 BY FH

GEORGIA INSTITUTE OF TECHNOLOGY
Engineering Experiment Station
Atlanta, Georgia

REPORT 5

PROJECT B-133
HPS-1(53)

THE STUDY OF STRESSES IN A FLEXIBLE PAVEMENT SYSTEM

By

GEORGE F. SOWERS

DECEMBER 31, 1961 through DECEMBER 31, 1963

Contract with
THE STATE HIGHWAY DEPARTMENT OF GEORGIA
in cooperation with
THE BUREAU OF PUBLIC ROADS

TABLE OF CONTENTS

This report contains 27 pages.

LIST OF FIGURES

I. INTRODUCTION

A. Scope of report

This series of tests was conducted to complete the investigation of subgrade stresses in flexible pavement systems by applying static wheel loads directly to a subgrade. Previous reports included a review of theoretical methods for analyzing stresses in elastic masses followed by full scale static load tests of pavement-base subgrade systems. The results of tests of pavement systems utilizing an elastic silt subgrade material, with topsoil, soil-bound macadam, sand asphalt, and soil macadam cement base courses, and asphaltic concrete surfaces of varying thicknesses were presented in Annual Reports 1 and 2 and "Final Report". The results of supplementary tests of a pavement system consisting of a sand asphalt base and asphaltic concrete surface on a sand subgrade were given in Report 4.

B. Summary of present phase

Previous tests of flexible pavement systems supported by elastic silt subgrade have tacitly assumed that the Boussinesq theory for a homogeneous, isotropic, semi-infinite elastic solid applied to the subgrade material; and investigations were conducted to determine the load spreading ability of various base materials and surface and base thicknesses in the systems.

Tests by the U. S. Waterways Experiment Station on a homogeneous elastic clay soil with a uniform circular load have verified the validity of the Boussinesq theory for that soil. In effect this investigation is a duplicated test of stress distribution in elastic silt subgrade as the 3 inch asphaltic concrete surface used in the initial test was found to have no additional load spreading abilities over 3 inches of silt subgrade used to replace the asphaltic concrete in the second test.

The sand subgrade system from the previous tests was removed and a new subgrade system was constructed from elastic silt of similar properties to that used in Reports 1 and 2 and "Final Report". Improved instrumentation gave consistent results which are reported in the stress distribution graphs without embellishment.

The results indicate that stress distribution by the Boussinesq theory for a homogeneous, isotropic, semi-infinite elastic solid is a valid representation of stresses in an elastic silt. As with the sand subgrade, stresses are higher under greater stress concentration; but are still close to theoretical.

II. MATERIALS AND THEIR PROPERTIES

A. Material classification

The asphaltic concrete surface material was the same hot mix secured from an asphalt plant in Atlanta. No previous tests were made on this material and since it was purchased under the same specifications from the same source and placed in the same manner it was considered comparable.

The subgrade soil was found to be a micaceous sandy silt typical of the poorer soils found in North Georgia and similar to the subgrade material used in previous tests. The grain size distribution curve shown in figure 1 is comparable to that of the original silt subgrade material shown in figure 1, page 5, of Report 2. The Liquid Limit of 39 would fall just outside the A-5 class of the original silt, and is properly classed A-4; however, the micaceous nature should justify the A-5 classification. The new material had a slightly lower PI of 6 vs. 8 for the previous subgrade.

A standard compaction test ASTM D698-58T was made. The results are given in figure 2 with an optimum moisture content of 24 vs. 24.8 per cent and a maximum dry density of 96.2 vs. 94.4 lb/cu ft for this material as compared to the properties of the former subgrade given in Report 1, page 34.

B. Triaxial tests

Triaxial tests were made of undisturbed samples taken from the subgrade after testing with the pavement removed. These samples were 4 inches in diameter by 8 inches in height and were run under the same conditions in the large triaxial cell previously used.

Results are given in the form of stress-strain curves, figure 3, and a Mohr envelope, figure 4. The shear parameters are a "cohesion" of 11.5 psi and an angle of internal friction of 24.5 degrees compared with a cohesion of 9 psi and an angle of 23 degrees for the silt subgrade of the previous report.

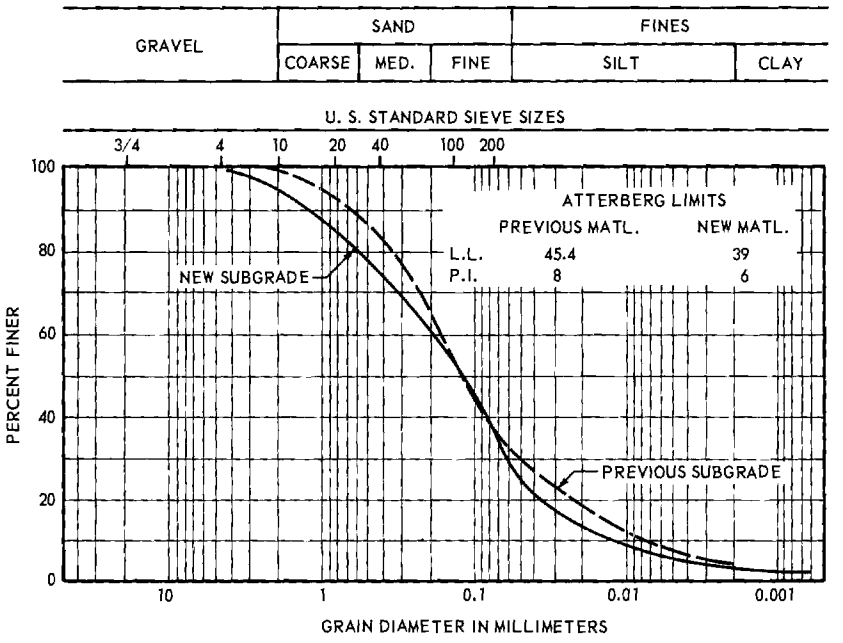

Figure 1. Grain size curves; subgrade silt.

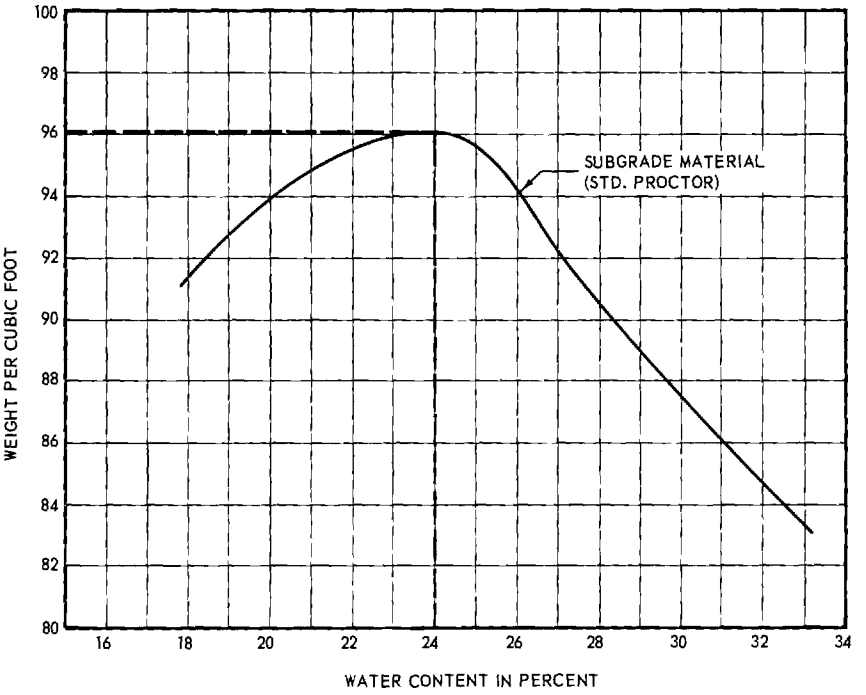

Figure 2. Compaction test; subgrade silt.

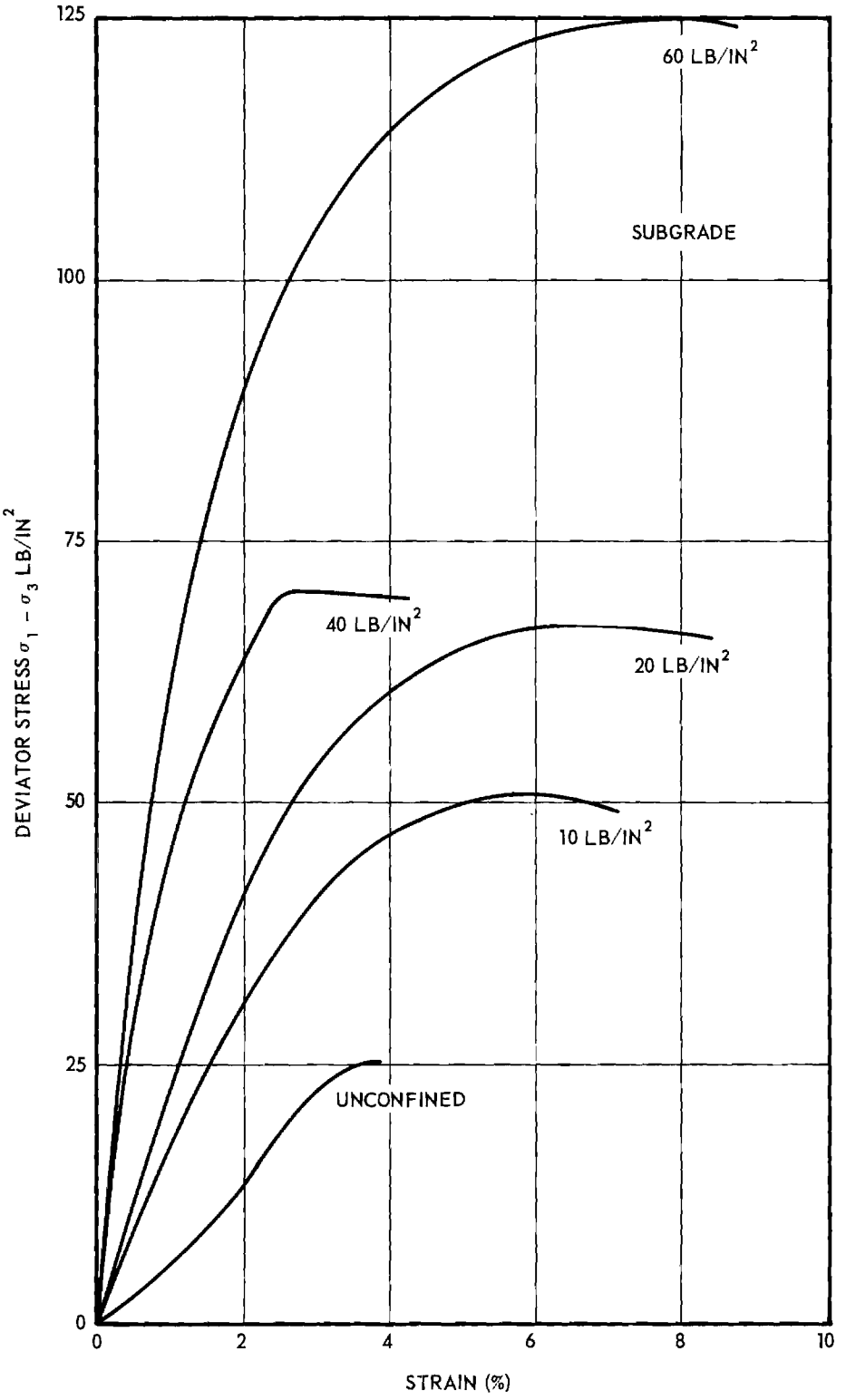

Figure 3. Stress strain curves from triaxial tests on the silt subgrade.

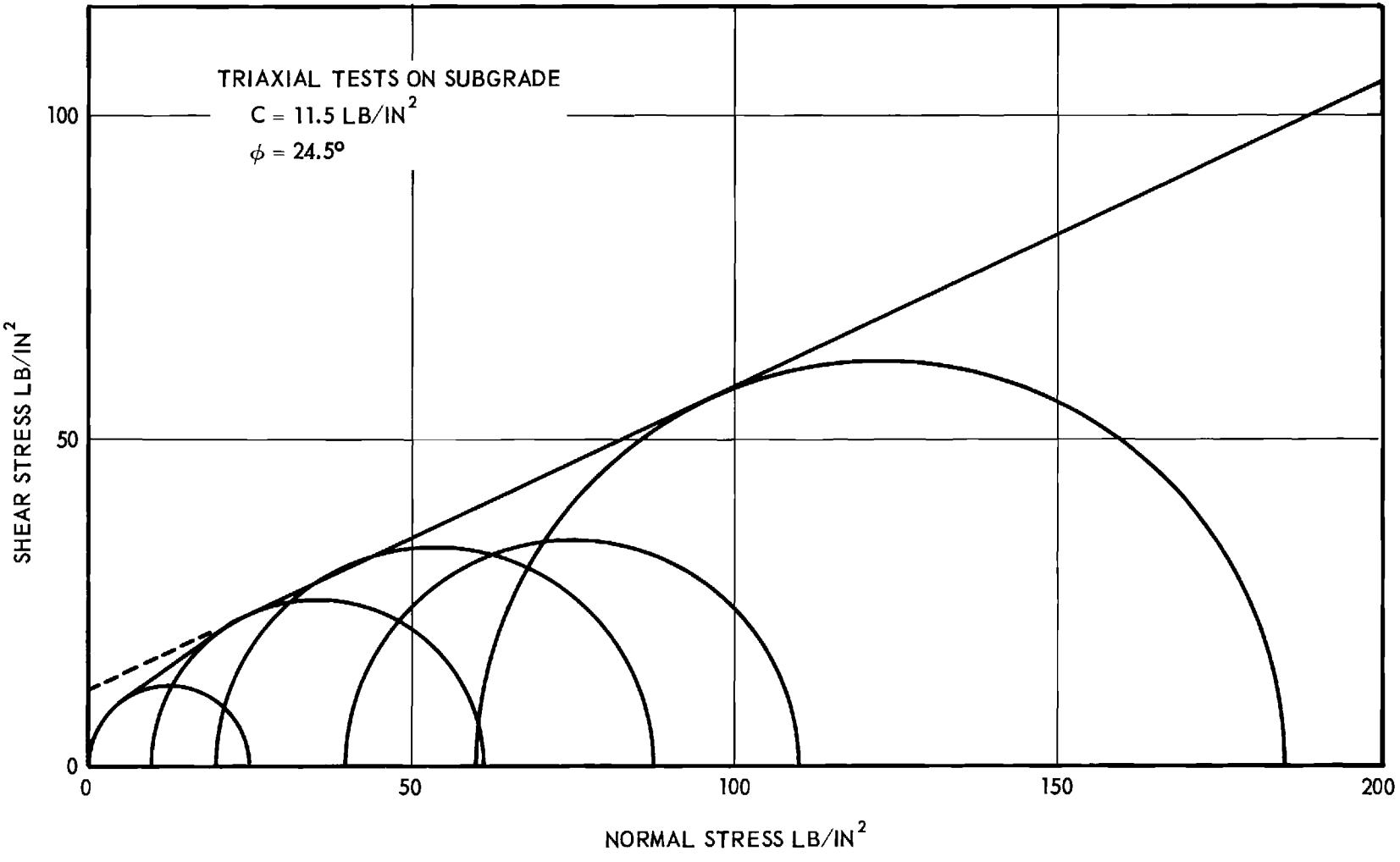

Figure 4. Triaxial test results; Mohr envelope of silt subgrade.

This indicated that the new subgrade is similar in characteristics but has a greater strength than the previous one. The initial tangent modulus of elasticity, figure 5, is higher than for the original silt subgrade. More important the modulus increases more with increasing confining pressure than that of the original silt.

C. In-place tests

In-place tests were made on the subgrade after completion of all the wheel tests. The plate load test was run using an 18 inch diameter circular plate. The results, shown in figure 6, show generally greater rigidity or less deflection than those found in Report 2, figure 16, page 34. The ratios of increase of contact pressure of the new subgrade over the previous for a given deflection are:

Total Deflection (inches)	Ratio
0.1	1.4
0.2	0.8
0.3	0.5

A California Bearing Ratio test was made on the subgrade after wheel load tests were completed. The results indicated in figure 7 are high. This is partially due to densification imposed by repeated deformation of the soil under wheel loads, but is also due to desiccation of the soil. The initial tangent modulus computed from the deflection was comparable to that found by the plate load test.

No tests were made of the asphaltic concrete. It was purchased from the same source and under the same specifications as before.

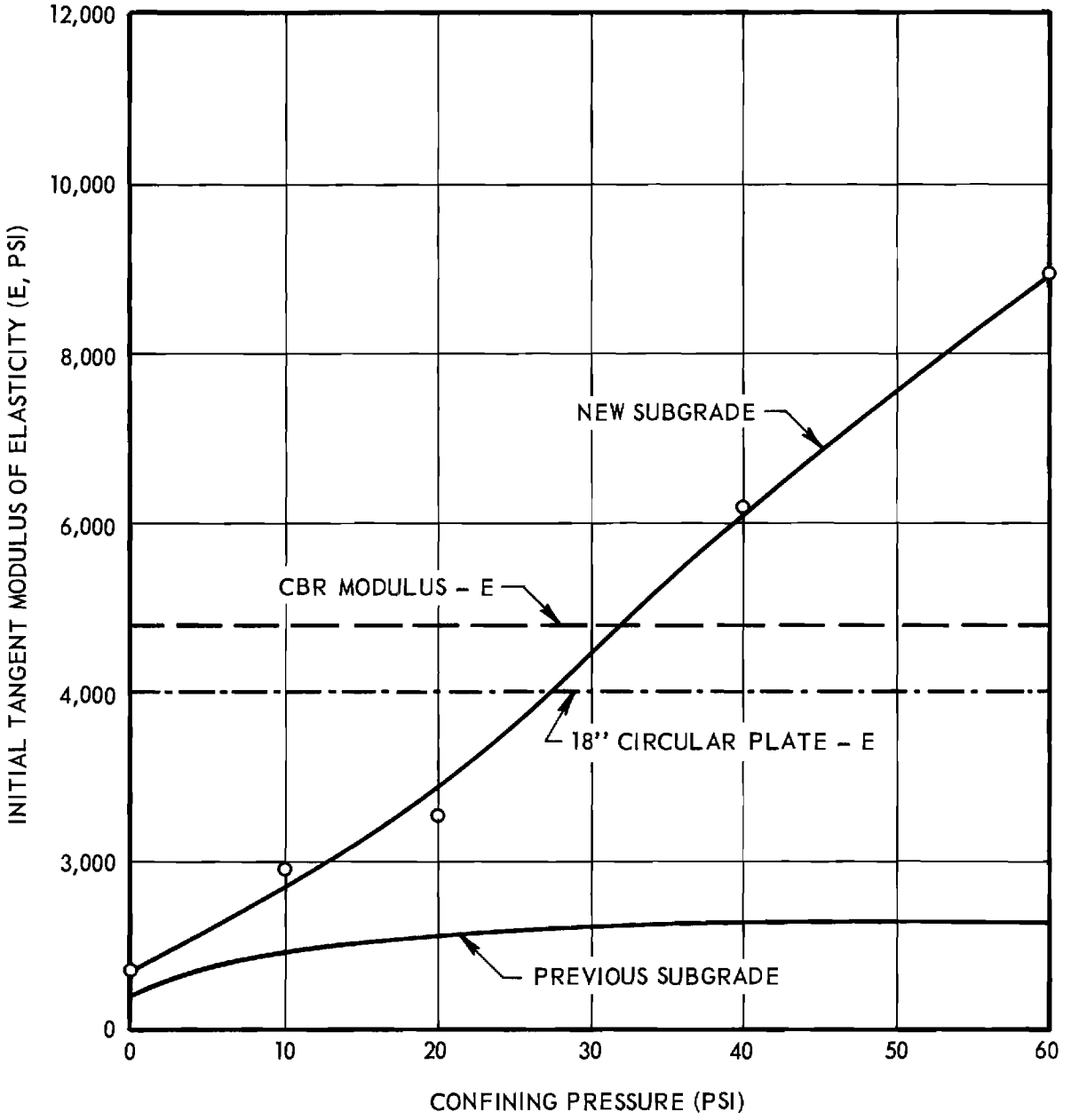

Figure 5. Initial tangent modulus of elasticity from triaxial tests of silt subgrade.

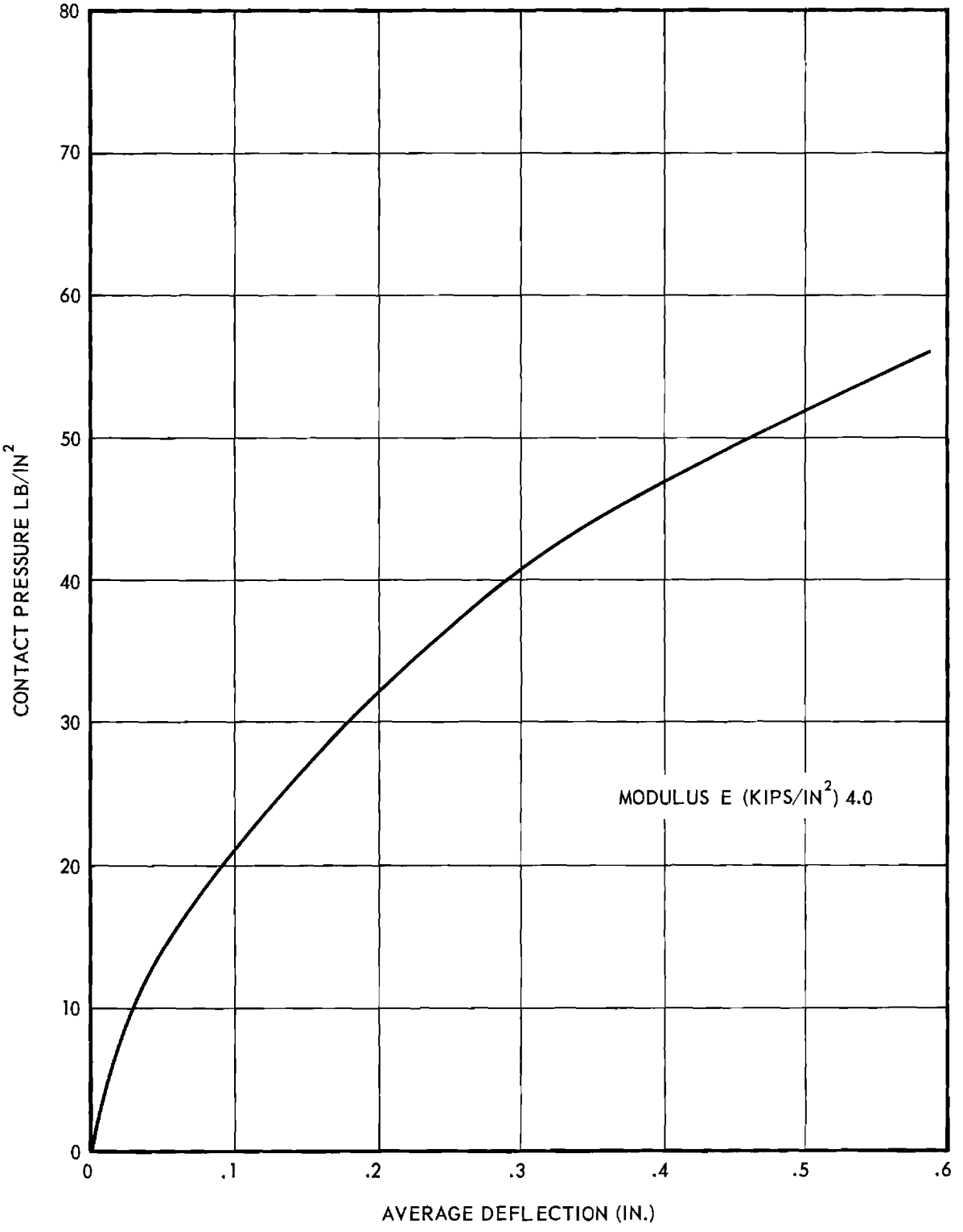

Figure 6. Load deflection curve for 18 inch circular plate load test of silt subgrade.

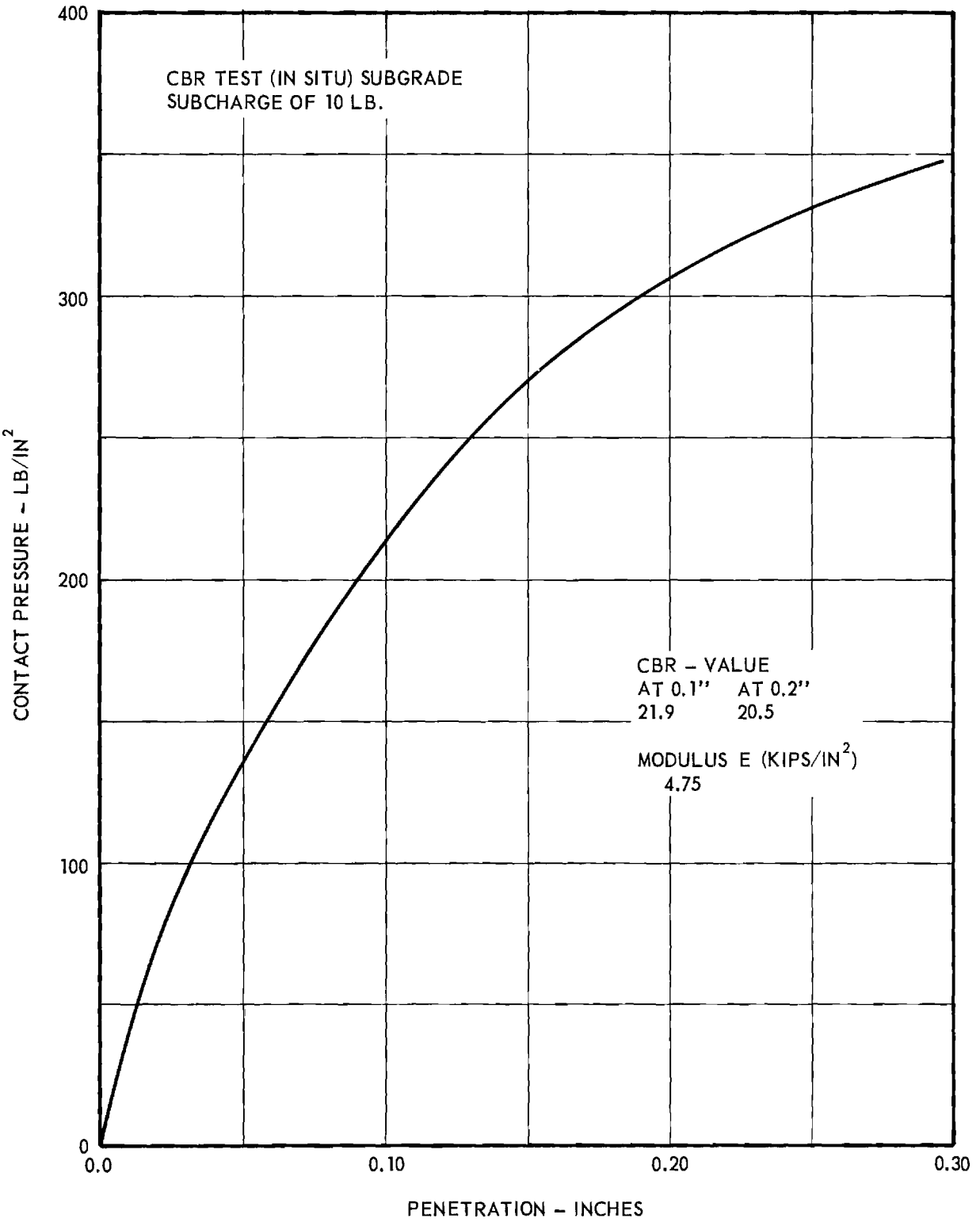

Figure 7. California bearing ratio test of silt subgrade.

III. LOAD TESTS ON PAVEMENTS

A. Pavement system construction

The same 8 ft wide, 12 ft long and 7 ft deep test pit used for previous tests was used for the construction of this system. The pit was completely emptied and a 2 to 8 inch thick layer of coarse material was placed on the bottom to facilitate flooding of the pit if required. The pit was then filled with the new silt subgrade material comparable with that used in previous tests. The bottom 2.5 ft of subgrade was compacted to 90 per cent of the maximum as specified by ASTM D698-58T and the remaining 3 ft to 95 per cent or greater by a vibrating tamper, the Jay-Tamp. No base course was employed. The 3 inch asphaltic concrete surface was compacted in two layers until no further densification was observed. After the initial test was run, the 3 inch layer of asphaltic concrete was replaced with 3 inches of silt subgrade compacted to 98 per cent.

B. Pressure cell installation

Cells from the test given in Report 4 were reused and rebuilt where damage had occurred. Figures 19 and 20, pages 42 and 43 of Report 1 show the typical cells. A high percentage of failures had eventually occurred in the previous tests due to moisture entering the cells, so these cells were rebuilt with a rigid epoxy resin connecting the thin aluminum diaphragm to the rigid base. A complete series of wheel load tests were run using cells thus constructed and the previous arrangement of switching unit and SR-4 strain indicator. Results were erratic due to the failure of 30 per cent of the cells when the diaphragm separated from the base, probably because of the vibration involved in compaction.

All cells were rebuilt a second time with a more flexible epoxy made of Epon resin 828 and curing agent 235. A mercury switch system was used which proved to be very sensitive and less subject to dust damage. The cells were installed in four layers as shown in figure 8. More sensitive instrumentation enabled detection of some arching in the elastic silt, so the cells were re-calibrated by being submerged in the silt of the calibration tank.

C. Wheel load tests

Identical test loads of 9000 and 13,500 lb for the single wheel and 9000, 13,500, and 18,000 lb for the dual wheels were applied both to the subgrade with a 3 inch asphaltic concrete pavement and to the subgrade alone with no surfacing. The loads were statically applied with 9 by 20 inch truck tires and the stresses in the subgrade were measured by pressure cells, using essentially the same equipment and procedures as employed in the previous tests. Two passes were made in each series and results were so close that the two passes were averaged to expedite plotting. The test results of load distribution with respect to depth are given in figures 9 through 18, with each plotted point accounting for the average of two tests under identical conditions. Four graphs are given on each figure corresponding to the depths of cell location.

The theoretical stress distribution for each depth is shown by the solid or dashed curves on each graph. These were computed by the Boussinesq theory for a semi-infinite homogeneous, isotropic, elastic solid. They are based on a rectangular approximation of the actual loaded area and a uniform tire pressure equivalent to the inflation pressure. Where two curves are shown on the graphs the solid line represents the theoretical stress distribution at the horizontal depth below the pavement surface for that graph and on a line parallel to the axle (or east-west variation of load center location), while

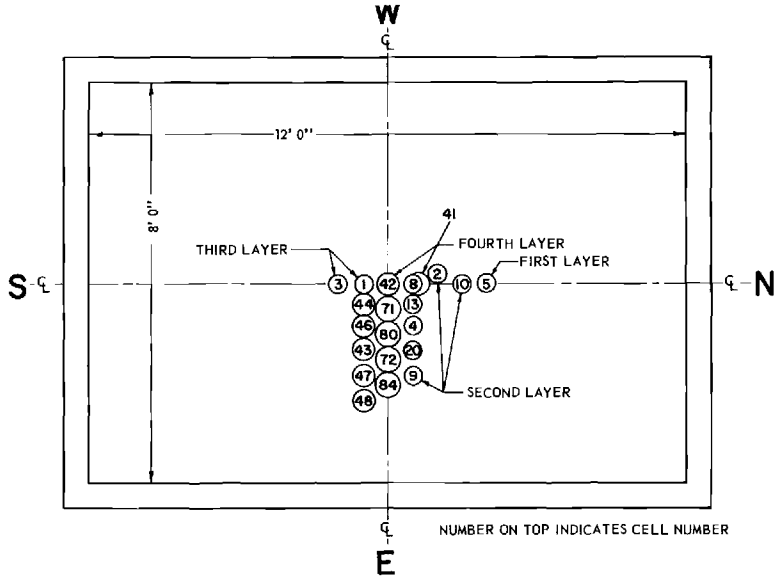

CELL SPACING

LAYER	CELL NO.	SPACING (INCHES) E-W	N-S
1	5	0	24 N
2	10	0	18 N
	2	2 W	12 N
	8	0	6 N
	13	5 E	6 N
	4	10 E	6 N
	20	16 E	6 N
	9	22 E	6 N
3	3	0	12 S
	1	0	6 S
	44	5 E	6 S
	46	10 E	6 S
	43	16 E	6 S
	47	22 E	6 S
	48	28 E	6 S
4	41	0	8 N
	42	0	0
	71	6 E	0
	80	12 E	0
	72	18 E	0
	84	24 E	0

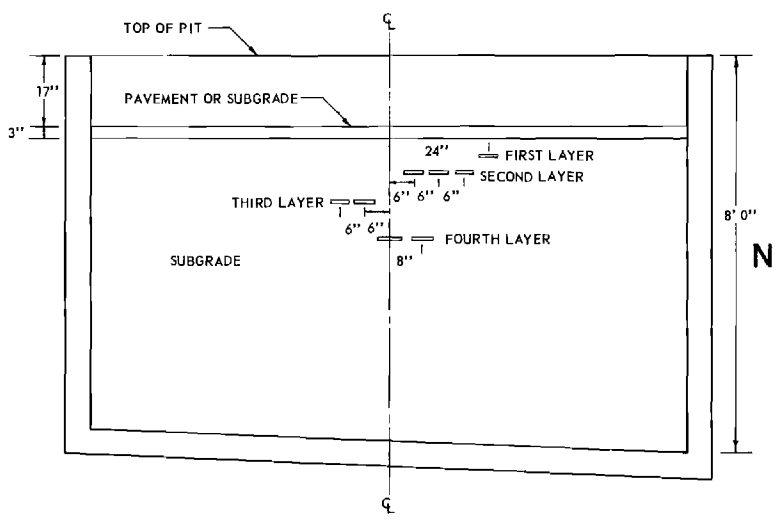

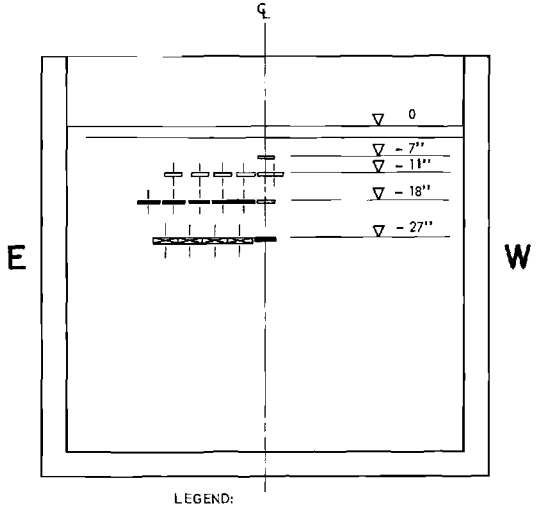

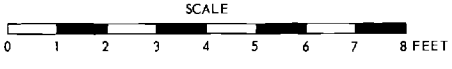

LEGEND:
- INDICATES 4" DIAMETER CELL (NUMBERS 1 THRU 20)
- INDICATES 5" DIAMETER CELL (NUMBERS 41 THRU 48)
- INDICATES 6" DIAMETER CELL (NUMBERS 71 THRU 84)

Figure 8. Position of pressure cells and cross section of the test section.

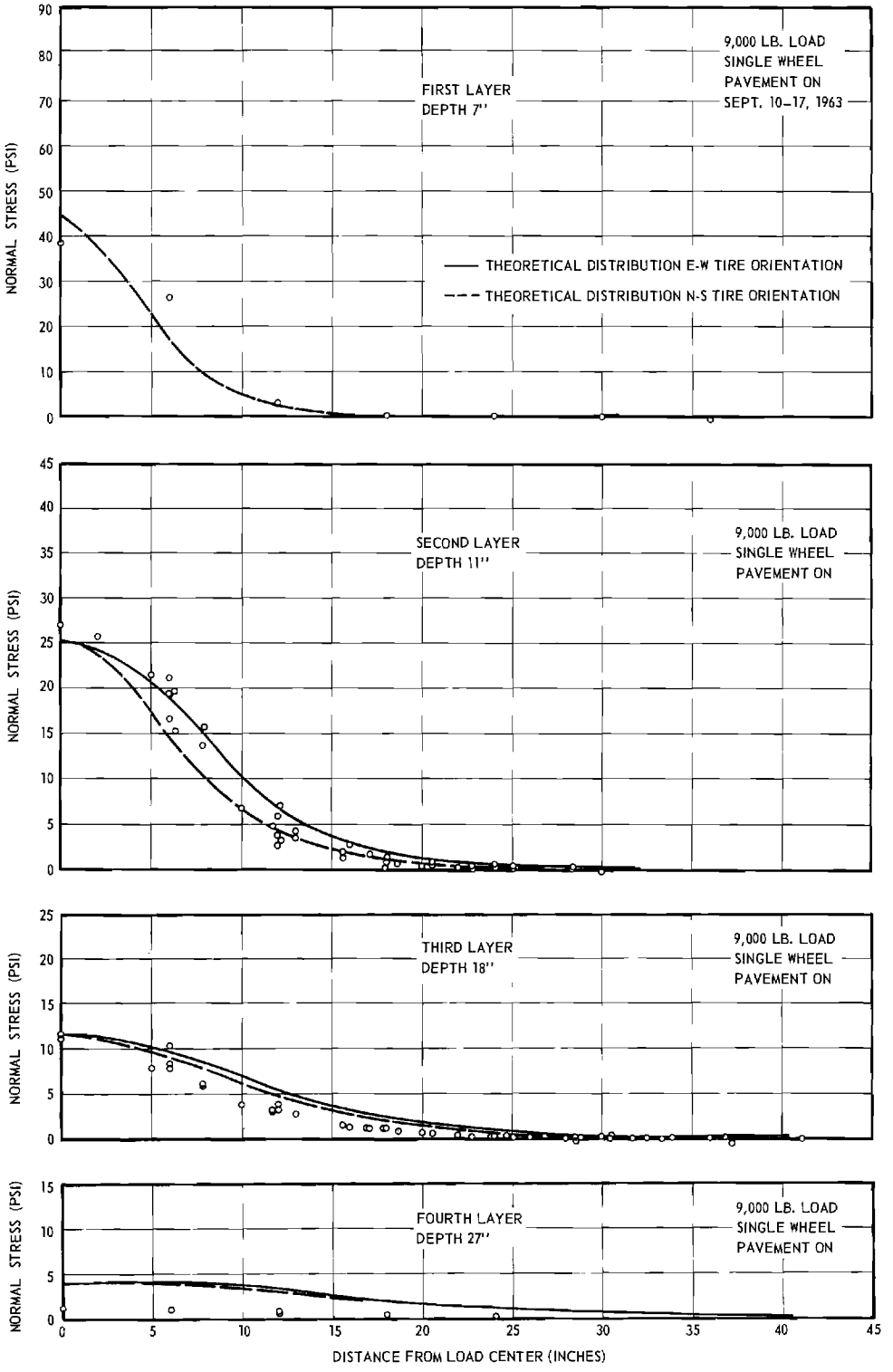

Figure 9. Measured stresses in silt subgrade; 9000 lb single wheel, 3 inch asphalt pavement.

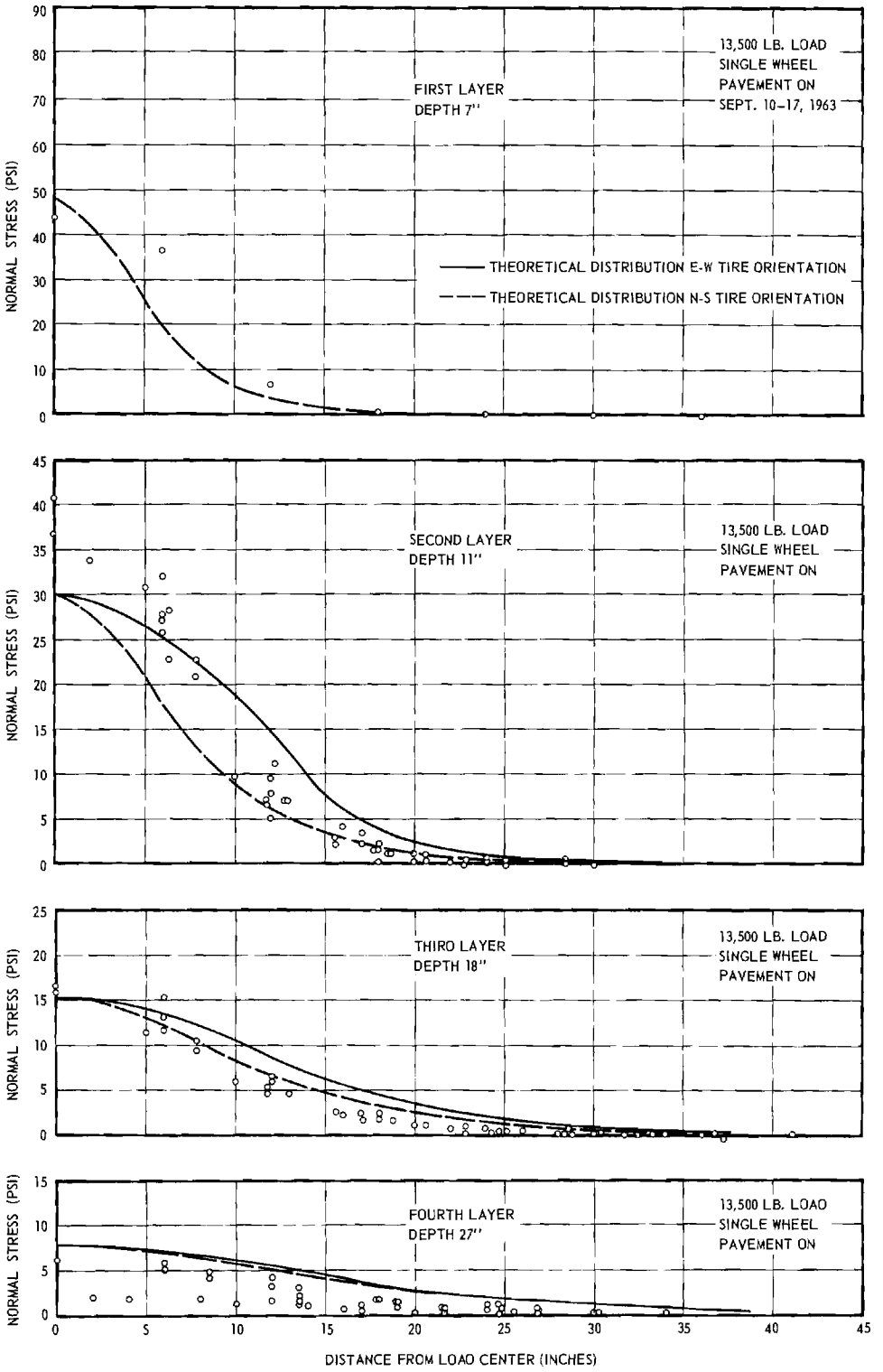

Figure 10. Measured stresses in silt subgrade; 13,500 lb single wheel, 3 inch asphalt pavement.

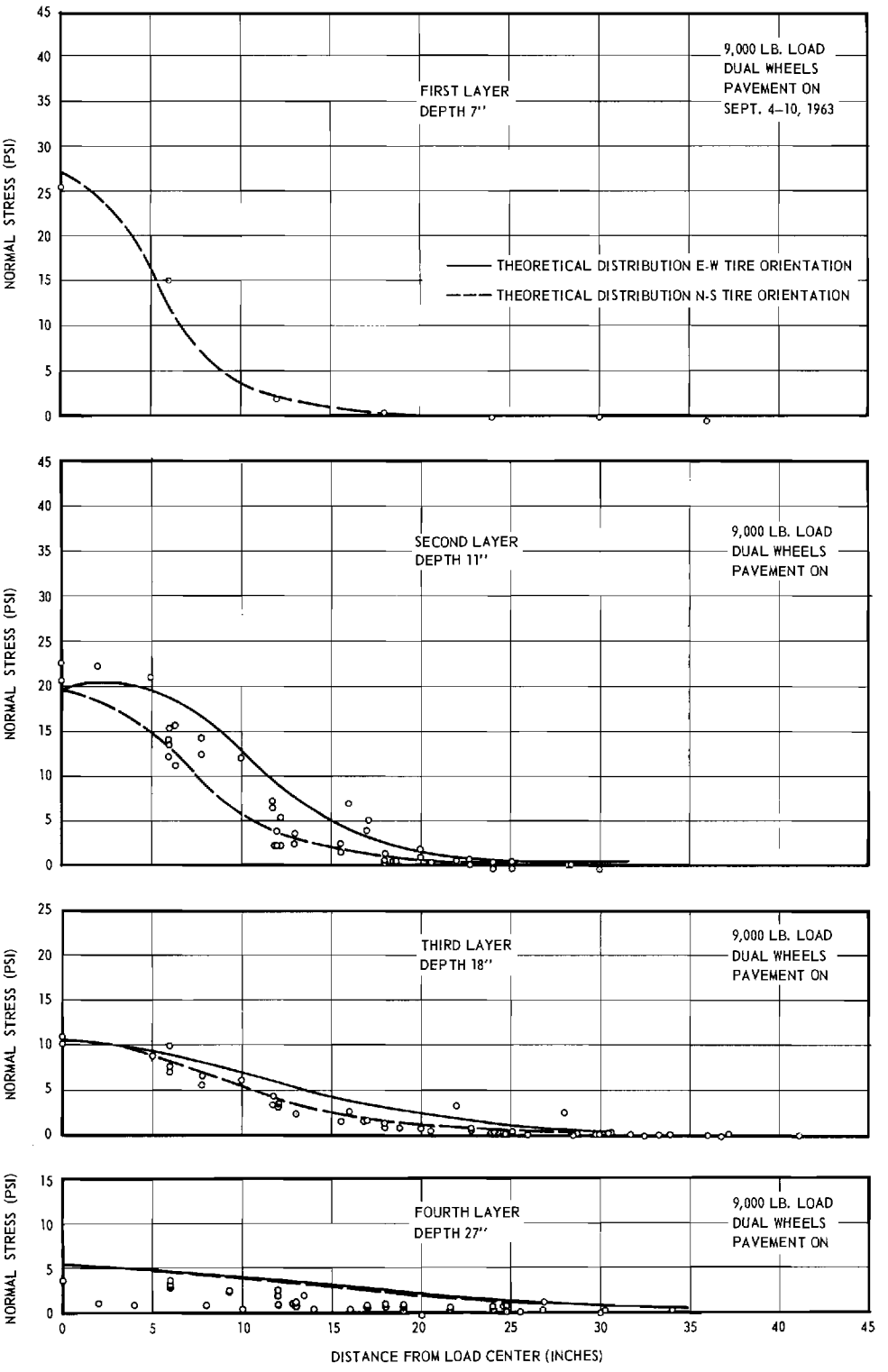

Figure 11. Measured stresses in silt subgrade; 9000 lb dual wheel, 3 inch asphalt pavement.

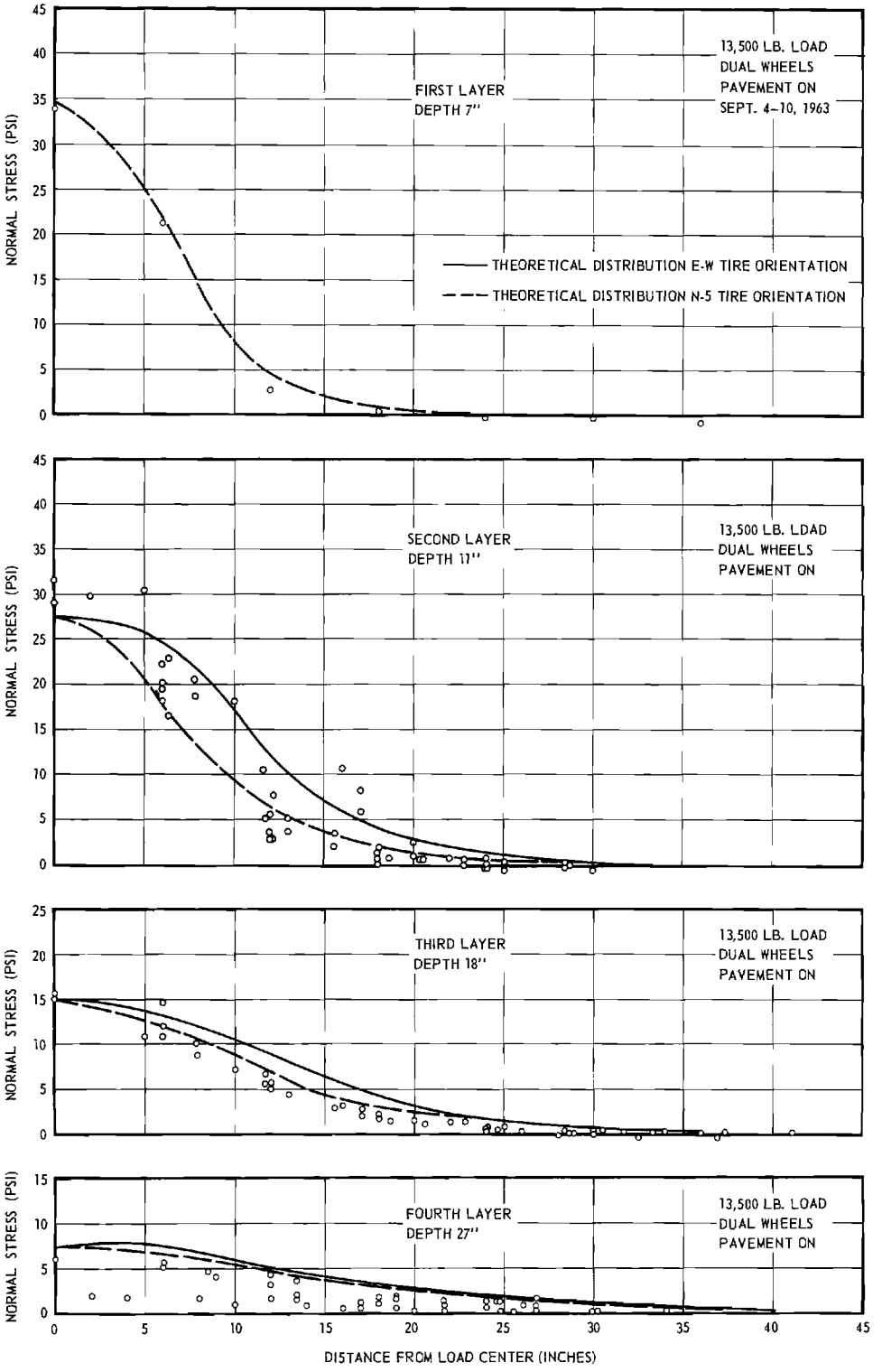

Figure 12. Measured stresses in silt subgrade; 13,500 lb dual wheel, 3 inch asphalt pavement.

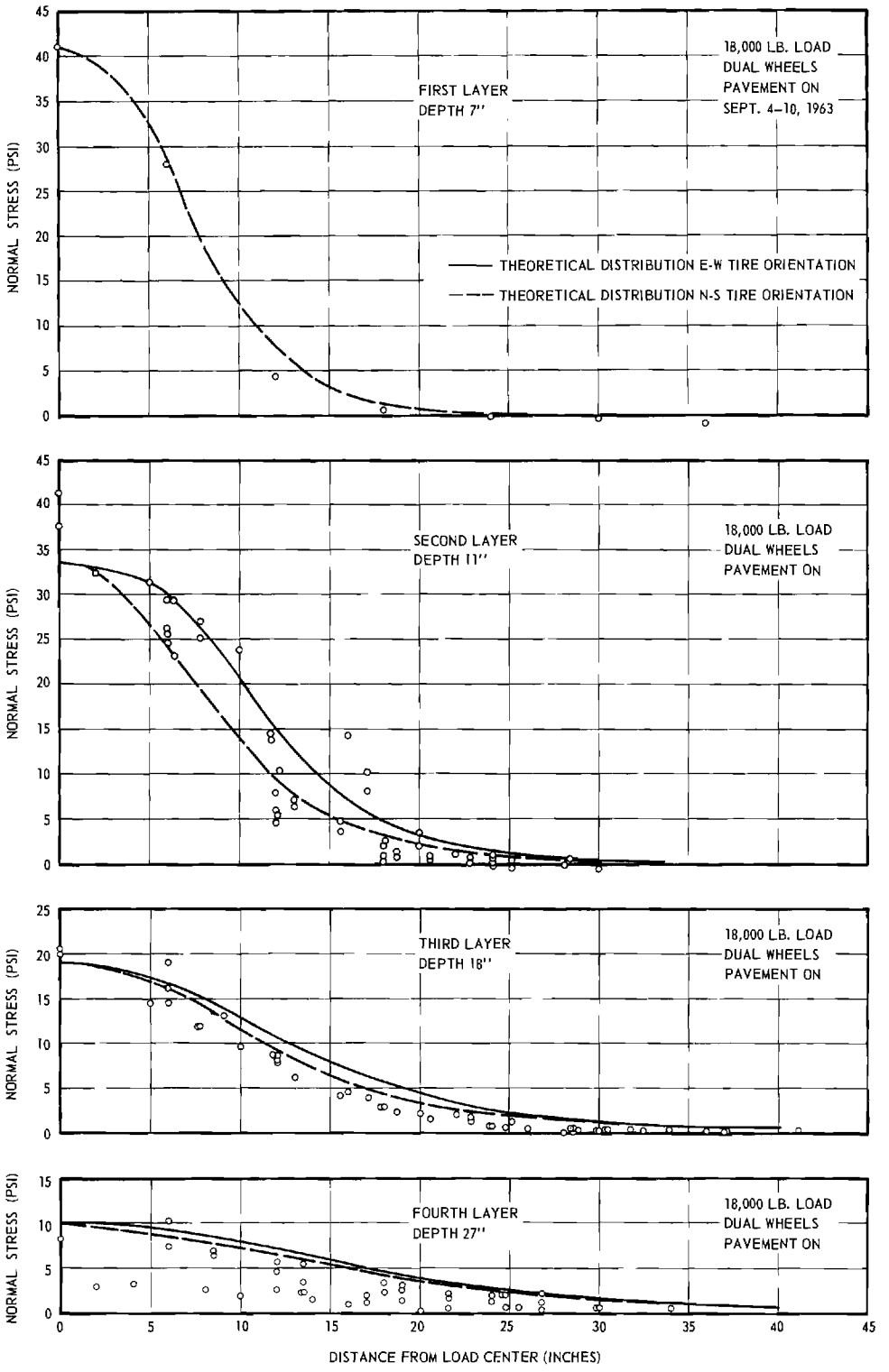

Figure 13. Measured stresses in silt subgrade; 18,000 lb dual wheel, 3 inch asphalt pavement.

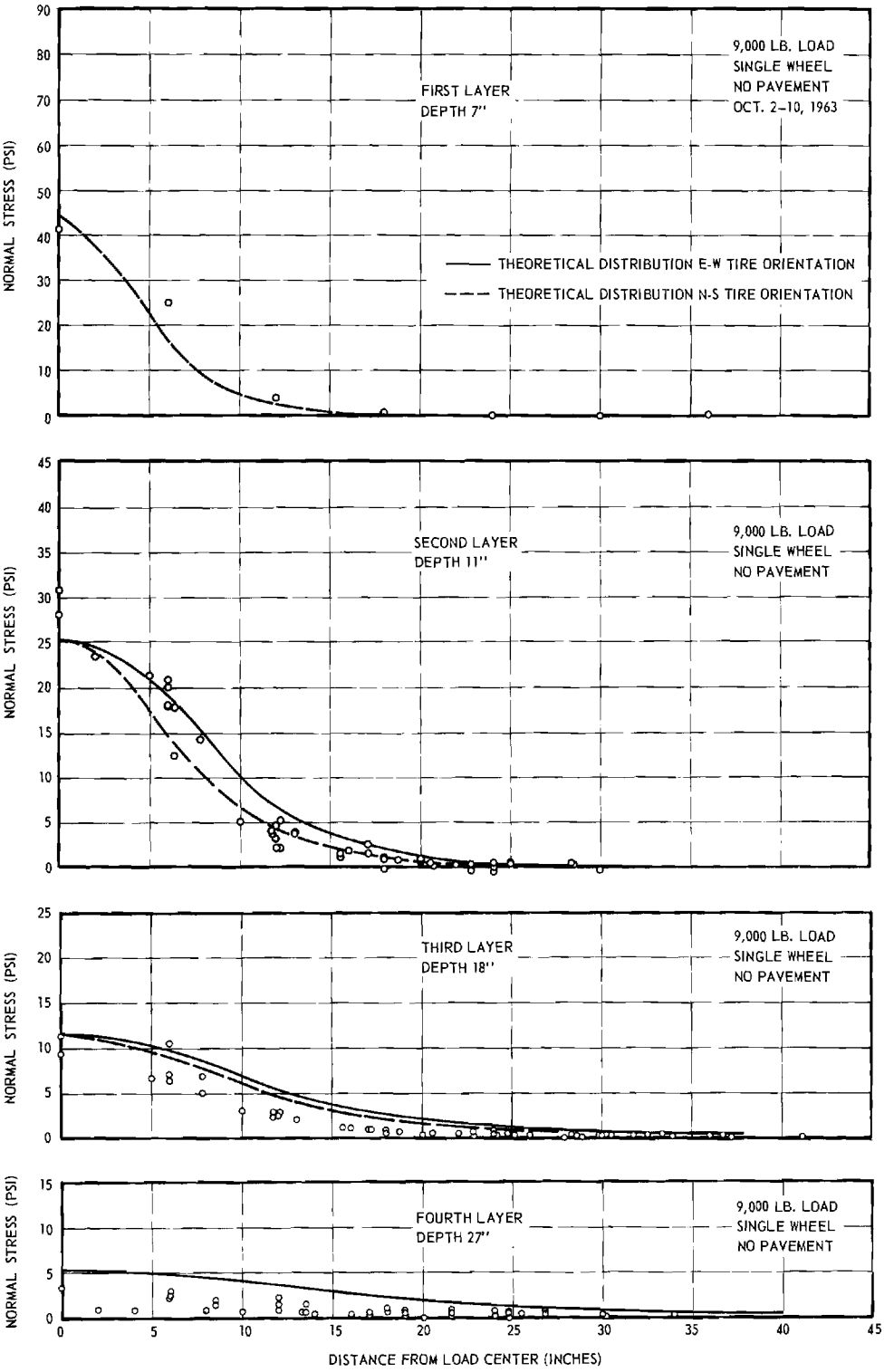

Figure 14. Measured stresses in silt subgrade; 9000 lb single wheel, directly on subgrade.

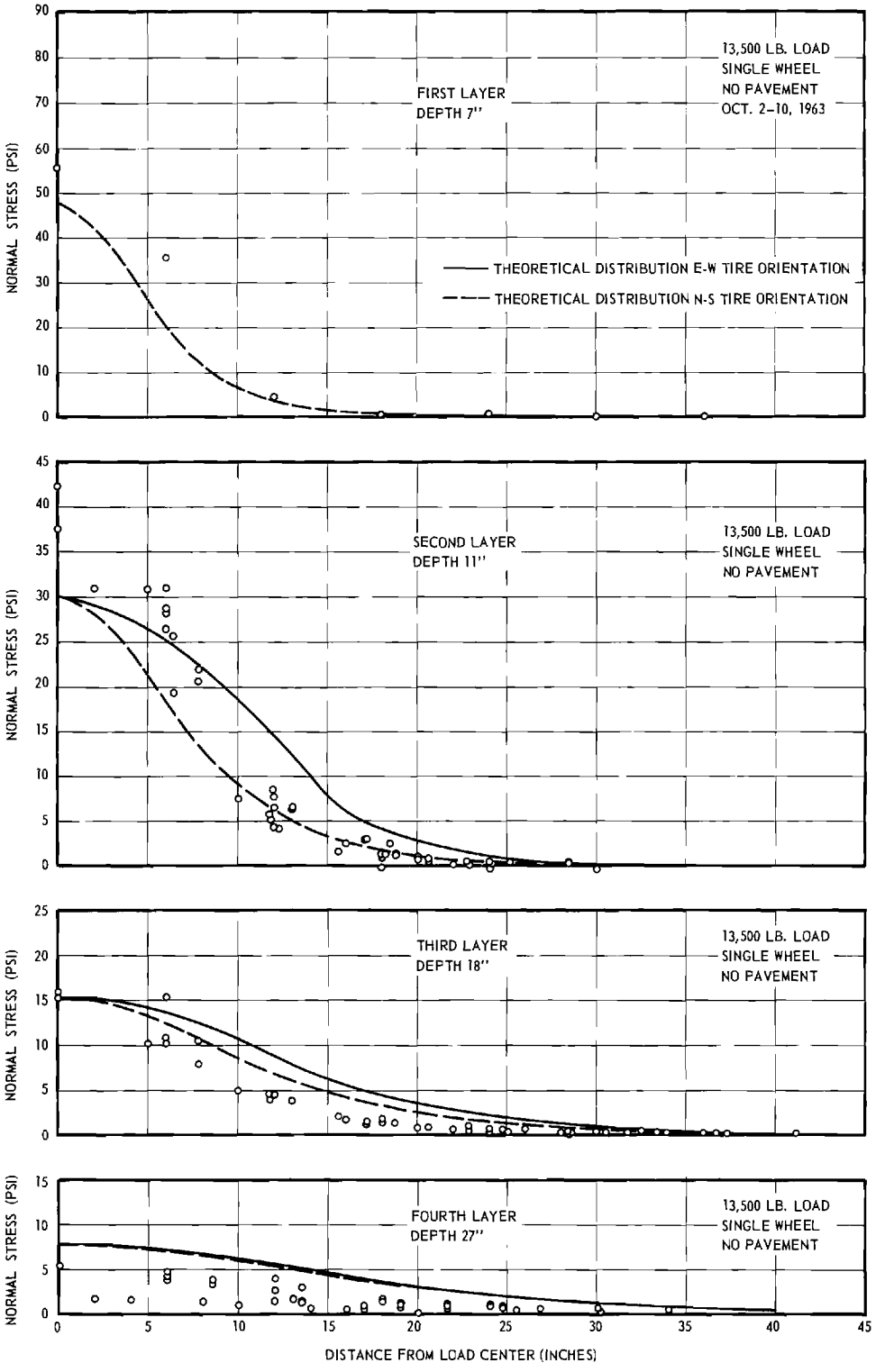

Figure 15. Measured stresses in silt subgrade; 13,500 lb single wheel, directly on subgrade.

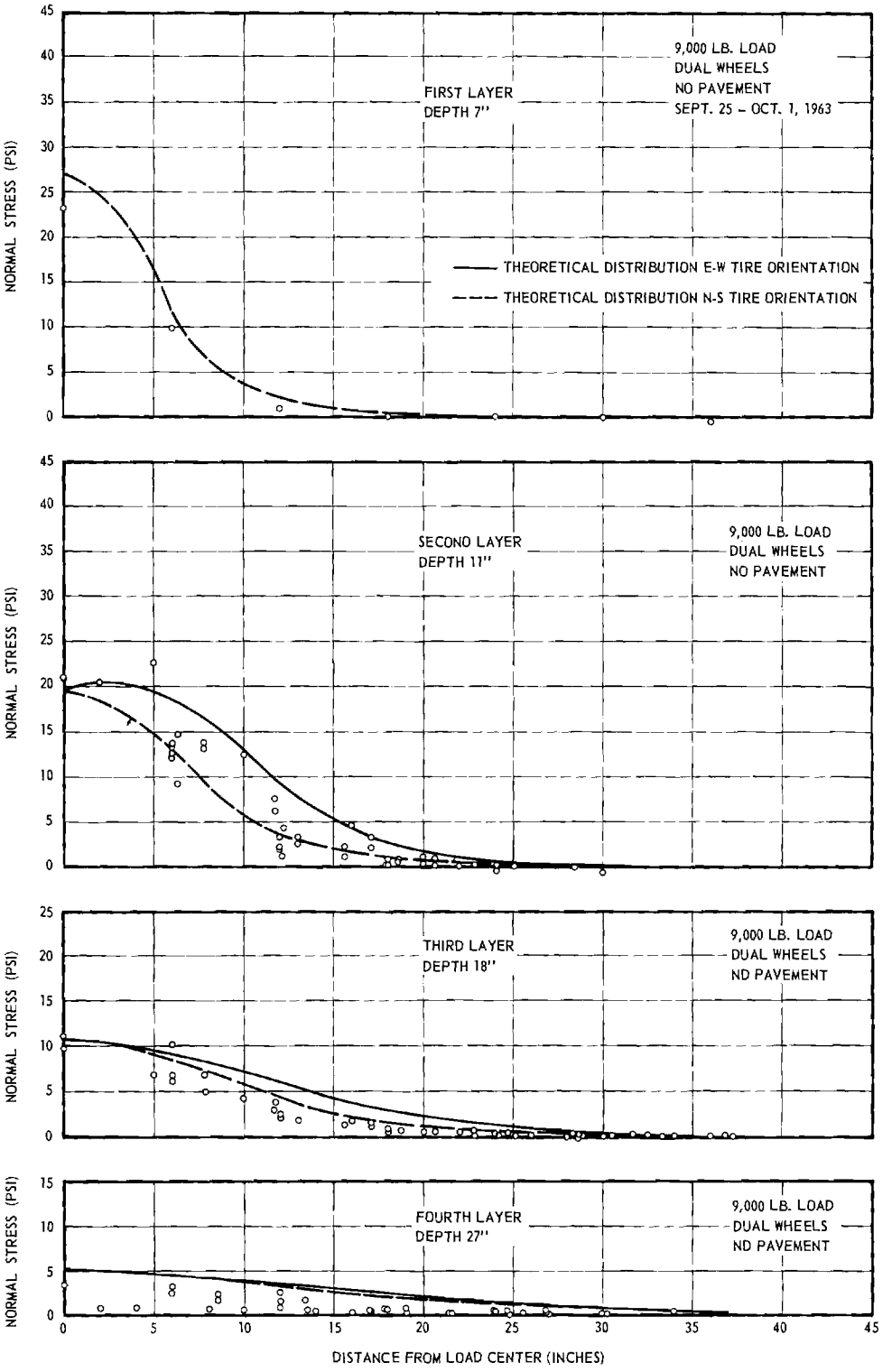

Figure 16. Measured stresses in silt subgrade; 9000 lb dual wheel, directly on subgrade.

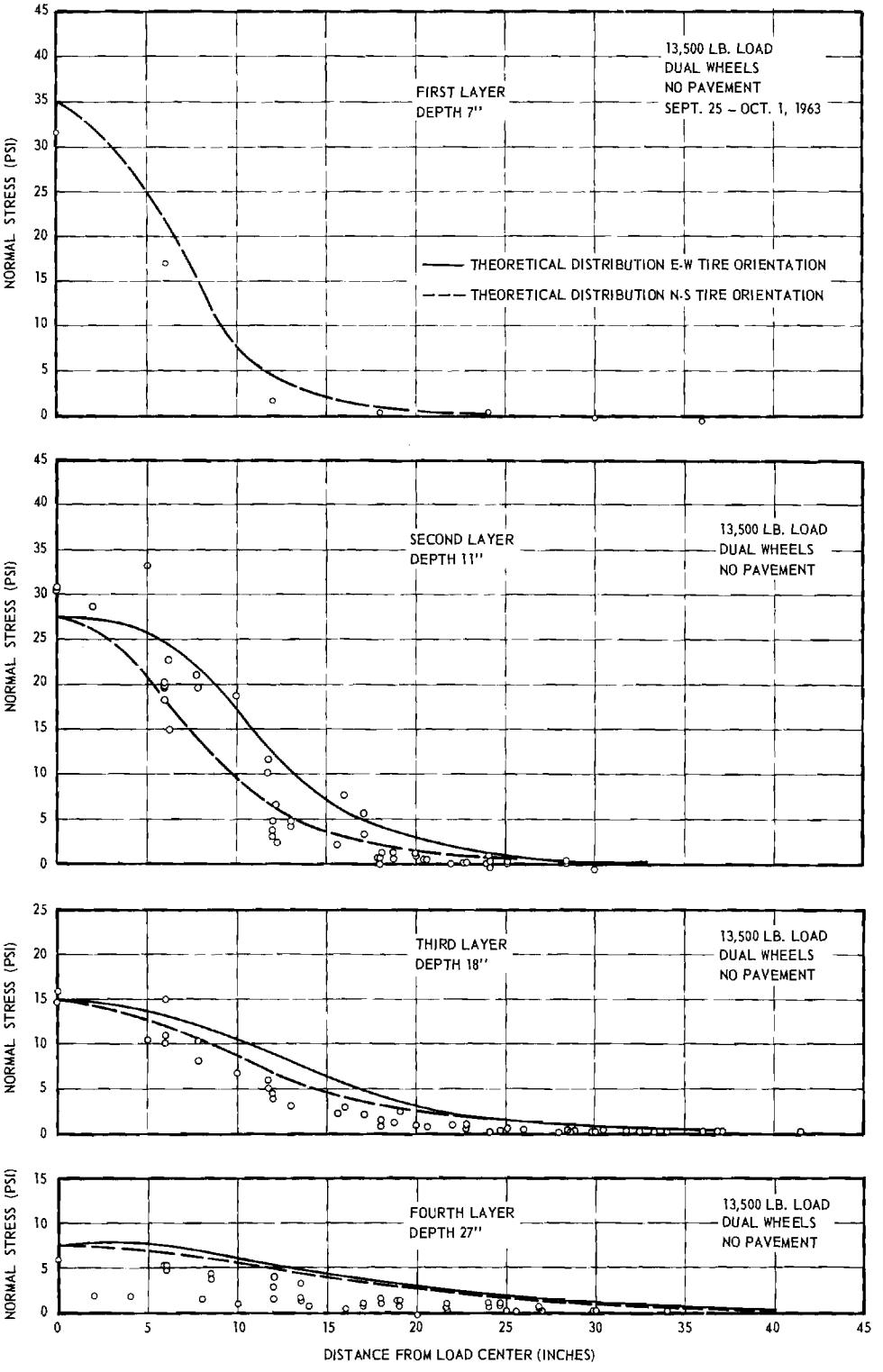

Figure 17. Measured stresses in silt subgrade; 13,500 lb dual wheel, directly on subgrade.

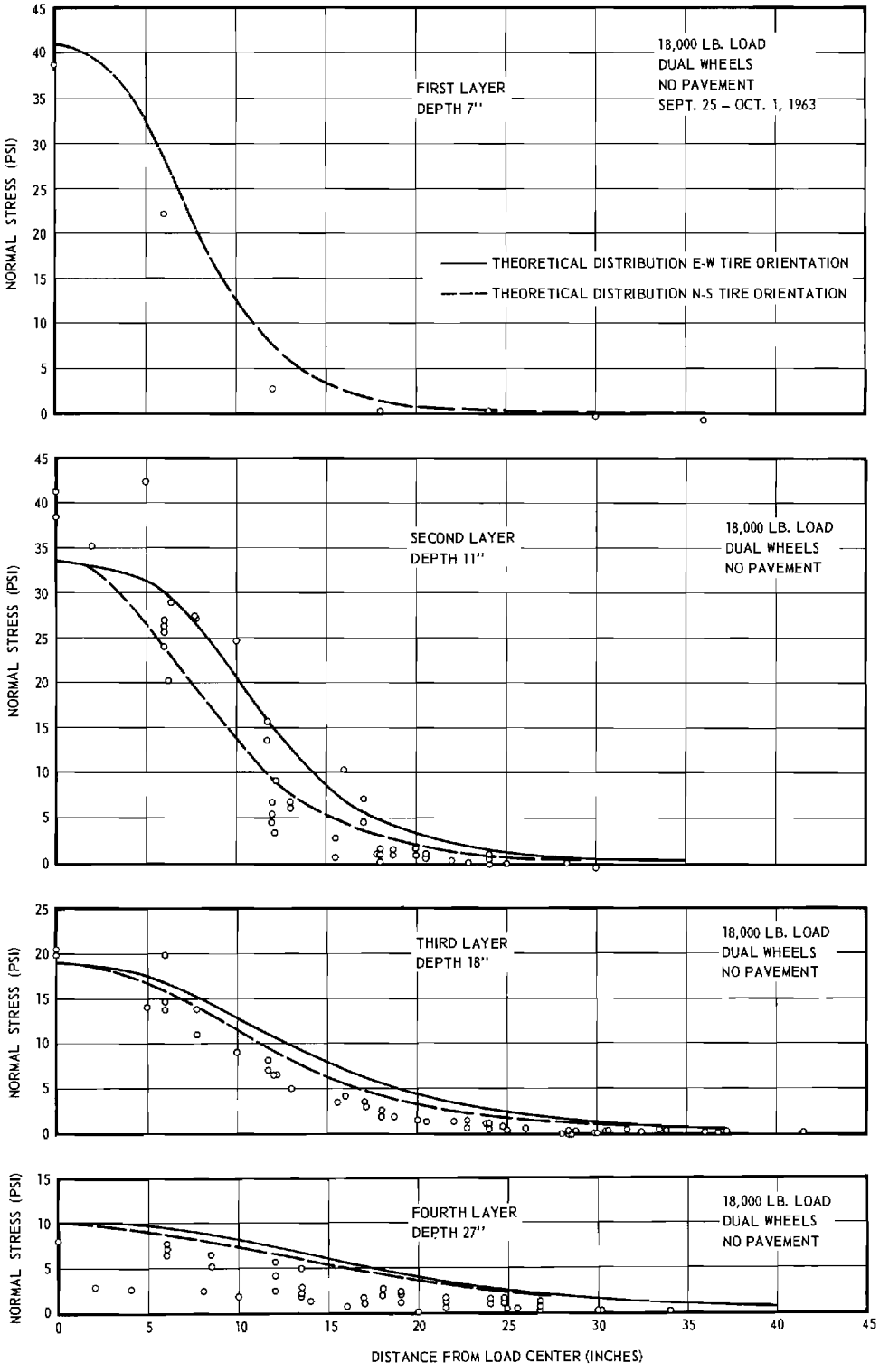

Figure 18. Measured stresses in silt subgrade; 18,000 lb dual wheel, directly on subgrade.

the dashed line represents the theoretical stress distribution at that same horizontal depth and on a plane perpendicular to the axle and midway between the tires (or north-south variation of load center location). The first layer has only a dashed line as it measured stresses only in a north-south variation of load center. It should be noted that this layer consisted of a single cell at the shallowest depth and did not have the averaging effect of several cells.

D. Discussion of test results--3 inch pavement

The results of the wheel load tests for a 3 inch asphaltic concrete surfacing laid directly on the elastic silt subgrade, figures 9 through 13, indicate that the stresses in the vertical subgrade are distributed in approximately the same manner as those computed by the Boussinesq theory. The stresses are greatest directly beneath the load and they become rapidly less with increasing horizontal distance from the load and with increasing depth.

The tests with the single tire found stresses of a depth of 7 or 4 inches below the underside of the pavement within about 10 per cent of the Boussinesq: less than the Boussinesq directly under the tire and more at a distance of 6 inches. This may be the result of the method used for computing the Boussinesq stress in which a uniform contact pressure was assumed to be acting over a rectangular area. Although the published data are not altogether conclusive, they do indicate that the actual pressure is somewhat greater at the edge of the tire than beneath the center, due to the rigidity of the carcass. The effect of such a nonuniform contact pressure ordinarily is significant at depths of less than 1.5 times the width of the loaded area. This is the case with the pressure measurements of a 7 inch depth because the tire contact area is approximately 7 inches wide and 14 inches long.

The stresses at depths of 11 and 18 inches below the single tire are generally within 5 to 10 per cent of the Boussinesq value. The stresses in the fourth layer of cells, at 27 inches was considerably less than the Boussinesq value, with the higher readings 20 to 25 per cent lower. It is suspected that the cause is under-registry of the pressure cells where the stress increase due to the wheels (5 or 6 psi maximum) is small compared to the possible residual stresses in the ground remaining from compacting the soil.

The stresses found beneath the dual wheels show similar agreement with those computed by the Boussinesq theory. At a depth of 7 inches the measured stresses are within 5 per cent of the theoretical values. Since the stresses were found for a point midway between the two wheels the effect of the local stress concentrations should be less than for the single tire. The stresses immediately under the tires in the 11 inch layer are about 16 per cent greater than the theoretical curve but close to it (and slightly lower) at greater distances. There is better agreement in the 18 inch layer, but the variation from the theoretical with the stresses under the tire is slightly greater and the stresses at larger distances are slightly less than the computed values. It is possible that the variation from the theoretical distribution reflects stress concentration arising from the fact that the modulus of elasticity of the soil increases with increasing confining pressure (figure 5). According to the Griffith-Frohlich theory (Report 1, pp 11-12) such a concentration of stress directly beneath the load should develop in a material whose E increases with confinement. This effect was very prominent in the results of the tests on the sand subgrade (Report 4, figure 6 and discussion pp 27-28). The present silt subgrade, with a greater increase in E with confinement than the original silt, should be expected to exhibit some stress concentration, but not to the same degree as the sand subgrade.

The stresses in the soil at a depth of 27 inches are still less than the theoretical but are closer to it, with the greater total wheel loads and greater stress increases.

E. Discussion of test results-- no pavement

The test results for loads placed directly on the subgrade without a pavement, figures 15 through 18, also are in general agreement with stresses computed by the Boussinesq theory. Again the stress measurements made at a depth of 7 inches reflect a smaller stress immediately beneath the load for the single 9000 lb wheel load but a greater stress beneath the 13,500 lb wheel load. The latter possibly is the result of excessive shear strains, because the subgrade appeared to be commencing to fail under the high stress without the benefit of the asphaltic concrete pavement.

The stresses measured at a depth of 11 inches in all cases show appreciable stress concentration, with the vertical stress directly under the load center as much as 20 per cent more than the theoretical Boussinesq value for the single wheel at 9000 lb and the dual wheels at 18,000 lb (or 9000 lb per wheel) and 33 per cent more for the single wheel loaded to 13,500 lb. This increase of stress concentration with increasing load probably reflects the excessive shear strains of incipient failure, because all of these loads produced increased rutting of the unprotected subgrade surface. Some part of the concentration can also be attributed to the reduced depth to the cells brought on by rutting. No correction was made further although the rut depth for the 13,500 lb single wheel was 0.7 inch. (The cell movement, in contrast, was much less.)

IV. CONCLUSIONS

The load tests made on the pavement without a base course and in the subgrade without a pavement confirm the conclusions reached in the tests previously reported.

1. The stresses in the homogeneous elastic subgrade can be approximated by the Boussinesq theory.

2. The 3 inch asphaltic concrete surface is not appreciably more effective in spreading the static wheel loads to the soil subgrade than an equal thickness of compacted subgrade. The tendency toward local shear failure, however, is greatly reduced by an asphaltic concrete surface only 3 inches thick.

Respectfully submitted:

George F. Sowers
Project Director

B-133

REPORT 6

PROJECT B-133 HPS-1(53)

STRESS, BEARING CAPACITY, AND FLEXIBLE PAVEMENT THICKNESS DESIGN BASED ON THE AASHO ROAD TEST AND GEORGIA PAVEMENT EVALUATION TESTS

GEORGE F. SOWERS

December 31, 1961 through February 15, 1964

Contract with
The State Highway Department of Georgia
in cooperation with
The Bureau of Public Roads

Engineering Experiment Station
GEORGIA INSTITUTE OF TECHNOLOGY
Atlanta, Georgia

REVIEW
PATENT 3-25 19 64 BY RAM(sc)
FORMAT 3-25 19 64 BY HH

GEORGIA INSTITUTE OF TECHNOLOGY
Engineering Experiment Station
Atlanta, Georgia

REPORT 6

PROJECT B-133
HPS-1(53)

STRESS, BEARING CAPACITY, AND FLEXIBLE PAVEMENT THICKNESS DESIGN BASED ON THE AASHO ROAD TEST AND GEORGIA PAVEMENT EVALUATION TESTS

By

GEORGE F. SOWERS
Research Associate and Professor of Civil Engineering

December 31, 1961 through February 15, 1964

Contract with
THE STATE HIGHWAY DEPARTMENT OF GEORGIA
in cooperation with
THE BUREAU OF PUBLIC ROADS

TABLE OF CONTENTS

(Continued)

TABLE OF CONTENTS (Continued)

LIST OF FIGURES

I. INTRODUCTION

1. Objective

The design of flexible pavements in Georgia has been largely based on experience expressed in the form of correlations between soil class, traffic, and base course thickness and character. While this method has been reasonably successful in the past, the rapid increases in the number of heavy axle loads and in the variety of subgrades that must support the heaviest loads have outrun the past experience.

It was the object of this research to provide a rational background for extending both Georgia experience and the results of the AASHO Road Test program to the design of new pavements in the state. First, this required an evaluation of the performance of pavements throughout Georgia, particularly in terms of subgrade capacity. Second, this involved a correlation of the AASHO Interim Guide for the Design of Flexible Pavements (1) with the properties of Georgia highway construction materials.

2. Method of Investigation

The evaluation of the Georgia pavements began with a field examination of typical examples of both satisfactory and unsatisfactory performance. Samples were secured of the subgrade from each, and these were tested to determine the subgrade's elasticity and strength. Computations were made to determine the subgrade's deflection and safety against shear failure. The results were then correlated with the pavement performance to establish the requirements for a safe design.

---

(1) Liddle, W. J., "Application of AASHO Road Test Results to the Design of Flexible Pavements," Preprint Volume Supplement, International Conference on the Structural Design of Asphalt Pavements, Univ. of Michigan, Ann Arbor, Michigan, 1962.

The correlation with the AASHO Test Road data was centered on tests of four undisturbed samples from the Test Road subgrade. Deflection and bearing capacity were correlated with the Serviceability Index or Rating in the same way as the data for the Georgia pavements. A comparison of the correlations permits a comparison of the supporting qualities of the Georgia subgrades with those of the AASHO subgrade.

Finally, the Georgia performance and soil support data were utilized independently to develop a semi-rational design method for Georgia pavements. While this is incomplete and requires further development, it appears to have some advantages that cannot be realized from the AASHO-derived design method.

3. Summary of Conclusions

The following conclusions have been reached in this investigation:

1. There are numerous causes or factors involved in the failure of a pavement to perform adequately. Of the pavements studied, however, most were load related.

2. The study of the performance of Georgia pavements disclosed a correlation between the Serviceability Rating or Index, traffic, and both deflection and bearing capacity of the subgrade.

3. The study of the AASHO data similarly disclosed a correlation between the Serviceability Rating or Index, traffic, and both deflection and bearing capacity.

4. The AASHO subgrade had an ultimate bearing capacity of 99 psi. For comparable load, traffic and performance Georgia roads required an ultimate bearing capacity of 31 psi. The difference is probably the result of differences in environment. The 31 psi required bearing capacity for Georgia subgrades corresponds to the Soil Support Number 3 of the AASHO design.

5. Georgia pavement thicknesses can also be designed by the use of triaxial tests on subgrade soils tested under field moisture conditions. The required safety factor against a bearing capacity (shear) failure is found by Fig. 8, and the required thickness to reduce the stress to that necessary to provide the safe bearing is given by Fig. 5.

II. PAVEMENT PERFORMANCE AND FAILURE

1. Definition of Failure of Pavement

Failure of a pavement is difficult to define. The failure of anything is defined as its coming to an end, its decay, decline, falling short, or deficiency (2). These criteria are easy to apply to a simple structural element, where failure is generally synonymous with rupture, and, of course, could easily be applied to a pavement that had ruptured or broken sufficiently that it was no longer usable. However, many structural systems, including pavements, may be deficient long before rupture is reached. In such cases, failure must be defined in terms of the ability of the structure, in the present case, the pavement, to perform its required function. In this case failure cannot be defined as an absolute quantity or point, but rather an arbitrary degree of impairment of function.

Failure of a pavement, therefore, must be defined in terms of pavement function, and the degree of impairment of that function. A modern pavement is a multi-purpose structure. It includes as its functions the following:

1. Spread the concentrated wheel load to match the supporting power of the subgrade.

2. Provide traction.

3. Provide a smooth riding surface.

4. Protect subgrade from deterioration brought on by weather.

The relative importance of these depends on both the vehicle and its physical requirements and on the person using the vehicle, including his needs, physical and psychological. Therefore, the relative importance would be different

(2) Webster's Collegiate Dictionary, G. C. Merriam Company, Springfield, Second Edition.

for a jeep and a heavily loaded inter-city truck; or for a inter-city traveller and a man visiting his neighbor on the next block. The relative importance would also be different for a person who had been accustomed all his life to muddy country roads compared to a man who was accustomed only to city streets.

It is impossible, therefore, to define pavement failure precisely; instead, it must be considered to be a deficiency in any one or more of the required functions. It is impossible to define failure as an absolute quantity or point; instead, it is a matter of degree. Finally, it is impossible to define failure objectively; instead it depends on the needs and whims of the users.

2. Performance - Serviceability

A new concept of pavement performance was developed in the AASHO Road Test in an attempt to express all the functions of the pavement in terms of the needs and demands of the using public. This is the Pavement Serviceability Rating (3) abbreviated PSR, which is a subjective evaluation of the ability of the pavement to serve high-speed high volume mixed truck and automobile traffic in its existing condition in terms of a numerical grade from 0 (or no quality) to 5 (the maximum). The rating is established by the means of individual ratings by a cross section of users: highway administrators, maintenance men, materials suppliers, truckers, highway educators, designers, automotive manufacturers, and researchers.

The Pavement Serviceability Index, PSI, is a synthesis of the PSR from measurements of the shape of the pavement surface and its physical condition, based on emperical correlations with the PSR established from the opinions of a group of individuals and tests of the same pavements. The major factors

(3) Carey, W. N. and P. E. Irick, "The Pavement Serviceability Performance Concept," Highway Research Board Bulletin 250, 1960

in the PSI were found to be the longitudinal profile of the surface and the mean depth of the ruts. The amount of cracking and patching were found to be factors, but not to the same degree as the first two. The longitudinal profile is expressed by the Slope Variance, $\overline{SV}$, which is the mean variance of the pavement surface slope (measured between two points 9 in. apart and the horizontal). The deterioration in PSI due to this factor was found to be 1.9 log $(1+\overline{SV})$. The deterioration in rating due to rutting was found to be 1.38 $\overline{RD}^2$ where $\overline{RD}$ is the mean rut depth in inches. Of these two, mean rut depth appears the more significant.

A simple expression for the Serviceability Index based only on rut depth was derived from the same data on which the AASHO PSI was based (4), by the writer.

$$PSI = 4.5 - 7\,\overline{RD}^2 \qquad (1)$$

Although the scatter of the data from this simplified relation is great, the equation agrees reasonably well with the observation that many of the Test Road pavements reached a PSI rating of 1.5 when the mean rut depth reached 0.6 to 0.7 in.

3. Causes of Pavement Deterioration and Failure

The subjective Pavement Service Rating gives no clue as to the cause of the deterioration of a pavement from the initial high value which it presumably possessed when it was built. The emperical Pavement Serviceability Index indicates that longitudinal variations and rut depth are major factors and cracking and patching are minor factors in the loss of the initial Serviceability but similarly does not define the mechanism by which they develop. In addition the scatter of the data suggest that there are other factors than those enumerated.

---

(4) , "The AASHO ROAD TEST -- Report 5 Pavement Research," Highway Research Board. Special Report 61E, Washington, 1962, p. 304.

While deterioration or failure of the pavement to perform its function may be reflected in the surface condition, the seat of the trouble may be in any of the layers which make up the flexible pavement system: the surface course, the base course, the sub-base (if any) and the subgrade or embankment. Furthermore the initial failure of one may lead to a failure (often in a different form) in another. For example, cracking of the asphaltic surface may let surface water into the subgrade and cause its softening and eventual shear.

The following mechanisms for pavement deterioration can be suggested:

Surface	Base and Sub-base	Subgrade
*Elastic deformation - rebound	*Densification - Consolidation	*Densification - Consolidation
*Densification - Consolidation	*Elastic deformation	*Elastic deformation
Thermal expansion and contraction	*Shear failure - bearing capacity	*Shear failure - bearing capacity
*Longitudinal shear failure (shoving)	Deterioration of aggregate	Swell-Shrink
*Curvilinear shear (bearing failure)	Deterioration of cementing agent	Pumping
Deterioration of the bitumen	Swell-Shrink	Settlement of deep strata
Separation of courses	Pumping	Mass shear failure - landslide
Bleeding		Limited mass shear (due to weak culverts, trenches)

Of these, the mechanisms marked * are primarily related to the traffic loads. The remainder are either independent of the traffic load or are related to the load only in that the failure is intensified or aggravated by the load rather than caused by it.

Deterioration and failure in the surface is not within the scope of this investigation. The causes are listed because they must be considered in diagnosing the mechanism of deterioration of existing pavements and deciding which failures are the result of inadequate pavement thickness.

Deterioration and failure of the base and sub-base is similarly beyond the scope of this study except when the base is so similar to the subgrade in its properties that the base and subgrade must be considered as a unit. This is the case with topsoil and sand bases. The failure of the higher types such as sand-asphalt and soil cement is not considered.

A major and possibly the most important function of the pavement is to distribute the concentrated wheel load so that the stress does not exceed the supporting capabilities of the subgrade. Of course the deformation and failure of the subgrade are reflected in the surface condition and thereby in the Pavement Serviceability Rating or Index. The elastic deformation, consolidation (densification) and shear (bearing capacity) failure of the subgrade are directly related to the wheel load and the resulting stress distributed through the surface and base courses.

The remaining mechanisms are not directly caused by the wheel loads. Swelling and shrinking of the subgrade depends on the moisture changes as well as the mineralogy of the soil. The effect may be bumps and hollows at irregular intervals not related to the traffic or load pattern. Swelling may have a secondary effect in that softening or weakening of the subgrade can lead to deflection or shear failure that is load-related. Similarly shrinkage has a secondary effect in producing tension and shear cracks in the pavement courses above. While these are not necessarily load-related, they may be aggravated by the load. Therefore it is difficult to isolate the effects of deterioration due to swelling and shrinking although the basic mechanism is different from the others.

Pumping is a complex phenomenon that is indirectly related to load, but which arises from the effect of free, available moisture on a susceptible subgrade or base. The load of the moving wheel causes the pavement components to deflect. After the load passes, the components rebound. If the upper layers rebound faster or more than the lower layers (which is likely because in the typical flexible pavement system the upper layers are more rigid and possibly more nearly elastic) a temporary void is formed between the layers. If free water is available, it is sucked into the void, only to be expelled at the next loading. If the base or subgrade is easily softened or eroded, the pumping of water in and out creates an erosion cavity and eventually a structural failure.

Settlement of the roadway (ordinarily an embankment) because of consolidation of deeper strata, landslides and localized shear failures caused by weak culverts or improperly compacted backfills behind bridge abutments or in trenches can cause disruption of the pavement surface and a loss of serviceability. None of these, however, are directly related to the design or adequacy of the pavement. Furthermore, the traffic loads are often not major factors in these phenomena, for they may be small compared to the weight of the soil mass that is involved. Pavement deterioration due to these phenomenon, therefore, must be discounted in evaluating observed pavement condition for the purpose of developing a pavement design.

The major subgrade mechanisms that contribute to pavement deterioration are deformation and shear failure. These are discussed in more detail in the following sections of the report.

4. Subgrade Deflection

The deflection of the subgrade under traffic load results from the stresses transmitted through the pavement system, particularly the vertical stresses.

These stresses have been the subject of the major part of this research project. Both theory and stress measurements show that the vertical stresses become smaller with increasing depth below the pavement surface and with increasing horizontal distance from the center of the line of load application (see Reports 1, 2, 3, 4, and 5, Project B-133) depending on the elastic characteristics of the subgrade and the base course.

These stresses have a two-fold effect on the subgrade (and on the other pavement layers, similarly). First, they produce a downward deflection of the subgrade surface due to the deformation of the soil without appreciable volume change. This can be visualized as the elastic shortening and lateral bulging of the column of soil immediately below the load similar to the shortening of any axially loaded structural member. If it is assumed that the subgrade is a semi-infinite homogeneous elastic mass with a modulus of elasticity of E and is momentarily incompressible, and that a uniform pressure of q is applied to a square area of width, b, the deflection, ρ, due to deformation will be

$$\rho = \frac{0.6qb}{E} \qquad (2)$$

In other words, the deflection is the same as for a free-standing column of soil whose height is 0.6 times the width of the column. Of course neither the distribution of the load nor the shape of the loaded area of the subgrade are as simple as the conditions assumed in this equation. More accurate (and more elaborate) mathematical representations of the deformation deflection of a subgrade are available and were discussed in Report 1, p. 13 and 29 - 30. All are of the same general form as Eq. 1; therefore, this will suffice as a

model for illustrating the effects of the different factors involved. (More recent methods have been developed (5) but none have been adequately verified.) The deflection in any case is directly proportional to the pressure and the size of the loaded area and inversely proportional to the modulus of elasticity.

The second deflection mechanism is the consolidation or densification of the subgrade. Although the theories of soil settlement due to reduction in the voids volume have been primarily applied to foundations of structures, they apply also to the consolidation of the subgrade. The relation between void ratio change and stress increase is more complex than that for elastic deformation and a simple expression for consolidation settlement is not available even for homogeneous soils. However, consolidation settlement does increase with increasing stress, not in direct proportion but more nearly in proportion to the log of the increase compared to the original stress due to the soil weight. Methods for analyzing the consolidation of pavement components await future development.

Under repeated loadings, progressive consolidation occurs. With each successive cycle of load and unload, the reduction in voids becomes less. However, it appears to continue indefinitely, but at an ever decreasing rate.

Subgrade deflection causes an elongated depression in the wheel path that is entirely below the original surface level. The deformation deflection is temporary and is recovered after the wheel passes. The major effect will be an "alligator" cracking of the surface course if the deflection is sufficiently great. The estimated limiting deflection, based on the U. S. Navy airfield design is 0.2 in. although some highway departments have suggested limiting deflections of about 0.05 in. for major highways. Consolidation

---

(5) "Preprints," International Conference on the Structural Design of Asphalt Pavements, Univ. of Michigan, Ann Arbor, 1962, Vol. 1, 2.

deflection causes a permanent rut that is entirely below the original surface. The rut may be accompanied by longitudinal and possibly transverse cracks. In addition, long longitudinal waves in the rut may be observed where there is severe consolidation.

5. Shear Failure

Shear failure of the subgrade, similar to the bearing capacity failure of a foundation, can result if the stresses transmitted to the subgrade through the base and surface courses is sufficiently great. If it is assumed that the subgrade is homogeneous and its properties can be described by the unit weight, γ, the cohesion, c, and the angle of internal friction, φ, and if it is assumed that the pressure transmitted to the subgrade is vertical, and uniform over an area of width, b, the pressure at which the soil will shear, q_o, is defined by

$$q_o = \frac{\gamma b}{2} N_\gamma + cN_c + q' N_q \qquad (3)$$

In this expression N_γ, N_c, and N_q are dimensionless functions of the angle of internal friction and q' is the weight of the pavement and base above the subgrade.

Many variations of this expression, originally proposed by Terzaghi (6), have been published. The differences are in the assumed character of the zone of shear failure and they are manifested in differences in the values of the N-factors. So far no analysis has been developed for a non-uniform loading of indefinite width such as that transmitted to the subgrade. However, it is

(6) Terzaghi, K., Theoretical Soil Mechanics, John Wiley and Sons, New York, 1941.

to be expected that the general form of the equation will be little changed; instead the values of N will reflect the non-uniform loading. If this is the case, then bearing capacities for subgrades computed by Equation 3 and utilizing the N-values for one of the existing methods of analysis, should be approximately proportional to the true bearing capacities. Or, conversely the safety factor with respect to shear failure computed by Equation 3 and utilizing some existing N-factors and the stresses transmitted to the subgrade through the pavement system should have some reasonably constant relation to the true safety factors.

While the strength parameters c and φ reflect complete soil failure, they may not indicate the development of limited but accumulating failure under repeated loads that are not great enough to produce complete failure. Although little is known about the effects of repeated loading on progressive shear, the indications are that the magnitude of progressive failure increases with the increasing ratio of the actual stress to the failure stress. In other words, progressive failure increases with a decrease in safety factor.

Shear in the subgrade is accompanied by a broad, deep depression or rut in the wheel path with the upheaval occurring beyond it. Longitudinal cracking may be severe, and eventually leads to transverse cracking which forms a blocky pattern (7). Shear along the pavement edge may be accompanied by curved cracking and outward movement of the base and surface and sometimes by severe outward tilting.

6. Summary

Pavement deterioration and failure is the result of a series of complex processes, none of which are clearly understood and only part of which are

(7) Hveem, F. N., "Types and Causes of Pavement Distress," Bulletin 187, Highway Research Board, 1958.

directly related to the loads supported. Although exact methods of analyzing the mechanical processes of subgrade deflection and shear failure are not available, approximations can be made that point out the relative importance of the different factors involved and also indicate the relative magnitude of possible deformation and the safety against shear failure.

The greatest unknown factors are those which involve the environment: temperature, ground water, surface water infiltration, and other moisture changes, and frost action. These profoundly influence the deformation and shear failure characteristics of all the pavement components but particularly those of the subgrade. At the present time little is known about the direct effects of the environment on the soil and too few facts are available to permit valid emperical correlations to be made.

III. SURVEY OF GEORGIA PAVEMENTS

1. Locations

A survey of Georgia pavements was undertaken in 1961 to locate typical areas in all four of the geologic regions (Coastal Plain, Piedmont, Blue Ridge, and Appalachian Ridge - Valley) in which comparable pavements had both exhibited good performance and had deteriorated badly. An inquiry was sent to each of the Georgia Highway Department Field Divisions asking for their suggested locations for study. From these a list of 84 was compiled for examination and testing. The locations are described in Table 1a.

2. Field Survey

A field survey was undertaken of these locations in the late summer, fall, and early winter of 1961 by A. E. Schwartz and D. Wheeless, Research Engineers, assisted by the appropriate Field Division Engineers and their staffs. The pavement was examined visually and data on the roadway environment and pavement condition obtained. A typical example of a completed survey data form is shown in Appendix A.

A survey of the traffic was made during the period of pavement examination in which the total number of vehicles in the lane under study was counted and the percentage of heavy trucks estimated. While such a short count is not a valid indication of the total traffic it does give some picture of the character of the traffic on pavements for which no accurate information is available.

The typical depth of rutting was measured using a 4 ft. long straight edge placed over the wheel paths. The segment so measured was then photographed and a sketch made of the pattern of cracking, if any.

The dates of construction and repair (if any) were obtained from the Field Division Engineer. He also provided information on the design and construction of the pavement, where it was available.

The pavement was marked at the location samples were to be made, usually in the zone of the failure but not where the failure itself might have disrupted the soil. Finally, a Serviceability Rating was assigned utilizing the criteria described by Carey (3) and based on the visual observations of the surface condition and its riding qualities.

3. Sampling

Samples were secured in most of the locations by the Georgia Highway Department Division of Materials and Tests. The sampling program was necessarily interspersed with the routine drilling and sampling work for new construction and thus was spread out over several months. Practically all was done in the late winter and spring of 1962 when the soil moisture conditions were likely to be at the highest.

The bituminous pavement was cored, where possible, and its thickness measured. The thickness of each deeper pavement course was measured and the materials described visually. Undisturbed samples were secured of each base course layer that contained no gravel and of the topmost 2 to 3 ft. of the subgrade, utilizing 3 in. O.D. thin wall sample tubes. The samples were sealed in the field with plastic end caps and brought to the Georgia Tech Soil Mechanics Laboratory.

4. Laboratory Tests

The samples were cut into 6 in. sections using either a high speed abrasive saw or a metal-cutting band saw. Unfortunately some of the samples were unsatisfactory because of gravel which caught under the edge of the tube

and disturbed the soil or because of faulty sealing. Most, however, were suitable for testing.

Because of the limited amounts of sample available only one form of test could be utilized. That which was considered the most representative of field conditions was the undrained triaxial, utilizing the full sample diameter of approximately 2.8 in. and without any changes in moisture. Where possible three confining pressures were employed: 10, 20, and 40 psi; however, in some cases only 10 and 20 psi were used when the amount of sample was limited. The samples, each about 6 in. long, were loaded axially at a controlled strain rate of 0.8 per cent to 1 per cent per min. The test data were analyzed on a computer and the results plotted in the form of stress-strain curves from which the initial tangent modulus of elasticity for a combining pressure of 10 psi was found. These values are given in Table 1. Mohr diagrams were plotted and the "cohesion" and angle of internal friction, c and φ, respectively, were found. These are also given in Table 1.

The visual descriptions of the materials are included in the table.

IV. AASHO SUBGRADE TESTS

The AASHO Test Road was constructed so as to provide as uniform a subgrade as possible, so that initial subgrade variability would not influence the pavement performance. Therefore the materials utilized were selected so as to be as nearly uniform as possible in composition, and the construction was controlled so that the moisture contents and densities could be kept within narrow limits.

1. Previous Tests

Tests of the subgrade (embankment) base and surface materials were summarized in the AASHO Test Road reports and in other published data on the road (8). These included control tests for quality and physical tests by the Bureau of Public Roads to determine the structural qualities of the compacted materials. In addition, samples were furnished to many state highway departments who tested them by the same procedures they commonly employed for their own design work. The results of these have also been published (9). Limited tests were made of soils in certain of the road embankments which had been removed from test because of deterioration, or at the programmed end of testing. These include moisture, density, CPR and K-factor tests. These data were included in AASHO Report 5, previously referenced.

2. Sampling

None of the data included strength tests of samples of the subgrades as constructed. Four undisturbed samples were secured by the Illinois Division

(8) "The AASHO Road Test Report 2, Materials and Construction," Special Report 61 B, Highway Research Board, 1962.

(9) Shook, J. F. and A. Y. Fang, "Cooperative Materials Testing Program at the AASHO Road Test," Special Report 66, Highway Research Board, 1961.

of Highways through the courtesy of Mr. W. E. Chastain, Jr., Engineer of Research and Development. All were obtained on about May 1, 1963, well after the spring thaw. These were of the subgrade, commencing 3 in. below the sub-base. All were 24 in. long, in 2 in. O.D. thin walled tubes. They were sealed at the site and shipped to the Georgia Institute of Technology Soil Laboratory.

3. Laboratory Tests

Triaxial tests were made of all four samples utilizing the same method and pressures as for the tests of Georgia subgrades. The results were expressed in stress-strain curves and Mohr diagrams, Fig. 1, 2, 3, and 4. As can be seen the results are not uniform. There is considerable variation in the densities and moistures as well as in the strengths. With the exception of the samples from Sta 60+00, where gravel made a full program of tests impossible, the samples exhibit comparable angles of internal friction of about 20 deg and cohesions of from 6.5 to 20 psi. A composite plot of all the data shows the weaker materials exhibit an average cohesion of 9.5 deg and an angle of internal friction of 20 deg. These values were used in subsequent analyses.

For comparison, the BPR tests of subgrade samples laboratory-compacted to 95 per cent of AASHO T 99-49 maximum (the specified value) found c and φ values of 11 psi and 31 deg respectively for Borrow Pit 1 and 8.9 psi and 21 deg for Pit 2. The corresponding CBR values were 2.7 and 2.5. The cooperative test data (9) results were comparable in those cases where the soil was tested under similar conditions of compaction and moisture content.

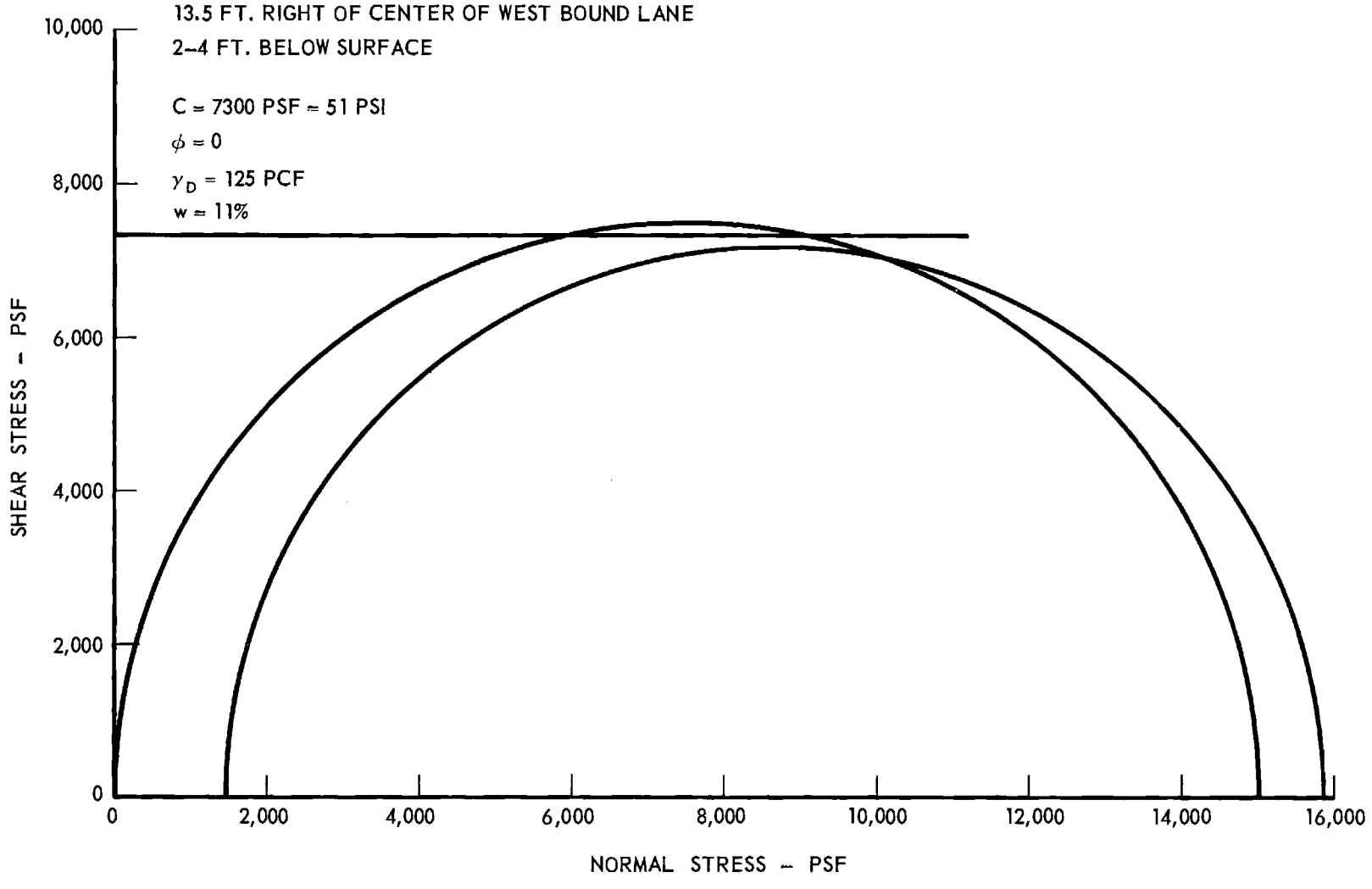

Figure 1. Triaxial Test Results - AASHO Subgrade Sta. 60+00.

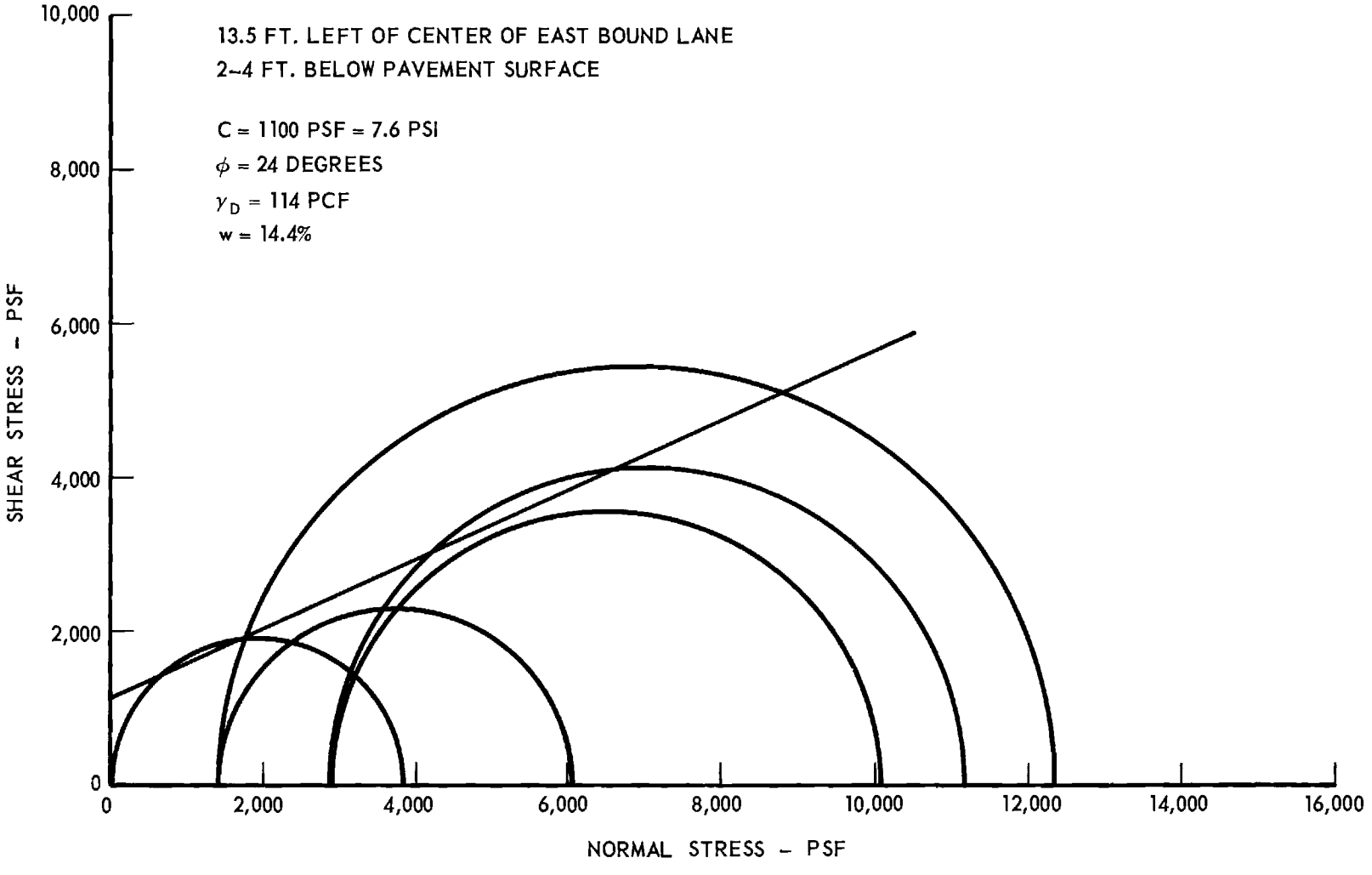

Figure 2. Triaxial Test Results - AASHO Subgrade Sta. 149+00.

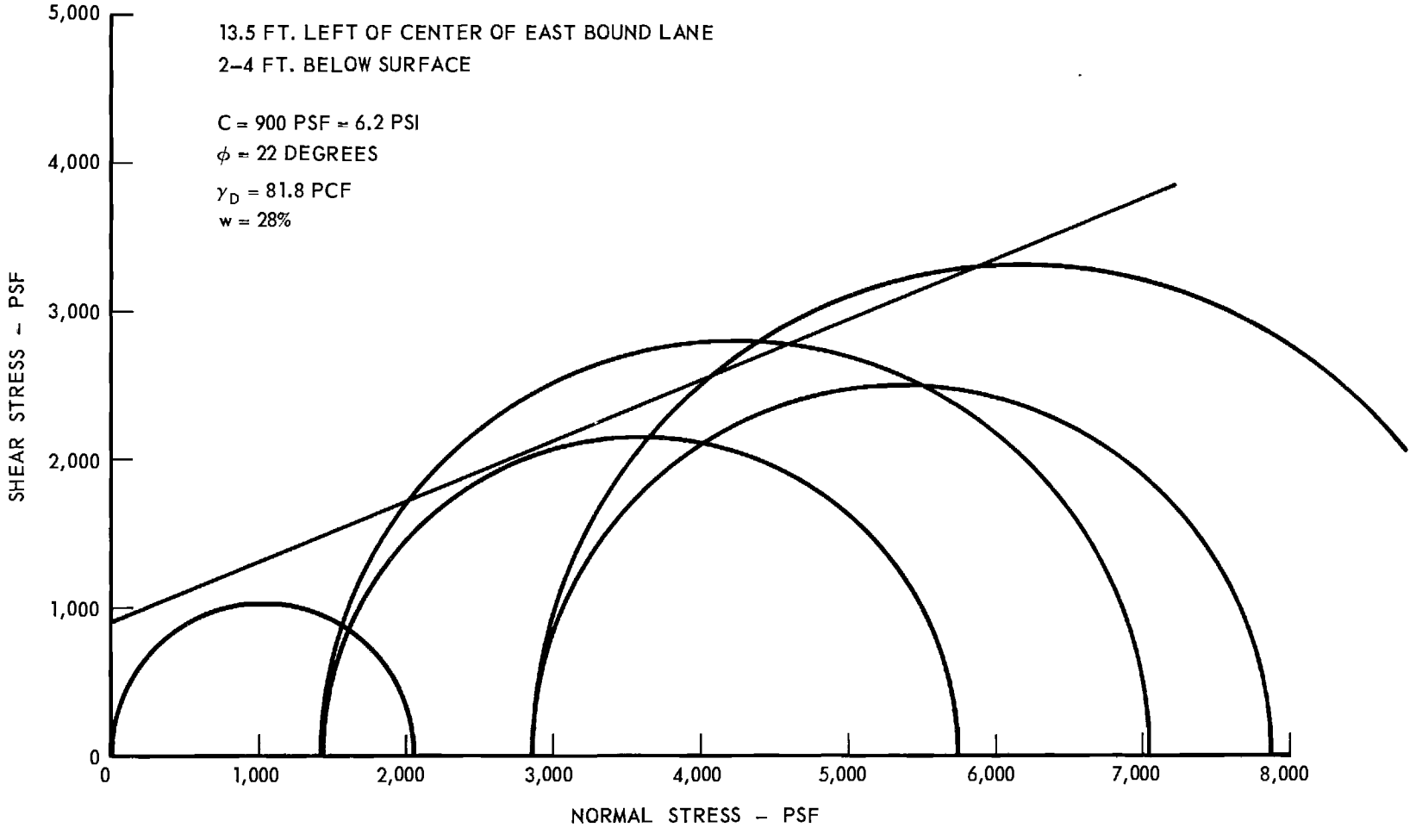

Figure 3. Triaxial Test Results - AASHO Subgrade Sta. 229+00.

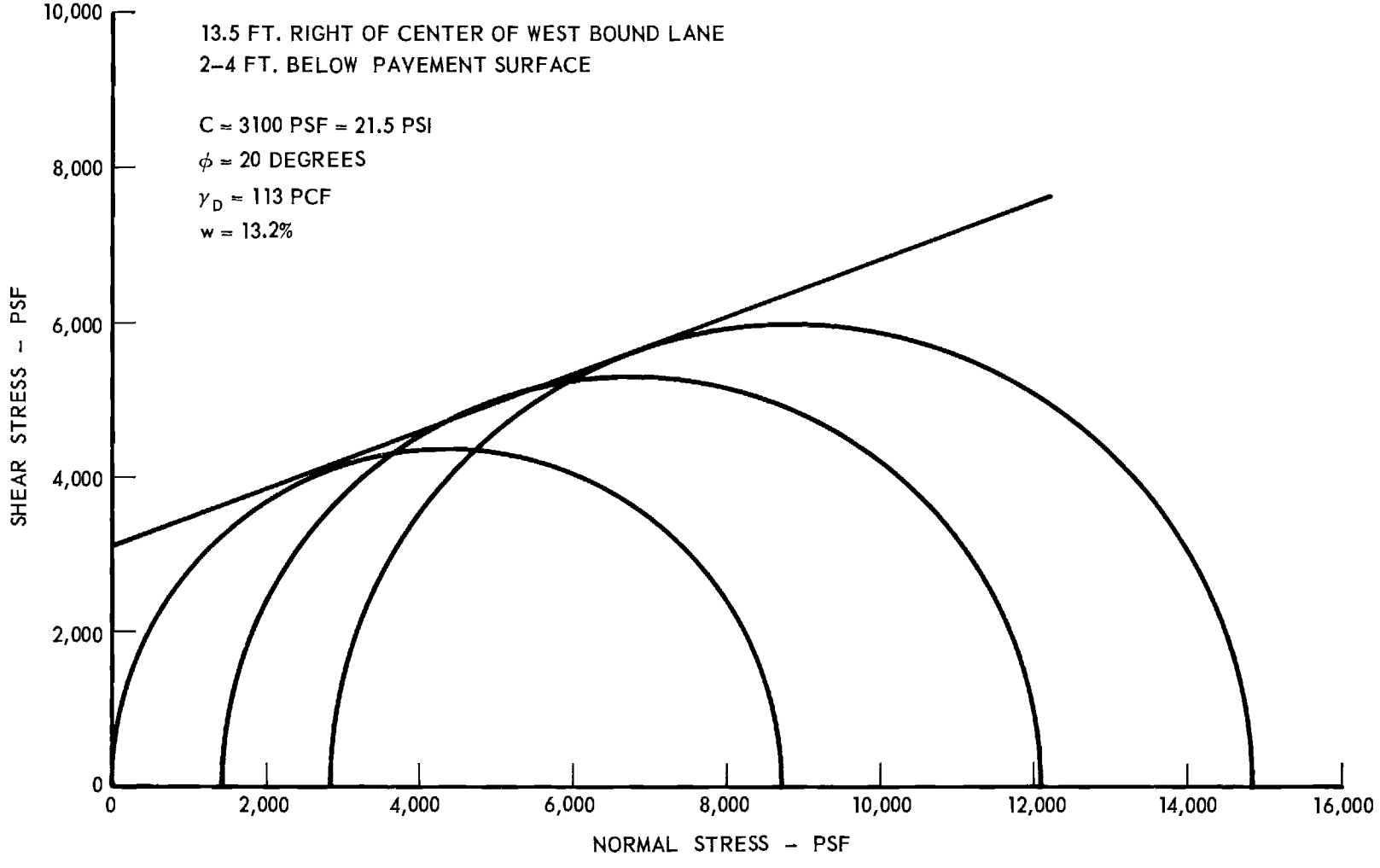

Figure 4. Triaxial Test Results AASHO Subgrade Sta. 357-368+00.

V. ANALYSIS OF GEORGIA PAVEMENT PERFORMANCE

The performance of the Georgia pavements was analyzed utilizing the pavement descriptions and Serviceability Rating. The theoretical bearing capacity and deflection of the subgrade were computed utilizing the methods described in Chapter II. These were correlated to form a semi-rational basis for pavement design evaluation.

1. Depth-Stress-Width

The previous reports of this project presented data on the vertical stresses at different depths beneath different pavement systems utilized in Georgia. These tests all found that the vertical stress was greatest immediately under the tire and it became rapidly less with increasing horizontal distance and increasing vertical depth below the ground surface. For the purpose of analysis it was assumed that the significant vertical stresses at any depth were those equal to or greater than 1/2 the maximum vertical stresses at that depth.

The average significant vertical pressures for a 9 kip dual wheel load were found from the test data presented in Reports 1 - 4 of this project. These were increased by 10/9 to find the average significant vertical pressures for a 10 kip dual wheel which is the present Georgia load limit of 20 kips per axle. A plot of these stresses is given in Fig. 5. It shows the significant vertical stresses beneath different bases as a function of depth beneath the pavement surface. For most Georgia pavement systems, the curve for the 3 in. asphaltic surface and 8 in. topsoil-soil-macadam, or silt base applies. This is almost identical to the stress distribution computed by the Boussinesq Theory and should apply reasonably well to all but soil cement and sand-asphalt bases. For the latter, their special curves are shown in Fig. 5.

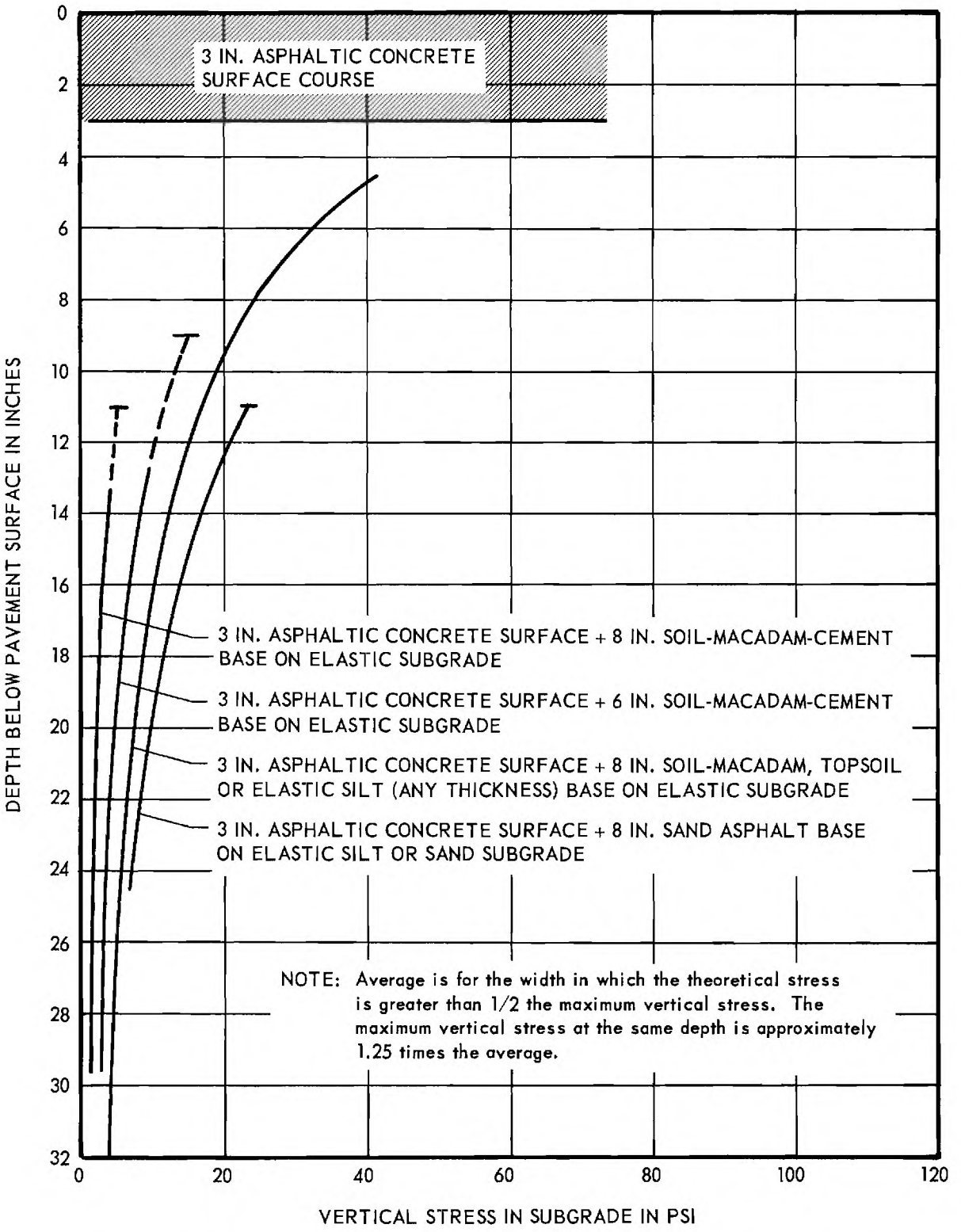

Figure 5. Average Significant Vertical Stress in Subgrade for Different Georgia Base Courses and 20 Kip Axle Loads on Dual Tires.

The width of the zone of significant vertical stresses was found from the stress distribution curves of the previous reports. This is shown in Fig. 6. The curve can be approximated by the straight line whose equation is

$$b = 15 + 0.7\,z \qquad (4)$$

where b is the equivalent width in inches and z is the depth below the pavement surface in inches.

2. Deflection - Bearing Capacity

The elastic deformation of each subgrade under a 20 kip axle load was computed utilizing the modulus of elasticity for the subgrade at a containing pressure of 10 psi and Equation 2 previously discussed in this report. The width, b, utilized in the computation was that shown in Fig. 6. The stress was that shown for the depth of the top of the subgrade by Fig. 5. Of course it would be false to conclude that this represents the true base deflection of the subgrade. However, it should be proportional to the true deflection if the modulus of elasticity determined by the laboratory tests is correct.

The bearing capacity of the subgrade, and in some cases the bearing of each different subgrade layer where the test data differed greatly, was computed utilizing Equation 3. The c and φ values were those of the soil tests and the b was found from Fig. 6. The values of the bearing capacity factors were those computed from the old, simple Bell-Terzaghi equations as modified by the author (10). These are tabulated in Appendix B for reference. For use in these computations the relation was simplified slightly. This simplification, shown in Appendix B, is based on the observation that the total thickness of

(10) Sowers, G. B. and G. F. Sowers, Introductory Soil Mechanics and Foundations, Macmillan Company, New York, Second Edition, 1961.

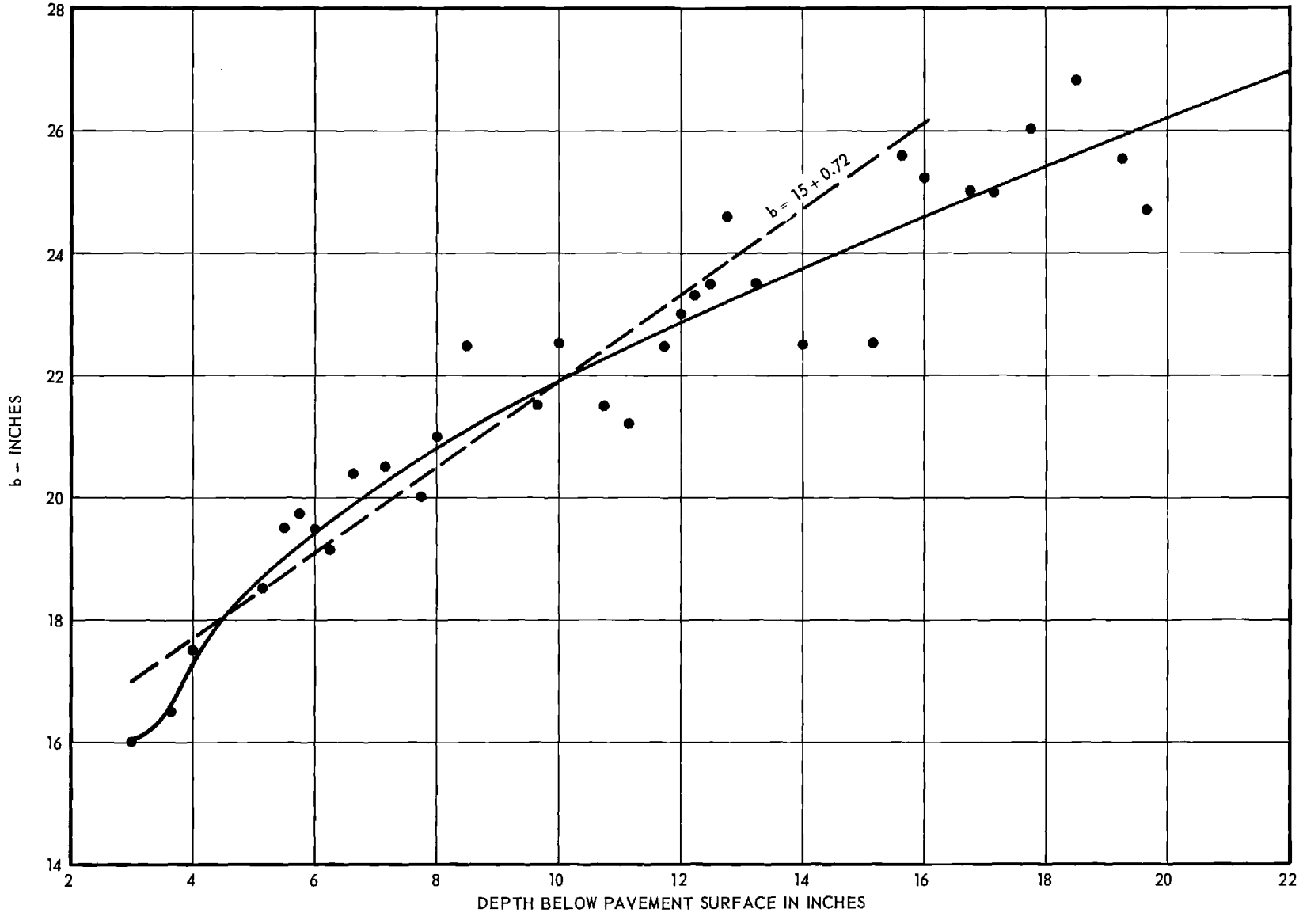

Figure 6. Equivalent Width of Area of Significant Vertical Pressure in Georgia Subgrade.

pavement and base for Georgia is ordinarily 10 to 12 in. In such cases constants can be introduced in the terms involving b, d, and γ with little sacrifice in accuracy (considering the greater error involved in utilizing this or any other existing bearing capacity expression in analyzing pavement capacity).

The vertical stress exerted on the subgrade by the 20 kip axle was found from Fig. 5. The ratio of the computed bearing capacity to the stress is the apparent safety factor. While this is probably not the true safety factor it should be proportional to it. Further it would be reasonable to conclude that the lower the safety factor, the greater the possibility of shear failure of the subgrade and the greater the amount of progressive shear. The data utilized and the results of these computations are given in Table 1.

3. Traffic

A short term traffic count was made of each sample section. Data on estimated daily total traffic was obtained from the Division of Highway Planning. In most cases these estimates were based on actual traffic counting at the regular stations in the area. However, in some cases, particularly the secondary roads in remote areas, the estimate was based largely on experience. In no case was the pavement failure close enough to a point of long term traffic study that the count can be considered accurate. Both the short term count at the sample section and the Georgia Highway Department estimate were utilized in determining the number of trucks per day (other than pickups) on the lane under study. This was converted to an equivalent number of 20 kip axles utilizing a relationship established by the Alabama Highway Department in their Loadometer Studies (11). The total number of trucks is multiplied by

(11) Eiland, E., "Alabama Highway Departments Use of the AASHO Data," Proceedings Sixth Alabama Joint Highway Conference, Auburn, April, 1963.

the weighting factorgives the equivalent 20 kip axles. The values of the factors used were

Interstate - Primary	0.43
Secondary	0.32

(These are average values from the Alabama studies, based on their use of load equivalents from the AASHO studies of mixed loads -- they are only an indication of the typical traffic distribution.)

The daily equivalent 20 kip axle load figure multiplied by the number of days the pavement was in service gives the total axle loads at the time of the evaluation. This figure is given on Table 1.

Considering the degree of estimating in establishing this traffic figure, it is likely that it may differ from the true value by 50 per cent. An even greater variation is likely on the secondary roads with light traffic where even a moderate use by pulpwood trucks or other local, highly specialized vehicles represents the major loading of the pavement.

4. Serviceability-Safety-Traffic

The Serviceability for each pavement area was checked by the writer utilizing the photographs, the measured rut depths, and the crack patterns. Greatest weight was given to those factors which reflect the subgrade behavior. For example, while the all-over Serviceability of a pavement suffering from the peeling of an overlay due to bad bond with the old pavement might be low, the Serviceability of the pavement considering the rut depth and longitudinal profile might be high. Since this investigation is concerned with the design of a pavement to fit the subgrade, the subgrade behavior was given greatest weight.

Plots of the serviceability as a function of computed bearing capacity, apparent safety factor, and traffic were made to determine which of these factors (discussed in Chapter II) were most significant in determining the behavior of the Georgia pavements.

A plot of Computed Deflection vs. Computed Safety Factor is shown in Fig. 7. Although there is considerable scatter, the relation shows that those pavements having the greatest safety factor against shear failure also exhibit the least elastic deflection. In other words, those soils having the greatest strength are also likely to be the most rigid. This relation also suggests that either deflection or bearing capacity alone might be a satisfactory criterion for design in that it reflects the other to some degree.

Because of the limited time available for study and the many factors in both deflection and bearing capacity for which no data are available, no attempt was made to analyze the cause of the scatter.

The plot of Serviceability vs. Apparent Safety Factor, Fig. 8, also exhibits considerable scatter. However, a general trend is apparent with serviceability decreasing with decreasing safety factor. If the traffic is considered, the trend becomes fairly well defined, with the lighter traffic requiring smaller safety factors than the heavier. Curves were drawn reflecting the largest safety factors required to maintain a given Serviceability, for different levels of traffic. In reality, therefore, each curve represents an envelope. There are a few points that do not fit the relations. Some of these with high serviceabilities undoubtedly represent different qualities of initial construction, rather than any deterioration of the pavement. A few exhibit lower serviceabilities because of deterioration other than of the subgrade.

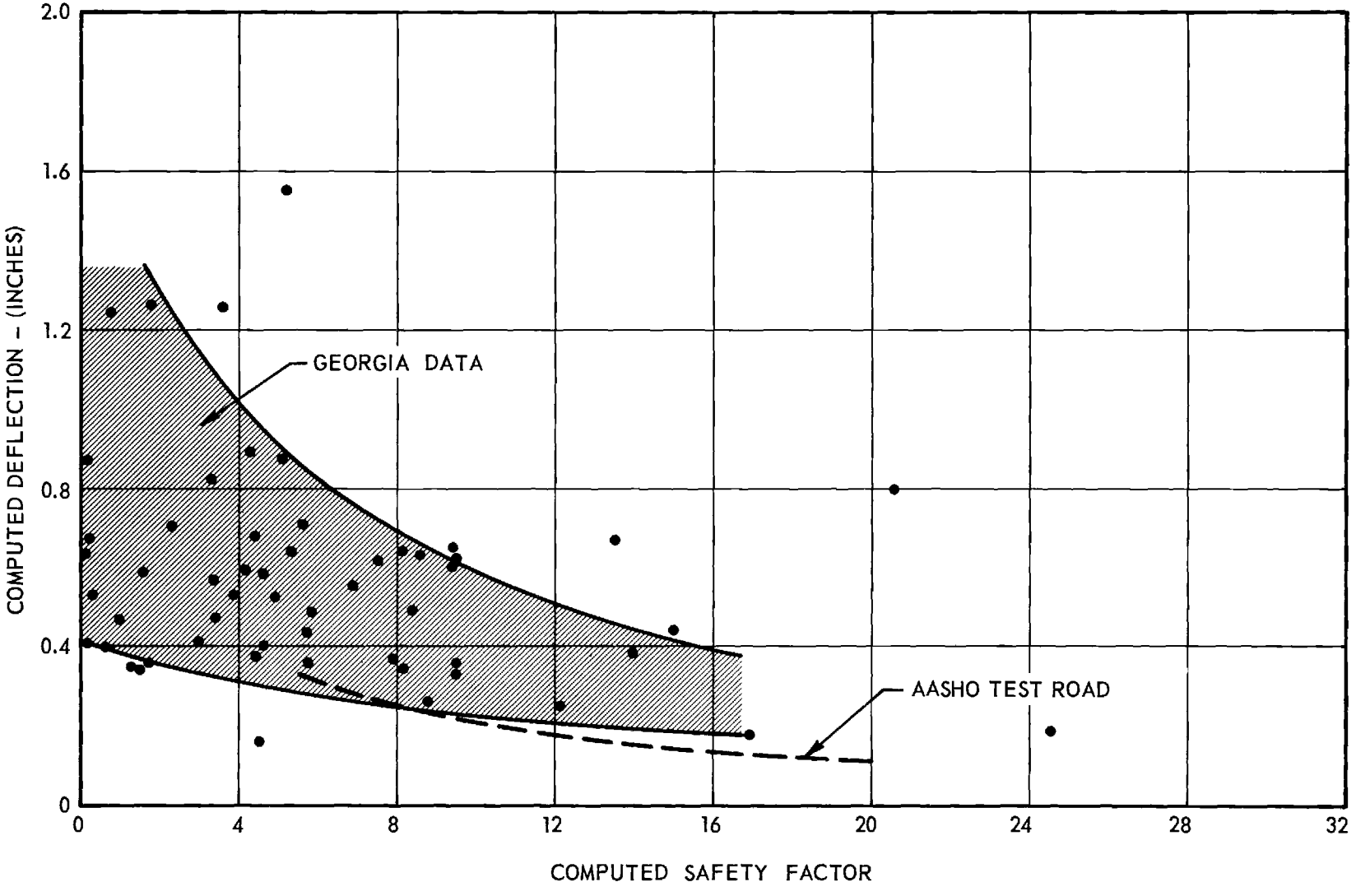

Figure 7. Computed Elastic Deflection vs. Computed Safety Factor of Subgrades of Georgia Pavements with 20 Kip Axle Loads.

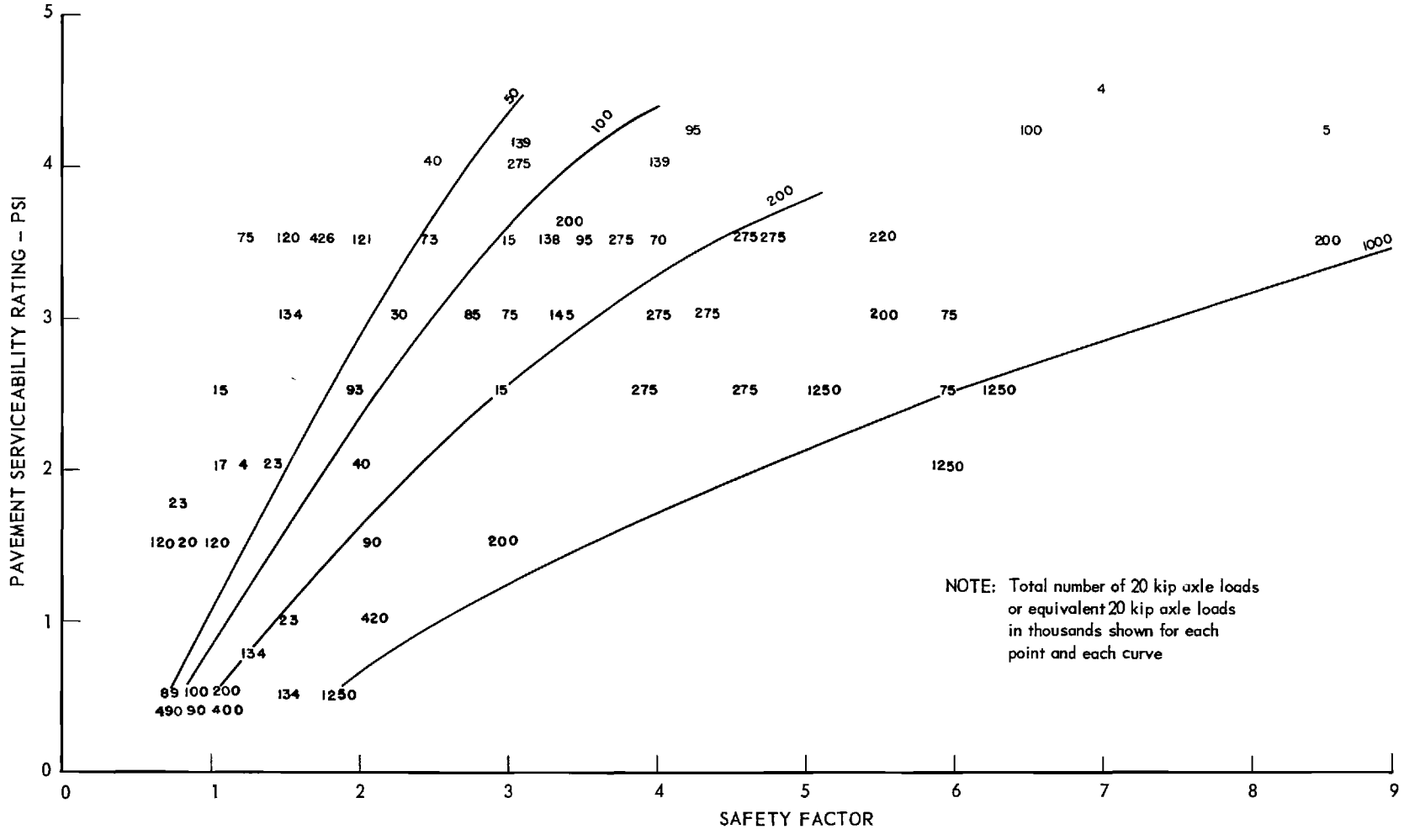

Figure 8. Required Safety Factors for Different Pavement Serviceability Indexer at End of Service Period for Georgia Pavements and 20 Kip Axle Loads.

A major, unknown factor in the scatter is the fact that the soil test data may not reflect the environmental conditions that are representative of deterioration and failure. For example, if the subgrade moisture increases in the winter and spring and if failure is more rapid during this period then the tests should be made of samples obtained during the critical period. While an attempt was made to do this, in obtaining the samples during the winter and spring, it is not known whether the soil at each location was sampled at its worst condition. Moreover, this might not be fair if the traffic during this period of soil weakening was materially less than the averages.

Considering the variable factors which could not be evaluated in this investigation, the degree of correlation shown in Fig. 8 is surprising.

VI. AASHO DATA ANALYSIS

1. AASHO Flexible Pavement Evaluation

The evaluation of the AASHO flexible pavement tests is given in detail in Report 5 (4) and has been discussed in numerous reports and papers, and will probably be the subject of much future study and debate. A brief review of the program, however, is necessary here to provide the background for the analysis made.

The entire flexible pavement test program utilized a single subgrade soil, a silty clay classified as A-6 by the AASHO system. This was compacted under close control to densities of between 95 and 100 per cent of T99-49 maximum so as to provide as uniform a subgrade as possible, and to eliminate the factor of variable subgrade support from the study.

The controlled variables were pavement component thickness and traffic. Although a few different base course materials were tested in limited sections, the major emphasis was on the effects of different combinations of surface, base, and sub-base thickness under different axle loads ranging from 2000 lb. to 48000 lb., with and nearly continuous traffic. The Serviceability of each pavement section was measured from time to time and a plot of serviceability as a function of the total number of axle loads made for each pavement section. The results were analyzed statistically to develop emperical relations between axle load, number of axles, pavement design, and performance. The tests effectively demonstrated that serviceability decreased with increasing load, increasing numbers of loads, and with decreasing pavement thickness. Curves showing these relationships were developed by assuming a mathematical form for them and by finding the best fit for the assumed curve by statistical methods.

The method of analysis employed in the AASHO studies does not take into consideration the mechanisms contributing to deterioration or the relative contribution of each. The effect of variable subgrade support is not considered. The effect of environment, particularly moisture variation, is also ignored in the primary analysis. Therefore, the AASHO test results cannot be directly applied to the design of Georgia Highways. Instead the AASHO data for the 18 kip axle loads (which is nearly equal to the present Georgia legal limit of 20 kips) was analyzed in the same manner as the Georgia data in this report.

2. Deflection-Bearing Capacity-Traffic

The elastic deflection and bearing capacity of the AASHO subgrade were computed in the same way as for the Georgia subgrades. A single value was utilized for c, φ, and E in all segments, corresponding to the poorer soils tested.

A plot of computed elastic deflection vs. computed safety factor, Fig. 9, is well defined, as might be expected because the only variable involved is pavement thickness. This does, however, suggest the validity of using a single index, either bearing capacity or deflection, as a basis for evaluating subgrade support. A comparison of Fig. 9 with Fig. 7 is interesting. The AASHO curve (superimposed in Fig. 7) approximately coincides with the lower limit of the Goergia data. This suggests that many of the Georgia soils are more elastic than those of the AASHO subgrade.

A plot of the safety factor of the AASHO pavements vs. number of 18 kip axle loads required to reduce the serviceability to 1.5 is shown in Fig. 10. A well-defined trend is evident showing that as the safety factor increases, so does the number of axle loads required to reduce the serviceability to 1.5. Conversely if, a serviceability of 1.5 is demanded at the end of the service life of a pavement, the required safety factor must increase with increasing traffic.

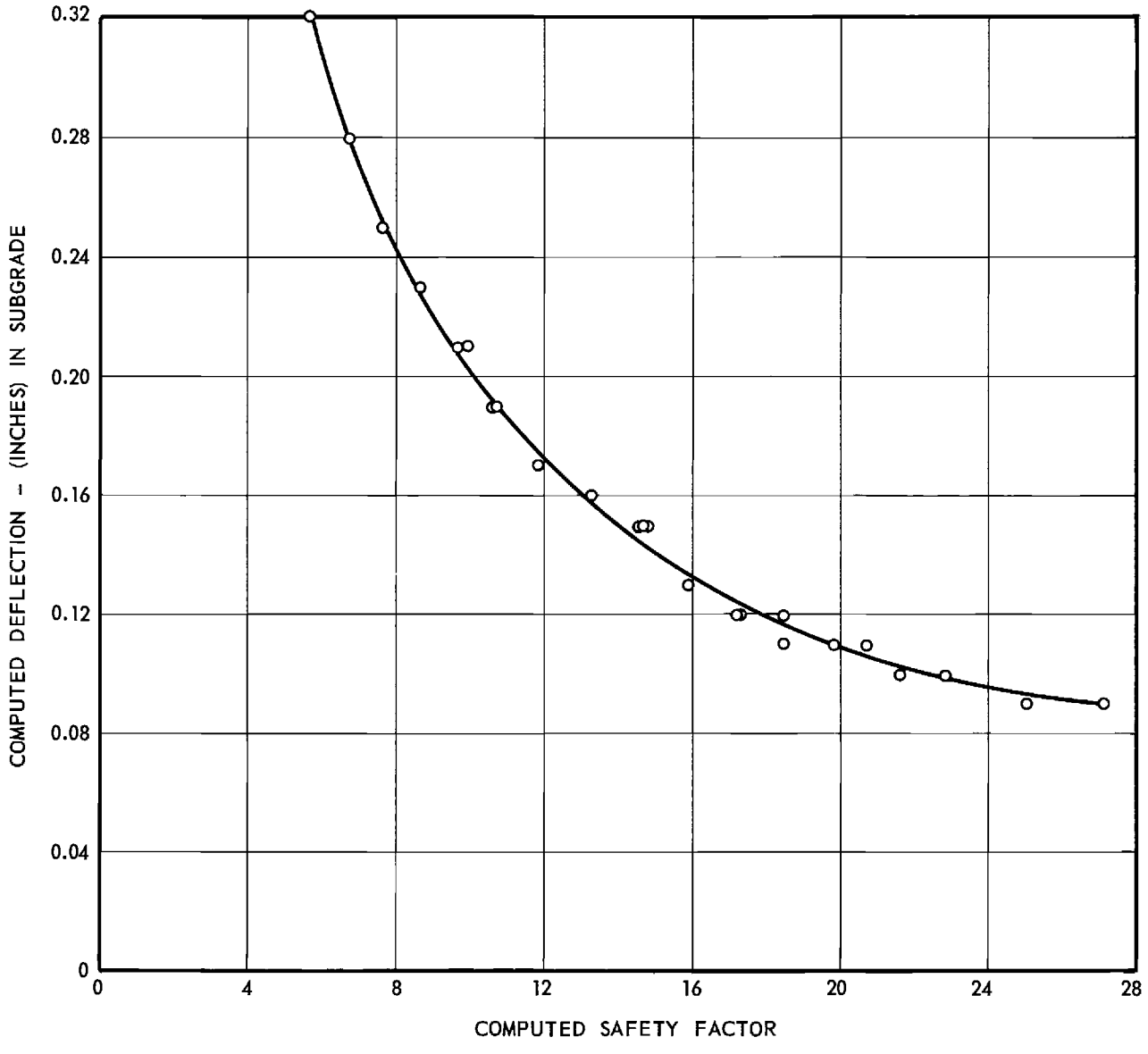

Figure 9. Computed Elastic Deflection vs. Computed Safety Factor of Subgrades of AASHO Road Test and 18 Kip Axle Loads.

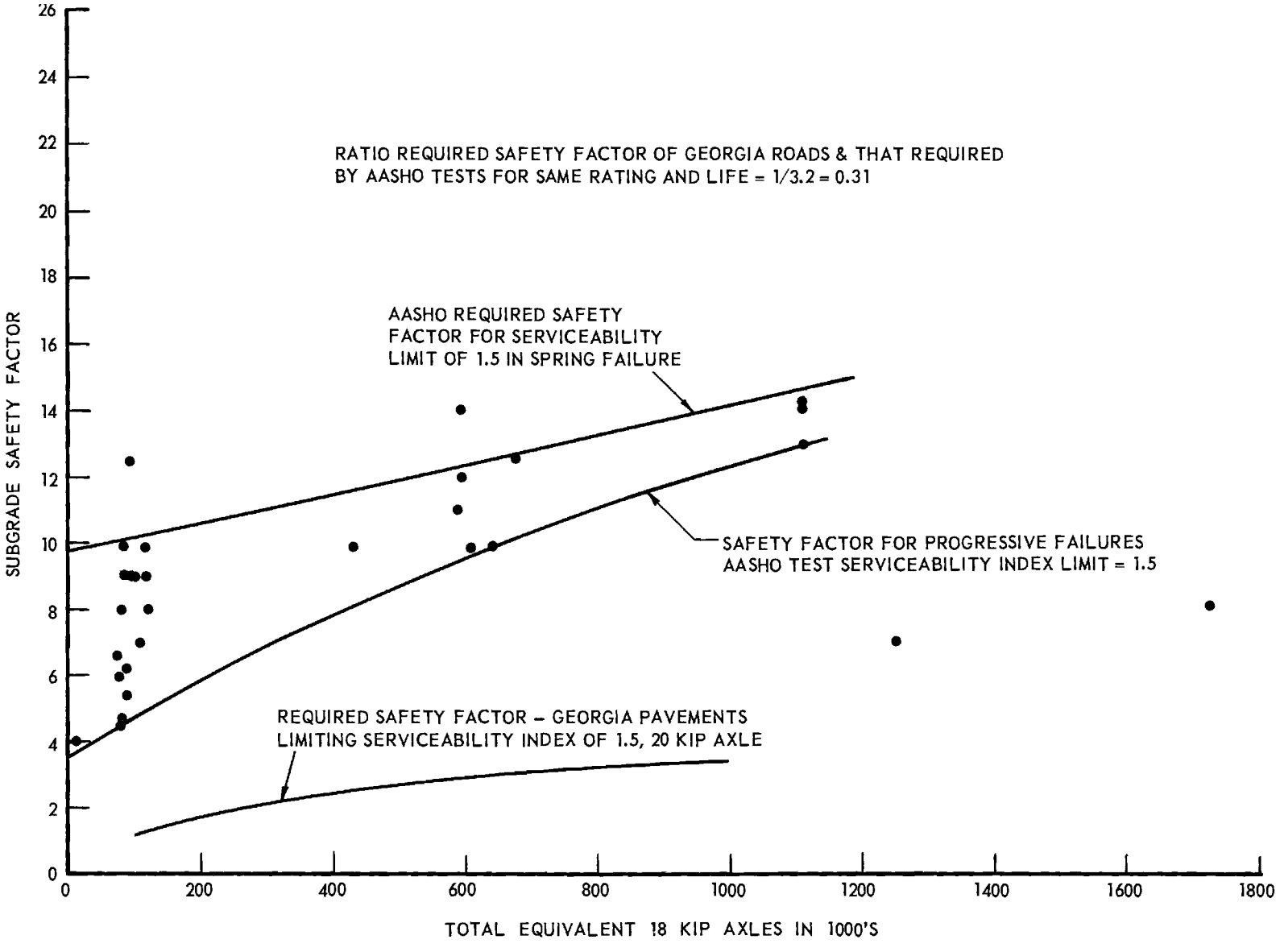

Figure 10. Required Safety Factor of AASHO Pavement to Provide a Serviceability Index of 1.5 After Different Numbers of 18 Kip Axle Loads.

The relationship exhibits considerable scatter, particularly of the lower numbers of axle loads. A study of the individual points shows that those exhibiting the higher safety factors failed suddenly in the spring of 1959 immediately after the thaw period. Two interpretations may be placed on this: (1) the failures were not the result of progressive failure or load or (2) the soil strength at this time was less than that indicated by the tests of samples made in the late spring of 1963. Those pavements which survived the spring break-up of 1959 exhibited a much better correlation between safety factor and traffic. Of these, however, those points above the lower line represent, for the most part, rather sudden failures corresponding to the spring break up. In the writer's opinion, the lower curve represents the more valid relationship between safety factor and traffic. If strength data were available for each test section for the period in which failure developed, the scatter would probably have been much less.

VII. PAVEMENT DESIGN

1. AASHO Pavement Design

A pavement design method has been derived from the AASHO Road Test results by the AASHO Operating Committee on design. A draft of this was published by W. J. Liddle of the U. S. Bureau of Public Roads. The basis for this development is outlined in this paper (1).

The major Road Test correlation is pavement serviceability deterioration (from the initial, constructed value) as a function of the pavement design, the axle load, and the number of axle loads. Thus for a given initial serviceability and a desired serviceability level at the end of the pavement life, and for a required axle load and total traffic, the required pavement design can be found. The correlation is entirely emperical, based on curve fitting, and does not necessarily reflect any consideration of the mechanisms that contribute to failure. The correlation is valid only for the Test Road subgrade and only if the subgrade properties are uniform and unchanging. An attempt was made to include the variation of the subgrade with the season by assigning a greater weight to the number of load applications occurring during seasons of more rapid deterioration than to those of less rapid deterioration. The method of determining the factor is incompletely described in Report 5. Apparently the process was purely emperical -- the weighting factors were adjusted until the serviceability -- total load application data fit the assumed mathematical model with the least variation. This procedure does not indicate the mechanism by which the deterioration is accelerated. In fact, it applies the correction to the traffic, rather than to the pavement design factors to which it should apply. Therefore, while it may improve the fit of the AASHO data to an assumed mathematical curve, there is no reason to believe that it might be valid elsewhere.

The pavement design in the main load-performance-traffic-design relationship is expressed in terms of the structural Number $\overline{\overline{SN}}$ or Equivalent Thickness, D, (both definitions and symbols are used for the same thing, the first in Liddle's paper and other design memoranda, and the second in Report 5). This is related to the actual pavement components by

$$D = \overline{\overline{SN}} = a_1D_1 + A_2D_2 + A_3D_3 \qquad (5)$$

where D_1, D_2, and D_3 are the thicknesses of the surface course, the base course and the sub base, respectively, in inches.

The coefficients a_1, a_2, and a_3 are assumed to be indexes of the relative load spreading or supporting qualities of each corresponding pavement course. The values found for the AASHO Test Road components varied with the traffic load and the component thicknesses. The values for the 18 kip axle load section were

Asphaltic concrete surface	$a_1 = 0.44$
Crushed stone base	$a_2 = 0.14$
Sand, gravel sub base	$a_3 = 0.11$

While the Report 5 (p. 36) states that these values indicate that an inch of surfacing ($a_1 = 0.44$) is about 3 times as effective as an inch of base ($a_2 = 0.14$) or four times as effective as an inch of sub base ($a_3 = 0.11$) this does not necessarily mean that these <u>materials</u> have support qualities or load spreading abilities in the same ratio. For example, one design of the AASHO Loop 4, where the 18 kip axle load was employed consisted of the following:

Course	Thickness	Stress in Course		Stress Reduction in Layer		
		Top	Bottom	Total	Per Inch	Comparative
Surface	4	90	44	46	11.5	1:1
Base	3	44	27	17	5.7	1:2
Sub base	4	27	17	10	2.5	1:4.6

If the vertical stresses are computed at the top and bottom of each layer using the Boussinesq equation, which applies to a semi-infinite, homogeneous elastic mass they will be seen to be less at the bottom of each successive course, as shown in the above table. The stress reduction in each layer and stress reduction per inch of layer are also shown. The comparison indicates that the first layer is 2 times more effective than the second and 4.6 times more effective than the third. Other combinations of thickness give different comparative values including the average comparative effectivenesses found by the Test Road Analyses. Therefore, it must be concluded that the relative values of a_1, a_2, and a_3 do not entirely reflect the load spreading or supporting qualities of the pavement materials but also their relative position with respect to the pavement surface.

The Road Test correlation does not include any terms reflecting the subgrade soil support, because it was assumed that this was constant and uniform. However, a possible "second" subgrade soil value might be inferred from the pavement section with such thick crushed stone bases that the base, in effect, was the subgrade. This inference was not checked by any rational procedure. Arbitrary "soil support values," S, were assigned to the subgrade and the thick stone base of 3 and 10, respectively. Of course, these values do not necessarily reflect relative support but instead are points of reference.

Nomographic design charts were constructed for the Road Test Correlation utilizing an axle load of 18 kips. These charts, for terminal serviceabilities

of 2 and 2.5 have tentatively been proposed for use in design. They are reproduced in Appendix C, from the "AASHO Interim Guide for the Design of Flexible Pavements" by the AASHO committee on design dated October 12, 1961. The same charts are included in Liddle's paper (1).

2. Design Constants, Georgia Pavements

The use of the AASHO design charts requires calibration of the soil support scale in terms of some quantitative index or measure of the appropriate property of the subgrade soil for which the pavement is designed.

While the AASHO test results do not directly point to the mechanism of pavement deterioration and failure, clues are given by the results of the trenching program. Trenches were cut into pavement sections that had deteriorated to the point of removal from test in 1959. An extensive trench program was undertaken in 1960 when 39 pavement sections were investigated. In each the transverse profile of the boundary between each of the pavement components was obtained accurately, and the densities of each layer in the wheel path and beyond the wheel path. These tests indicated that about 25 per cent of the thickness change of the pavement layers could be attributed to densification or consolidation of the layers. The remaining change, therefore, must be shear displacement. Such shear displacements can be clearly seen in the transverse profiles of the subgrade surface. Therefore, because it is shown that the major part of the subgrade's contribution to the deterioration of the pavement surface is shear failure, it appears reasonable to presume that the subgrade bearing capacity (its resistance to shear displacement) would be a valid index to the subgrade support of "Soil Support Value," S. On this basis the AASHO support value would represent an ultimate bearing capacity of 99 psi, based on tests of samples secured some time after the critical period of spring softening.

This value probably does not represent the bearing capacity during the periods of most rapid deterioration. This is confirmed by the plot of safety factor vs. traffic for the AASHO Test Road. The lowest curve, which represents the more valid traffic-related deterioration, shows a safety factor of 3.6 required under conditions of very little traffic. The corresponding Georgia data found a safety factor of about 1 for the same low traffic. Therefore, it is concluded that the actual bearing capacity of the AASHO Road was less than 99 psi during the critical periods of the Road Test.

A plot of the required Georgia subgrade safety factors for the same level of serviceability (1.5) based on Fig. 8, is shown in Fig. 10 for comparison. The Georgia values everywhere are $\frac{1}{3.2}$ or 31 per cent of the indicated AASHO values. On this basis the equivalent Georgia ultimate bearing capacity would be 0.31 x 99 or 31 psi. This value is recommended for use of pavement design in Georgia as the equivalent of the subgrade support value of 3.

Other values on the subgrade support value scale were computed from this key bearing capacity utilizing the AASHO pavement thickness relation for an 18 kip axle load and 100 equivalent axle loads per day. The required safety factors for Georgia pavements for different amounts of traffic and different serviceabilities at the end of the pavement life were found from Fig. 8 and plotted in Fig. 11. One hundred axles per day for 20 years is a total of 730,000 axle loads. For a serviceability limit of 2.0 the required Georgia Safety Factor is 4. The safe limit of stress for the correct design would be 1/4 x 31 or 7.75 psi. The total pavement thickness required to maintain the stress at this level, from Fig. 5, is 19.5 in. From the AASHO chart for a serviceability of 2, a soil "S" value of 3 and 100 axles per day require a pavement structural number, $\overline{SN}$, of 3.58. The weighted average "a" for the Georgia pavement, therefore, is $\frac{3.58}{19.5}$ or 0.184. Now if the Georgia subgrade has a bearing

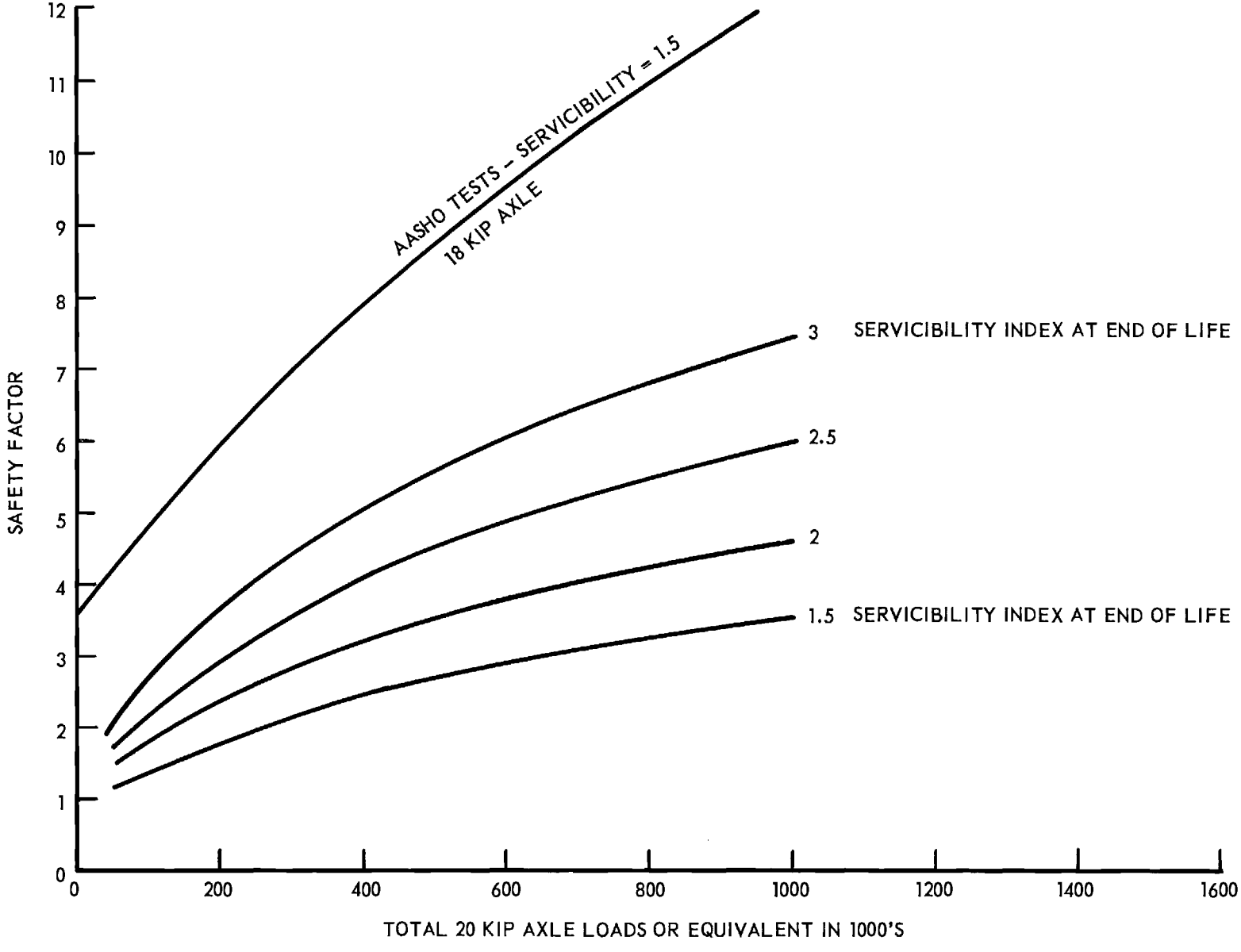

Figure 11. Required Safety Factors for Georgia Subgrades for Different Numbers of 20 Kip Axle Loads.

capacity of 50 psi the actual stress on the subgrade would be limited to $\frac{50}{4}$ = 12.5 psi. This corresponds in Fig. 5 to a total thickness of 13.7 in. Utilizing the same weighed average "a" the $\overline{SN}$ would be 13.7 x .184 = 2.52. From the AASHO chart the soil support number corresponding to $\overline{SN}$ = 1.52 and 100 axle loads daily would be 5.7. Therefore the "S" value corresponding to a bearing capacity of 50 psi would be 5.7. By this process the bearing capacities corresponding to various "S" values were found and are given below.

Table 3. Relation of "S" to Computed Bearing Capacity

Bearing Capacity	S	Bearing Capacity	S
15 psi	-0.7	60 psi	6.6
20	+0.9	70	7.4
30	2.9	80	8.2
40	4.5	90	8.9
50	5.7	100	9.5

These values apply to the 100 axle loads daily and the performance rating of 2.0 at the end of the pavement life. However their applicability to other conditions is as valid as the other assumptions made in developing the design method.

In utilizing these values for design, consideration must be given to the test method on which the Georgia evaluations were based. The samples were secured in actual subgrades during the winter and the time of greatest soil moisture and lowest strength. Until data are available on the variations in soil moisture with the season, it is safe only to assume that the limit of capillary saturation is the limiting moisture corresponding to the Georgia test data. It is recommended that the bearing capacity be determined from c and φ values determined as follows:

1. Compact two specimens of the subgrade to the lowest density and highest moisture permitted by the construction specifications.

2. Confine each in a triaxial chamber, one at a confinement of 10 psi and the other at 20 psi.

3. Subject each to a head of 1 ft. of water from the bottom and allow to saturate until no more water is absorbed. (The period of saturation to be found by experiment.)

4. Load axially until failure occurs, without further change in moisture. For design utilize a seasonal weighting factor of 1 throughout.

Determination of the "a" coefficients for use in the AASHO design method is more difficult because there is little on which to base a correlation. The AASHO values are 0.44 for the asphaltic concrete and 0.14 for the crushed stone base. The weighted "a" for a typical Georgia pavement of 3 in. surface and 8 in. soil bound macadam base would be $\frac{3}{11} \times .44 + \frac{8}{11} \times .14 = 0.22$. This compares reasonably well with the average figure, 0.183, deducted from the equivalent thicknesses utilizing the AASHO design chart as previously described.

Based on the subgrade stress studies of this investigation, the value of 0.44 for the surface appears large. Considering the stress spreading value of the layers alone we suggest 0.35 for the asphaltic surface and 0.14 for the base. The weighted average of these is .197 which is closer to that of the value computed from the bearing study and the values have a ratio of 2.5 to 1 which is close to that found on the basis of the Boussinesq distribution. (The previous research in this project found that the Boussinesq distribution was applicable to a flexible pavement system employing a granular base.

The value of the soil macadam cement base can be found indirectly from the stress-depth chart, Fig. 5. This shows that an 8 in. soil macadam cement base (5psi on subgrade) is equivalent to 22 in. of soil-bound macadam, etc. In other

words it would have an "a" of $\frac{22}{8}$ x .14 = 0.38. The 6 in. soil macadam cement (15 psi) is as effective as 9 in. of soil bound macadam or it has an "a" of $\frac{9}{6}$ x 0.14 = 0.21. At first glance the different "a" values for the same material might appear contradictory. However, stress theory indicates that the load spreading ability of a layer that is capable of supporting tension is not a linear function of the layer thickness. For an all-over design value, an "a" of 0.25 to 0.30 for soil macadam cement would appear reasonable. This is not greatly different from the value of 0.23 estimated for the AASHO pavements.

The sand-asphalt base 8 in. thick stressed the subgrade to 23 psi which is equivalent to a soil bound macadam base 5.5 in. thick. The equivalent "a" value for the sand asphalt, therefore, would be $\frac{5.5}{8}$ x 0.14 = 0.10. This is considerably less than the 0.25 estimated from the AASHO test results. (Of course, the AASHO tests did not include a sand asphalt base.) The great difference is probably the result of the higher Georgia temperatures and resulting lower rigidity as well as the rate of loading.

3. Alternate Georgia Design Method

An alternate design procedure can be evolved from the Georgia pavement evaluation data.

1. Determine the c and φ of the soil as outlined in the previous section.

2. Compute the ultimate bearing capacity as given in Appendix B. Use an assumed tentative pavement thickness, D.

3. Find the appropriate safety factor from Fig. 11.

4. Compute the safe bearing capacity by dividing the ultimate bearing capacity, Step 2, by the safety factor, Step 3.

5. Find the total pavement thickness from Fig. 5 utilizing the appropriate curve for the type of base course to be employed.

This procedure is no more complicated than that of the AASHO Interim Guide. It makes use of the AASHO serviceability concept and the traffic-serviceability decline principle. It is based on Georgia performance and on the stress spreading ability of the Georgia base courses. Finally, it is a more nearly rational approach to design than to AASHO.

4. Recommendations for Further Study

Based on the experience gained in this investigation a number of recommendations can be made.

1. Test sections of pavement should be constructed specifically for serviceability-performance studies.

a. These should be a part of the Georgia Highway system so as to reflect the use and traffic patterns of real highways.

b. These should be placed on typical subgrades in each geologic region.

c. These should be constructed with varying pavement thicknesses and typical Georgia bases.

d. These should be accompanied by a traffic count station where periodic Loadometer studies can be made to determine the distribution of the heavier axle loads.

e. The soil moisture variation should be measured periodically.

f. The bearing capacity should be determined by laboratory tests of samples secured so as to reflect the typical range of moistures.

g. Measure the pavement serviceability accurately from time to time.

2. Subgrade moisture studies should be undertaken to define the range in moisture content changes for the typical subgrades in each geologic region.

3. Triaxial tests should be made on typical Georgia subgrade materials.

a. Utilize the procedure outlined in this report for "saturating" the soils, or

b. When more realistic subgrade moisture data became available from Recommendations 1e and 2 make the tests at those moistures.

c. Compute the beating capacities and deflections of these materials.

d. Correlate the bearing capacities and deflections with the geology, soil classification, and region for use in preliminary design.

4. Develop more realistic theories for the bearing capacity and deflection of the subgrade and each of the pavement components.

5. Extend the present analysis to include the effects of deflection.

Table 1a. Georgia Pavement Evaluation Data

Test No.	County	Highway Number	Lane	Location	Topography	Drainage
1	Taylor	Ga. 22	E. bnd.	2.75 mi. west of junction of Ga. 3 and Ga. 22	Gently rolling wooded area	External ditch
2	Talbot	Ga. 22	E. bnd.	6.4 mi. west of Talbot-Taylor Co. line	Rolling	External ditch
3	Worth	Ga. 50	E. bnd.	0.15 mi. east of Worth-Dougherty Co. line	Flat and level	External ditch
4	Worth	Ga. 50	E. bnd.	0.30 mi. east of RR crossing on east side of Sylvester at end of 4 lane	Gently rolling	External ditch
5	Mitchell	S 947	E. bnd.	1.25 mi. east of Ga. 333, near Baconton	Flat	External ditch
6	Mitchell	S 947	E. bnd.	4.50 mi. east of Ga. 333, also 0.80 mi. west of Ga. 112	Gently rolling	External ditch severe eroded
7	Early	Ga. 39	So. bnd.	150 ft. west of intersection of US 27 and Ga. 39 in Blakely	Level	External ditch
8	Early	Ga. 39	So. bnd.	800 ft. west of intersection of US 27 and Ga. 39	Level	Ditch in poor condition
9	Early	Ga. 39	So. bnd.	0.75 mi. south of intersection of US 27 and Ga. 39	Level	External ditch
10	Early	Ga. 39	No. bnd.	0.50 mi. south of intersection of US 27 and Ga. 39	Level	External ditch
11	Decatur	Ga. 309	So. bnd.	4.50 mi. south of Bainbridge city limits, in front of white house	Gently rolling	External ditch
12	Decatur	Ga. 309	So. bnd.	10.3 mi. south of Bainbridge city limits, 150 ft. south of county road intersection	Slightly rolling	External side ditch
13	Decatur	Ga. 309	So. bnd.	13.8 mi. south of Bainbridge city limits, 300 ft. south of intersection of Ga. 309 and Ga. 241	Flat	External wide side ditches
14	Decatur	Ga. 309	No. bnd.	0.25 mi. north of Fla. state line	Slightly rolling	External side ditches

(Continued)

Table 1a (Continued). Georgia Pavement Evaluation Data

Test No.	County	Highway Number	Lane	Location	Topography	Drainage
15	Decatur	Ga. 309	No. bnd.	0.25 mi. north of Fla. state line	Slightly rolling	External side ditches
16	Decatur	Ga. 309	No. bnd.	0.30 mi. north of intersection of Ga. 241 and Ga. 309	Slightly rolling	External side ditch
17	Grady	Ga. 112	No. bnd.	0.85 mi. north of intersection of US 84 and Ga. 112; 12.25 mi. south of intersection of Ga. 262 and Ga. 112	Gently rolling	External side ditches
18	Grady	Ga. 112	No. bnd.	2.1 mi. north of intersection of US 84 and Ga. 112, at dirt road intersection on top of hill	Gently rolling	Side slope and side ditch
19	Grady	Ga. 112	No. bnd.	3.5 mi. north of intersection of US 84 and Ga. 112; 0.15 mi. south of concrete bridge	Flat	Side slopes
20	Grady	Ga. 112	No. bnd.	11.0 mi. north of intersection of US 84 and Ga. 112; 2.1 mi. south of intersection of Ga. 262 and Ga. 112	Rolling	Very shallow side ditches
21	Thomas	Ga. 133	So. bnd.	1.05 mi. south of intersection of Ga. 133 and Ga. 38, south of Boston	Flat	Side ditches
22	Thomas	Ga. 133	So. bnd.	8.35 mi. south of intersection of Ga. 133 and Ga. 38, south of Boston	Flat	Side culvert on both sides
23	Lowndes	S 951	E. bnd.	2.8 mi. east of intersection of S 951 and Ga. 33; 9.55 mi. west of intersection of S 951 and Ga. 31	Flat	Side ditches
24	Lowndes	S 951	W. bnd.	3.7 mi. east of intersection of S 951 and Ga. 33; 6.65 mi. west of intersection of S 951 and Ga. 31	Rolling	Side ditches

(Continued)

Table 1a (Continued). Georgia Pavement Evaluation Data

Test No.	County	Highway Number	Lane	Location	Topography	Drainage
25	Echols	Ga. 94	E. bnd.	6.6 mi. east of intersection of US 129 and Ga. 94 in Statenville	Flat	Side ditches
26	Echols	Ga. 94	E. bnd.	6.75 mi. east of intersection of US 129 and Ga. 94 in Statenville; opposite Ga. Power Co. transformer station	Flat	Side ditches
27	Echols	Ga. 94	E. bnd.	7.7 mi. east of intersection of Ga. 94 and US 129 in Statenville	Flat	Side ditches
28	Echols	Ga. 94	E. bnd.	10.2 mi. east of intersection of Ga. 94 and US 129	Flat	Side ditches
29	Clinch	Ga. 38 (US 84)	E. bnd.	1.7 mi. east of intersection of US 84 and Ga. 89	Flat	Side ditches
30	Clinch	Ga. 38	E. bnd.	2.1 mi. east of intersection of US 84 and Ga. 89	Flat	Side ditches
31	Clinch	Ga. 38	E. bnd.	6.6 mi. east of intersection of US 84 and Ga. 89, on east side of Argyle	Flat	Side slopes
32	Bibb	Ga. 247	So. bnd.	1.60 mi. south of US 41 turn-off, 150 ft. north of Borden's Milk bill board	Slightly rolling	Ditch
33	Bibb	Ga. 247	So. bnd.	1.75 mi. south of US 41 turn-off, 30 ft. north of entrance to Southeastern Metal and Parts Co.	Gently rolling	External ditch
34	Bibb	Ga. 247	So. bnd.	2.40 mi. south of US 41 turn-off, 300 ft. north of beginning of curve	Gently rolling	External ditch
35	Bibb	Ga. 247	So. bnd.	2.75 mi. south of US 41 turn-off, 300 ft. north of railroad overpass	Gently rolling	External ditch
36	Bibb	Ga. 247	So. bnd.	3.10 mi. south of US 41 turn-off, 150 ft. south of Phillips 66 gas station	Gently rolling	Ditch -- poorly maintained

(Continued)

Table 1a (Continued). Georgia Pavement Evaluation Data

Test No.	County	Highway Number	Lane	Location	Topography	Drainage
37	Bibb	Ga. 247	So. bnd.	3.10 mi. south of US 41 turn-off, 300 ft. south of Phillips 66 gas station	Gently rolling	Ditch -- poorly maintained
38	Bibb	Ga. 247	So. bnd.	3.15 mi. south of US 41 turn-off at intersection of dirt road	Gently rolling	External ditch
39	Bibb	Ga. 247	So. bnd.	4.70 mi. south of US 41 turn-off, opposite Macon Airport runways	Flat	External ditch
40	Wayne	Ga. 27 (US 341)	W. bnd.	4.4 mi. west of Jesup (west) city limits; 1.25 mi. east of Appling-Wayne Co. line	Flat	External side ditches
41	Appling	Ga. 27	W. bnd.	15.95 mi. west of Jesup city limits; 7.05 mi. west of traffic light in Odum, Ga.; 100 ft. east of bridge	Flat	Side slopes
42	Appling	Ga. 27	W. bnd.	Same as No. 41	Flat	Side slopes
43	Appling	Ga. 27	W. bnd.	16.25 mi. west of Jesup city limits; 0.25 mi. west of bridge	Flat	Side ditches
44	Appling	Ga. 27	W. bnd.	16.30 mi. west of Jesup city limits	Flat	Side ditches
45	Appling	Ga. 27	W. bnd.	Same as No. 44	Flat	Side ditches
46	Appling	Ga. 27	W. bnd.	17.10 mi. west of Jesup; 1.40 mi. west of Appling-Wayne Co. line	Flat swampy	External ditch
47	Appling	Ga. 27	W. bnd.	19.6 mi. west of Jesup city limits; 0.7 mi. east of Surrency city limits	Flat	Side ditches
48	Ware	Ga. 4 (US 1,23)	So. bnd.	2.70 miles south of intersection of Ga. 177 and Ga. 4; 9.00 miles north of Ware-Charlton Co. line	Flat swampy	External ditch
49	Ware	Ga. 4	So. bnd.	Same as No. 48	Flat swampy	External ditch

(Continued)

Table 1a (Continued). Georgia Pavement Evaluation Data

Test No.	County	Highway Number	Lane	Location	Topography	Drainage
50	Bacon	Ga. 4	No. bnd.	2.40 mi. north of Ware-Bacon Co. line	Gently rolling	External ditch
51	Putnum	Ga. 24	So. bnd.	6.80 mi. south of intersection of Ga. 24 and US 129; 3.25 miles north of Putnum-Hancock Co. line	Rolling	External ditch
52	Putnum	Ga. 24	So. bnd.	6.85 mi. south of intersection of Ga. 24 and US 129; 3.20 mi. north of Putnum-Hancock Co. line	Rolling	Side ditches
53	Hancock	Ga. 16	W. bnd.	7.2 mi. west of Sparta Court house; 6.5 mi. west of intersection of Ga. 15 and Ga. 16	Gently rolling	Side ditches
54	Hancock	Ga. 16	W. bnd.	Same as No. 53	Rolling	Side ditches
55	Hancock	Ga. 16	W. bnd.	Same as No. 53	Rolling	Side ditches
56	Morgon	Ga. 12 (US 278)	W. bnd.	0.4 mi. west of intersection of Ga. 83 and Ga. 12, west of Madison	Rolling	Side slopes
57	Morgon	Ga. 12	W. bnd.	1.3 mi. west of intersection of Ga. 12 and Ga. 83, west of Madison	Rolling	External ditch
58	Morgon	Ga. 12	W. bnd.	1.8 mi. west of intersection of Ga. 83 and Ga. 12, west of Madison	Rolling	Side ditch on north, culvert on south
59	Morgon	Ga. 12	W. bnd.	Same as No. 58	Rolling	Side ditch on north, culvert on south
60	Morgon	Ga. 12	W. bnd.	1.85 mi. west of intersection of Ga. 83 and Ga. 12, west of Madison	Rolling	Side ditches

(Continued)

Table 1a (Continued). Georgia Pavement Evaluation Data

Test No.	County	Highway Number	Lane	Location	Topography	Drainage
61	Morgon	Ga. 12	W. bnd.	3.30 mi. west of intersection of Ga. 12 and and Ga. 83, west of Madison	Rolling	External ditch
62	Morgon	Ga. 12	W. bnd.	6.05 mi. west of intersection of Ga. 12 and Ga. 83		External ditch
63	Union	Ga. 11	No. bnd.	1.25 mi. north of intersection of Ga. 2 and Ga. 11; 0.85 mi. north of Blairesville city limits	Hilly	Side ditches
64	Union	Ga. 11	No. bnd.	1.7 mi. north of intersection of Ga. 2 and Ga. 11	Hilly	Side slopes
65	Union	Ga. 11	No. bnd.	1.75 mi. north of intersection of Ga. 2 and Ga. 11	Hilly	Side slopes
66	Union	Ga. 11	No. bnd.	2.45 mi. north of intersection of Ga. 2 and Ga. 11	Hilly	Side ditch on east, side slope on west
67	Union	Ga. 11	No. bnd.	2.50 mi. north of intersection of Ga. 2 and Ga. 11	Hilly	Side slopes
68	Union	Ga. 11	No. bnd.	2.75 mi. north of intersection of Ga. 2 and Ga. 11; 2.35 mi. north of Blairesville city limits	Hilly	Side ditches
69	Lumpkin	Ga. 60	No. bnd.	4.50 miles north of Lumpkin-Hall Co. line; 2.70 miles south of Dahlonega city limits	Rolling	External ditch
70	Lumpkin	Ga. 60	No. bnd.	Same as No. 69	Rolling	External ditch
71	Lumpkin	Ga. 60	So. bnd.	0.15 miles south of Dahlonega city limits	Mountainous	External ditch
72	Lumpkin	Ga. 60	So. bnd.	Same as No. 71	Hilly	Side slope
73	Lumpkin	Ga. 60	So. bnd.	4.45 mi. south of Dahlonega city limits	Hilly on east side flood plain on west	External ditch

(Continued)

Table 1a (Continued). Georgia Pavement Evaluation Data

Test No.	County	Highway Number	Lane	Location	Topography	Drainage
74	Cherokee	Ga. 140	E. bnd.	10.9 mi. east of intersection of US 411 and Ga. 140; 0.5 mi. west of intersection of Ga. 156 and Ga. 140; next to "Welcome to Waleska" sign	Mountainous	Side ditch
75	Cherokee	Ga. 140	E. bnd.	Same as No. 74	Mountainous	Side ditch
76	Cherokee	Ga. 140	E. bnd.	7.5 mi. east of intersection of US 411 and Ga. 140; approximately 1/4 mi. east of Standard Oil station	Mountainous	Side ditch
77	Cherokee	Ga. 140	E. bnd.	Same as No. 76	Mountainous	Side ditch
78	Cherokee	Ga. 140	W. bnd.	0.35 mi. east of intersection of US 411 and Ga. 140	Hilly	Side ditch
79	Bartow	US 41	So. bnd.	1.0 mi. south of the Bartow-Gordon Co. line	Rolling	Side ditch
80	Bartow	US 41	So. bnd.	1.9 mi. south of Bartow-Gordon Co. line; 200 ft. north of north city limit of Adairsville, Ga.	Flat	Side ditch on east side
81, 82	Bartow	US 41	So. bnd.	1.7 mi. south of Bartow-Gordon Co. line; 500 ft. north of Shell station	Flat	Side ditch
83	Bartow	US 41	So. bnd.	5.8 mi. south of Bartow-Gordon Co. line	Mountainous	Side ditch and slope
84	Bartow	US 41	So. bnd.	5.85 mi. south of Bartow-Gordon Co. line	Mountainous	Side slopes

Table 1b. Georgia Pavement Evaluation Data

Test No.	Condition of Pavement: Rut Depth Avg.	Rut Depth Max.	Cracking	Pavement Service Rating	History: Const.	Repaired	Examined	Days in Service
1			One longitudinal crack -- curved on ends -- 15' long Landslide not a subgrade failure	3.5	Dec. 1959		9-11-61	671
2	1/16"	1/8"	None	4	Dec. 1959		9-11-61	671
3	5/8"	7/8"	Longitudinal cracking -- concealed by surface treatment	1	Sept. 1949		9-12-61	4060
4	3/8"	3/8"	None	3.5	Sept. 1949		9-12-61	4060
5	1/8"	1/4"	None	4.5	Sept. 1960	July 1962	9-12-61	370
6	1/8"	1/4"	Pot holes -- broken pavement. Surface failure, not subgrade	2	Sept. 1960	July 1962	9-12-61	370
7	1/4"	3/8"	Longitudinal cracking -- transverse cracks spaced 6' apart	2.5	Aug. 1953	Sept. 1961	9-12-61	2990
8	1/16"	1/8"	Longitudinal with transverse cracks	3.5	Aug. 1953	Sept. 1961	9-12-61	2990
9			Irregular, Angular	3	Aug. 1953	Sept. 1961	9-12-61	2990
10			Closely spaced -- small alligator cracking	3	Aug. 1953	Sept. 1961	9-12-61	2990
11	7/8"	13/8"	Closely skewed cracks	1	Sept. 1955		9-12-61	2592
12			Numerous holes in surface -- 2" - 5" in diameter	2	Sept. 1955		9-13-61	2592

(Continued)

Table 1b (Continued). Georgia Pavement Evaluation Data

Test No.	Condition of Pavement			Pavement Service Rating	History			
	Rut Depth		Cracking		Const.	Repaired	Examined	Days in Service
	Avg.	Max.						
13	3/8"	3/8"	Large, long, longitudinal crack, widely spaced, slight transverse cracks	2	Sept. 1955		9-13-61	2592
14	1/8"	1/8"	Transverse with irregular longitudinal	3.5	Sept. 1955		9-13-61	2592
15			None	4	Sept. 1955		9-13-61	2592
16			None	4	Sept. 1955		9-13-61	2592
17	3/16"	1/4"	Longitudinal, 4-6" apart, parallel, 2' from shoulder	3.5	Aug. 1950	1963	9-13-61	4090
18	3/16"	1/4"	Blocks -- 4' long 3' transverse	3	Aug. 1950	1963	9-13-61	4090
19			None	4.2	Aug. 1950	1963	9-13-61	4090
20	1"	11/8"	Closely spaced transverse and longitudinal	0.5	Aug. 1950	1963	9-13-61	4090
21			No cracks, severe wash-board, 2' - 4' apart	2	Nov. 1955		9-13-61	2170
22			None	4.5	June 1958		9-13-61	1220
23	3/16"	1/4"	None	3			9-14-61	
24	1"	13/8"	Longitudinal, 4' from edge, deep rutting	0.5			9-14-61	
25	13/16"	5/4"	Block, longitudinal cracks 1' apart, transverse -- 3' apart	0.5	Aug. 1951		9-14-61	3720

(Continued)

Table 1b (Continued). Georgia Pavement Evaluation Data

Test No.	Condition of Pavement: Rut Depth Avg.	Rut Depth Max.	Cracking	Pavement Service Rating	History: Const.	Repaired	Examined	Days in Service
26	17/16"	1/8"	Block, longitudinal cracks 1' - 2' apart transverse 2' - 3' apart	0.5	Aug. 1951		9-14-61	3720
27	11/16"	1"	Longitudinal, straight, 1' apart	0.5	Aug. 1951		9-14-61	3720
28	13/16"	1"	None, deep rutting	1.5	Aug. 1951		9-14-61	3720
29	5/16"	3/8"	Mostly longitudinal with irregular small transverse	1	Feb. 1950		9-14-61	4270
30	5/16"	3/8"	Wide 1/4" longitudinal cracks in ruts, transverse cracks every 2'	1	Feb. 1950		9-14-61	4270
31	3/4"	1"	Closely spaced hairline longitudinal cracks, larger transverse cracks also	1	Feb. 1950		9-14-61	4270
32	1/16"	1/16"	None	4	Aug. 1955		9-15-61	2260
33	5/16"	3/8"	Waves spaced 8' apart, 1/8" max. depth between	3	Aug. 1955		9-15-61	2260
34	1/8"	1/4"	Longitudinal with occasional transverse	3	Aug. 1955		9-15-61	2260
35	3/16"	1/4"	45° cracks -- 6" apart connected by longitudinal cracks	2.5	Aug. 1955		9-15-61	2260
36	5/16"	3/8"	Hairline cracks from 1 to 3" apart in OWP	2.5	Aug. 1955		9-15-61	2260

(Continued)

Table 1b (Continued). Georgia Pavement Evaluation Data

Test No.	Condition of Pavement			Pavement Service Rating	History			
	Rut Depth		Cracking		Const.	Repaired	Examined	Days in Service
	Avg.	Max.						
37	3/16"	1/4"	Slight longitudinal crack with short transverse cracks	3.5	Aug. 1955		9-15-61	2260
38	3/16"	1/4"	Longitudinal crack in OWP changing to transverse crack connected by circular arc	3.5	Aug. 1955		9-15-61	2260
39			8' x 12' blocks	3.5	Aug. 1955		9-15-61	2260
40	1/4"	1/4"	One longitudinal crack in OWP 1/4" wide for 4'	3	Sept. 1957		9-18-61	1490
41	3/16"	1/4"	Longitudinal starting at edge of pavement and running toward bridge	3.5	Sept. 1957		9-18-61	1490
42	3/16"	1/4"	Longitudinal crack down ℄ ≈ 10 yards long	3	Sept. 1957		9-18-61	1490
43	3/8"	3/8"	Short longitudinal parallel cracks 2' apart also hair-line cracks 1" apart	2.5	Sept. 1957		9-18-61	1490
44	1/4"	1/4"	Longitudinal -- parallel 6" apart	2.5	Sept. 1957		9-18-61	1490
45	1/4"	1/4"	Short transverse, 2" - 3" apart, 6" long across ℄	2.5	Sept. 1957		9-18-61	1490
46	1/4"	1/4"	None	3	Sept. 1957		9-18-61	1490
47	1/4"	1/4"	Transverse cracks extend 3' into pavement from edge, to edge spaced evenly at 10'	2.5	Sept. 1957		9-18-61	1490
48	13/16"	7/8"	None	0.5	Sept. 1955		9-19-61	2230

(Continued)

Table 1b (Continued). Georgia Pavement Evaluation Data

Test No.	Condition of Pavement: Rut Depth Avg.	Rut Depth Max.	Cracking	Pavement Service Rating	History: Const.	Repaired	Examined	Days in Service
49	13/16"	7/8"	4" transverse cracks on ℄ of roadway 6" to 8" apart	0.5	Sept. 1955		9-19-61	2230
50	3/16"	3/16"	None	3	April 1957		9-19-61	1650
51	1/8"	1/8"	Longitudinal with transverse cracks	3.5	Sept. 1952		9-19-61	3320
52	3/16"	1/4"	Transverse every 10' perpendicular to edge	3.5	May 1956		9-19-61	2010
53	7/16"	1/2"	Longitudinal crack ≈ 1.5' from edge and parallel to edge	2	May 1956		9-20-61	2010
54	0	0	None	4	May 1956		9-20-61	2010
55	1/16"	1/8"	Surface layer ≈ 1" thick separated from layer beneath and has been pushed forward, causing separation in top layer	3*	July 1949		9-20-61	4480
56	3/16"	1/4"	Transverse -- 5' apart -- longitudinal 4' apart	2	July 1949		9-20-61	4480
57	1/8"	1/4"	Alligator cracking in OWP with transverse crack extending from center of westbound lane to shoulder	2	July 1949		9-20-61	4480

*Neglecting asphaltic surface condition

(Continued)

Table 1b (Continued). Georgia Pavement Evaluation Data

Test No.	Condition of Pavement: Rut Depth Avg.	Rut Depth Max.	Cracking	Pavement Service Rating	History: Const.	Repaired	Examined	Days in Service
58	1/4"	3/8"	Longitudinal in bottom of both wheel paths, and longitudinal along ℄	1	July 1949		9-20-61	4480
59	3/8"	1/2"	Parallel longitudinal 4" - 6" apart. Transverse 2' apart	1.5	July 1949		9-20-61	4480
60	3/8"	5/8"	Longitudinal crack 4' long with 180° turns on ends	2	July 1949		9-20-61	4480
61	1/4"	1/2"	Alligator cracking in OWP	1.5	July 1949		9-20-61	4480
62	1/4"	1/4"	Longitudinal crack down ℄ pavement	3	July 1949		9-20-61	4480
63	5/16"	3/8"	Parallel longitudinal 3" apart. Pattern extends ~ 1.5' from pavement edge over to edge	2.5	Aug. 1952		9-21-62	3360
64	3/16"	3/8"	Small blocks 2" x 2" extend 6 1/2' from edge	2	Nov. 1942		9-21-61	7900
65	1/8"	1/4"	Alligator -- small blocks -- 4" x 4"	1.5	Nov. 1942		9-21-61	7900
66	1/4"	1/2"	Diagonal starting on west side of road and running north-east to east side of road, 20 yards long	1.5	Nov. 1942		9-21-61	7900
67	1/4"	1/4"	None	3.5	Nov. 1942		9-21-61	7900

(Continued)

Table 1b (Continued). Georgia Pavement Evaluation Data

Test No.	Condition of Pavement: Rut Depth Avg.	Rut Depth Max.	Cracking	Pavement Service Rating	History: Const.	Repaired	Examined	Days in Service
68	3/16"	3/8"	Parallel longitudinal 6" apart with block 6" x 4"	1.5	Nov. 1942		9-21-61	7900
69	3/8"	1/2"	Parallel longitudinal cracks 2" to 6" apart located 4' from ℄ of roadway	1.5	Nov. 1949		9-22-61	4360
70	9/8"	2 1/4"	Parallel longitudinal with deep depression in OWP with fat spot	0.5	Nov. 1949		9-22-61	4360
71	1/8"	1/4"	Diagonal and longitudinal cracking in area	3.5	Nov. 1949		9-22-61	4360
72	3/16"	1/4"	Longitudinal making 90° turn toward west side of pavement	3.5	Nov. 1949		9-22-61	4360
73	1/4"	1/2"	None	3.5	June 1950		9-22-61	4150
74	7/8"	1 3/4"	3" x 5" blocky cracking with depression	0.5	Nov. 1952	June 1962	12-29-61	3360
75	1/8"	1/4"	3" x 5" blocky cracking	3	Nov. 1952	June 1962	12-29-61	3360
76	1 1/4"	1 5/8"	Irregular cracking in depression in center of road	0.5	Nov. 1952	June 1962	12-29-61	3360
77	1 1/4"	1 5/8"	Single longitudinal crack in depression 1' from edge of pavement	0.5	Nov. 1952	June 1962	12-29-61	3360
78	0	0	None	4.2	Nov. 1952	June 1962	1-26-62	3360
79	1/2"	7/8"	Longitudinal with transverse, long crack in center of 2' wide depression	2.5	June 1953		12-29-61	3140

(Continued)

Table 1b (Continued). Georgia Pavement Evaluation Data

Test No.	Condition of Pavement			Pavement Service Rating	History			
	Rut Depth		Cracking		Const.	Repaired	Examined	Days in Service
	Avg.	Max.						
80	7/16"	5/8"	Blocky with 1/4" openings	2.0	June 1953		12-29-61	3140
81	29/16"	2 1/8"	Alligator cracking in deep ruts in wheel paths	0.3	June 1953		12-29-61	3140
82	29/16"	2 1/8"	Alligator cracking in deep ruts in wheel paths	0.3	June 1953		12-29-61	3140
83	1/4"	3/8"	Longitudinal crack near ℄ highway	2.5	June 1953		12-29-61	3140
84	1/4"	1/4"	Transverse crack across entire roadway	3	June 1953		12-29-61	3140

Table 1c. Georgia Pavement Evaluation Data

Test No.	Design				Traffic			
	Subgrade	Sub base	Base	Surface	Traffic Count in Traffic Lane cars/day	trks/day	Equiv. Daily 20 Kip Loads	Est. Total 20 Kip Loads (1000's)
1	Yellow clayey sand 8"		Clayey sand & gravel 7"	Asphalt 5 1/2"	300	40	13	8
2				Asphalt Paving	300	40	13	8
3	Brown & yellow clayey sand 16"		Bituminous stabilized black silty clay, sand & gravel 8"	Asphalt 2 1/8"	2220	336	105	426
4	Brown clayey sand 7"		Brown clayey sand & pebbles 8 1/2"	Asphalt 3 3/4"	2220	336	105	426
5	Brown silty clayey sand 7"		Yellow sandy clay 5"	Asphalt Surface Treatment 1/2"-3/4"	85	35	11	4
6	Silty clay, sandy clay		Sandy clay 6"	Asphalt Surface Treatment 1/2" - 3/4"	35	35	11	4
7	Red silty clay		Clayey sand 9"	Asphalt Paving 1"	32	16	5	15
8	Orange plastic clay		Clayey sand 8 1/2"	Asphalt Paving 1"	32	16	5	15
9				Asphalt	32	16	5.0	15
10				Asphalt	175	32	10.0	30
11	White and red mottled clay		Red clayey sand 2"	Asphalt Paving 1 3/4" Patch 1"	364	28	8.7	23

(Continued)

Table 1c (Continued). Georgia Pavement Evaluation Data

Test No.	Design				Traffic			
	Subgrade	Sub base	Base	Surface	Traffic Count in Traffic Lane cars/day	trks/day	Equiv. Daily 20 Kip Loads	Est. Total 20 Kip Loads (1000's)
12	Yellow clayey sand		Red clayey sand 5 1/2"	Asphalt Pavement 1 3/4"	364	28	8.7	23
13	Brown silty sand		Red clayey sand 3 3/4"	Asphalt Paving 2"	364	28	8.7	23
14	Orange silty clay		Red clayey sand 3"	Asphalt Paving 2"	170	178	55.6	139
15	Yellow silty sandy clay		Red clayey sand 5"	Asphalt 2 1/2"	170	178	55.6	139
16	Yellow clayey silt		Red clayey sand 7 1/4"	Asphalt Paving 2 1/2"	170	178	55.6	139
17	Red sandy clay		Yellow sand & pebbles 6"	Asphalt Surface Treatment 1/2" - 3/4"	260	74	23.1	95
18			Yellow clayey sand & pebbles 5"	Asphalt Surface Treatment 1/2" - 3/4"	260	74	23.1	95
19	Clayey silt & sandy clay		Yellow clayey sand & pebbles 8 1/2"	Asphalt Surface Treatment 1/2" - 3/4"	260	74	23.1	95
20				Asphalt	260	74	23.1	95
21	6" red clay & clayey silt		Stabilized sand & gravel - 4" Yellow sandy clay - 4"	Asphalt Surface Treatment 1/2" - 3/4"	150	30	8	17
22	Clayey sand		Lime rock, stabilized sand 4" clay & pebbles 4"	Asphalt Surface Treatment 1/2" - 3/4"	75	15	4.1	5

(Continued)

Table 1c (Continued). Georgia Pavement Evaluation Data

Test No.	Design				Traffic			
	Subgrade	Sub base	Base	Surface	Traffic Count in Traffic Lane cars/day	trks/day	Equiv. Daily 20 Kip Loads	Est. Total 20 Kip Loads (1000's)
23	Clayey sand		Brown clayey sand 8"	Asphalt Surface Treatment 1/2" - 3/4"	175	50	15	30
24	Black sand		Brown sandy clay 6"	Asphalt Surface Treatment 1/2" - 3/4"	175	50	15	100
25	Organic sand		Asphalt stabilized sand 5"	Asphalt Surface Treatment 1/2" - 3/4"	230	77	24.0	90
26	Organic fine sand		Asphalt stabilized sand 5 1/2"	Asphalt Surface Treatment 1/2" - 3/4"	230	77	24.0	90
27	Organic fine sand		Asphalt stabilized sand 6"	Asphalt Surface Treatment 1/2" - 3/4"	230	77	24.0	90
28	Black silt fine sand		Asphalt stabilized sand 6"	Asphalt Surface Treatment 1/2" - 3/4"	230	77	24.0	90
29			Slag stabilized sand & pebbles 14"	Asphalt Pavement 4 1/2"	530	93	29.0	124
30			Slag stabilized sand & pebbles 8"	Asphalt Pavement 4 3/8"	530	93	29.0	124
31			Slag stabilized sand & pebbles 5"	Asphalt Pavement 4 1/2"	530	93	29.0	124
32	Silty clay	Brown sand & Quartzy pebbles 4"	Well graded sand Agg. 4"	Asphalt Pavement 3 1/4"	2050	390	121.7	275

(Continued)

Table 1c (Continued). Georgia Pavement Evaluation Data

Test No.	Design				Traffic			
	Subgrade	Sub base	Base	Surface	Traffic Count in Traffic Lane cars/day	trks/day	Equiv. Daily 20 Kip Loads	Est. Total 20 Kip Loads (1000's)
33	Clayey sand	Brown sand quartzy pebbles 5 1/4"	Well graded sand Agg. 5"	Asphalt Pavement 3"	2050	390	121.7	275
34	Red clay, clayey sand		Red clayey sand & quartz pebbles 6"	Asphalt Pavement 3 1/2"	2050	390	121.7	275
35	Multicolored sand & clay 10 1/2"		Red clayey sand & quartz pebbles 8"	Asphalt Pavement 3"	2050	390	121.7	275
36	Multicolored sand & clay 16"		Red clayey sand & quartz pebbles 9"	Asphalt Pavement 4 1/4"	2050	390	121.7	275
37	Multicolored sand & clay 14"		Red clayey sand & quartz pebbles 6 1/2"	Asphalt Pavement 3" Asphalt Surface Treatment 1/2"-3/4"	2050	390	121.7	275
38	Brown clayey sand 4 1/4"		Red clayey sand & pebbles 11 1/4"	Asphalt Pavement 4 3/4" Asphalt Surface Treatment 1/2"-3/4"	2050	390	121.7	275
39	Black silty clayey sand 9 1/2"		Red clayey sand & quartz pebbles 7"	Asphalt Pavement 3" Asphalt Surface Treatment 1/2"-3/4"	2050	390	121.7	275
40	Red white & yellow clayey sand 5"		Lime rock crushed 5 1/2"	Asphalt Pavement 5 1/2" Asphalt Surface Treatment 1/2"-3/4"	600	125	40	60

(Continued)

Table 1c (Continued). Georgia Pavement Evaluation Data

Test No.	Design				Traffic			
	Subgrade	Sub base	Base	Surface	Traffic Count in Traffic Lane cars/day	trks/day	Equiv. Daily 20 Kip Loads	Est. Total 20 Kip Loads (1000's)
41	Red white & yellow clayey sand 16"		Cement stabilized Brown sand & pebbles 10 3/4"	Asphalt Pavement 2 3/4"	600	125	50	75
42	Red white & yellow clayey sand 5 3/4"		Cement stabilized Brown sand & pebbles 10 1/4"	Asphalt Pavement 4"	600	125	50	75
43	Black organic soil		Crushed lime rock 5"	Asphalt Pavement 10"	600	125	50	75
44	Clayey sand		Crushed lime rock 4 3/4"	Asphalt Pavement 10" Asphalt Surface Treatment 1/2" - 3/4"	600	125	50	75
45	Clayey sand		Crushed lime rock 5 3/8"	Asphalt Pavement 9 5/8"	600	125	50	75
46	Clayey sand		Crushed lime rock 5 3/4"	Asphalt Pavement 4 1/4"	600	125	50	75
47	Loose, wet sand		Cement stabilized Brown sand & pebbles 9"	Asphalt Pavement 2 3/4"	600	125	50	75
48	Loose organic silty sand		Asphalt stabilized sand 6"	Asphalt Pavement 3 1/2"	1800	690	220	490
49	Loose organic black sand		Asphalt stabilized sand 7"	Asphalt Pavement 3 1/2"	1800	690	220	490
50	Sandy clay & Clayey sand	Brown silty sand, 4" clayey sand	Crushed lime rock 6 1/2"	Asphalt Pavement 3 1/2" Surface Treatment 1/2" - 3/4"	1200	280	88	145

(Continued)

Table 1c (Continued). Georgia Pavement Evaluation Data

Test No.	Design				Traffic			
	Subgrade	Sub base	Base	Surface	Traffic Count in Traffic Lane cars/day	trks/day	Equiv. Daily 20 Kip Loads	Est. Total 20 Kip Loads (1000's)
51	Brown silty sand 8"		Graded Sand Agg. 6 1/2"	Asphalt Pavement 2 1/2"	1170	117	36.5	121
52	Brown silty sand 6 1/4"		Graded Sand Agg. 7 5/8"	Asphalt Pavement 2 1/8"	1170	117	36.5	73.1
53	Mica clay, silt		Brown clayey sand 7"	Asphalt Pavement 3"	300	60	19	40
54	Silty, highly micaceous clayey saprolite 17"		Brown clayey sand 7"	Asphalt Pavement 2 1/4"	300	60	19	40
55			Brown clayey sand 6 3/4"	Asphalt Pavement 3 1/4"	300	60	19	85
56					692	154	48.1	215.5
57					692	154	48.1	216
58					692	154	48.1	216
59					692	154	48.1	216
60					692	154	48.1	216
61					692	154	48.1	216
62					692	154	48.1	216
63	Micaceous silty clay		Brown sandy micaceous silt & quartz creek pebbles 7 3/4"	Asphalt Surface Treatment 1/2"-3/4"	400	89	27.8	93
64					400	89	27.8	220

(Continued)

Table 1c (Continued). Georgia Pavement Evaluation Data

Test No.	Design				Traffic			
	Subgrade	Sub base	Base	Surface	Traffic Count in Traffic Lane cars/day	trks/day	Equiv. Daily 20 Kip Loads	Est. Total 20 Kip Loads (1000's)
65	Micaceous silt		Brown silty sand & gravel 7"	Asphalt Surface Treatment 1/2" - 3/4"	400	89	27.8	120
66	Micaceous silt		Brown sandy micaceous silt & gravel 4 1/2"	Asphalt Surface Treatment 1/2" - 3/4"	400	89	27.8	120
67	Micaceous silt		Red silty sand & gravel 6"	Asphalt Surface Treatment 1/2" - 3/4"	400	89	27.8	120
68	Micaceous silt		Brown silty sand & gravel 6"	Asphalt Surface Treatment 1/2"-3/4"	400	89	27.8	120
69	Brown slightly micaceous silt		Silty, slightly micaceous sand & quartz gravel 6 1/2"	Asphalt Surface Treatment 1/2"-3/4"	690	147	45.9	200
70	Micaceous silt		Micaceous sandy silty clay quartz pebbles 4"	Asphalt Surface Treatment 4 1/2" - 5"	690	147	45.9	200
71	Brown & black silty clayey sand 3", Mica silt		Silty, slightly clayey micaceous sand & quartz 7"	Asphalt Surface Treatment 1/2" - 3/4"	400	150	50	220
72	Tan micaceous silt		Silty, slightly clayey micaceous sand & quartz 7 1/2"	Asphalt Surface Treatment 1/2" - 3/4"	400	150 (est)	50	220

(Continued)

Table 1c (Continued). Georgia Pavement Evaluation Data

Test No.	Design				Traffic			
	Subgrade	Sub base	Base	Surface	Traffic Count in Traffic Lane cars/day	trks/day	Equiv. Daily 20 Kip Loads	Est. Total 20 Kip Loads (1000's)
73	Red sand clay micaceous 7"		Silty micaceous sand & quartz gravel 8 1/2"	Asphalt Surface Treatment 1/2" - 3/4"	376	150	50	220
74	Red sand clay micaceous 2"		Silty micaceous sand & quartz gravel 5 3/4"	Asphalt Surface Treatment 1/2" - 3/4"	300	128	40.0	134
75	Red clayey silty sandy micaceous soprolite 7"		Silty clayey micaceous sand & quartz gravel 5"	Asphalt Surface Treatment 1/2" - 3/4"	300	128	40.0	134
76	Clayey sand		Silty slightly clayey sand & Quartz gravel 7"	Asphalt Surface Treatment 1/2" - 3/4"	300	128	40.0	134
77	Clayey sand		Silty slightly clayey sand & quartz pebbles 4"	Asphalt Surface Treatment 1/2" - 3/4"	300	128	40.0	134
78	Red silty clay		Silty clayey sand & Quartz pebbles 5"	Asphalt Surface Treatment 1/2" - 3/4"	200	90 (est)	30	100
79	Silty clay		Cement stabilized clayey sand & Agg. 8 1/4"	Asphalt Pavement 4"	3000	1200 (est)	400	1250

(Continued)

Table 1c (Continued). Georgia Pavement Evaluation Data

Test No.	Design				Traffic			
	Subgrade	Sub base	Base	Surface	Traffic Count in Traffic Lane cars/day	trks/day	Equiv. Daily 20 Kip Loads	Est. Total 20 Kip Loads (1000's)
80	Red silty clay		Cement stabilized sand & Agg. 6"	Asphalt Pavement 4"	3000	1200	400	1250
81	Red silty clay		Cement stabilized clayey sand & Agg. 8"	Asphalt Pavement 2 1/2"	3000	1200	400	1250
82	Red silty clay		Cement stabilized clayey sand & Agg. 8 3/4"	Asphalt Pavement 2 1/2"	3000	1200	400	1250
83	Gravelly clay		Cement stabilized clayey sand & Agg. 6 1/4"	Asphalt Pavement 4 3/4"	3000	1200	400	1250
84			Cement stabilized clayey sand & Agg. 7"	Asphalt Pavement 3 1/2"	3000	1200	400	1250

Table 1d. Georgia Pavement Evaluation Data

Test No.	Average Vertical Stress on Subgrade in psi	Physical Properties From Tests			Bearing Capacity (psi)	Safety Factor	Location of Samples in Pavement System
		c(psi)	φ	E(psi)			
1	32	1.0	16	405	13	0.42	Base
2							
3	62	31.2	0°	1330	1322	2.1	Base
	22	25.0	0°	1280	106	4.9	S. G.
	7	13.9	0°	1160	587	8.9	S. G.
4	17.5	0	36.0°	1400	30	1.7	S. G.
		0	23.8°	1330			
5							
	9	0	41.1°	2140	63	6.9	S. G.
6	80	21.5	0°	1380	89	1.1	Base
	28	12.5	0°	1200	52	1.9	S. G.
	10	0	27°	1180	13	1.4	S. G.
7	80	0	39°	1310	24	0.3	Base
	22	0	34°	2160	20	0.9	S. G.
	9	13.6	15°	3090	121	13.5	S. G.
8	22	0	47°	2020	63	2.9	Base
		0	50.7°	2420			S. G.
							S. G.
9							

(Continued)

Test No.	Average Vertical Stress on Subgrade in psi	Physical Properties From Tests			Bearing Capacity (psi)	Safety Factor	Location of Samples in Pavement System
		c(psi)	φ	E(psi)			
10							
	66	18.1	4°	850	106	1.6	Base - S. G.
11	20	19.3	0°	660	82	4.1	S. G.
	10	17.7	0°	1110	75.1	7.4	S. G.
12	23	32.1	0°	1250	135.4	5.9	S. G.
	10	0	32°	950	13.3	1.3	S. G.
	69	0	34°	1070	12.0	0.2	Base - S. G.
13	21	0	32°	960	16.7	0.8	S. G.
		0	45.1°	2380			
	63	6.4	16°			3	
14	19	6.4	16°	2020	55.5	3	S. G.
	8	6.4	16°			3	S. G.
		3.4	28°		59.0		
15	18	3.4	28°	930	59.0	3.3	S. G.
	8	3.4	28°		59.0		
	58	0	44.4°	720	53	0.9	Base
16	18	15.3	5°	1190	74	4.1	S. G.
	8		19.2°	2880			S. G.
17	23	18.7	0°	1470	79.5	3.5	S. G.
	11	25.7	0°	1010	108.6	10.3	S. G.
18	Samples no good						
	80	0	40.6°	1270			Base
19	23	6.9	20°	1930	70.8	3.1	S. G.
	8	6.9	20°	2350	70.8	8.9	S. G.

(Continued)

Table 1d (Continued). Georgia Pavement Evaluation Data

Test No.	Average Vertical Stress on Subgrade in psi	Physical Properties From Tests			Bearing Capacity (psi)	Safety Factor	Location of Samples in Pavement System
		c(psi)	φ	E(psi)			
20	Samples no good						
	80	3.5	34°	490	84.0	1.1	Base
21	32	17.0	8°	1700	116.6	3.6	S. G.
	10	0	34°	1010	29.3	3.1	S. G.
	77	0	39.2°	472	20.1		Base
22	32	2.0	39°	830	270.8	8.5	S. G.
	11	2.0	39°	2310	270.8	2.5	Base
	80	0	41.6°	1310	26.5	0.3	Base
23	32	14.6	0°	1490	69.4	2.2	S. G.
	80	0	45°	1460	42.9	0.5	Base
24	27	4.2	0°	770	18.1	0.7	S. G.
	10	0	36.2°	3310	39.0	4.1	S. G.
25	23	0	40.4°	1240	42.2	1.8* 1 (est)	S. G.
26	Samples no good						
	80	5.6	19.6°	870	55.6	0.7	Base
27	27	0	39.1°	1690	46.0	1.7* 1 (est)	S. G.

*Too high -- most of sample too weak to test

(Continued)

Test No.	Average Vertical Stress on Subgrade in psi	Physical Properties From Tests			Bearing Capacity (psi)	Safety Factor	Location of Samples in Pavement System
		c(psi)	φ	E(psi)			
28	80	0	14.7°	1260	1.8		Base
	23	0	39.7°	1500	47.8	2.1	S. G.
29	Samples no good						
30	Samples no good						
31	Samples no good						
	28	16.6	6.9°	870	83.3	3	Sub base
32	15	22.8	0°	1000	96.5	6.6	S. G.
33	17	0	45.8°	906	75.6	4.1	S. G.
	53	0	39.3°	2180	26.7	0.5	Base
34	18	15.9	24.0°	2740	208.9	11.6	S. G.
	8	9.4	0°	4630	31.7	3.9	S. G.
	63	47.9	0°	1640	240.2	3.8	Base
35	19	27.1	0°	1280	135.2	7.1	S. G. - Base
	9	32.5	0°	2190	168.7	18.8	S. G.
	51	0	42.5°	830	42.4	0.8	Base
36	15	13.5	3.3°	1270	66.9	4.6	S. G.
	7	7.6	9.5°	2270	59.0	8.7	S. G.
	57	22.9	0°	1290	114.5	2.0	Base
37	17	6.9	14°	2040	61.9	3.8	S. G.
	6	2.1	30.2°	1120	60.6	10.1	S. G.
	25	22.6	0°	80.0	113.1	4.6	Base
38	12	22.5	0°	2850	113.1	9.4	Base - S. G.

(Continued)

Table 1d (Continued). Georgia Pavement Evaluation Data

Test No.	Average Vertical Stress on Subgrade in psi	Physical Properties From Tests			Bearing Capacity	Safety Factor	Location of Samples in Pavement System
		c(psi)	φ	E(psi)	(psi)		
	57	0	32.4°	820	11.5	0.2	Base
39	16	15.2	0°	830	76.4	4.8	S. G.
	8	0.6	37.0°	2290	37.8	4.7	S. G.
40	15	0	50.2°	2110	88.8	6.0	S. G.
	52	20.1	8.2°	330	188.5	3.7	Base
41	19	9.0	33.4°	1260	205.6	10.9	S. G.
	53	13.0	0°	444	64.9	1.2	Base
42							
43							
44	12	0	45°	1620	69.4	5.9	S. G.
		0	37.8°	1130			
45	11	0	35.9°	2140	29.4	2.8	S. G.
	25	0	44.1°	1100	72.8	3.0	Base - S. G.
46							
47							

(Continued)

Table 1d (Continued). Georgia Pavement Evaluation Data

Test No.	Average Vertical Stress on Subgrade in psi	Physical Properties From Tests			Bearing Capacity (psi)	Safety Factor	Location of Samples in Pavement System
		c(psi)	φ	E(psi)			
48	16	0	39.8°	1100	34.6	2.2	S. G.
	10	1.3		150	6.3	0.6	S. G.
	58	0	40°	1820	28	0.4	Base
49	Samples no good					1	
						1 (est)	
	47	12	23.8°	2080	156	3.3	Base - S. B.
50	15.7	7	29°	1690	138	8.8	S. B. - S. G.
		20	0°	670			
	58	19	0°	1150	102	1.8	Base - S. G.
51	21	0	39.6°	1320	41	2.0	S. G.
		15	0°	480			
	72	0	35.8°	410	13.5	0.2	Base
52	17.5	0	38.6°	370	40	2.3	S. G.
	12.5	0	24.7°?	590	11.3	0.9?	S. G.
	18	7	11°	550	36	2	S. G.
53	10	19	0°	740	95	2	S. G.
	71	15	9°	910	107	1.5	Base
54	23	11	0°	740	56	2.4	S. G.

? Poor sample

(Continued)

Table 1d (Continued). Georgia Pavement Evaluation Data

Test No.	Average Vertical Stress on Subgrade in psi	Physical Properties From Tests			Bearing Capacity (psi)	Safety Factor	Location of Samples in Pavement System
		c(psi)	φ	E(psi)			
	60	17	3°	440	87	1.4	Base
55	21	5.4	18.6°	570	60	2.9	S. G.
56	Samples no good						
57	Samples no good						
58	Samples no good						
59	Samples no good						
60	Samples no good						
61	Samples no good						
62	Samples no good						
63	47	18.3	0°	1070	91	1.9	Base - S. G.
64							
	80	0	32.2°	1310	7.6	0.1	Base
65	32	0	38.9°	790	33	1.0	S. G.

(Continued)

Table 1d (Continued). Georgia Pavement Evaluation Data

Test No.	Average Vertical Stress on Subgrade in psi	Physical Properties From Tests			Bearing Capacity (psi)	Safety Factor	Location of Samples in Pavement System
		c(psi)	φ	E(psi)			
66	32	0	24.6°	550	7.2	0.2	S. G.
	14	0	22.7°	1130	12	0.9	S. G.
	80	0	35.4°	1340	12	0.2	Base
67	39	0	46.1°	940	59	1.5	S. G.
	67	9.4	1.3°	420	47	0.7	Base - S. G.
68	23	0	32.3°	760	13	0.6	S. G.
	80	7.45	13.4°	840	69	0.9	Base
69	32	195	0°	630	93	2.9	S. G.
	14	19	0°	1010	94	6.7	S. G.
	46	8.3	11°	980	50	1.1	Base - S. G.
70	17.2	15.2	6°	1090	76	4.4	S. G.
	57	9.4	31°	1750	169	2.9	Base
71	20	9.4	31°	1710	171	8.6	S. G.
	10	6.25	29°	1560	126	12.7	S. G.
	57	13.2	0°	600	65	1.2	Base - S. G.
72	20	10	23°	1880	110	5.5	S. G.
	12	7.6	23°	900	105	8.7	S. G.
73	12	4.9	22°	1700	69	5.5	S. G.
74	Samples not obtained						

(Continued)

Table 1d (Continued). Georgia Pavement Evaluation Data

Test No.	Average Vertical Stress on Subgrade in psi	Physical Properties From Tests			Bearing Capacity (psi)	Safety Factor	Location of Samples in Pavement System
		c(psi)	φ	E(psi)			
	80	0	35.7°	580	12	0.2	Base
75	32	11.5	0°	1750	48	1.5	S. G.
	67	24.3	0°	790	98	1.5	Base
76	28	27.8	0°	1630	112	4.0	S. G.
	67	0	42.0°	360	26	0.4	Base - S. G.
77	28	6			26	0.9	S. G.
	67	6.1	1.5°	2220	31	0.5	Base
78	32	41	0°	3440	165	6.4	S. G.
	14	44	0°	2700	222	15.9	S. G.
	53	30	0°	1800	150	2.8	Base
79	16	20	5.3°	1450	100	6.2	S. G.
	53	14.7	9.5°	880	105	2.0	Base
80	19	22	0°		111	5.8	S. G.
	63	22.5	0°	1010	113	1.8	Base
81	24	3.5	15°	1150	42	1.7	S. G.
	12	65	0°	750	344	27.6	S. G.
	63	15	16.2°	1410	111	1.7	Base
82	22	7.6	17°	1230	66	3.0	S. G.
	11	25.7	2°	1550	128	12.1	S. G.
	31	14.6	18° (est)	710	121	3.9	Base
83							
	12	14.6	0°	1970	5	6.9	S. G.
84							

Table 2a. AASHO Road Test Data

Construction Block	Days In Service	Condition of Pavement			Design of Pavement			Traffic	
		Rut Depth		PSI Rating	Sub-base	Base	Surface	Avg. Daily 18^k Applications	Total 18^k Applications (1000's)
		Avg.	Max.		Sand-Gravel Mulch	Crushed Stone	Asphalt		
569	225	0.6"	0.8"	1.5	12"	0"	3"	512	1.15
571	182	0.3"	0.5"	1.5	12"	0"	3"	451	82.0
573	182	0.2"	0.5"	1.5	8"	3"	3"	451	82.0
575	789	0.6"	0.7"	1.5	12"	3"	4"	1407	1110.0
577	792	0.7"	0.7"	1.9	8"	6"	4"	1407	1110.0
579	242	0.5"	0.5"	3.0	4"	3"	5"	517	109.0
581	792	0.5"	0.5"	3.3	12"	6"	5"	1407	1110.0
583	176	0.2"	0.2"	3.5	4"	0"	4"	443	77.0
585	178	0.3"	0.3"	1.5	4"	6"	3"	449	80.0
587	222	0.7"	1.0"	1.5	8"	0"	5"	536	119
589	210	0.6"	0.9"	1.5	8"	3"	4"	476	100
591	792	0.5"	0.5"	4.3	12"	6"	5"	1000	1110.0
593	554	0.4"	0.4"	3.5	12"	3"	5"	1069	100
595	199	0.2"	0.3"	1.5	4"	6"	4"	452	90.0
597	225	0.5"	0.6"	1.5	8"	3"	4"	493	1110.0
599	163	0.4"	0.5"	1.5	4"	3"	3"	454	74.0
601	792	0.6"	0.7"	1.6	12"	6"	3"	1407	1110.0
603	505	0.7"	0.9"	3.0	12"	0"	4"	844	106
605	196	0.1"	0.1"	1.5	4"	0"	5"	449	88.0

(Continued)

Table 2a (Continued). AASHO Road Test Data

Construction Block	Days In Service	Condition of Pavement			Design of Pavement			Traffic	
		Rut Depth		PSI Rating	Sub-base	Base	Surface	Avg. Daily 18^k Applications	Total 18^k Applications (1000's)
		Avg.	Max.		Sand-Gravel Mulch	Crushed Stone	Asphalt		
607	157	0.3"	0.5"	1.5	8"	0"	3"	459	72.0
615	560	0.7"	0.9"	1.5	4"	6"	5"	1091	611.0
617	547	0.5"	0.7"	1.5	12"	3"	3"	1066	583.0
619	220	0.6"	0.8"	1.5	8"	0"	4"	486	107.0
621	588	0.8"	1.0"	3.5	12"	0"	5"	1150	104
623	204	0.4"	0.6"	1.5	8"	6"	3"	443	92
625	792	0.8"	0.8"	3.8	12"	6"	4"	1407	233
627	194	0.4"	0.6"	1.5	4"	3"	4"	448	87.0
629	573	0.8"	1.0"	3.5	5"	6"	4"	1119	519
631	549	0.7"	0.7"	1.5	8"	3"	5"	1073	589.0
633	41	0.5"	0.7"	1.5	4"	0"	3"	49	2.0

Table 2b. AASHO Road Test Data

Construction Block	Stress on Subgrade Avg. (psi)	Physical Properties of Embankment c (psi)	φ	E (psi)	Bearing Capacity Pressure psi	Safety Factor
569	10	9.5	20	1040	99	9.9
571	10	9.5	20	1040	99	9.9
573	11	9.5	20	1040	99	9
575	7	9.5	20	1040	99	14
577	7	9.5	20	1040	99	13
579	14	9.5	20	1040	99	7
581	6	9.5	20	1040	99	16.5
583	22	9.5	20	1040	99	4.5
585	13	9.5	20	1040	99	8
587	13	9.5	20	1040	99	8
589	11	9.5	20	1040	99	9
591	7	9.5	20	1040	99	14
593	7	9.5	20	1040	99	14
595	11	9.5	20	1040	99	9
597	11	9.5	20	1040	99	9
599	16	9.5	20	1040	99	6
601	7	9.5	20	1040	99	14
603	10	9.5	20	1040	99	9.9
605	18	9.5	20	1040	99	5.4

(Continued)

Table 2b (Continued). AASHO Road Test Data

Construction Block	Stress on Subgrade Avg. (psi)	Physical Properties of Embankment c (psi)	Φ	E (psi)	Bearing Capacity Pressure psi	Safety Factor
607	15	9.5	20	1040	99	6.6
615	10	9.5	20	1040	99	9.9
617	8	9.5	20	1040	99	12
619	14	9.5	20	1040	99	7
621	8	9.5	20	1040	99	12.5
623	8	9.5	20	1040	99	12.5
625	6	9.5	20	1040	99	16
627	16	9.5	20	1040	99	6.1
629	10	9.5	20	1040	99	9.9
631	9	9.5	20	1040	99	11
633	24	9.5	20	1040	99	4

Appendix A. Typical Pavement Survey Data

PAVEMENT SURVEY - Project B-133

Date 9/20/61 By AES Photo No. 19

Morgan County No. Ga. 12 Hwy No. U. S. 278 Sample No. 58

Location 1.8 mi. west intersection Ga. 83 -- west of Madison -- west bound lane

Percent grade 1 1/2 per cent (uphill, downhill)

Curvature --- Superrelevation ---

Foundation (cut, fill, transition, at grade) 4 ft.

Fill/cut Exposure Red, gravelly, clay

Vehicle Speed Change Truck stop opposite sample on south side of road

Topography Rolling

Vegetation Open field (grass), pine, sweet gum

Surface Water None

Ground water/seepage None

Is area frequently flooded? No

Drainage: external Side ditch on north, culvert on south

internal

Crack Pattern Longitudinal in bottom of both wheel paths, longitudinal along ℄

Longitudinal Alignment Good

Deformation: OWP 3/8 - 3 1/2' from edge IWP 1/8

Rut Spacing 5.5'

Condition of Shoulder Bare clay, 1" below pavement edge

Extent of Failure Continuous

Number of Vehicles per hour per day 692

Percent heavy trucks 22

Comment: Longitudinal crack in OWP has been patched. Noticeable rutting.

Estimated Pavement Serviceability = 2.

Appendix B. Bearing Capacity Equation

The basic expression for the bearing capacity, q_o, of a uniformly loaded, homogeneous soil mass is

$$q_o = \frac{\gamma b}{2} N_\gamma + cN_c + q' N_q$$

where γ is the soil unit weight, c, the cohesion, b, the width of the load and q' the weight of materials above the load level. The factors N_γ, N_c, and N_q are functions of φ. Each must also be corrected for the shape of the loaded area.

The loaded area developed by dual tires is approximately a square whose effective width increases with the distance, D, below the surface. For most base courses the effective width, b, (in inches) is

$$b = 15 + 0.7\ D$$

For a subgrade D is the pavement thickness in inches and q' the pressure exerted by the weight of the pavement. If the pavement components weigh 144 pcf and the subgrade 120 pcf

$$q_o = \frac{60}{1728} (15 + .7\ D)\ N_\gamma + cN_c + \frac{144\ D}{1728} N_q \quad \text{(in psi)}$$

$$q_o = .035\ (15 + .7\ D)\ N_\gamma + cN_c + .083\ D\ N_q \quad \text{(in psi)}$$

For a typical 12 in. thick pavement the expression simplifies to

$$q_o = .81\ N_\gamma + cN_c + N_q \quad \text{(in psi)}$$

Table 4. Values of N-Corrected for Square(Bell Terzaghi)

φ	N_γ	N_c	N_q	φ	N_γ	N_c	N_q
0	1	5	1	30	13	17	9
5	1	6	1	33	18	20	12
10	2	7	2	36	25	24	15
15	3	9	3	39	34	28	19
20	5	11	4	42	48	34	25
25	8	14	6	45	69	40	34

Appendix C - Proposed Design Nomographs
From AASHO Interim Guide for the Design of Flexible Pavement Structures
October 12, 1961

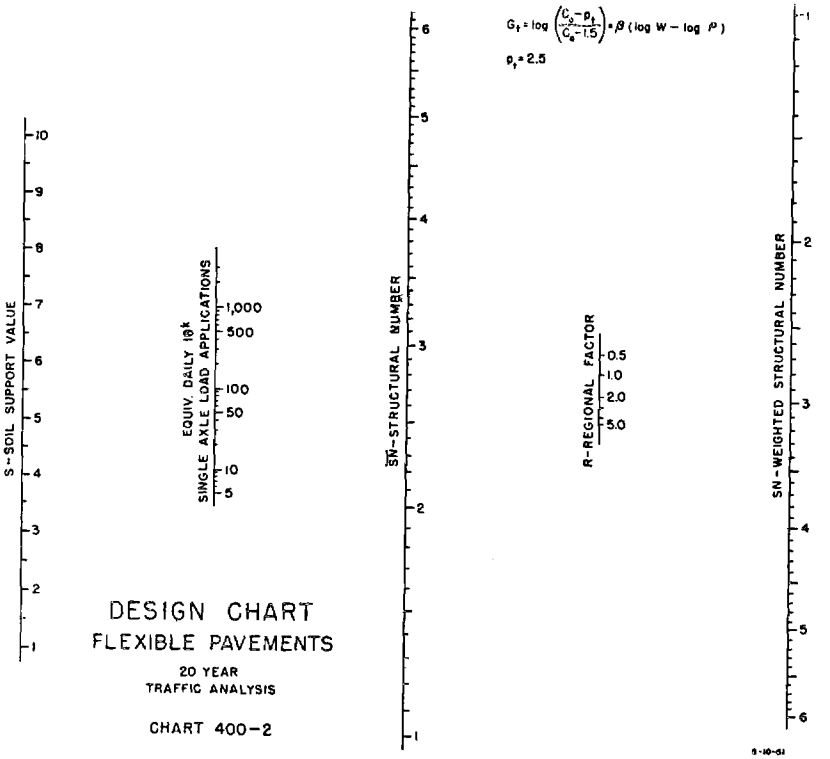

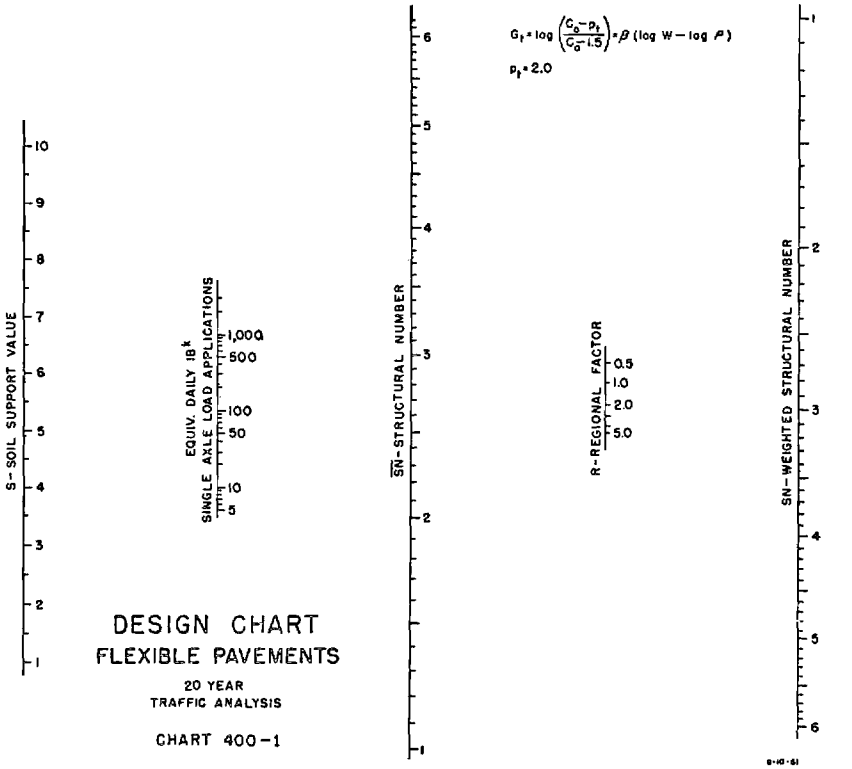

B-133

VERTICAL STRESSES IN SUBGRADES BENEATH STATICALLY LOADED FLEXIBLE PAVEMENTS

By

George F. Sowers, Professor of Civil Engineering
and
Aleksandar B. Vesic, Associate Professor of Civil Engineering
Georgia Institute of Technology

Vertical Stresses in Subgrades Beneath Statically Loaded Flexible Pavements

By

George F. Sowers, Professor of Civil Engineering
Aleksandar B. Vesić, Associate Professor of Civil Engineering
Georgia Institute of Technology

Summary

Full scale static load tests have been made of single, dual and dual tandem ıck tire loads on flexible pavements in order to determine the stress distri- ion in the subgrade and the relative load spreading ability of different base rse materials now in use by the Georgia Highway Department.

The measured stresses below topsoil and soil bound macadam base pavements comparable to those computed by the Boussinesq theory. The measured stresses ow the sand asphalt are comparable to or slightly more than those computed by Boussinesq. The stresses found below the soil cement base are much lower than se given by Boussinesq and are comparable to the stresses found by the two layer stic theories. Asphaltic concrete overlays reduce the stresses to the same ree as an equal thickness of the topsoil or soil bound macadam.

Introduction

The rational design of any structural system, including pavements, requires ıowledge of the stresses induced by the imposed loads. However, little infor- on is available regarding the stresses developed in the underlying soils by led vehicles supported by pavements. It was the purpose of this research to stigate the stresses produced in soil subgrades by wheel loads such as truck s on flexible pavements.

A major function of any pavement is to sufficiently spread the concentrated delivered to it by the wheel so that the stress ultimately transmitted to the rlying soil will not cause shear nor excessive deformation. The rigid

vement does this by beam or slab action. The flexible pavement system action more complex; the load is spread through a mass of discrete particles that act like an elastic continuum when they are confined. The flexible pavement is mposed of layers, all of which contribute to the load spreading, but some with re specialized functions. The surface resists the vertical and tractive loads well as the wear of the wheels and provides a smooth roadbed. The base course the main load spreading member. It is usually the thickest layer and the one ich involves the greatest variety of materials and methods of construction. subgrade, either natural soil or compacted fill, furnishes the ultimate sup-t for the load. Some pavements include a sub-base course that serves as a nsition between base and subgrade. Resurfacing or overlaying with asphaltic crete restores a damaged surface. It also adds another load spreading layer the pavement system.

Of course, the stresses at any point in the subgrade consist of combinations shear and normal stress. Whether all the components of stress or only certain s need be evaluated depends on the criteria established for pavement perfor-ce and design. The earliest methods of design were related to shear and ar failure in the subgrade; therefore in these methods shear stresses have n considered the most important. Recent studies indicate that deflection may the better index to design; and therefore the vertical normal stress is of atest significance. In this project, only the vertical normal stress has n investigated.

Although flexible pavements enjoy widespread use, little information has n available regarding the way in which vertical stresses are transmitted through n into the subgrade. Various simple assumptions have been proposed. One such od assumes that the wheel is concentrated at a point on the pavement surface. vertical component of the load spreads uniformly over an area defined by a whose vertex is at the pavement surface and whose sides slope at 45 degrees the vertical. A second method assumes the contact area of the tire to be a

rcle and the vertical component of the load is spread uniformly over an area fined by the frustum of a cone whose upper base is the circle of tire contact d whose sides slope at an angle of 30 degrees with the vertical.

Various elastic theories have also been proposed for evaluating subgrade resses beneath pavements. In all of these the pavement is represented by a mplified model whose physical properties can be described mathematically. The resses in the model are analyzed by the laws of mechanics, and are assumed to the same as those in the real pavement it represents. Certainly their validity ends on how accurately the model represents the real pavement.

Few data are available to confirm or reject any of the proposed theories determining vertical stresses in the subgrade. One purpose of this investi-ion was to compare the measured stresses beneath pavements with those computed oretically and if possible verify the theoretical methods.

The loads encountered in highway work are predominantly moving and vertical cept at points of braking and acceleration). The rate varies from a standstill 70 mph or more. However, present knowledge of the behavior of soils and simi-fragmental materials indicates that maximum deflections and stresses are more ely to occur with sustained load rather than rapidly changing load. Therefore, y static loading was investigated experimentally.

oretical Stress Distribution

The analysis of stress distribution in loaded soil masses or pavements is, erally, a problem that is being solved, for ideal materials, by the theory of sticity.

The basic solution of this problem is the well known Boussinesq solution [1] a single, vertical point load acting on the horizontal surface of a semi-nite, homogeneous, isotropic, elastic solid. This solution was extended to case of load uniformly distributed over any finite area by Love [2]. Particular

lutions have been worked out, evaluated and presented in tables or graphs by ny authors. The work by Steinbrenner [3], Newmark [4], [5], Fadum [6], Fergus d Miner [7], Foster and Ahlvin [8], Dereśiewicz [9] should be cited as perhaps e most important for stress evaluation in pavements.

A semi-empirical modification of the Boussinesq solution by introduction of e concentration index has been proposed by Griffith [10] and Fröhlich [11] for ni-infinite soil masses which are non-homogeneous in a vertical direction or n-isotropic. Their work was further extended by Ohde [12].

The stress distribution in semi-infinite, homogeneous, orthotropic solid, ing different deformation moduli in horizontal and vertical directions was estigated by Buisman [13], Wolf [14], Jelinek [15, 16, 17] and Koning [18]. sman also investigated the case of an orthotropic and non-homogeneous mass ing a modulus of deformation linearly increasing with depth. The problem of emi-infinite solid reinforced by horizontal perfectly flexible membranes was ved by Westergaard [19] and integrated by Fadum [6].

Of particular interest for stress distribution in pavement sytems is the blem of a multi-layered elastic solid (Fig. 1). The basic solution of this blem is that found by Burmister for a circular, uniformly distributed load at surface of a two-layer system [20]. This solution was extended by the same hor to the case of a three-layer system [21] and generalized by Schiffman for case of surface loading [22]. Numerical evaluation of stresses in a two-layer em was performed by Fox [23] and Hank and Scrivner [24]. Evaluation of sses at the interfaces of a three layer system was made by Acum and Fox [25]. hould be noted that all mentioned evaluations of stresses were performed for ts beneath the center of the loaded circular area only.

Previous Experiments on Stress Distribution

The mentioned theories of stress distribution are based on several simplifying assumptions which, to a greater or lesser degree, always deviate from the real behavior of materials. Assumptions are made, for instance, that the materials are perfectly elastic and have linear relationship between stresses and strains defined, generally, by constant Young's moduli E and Poisson's ratios ν . However, soils and other pavement materials are only partly elastic and do not have linear stress-strain relationship. Neither E nor ν are constant but vary with the applied load. Both E and ν may have quite different values in tension than in compression (many soils and base materials have practically no tensile strength at all). Also, most solutions are based on assumption of perfect homogeneity and isotropy of different layers. Whereas pavement layers are usually reasonably homogeneous, they normally possess a structural aniostropy. Subgrades often display a decrease of compressibility with depth; they also may be stratified or laminated.

Consequently, discrepancies have to be expected between theoretical and actual stress in loaded soil masses or pavement systems. Several investigators have undertaken so far the task of checking to what extent the actual stresses follow the stress pattern indicated by the theories.

The early investigations of this kind, made on homogeneous sand fills in large boxes [26-31] as well as on layered pavement models [32], gave somewhat misleading results concerning the concentration of stresses under the applied loads, as compared with the Boussinesq theory for homogeneous solids. Namely, due to the limited dimensions of test boxes the bottom acted as a rigid base and caused additional stress concentration.

Very thorough experimental studies of stress distribution in homogeneous silt and sand masses were made at the Waterways Experiment Station at Vicksburg, Miss. [34-35]. It was found that the pattern of measured stresses for both kinds of

omogeneous soil followed closely the general shape indicated by the Boussinesq heory. There was somewhat higher concentration of stresses under the loads, articularly in sand; however, the use of the Fröhlich concentration index did ot improve the agreement between the theoretical and measured stresses.

Experimental studies were made by McMahon and Yoder [36] on stress distri- tion in homogeneous clay as well as in a two-layered mass consisting of crushed one base of variable thickness and a clay subgrade. This investigation showed thin the homogeneous clay mass a stress pattern close that predicted by the ussinesq theory. At the same time the stresses in the two-layer system were newhat reduced directly under the interface; however, only with a distance t greater than the radius of the loaded plate. Nevertheless, stresses were nsiderably higher than those predicted by the Burmister two layer theory, and general closer to values obtained by the Boussinesq theory for homogeneous l.

Test Apparatus

Full scale models of flexible pavement systems, including the subgrade were structed in a test pit. Static loads were applied to the pavement by truck es and the vertical stresses in the subgrade were measured by pressure cells.

t Pit and Load Frame

In order to control moisture content changes in the subgrade the entire model built in a test pit, Fig. 2a and 2b. The inside dimensions are 8 ft wide, 7 leep and 12 ft long, so the volume of the model was 25 cu yd. At a 9000 lb el load the approximate diameter of the tire contact area was 11 inches. The h and width of the pit were 7.6 and 8.7 diameters respectively which means the rigid boundary effects should not be significant. A steel frame, ened to the ends of the pit with a heavy beam spanning the center line, ished the reaction for loading the tires.

A hydraulic jack mounted beneath a carriage riding on the beam supplied ıe load. The load was measured by the hydraulic pressure with a calibration ;ror of less than 2 per cent.

ıeel Assemblies

Single, dual, and dual tandem wheel assemblies were employed, with 9"x 20" ;avy duty truck tires inflated to pressures between 70 and 90 psi. These tires 'e designed for a maximum load of 9000 lb each although they are occasionally erloaded in practice. The tire spacings were 10.5 in. center to center in e dual configuration and 54 in. axle to axle in the dual tandem. These are andard spacings in U. S. Highway trucks.

ɜssure Cells

A simple diaphram type pressure cell, Fig. 3, previously developed in the ›rgia Tech soil laboratory, was employed to measure the vertical normal stresses the subgrade. It consists of an elastic membrane, a thin disk of aluminum, ɛd at its perimeter to a thicker circular base plate. The membrane responds normal stresses by bending and stretching slightly. A SR-4 electrical strain e, bonded to the membrane, measures the strain induced by the pressure. A ond compensating gage is mounted in the base plate at a point where it under- s little strain under load. The individual gages are internally waterproofed ɑ petrosene wax. The entire assembled cell, with its vinyl insulated lead ɛs, is waterproofed by dipping in a solvent type vinyl cement. From three to ' coats of the cement provide a waterproof, flexible jacket that can resist ɜrsion in water for a month or more. Three different cell diameters were ., 4 in., 5 in., and 6 in., with diaphrams 0.19 in. and 0.12 in. thick in r to provide a range in sensitivities. The cells were 0.4 in. thick or less. cell diameter to thickness ratios were between 10 and 15 which minimized the able effects of soil arching over the deflecting diaphrams.

Each cell was individually calibrated by the application of a uniform essure by means of an air loaded rubber membrane in a soil filled calibration amber. Initially the cells were calibrated completely surrounded by subgrade il compacted to the same density as in the test section. Comparative tests, wever, showed that virtually the same results were obtained for pressures thin the middle range for each cell if the cell were placed on a surface of mpacted soil and loaded directly with the rubber membrane. Subsequent cali- ation was performed in this manner.

From 25 to 30 cells were employed, arranged in 4 (or 3) straight lines rpendicular to the axis of the pit, with each line at a different depth below surface and at a different position along the pit axis. In this way no cell directly below another so as to minimize any arching or load concentration sed by their rigidity. The exact depths varied from test to test. In the st series, on the topsoil base, the upper layer was in the base at a depth of 1. below the surface, and the remainder in the subgrade at depths of 15.7, 27.6, 45.6 inches below the surface or respectively 0.8, 1.4, 2.5, and 4.1 diameters sed on an equivalent circular 9000 lb wheel load). In the remainder of the s the upper cell layer was in the subgrade, just below the base course at pth of 11 to 13 inches (1 to 1.2 diameters) with a 3 inch asphaltic surface 5 inches (1.4 diameters) with a 6 inch asphaltic surface. The other layers at depths of about 17, 23, and 29 inches (1.5, 2.1, and 2.7 diameters) with inch asphaltic surface and correspondingly greater depths with the 6 in. thick ace. The exact depths for each test series are shown on the plots of the results.

Pavements Systems

The pavement systems tested were typical of those currently employed by the gia State Highway Department. The subgrade soil for all tests was a micaceous

andy silt, a residual material derived from granite gneiss. This type of soil s widespread in the northern half of the state and is characterized by a low esistance to deformation, particularly under load. It is far from an ideal ubgrade and is typical of the poorer materials in the state on which roads ust be built. Four types of bases were used: topsoil, (silty well graded unds from two locations in Central Georgia); soil bound macadam consisting of) per cent by weight of the topsoil and 60 per cent by weight of size 467 rushed granite; soil cement, consisting of 4 per cent by weight Type 1 port- nd cement and 96 per cent of the soil bound macadam; and sand asphalt, a iform subangular quartz sand with 5 per cent RC-3 cut back asphalt.

Standard laboratory tests were run on all these materials to determine their ysical properties. Because of the coarse aggregate size it was impossible to n the ordinary compaction test on the soil bound macadam and soil cement macadam terials. These materials were compacted in an 8 in. diameter by 16 in. high ld in 2 in. layers by a 5.5 lb hammer filling 12 inches using sufficient blows each layer to provide the same 12,400 ft lb per cu ft as in the Standard AASHO st. The physical properties of these materials are summarized in Table I. The rface in all cases was a plant mix asphaltic concrete.

ement Construction

Different combinations of base, base thickness and pavement thickness were ted as summarized in Table II. The initial work employed 8 in. thick base rses and 3 inch asphaltic concrete surface courses (laid in two layers). Later ts included 3 to 3.5 in. thick asphaltic concrete overlays on the 3 inch sur- es, as well as 6 in. base thickness.

The subgrades were constructed in accordance with the current Georgia Highway artment practice for embankments. The lower 3 ft. was compacted to 90 per t of the maximum density as specified by ASTM D-698 - 58T - C . Compaction test to the upper 3 ft to a density of between 95 and 100 per cent of the same

TABLE I

PROPERTIES OF SUBGRADE AND BASE MATERIALS

ıl	Detailed Description	Liquid Limit	Plastic Index	Percentage Passing No.10	Percentage Passing No.200	Maximum Density*	Class
ıb-	Micaceous fine sandy silt	45	8	98-100%	36-40%	95-97 pcf	A-5
	Silty well graded sand	14.5	0	98	12-15	128	A-1
und	Subangular to angular granite gneiss sizes 467** 60% plus 40% topsoil			40	6-8	131	
ment	4% Type 1 cement plus 96% soil bound Macadam (above)					135	
phalt	Uniform subangular quartz sand 95% plus 5% RC-3 cutback asphalt	0	0		0	105	A-3***
ic ɜ	Plant Mix, 5% Bitumen					140	

ASTM D 698-58T Method C for sand, topsoil, mica silt. For others a special ıction test was employed -- see text.

D 448

alone

Test Series	Subgrade Soil	Surface-Plant Mix Asphalt Conc. Thickness	Base Course Composition	Base Course Thickness	Loading Wheel	Loading Total Load, Kips
I	Mica Silt	3"	Topsoil I	8"	Single Dual Dual Tandem	5, 9, 13.5 5, 9, 13.5, 18 18, 27, 36
II	Mica Silt	3	Soil Bound Macadam	8	Single Dual	5, 9, 13.5 9, 13.5, 18
III	Mica Silt	3	Soil Cement Macadam	8	Single Dual	5, 9, 13.5 9, 13.5, 18
IV-1	Mica Silt	3	Sand Asphalt	8	Single Dual	5, 9, 13.5 9, 13.5, 18
IV-2	Mica Silt	6 (3" overlay)	Sand Asphalt	8	Single Dual	5, 9, 13.5 9, 13.5, 18
V-1	Mica Silt	3	Topsoil II	8	Dual	9, 13.5, 18
V-2	Mica Silt	6.5(3" overlay)	Topsoil II	8	Single Dual	8.5, 12.5, 17 9, 13.5, 18
VI-1	Mica Silt	3	Soil Cement Macadam	6	Single Dual	5, 9, 13.5 9, 13.5, 18
VI-R	Mica Silt	3	Soil Cement Macadam	6	Single	13.5 (1000 cycles)
VI-2	Mica Silt	6.5 (3" overlay)	Soil Cement Macadam	6	Single Dual	5, 9, 13.5 9, 13.5, 18
VI-F	Mica Silt	6.5 (3" overlay)	Soil Cement Macadam*	6	Dual	9, 13.5, 18

*Subgrade and base inundated.

ximum. Both were tamped in 2 in. thick layers with a gasoline-driven dy-
mic device, the "Jay Tamp" at a moisture content equal to or slightly below
e optimum. The topsoil and sand asphalt base courses were compacted to 100
r cent of the ASTM D698-58T-C max.; the soil bound macadam and the soil cement
:adam were compacted to 100 per cent of the maximum density found on the large
mpaction molds. The asphaltic surface was compacted with the Jay Tamp in 1.5
:h thick layers to as great a density as possible. Tests of cores from one
:ies showed a mean density of 131 pcf which is slightly less than that ob-
ned by rolling the same mix on a highway job.

;ineering Properties of Pavement Components

Tests were run on each of the pavement components to determine their modulus
elasticity and strength properties. Triaxial shear tests were made of all
materials in which both stress-strain characteristics and stresses at failure
e determined. The tests of the subgrade, topsoil, and sand asphalt were run
both laboratory specimens compacted in a 4 in. diameter 8 in. high mold and
undisturbed samples cut from the test section. The tests on the soil bound
adam were made on specimens compacted in the 8 in. diameter 16 in. high mold
the laboratory. All were tested in a large triaxial cell with interchangeable
5, and 8 in. diameter sample bases. In all cases the undrained (quick) pro-
ure was used, with a constant axial deformation rate of 0.02 in. per min.
sand asphalt was also tested at a rate of 0.01 in. per min. to determine if
r rate had any effect on its deformation properties. It was tested at tempera-
s comparable to those measured in the base course at the time of stress measure-
. The elasticity test results are shown in Fig. 4a, 4b, 5a, and 5b. They
the initial or tangent modulus of elasticity of each material as a function
he minor principal stress and the ratio of the modulus of elasticity of the
to that of the silt subgrade at equal minor principal stresses. The strength
elasticity data are summarized in Table III.

STRENGTH AND DEFORMATION CHARACTERISTICS OF MATERIALS

Material	Weight (lb/ft^3)	Water Content (%)	Strength Characteristics c (lb/in^2)	Strength Characteristics Ø	Deformation Characteristics: Elasticity Modulus, lb/in^2, (First no.) Strain at Failure in %(Second no.) from Triaxial Tests, at Confining Pressures of: 0 lb/in^2	20 lb/in^2	40 lb/in^2	60 lb/in^2	Modulus of Elasticity from Plate Load Tests ($lb/in.^2$)	Tangent Modulus from CBR-Tests (lb/in^2) and CBR-Value: Without Surcharge	With Surcharge 0.40 lb/in^2
Subgrade	79.1	26.8	9.0	23°	328 2.5	1,104* 13.7	1,160** 14.3	1,346 17.6	1,300	691 3.4	1,237**** 4.2
Topsoil samples from the actual base	121.2	10.2	20.2	33°	1,640 4.9	4,910 6.3	4,800 8.2	--	10,400***	4,400 29.1	6,650 44.1
Topsoil samples prepared in the laboratory	123.0	10.6	5.1	33°	545 3.8	2,700 10.4	3,140 13.2	3,970 23.9	--	--	--
Soil bound Macadam	131.1	3.9	2.5	37°	2,940 0.6	10,520 2.9	12,360 8.2	--	11,200***	12,660 34.5	--
Soil Cement	134.5	3.5	51.3	50°	49,400 0.8	61,500 0.7	74,000 0.9	91,000 0.9	130,000	--	---
Sand Asphalt: loading rate 0.02 in/min	103.4	8.5	2.2	35°	1,245 1.4	5,970 4.8	10,520 4.4	15,380 5.9	5,590	2,370 9.2	3,820 19.3
Sand asphalt: loading rate 0.01 in/min	105.2	8.8	1.0	33°	1,080 2.9	5,670 6.2	9,450 8.2	12,350			

*At 15 lb/in^2

**At 30 lb/in^2

***With 3 inches of pavement above

****Surcharge 0.80 lb/in^2

The modulus of elasticity curves all show an increase in E with an increase n confining pressure. The curve for the sand asphalt shows a continuing, nearly inear increase while for the others E increases rapidly at low pressures but pproaches a constant of higher pressures. The ratios of the E of the base to ie E of the subgrade, however, are nearly constant regardless of confining ressure for all except the sand asphalt base. For the latter, the ratio in- reases with increased confinement. These variations in E are significant be- use most theoretical analyses, including the Boussinesq and the two layer and ree layer theories assume that E is a constant that is independent of confine- nt.

Two types of in-place tests were conducted on the pavement components: lifornia Bearing Ratio (CBR) and plate load tests. The CBR tests were made the upper surfaces of the subgrade and base courses using the standard methods the Corps of Engineers with a nominal surcharge load equivalent to 3 in. of vement.

Plate load tests were made on the subgrade, all base courses, and the rface course for all but the sand asphalt base pavement. An 18 in. diameter ate was employed, that was rigidly reinforced so as to have negligible deflec- on.

An effective modulus of elasticity was computed from each CBR and plate d test using the theory of the deflection of a rigid circular load on an stic medium. The plate load modulus of elasticity data for the base courses e computed from the two layer elastic theory using the elastic modulus of the grade as computed from the subgrade load tests. The results of these compu- ions, which must be considered as rough indications at best, are also summarized Table III.

Wheel Load-Subgrade Stress Tests

The full scale model tests of truck tires on the pavement included more han sixty combinations of load, wheel configuration and pavement design. In eneral the single tire was subjected 5, 9 and 13.5 Kips equivalent to 10, 18, nd 27 Kip axle loads while the dual tires were subjected to 9, 13.5, and 18 ips total or 18, 27, and 36 Kips per axle. The range selected includes the egal loads permitted in many states and anticipates possible larger maximum oads of the future.

ire Contact Area

The tire selected is designed for a maximum load of 9000 lb at an inflation ressure between 80 and 90 psi. The size and shape of the tire contact was termined for loads of 4500, 6750, 9000, and 13,500 lb in order to compute the resses in the soil theoretically. The tire prints and the load-contact pres- re curve are shown in Figs. 6 and 7. The prints show a nearly circular contact one half the design tire load and a rectangle whose length is 2.5 times the dth for 1.5 times the design tire load.

st Procedure

Each load was placed on the pavement of ten different positions on the long- idinal axis of the pit: center, 3, 6, 12, 24 in. each side of center, and 36 . north of the center. The vertical pressures were measured by each cell in h position. The results are shown graphically on the attached charts. They plotted with vertical stress as a function of distance from the center of the d, regardless. The variable positioning of the tire made it possible for each l to contribute more than one point to the curve. Only the center pressure h a distance from the load of 0 was measured by one cell alone at each depth. least two and sometimes five sets of identical independent loadings and stress surements were made for each tire load. All the individual stress measurements plotted rather than averages in order to show the range of variability in the

readings. In this paper only the data for the 9000 lb single tire and the 13,500 lb dual are included. The data from the other loads are in direct proportion.

Theoretical Stresses

The theoretical stresses for each loading were computed from the load-tire contact area data using an equivalent rectangular or circular loaded area. The Boussinesq analysis of a semi infinite homogeneous isotropic elastic solid was used for all. In addition the two layer theory was employed for the soil cement pavements by assuming that the modulus of elasticity of the asphaltic concrete surface was the same as that of the soil cement. Three different ratios of the elasticity of the upper layer to that of the lower layer were assumed: 1 to (which is the same as the Boussinesq), 10 to 1, and 100 to 1. The stress computations for the dual tires were made in two directions: (1) along the axis of the pit---in the direction of wheel travel; and (2) on the line of the axle at right angles to the direction of wheel travel. (The actual stress measurements include both these directions and many others in between, and are not differentiated in the graphical presentation.) The theoretical stress distribution is shown in Figs. 8 through 26 by the continuous curves. In the dual tire results, the solid curve represents the stress distribution in line with the axle and the dashed curve at right angles to the axle.

Topsoil Base Pavements

The measured vertical stresses for the topsoil base pavement systems are shown in Figs. 8 through 12 as individual points on the graphs. They show that the vertical pressures in the subgrade decrease rapidly with increasing depth. The pressure distribution is seen to be close to that given by the Boussinesq theory. The maximum pressure in the subgrade, under the center of the load is equal to the Boussinesq for Topsoil I and equal to or slightly greater (up to 15 percent more) for Topsoil II. For the topsoil subgrades, therefore the Boussinesq

heory, based on a semi-infinite homogeneous isotropic elastic mass, is found
› be a reasonably accurate representation. This is somewhat surprising because
ıe ratio of the modulus of elasticity of the base to the subgrade is 3 to 4
ıich, by the two layer theory, should yield slightly lower stresses directly
:neath the center of the load. Two factors are undoubtedly responsible. First,
ı order for the two layered theory to be valid theoretically, there must be
nsile stresses in the interface between the two layers. The Mohr envelopes
ow a cohesion of only 15 psi for the topsoil (based on a curved envelope)
20 psi (based on an approximate stright line) for the samples taken from
ɜ model pavement and 5 psi for the laboratory compacted samples. The cohesion
the subgrade is 9 psi. Neither material, therefore, is capable of resisting
:h tension, which invalidates, to some degree, the two layer theory. Second,
ither modulus of elasticity is a constant although both the two layer theory
ı the Boussinesq theory assume unchanging E values. It is possible the in-
:ase in E with increasing confinement causes a stress concentration, as noted
Griffith and Fröhlich and partially offsets the gain in load spreading pro-
ed by the more rigid base. However, it also may be argued that the ratio
the E of the base to that of the subgrade is nearly constant so that the
iation in E with confinement is not so significant. A theoretical analysis
the effects of varying E would be instructive, but is not available.

ı Bound Macadam Base Pavements

The test results for the wheel loads on the Macadam base pavement are
ın in Figs. 13 and 14. The results are almost identical to those of the
:oil base: A marked decrease in vertical stress with increasing depth and
ɾessure distribution that is very close to that given by the Boussinesq
ry. The modulus of elasticity data, Fig. 5a, shows that the soil bound
dam base has a modulus of elasticity 9 times that of the subgrade. According
he two layer elastic theory the stresses in the upper surface of the subgrade

should be slightly less than half the measured vertical stresses (or slightly less than half the Boussinesq). As in the case of the topsoil base, two factors appear responsible. First, the cohesion of the soil bound Macadam is only 2 psi which with its high angle of friction means negligible tensile resistance. Tensile cracks develop at the bottom of the base course along the interface which destroy the continuity of the elastic layer and invalidate the theory. Second, the modulus of elasticity increases with increasing confining pressures, although the ratio of the E of the base to that of the subgrade is nearly constant. The result may be a stress concentration that offsets the gain in load spreading of the more rigid base, as also may be in the case of the topsoil.

and Asphalt Base

The stresses beneath the pavements with sand asphalt bases on the micaceous silt subgrade are shown in Figs. 15 through 18. While all the tests show a marked reduction in vertical stresses with increasing depth, the maximum vertical stress directly under the load center and 0.3 in. below the base-subgrade interface was found to be considerably greater than that at an equivalent location in the topsoil and soil bound Macadam base pavements. The ratios of these maximum measured stresses just below the interface to the theoretical stresses computed by the Boussinesq theory at the same point are tabulated below.

Single Tire			Dual Tire		
Load	3 in. Surf.	6 in. Surf.	Load	3 in. Surf.	6 in. Surf.
5000	1.72*	1.52*	9000	1.31*	1.33*
9000	1.61	1.42	13500	1.23	1.36
13500	1.38*	1.23*	18000	1.25*	1.32*
Avg.	1.57	1.39		1.26	1.34

*Not shown in the figures included with this report.

As can be seen the ratios are greater for the single tire than for the dual and for the smaller loads than for the larger ones. Deeper in the subgrade, 6 inches below the interface the measured stresses are approximately the same as those computed by the Boussinesq theory.

The modulus of elasticity data, Fig. 5a, show that the E of the sand asphalt base is 4 or more times that of the subgrade and on that basis it would be presumed that the subgrade stresses, in accordance with the two layer theories would be appreciably less than those computed by the Boussinesq theory. Instead, they are considerably greater. The Griffith-Fröhlich theories demonstrate that in a material whose modulus of elasticity increases in direct proportion to the confining pressure there is a concentration of stress immediately below the load. A concentration factor of 4 in the G-F equations (which has been verified by limited tests of cohesionless sands) gives a maximum stress 1.33 times the Boussinesq; a concentration factor of 5 gives a maximum stress 1.63 times the Boussinesq. Of all the base materials tested the sand asphalt has a modulus of elasticity that most nearly resembles that of a cohesionless sand -- a nearly linear increase of E with increasing confining pressure. Further, it is the only base material in which the ratio of the base E to the subgrade E increases substantially with increasing pressure. It is the authors' opinion that the stress concentration found just below the interface of the sand asphalt base is similar to the stress concentration described by the Griffith-Fröhlich equations. Deeper in the elastic subgrade, the stresses return to the Boussinesq as might be expected.

Soil Cement Bases

The test results for the 8 in. soil bound Macadam-cement are given on Figs. 19 and 20 and the 6 in. soil bound Macadam cement on Figs. 21 through 26. The stresses in the subgrade are considerably less than those found below the topsoil, soil bound Macadam, and sand asphalt bases. The reduction is greater beneath the

in. thick base than the 6 in. thick base as might be expected. Each graph shows ıe stresses computed by the two layer elastic theory by assuming that the asphaltic ırface has the same modulus of elasticity as the base. This is not strictly valid ecause the asphaltic concrete is less rigid than the soil cement, but it will erve as an index for comparison. The stresses beneath the 8 in. thick soil cement ıse (where the base thickness is 73 per cent of the total pavement) are between ıose computed for a ratio of base E to subgrade E of 10 and those for a ratio of 0. The laboratory tests, Figs. 5, 6 show an E ratio of 100 or more for very all confining pressures dropping to about 55 for confining pressures between and 40 psi. Plate load tests on the base found a ratio of 100 (computed by e elastic layer theory). Since the surface is not as rigid as the base, the fective ratio would appear to be 50 or slightly less which agrees with the st results.

The results for the 6 in. base and 3 in. surface are equivalent to an elas- city ratio between 10 and 100, but closer to 10. This is to be expected because e less rigid surface is one third the total pavement thickness. The measured esses with the 6 in. base and 6 in. thick surface correspond to a slightly er elasticity ratio, approximately 10. These differences are to be expected ause the effective rigidity of the pavement (base plus surface) becomes less the proportion of surface to base increases.

The agreement between the measured stresses and the stresses computed by the layered elastic theory for the soil cement tends to verify the authors' ex- nation of the lack of validity of the layered theory for the other bases. The ar tests show that the soil cement is capable of withstanding appreciable sile stresses while the others are not. In addition, the modulus of elasci- y of the soil cement, while increasing with increasing confining pressure, s not change as much relatively as the others. This can be seen by the per- cage increase of E with respect to E measured at 0 confining pressure produced

y increasing the confining pressure from 0 to 20 psi.

Base	E at 0 psi	E at 20 psi	ΔE	Increase
opsoil (Actual)	1.6 ksi	4.9 ksi	3.3 ksi	206%
oil Bound Macadam	3.0	10.6	7.6	254
and Asphalt	1.2	5.8	4.6	384
oil Cement	49	62	13	26

epeated Load-Soil Cement Base

Some concern was felt about the continued load spreading efficiency of the oil cement after repeated loading. It has been observed that soil cement pavements tend to develop hair cracks that divide the surface into large poly gonal ocks. In order to investigate this possibility the 6 in. thick soil cement base in. surface pavement was subjected to 1000 cycles of load-unload with the 13,500 single tire. In employing this gross overload on a single tire, equivalent a 27,000 lb axle, it was hoped to magnify any effects of base cracking. The sults, Fig. 25, show no change of stresses in the subgrade 3 in. below the ograde-base interface.

fect of Inundation.

All the tests had been made with the moisture content of the soil subgrade l the base near the respective optimum moistures. Holes were drilled through 6 in. base soil cement, 6.5 in. surface pavement and through the entire depth the subgrade. These were filled with water and kept full so as to inundate subgrade and base. Moisture tests made at regular intervals in observation es between the inflow holes showed an increase in saturation from the original ue of about 75 per cent to an average of 96.5 per cent in one week, after which remained constant. Tests were conducted with dual wheels and loads of 9000, 00, and 18000 lb. The results (data for the 13500 lb load are given on Fig. showed possibly a slight reduction in the stresses just below the subgrade- interface. Since inundation caused a small reduction in the modulus of sticity of the subgrade but little change in the soil cement base, the elasticity

'atio was increased. Theoretically, the stress should have decreased slightly, nd the tests verify it.

ffect of Overlay

A number of the pavement systems were tested with both 3 in. thick and 6 n. thick asphaltic surfaces to determine the load spreading effects of a 3 in. hick overlay. The results can be seen by comparing the graphs of the 3 in. and in. surfaces for the topsoil II, sand asphalt, and 6 in. soil cement base pave- ents. They show that the overlay causes a stress reduction slightly less than iat produced by an equal thickness of a homogeneous, isotropic elastic solid. ı other words, the stress reduction was comparable to that produced by an equal ıickness of topsoil or soil bound Macadam base and somewhat more effective than iat of an equal thickness of sand asphalt.

Acknowledgments

This work has been sponsored by the Georgia State Highway Department and e U. S. Bureau of Public Roads, through the Engineering Experiment Station the Georgia Institute of Technology. The authors are indebted to Messrs. E. Hedges, W. H. Johnson, F. Chabrol, C. E. Snepp, W. L. Boyd, A. Schwartz, ł D. Wheeless, Graduate Research Assistants for their part in these investigations.

References

Boussinesq, J., Application des Potentiels a l 'Etude de l'Equilibre et du Mouvement des Solides Elastiques; Paris, 1885. (Gauthier-Villars.)

Love, A. E. H., The Stress Produced in a Semi-infinite Body by Pressure on Part of the Boundary, Phil. Trans. Roy. Soc., series A Vol. 228 (1928) pp. 377-420.

Steinbrenner, W., Tafeln zur Setzungsberechung; Die Strasse Vol. 1 (1934).

Newmark, N. M., Influence Charts for Computation of Stresses in Elastic Foundations, Univ. of Illinois Eng. Exp. Sta. Bull. No. 338, Urbana, 1942.

Newmark, N. M., Influence Charts for Computation of Vertical Displacements in Elastic Foundations, Univ. of Illinois Eng. Exp. Sta. Bull. No. 367, Urbana, 1947.

Fadum, R. E. Influence Values for Vertical Stresses in a Semi-Infinite Solid due to Surface Loads, Harvard University, 1941.

Fergus and Miner, Distributed Loads on Elastic Foundation, Proc. Hwy. Res. Board, Vol. 34 (1955) pp. 582-597.

Foster & Ahlvin (1954), Stresses and Deflections Induced by a Uniform Circular Load, Proc. Hwy. Res. Board, Vol. 33 (1954), pp. 467-470.

Deresiewicz, H., The Half-Space Under Pressure Distributed Over an Elliptical Portion of its Plane Boundary, Trans. ASME, Journal of Applied Mechanics, 1960.

Griffith, J. H., The Pressures Under Substructures; Engineering and Contracting, Vol. 1 (1929), pp. 113-119.

Fröhlich, O. K., Druckverteilung im Baugrunde; Berlin, 1934, (J. Springer).

Ohde, J., Zur Theorie der Druckverteilung im Baugrunde, Der Bauingenieur, Vol. 20 (1939), pp. 451-459.

Buisman, A. S., Druckverdeeling in bouwgrond in verband met ongelijke samendrukbaarheid in horizontale en verticale richting; De Ingenieur 47 (1932), pp. B175-180.

Wolf, K., Ausbreitung der Kraft in der Halbebene und im Halbraum bei anisotropem Material, Zeitschift angew. Math. und Mech. Vol. 15 (1935) pp. 249-254.

Jelinek, R., Der Boden als querisotropes Medium, Abhandlungen über Bodenmechanik und Grundbau, Berlin 1948 (E. Schmidt) pp. 19-24.

Jelinek, R., Die Kraftausbreitung im verallgemeinerten ebenen Spannungszustand für querisotrope Böden; Abhandlungen über Bodenmechanik und Grundbau Berlin 1948 (E. Schmidt) pp. 24-27.

Jelinek, R., Die Kraftausbreitung im Halbraum für querisotrope Böden; Abhandlungen über Bodenmechanik und Grundbau Berlin 1948 (E. Schmidt) pp. 28-33.

3. Koning, H., Stress Distribution in a Homogeneous, Anisotropic, Elastic Semi-Infinite Solid; Proceedings, Fourth Int. Conf. Soil Mech. and Found. Engrg. London, 1957, Vol. 1, pp. 335-338.

). Westergaard, H. M., A Problem of Elasticity Suggested by a Problem in Soil Mechanics, Soft Material Reinforced by Numerous Strong Horizontal Sheets, Contribution to Mechanics of Solids, Stephen Timoshenko 60th Anniversary Volume, New York, 1938 (MacMillan).

. Burmister, D. M., The Theory of Stresses and Displacements in Layered Systems and Application to the Design of Airport Runways, Proceedings, Highway Research Board, Vol. 23 (1943) pp. 126-148.

. Burmister, D. M., The General Theory of Stresses and Displacements in Layered Systems, Journal of Applied Physics, Vol, 16, (1945) pp. 296-302.

. Schiffman, R. L., The Use of Integral Transforms in the Solutions of Three-layer Soil Problems (unpublished).

. Fox, L., Computation of Traffic Stresses in a Simple Road Structure, Road Research Laboratory (England), Road Research Paper No. 9, London, 1948, (H. M. Stationary Office), also, Proc. Sec. Inf. Conf. Soil Mech. and Found. Engrg. Vol II, pp. 236-246.

. Hank and Scrivner, Some Numerical Solutions of Stresses in Two and Three Layered Systems, Proceedings Highway Research Board, Vol. 28, 1948, pp. 457-468.

Acum, W. E. A. and Fox L., (1951) Computation of Load Stresses in a Three-Layer Elastic System, Geotechnique Vol. II, No. 4, pp. 293-300.

Steiner, Handbuch der Ingenieurwissenschaften II Bd., Der Bruckenbau, p. 195, Leipzig, 1882, (W. Engelmann).

Strohschneider, O., Elastische Druckverteilung und Drüchüberschreitung in Schüttungen, Sitz. Berichte der K. K. Akad. Wiss. Wien, Vol. 121 (1912) p. 301.

Moyer J. A., Distribution of Vertical Soil Pressure; Eng. Record, Vol. 69 (1914) p. 608 and Vol. 71 (1915) p. 330.

Enger, M. L., High Unit Pressures Found in Experiments on Distribution of Vertical Loading through Sand; Eng. Record, Vol. 73 (1913) p. 106.

Goldbeck, A. T., Distribution of Pressures through Earth Fills, Proc. ASTM, Vol. 17 (1917) p. 640.

Kögler, F. & Scheidig, A., Druckverteilung im Baugrunde, Bautechnik Vol. 5, (1927) p. 418, Vol. 6, (1928) p. 205, Vol. 7 (1929), p. 268.

Spangler, M. G. and H. O. Ustrud, Wheel Load Stress Distribution through Flexible Type Pavements; Proceedings, Highway Research Board, Vol. 20 (1940) pp. 235-257.

Waterways Experiment Station, Investigations of Pressures and Deflections for Flexible Pavements, Report No. 1, Homogeneous Clayey-Silt Test Section, Vicksburg, Miss., 1951.

4. Waterways Experiment Station, Investigations of Pressures and Deflections for Flexible Pavements, Report No. 4, Homogeneous Sand Test Section, Vicksburg, Miss., 1954.

5. Turnbull, W., A. A. Maxwell and R. G. Ahlvin, Stress Distribution in Homogeneous Soil Masses, Proceedings, Fifth Int. Conf. Soil Mech. and Found. Engrg., Paris, 1961 Vol. II, pp. 337-345.

6. McMahon, T. F. and E. J. Yoder, Design of a Pressure-Sensitive Cell and Model Studies of Pressures in a Flexible Pavement Subgrade, Proceedings, Highway Research Board, Vol. 39 (1960) pp. 650-682.

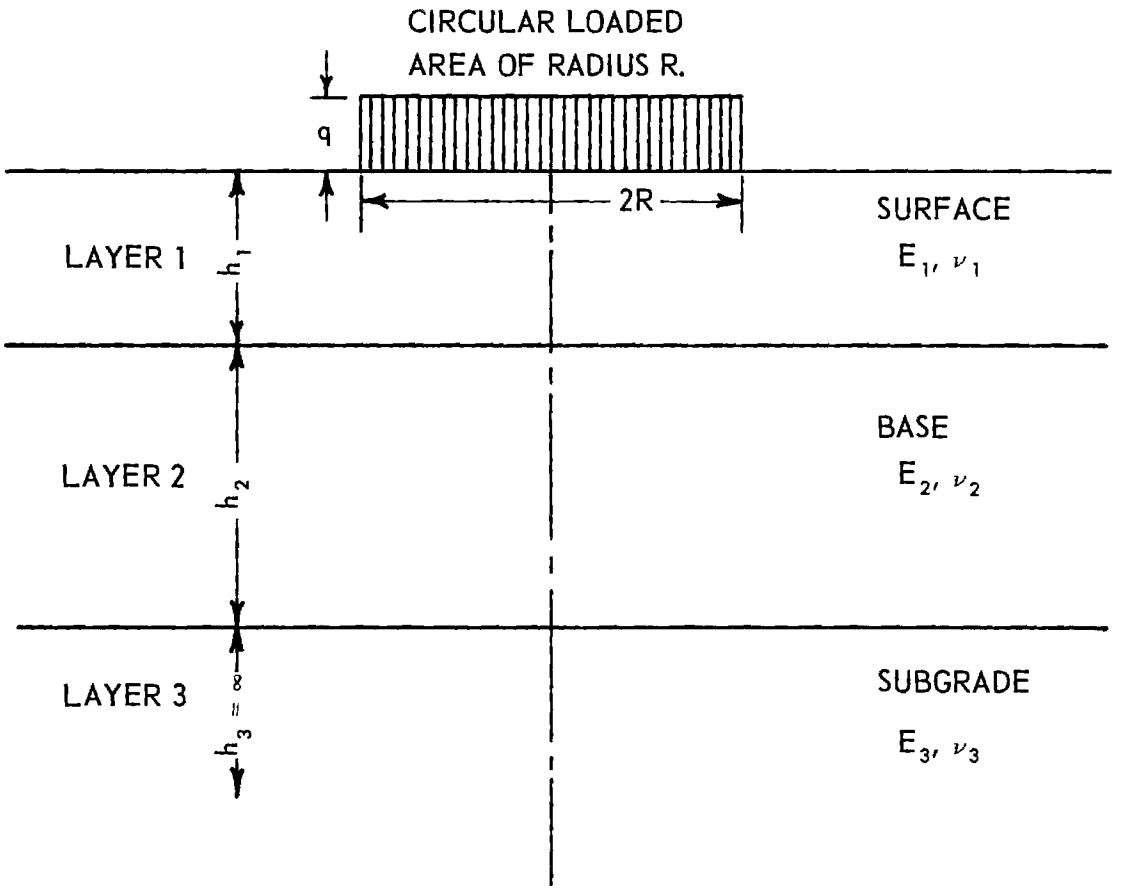

Figure 1. A flexible pavement system.

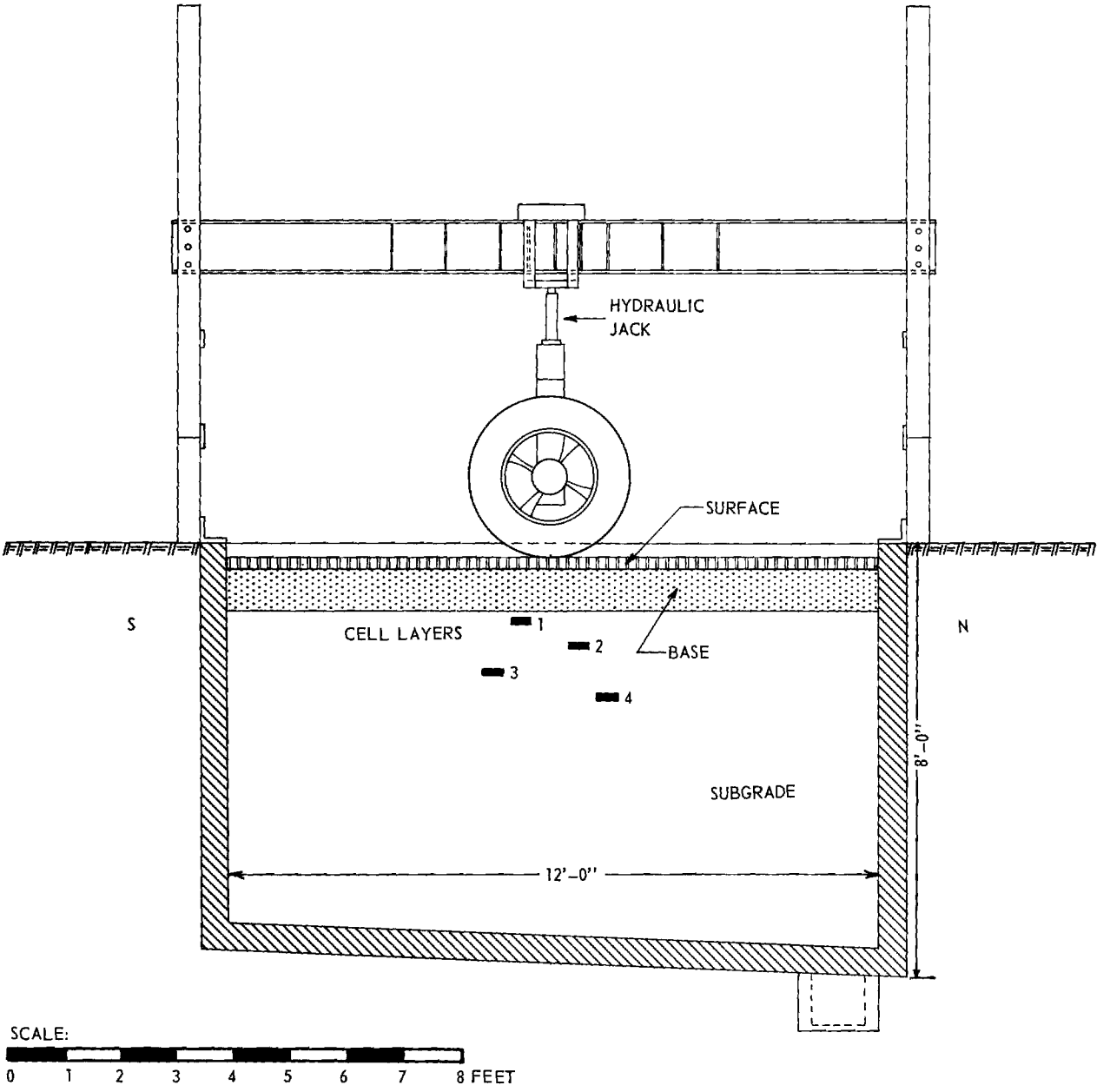

Figure 2b. Cross-section of the test pit showing position of layers of pressure cells and the loading equipment.

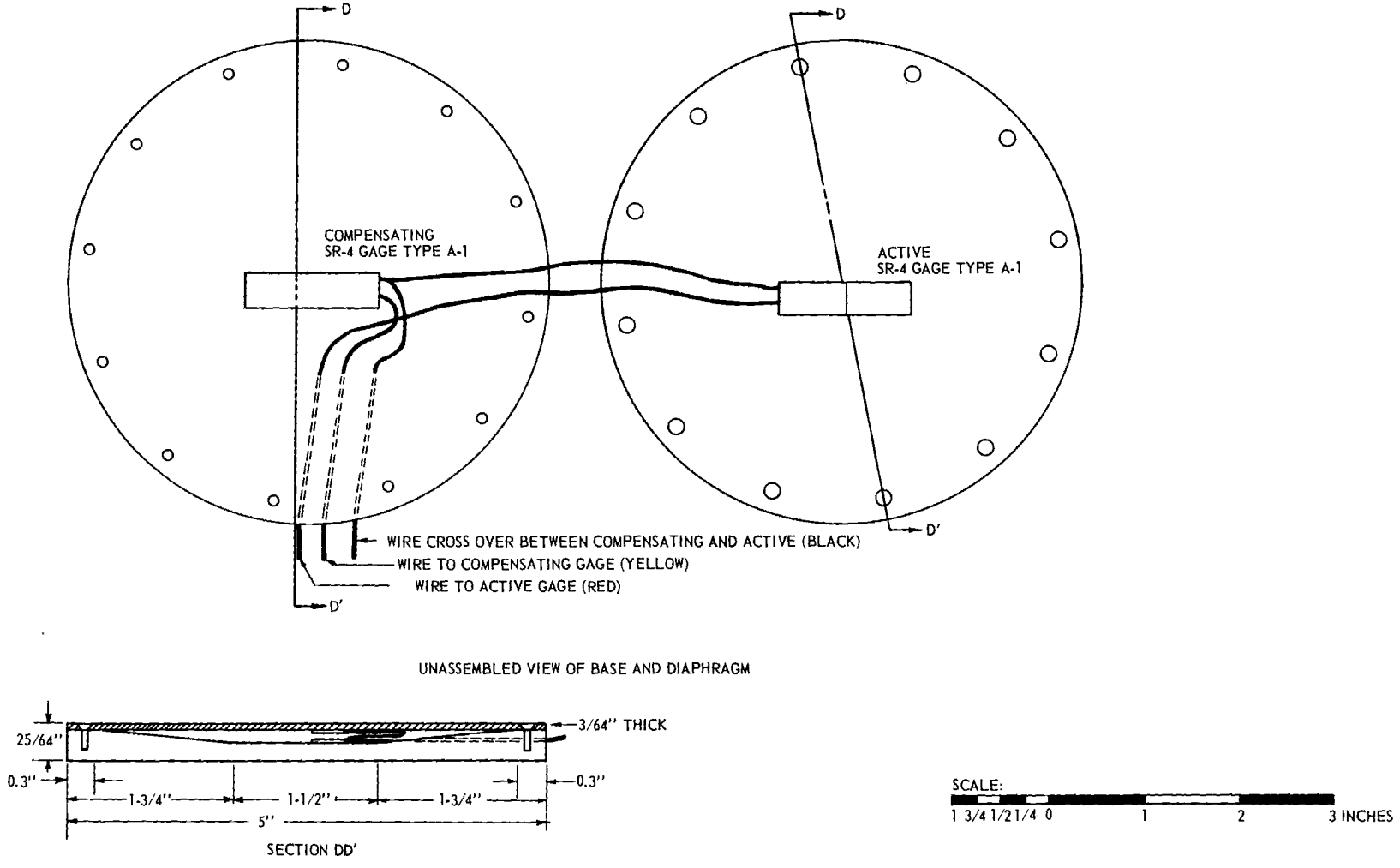

Figure 3. Typical pressure cell.

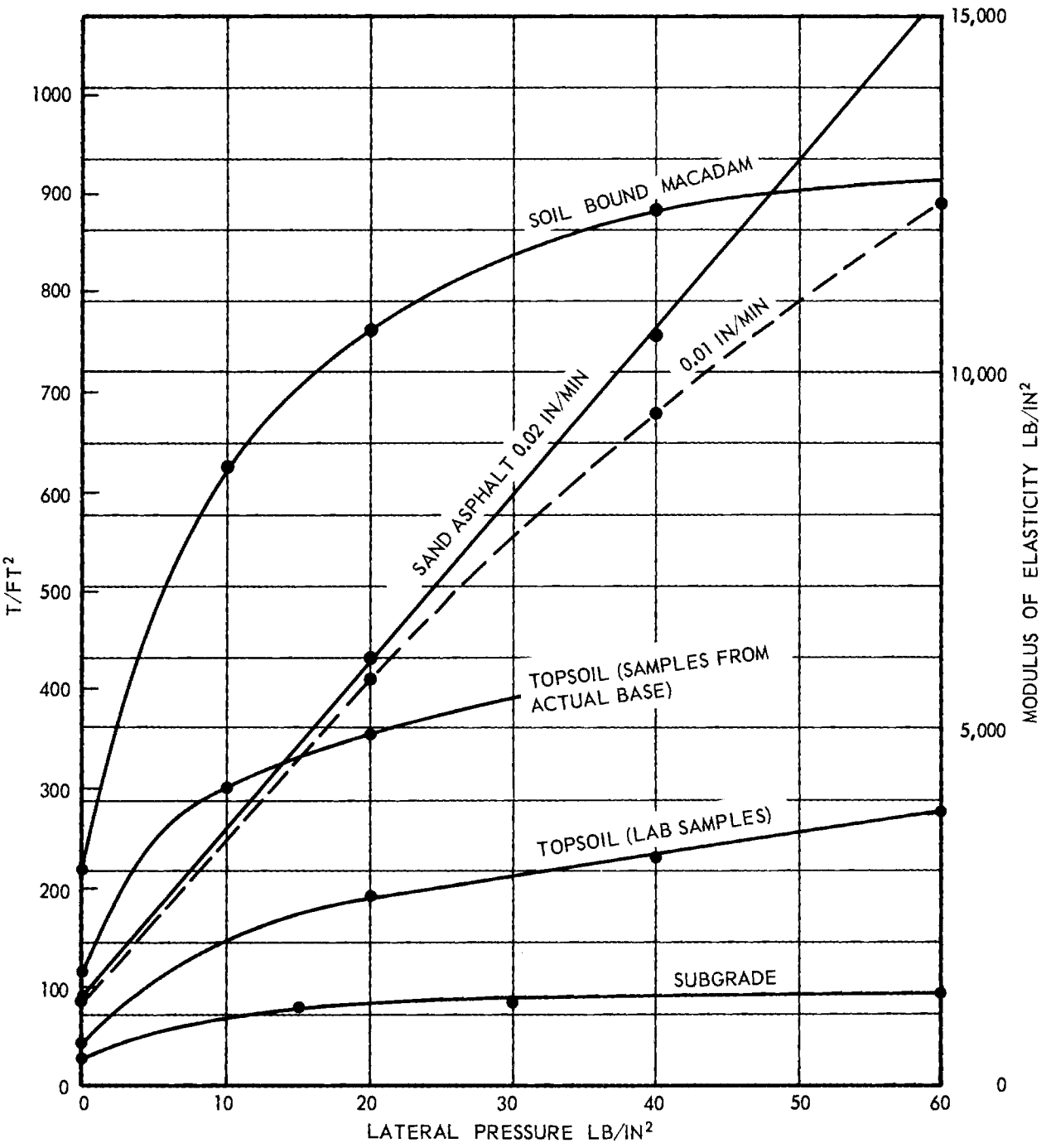

Figure 4a. Modulus of elasticity, E, of base and subgrade materials obtained by triaxial tests at different confining pressures.

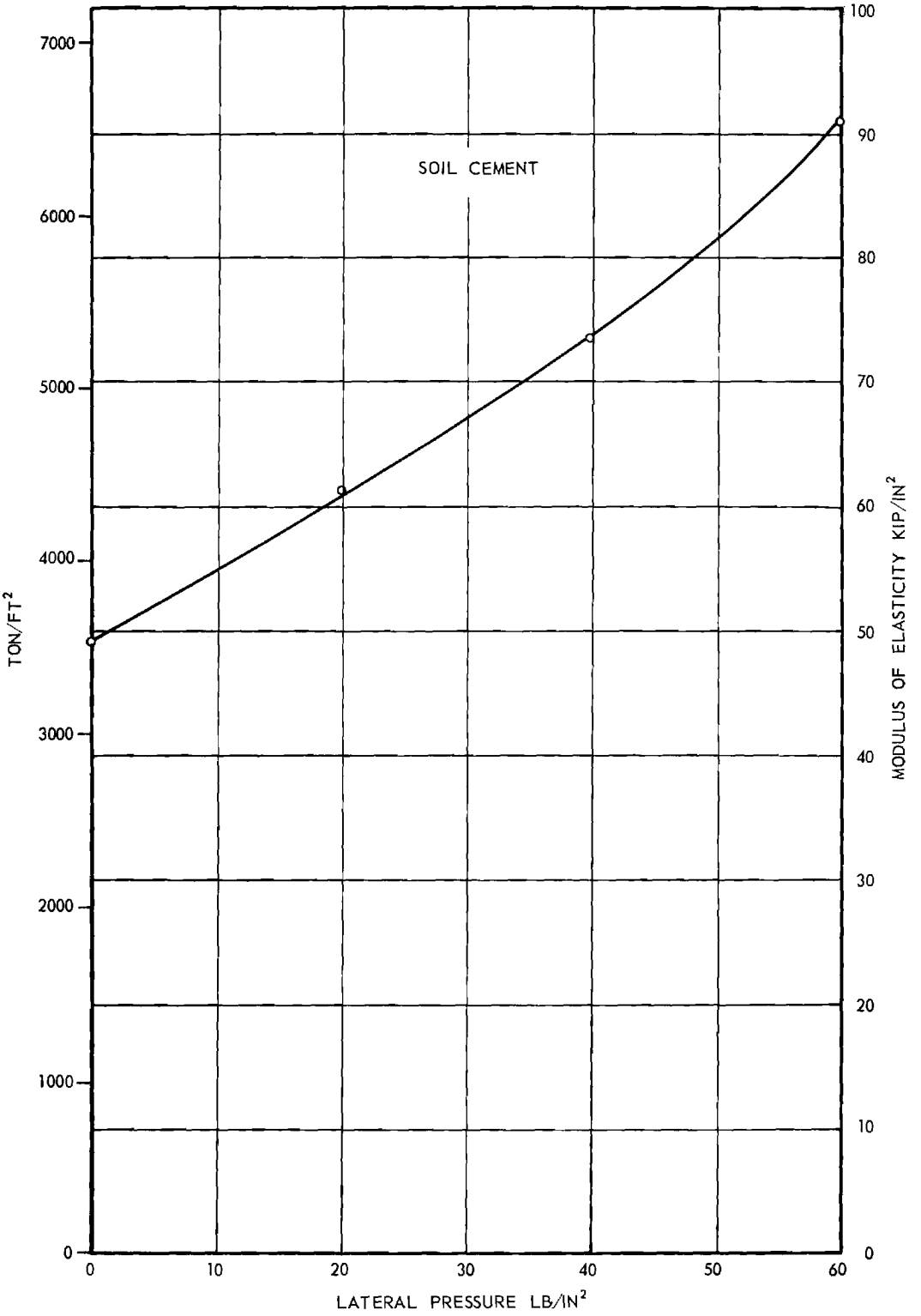

Figure 4b. Modulus of elasticity, E, of soil cement base material obtained by triaxial tests at different confining pressures.

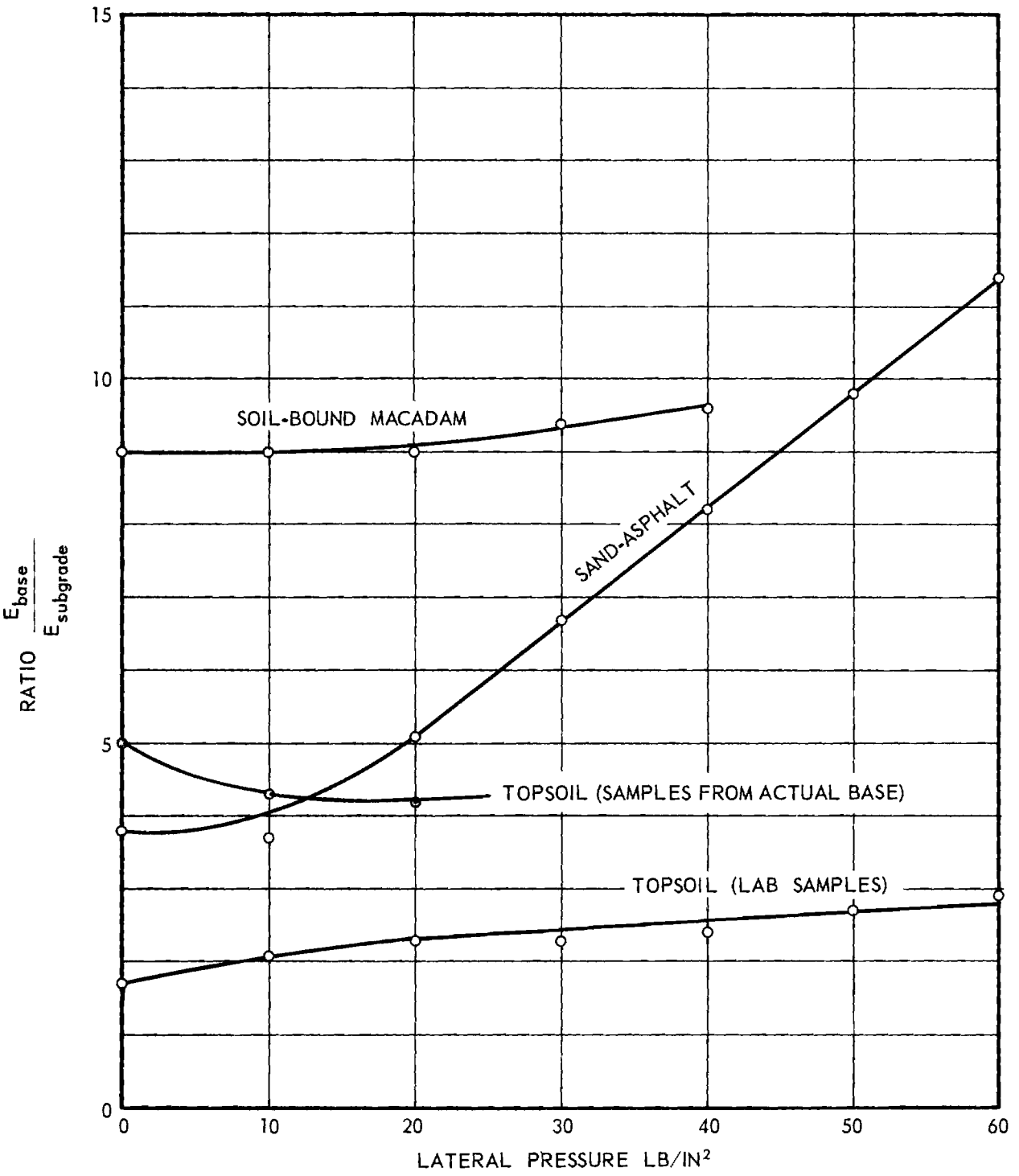

Figure 5a. Ratio of modulus of elasticity of base material to subgrade soil at different confining pressures.

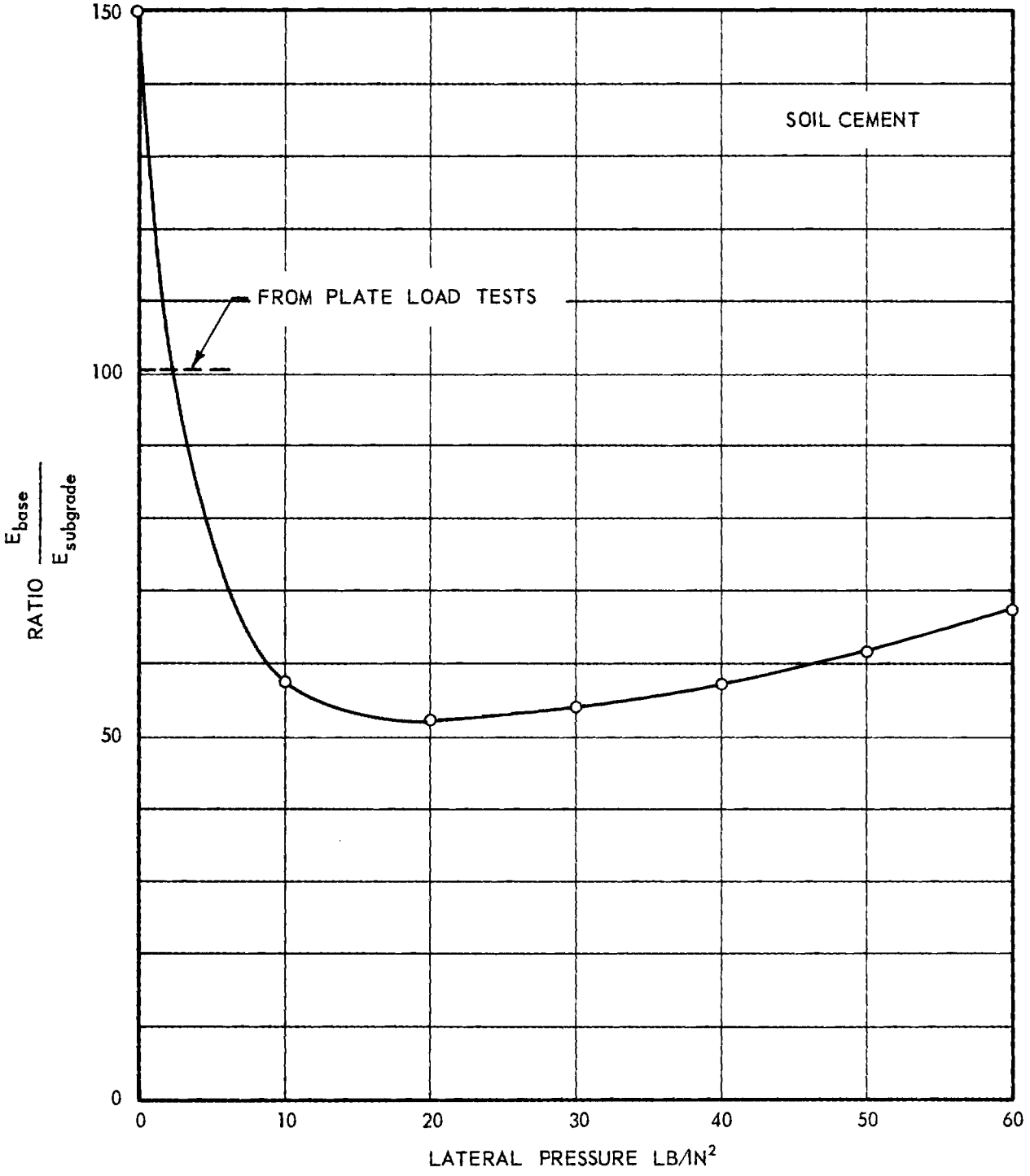

Figure 5b. Ratio of modulus of elasticity of soil cement base to subgrade at different confining pressures.

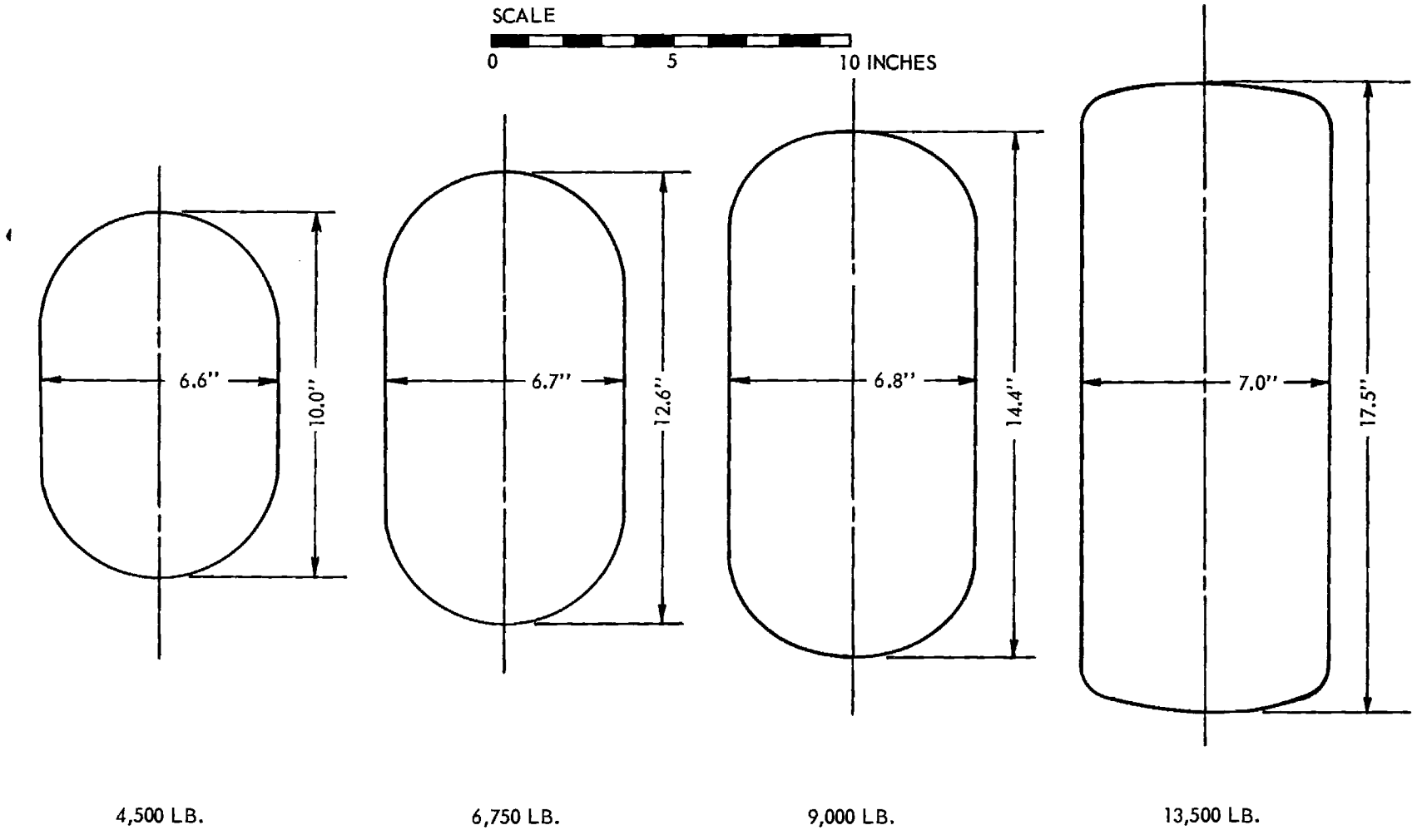

Figure 6. Typical tire prints for new 9 x 20 truck tire inflated to recommended pressure of 86 psi.

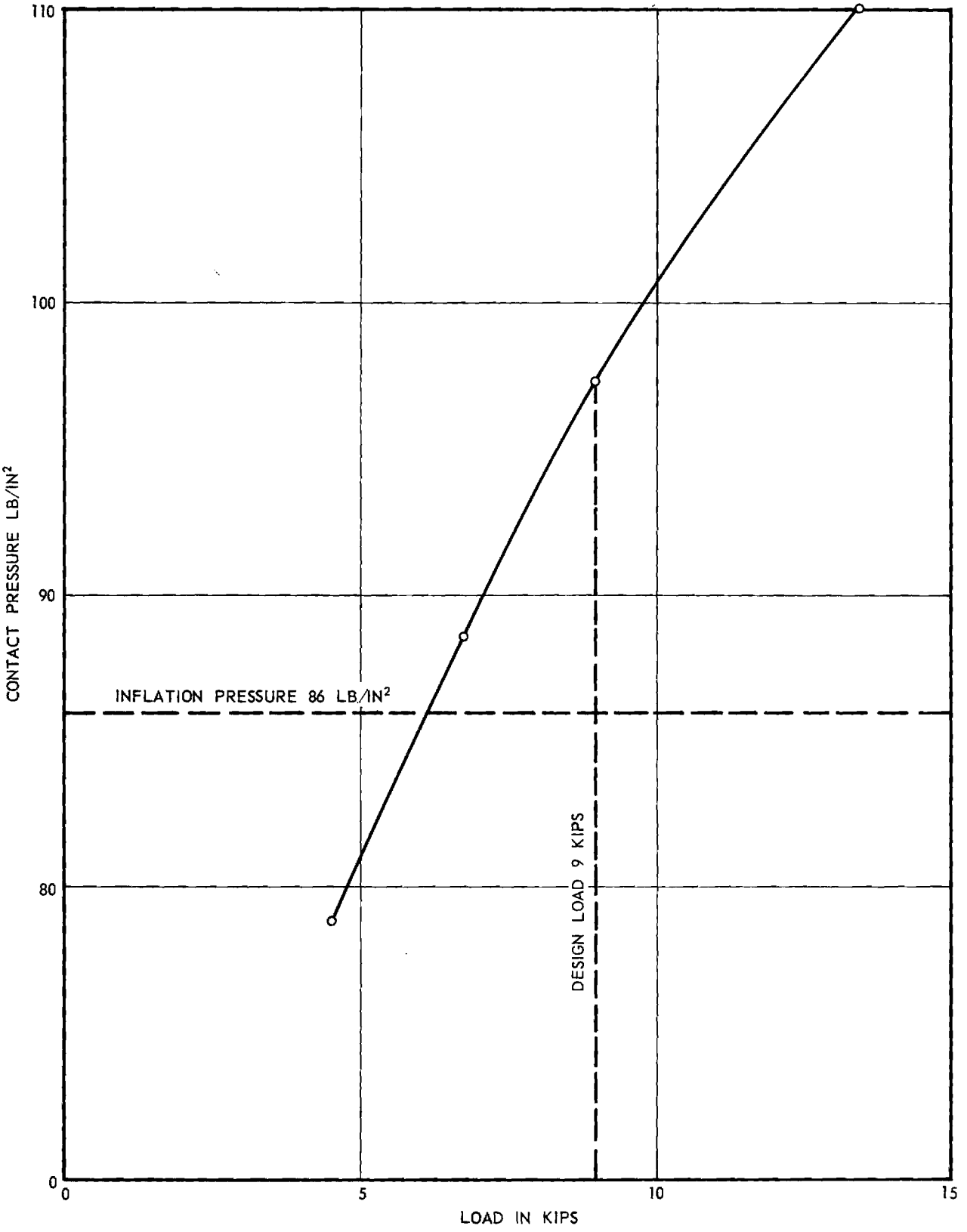

Figure 7. Variation of average contact pressure of a 9 x 20 truck tire as a function of tire load, at recommended inflation pressure of 86 psi.

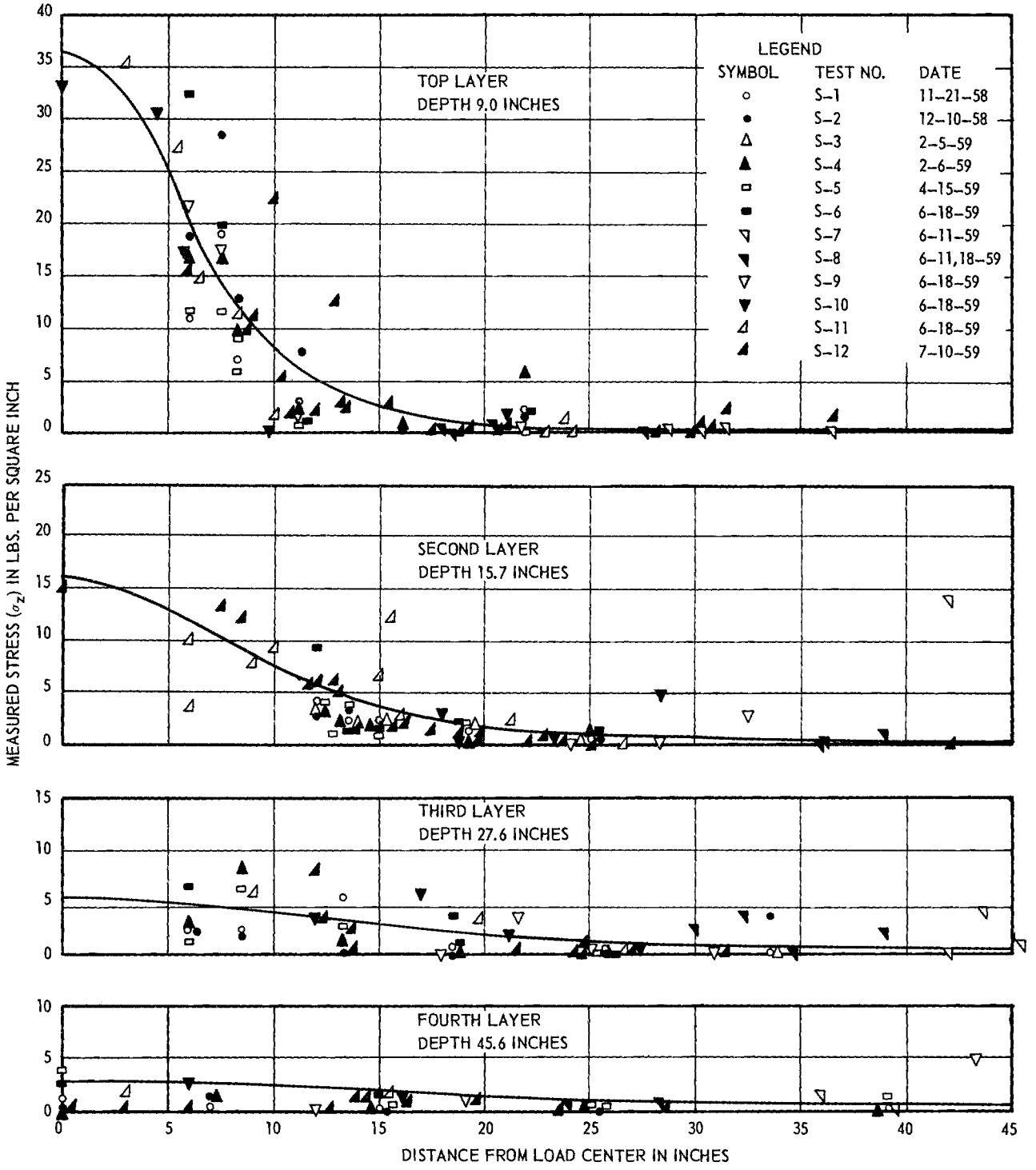

Figure 8. Measured stresses; single load 9000 lbs. topsoil I base 8 in. thick, 3 in. surface. Solid line is Boussinesq stress distribution.

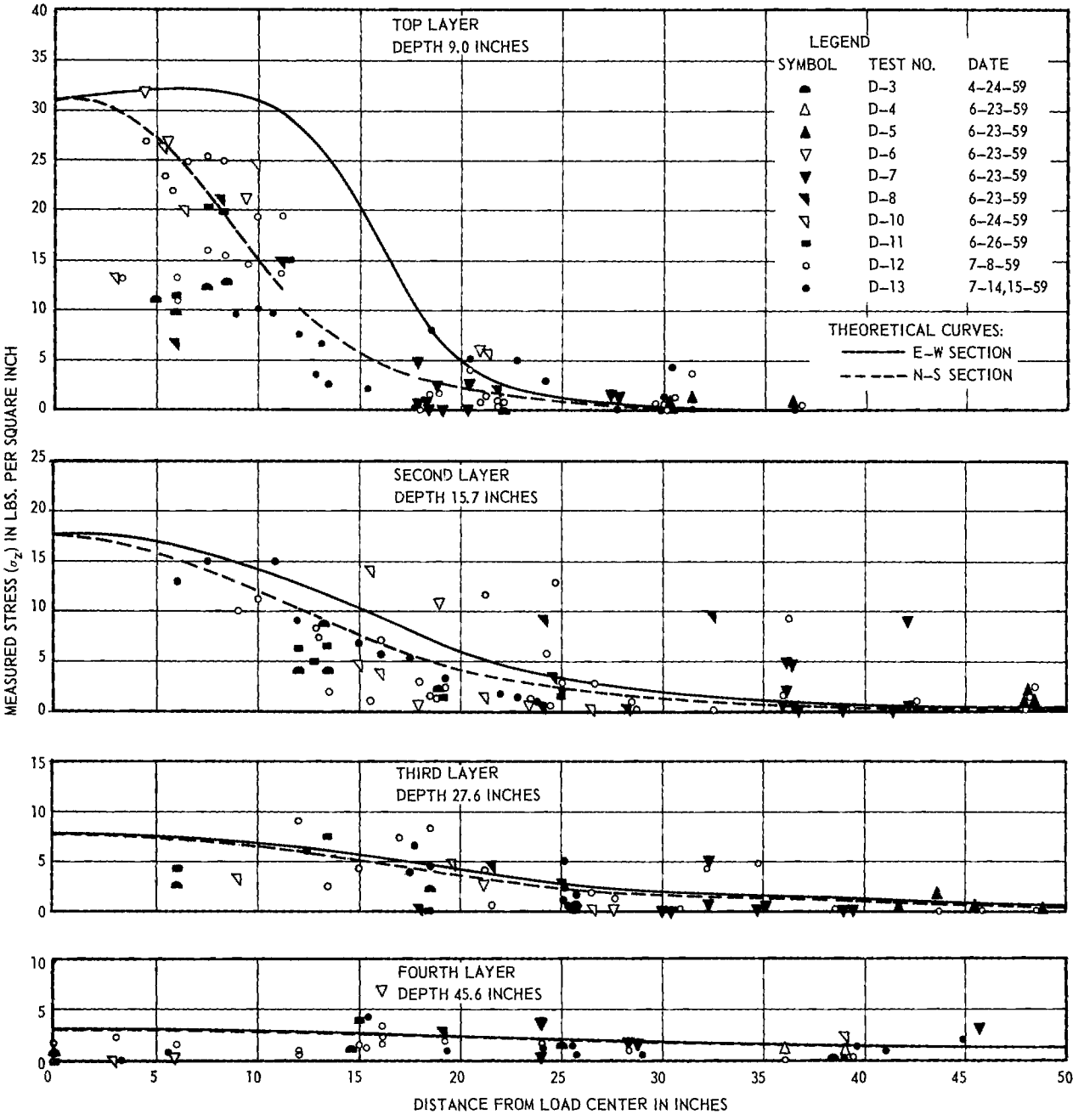

Figure 9. Measured stresses; dual load 13,500 lbs. topsoil I base 8 in. thick; 3 in. surface. Solid line is Boussinesq stress distribution parallel to the axle; dotted line is Boussinesq stress perpendicular to the axle.

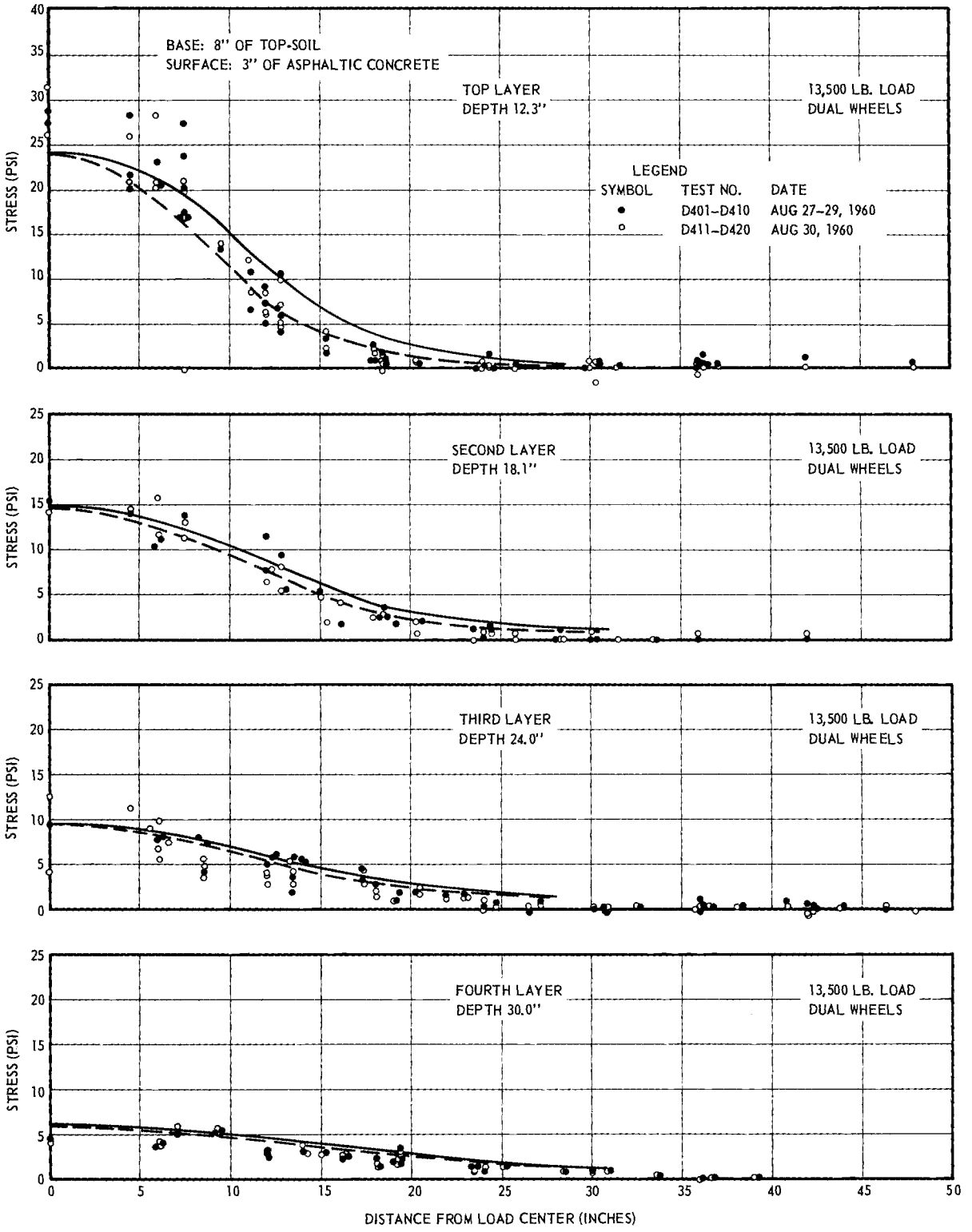

Figure 10. Measured stresses; dual load 13,500 lbs. topsoil II base 8 in. thick, 3 in. surface.

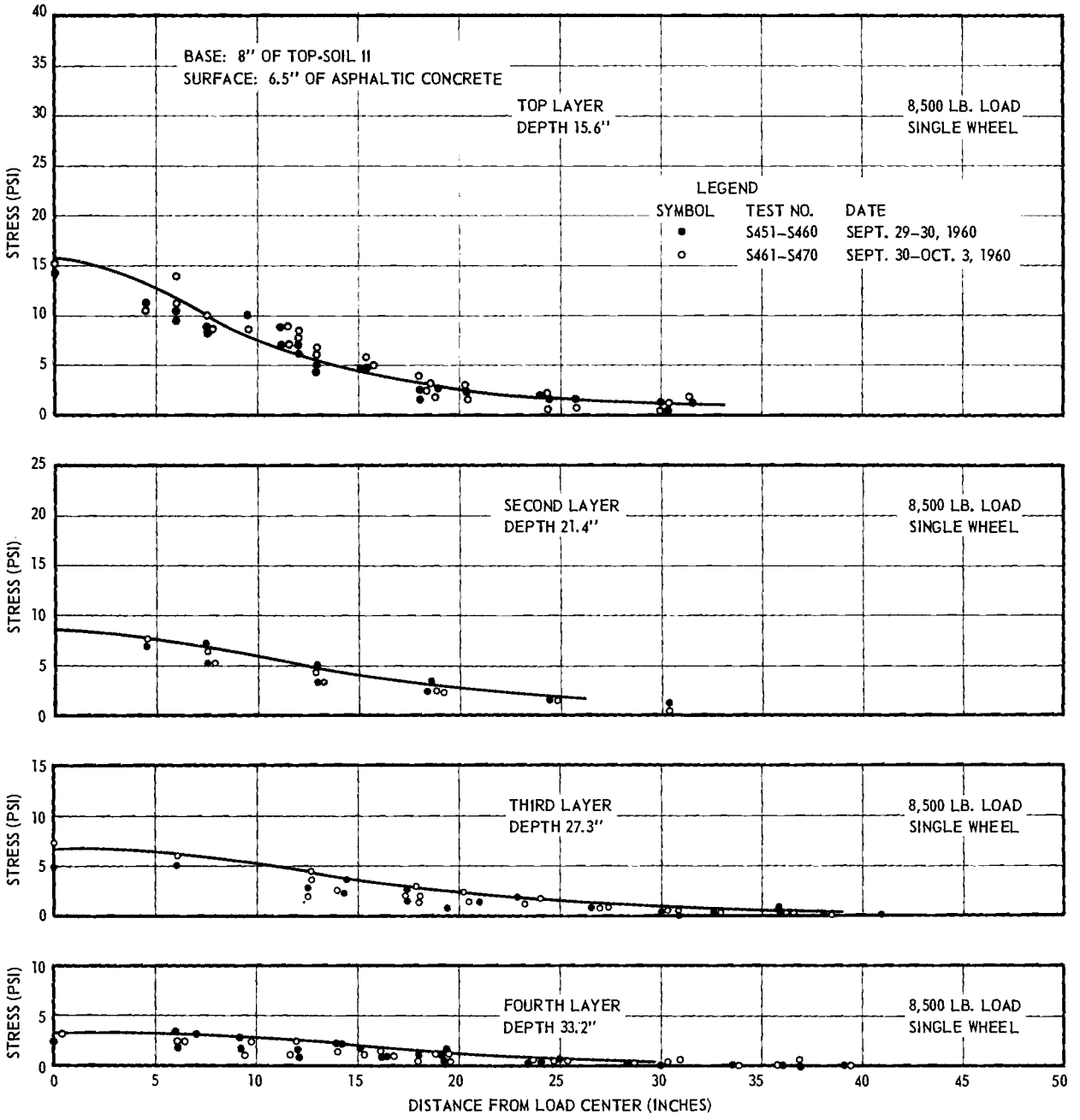

Figure 11. Measured stresses; single load 8,500 lbs. topsoil II base 8 in. thick, with 3 in. asphaltic concrete surface and 3.5 in. asphaltic concrete overlay.

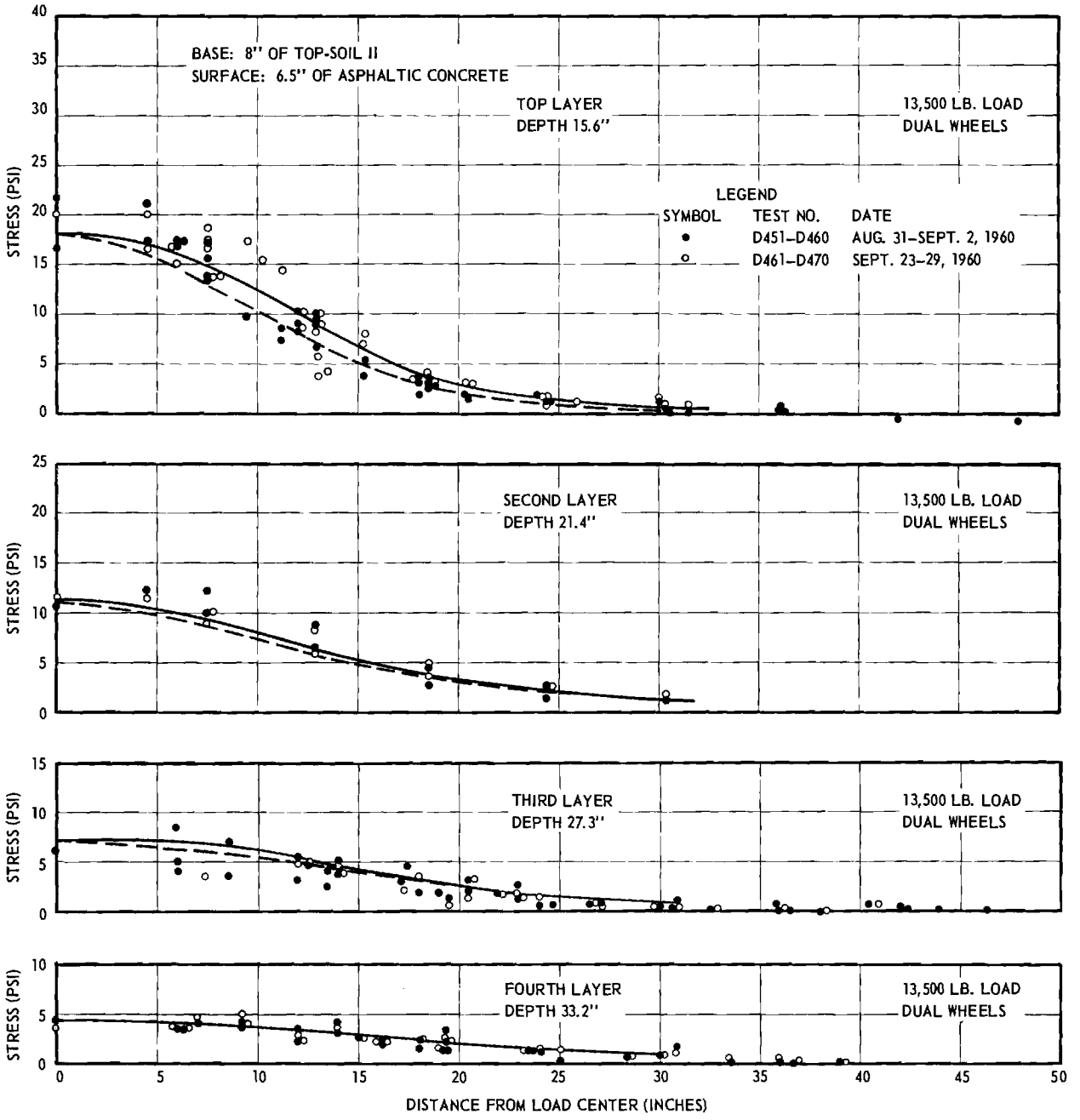

Figure 12. Measured stresses; dual load 13,500 lbs. topsoil II base 8 in. thick, 3 in. thick asphaltic concrete surface with 3.5 in thick asphaltic concrete overlay.

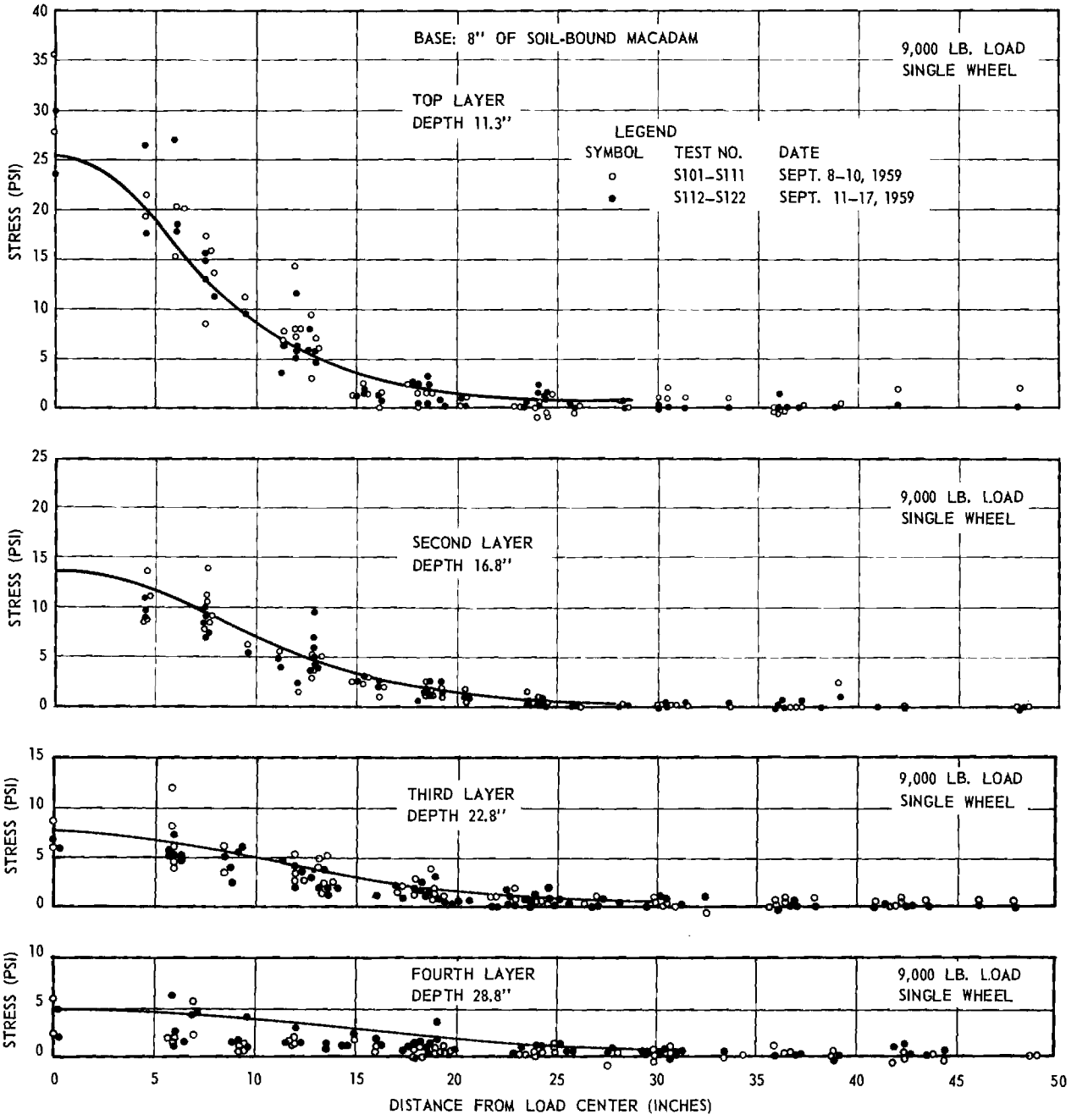

Figure 13. Measured stresses; single load 9,000 lbs soil-bound macadam base 8 in. thick; 3 in. asphaltic concrete surface.

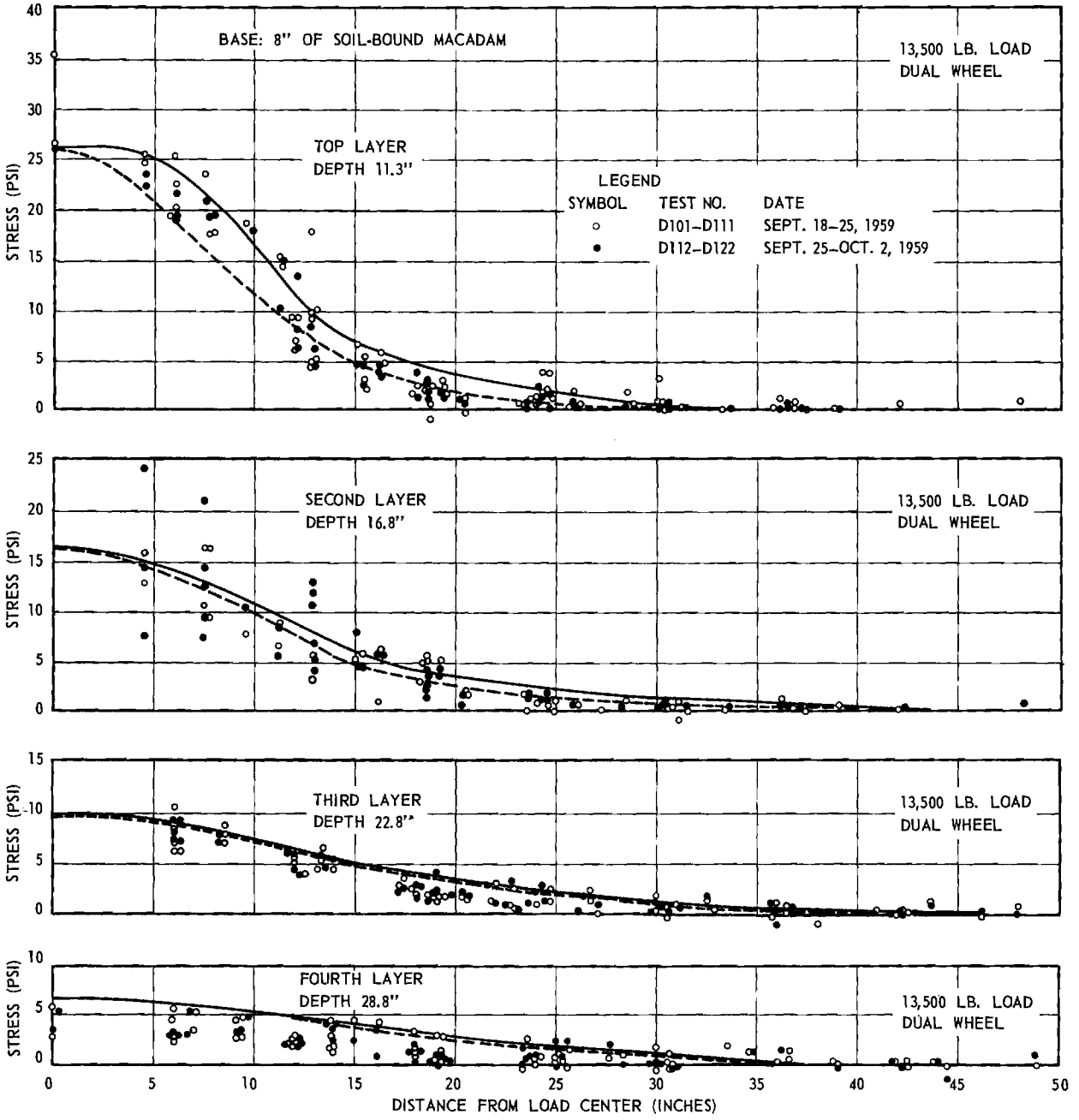

Figure 14. Measured stresses; dual load 13,500 lbs soild-bound macadam base 8 in. thick; 3 in. asphaltic concrete.

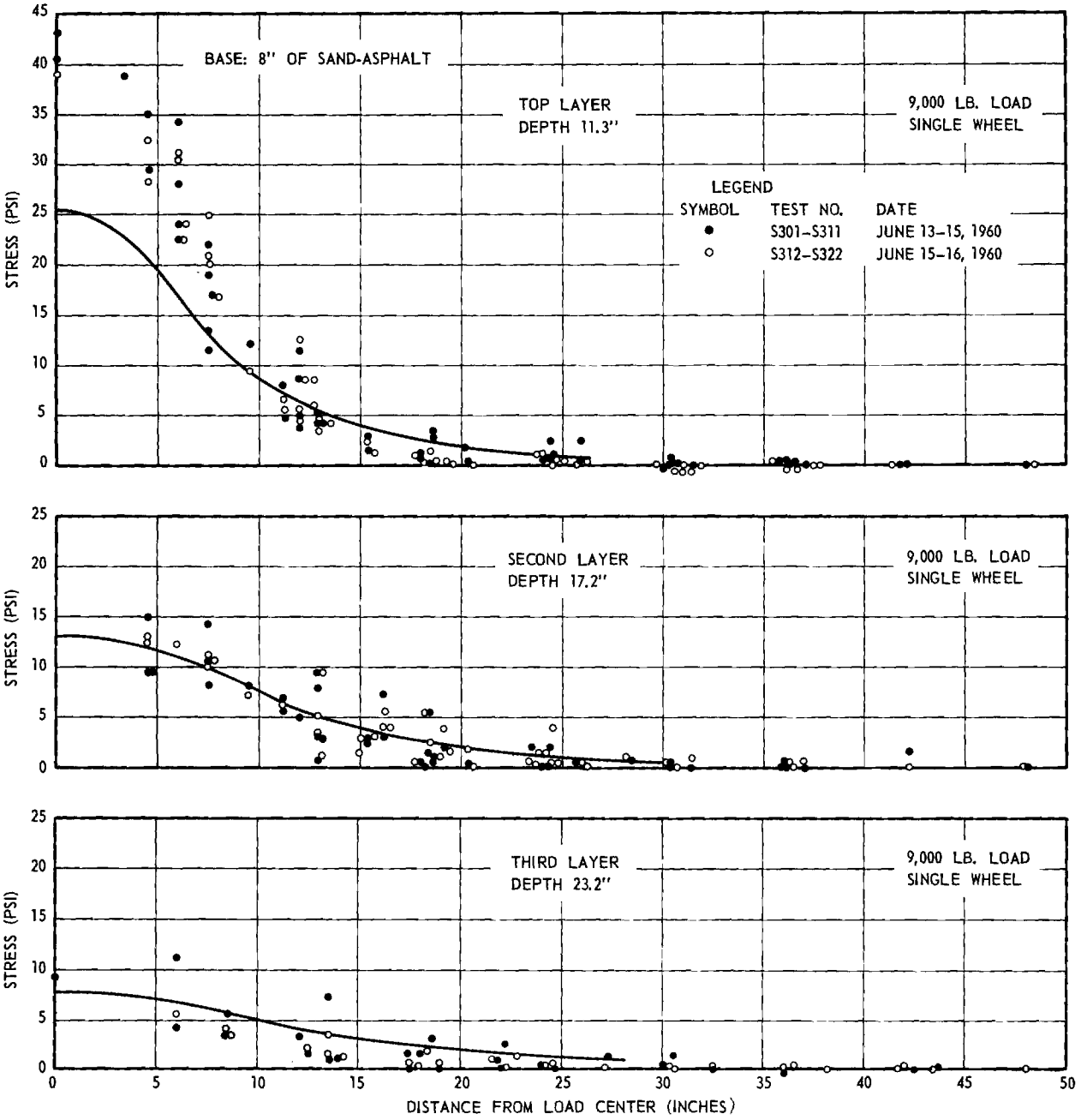

Figure 15. Measured stresses; single load 9,000 lbs sand-asphalt base 8 in. thick; 3 in. thick asphaltic concrete surface.

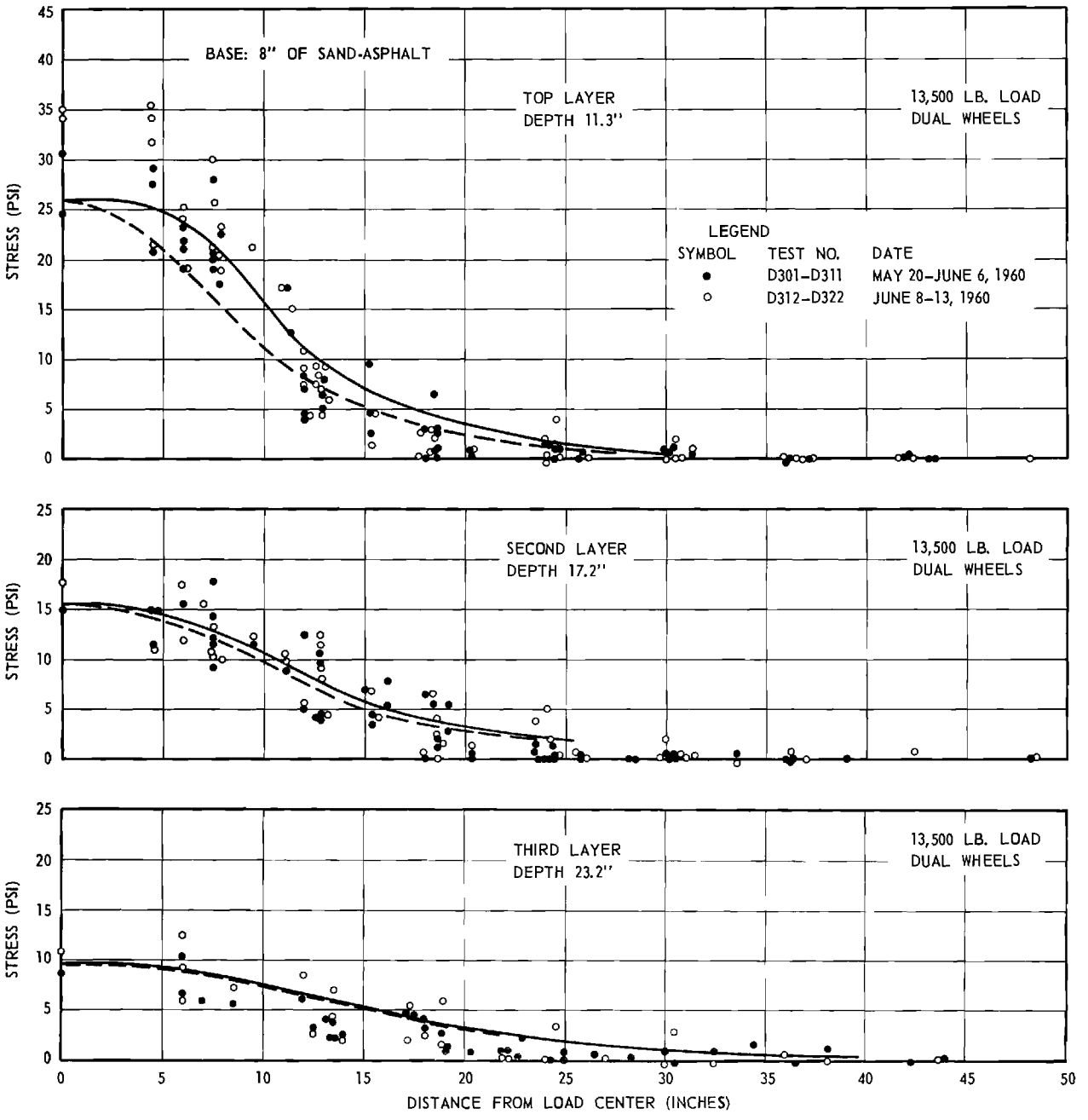

Figure 16. Measured stresses; dual load 13,500 lbs. sand-asphalt base 8 in. thick; 3 in. thick asphaltic concrete surface.

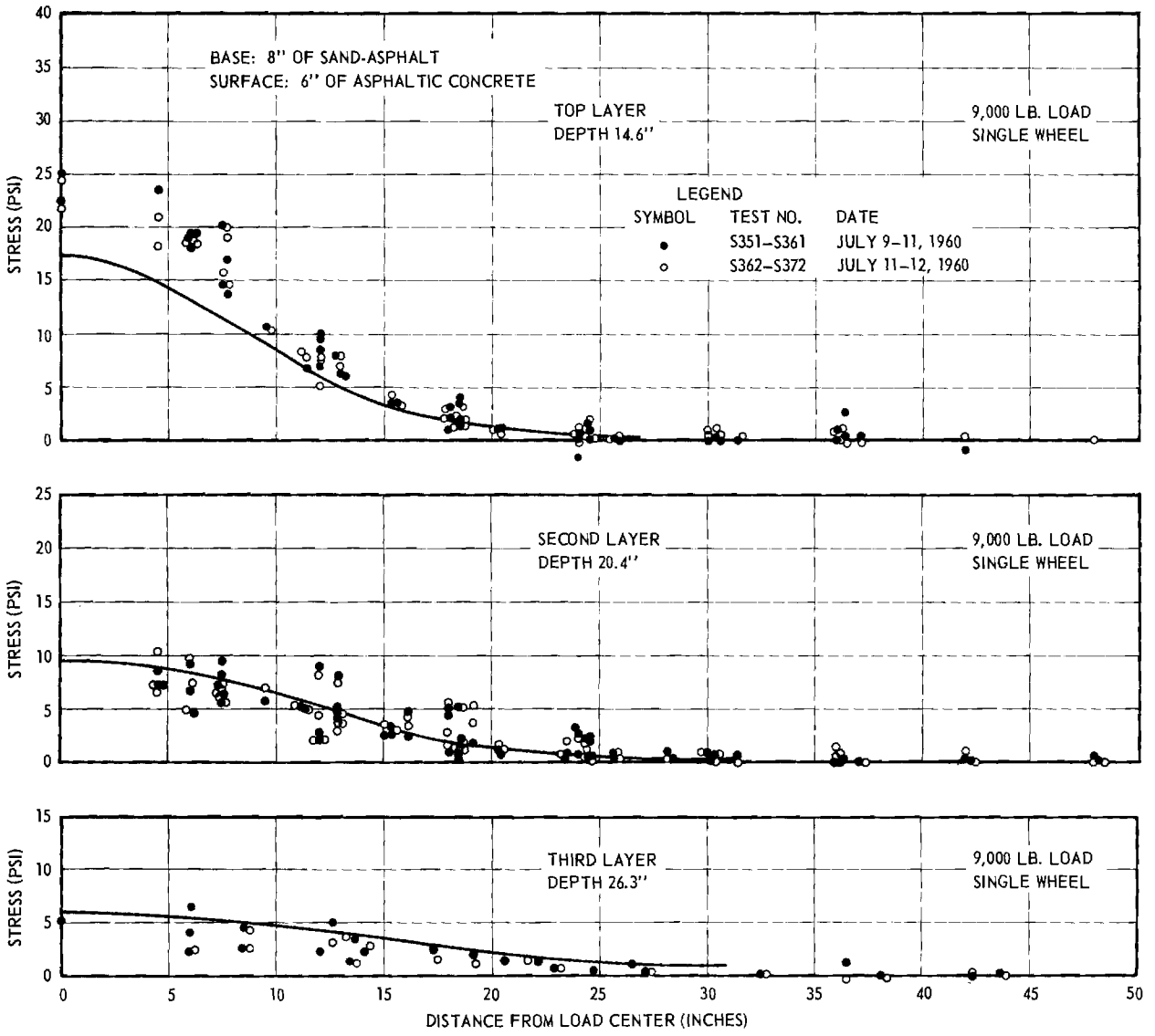

Figure 17. Measured stresses; single load 9,000 lbs. sand-asphalt base 8 in. thick; 3 in. asphaltic concrete surface with 3 in. asphaltic concrete overlay.

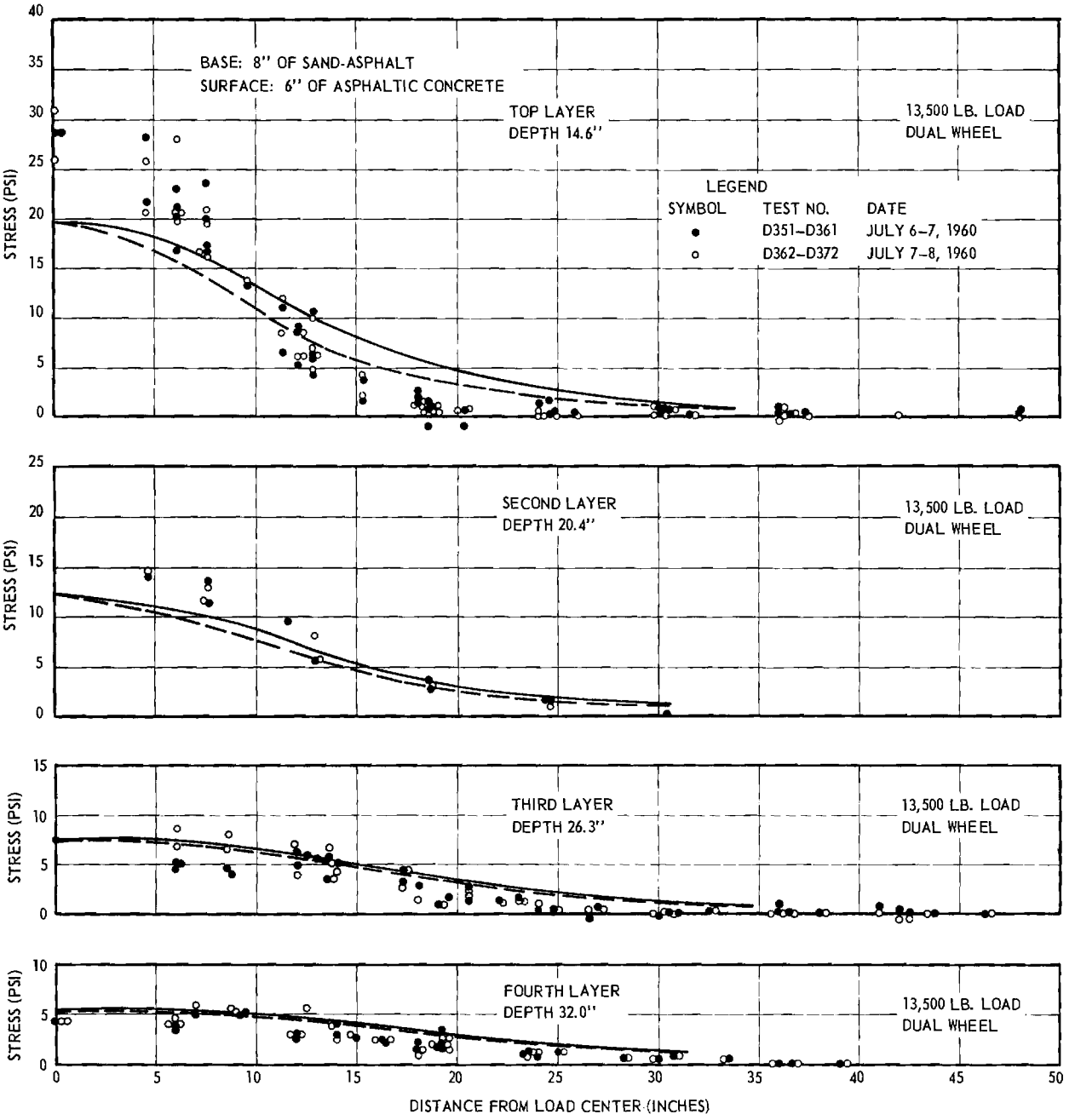

Figure 18. Measured stresses; dual load 13,500 lbs. sand-asphalt base 8 in. thick; 3 in. asphaltic concrete surface and 3 in. asphaltic concrete overlay.

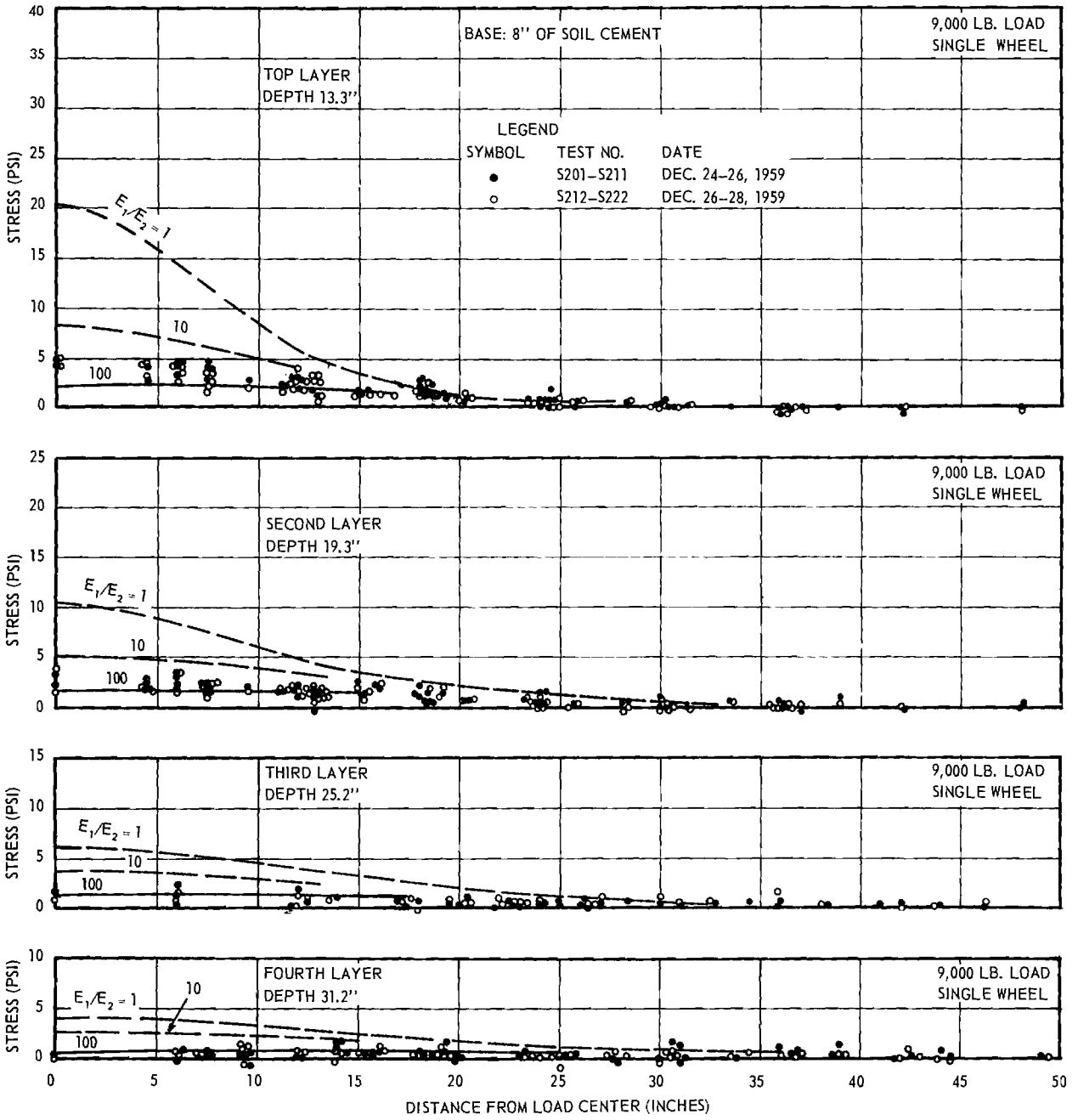

Figure 19. Measured stresses; single load 9,000 lbs. soil-cement base 8 in. thick; 3 in. asphaltic concrete surface. Curves are for theoretical stresses computed by the two elastic layer theory, for different elasticity ratios; upper curve is equivalent to Boussinesq distribution.

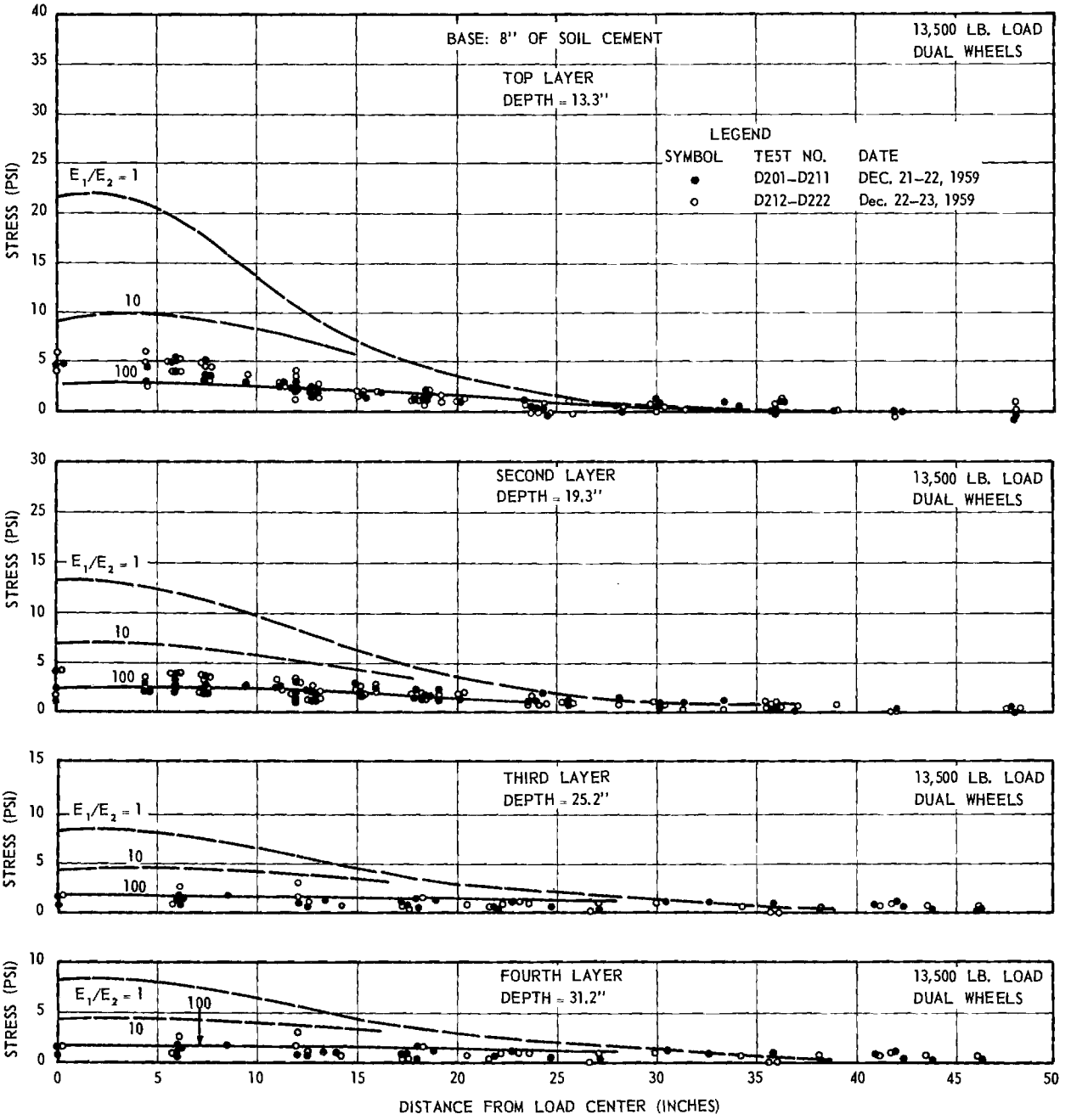

Figure 20. Measured stresses; dual load 13,500 lbs. soil-cement base 8 in. thick; 3 in. asphaltic concrete surface.

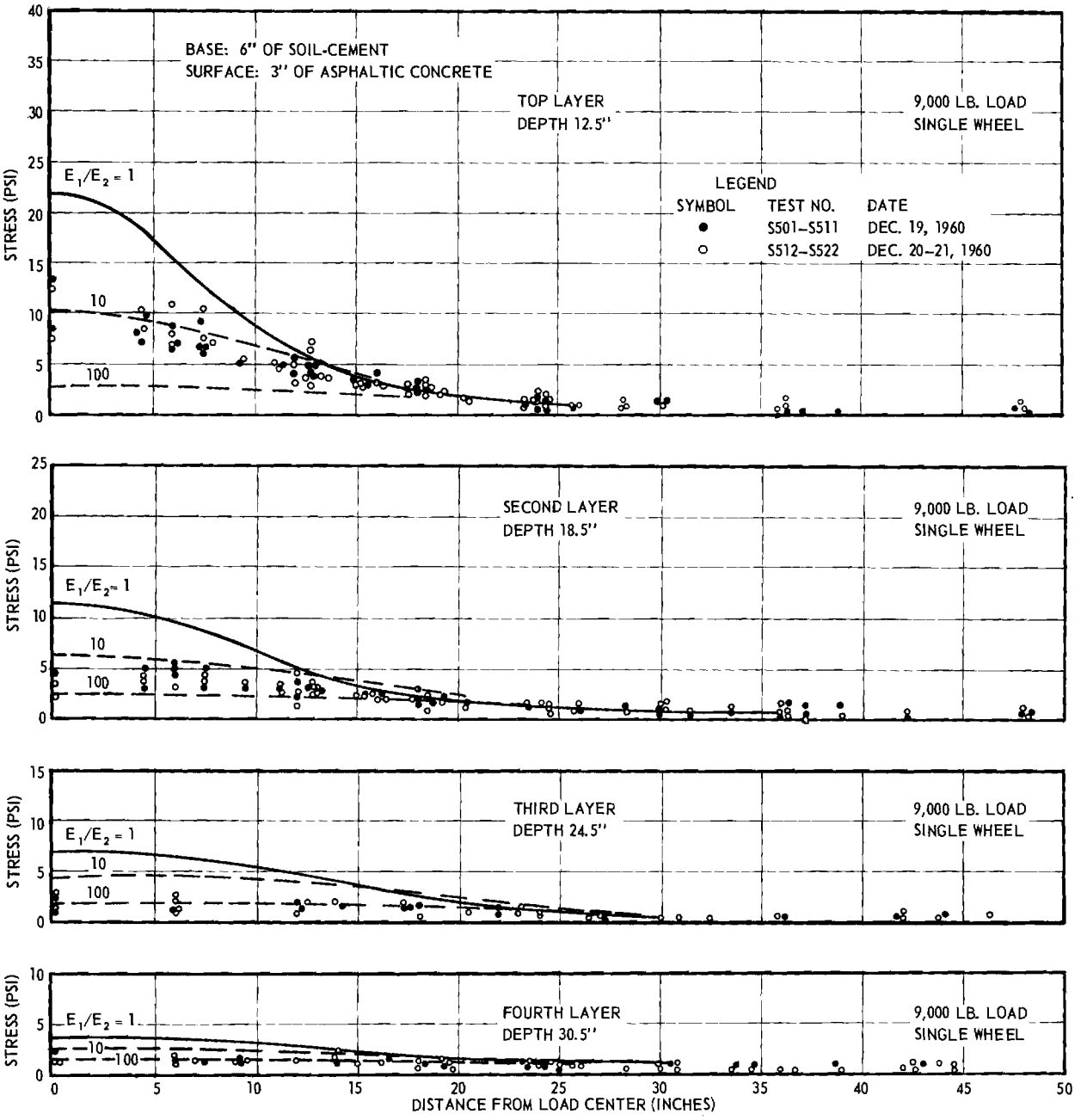

Figure 21. Measured stresses; single load 9,000 lbs. 6 in soil-cement base; 3 in. asphaltic concrete surface.

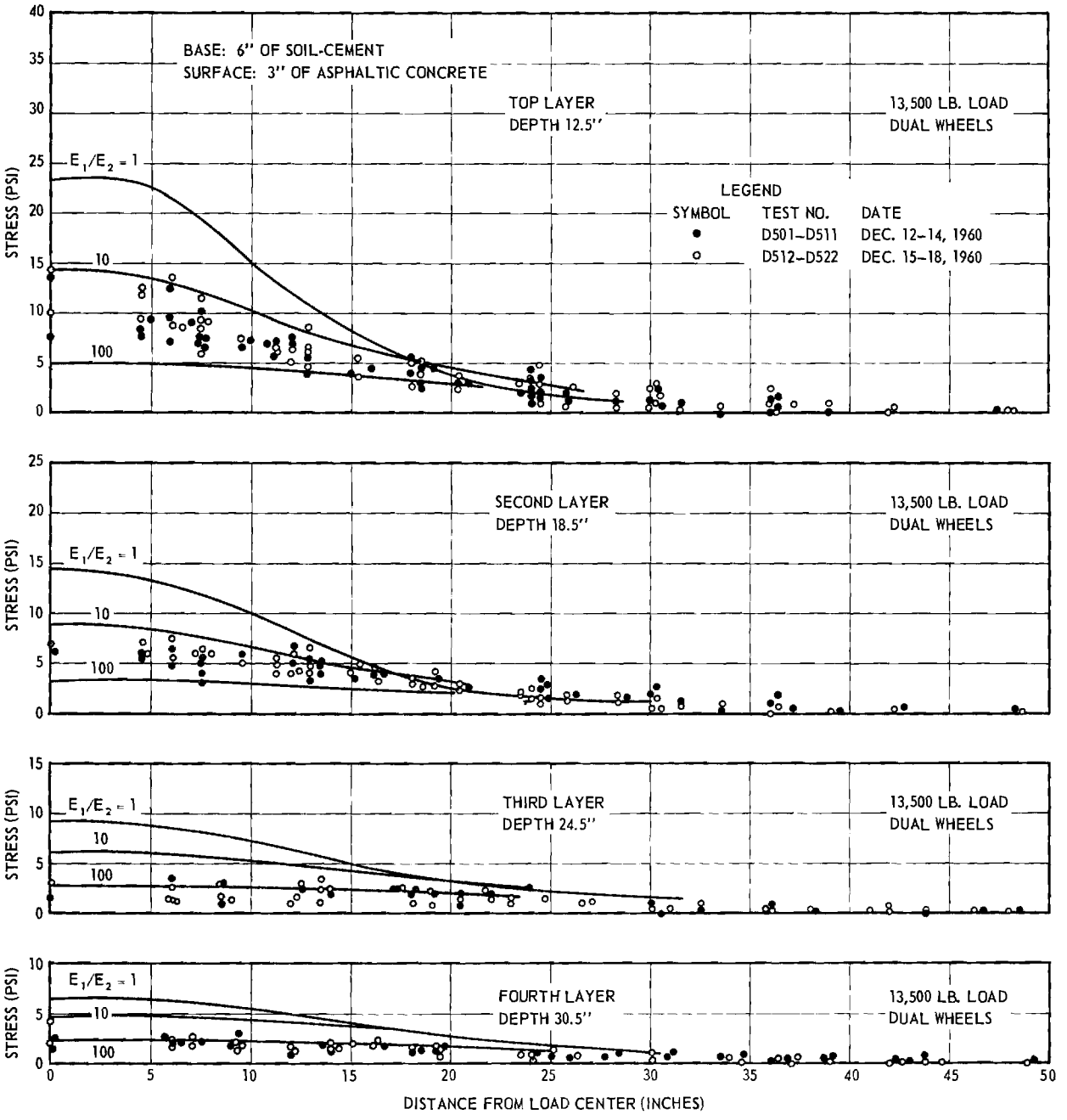

Figure 22. Measured stresses; dual load 13,500 lbs. 6 in. soil-cement base; 3 in. asphaltic concrete surface.

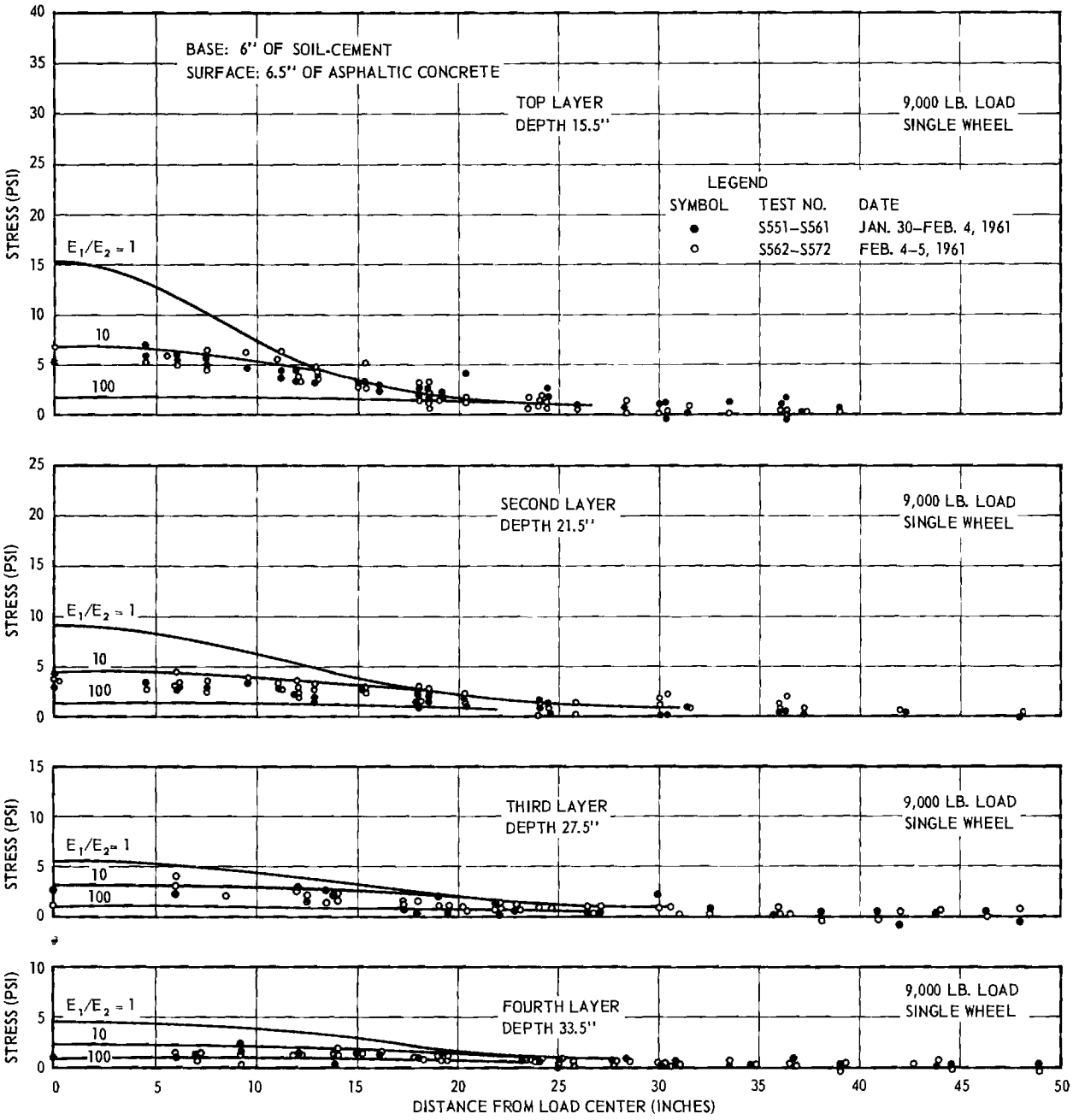

Figure 23. Measured stresses; single load 9,000 lbs. 6 in. soil-cement base; 3 in. asphaltic concrete surface and 3.5 in. asphaltic concrete overlay.

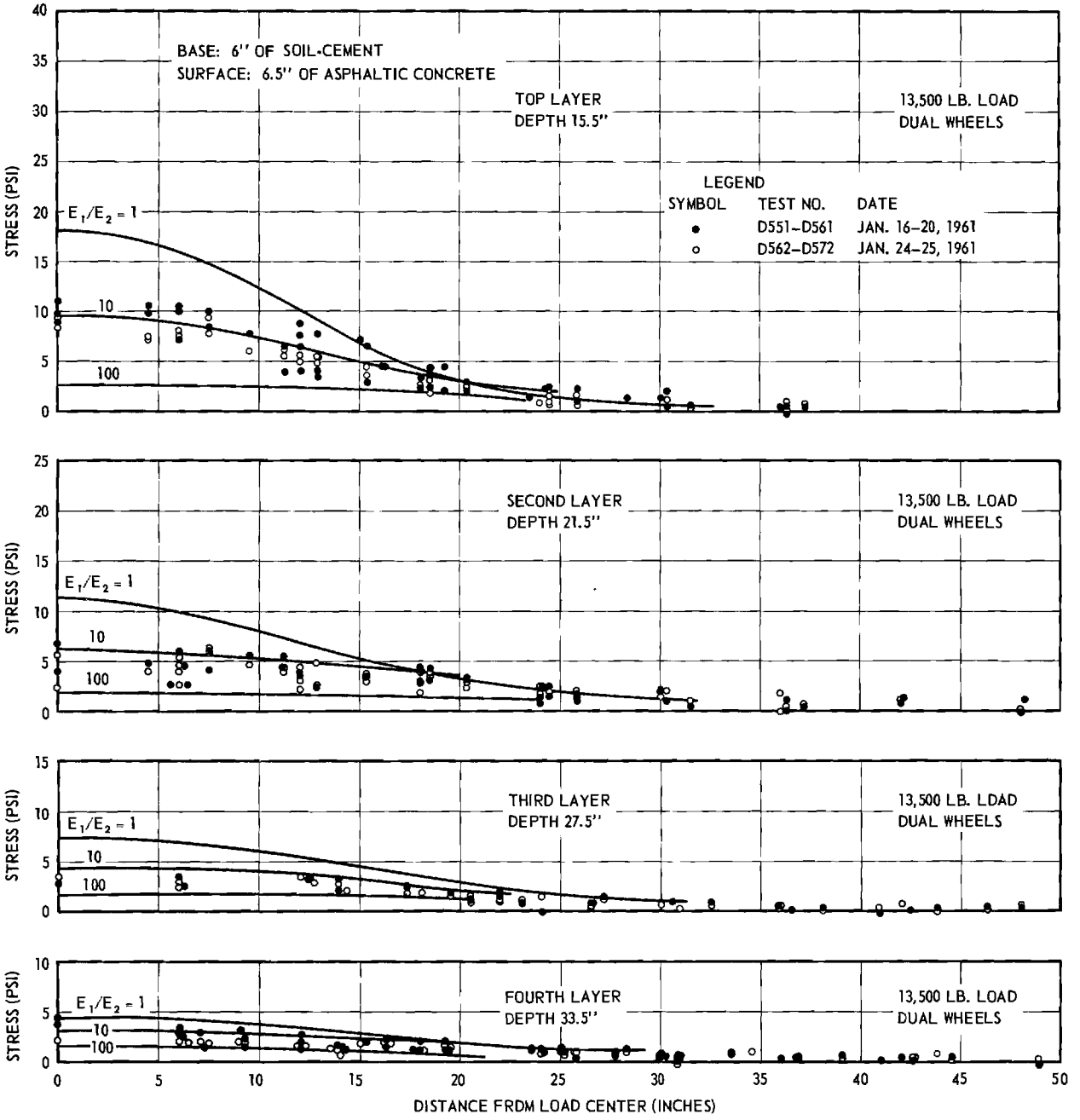

Figure 24. Measured stresses; dual load 13,500 lbs. 6 in. soil-cement base; 3 in. asphaltic concrete surface and 3.5 in. asphaltic concrete overlay.

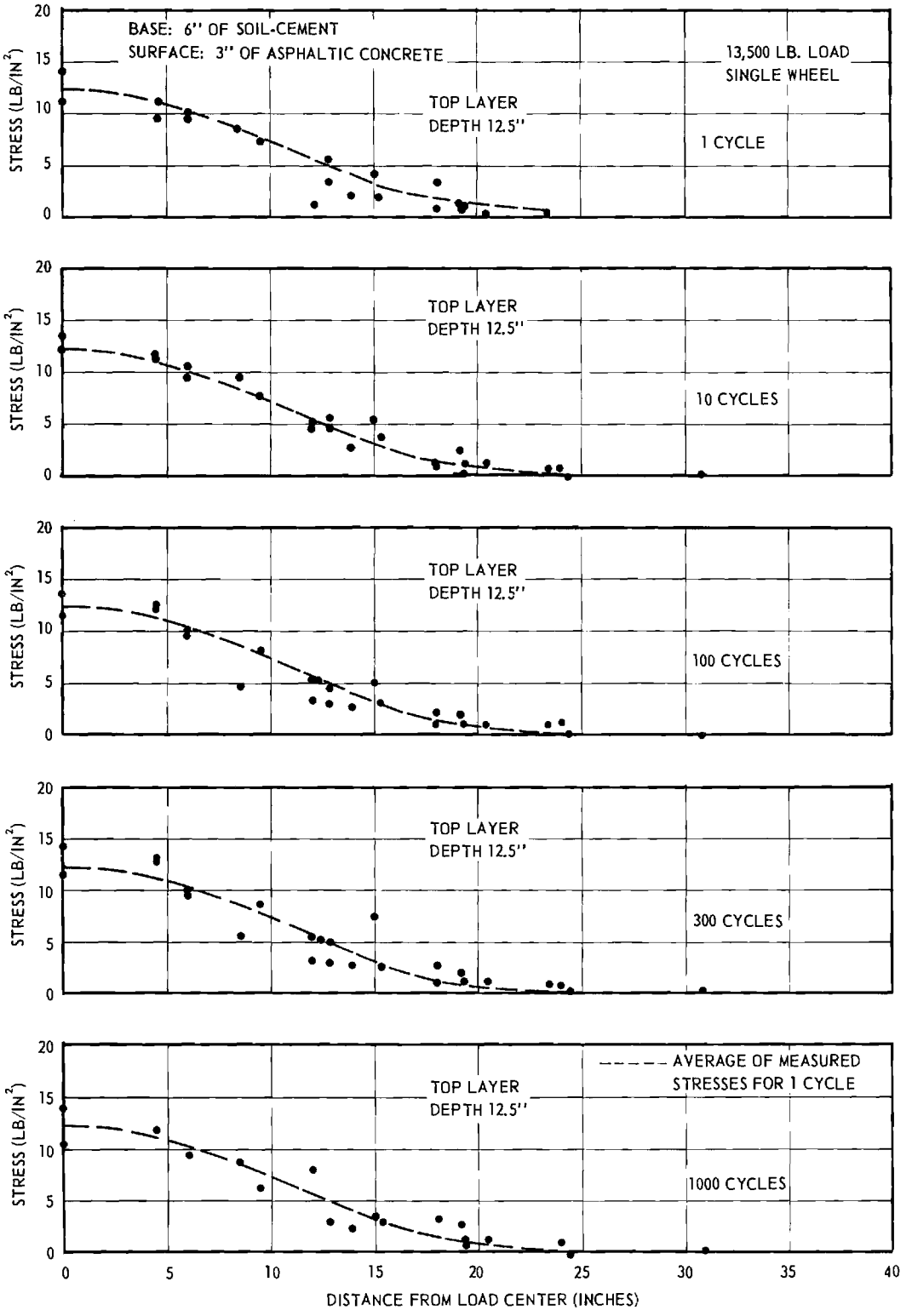

Figure 25. Measured stresses; repeated single wheel load 13,500 lbs. on 6 in. soil-cement base; 3 in. thick asphaltic concrete surface. Curve is average of measured stresses for one load cycle.

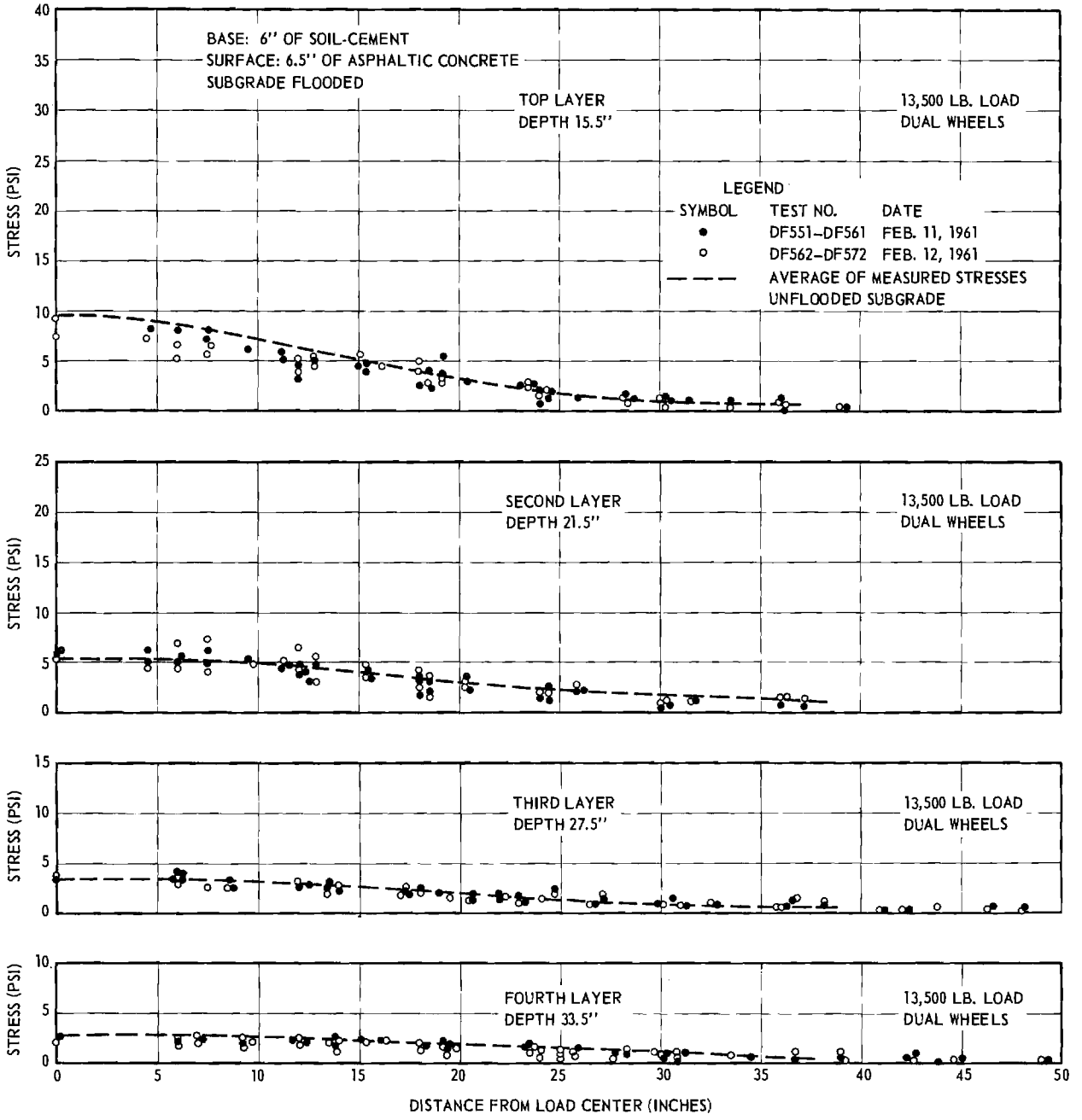

Figure 26. Measured stresses; dual load 13,500 lbs. 6 in. soil-cement base; 3 in. thick asphaltic concrete surface and 3.5 in. asphaltic concrete overlay, subgrade flooded. Curves are average measured stresses in unflooded subgrade.

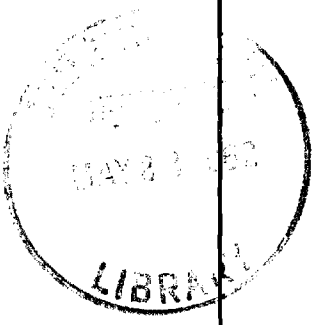

ANNUAL REPORT NO. 1

PROJECT B-133

THE STUDY OF STRESSES IN A FLEXIBLE PAVEMENT SYSTEM

By

GEORGE F. SOWERS and ALEKSANDAR B. VESIĆ

CONTRACT WITH THE STATE HIGHWAY
DEPARTMENT OF GEORGIA IN COOPERATION
WITH THE BUREAU OF PUBLIC ROADS

JANUARY 1, 1958 through MARCH 1, 1959

Engineering Experiment Station
Georgia Institute of Technology
Atlanta, Georgia

ENGINEERING EXPERIMENT STATION
of the Georgia Institute of Technology
Atlanta, Georgia

ANNUAL REPORT NO. 1

PROJECT B-133

THE STUDY OF STRESSES IN A FLEXIBLE PAVEMENT SYSTEM

By

GEORGE F. SOWERS and ALEKSANDAR B. VESIĆ

CONTRACT WITH THE STATE HIGHWAY
DEPARTMENT OF GEORGIA IN COOPERATION
WITH THE BUREAU OF PUBLIC ROADS

JANUARY 1, 1958 through MARCH 1, 1959

TABLE OF CONTENTS

CHAPTER I

INTRODUCTION

Objectives

The design of a pavement system to support heavy wheel loads is one of the most critical problems facing any highway department. In the past, most design has been based on tradition and empirical rules or on the results of simple but crude tests of the soil physical properties. Design on such bases, therefore, must be ultra-conservative or else must risk pavement failure. The high cost of highway construction and the growing incidence of failures are both indications that the present design methods need improvement.

Existing pavements are suffering from the increased wheel loadings developed by modern equipment. The old methods of design evaluation, based on past experience, do not include the effects of these newer, heavier loads. Therefore there is no way to determine what the consequences of these increased loadings will be, or what limitations should be imposed on wheel and axle loads in the future.

The rational design of any structural system, including pavements, must begin with stresses developed. It is the object of this research project to investigate the stresses produced in a flexible pavement system, including the pavement itself and the soil beneath, by heavy loads such as those imposed by large trucks. The local spreading ability of different types of pavements will be investigated to provide a scientific basis for the design of new pavements and the re-evaluation of existing ones.

Technical Background

By far the largest highway mileage existing and planned in Georgia employs

flexible pavements. The major purpose of any pavement is to spread the relatively intense pressure delivered by the wheels sufficiently that the stresses delivered to the underlying soil will not exceed its ability to absorb them. A rigid pavement does this by beam action. It is a continuous solid whose greater rigidity compared to the soil spreads the stresses over a broad area.

The flexible pavement, on the other hand, is made up of discrete particles which form a discontinuous solid. These particles are sometimes partially bonded together but they depend to a large extent on their position and shape to spread the load, much as do the individual stones in an arch.

Little is known about the load spreading ability of such discontinuous solids because their structures are so complex that they have so far defied exact mathematical analysis. Various approximations have been developed but all are based on certain idealized conditions or properties which do not fully represent the real materials. It is the basic objective of this project to develop quantitative information regarding the stress distribution in such materials produced by relatively concentrated surface loads, to determine which, if any, of the idealized analyses is a reasonable approximation of the real material, and to develop either better approximations or empirical corrections and constants to be used with the present ones.

A flexible pavement is a layered system composed of a wearing surface, a load spreading layer (usually termed the base), and the soil which ultimately supports the load (the subgrade). The stresses of interest in pavement design and therefore the focal point of this investigation are the stresses spread by the wearing surface and base and finally distributed into the subgrade.

The depth to which the significant stresses extend in the subgrade is important for it influences the depth to which the subgrade strength must be

evaluated and the depth to which corrective treatment must extend. This also is a part of the problem being investigated.

The stresses at any point, of course, consist of combinations of shear and normal stresses. Whether all of these or only certain ones need be evaluated for pavement design depends on the criteria established for pavement performance. The earlier methods of design require that the stresses distributed into the subgrade do not produce soil failure or shear. The shear stresses, therefore, are of greatest importance for such analyses. The most recent studies, however, indicate that vertical deflection of the subgrade is the best index of pavement performance. This is largely a function of the vertical stresses. In this project, therefore, the emphasis is on vertical normal stresses, although others may be investigated in the later phases of the work.

Deflection of the pavement and subgrade is obviously related to the stresses developed in them. As in the case of stresses no exact analysis is available, although various idealized mathematical solutions have been developed for this purpose. An objective of this investigation, therefore, will be to develop quantitative data regarding deflections to verify the present theories and to provide a better solution.

The loads encountered in highway work are predominately moving, but vertical (except at points of braking and acceleration). The rate of movement varies from a standstill to greater than 60 mph. However, the present knowledge of the characteristics of soils and similar fragmental materials indicates that both the maximum deflection and failure are more likely to occur under sustained load than under a dynamic load. Therefore, only static loading, the most severe condition, is being investigated. The relation between the effects of static

and dynamic loadings could form a separate study or a future part of this one.

The little data available indicate that repeated loadings are somewhat more severe in their effect on pavements than single loadings. This point is not being considered in the present project. Depending on the results of such investigations as the Illinois Test Road some tests with repeated loadings may be attempted.

The question of what constitutes pavement failure, while vital to design, will not be considered in this work. It could be a part of a future development of a design method.

Outline of Project

The entire project will consist of four phases:

1. Analytical study of stresses in layered systems.
2. Experimental evaluation of stresses in typical flexible pavements.
3. Evaluation of the physical properties of typical flexible pavement courses.
4. Correlation of analytical study with the experimental results.

The analytical phase is largely a review of existing literature on the subject of stresses in large masses which are similar to soils in their physical properties. The stresses which are developed in a base course and subgrade by wheel loads will be computed by these methods using the physical properties of the soil and pavement materials.

The experimental phase consists of tests on actual pavement systems such as are being used on Georgia Highways today. The testing facility consists of a large concrete pit that is spanned with a steel beam mounted on adjustable supports. A full-scale model of an embankment, prepared subgrade (or sub-base),

base course, and asphaltic surface are constructed in the pit. Pressure measuring cells are installed at different levels in the subgrade and embankment to determine the stresses.

The pavements systems to be tested consist of the following layers:

1. Embankment - Micaceous sandy silt typical of the poorer soils of north Georgia.

2. Controlled Subgrade (Sub-base) - Micaceous sandy silt compacted as specified by the Georgia State Highway Department specifications.

3. Base Courses

   a. Soil bound Macadam, 40% soil and 60% No. 467 stone.
   b. Sand clay or "topsoil."
   c. Sand bituminous road mix.
   d. Soil cement.
   e. Water bound Macadam and other types not included in the current Georgia specifications. Thicknesses of 6, 8, and 10 inches to be tested.

4. Surface Course - 2.5 to 3 inches of asphaltic concrete.

The loads employed are comparable to and greater than those permitted by the present Georgia laws. The greater loads are in anticipation of future increases in truck weights and the possibility of permitting them on certain highways. Single, dual and dual tandem truck wheels with loads of 4500, 9000, and 13500† lb. per tire are being used corresponding to axle loads of up to 36,000 lb.

The physical properties of the base, subgrade, and embankment will be evaluated to serve as a basis for the analytical computations of stresses. Tests for shear strength, modulus of elasticity, compressibility, and Poissons' ratio are included. Because of the particle sizes of the base course materials

†Not on dual tandem. Dual Tandem limit of 9000 lb. per tire.

special large testing devices are necessary. Their development is a part of this project. Routine tests of the classification of these materials are also included to aid in correlating the test results with similar studies being made elsewhere.

The last phase is correlating the measured stresses with stresses computed by the analytical methods. From these correlations a method for analyzing future pavements and loads will be developed to serve as a basis for evaluating pavements from the results of laboratory tests of the physical properties of the materials.

Work to Date

The work to date includes the following:

1. A complete review of past literature on stresses.
2. The construction of the pavement test facilities including
   a. Test pit
   b. Loading frame and wheel supports
   c. Pressure cells
3. A series of tests on a pavement system employing a sand clay (topsoil) base course.

These will be discussed in detail in the following chapters.

CHAPTER II

A STUDY OF PAST RESEARCH

INTRODUCTION

This study is divided into three sections.

In Section 1 past research on theoretical distribution of stresses in loaded soils is reviewed.

Section 2 contains a review of tests on stress distribution in loaded soils.

Finally, a classification and general description of design methods for flexible pavements is presented in Section 3.

The Appendix at the end contains tables and graphs for stresses and displacements in loaded soil masses.

I. THEORETICAL DISTRIBUTION OF STRESSES IN LOADED SOIL

A. Stresses in a homogeneous semi-infinite soil mass

The basic solution for the analysis of stress distribution in a homogeneous soil is the solution of the problem of a single, vertical point load P acting on the horizontal surface of a semi-infinite elastic solid[1].† The following notation is used, as shown in Figure 1:

σ_z, σ_r, σ_θ: respectively vertical, horizontal radial and horizontal circumferential normal stresses in any point N of the solid;

τ_{rz}: shearing stress in the directions of r and z;

z: vertical co-ordinate of the point N;

†See the list of references at the end.

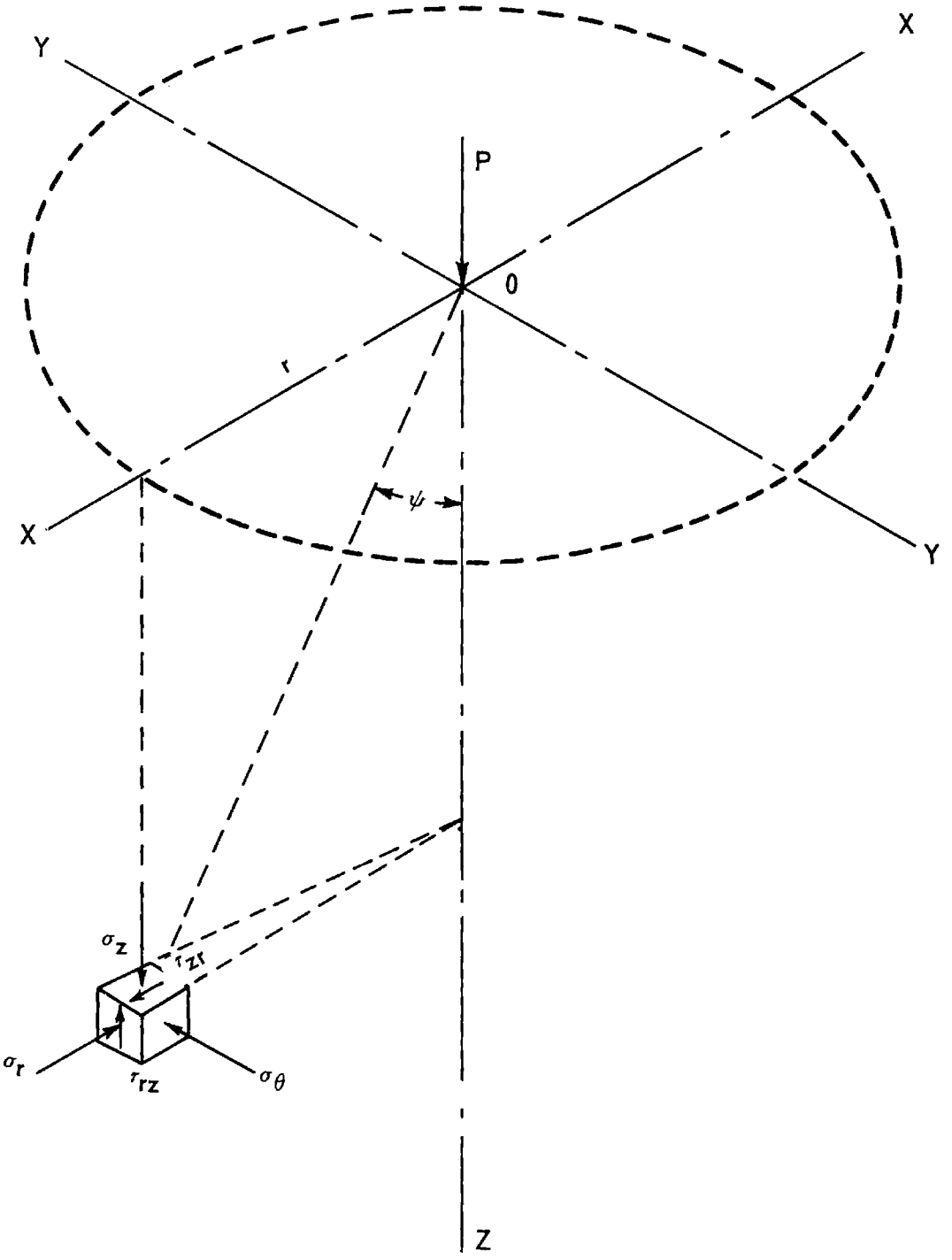

Figure 1. Stresses at a Point of Semi-Infinite Solid Acted Upon by a Point Load P.

r: horizontal radial distance between a vertical axis through the point O of application of P and the point N;

ψ: the angle between the vertical axis and ON

μ: Poisson's ratio of the solid;

The following expressions for the stresses are found:

$$\sigma_z = \frac{3P}{2\pi z^2} \cos^5\psi = \frac{3P}{2\pi}\frac{z^3}{(z^2+r^2)^{5/2}} = \frac{P}{z^2} I_\sigma \tag{1}$$

$$\sigma_r = \frac{P}{2\pi z^2}\left[3\cos^3\psi\sin^2\psi - (1-2\mu)\frac{\cos^2\psi}{1+\cos\psi}\right] \tag{2}$$

$$\sigma_\theta = -(1-2\mu)\frac{P}{2\pi z^2}\left[\cos^3\psi - \frac{\cos^2\psi}{1+\cos\psi}\right] \tag{3}$$

$$\tau_{rz} = \frac{3P}{2\,z^2}\cos^4\psi\sin\psi \tag{4}$$

The numerical values of the influence factor

$$I_\sigma = \frac{3}{2\pi}\left[\frac{1}{1+(r/z)^2}\right]^{5/2} \tag{5}$$

as computed by Gilboy[2] are given in the Appendix (Table A).

Also, the following expression for vertical displacement w at any point of the soil mass can be derived:

$$w = \frac{P}{2\pi E}\left[\frac{(1+\mu)z^2}{(r^2+z^2)^{3/2}} + \frac{2(1-\mu^2)}{(r^2+z^2)^{1/2}}\right] \tag{6}$$

where E is the Young's modulus of the solid and other symbols have the same meaning as in equations (1) - (4).

The values of stresses in any point of a solid acted upon by a load p distributed over a certain finite area on the horizontal surface can be found, in principle, by integration of the Boussinesq equations. The computations

are, however, rather complicated. The results cannot be obtained, even for simple cases of a rectangular or a circular area, in a closed, simple form. The general solution of this problem is due to Love[3].

Particular solution for the stresses σ_z along a vertical line passing through the corner of a rectangular loaded area has been worked out and presented in very useful graphs by Steinbrenner[4]. Table B in the Appendix contains numerical values of influence factors for this case of loading. Newmark[5] developed a similar solution. It is presented in the form of a chart that may give the stress σ_z at any point of the mass due to any shape of the loaded area (see the Appendix, Figure 32).

Particular solution for stresses σ_z, σ_r, σ_θ beneath the center of a circular loaded area of radius R was found by Boussinesq[1] to be:

$$\sigma_z = q \left[1 - \frac{z^3}{(R^2+z^2)^{3/2}} \right] = q\, I_\sigma \tag{7}$$

$$\sigma_r = \sigma_\theta = \frac{q}{2} \left[(1+2\mu) + \left(\frac{z}{\sqrt{R^2+z^2}} \right)^3 - \frac{2(1+\mu)^2 z}{\sqrt{R^2+z^2}} \right] \tag{8}$$

The numerical values of I_σ are given on the Appendix (Table C).

The maximum shearing stress at any point on the z axis is:

$$\tau_{max} = \frac{q}{2} \left\{ \frac{(1-2\mu)}{2} + (1+\mu) \frac{z}{\sqrt{R^2+z^2}} - \frac{3}{2} \left(\frac{z}{\sqrt{R^2+z^2}} \right)^3 \right\} \tag{9}$$

This expression has a maximum when

$$\frac{z}{\sqrt{a^2+z^2}} = \frac{1}{3} \sqrt{2(1+\mu)}$$

or

$$z = R \sqrt{\frac{2(1+\mu)}{7-2\mu}} \tag{10}$$

at what depth

$$\tau_{max} = \frac{q}{2} = \left[\frac{1-2\mu}{2} + \frac{2}{9}(1+\mu)\sqrt{2(1+\mu)} \right] \qquad (11)$$

Boussinesq also found the following expression for the deflection of the surface of a semi-infinite solid with a circular loaded area of radius R:

$$w = \frac{4(1-\mu^2)\, q\, R}{\pi E} \left[\int_0^{\pi/2} \sqrt{1 - \frac{R^2}{r^2} \sin^2\theta}\, d\theta + \left(1 - \frac{R^2}{r^2}\right) \int_0^{\pi/2} \frac{d\theta}{\sqrt{1 - \frac{R^2}{r^2} \sin^2\theta}} \right] \qquad (12)$$

A more general solution for stresses and displacements at any point of a semi-infinite solid loaded by a flexible, circular, uniformly distributed load at the surface was developed from the already mentioned Love's solution[3] by Fergus and Miner at the Waterways Experiment Station at Vicksburg.[7,8]

Useful graphs of stresses and displacements for this case of loading, based on Newmark's charts[5,6] were published by Foster and Alvin[9]. These charts give directly the values of stresses σ_z, σ_r, σ_θ, τ_{rz} and deflection at any point situated within depth $z \leq 10R$ and distance $r \leq 10R$ from the center of the circular load. They are reproduced in the Appendix, (Figures 33-35).

B. Stresses in Non-Homogeneous or Non-Isotropic Semi-Infinite Soil Masses

For semi-infinite soil masses which are non-homogeneous in a vertical direction or non-isotropic Griffith[10] and Fröhlich[11] proposed a semi-empirical modification of Boussinesq's equations for stresses. They assumed $\mu = 0.50$ and replaced at the same time the exponent 3 for principal stresses acting in any point of the mass by ν. Or, instead of

$$\sigma_I = \frac{3Q}{2\pi z^2} \cos^3\psi \qquad (13)$$

as obtained by Boussinesq, they took

$$\sigma_I = \frac{\nu Q}{2\pi z^2} \cos^{\nu}\psi \tag{14}$$

satisfying at the same time the basic requirement for equilibrium in a vertical direction. In this way they obtained for the stress components the following expressions:

$$\sigma_z = \frac{\nu Q}{2\pi z^2} \cos^{\nu+2}\psi \tag{15}$$

$$\sigma_e = \frac{\nu Q}{2\pi z^2} \cos^2\psi \sin^2\psi \tag{16}$$

$$\sigma_\theta = 0 \tag{17}$$

$$\tau_{rz} = \frac{\nu Q}{2\pi z^2} \cos^{\nu+1}\psi \sin\psi \tag{18}$$

The value ν they named concentration index. Evidently, for $\nu = 3$ Frohlich's expression[13] becomes identical with the expression (14) for homogeneous soils; if $\nu > 3$ greater concentration of stresses immediately beneath the load occurs.

The Frohlich's expressions for stresses were integrated for $\nu = 4$ for different cases of loading, strip, rectangle, circle and presented in graphs and charts similar to those that exist for the Boussinesq case.[12]

According to the results of some older stress measurements (see Section II) values of ν varying from 4 to 6 have been proposed for sand. However, most of the recent measurements, especially those made at the Waterways Experiment Station at Vicksburg, showed that values of ν greater than 4 are exaggerated; and that even $\nu = 4$ does not give, in general, better agreement of theoretical and experimental values than $\nu = 3$.

The stress distribution in semi-infinite homogeneous, orthotropic solid, having a different modulus (E_h) in a horizontal direction than in a vertical direction. (E_v) was investigated by Wolf (13), Jelinek (14), (15), (16) and Koning (17). These investigations showed that if $E_h > E_v$ the vertical stresses σ_z immediately beneath the load decrease more rapidly with depth than in homogeneous solids.

A similar result was obtained by Westergaard[18] who investigated the case of a semi-infinite solid reinforced by horizontal, perfectly flexible membranes, which prevent completely any deformation in a horizontal direction without interfering with deformations in a vertical sense.

The Westergaard solution for point load Q, has the form:

$$\sigma_z = \frac{Q}{z^2} \frac{C}{2\pi} \frac{1}{C^2 + (r/z)^2}^{3/2} \tag{19}$$

where

$$C = \frac{1 - 2\mu}{2(1-\mu)} \tag{20}$$

It was integrated, on an assumption $\mu = 0$ by Fadum.[19] Different influence values were tabulated and presented on graphs as for instance: point load, circular load, rectangular load. Newmark-type charts for this analysis have also been developed.

C. Stresses in Layered Soil Masses

The rigorous analysis of stresses in layered soil masses started with a work by Melan.[20] He analyzed an elastic layer overlying a rigid base and loaded at the surface by point and line loads, on the assumption that there is neither friction nor adhesion between the layer and the base.

Marguerre[21] solved the same problem for a line load and a rough base and Biot[22] for a point load and a rough base. A more complete analysis of the same problem was done by Picketts.[23]

All these solutions show that the influence of a rigid base results in concentration of vertical stresses towards the loaded area.

A general solution of a two-layer problem in a form permitting evaluation of all stresses and displacements throughout both layers was found by Burmister[24] for an arbitrary ratio of moduli of elasticity of the two layers (see Figure 2). The assumptions on which this solution was based are:

a. The soils of each of the two layers are homogeneous, isotropic, elastic materials for which Hooke's law is valid; the surface layer has a finite thickness h_1 and is infinite in extent in the horizontal direction; the subgrade layer 2 is infinite in extent both horizontally and vertically downward.

b. At the interface between two layers exists a perfect continuity of both stresses and displacements.

c. The Poisson's ratio in both layers is equal to 0.50.

With the same basic assumptions this solution was extended later[25] to the case of a three-layered mass (Figure 3).

Burmister performed the numerical evaluation of his solution for the settlement at the center of a circular bearing area at the surface of a two layered system. The expression for this settlement reads:

$$W_c = \frac{1.5\ pR}{E_2} F_w \left(\frac{R}{h_1}, \frac{E_2}{E_1} \right) \qquad (21)$$

where p = unit load at the surface,

R = radius of the circular bearing area,

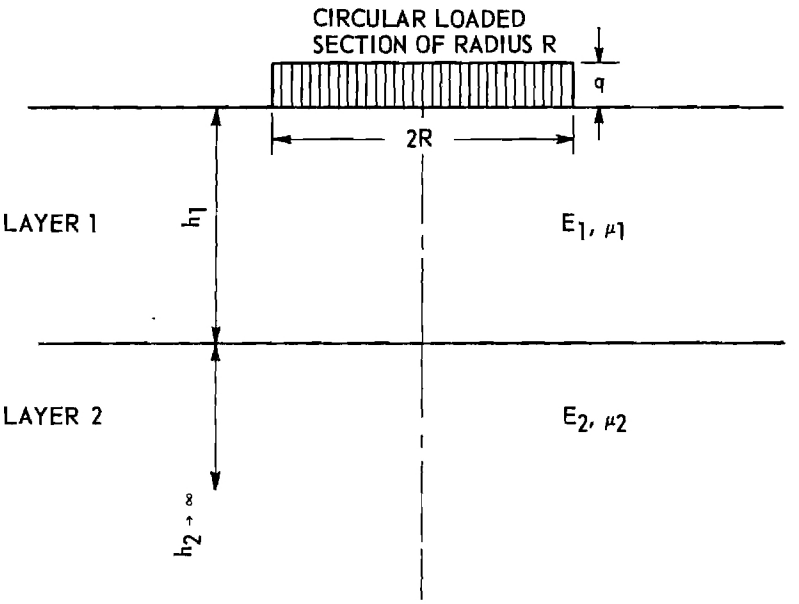

Figure 2. Two-Layer System.

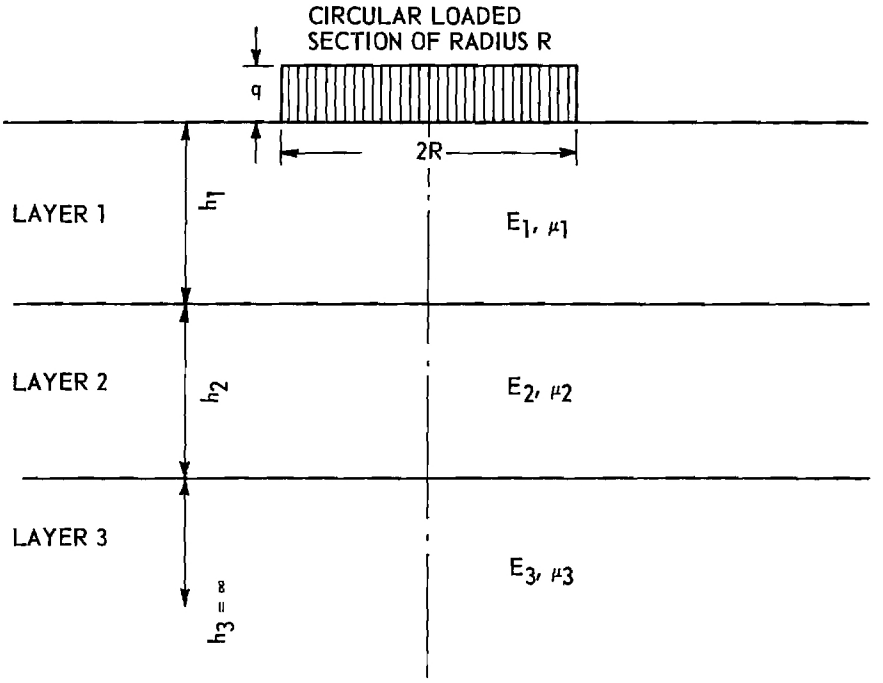

Figure 3. Three-Layer System.

E_2 = modulus of elasticity of the subgrade layer,

E_1 = modulus of elasticity of the surface layer,

h_1 = thickness of the surface layer,

F_w = a function of R/h_1 and E_2/E_1; (presented in Figure 4).

Fox[26] evaluated the stresses at the interface of a two-layer system under assumption of a perfect continuity between the layers. He found that for big ratios of moduli E_2/E_1 the shear stresses along the interface were negligible. The results of his computations are given in the Appendix, (Table D and Fig. 36-39).

Hank and Scrivner[27] evaluated also the stresses at the interface of a two-layer system for both possible extreme conditions at the interface: perfect continuity-rough interface and no continuity-smooth interface. The results of their computations are also given in the Appendix, (Table F).

Acum and Fox[28] evaluated the stresses at both interfaces of a three-layer system, assuming full continuity at all interfaces. The tables containing the results of their work are given in the Appendix (Table E).

It should be noted that all the mentioned evaluation of stresses was performed for points beneath the center of the loaded area only.

Finally Burmister[29] elaborated a complete series of influence diagrams of stresses and displacements in a two-layer system with a rigid base.

II. EXPERIMENTS ON STRESS DISTRIBUTION IN LOADED SOILS

The theory of stress distribution on loaded soils is based on several simplifying assumptions, which, to a greater or lesser degree, always deviate from the real behavior of soils:

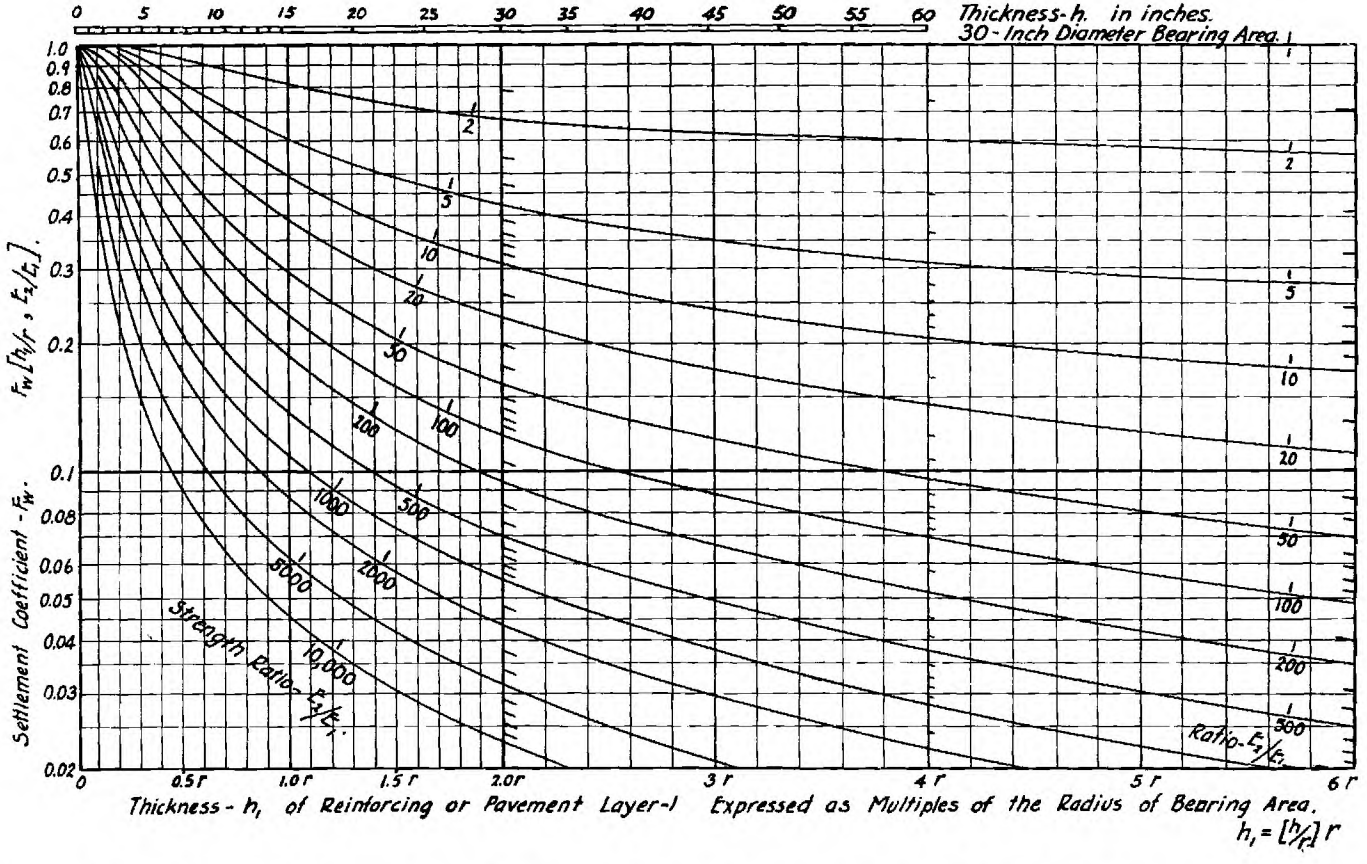

Figure 4. Influence Curves of the Settlement Coefficient - F_w for the Two-Layer System.

a. The solutions are based on assumption of perfect elasticity and linear relationship between stresses and strains. Soils are only partly elastic and do not have linear stress-strain relationship. Neither Young's modulus E nor Poisson's ratio μ are constant, but vary with the increase of the load. Also both E and μ may have quite different values on tension than in compression (some soils do not have tensile strength at all).

b. The solutions are based on assumption of perfect homogeneity of different layers. Whereas each pavement layers is usually reasonably homogeneous this is not the case with the subgrade, which very often displays a change of compressibility with depth.

c. Most of the solutions are based on assumption of isotropy. However, many of the natural soils are stratified or laminated and very often the methods of construction of pavement layers are such that a structural anisotropy is also created within them.

Consequently discrepancies are to be expected between theoretical and real stresses in loaded soil masses. Several investigators undertook the task of checking to what extent the real stresses follow the stress pattern indicated by the theory.

The early tests of this kind were made on sand fills in large boxes by Steiner-Kick[30], Strohschneider[31], Moyer[32], Enger[33], Goldbeck[34]. This work was continued by Kögler-Scheidig[35] and others.[36-40] The pressure-measuring devices in those tests were usually membranes or free diaphragms connected with some source of pressure (air or liquid) and manometers. The best known of these devices are the Goldbeck pressure cell (Figure 5) and the Freiberg pressure cell (Figure 6).

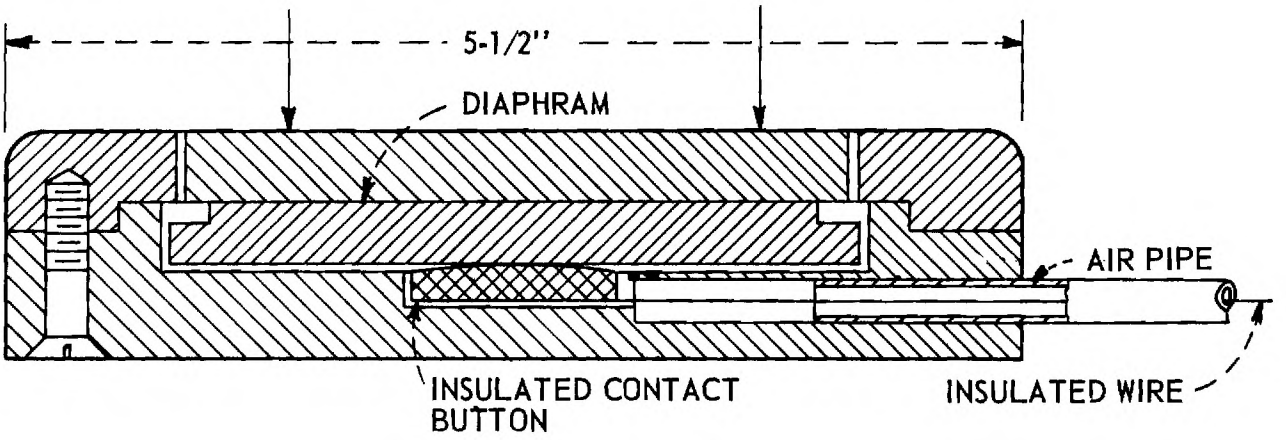

Figure 5. Goldbeck Pressure Cell.

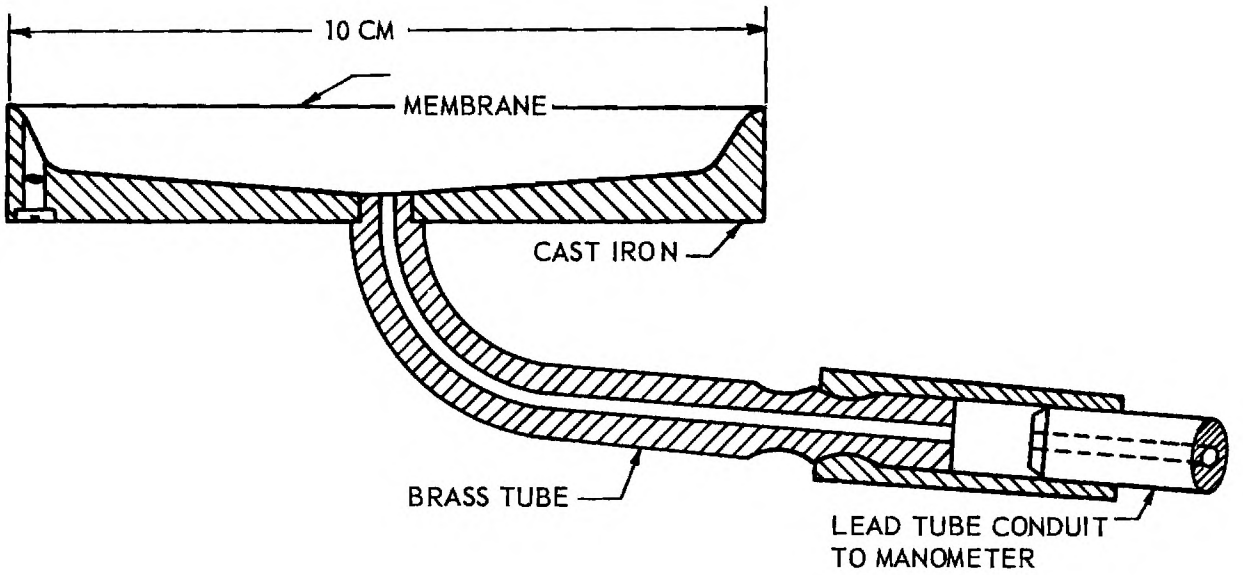

Figure 6. Freiberg Pressure Cell.

The results of these early investigations indicated that the stress distribution in the soil mass follows in a general way the theoretical stress distribution as obtained by Boussinesq solutions. However, the vertical pressure, σ_z seemed to be somewhat more concentrated under the footing and somewhat less spread out laterally than is indicated by the theory for homogeneous soil. Also, near the surface a zone of zero-stress was discovered. This was explained by the lack of tensile strength near the surface of a non-cohesive mall such as sand.

A greater concentration of stresses towards the axis of the load can be explained by the limited dimensions of the test boxes. In most of the experiments the depth of the sand layer was not greater than two diameters of the loaded area. Thus, the bottom of the box was a rigid base, causing concentration of stresses. This can easily be explained by the later theoretical investigation of stresses in layers of finite thickness on a rigid base. However, the analyses also show that a part of this stress concentration nevertheless is due to the increase of the modulus of elasticity of sand with depth, corresponding to the Griffith-Fröhlich analysis.

In some of the older tests the concentration of stresses is due to the presence of rigid cells in a sand mass. The result is non-homogeneity of the mass, arching and local increase of pressure on the cells. In Freiberg tests (Kögler and Scheidig 1927-29) this phenomenon was eliminated by using a very large number of closely spaced pressure cells in horizontal layers.

After a certain period of stagnation, the period of World War II saw a renewed and intensified interest in the problems of stress distribution connected with the design of airfield pavement. Concurrently with extensive theoretical

studies the U. S. Corps of Engineers and its Waterways Experiment Station at Vicksburg (Miss.) made numerous deflection and pressure measurements under various wheel loads and wheel assemblies.[40-42] The study of obtained data showed that the basic knowledge on real stress distribution is soils was not adequate.

Thus, a broad investigational program was planned and realized by the Waterways Experiment Station[43-44] on stress distribution in homogeneous clayey silt and sand masses loaded by single 1000 in^2 and dual 500 in^2 uniform, circular loads applied at the surface.

A large test section 50 x 26 ft. and 12 ft. deep of homogeneous clayey-silt resp. sand was constructed. Special WES pressure cells and deflection gages were installed throughout the section in different levels and positions (horizontal, vertical and inclined). Thus different normal stresses and deflections induced by static loads up to 60,000 lbs. were measured. The fact that pressure cells were installed at angles 0°, 45°, 90° and 135° to the horizontal permitted the computation of principal and shearing stresses.

The WES pressure cells used in these tests (Figure 7) have as principal part a steel diaphragm the strains of which are measured by SR-4 strain gages. The external pressure is transmitted to the diaphragm by means of oil contained in the fluid chamber. These cells possess a high accuracy of ±0.5% in laboratory conditions and can give in field conditions readings accurate to within 10%.

The principal conclusion of the thorough investigations made by the WES was that the distribution pattern of the measured stresses followed closely the same general shape as computed from the theory of elasticity for homogeneous

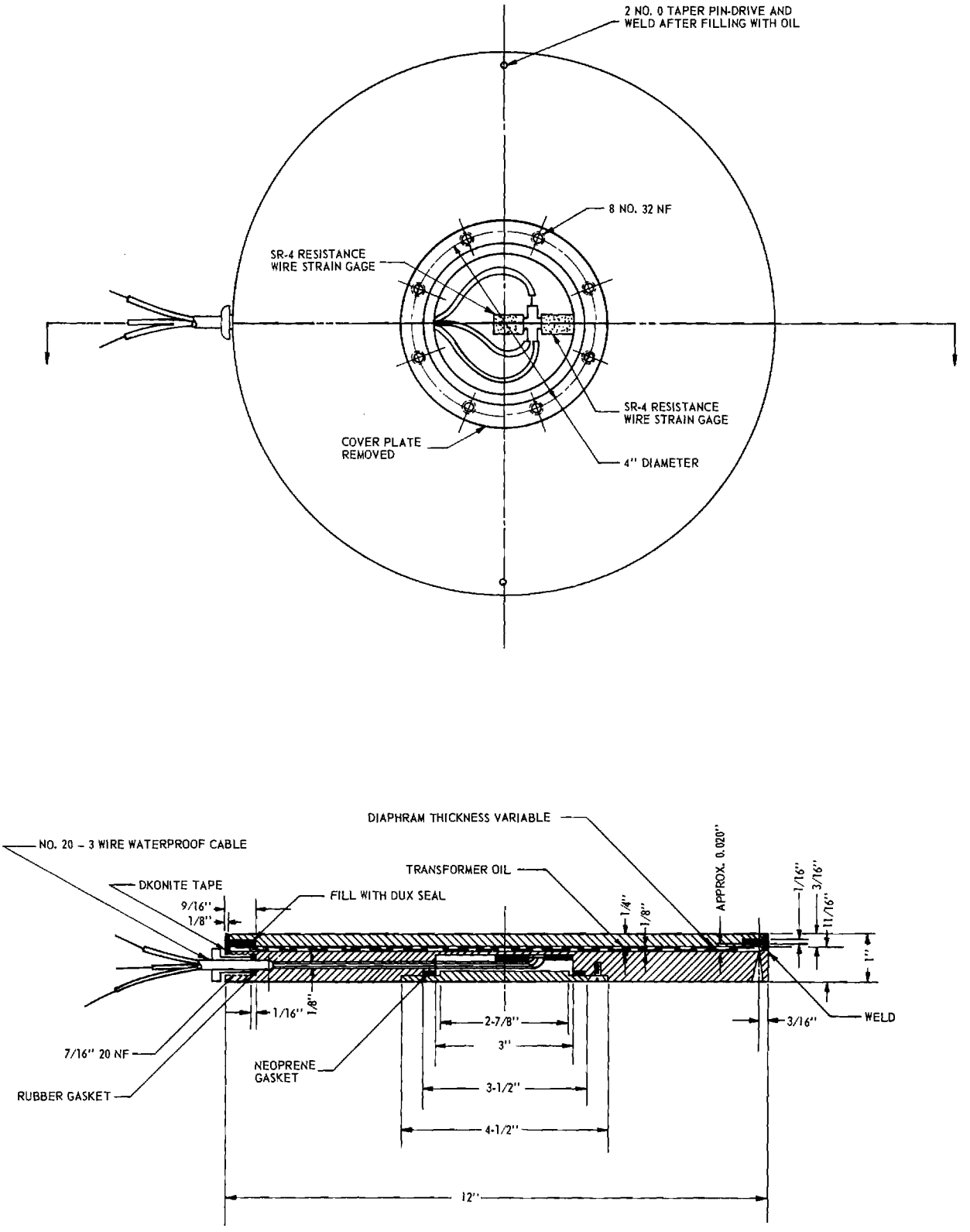

Figure 7. Waterways Experiment Station Pressure Cell.

isotropic materials. The use of the Fröhlich concentration index did not improve the agreement between the measured and theoretical stresses. Also computation of stresses and deflections with Poisson's ratios different from 0.5 did not improve the agreement between the measured and theoretical values. In the region of the load there was a constant tendency of vertical stresses to be a few percent larger and horizontal stresses to be somewhat smaller than expected following the theory for homogeneous soils.

The patterns of measured deflections did not conform to those predicted by the theory of elasticity using a constant modulus of deformation (elasticity). Larger deflections agreed generally with a smaller value of modulus of deformation than the smaller deflections.

The deflections were, however, proportional to the external load. This was also the case with smaller stresses (up to 10% of the contact pressure). At large stress values a variation of the ratio of measured stress to the external load was observed.

In general, the stress-strain curves developed from the load tests had a shape similar to that obtained from triaxial tests. It was found that a good correlation with the load and tests can be obtained by prestressing a sample of the test section material and varying the lateral pressure during testing in the manner in which it varied in the test section.

Attempts were made, too, to measure the residual stresses. The results were not completely understandable. It was found, however, that the stresses due to the overburden load form an appreciable part of total measured stresses after removal of the load. The differences between the total measured stresses and the overburden load did not exceed 3 psi. Contrary to what normally might

be expected it was noted that the horizontal residual stresses in no case did exceed the vertical residual stresses.

In conclusion, although the investigations during the past fifteen years throw a new light on the problem of stress distribution in soils in general, and in pavement systems in particular, a considerable experimental work still remains to be done, especially in the field of multi-layered systems.

III. DESIGN METHODS FOR FLEXIBLE PAVEMENTS

Design methods for flexible pavements which are now in use or proposed can be classified into four distinct groups:

A. The first group embraces empirical methods using no soil strength tests in order to estimate the value of a soil as a pavement support. The thickness of the pavement construction is determined from past experience on similar soils. Soil classification, based mostly on grain-size determination, Atterberg limits and compaction characteristics is the only rational criterion that figures in the methods. Methods of this type are used by many highway departments and some other institutions (e.g. Civil Aeronautics Administration) in the country.

The Georgia Design Method[46] may be taken as an example of this type.

The basis of this method is a soil classification[45] by which the foundation materials are divided into six classes. Two of the classes are further subdivided into sub-classes. These classes can normally be differentiated by field observation and examination, combined with grain-size, Proctor-density and volume change tests in the laboratory.

Each of these classes and sub-classes carries its own depth of subgrade treatment, which varies from 0 to 24" (materials of the IV class-peat, muck

or organic soils have to be removed completely). Over this prepared subgrade or sub-base a base of uniform thickness, usually 8", and a surface course (usually 3") are placed.

The principal advantage of the methods of this group is simplicity that enables an easy and expedient design of pavements.

The shortcomings of these methods are numerous. First, the safety factor of the pavement is unknown. The strength and stress-strain characteristics of soils falling into the same class may be quite different, while the design method assures safety for the weakest of them. Thus, the design thickness in many cases is uneconomical.

Second, diverse possible types of surface course, base, and treated subgrade may have quite different mechanical properties resulting in different ability of supporting and spreading the load to the foundation. Following the design method, however, the quality of these courses have no influence on the thickness of pavement.

Finally, the magnitude of maximum wheel load, tire pressure and intensity of traffic do not figure in the design method. Thus no rational extrapolations for heavier wheel loads or different assemblies of loads than those in use at present are possible.

B. In the second group are empirical methods based on experience and the use of a mechanical strength (penetration, plate load or triaxial) test for evaluation of the soil's supporting capacity. The best known and widest used of these methods is these methods is the California Bearing Ratio (CBR) method,[47,48] which will be described below. The other methods of this group are: North Dakota Cone-Method,[49] Canadian Department of Transport Method,[51, 52]

as well as the Kansas State Highway Department and Texas Highway Department methods.[53,54,55]

In the CBR method the quality of subgrade materials is evaluated by a standard laboratory penetration test. Thoroughly consolidated samples are soaked for 4 days under a surcharge representing the weight of the pavement. A penetration test, using a 3 in^2 piston, is then made. The resistance to penetration, expressed as a percentage of the resistance of a standard crushed stone base, is called CBR-value of the material.

Investigations made on pavements that failed furnished the design curves giving safe thickness of pavement above the material tested versus its CBR-value. Two curves were used by the California Division of Highways (see Figure 8), Curve A for average traffic conditions = light and medium traffic and Curve B for light traffic only.

During the World War II the CBR-method was adopted by the U. S. Corps of Engineers for the design of airfield pavements. The initial design curves were extrapolated tentatively to wheel loads up to 60,000 lb. A wide research program was initiated to provide information for verifying or revising these extrapolated curves. Finally, the tentative curves were modified. The final form of design curves is given in Figure 9. (See also 48 and 56.)

The methods of the second group have the advantage of being simple, both in the testing and design. They have stood the experimental check as well as the check by experience for many years (especially the CBR-method).

The shortcomings of this second group of methods is partly the same as that of the first group of purely empirical methods. Although these methods deal with a value which is correlated to the strength of the material, the actual safety factor of pavements is still not defined and unknown. Also,

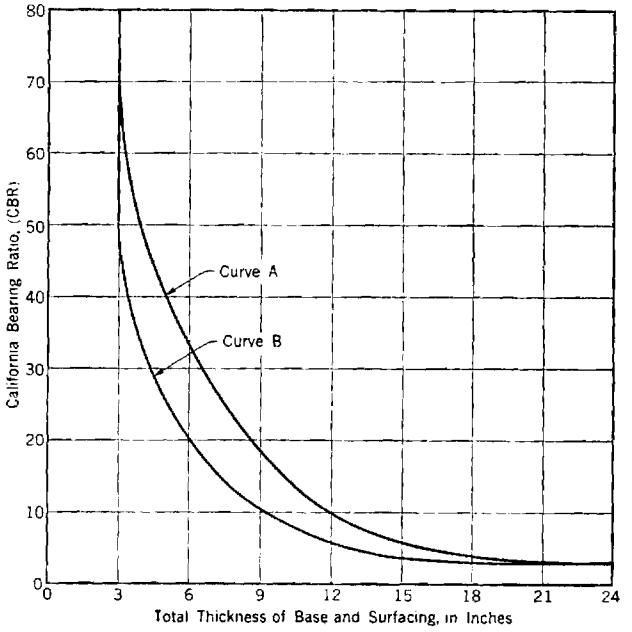

A = AVERAGE TRAFFIC CONDITIONS
B = LIGHT TRAFFIC CONDITIONS

Figure 8. CBR - Curves for Highways (California Division of Highways).

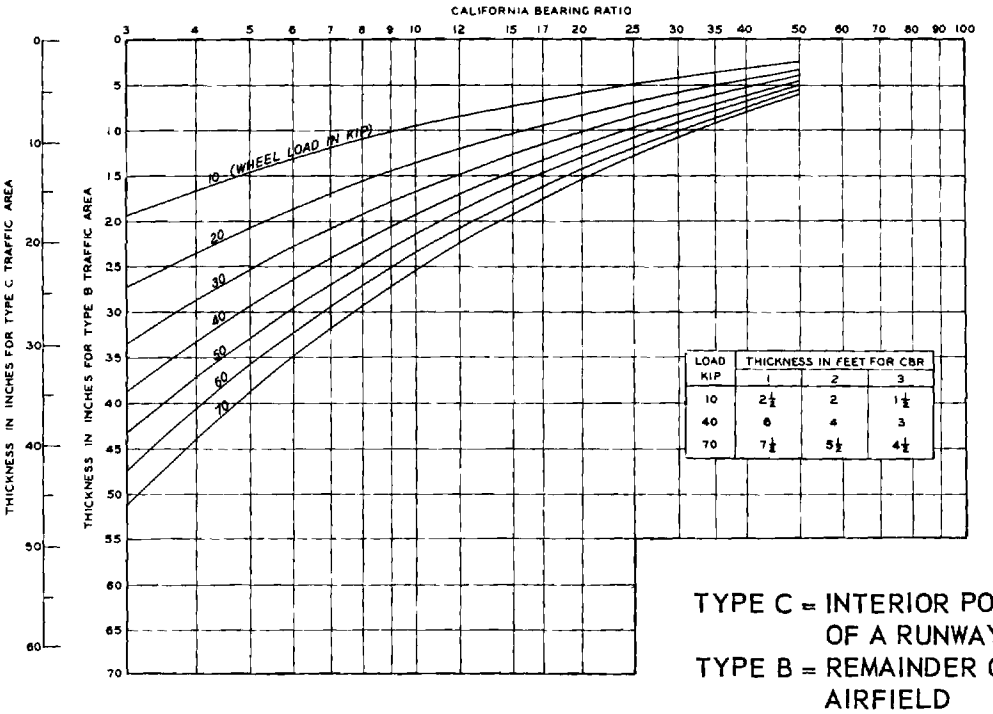

TYPE C = INTERIOR POSITION OF A RUNWAY
TYPE B = REMAINDER OF THE AIRFIELD

Figure 9. CBR - Curves for Airfields (Corps of Engineers).

the strength properties of the surface and base course do not influence their design thickness. For the CBR-method, the procedure of thorough soaking of samples before penetration testing was found in many instances to be too conservative and uneconomical.

In spite of all the shortcomings the methods of this group, especially the CBR, are considered to be the most reliable design methods for flexible pavements.

C. The third group are the methods based on the considerations of ultimate strength of the pavement system. This system must possess adequate thickness and shearing strength so that a defined safely factor exists against shear failure under the considered load.

The first attempt to establish a method of design of this type was made by Glossop and Golder;[57] their method was applicable to frictionless soils only; it was extended later by Golder,[58] to soils having both friction and cohesion. The mentioned methods are based on Prandtl-Terzaghi formulae for ultimate bearing capacity of shallow footings. The values of shear characteristics of the subgrade soil are determined by unconfined compression, respectively triaxial tests. In the original Glossop-Golder method it was assumed that the pavement has the same strength as the subgrade; Golder assumed later that the load is spread through the pavement at an angle 26 1/2° to the vertical and considered the shear failure of the subgrade only.

Similar to Glossop-Golder methods is the approach made by McLeod.[59] He considered, the pavement with the subgrade as a layered system and used the logarithmic-spiral method for determination of the ultimate bearing capacity of the system as a whole. He did not make, however, definite recommendation

concerning the choice of the safety factor to be adopted for design.

The methods of the third group offer the possibility of a rational definition of the safety factor for design. All different parameters that in the methods of the first and second group do not influence directly the design thickness, are introduced here: tire pressure and strength properties of the surface and base course too. Well defined characteristics of materials; cohesion and the angle of internal friction are dealt with in the design.

The principal shortcomings of the methods of the third group are:

1. They are not developed to such an extent that the application in the practice would be simple enough as when methods of the first and second group are used;

2. Only a limited study of behaviour of pavements in the light of these methods was made; the question of the safety factor to be used in design is still not cleared.

In conclusion, having a sure rational basis the methods of third group are very promising. However, they are still not developed enough to furnish immediate answer to design problems.

D. Finally the fourth group are the methods based on theoretical analysis of stresses and/or displacements inside the pavement structure and on the true stress-strain relationship of the various materials of the pavement.

Only one design method of this group was really developed - the Burmister method.[24] This method is based on his solution for displacements beneath a circular loaded area at the top of the surface-layer of a two-layer system (see p.14 of this report). Considering surfacing, base and sub-base as the surface layer, the thickness of this layer is selected so that the displacement under the load is limited to 0.2 in. The moduli of elasticity of the

subgrade and base are determined, by plate bearing tests. A similar method has been adopted by the U. S. Navy.[50]

Tentative design curves, proposed by Burmister for some standard crushed stone bases are given in Figure 10.

The principal virtue of the methods of this group consists in their sound scientific basis. They deal with well-defined characteristics of the materials, being at the same time as simple in testing and practical use as the methods of the second group.

However, there is no method of this type which has been perfected sufficiently for general use. The criterion adopted by Burmister to limit the settlement at the surface to an arbitrary quantity is not completely adequate and gives some nonconsistent results (cf. discussion on his paper). Experience to date indicates that the critical deflection should vary depending upon the type of subgrade, type of base wheel loads and some other factors. T. A. Middlebrooks in discussion of Burmister's paper expressed the opinion that it would be more accurate to use the curvature of the surface as a criterion rather than the deflection; however, that the best criterion should probably be based on shearing stress considerations.

Of course, as most of the pavement failures are due to overstressing-excessive deformation of the subgrade, the criterion should also contain some considerations on the stresses and displacements of the subgrade layer.

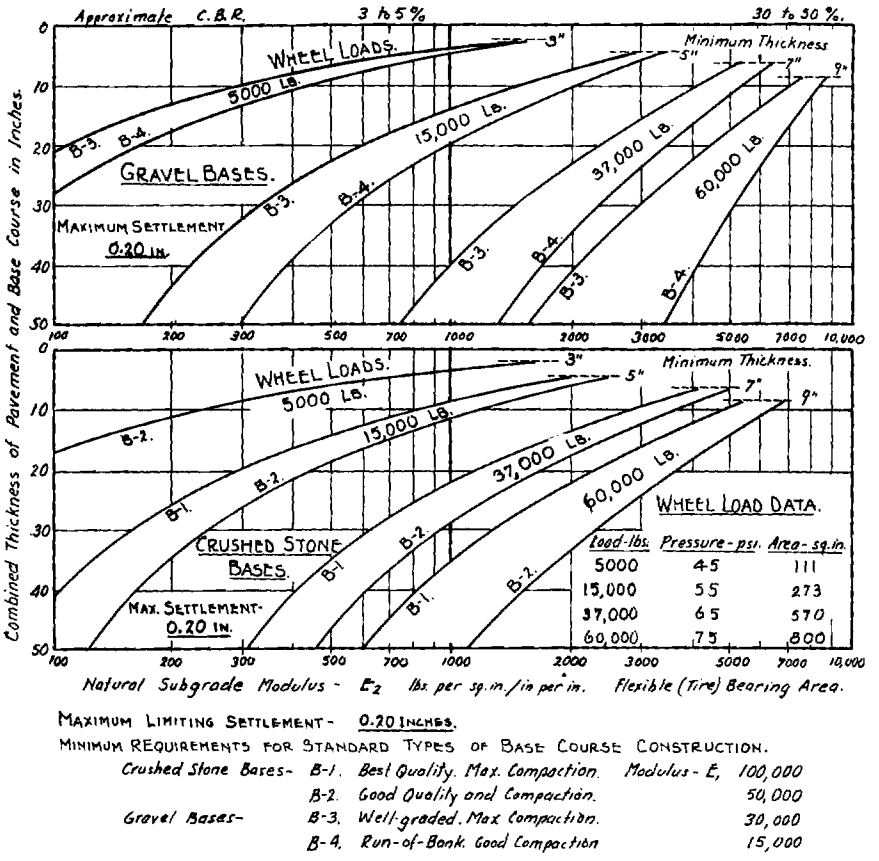

MAXIMUM LIMITING SETTLEMENT - 0.20 INCHES.

MINIMUM REQUIREMENTS FOR STANDARD TYPES OF BASE COURSE CONSTRUCTION.

Crushed Stone Bases-	B-1.	Best Quality. Max. Compaction.	Modulus - E, 100,000
	B-2.	Good Quality and Compaction.	50,000
Gravel Bases-	B-3.	Well-graded. Max Compaction.	30,000
	B-4.	Run-of-Bank. Good Compaction	15,000

Figure 10. Design Curves for Flexible Pavements (Burmister).

SUMMARY

The analysis of stresses and deformations of loaded soil masses is made by means of the Theory of Elasticity. Complete solutions, with tables, graphs and charts for immediate practical application exist for most important cases of loading of homogeneous masses. General solutions exist for important cases of loaded layered and orthotropic masses. However existing tables and graphs permit direct evaluation of stresses along the axis of the load only and evaluation of the maximum displacement of the surface only.

As the Theory of Elasticity deals with ideal elastic materials, deviations from the theoretical stress distribution have to be expected in real soils.

Considerable experimental work was done during the past fifty years with a view of checking to what extent the stresses in soil masses follow the stress pattern indicated by the theory. After some misleading conclusions of the early investigators, recent measurements and analyses showed that the Boussinesq theory represents the best possible approach to stress and deformation problems in homogeneous sandy and clayey soils. There is still not sufficient experimental evidence on the stress distribution in layered masses, which is of greatest importance in study of pavement systems.

The design methods for flexible pavements are in development now. There are several good empirical methods which, although not perfect, satisfy temporarily the needs of the engineering practice. More rational methods, based on thorough understanding of phenomena that occur on subgrades, bases and surface-courses under wheel loads, are still to be developed.

CHAPTER III

TEST SECTION, EQUIPMENT AND INSTRUMENTS

General

For the purpose of this research project a test section of a highway pavement was constructed in a test pit. Pressure cells were made and installed at different positions inside the test section. Static loads are applied by means of the loading equipment (jack against loading frame) through various wheel assemblies at different positions at the surface of the pavement. Stresses are measured by means of pressure cells. Simultaneously readings of air and pavement temperature are made.

Detailed description of the test section, equipment and instruments mentioned above is given in the following pages.

Test Pit

As constructed, the test pit is 8 ft. wide, 12 ft. long and 7 ft. deep (net dimensions). It has vertical 6 in. wide walls of concrete with wire reinforcements. A sump, consisting of a 12 in. clay pipe is placed in the northwest corner of the pit in order to allow control of water level in the test section. The bottom of the pit, consisting of 6 in. slab of concrete with wire reinforcement, is slightly inclined (4%) toward the bottom of the sump, for easier drainage of water.

The continuity between the vertical walls and the bottom slab of the pit is assured by 18 reinforcing bars No. 4. Two 2" by 2" vertical notches are provided on full height of the longer sides of the pit for possible division of the pit in smaller sections. Also, thirty-two anchor nuts are provided

along the top of the walls of the pit for the connection of different possible equipment (loading frame etc.). -- The plan of the test pit with the loading equipment is shown in Figure 11.

Test Section

The first test section of pavement in full scale was constructed as shown on Figure 12. It consists of a 3 in. surfacing of asphaltic concrete with an 8 in. sand ("topsoil") base. The surfacing and the base are underlain by a 37 in. layer of controlled subgrade (sub-base) and 36 in. of uncontrolled subgrade soil.

The grain-size and compaction curves of the "topsoil" used for base, as well as for the material of which both controlled and uncontrolled subgrade are constructed, are shown in Figure 13 and 14. Measured indexes of the soils used are given in the following table:

INDEXES OF THE SOILS USED

		Base	Subgrade
Liquid limit		14.5	45.4
Plastic limit		-	37.4
Plasticity index		0	8.0
Specific gravity of solids		2.61	2.69
Optimum moisture content	Standard Proctor	10.1%	24.8%
	Modified Proctor	-	16.4%
Maximum dry unit weight lb/cuft	Standard Proctor	128.0	94.4
	Modified Proctor	-	103.3

Wheel Assemblies

Three different wheel assemblies, shown on Figure 15 are used in loading

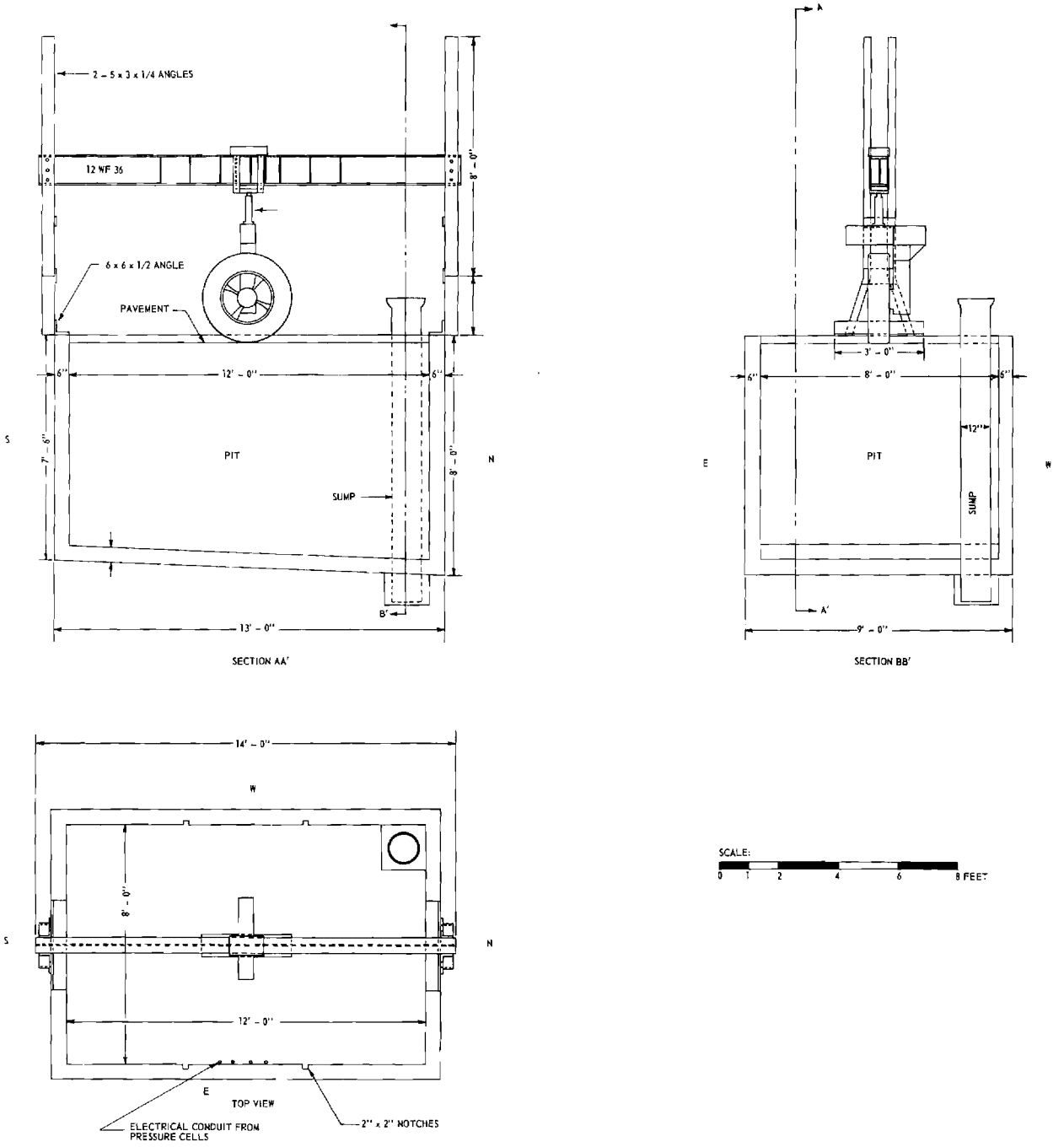

Figure 11. Test Pit and Loading Frame.

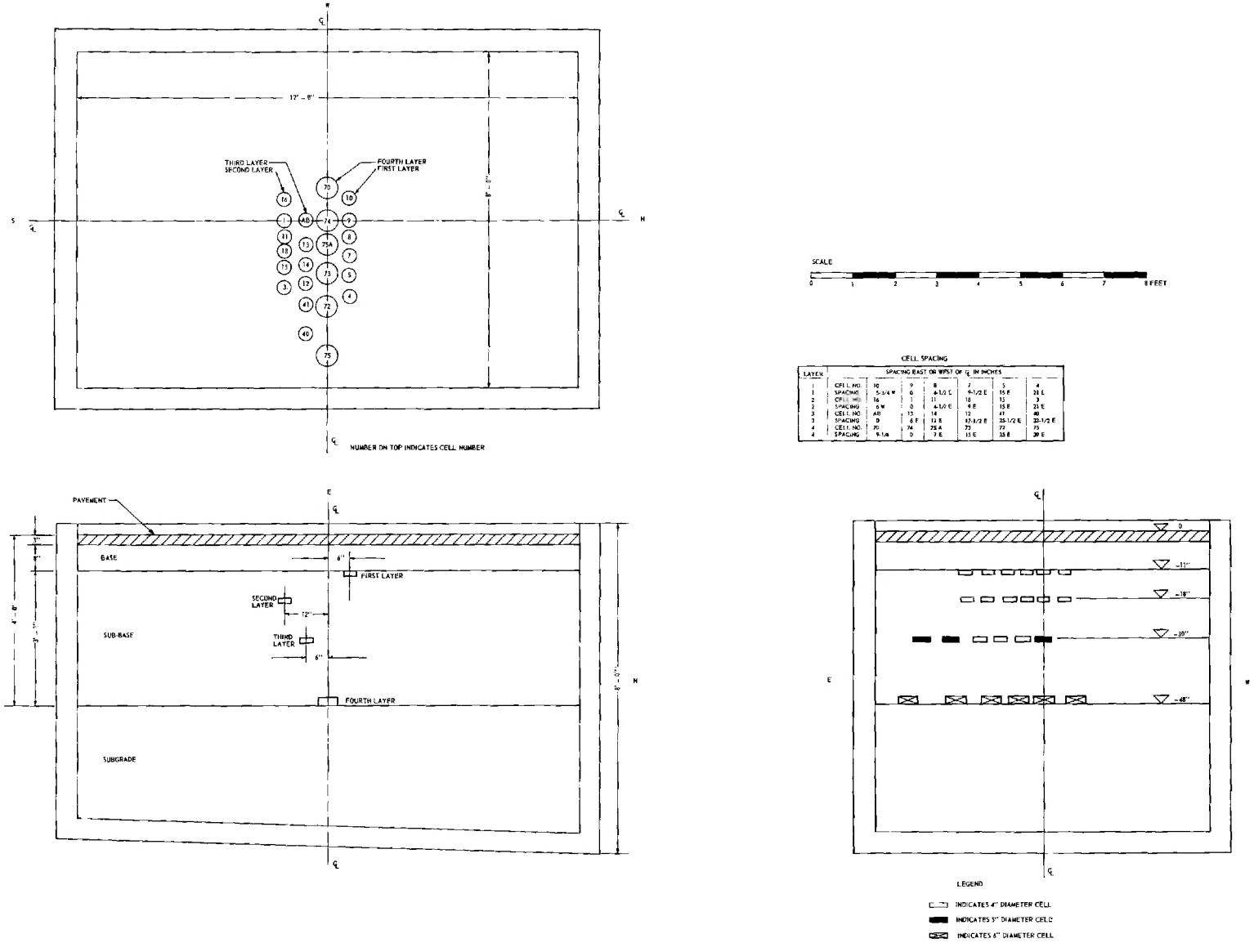

Figure 12. Position of Pressure Cells and Cross Section of the Test Section.

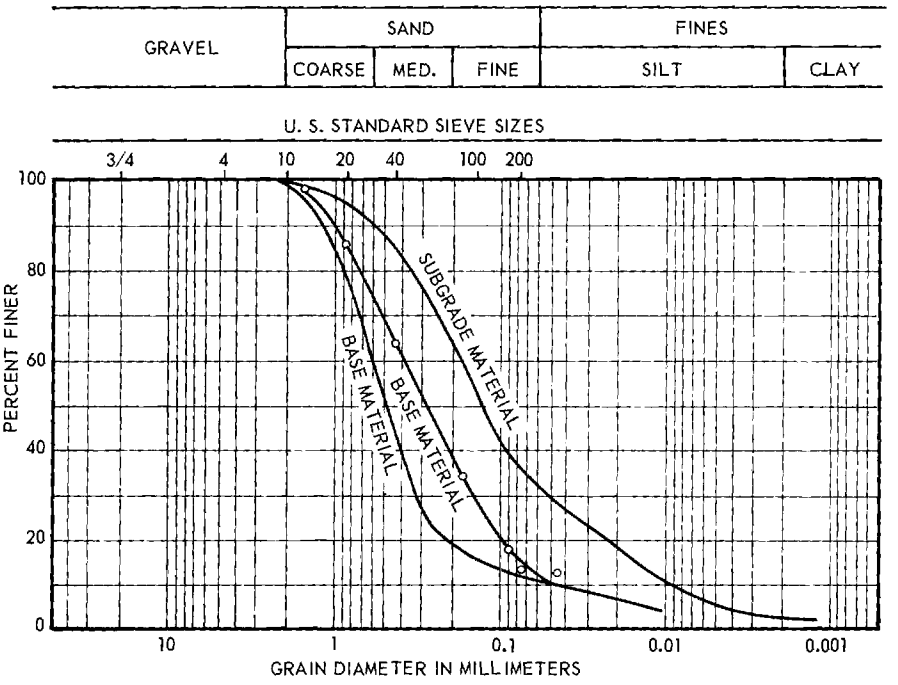

Figure 13. Grain-Size Curves.

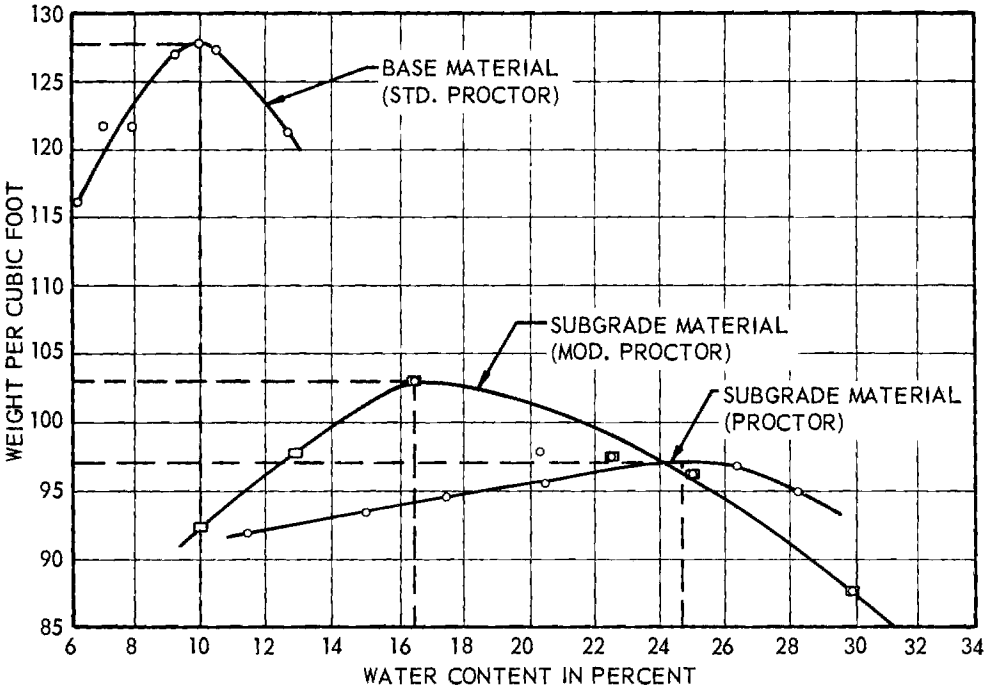

Figure 14. Compaction Curves.

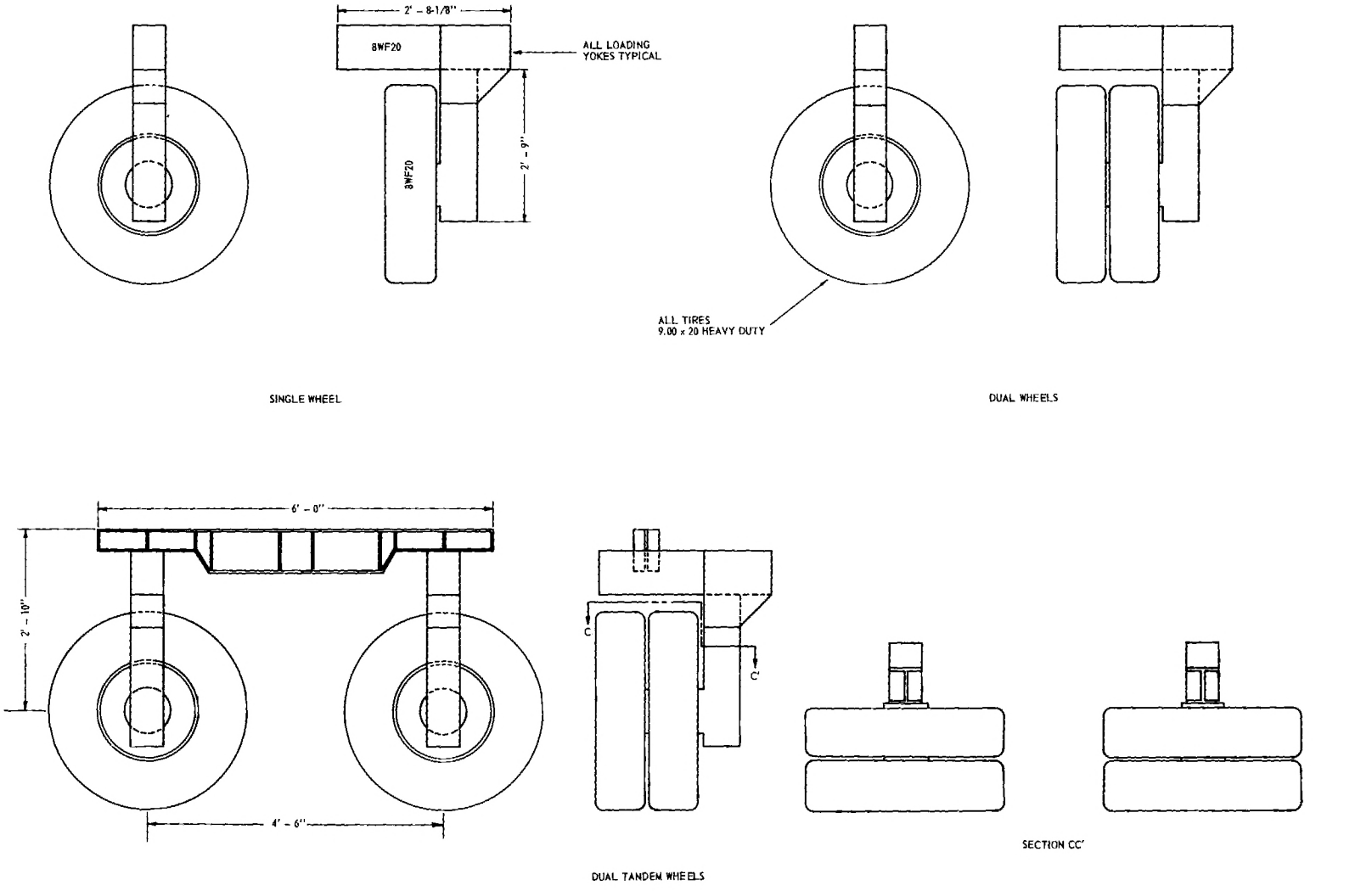

Figure 15. Wheel Assemblies.

tests: single, dual and dual-tandem. The tires used are standard 9/20 truck tires inflated to 70-90 psi pressure.

Imprints of these tires at an inflation pressure of 86 psi and at loads of 4500, 6750, 9000, 13500 lbs are presented in Figure 16.

Loading Equipment

Loads are applied to the wheel assemblies by means of a simple hydraulic jack (capacity 30 tons). The reaction for the loads is furnished by a steel frame, the view of which is given in Figure 11, together with the test section of the pavement and a single wheel ready for loading. The horizontal beam of the frame can be moved in vertical direction and placed at any desired height above the pavement. The jack is attached to a carriage that may be moved horizontally along the lower flange of the beam. The general view of the frame and of the loading equipment (carriage, jack) with a single wheel and the stress measuring instruments is shown on enclosed photographs (Figures 17, 18). The beam is designed for a single load of 36,000 lb at any position.

Pressure Cells

For the measurement of normal stresses in soil mass a simple pressure cell, shown in Figures 19& 20 was designed. It consists of a thin circular face plate-membrane fixed at its perimeter to a thicker base plate. The face plate-membrane responds to loading by stretching and bending. A SR-4 strain-gage fixed to the rear of this plate undergoes resistance changes proportional to these strains. As this plate is made of an aluminum alloy obeying Hooke's law, resistance changes are also nearly proportional to applied external pressure. Another, dummy, SR-4 gage is fixed to the base plate. It enables compensation for temperature and similar parasite strains.

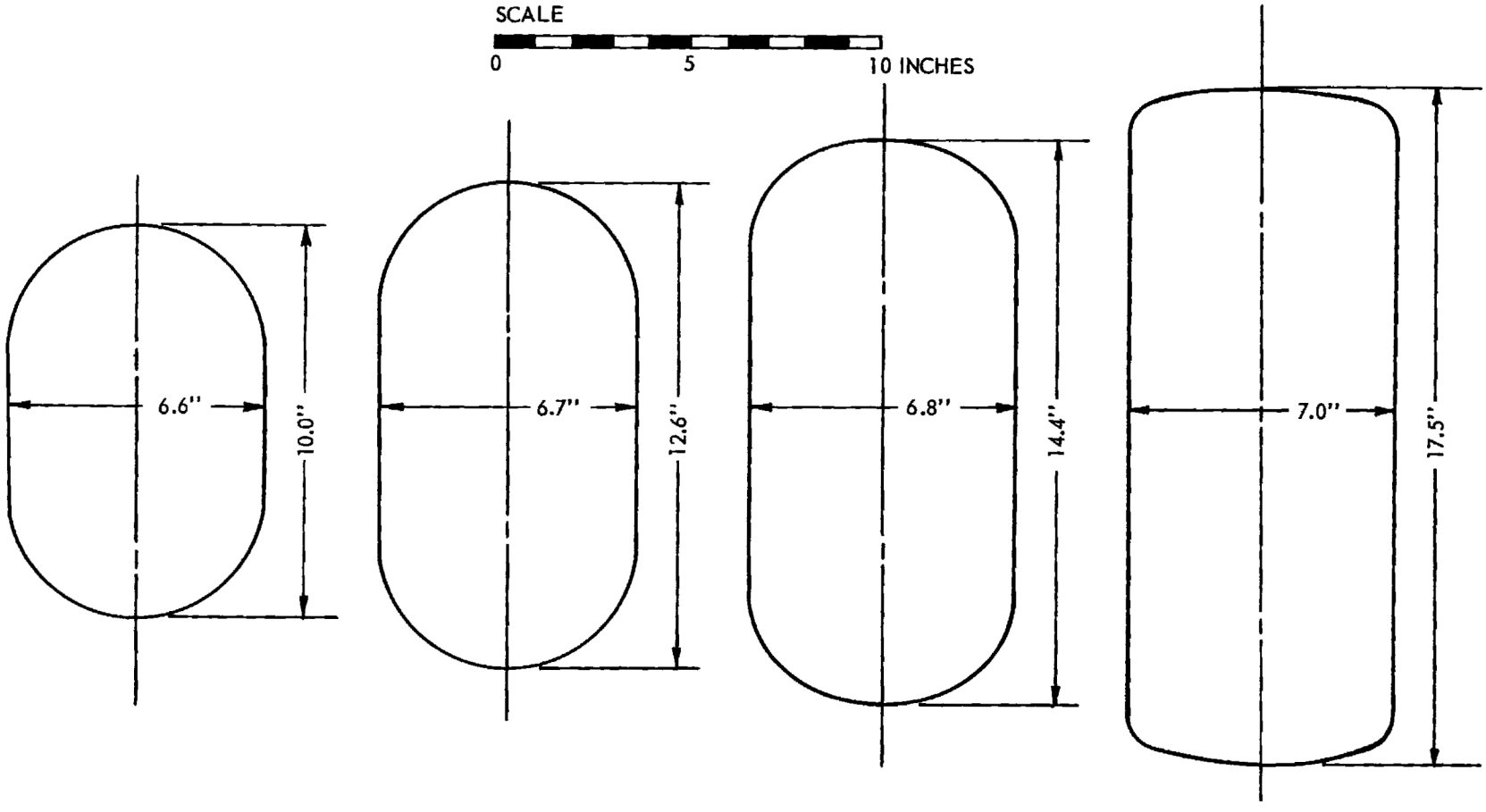

Figure 16. Typical Tire Prints.

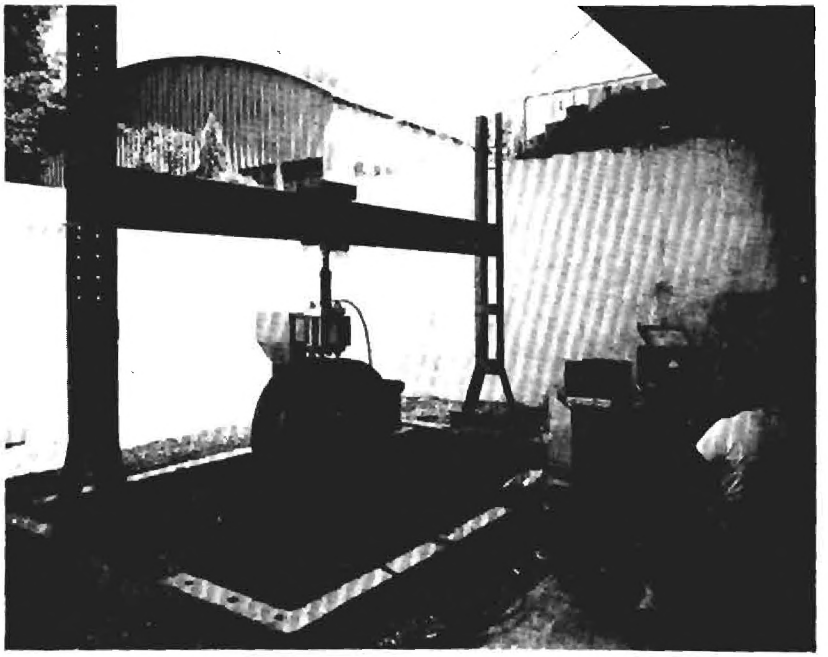

Figure 17. General View of the Test Pit and Loading Equipment.

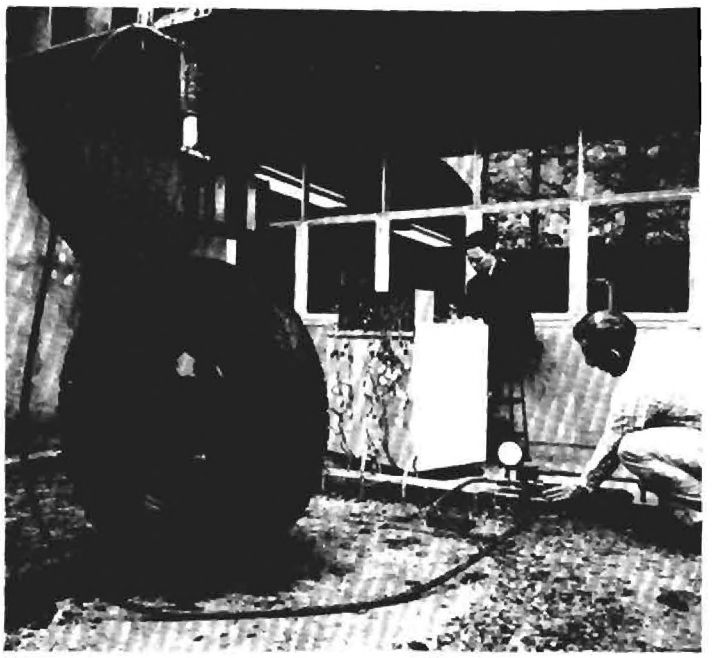

Figure 18. A Single Wheel, Loading Jack and Stress-Measuring Devices.

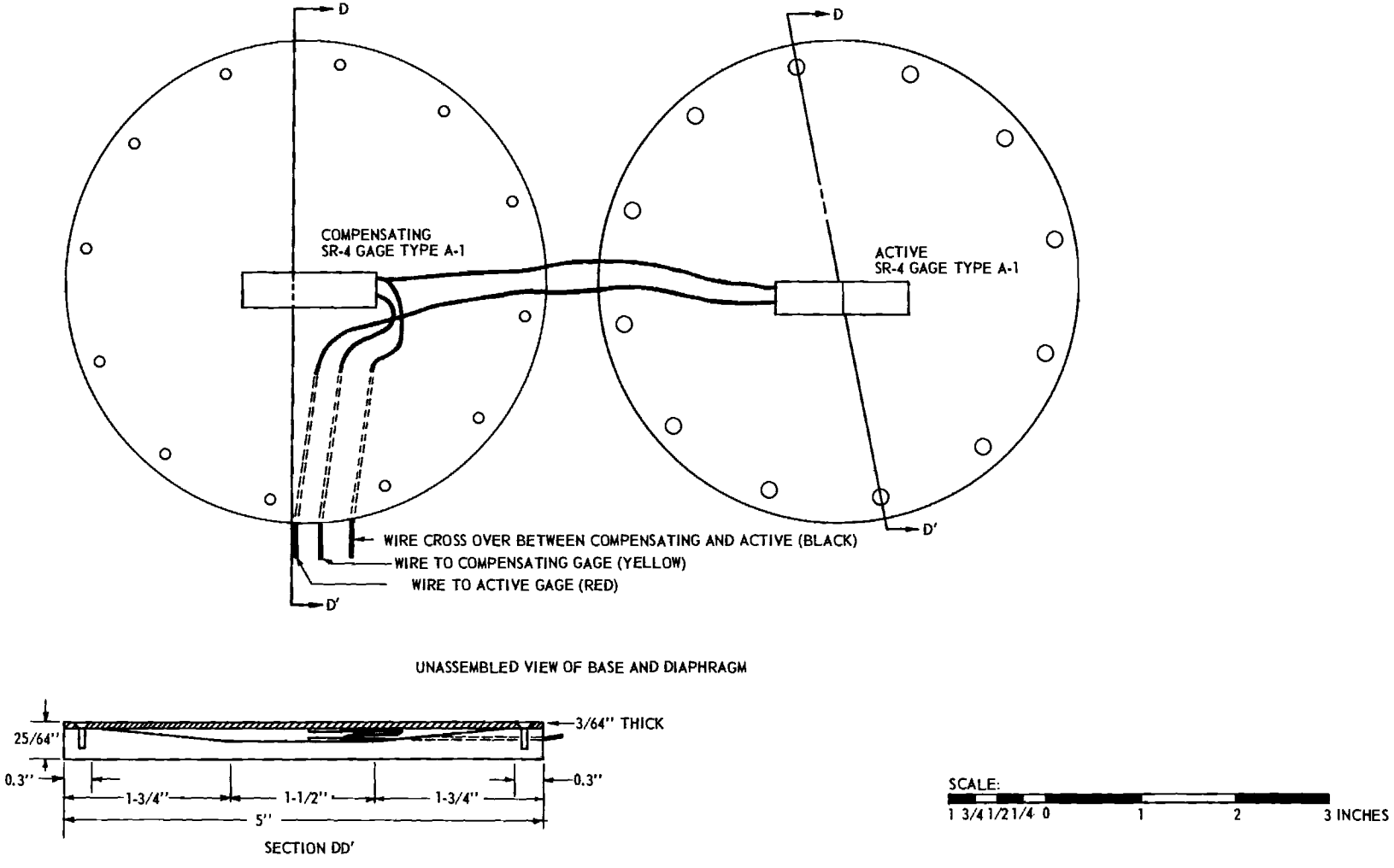

Figure 19. Typical Pressure Cell.

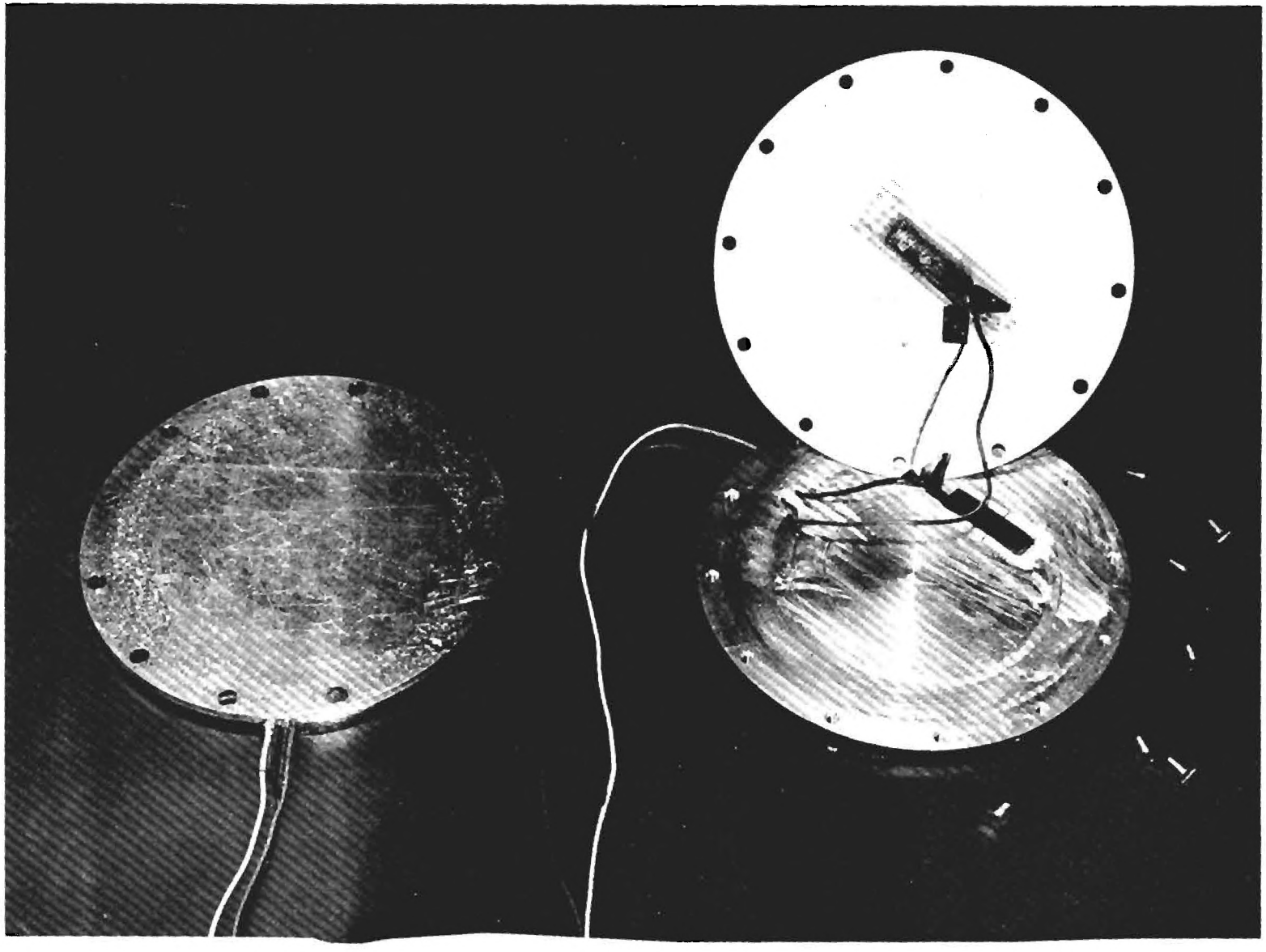

Figure 20. View of a Pressure Cell (left); Inside View of the Rigid Base and the Membrane of a Cell with Strain-Gages (right).

The installed gages are carefully waterproofed with Petrosene wax and connected in a circuit of the Wheatstone bridge type to the strain-indicator, a Baldwin L. Due attention was devoted to perfect sealing and waterproofing of the outside of the cells with polyvinyl cement. The leads were protected by steel conduits. Two switching and balancing units (a 20 channel Baldwin PSBA20 and a 6 channel Ellis BS6) permit quick reading of the 25 cells installed in this preliminary stage of testing.

Three different sizes of cells are used: 4-in., 5-in. and 6-in. diameter. Each cell was calibrated by direct application of a set of pressures in a calibrating chamber (see Figures 21 and 22). Air pressure was applied directly on the cells lying on a layer of compacted soil and covered with a rubber membrane. However, several comparative calibrations with cells completely embedded in soil showed little difference to the calibrations made by direct air pressure.

Calibration curves for three typical cells are shown in Figure 23. The results of a comparative calibration with air pressure applied directly respectively through a 1 1/2 in. layer of soil above the cell is shown in Figure 24.

A plan of position of installed cells is shown on Figure 12, together with the cross-section of the test section. Twenty-five cells were installed in 4 layers at depths shown.

Temperature Measurements

During stress measurements temperature changes were observed and recorded using a laboratory thermometer the end of which was placed in an insulated 4 in. deep hole in the pavement. Air-temperature was recorded too.

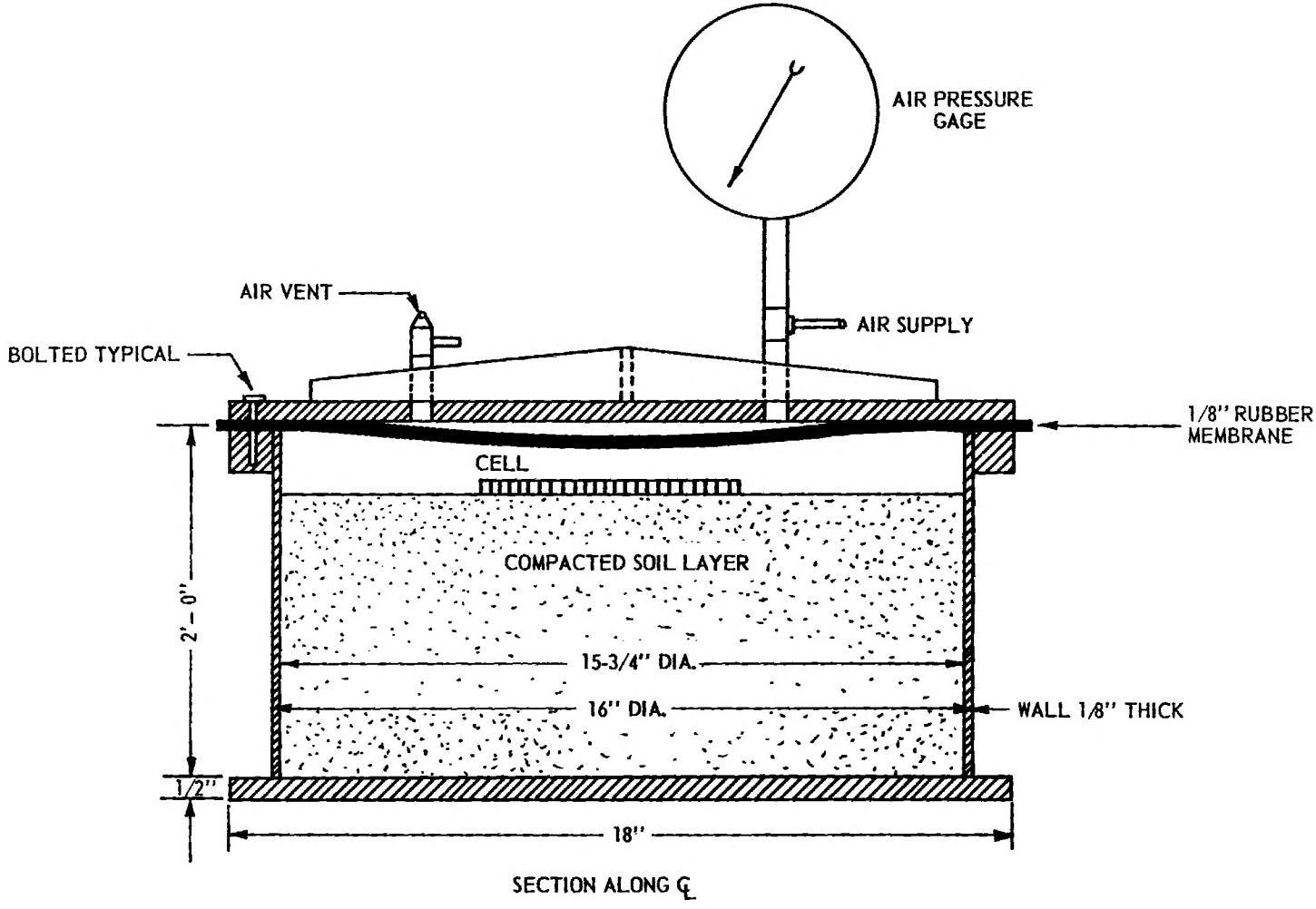

Figure 21. Pressure Cell Calibrating Chamber.

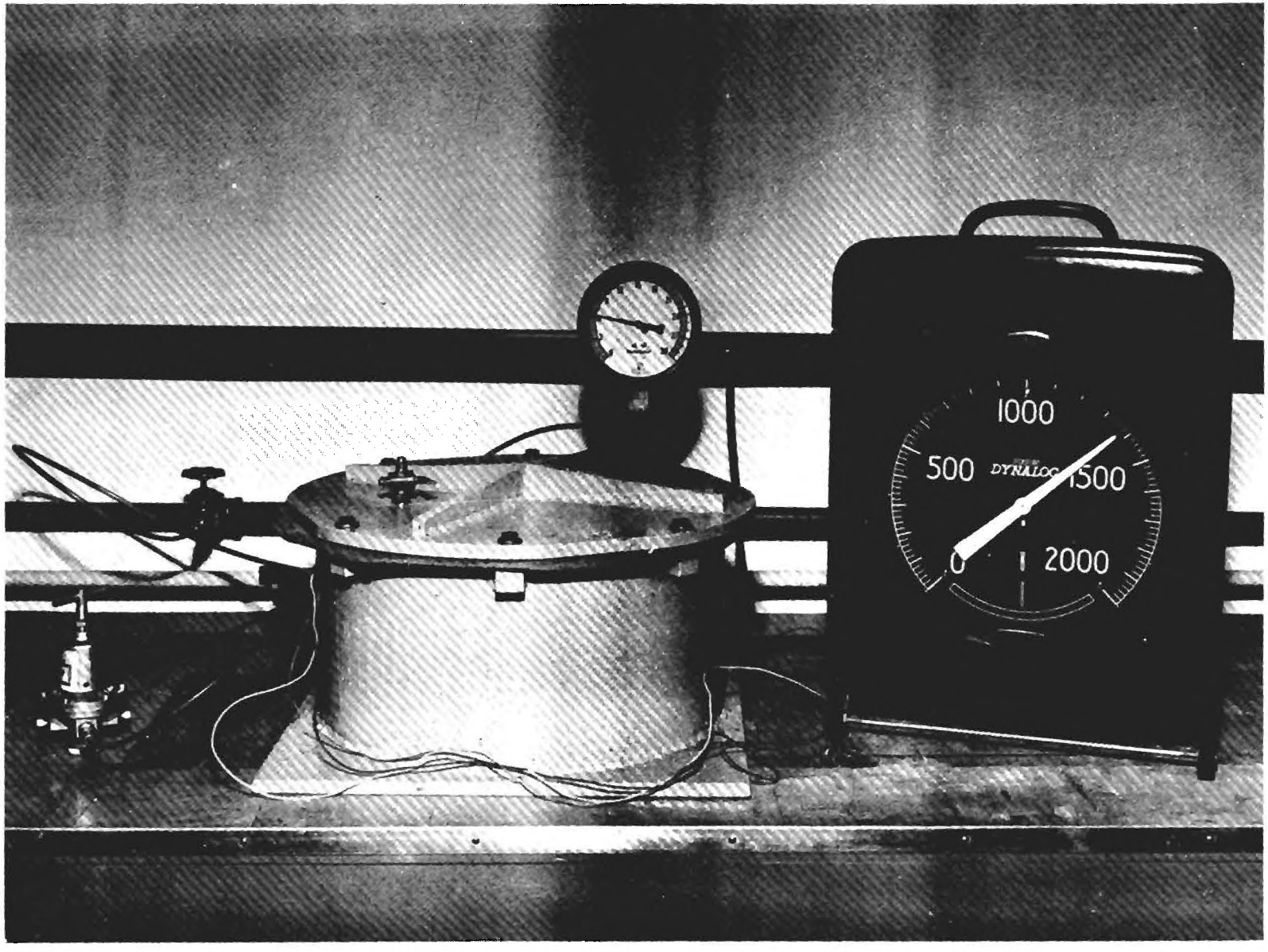

Figure 22. View of the Calibrating Chamber with Baldwin Dynalog Strain Recorder.

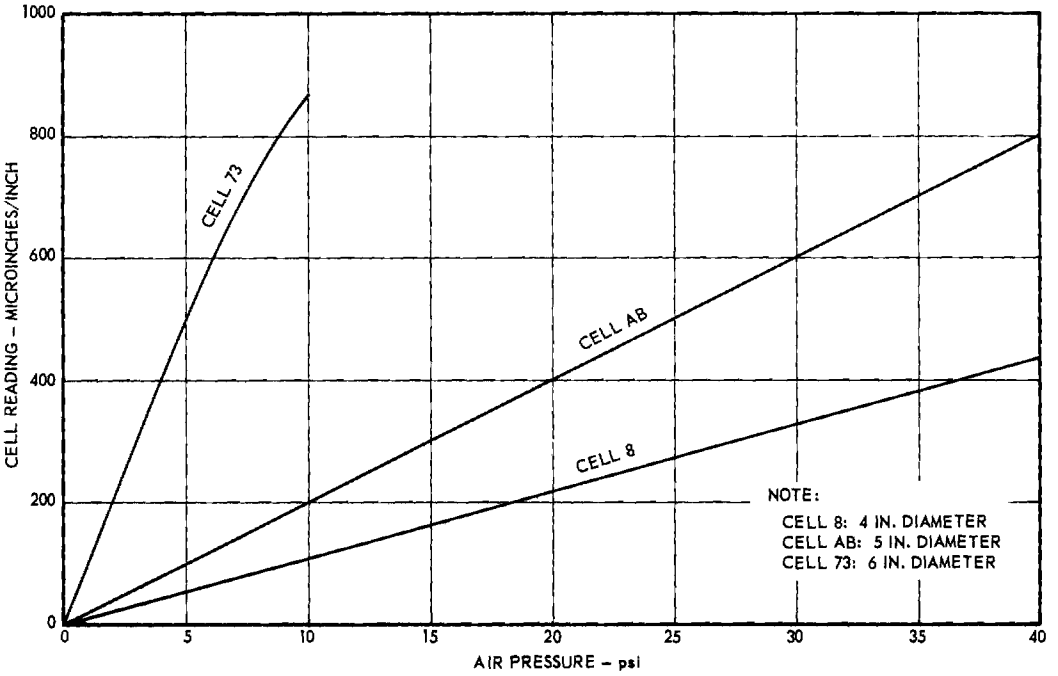

Figure 23. Typical Calibration Curves for Pressure Cells.

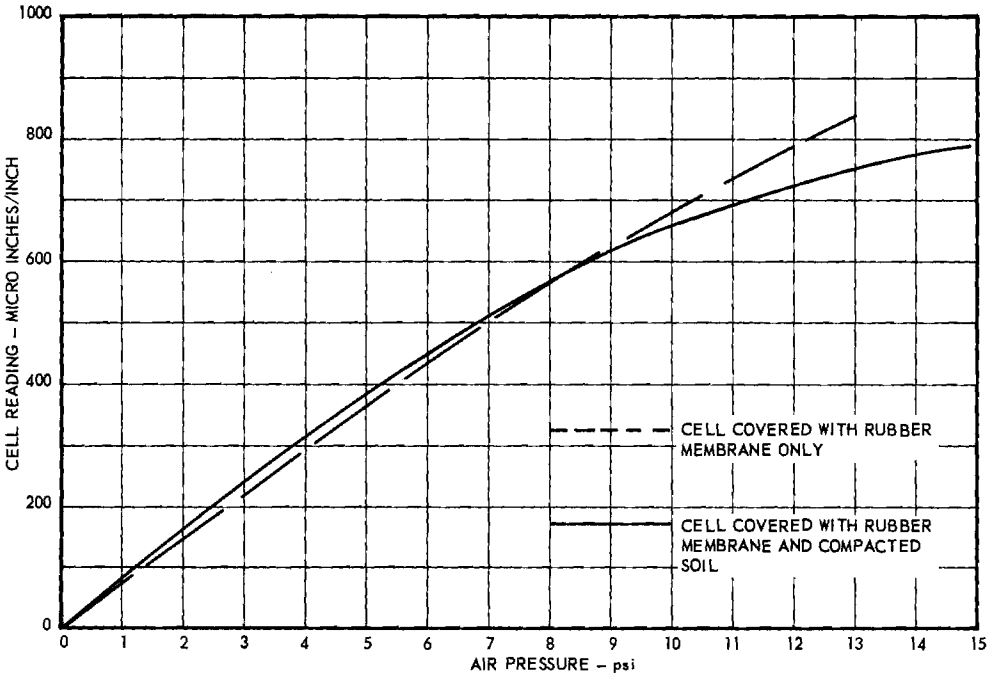

Figure 24. Calibration Curves for Cell No. 71.

Soil Testing Equipment

Laboratory tests on samples of soil used in construction of the test section are made using standard equipment.

Grain-size curves are determined by using standard U. S. sieves (for coarser-fractions) and soil hydrometers (for finer fractions).

Liquid limits are determined in a standard ASTM device.

Compaction tests are made in standard Proctor mold (4 in. in diameter), using 25 blows of standard hammer (5.5 lb) falling 12 in. on each of the three layers. (Standard ASTM or standard AASHO-test).

Consolidation tests will be made by using samples 2.375" in diameter and 1" high, subjected to pressures up to 32000 lb/ft^2 or 222 psi.

Triaxial shear tests will be made in a new constructed big triaxial shear apparatus, with samples 4, 6 and 8 in. in diameter as well as in the existing apparatus of the laboratory with standard samples 1.4 in. and 2.8 in. in diameter.

For detailed description of the equipment used in the mentioned standard tests see general references (58) (62).

CHAPTER IV

EXPERIMENTAL PROCEDURE

Construction of Test Section

Both uncontrolled and controlled subgrade were constructed of a local material - typical micaceous silt of the Piedmont Region. The base was constructed of a "topsoil" from Waverly Hall, Georgia, used currently by the Georgia Highway Department as a material for the base. The grain-size and compaction characteristics of these materials are shown in Figure 13 and 14; other measured indexes in a table on page 34.

Compaction of the subgrade as well as of the base was accomplished by using a mechanical light tamper ("Jay") with gasoline-engine. The water content of the material was kept slightly below the optimum. The material was placed in horizontal layers 2-3" thick. The controlled part (sub-base) was compacted to 95-100% of the Standard Proctor maximum dry unit weight, and the uncontrolled part to roughly 90% of the same.

The surface-course was constructed on a 3 in. layer of asphaltic concrete E, compacted by means of a plate-vibrator.

Cell Installation

As shown in Figure 12, 25 pressure cells were installed in the test section in four layers. The cells of one layer are arranged in rows placed longitudinally so as to minimize possible arching due to the presence of cells on the soil mass.

Installation of cells in the planned positions in the test section was done with greatest care. For each cell a small shallow pit was excavated to

the desired depth and the cell embedded in the right position. Backfill around the cells was then placed in and tamped carefully using a hand tamper. It is believed that good homogeneity of the soil was realized around the cells as well as in the rest of the backfill.

Stress Measurements

In this preliminary testing program tests were performed with single and dual loads, applied at ten different positions along the N-S axis of the test section. The positions for the loads were: at center-line, as well as 3", 6", 12", 24" and 36" north of center-line, and 3", 6", 12" and 24" south of center line.

Stress readings were made at loads of 2500, 5000, 9000 and 13500 lbs for single loads; 5000, 9000 13500 and 18000 lbs for dual loads. Particular attention was paid to balance the cells out to read zero just prior to the application of the load. Another control zero reading was made after the load has been released.

Soil Testing

In testing soil samples standard procedures were used. For details one may refer to general references (58) and (62).

CHAPTER V

TEST RESULTS

The results of stress measurements are presented in Figures 25-31.

Figures 25-27 show the measured stresses in psi at four depths (11", 18", 30", 48") versus distance in inches from the center of the applied single loads. Separate presentation of results for different intensities of the load (5000, 9000 and 13500 lb) was necessary due to the fact that the size and the shape of the loaded area as well as the intensity of the contact pressure varied with the load. The theoretical curves drawn represent stress distribution for a homogeneous and isotropic soil mass, due to corresponding loads evenly distributed over circular loaded areas.

Figures 28-31 show the measured stresses in psi at four depths versus distance in inches from the center of gravity of the applied dual loads. For the afore-mentioned reason, results for different load intensities (5000, 9000, 13500 and 18000 lb. total load) are presented separately. For comparison with the theoretical values two theoretical curves for stresses in a homogeneous and isotropic soil mass are drawn for each load intensity and depth. These curves represent stresses along the N-S and E-W vertical cross section through the center of gravity of the applied loads. These stresses were computed assuming rectangular loaded areas and uniformly distributed contact pressure, which, according to the data obtained from tire print measurements (Figure 16) varied with the applied load.

The analysis of test results shows that the scattering of pressure cell readings is in most cases within plus or minus 2 psi which is the probable

accuracy of the cells. The average error is probably in the order of ± 1 psi.

However some cell readings were, for a still unexplained reason, completely erratic. Also some of the cells showed accuracy less than normal. It will be decided after recalibration of all cells whether these less accurate cells will be used in the next phase of work.

It was remarked during the testing operations that the zero-shift in the pressure cells was occasionally very high. A particular study will be undertaken in order to explain fully the possible influences of temperature, barometric pressure and residual stresses in the soil mass on this phenomenon.

A comparison with the theoretical curves for homogeneous and isotropic soil shows that measured stresses follow the general distribution pattern indicated by the homogeneous theory. This indicates, that the "topsoil" base used has only limited ability to spread the load and reduce the stress on the subgrade.

In fact, although the modulus of deformation of the base appears greater than the modulus of the subgrade there was a consistent trend of stresses immediately beneath the load to be even higher than those indicated by the theory for homogeneous soils. This can be explained partly by the fact that the high applied loads (single 13500 lb and dual 18000 lb) caused some shear immediately beneath the wheels, resulting in relatively large deflections of the surface (maximum up to 0.9"). Also, some of the cells in the vicinity of the N-S axis of the pit seemed to show consistently higher readings. Thus, a final conclusion concerning the exact amount of possible stress concentration in this case will be reached in the next phase of work, after checking and recalibrating the cells.

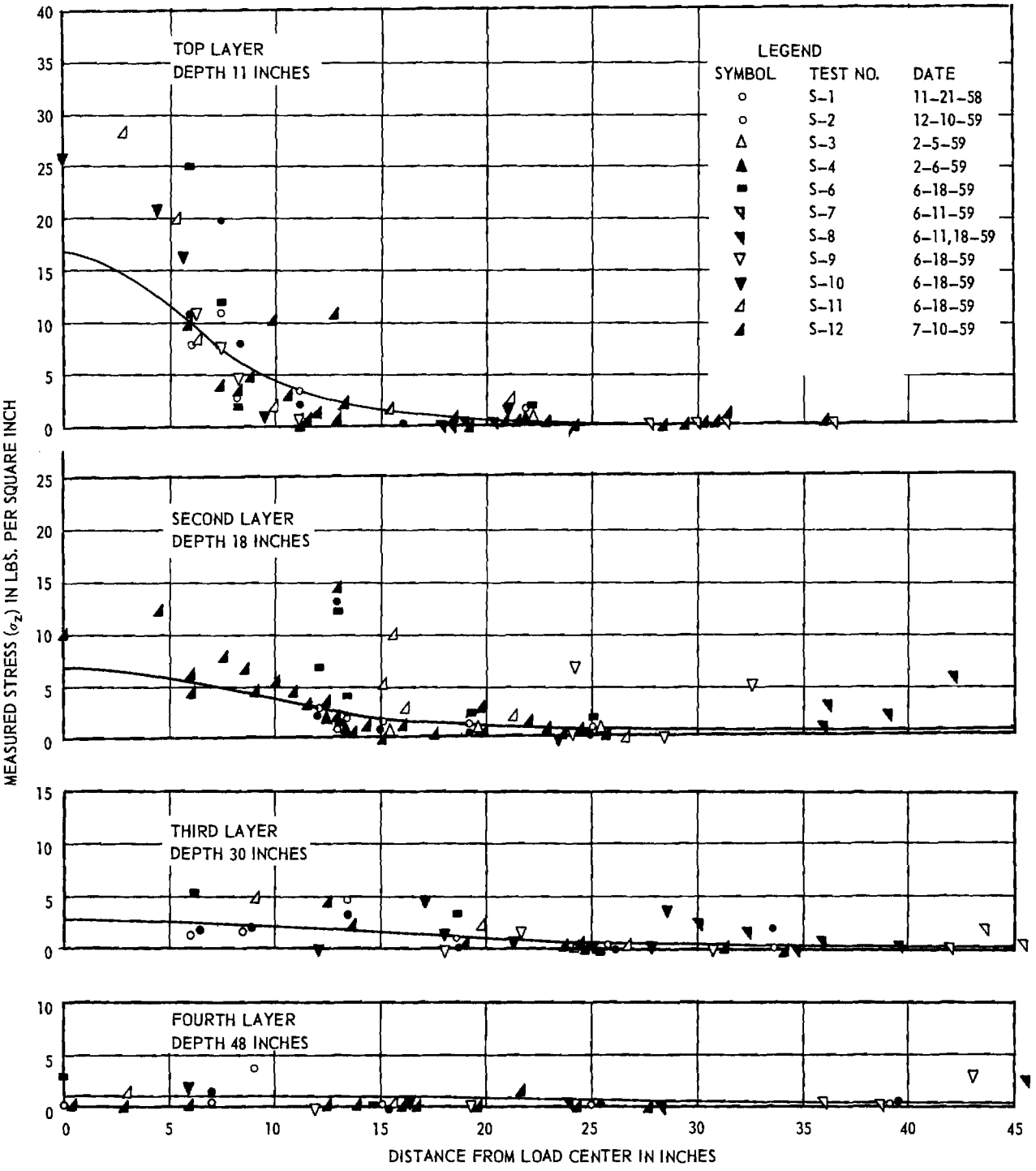

Figure 25. Measured Stresses; Single Load 5000 Lbs.

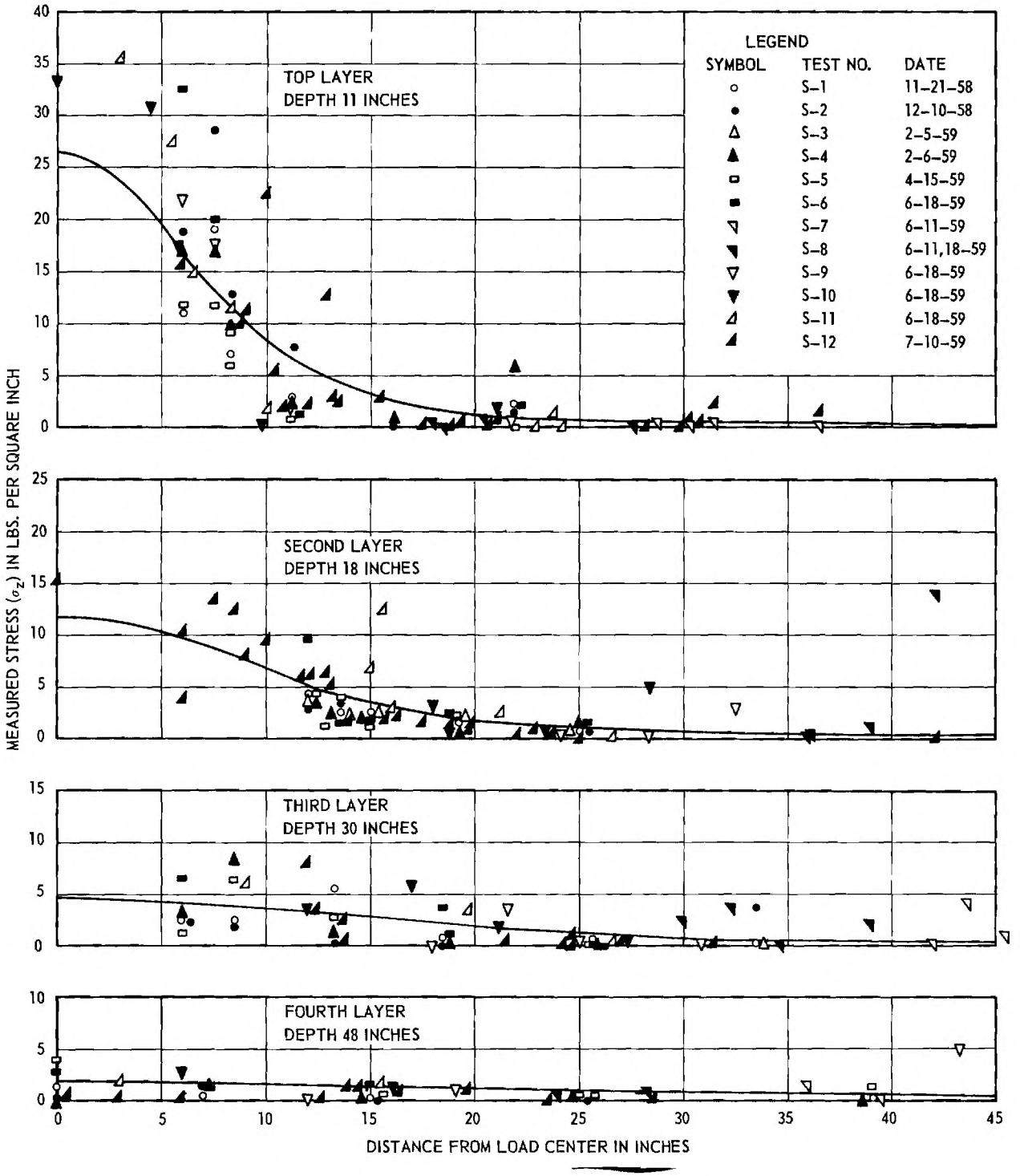

Figure 26. Measured Stresses; Single Load 9000 Lbs.

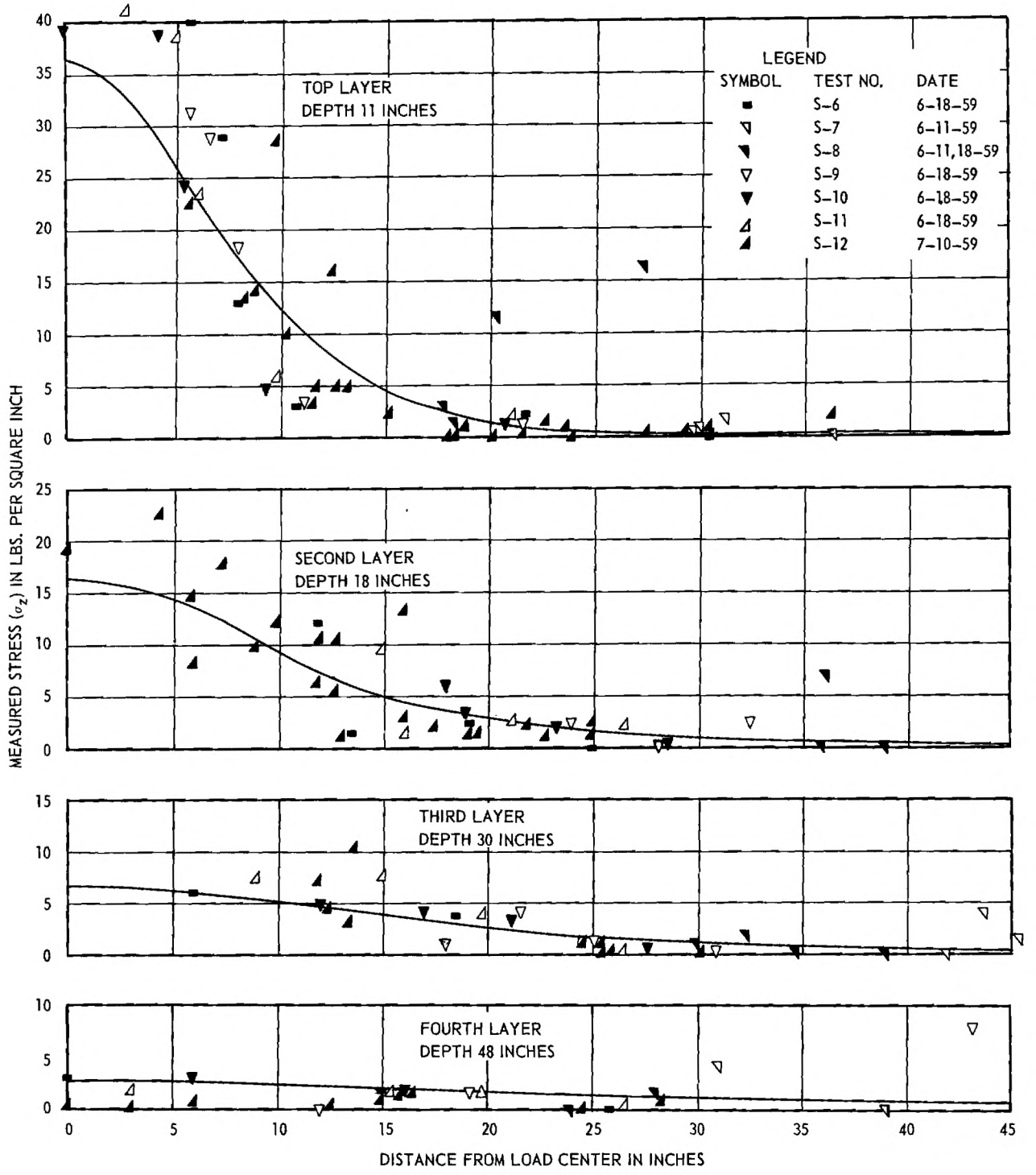

Figure 27. Measured Stresses; Single Load 13,500 Lbs.

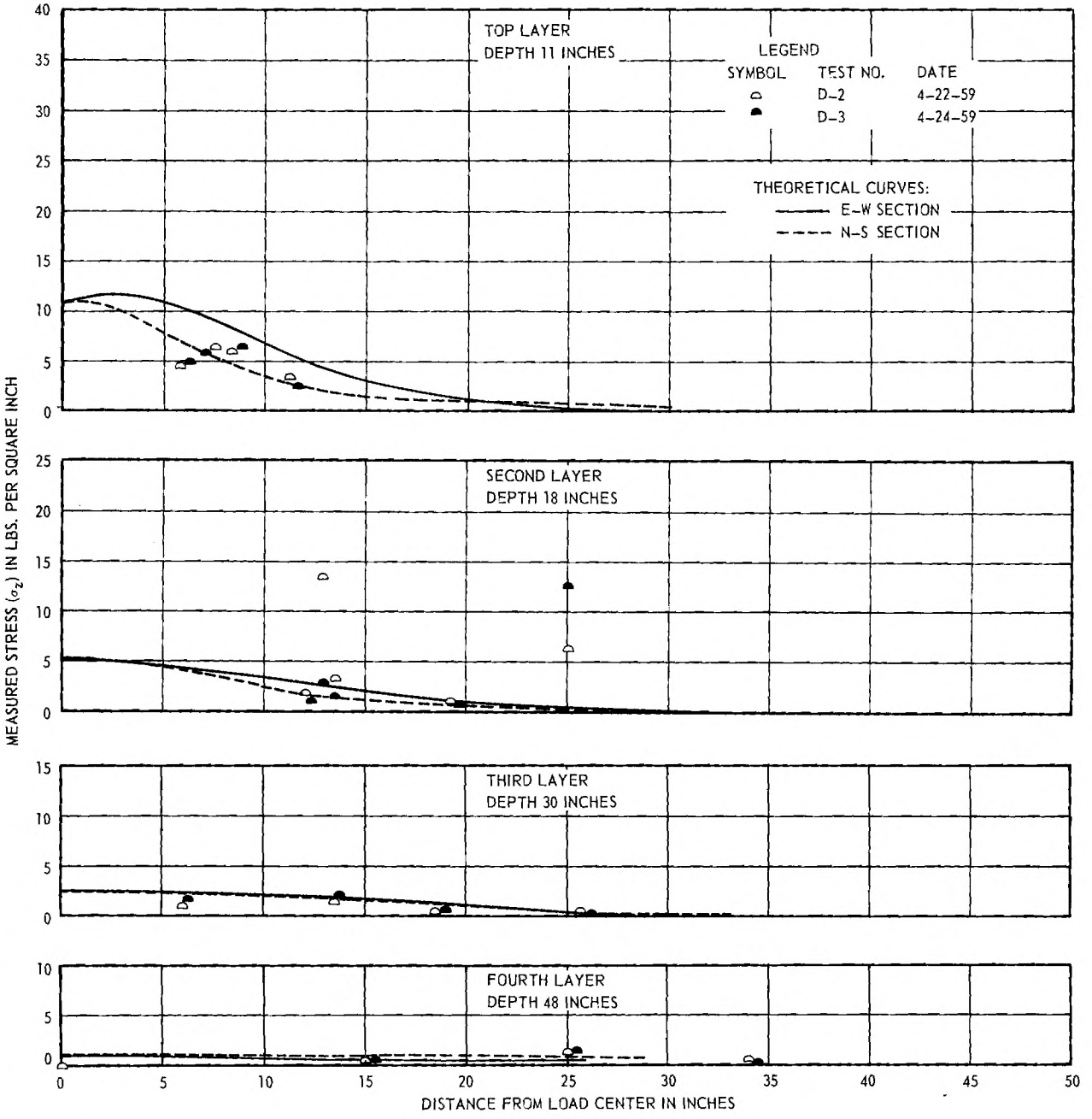

Figure 28. Measured Stresses; Dual Load 5000 Lbs.

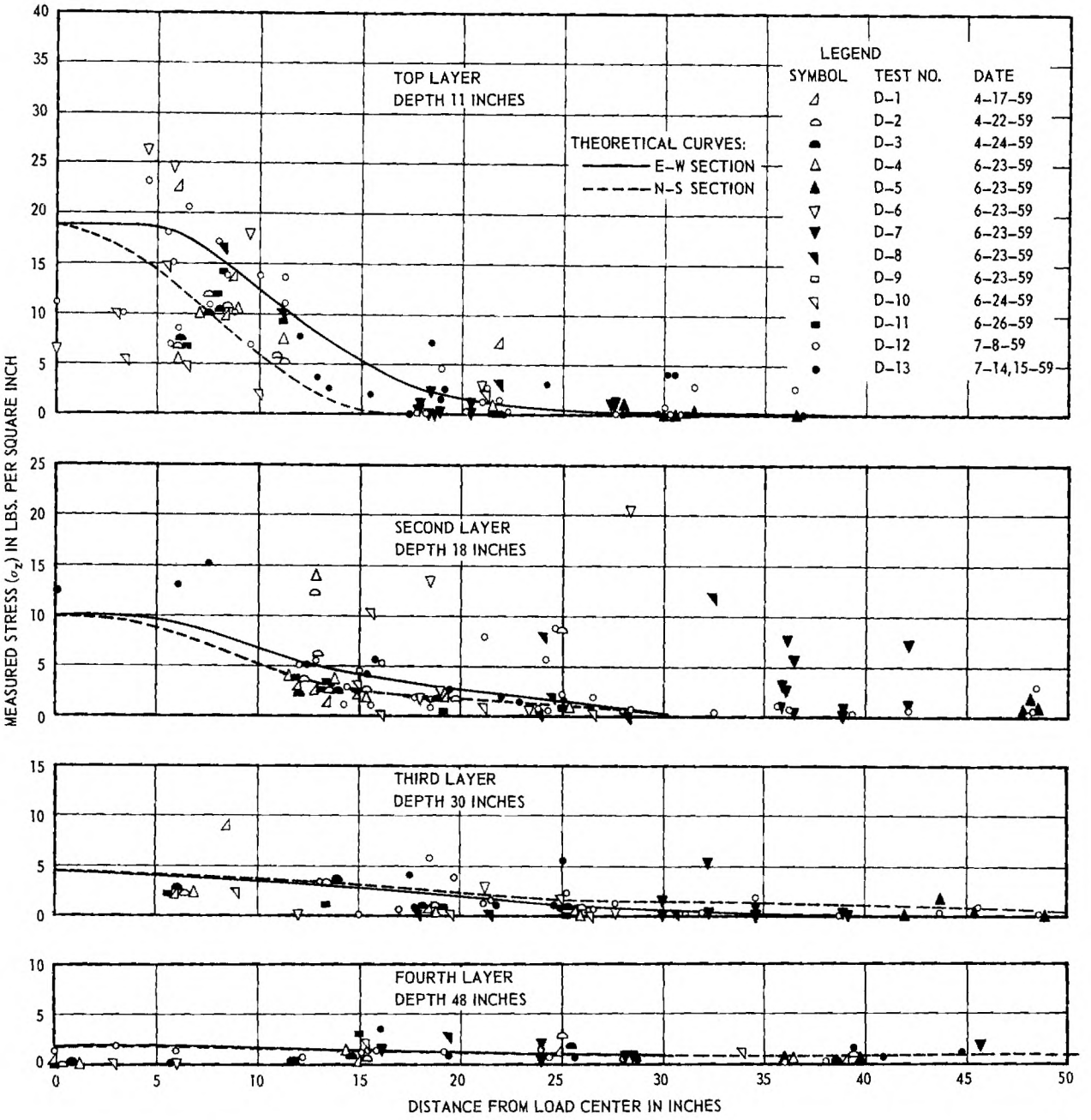

Figure 29. Measured Stresses; Dual Load 9000 Lbs.

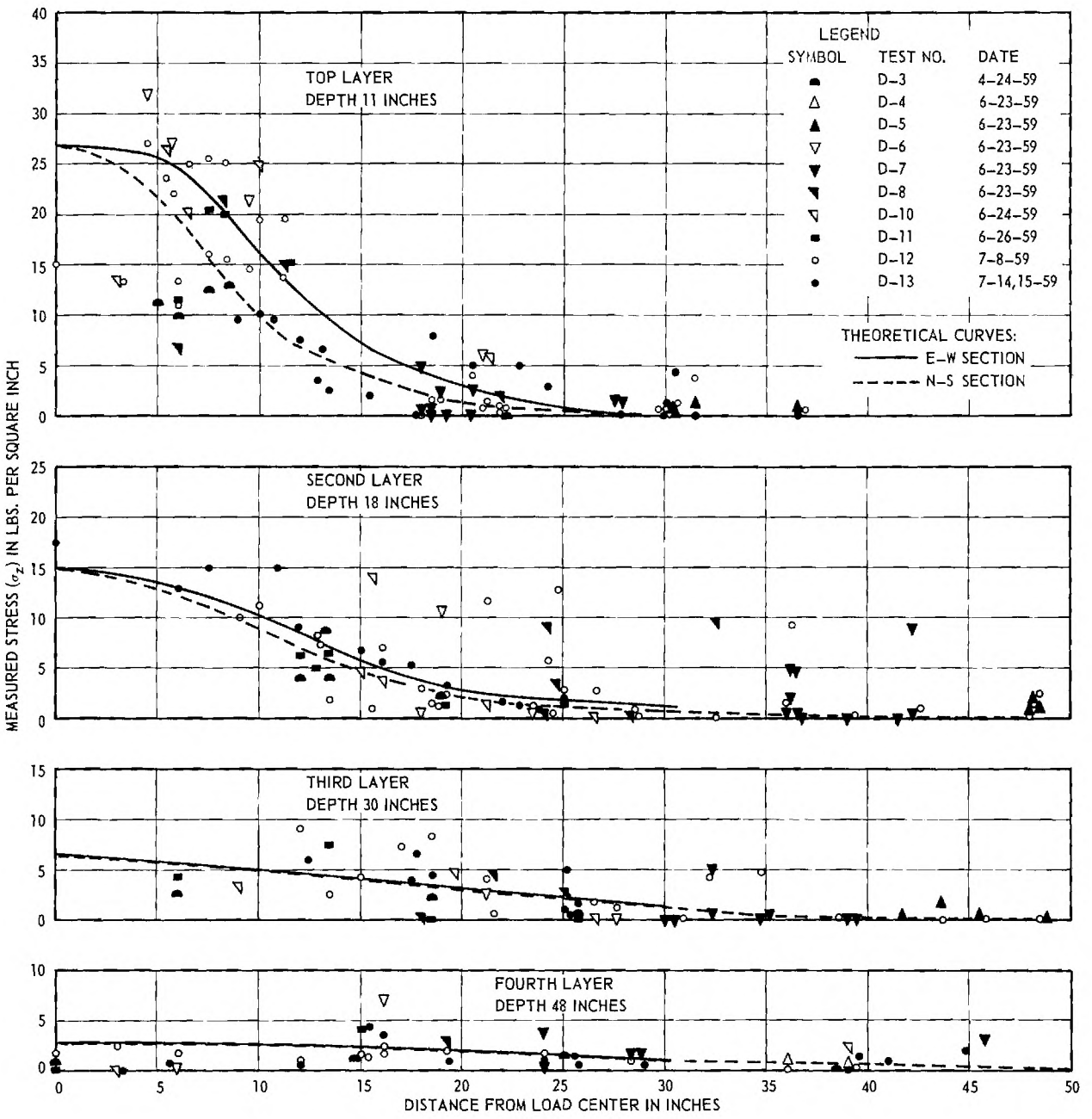

Figure 30. Measured Stresses; Dual Load 13,500 Lbs.

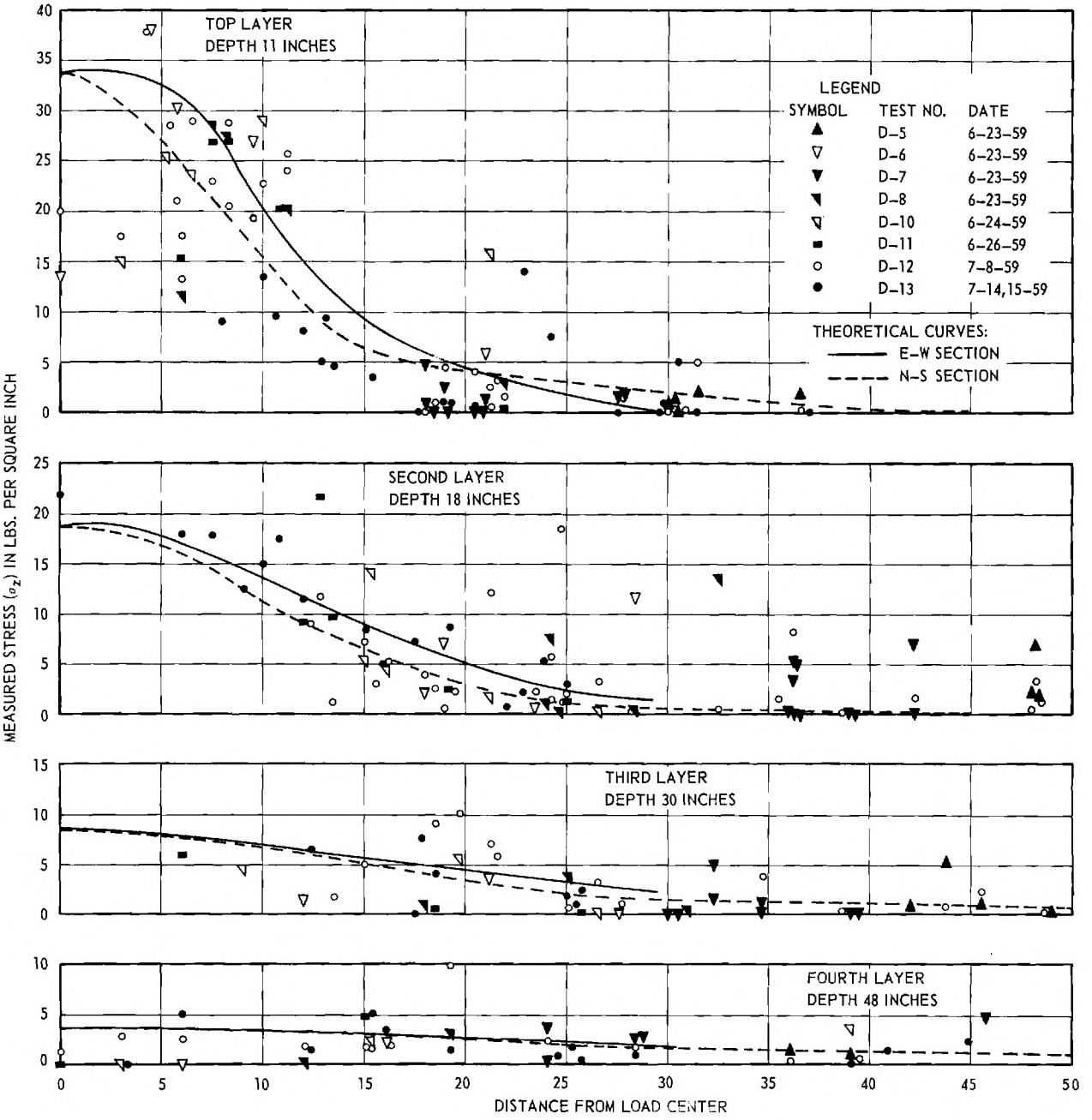

Figure 31. Measured Stresses; Dual Load 18,000 Lbs.

PREVIEW OF NEXT PHASES OF WORK

The first year's work has indicated weaknesses in some equipment designs and shortcomings in the test procedures. The first step in continuing the research will be to modify the loading equipment so it will provide greater loads and more stability during tests. The pressure cells will be recalibrated and re-waterproofed. Additional cells will be made to supplement the present ones.

Tests will then be made using different types of base courses:

Soil Bound Macadam
Soil Bituminous
Water-bound Macadam†
Limerock†

Single, dual, and dual tandem loads will be employed.

The first tests will be limited to the 8 in. base thickness. Varying base thicknesses will be employed later to determine the differences in stresses that result. This will be particularly necessary with the soil cement base which is expected to be more effective than the others.

The physical characteristics of the bases will be tested in the laboratory. A new triaxial cell is being constructed to accommodate the coarse grained materials of the base courses. It will permit a maximum sample diameter of 8 inches.

Plate load tests will be made in the pavement, base, and prepared subgrade to determine the modulus of deformation of each layer, similar to the plate test used in the U. S. Navy-Burmister flexible pavement design. This procedure holds some promise as a practical approach to design.

---

†Tentative

Prepared and submitted by

George F. Sowers
Project Director

and

Aleksandar B. Vesić
Research Associate

Approved by

Thomas W. Jackson, Chief
Mechanical Sciences Division

Released by

J. E. Boyd
Director

APPENDIX

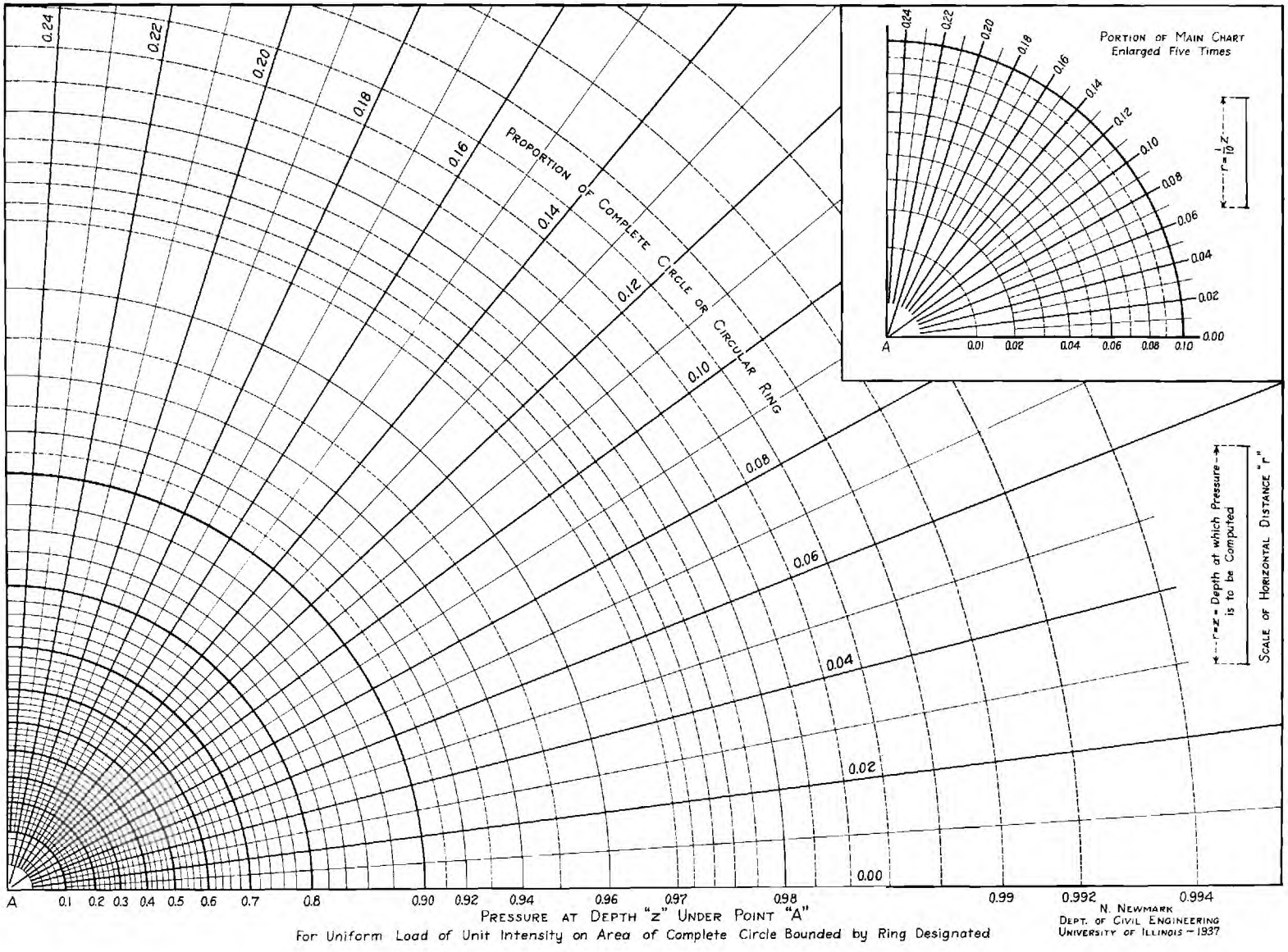

Figure 32. Newmark Chart.

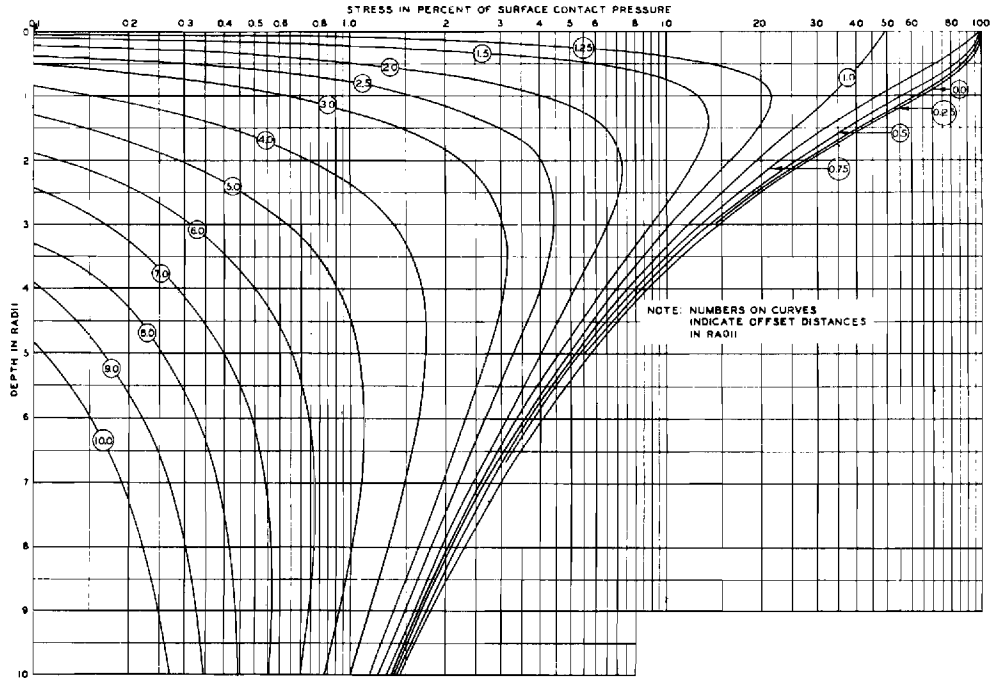

Figure 33. Vertical Stress σ_z Due to Uniform Circular Load. (Foster & Ahlvin).

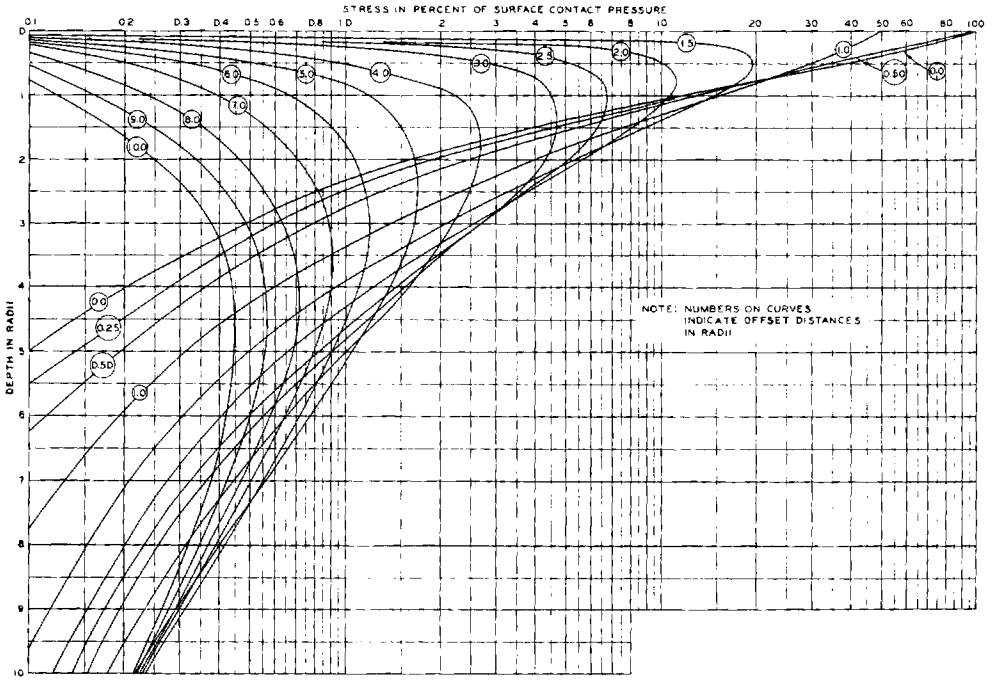

(A)

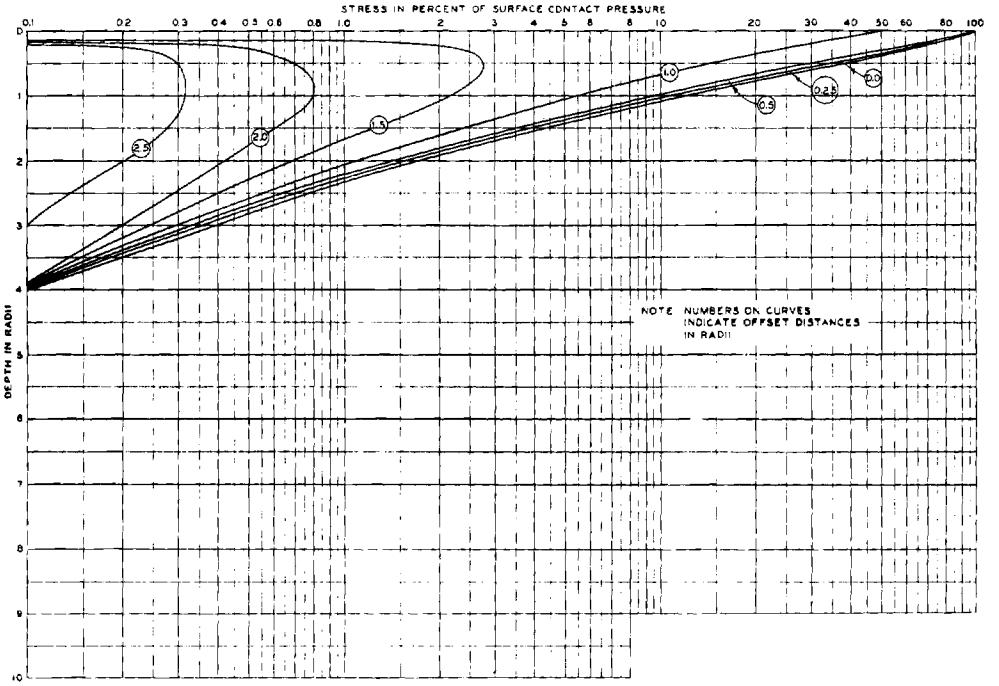

(B)

Figure 34. Horizontal Stresses σ_r (A) and σ_θ (B) Due to Uniform Circular Load. (Foster & Ahlvin).

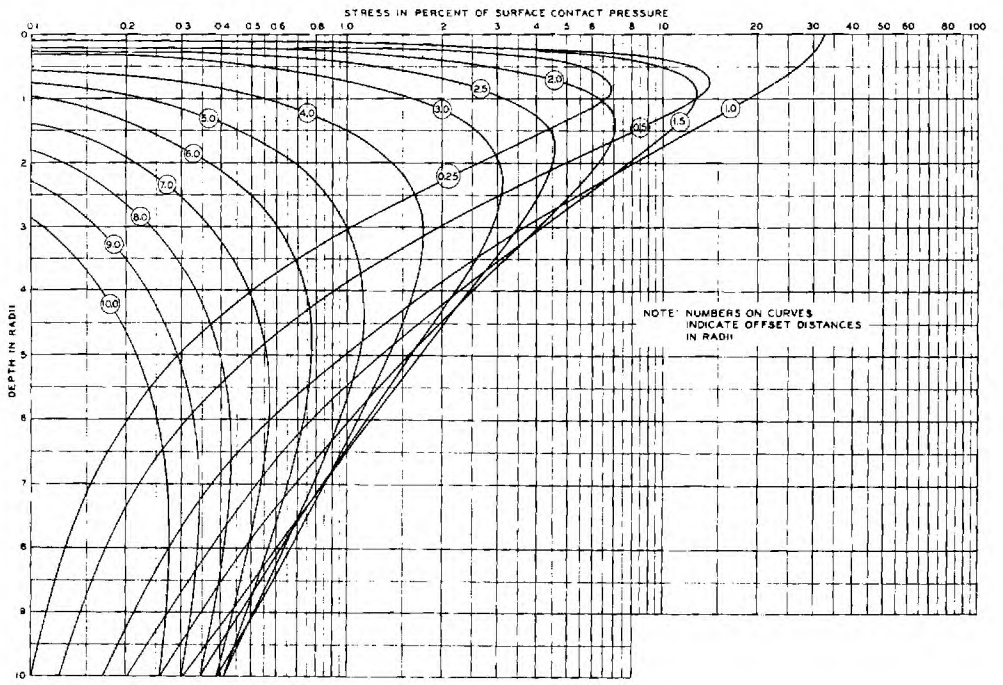

(A)

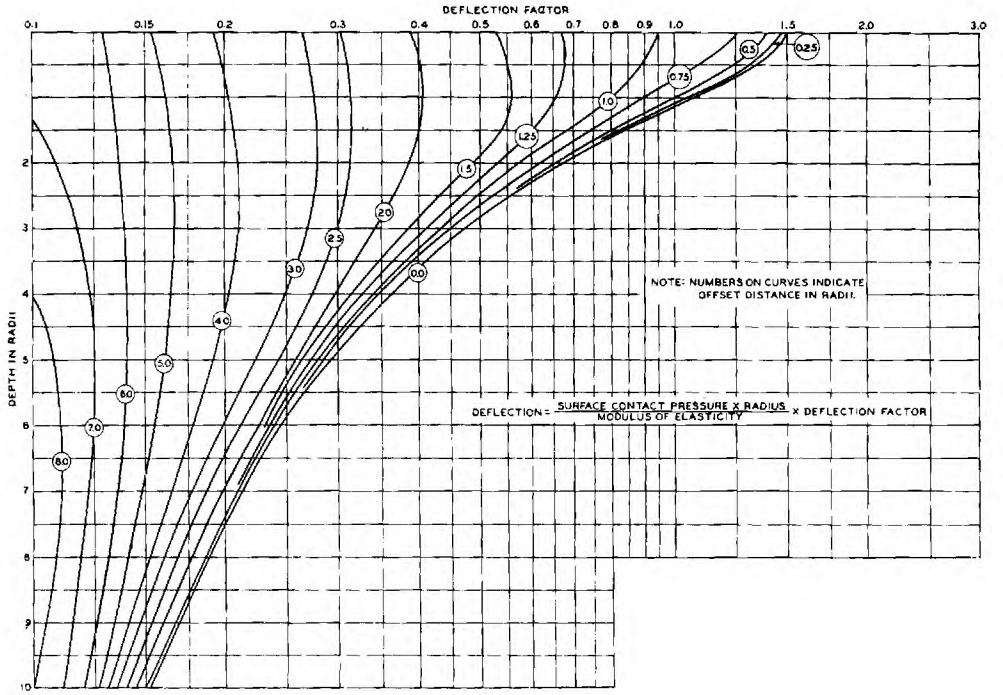

(B)

Figure 35. (A) Shear Stress; (B) Deflection - Due to Uniform Circular Load. (Foster & Ahlvin).

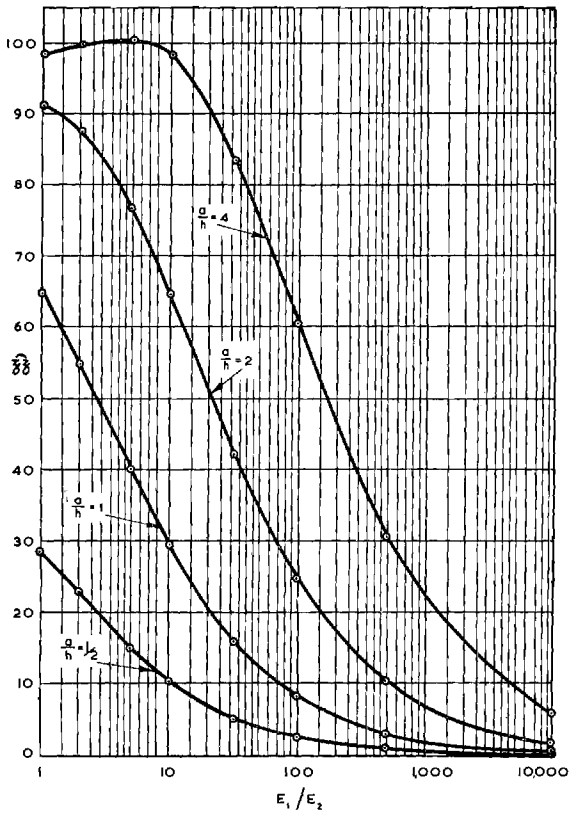

(A)

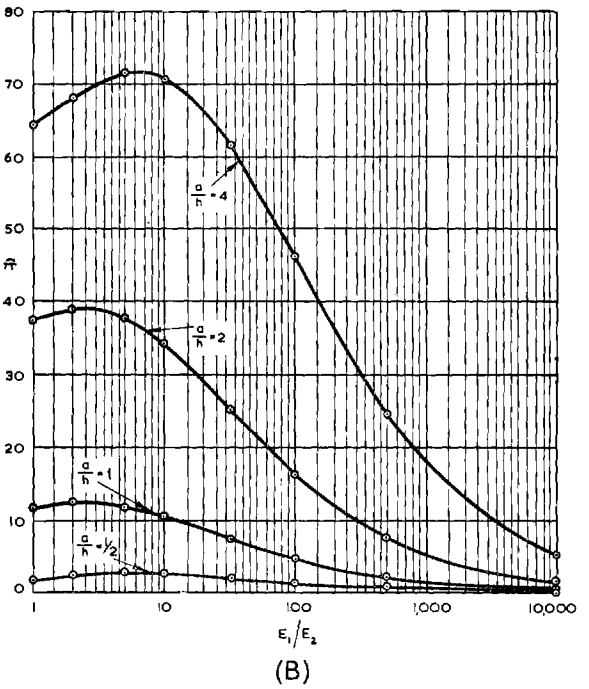

(B)

Figure 36. Normal Stresses at a Rough Interface σ_z (A); $\sigma_r = \sigma_\theta$ (B) as Percentage of Applied Uniform Circular Load. Two-Layer System. (Fox).

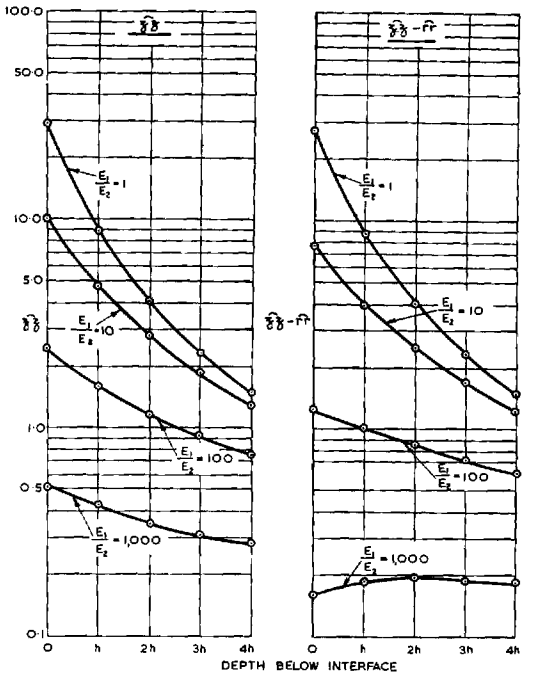

(A)

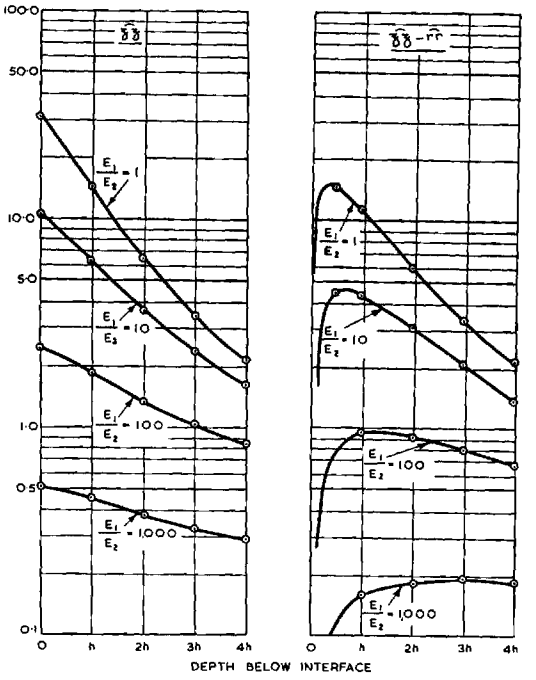

(B)

Figure 37. Normal Stresses in the Lower Layer of a Two-Layer System due to Uniform Circular Load (R/h = 1/2) (A) Rough Interface; (B) Smooth Interface. (Fox).

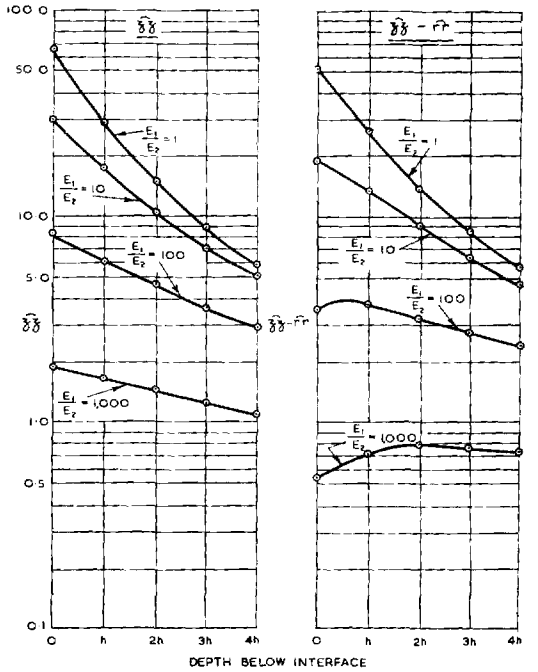

(A)

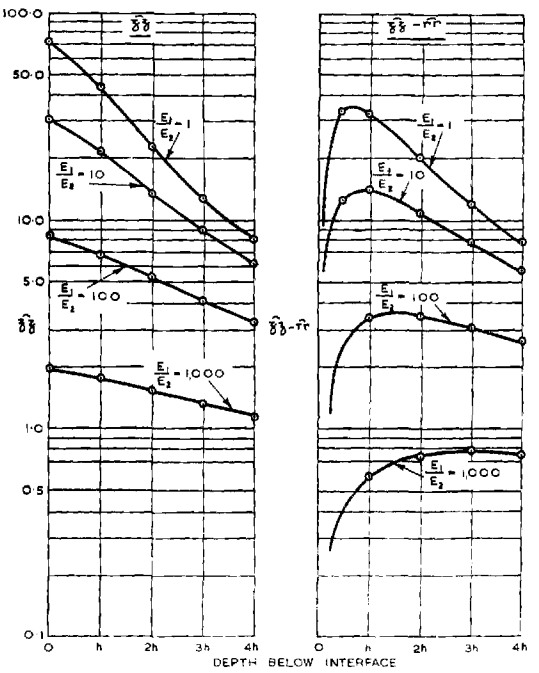

(B)

Figure 38. Normal Stresses in the Lower Layer of a Two-Layer System due to Uniform Circular Load (R/h = 1). (A) Rough Interface; (B) Smooth Interface. (Fox).

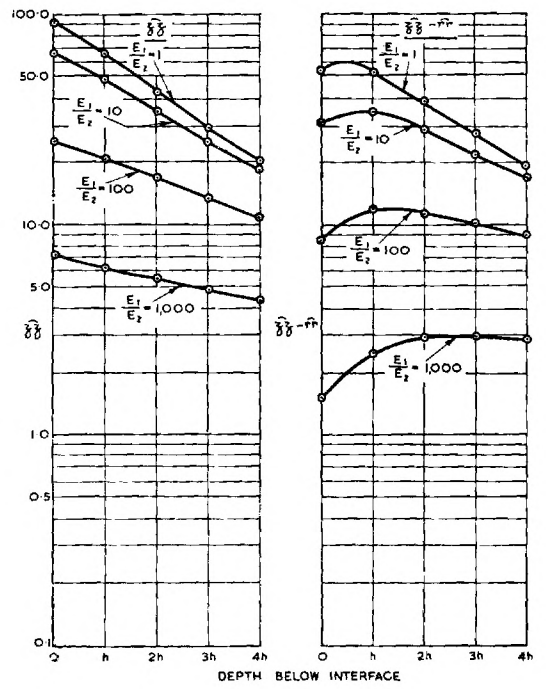

(A)

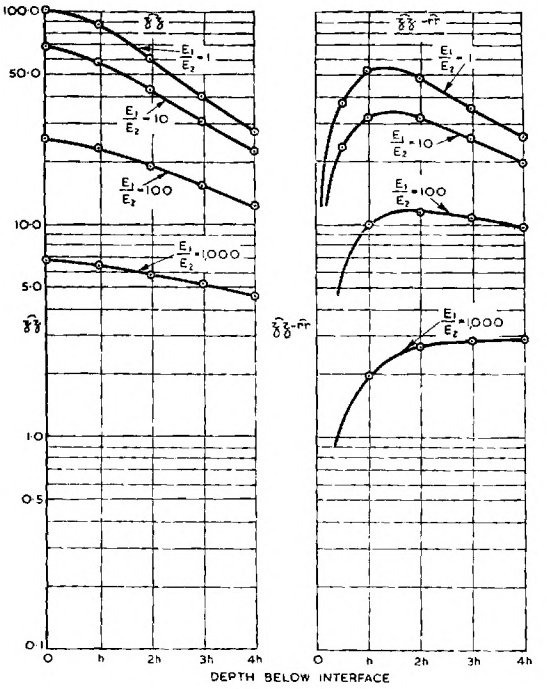

(B)

Figure 39. Normal Stresses in the Lower Layer of a Two-Layer System due to Uniform Circular Load (R/h = 2). (A) Rough Interface; (B) Smooth Interface. (Fox).

TABLE A

INFLUENCE FACTOR I_σ FOR VERTICAL STRESSES σ_z DUE TO A POINT LOAD

The vertical normal stress σ_z at a point located at a depth z below the surface of the solid at a horizontal distance r from the point of application of a point load Q (Figure 1) is given by the equation

$$\sigma_z = \frac{Q}{z^2} I_\sigma$$

wherein

$$I_\sigma = \frac{3}{2\pi}\left[\frac{1}{1 + (r/z)^2}\right]^{5/2}$$

The following table contains the values of I_σ for different values of r/z.

r/z	I_σ	r/z	I_σ	r/z	I_σ	r/z	I_σ
0.00	0.4775	0.20	0.4329	0.40	0.3294	0.60	0.2214
1	0.4773	1	0.4286	1	0.3238	1	0.2165
2	0.4770	2	0.4242	2	0.3181	2	0.2117
3	0.4764	3	0.4197	3	0.3124	3	0.2070
4	0.4756	4	0.4151	4	0.3068	4	0.2024
5	0.4745	5	0.4103	5	0.3011	5	0.1978
6	0.4732	6	0.4054	6	0.2955	6	0.1934
7	0.4717	7	0.4004	7	0.2899	7	0.1889
8	0.4699	8	0.3954	8	0.2843	8	0.1846
9	0.4679	9	0.3902	9	0.2788	9	0.1804
0.10	0.4657	0.30	0.3849	0.50	0.2733	0.70	0.1762
1	0.4633	1	0.3796	1	0.2679	1	0.1721
2	0.4607	2	0.3742	2	0.2625	2	0.1681
3	0.4579	3	0.3687	3	0.2571	3	0.1641
4	0.4548	4	0.3632	4	0.2518	4	0.1603
5	0.4516	5	0.3577	5	0.2466	5	0.1565
6	0.4482	6	0.3521	6	0.2414	6	0.1527
7	0.4446	7	0.3465	7	0.2363	7	0.1491
8	0.4409	8	0.3408	8	0.2313	8	0.1455
9	0.4370	9	0.3351	9	0.2263	9	0.1420

(Continued)

TABLE A (Continued)

r/z	I_σ	r/z	I_σ	r/z	I_σ	r/z	I_σ
0.80	0.1386	1.20	0.0513	1.60	0.0200	2.00	0.0085
1	0.1353	1	0.0501	1	0.0195	1	0.0084
2	0.1320	2	0.0489	2	0.0191	2	0.0082
3	0.1288	3	0.0477	3	0.0187	3	0.0081
4	0.1257	4	0.0466	4	0.0183	4	0.0079
5	0.1226	5	0.0454	5	0.0179	5	0.0078
6	0.1196	6	0.0443	6	0.0175	6	0.0076
7	0.1166	7	0.0433	7	0.0171	7	0.0075
8	0.1138	8	0.0422	8	0.0167	8	0.0073
9	0.1110	9	0.0412	9	0.0163	9	0.0072
0.90	0.1083	1.30	0.0402	1.70	0.0160	2.10	0.0070
1	0.1057	1	0.0393	1	0.0157	1	0.0069
2	0.1031	2	0.0384	2	0.0153	2	0.0068
3	0.1005	3	0.0374	3	0.0150	3	0.0066
4	0.0981	4	0.0365	4	0.0147	4	0.0065
5	0.0956	5	0.0357	5	0.0144	5	0.0064
6	0.0933	6	0.0348	6	0.0141	6	0.0063
7	0.0910	7	0.0340	7	0.0138	7	0.0062
8	0.0887	8	0.0332	8	0.0135	8	0.0060
9	0.0865	9	0.0324	9	0.0132	9	0.0059
1.00	0.0844	1.40	0.0317	1.80	0.0129	2.20	0.0058
1	0.0823	1	0.0309	1	0.0126	1	0.0057
2	0.0803	2	0.0302	2	0.0124	2	0.0056
3	0.0783	3	0.0295	3	0.0121	3	0.0055
4	0.0764	4	0.0288	4	0.0119	4	0.0054
5	0.0744	5	0.0282	5	0.0116	5	0.0053
6	0.0727	6	0.0275	6	0.0114	6	0.0052
7	0.0709	7	0.0269	7	0.0112	7	0.0051
8	0.0691	8	0.0263	8	0.0109	8	0.0050
9	0.0674	9	0.0257	9	0.0107	9	0.0049
1.10	0.0658	1.50	0.0251	1.90	0.0105	2.30	0.0048
1	0.0641	1	0.0245	1	0.0103	1	0.0047
2	0.0626	2	0.0240	2	0.0101	2	0.0047
3	0.0610	3	0.0234	3	0.0099	3	0.0046
4	0.0595	4	0.0229	4	0.0097	4	0.0045
5	0.0581	5	0.0224	5	0.0095	5	0.0044
6	0.0567	6	0.0219	6	0.0093	6	0.0043
7	0.0553	7	0.0214	7	0.0091	7	0.0043
8	0.0539	8	0.0209	8	0.0089	8	0.0042
9	0.0526	9	0.0204	9	0.0087	9	0.0041

(Continued)

TABLE A (Continued)

r/z	I_σ	r/z	I_σ	r/z	I_σ	r/z	I_σ
2.40	0.0040	2.80	0.0021	3.20	0.0011	3.75	
1	0.0040	1	0.0020	1	0.0011	to	0.0005
2	0.0039	2	0.0020	2	0.0011	3.90	
3	0.0038	3	0.0020	3	0.0011		
4	0.0038	4	0.0019	4	0.0011		
5	0.0037	5	0.0019	5	0.0011	3.91	
6	0.0036	6	0.0019	6	0.0010	to	0.0004
7	0.0036	7	0.0019	7	0.0010	4.12	
8	0.0035	8	0.0018	8	0.0010		
9	0.0034	9	0.0018	9	0.0010		
						4.13	
2.50	0.0034	2.90	0.0018	3.30	0.0010	to	0.0003
1	0.0033	1	0.0017	1	0.0009	4.43	
2	0.0033	2	0.0017	2	0.0009		
3	0.0032	3	0.0017	3	0.0009		
4	0.0032	4	0.0017	4	0.0009	4.44	
5	0.0031	5	0.0016	5	0.0009	to	0.0002
6	0.0031	6	0.0016	6	0.0009	4.90	
7	0.0030	7	0.0016	7	0.0009		
8	0.0030	8	0.0016	8	0.0009		
9	0.0029	9	0.0015	9	0.0009	4.91	
						to	0.0001
2.60	0.0029	3.00	0.0015	3.40	0.0009	6.15	
1	0.0028	1	0.0015	1	0.0008		
2	0.0028	2	0.0015	2	0.0008		
3	0.0027	3	0.0014	3	0.0008		
4	0.0027	4	0.0014	4	0.0008		
5	0.0026	5	0.0014	5	0.0008		
6	0.0026	6	0.0014	6	0.0008		
7	0.0025	7	0.0014	7	0.0008		
8	0.0025	8	0.0013	8	0.0008		
9	0.0025	9	0.0013	9	0.0008		
2.70	0.0024	3.10	0.0013	3.50	0.0007		
1	0.0024	1	0.0013	to			
2	0.0023	2	0.0013	3.61			
3	0.0023	3	0.0012				
4	0.0023	4	0.0012				
5	0.0022	5	0.0012	3.62			
6	0.0022	6	0.0012	to	0.0006		
7	0.0022	7	0.0012	3.74			
8	0.0021	8	0.0012				
9	0.0021	9	0.0011				

TABLE B

INFLUENCE FACTOR I_σ FOR VERTICAL STRESSES σ_z BENEATH ONE OF THE CORNERS OF A UNIFORMLY LOADED RECTANGULAR AREA

If B is the width and L the length of a rectangular area, which carries a load q per unit of area the vertical normal stress at a point N at a depth z below one of the corners of the area is equal to

$$\sigma_z = qI_\sigma$$

The influence value I_σ is determined by the equation

$$I_\sigma = \frac{1}{4\pi}\left[\frac{2mn\sqrt{m^2+n^2+1}}{m^2+n^2+m^2n^2+1}\cdot\frac{m^2+n^2+2}{m^2+n^2+1} + \tan^{-1}\frac{2mn\sqrt{m^2+n^2+1}}{m^2+n^2+1-m^2n^2}\right]$$

wherein

$$m = \frac{B}{z} \quad \text{and} \quad n = \frac{L}{z}$$

The values of I_σ for given values of m and n are contained in the following table.

m	n											
	0.1	0.2	0.3	0.4	0.5	0.6	0.7	0.8	0.9	1.0	1.2	1.4
0.1	0.00470	0.00917	0.01323	0.01678	0.01978	0.02223	0.02420	0.02576	0.02698	0.02794	0.02926	0.03007
0.2	0.00917	0.01790	0.02585	0.03280	0.03866	0.04348	0.04735	0.05042	0.05283	0.05471	0.05733	0.05894
0.3	0.01323	0.02585	0.03735	0.04742	0.05593	0.06294	0.06858	0.07308	0.07661	0.07938	0.08323	0.08561
0.4	0.01678	0.03280	0.04742	0.06024	0.07111	0.08009	0.08734	0.09314	0.09770	0.10129	0.10631	0.10941
0.5	0.01978	0.03866	0.05593	0.07111	0.08403	0.09473	0.10340	0.11035	0.11584	0.12018	0.12626	0.13003
0.6	0.02223	0.04348	0.06294	0.08009	0.09473	0.10688	0.11679	0.12474	0.13105	0.13605	0.14309	0.14749
0.7	0.02420	0.04735	0.06858	0.08734	0.10340	0.11679	0.12772	0.13653	0.14356	0.14914	0.15703	0.16199
0.8	0.02576	0.05042	0.07308	0.09314	0.11035	0.12474	0.13653	0.14607	0.15371	0.15978	0.16843	0.17389
0.9	0.02698	0.05283	0.07661	0.09770	0.11584	0.13105	0.14356	0.15371	0.16185	0.16835	0.17766	0.18357
1.0	0.02794	0.95471	0.07938	0.10129	0.12018	0.13605	0.14914	0.15978	0.16835	0.17522	0.18508	0.19139
1.2	0.02926	0.05733	0.08323	0.10631	0.12626	0.14309	0.15703	0.16843	0.17766	0.18508	0.19584	0.20278
1.4	0.03007	0.05894	0.08561	0.10941	0.13003	0.14749	0.16199	0.17389	0.18357	0.19139	0.20278	0.21020
1.6	0.03058	0.05994	0.08709	0.11135	0.13241	0.15028	0.16515	0.17739	0.18737	0.19546	0.20731	0.21510
1.8	0.03090	0.06058	0.08804	0.11260	0.13395	0.15207	0.16720	0.17967	0.18986	0.19814	0.21032	0.21836
2.0	0.03111	0.06100	0.08867	0.11342	0.13496	0.15326	0.16856	0.18119	0.19152	0.19994	0.21235	0.22058
2.5	0.03138	0.06155	0.08948	0.11450	0.13628	0.15483	0.17036	0.18321	0.19375	0.20236	0.21512	0.22364
3.0	0.03150	0.06178	0.08982	0.11495	0.13684	0.15550	0.17113	0.18407	0.19470	0.20341	0.21633	0.22499
4.0	0.03158	0.06194	0.09007	0.11527	0.13724	0.15598	0.17168	0.18469	0.19540	0.20417	0.21722	0.22600
5.0	0.03160	0.06199	0.09014	0.11537	0.13737	0.15612	0.17185	0.18488	0.19561	0.20440	0.21749	0.22632
6.0	0.03161	0.06201	0.09017	0.11541	0.13741	0.15617	0.17191	0.18496	0.19569	0.20449	0.21760	0.22644
8.0	0.03162	0.06202	0.09018	0.11543	0.13744	0.15621	0.17195	0.18500	0.19574	0.20455	0.21767	0.22652
10.0	0.03162	0.06202	0.09019	0.11544	0.13745	0.15622	0.17196	0.18502	0.19576	0.20457	0.21769	0.22654
∞	0.03162	0.06202	0.09019	0.11544	0.13745	0.15623	0.17197	0.18502	0.19577	0.20458	0.21770	0.22656

(Continued)

m	n										
	1.6	1.8	2.0	2.5	3.0	4.0	5.0	6.0	8.0	10.0	∞
0.1	0.03058	0.03090	0.03111	0.03138	0.03150	0.03158	0.03160	0.03161	0.03162	0.03162	0.03162
0.2	0.05994	0.06058	0.06100	0.06155	0.06178	0.06194	0.06199	0.06201	0.06202	0.06202	0.06202
0.3	0.08709	0.08804	0.08867	0.08948	0.08982	0.09007	0.09014	0.09017	0.09018	0.09019	0.09019
0.4	0.11135	0.11260	0.11342	0.11450	0.11495	0.11527	0.11537	0.11541	0.11543	0.11544	0.11544
0.5	0.13241	0.13395	0.13496	0.13628	0.13684	0.13724	0.13737	0.13741	0.13744	0.13745	0.13745
0.6	0.15028	0.15207	0.15326	0.15483	0.15550	0.15598	0.15612	0.15617	0.15621	0.15622	0.15623
0.7	0.16515	0.16720	0.16856	0.17036	0.17113	0.17168	0.17185	0.17191	0.17195	0.17196	0.17197
0.8	0.17739	0.17967	0.18119	0.18321	0.18407	0.18469	0.18488	0.18496	0.18500	0.18502	0.18502
0.9	0.18737	0.18986	0.19152	0.19375	0.19470	0.19540	0.19561	0.19569	0.19574	0.19576	0.19577
1.0	0.19546	0.19814	0.19994	0.20236	0.20341	0.20417	0.20440	0.20449	0.20455	0.20457	0.20458
1.2	0.20731	0.21032	0.21235	0.21512	0.21633	0.21722	0.21749	0.21760	0.21767	0.21769	0.21770
1.4	0.21510	0.21836	0.22058	0.22364	0.22499	0.22600	0.22632	0.22644	0.22652	0.22654	0.22656
1.6	0.22025	0.22372	0.22610	0.22940	0.23088	0.23200	0.23236	0.23249	0.23258	0.23261	0.23263
1.8	0.22372	0.22736	0.22986	0.23334	0.23495	0.23617	0.23656	0.23671	0.23681	0.23684	0.23686
2.0	0.22610	0.22986	0.23247	0.23614	0.23782	0.23912	0.23954	0.23970	0.23981	0.23985	0.23987
2.5	0.22940	0.23334	0.23614	0.24010	0.24196	0.24344	0.24392	0.24412	0.24425	0.24429	0.24432
3.0	0.23088	0.23495	0.23782	0.24196	0.24394	0.24554	0.24608	0.24630	0.24646	0.24650	0.24654
4.0	0.23200	0.23617	0.23912	0.24344	0.24554	0.24729	0.24791	0.24817	0.24836	0.24842	0.24846
5.0	0.23236	0.23656	0.23954	0.24392	0.24608	0.24791	0.24857	0.24885	0.24907	0.24914	0.24919
6.0	0.23249	0.23671	0.23970	0.24412	0.24630	0.24817	0.24885	0.24916	0.24939	0.24946	0.24952
8.0	0.23258	0.23681	0.23981	0.24425	0.24646	0.24836	0.24907	0.24939	0.24964	0.24973	0.24980
10.0	0.23261	0.23684	0.23985	0.24429	0.24650	0.24842	0.24914	0.24946	0.24973	0.24981	0.24989
∞	0.23263	0.23686	0.23987	0.24432	0.24654	0.24846	0.24919	0.24952	0.24980	0.24989	0.25000

TABLE C

INFLUENCE FACTOR I_σ FOR VERTICAL STRESSES σ_z BENEATH THE CENTER OF A UNIFORMLY LOADED CIRCULAR AREA

The vertical normal stress at depth z beneath the center of a circular area with a radius R carrying a load q per unit of area is

$$\sigma_z = qI_\sigma$$

wherein

$$I_\sigma = 1 - \left[\frac{1}{1 + (R/z)^2} \right]^{3/2}$$

The following table contains the values of I_σ for different values of R/z.

R/z	I_σ	R/z	I_σ	R/z	I_σ	R/z	I_σ
0.00	0.00000	0.20	0.05713	0.40	0.19959	0.60	0.36949
1	0.00015	1	0.06268	1	0.20790	1	0.37781
2	0.00060	2	0.06844	2	0.21627	2	0.38609
3	0.00135	3	0.07441	3	0.22469	3	0.39431
4	0.00240	4	0.08057	4	0.23315	4	0.40247
5	0.00374	5	0.08692	5	0.24165	5	0.41058
6	0.00538	6	0.09346	6	0.25017	6	0.41863
7	0.00731	7	0.10017	7	0.25872	7	0.42662
8	0.00952	8	0.10704	8	0.26729	8	0.43454
9	0.01203	9	0.11408	9	0.27587	9	0.44240
0.10	0.01481	0.30	0.12126	0.50	0.28446	0.70	0.45018
1	0.01788	1	0.12859	1	0.29304	1	0.45789
2	0.02122	2	0.13605	2	0.30162	2	0.46553
3	0.02483	3	0.14363	3	0.31019	3	0.47310
4	0.02870	4	0.15133	4	0.31875	4	0.48059
5	0.03283	5	0.15915	5	0.32728	5	0.48800
6	0.03721	6	0.16706	6	0.33579	6	0.49533
7	0.04184	7	0.17507	7	0.34427	7	0.50259
8	0.04670	8	0.18317	8	0.35272	8	0.50976
9	0.05181	9	0.19134	9	0.36112	9	0.51685

(Continued)

TABLE C (Continued)

R/z	I_σ	R/z	I_σ	R/z	I_σ	R/z	I_σ
0.80	0.52386	1.20	0.73763	1.60	0.85112	2.00	0.91056
1	0.53079	1	0.74147	1	0.85312	.02	0.91267
2	0.53763	2	0.74525	2	0.85507	.04	0.91472
3	0.54439	3	0.74896	3	0.85700	.06	0.91672
4	0.55106	4	0.75262	4	0.85890	.08	0.91865
5	0.55766	5	0.75622	5	0.86077	.10	0.92053
6	0.56416	6	0.75976	6	0.86260	.15	0.92499
7	0.57058	7	0.76324	7	0.86441	.20	0.92914
8	0.57692	8	0.76666	8	0.86619	.25	0.93301
9	0.58317	9	0.77003	9	0.86794	.30	0.93661
						.35	0.93997
0.90	0.58934	1.30	0.77334	1.70	0.86966	.40	0.94310
1	0.59542	1	0.77660	1	0.87136	.45	0.94603
2	0.60142	2	0.77981	2	0.87302	.50	0.94877
3	0.60734	3	0.78296	3	0.87467	.55	0.95134
4	0.61317	4	0.78606	4	0.87628	.60	0.95374
5	0.61892	5	0.78911	5	0.87787	.65	0.95599
6	0.62459	6	0.79211	6	0.87944	.70	0.95810
7	0.63018	7	0.79507	7	0.88098	.75	0.96009
8	0.63568	8	0.79797	8	0.88250	.80	0.96195
9	0.64110	9	0.80083	9	0.88399	.85	0.96371
						.90	0.96536
1.00	0.64645	1.40	0.80364	1.80	0.88546	.95	0.96691
1	0.65171	1	0.80640	1	0.88691		
2	0.65690	2	0.80912	2	0.88833	3.00	0.96838
3	0.66200	3	0.81179	3	0.88974	.10	0.97106
4	0.66703	4	0.81442	4	0.89112	.20	0.97346
5	0.67198	5	0.81701	5	0.89248	.30	0.97561
6	0.67686	6	0.81955	6	0.89382	.40	0.97753
7	0.68166	7	0.82206	7	0.89514	.50	0.97927
8	0.68639	8	0.82452	8	0.89643	.60	0.98083
9	0.69104	9	0.82694	9	0.89771	.70	0.98224
						.80	0.98352
1.10	0.69562	1.50	0.82932	1.90	0.89897	.90	0.98468
1	0.70013	1	0.83167	1	0.90021		
2	0.70457	2	0.83397	2	0.90143	4.00	0.98573
3	0.70894	3	0.83624	3	0.90263	.20	0.98757
4	0.71324	4	0.83847	4	0.90382	.40	0.98911
5	0.71747	5	0.84067	5	0.90498	.60	0.99041
6	0.72163	6	0.84283	6	0.90613	.80	0.99152
7	0.72573	7	0.84495	7	0.90726		
8	0.72976	8	0.84704	8	0.90838		
9	0.73373	9	0.84910	9	0.90948		

(Continued)

TABLE C (Continued)

R/z	I_σ	R/z	I_σ	R/z	I_σ	R/z	I_σ
5.00	0.99246	8.00	0.99809	18.00	0.99983	100.00	1.00000
.20	0.99327						
.40	0.99396	9.00	0.99865	20.00	0.99988	∞	1.00000
.60	0.99457						
.80	0.99510	10.00	0.99901	25.00	0.99994		
6.00	0.99556	12.00	0.99943	30.00	0.99996		
.50	0.99648						
		14.00	0.99964	40.00	0.99998		
7.00	0.99717						
.50	0.99769	16.00	0.99976	50.00	0.99999		

TABLE D-1

NORMAL STRESSES AT A PERFECTLY ROUGH INTERFACE OF A TWO-LAYER SYSTEM GIVEN AS PERCENTAGE OF APPLIED LOADING

σ_z

E_1/E_2	R/h = 1/2	R/h = 1	R/h = 2	R/h = 4
1	28.4	64.6	91.1	98.6
2	22.4	54.7	87.5	99.8
5	14.7	39.7	76.7	100.5
10	10.1	29.2	64.4	98.4
32-1/3	4.93	15.6	41.9	83.4
99	2.38	8.1	24.6	60.5
499	0.81	2.97	10.1	30.4
9999	0.104	0.41	1.58	5.75

$\sigma_z = \sigma_\theta$

E_1/E_2	R/h = 1/2	R/h = 1	R/h = 2	R/h = 4
1	1.62	11.6	37.4	64.3
2	2.30	12.3	38.8	68.0
5	2.64	11.7	37.6	71.4
10	2.49	10.4	34.0	70.6
32-1/3	1.83	7.2	24.9	61.5
99	1.12	4.53	16.2	46.1
499	0.51	1.99	7.50	24.6
9999	0.09	0.35	1.37	5.12

TABLE D-2

PERFECTLY ROUGH INTERFACE; NORMAL STRESSES σ_z AND $\sigma_z - \sigma_r$, AS PERCENTAGE OF APPLIED LOADING, IN THE LOWER LAYER OF A TWO-LAYER SYSTEM

	σ_z				$\sigma_z - \sigma_r$			
E_1/E_2	1	10	100	1000	1	10	100	1000
Depth below Interface	R/h = 1/2							
0	28.4	10.1	2.38	0.51	26.8	7.6	1.26	0.160
h	8.7	4.70	1.58	0.42	8.6	3.93	1.02	0.185
2h	4.03	2.78	1.17	0.35	4.00	2.48	0.85	0.195
3h	2.30	1.84	0.91	0.31	2.29	1.70	0.71	0.190
4h	1.48	1.29	0.74	0.28	1.48	1.23	0.61	0.185
	R/h = 1							
0	64.6	29.2	8.1	1.85	53.0	18.8	3.6	0.54
h	28.4	16.8	6.0	1.62	26.8	13.5	3.8	0.71
2h	14.5	10.5	4.6	1.43	14.1	9.2	3.3	0.79
3h	8.7	7.0	3.6	1.24	8.6	6.4	2.8	0.76
4h	5.7	5.0	2.9	1.10	5.6	4.7	2.4	0.73
	R/h = 2							
0	91.1	64.4	24.6	7.10	53.7	30.4	8.4	1.50
h	64.6	48.0	20.5	6.06	53.0	34.6	11.8	2.52
2h	42.4	34.0	16.5	5.42	38.4	28.2	11.4	2.90
3h	28.4	24.4	13.3	4.80	26.8	21.5	10.2	2.92
4h	20.0	18.1	10.8	4.28	19.2	16.6	8.8	2.82

TABLE D-3

PERFECTLY SMOOTH INTERFACE: NORMAL STRESSES σ_z AND $\sigma_z - \sigma_r$, AS PERCENTAGE OF APPLIED LOADING IN THE LOWER LAYER OF A TWO-LAYER SYSTEM

	σ_z				$\sigma_z - \sigma_r$			
E_1/E_2	1	10	100	1000	1	10	100	1000
Depth Below Interface	R/h = 1/2							
0	31.0	10.5	2.41	0.51	0.00	0.00	0.00	0.00
1/2h	--	--	--	--	14.5	4.49	--	--
h	14.1	6.3	1.83	0.45	11.5	4.32	0.96	0.16
2h	6.4	3.67	1.36	0.38	5.9	3.03	0.91	0.18
3h	3.46	2.35	1.05	0.33	3.32	2.08	0.79	0.19
4h	2.12	1.61	0.83	0.29	2.07	1.37	0.66	0.18
	R/h = 1							
0	72.2	30.5	8.2	1.90	0.00	0.00	0.00	0.00
1/2h	--	--	--	--	34.2	12.7	--	--
h	43.7	21.7	6.8	1.72	33.1	14.2	3.41	0.59
2h	22.5	13.6	5.25	1.51	20.2	11.0	3.47	0.74
3h	12.8	8.9	4.09	1.33	12.1	7.8	3.05	0.77
4h	8.1	6.2	3.26	1.17	7.8	5.7	2.61	0.75
	R/h = 2							
0	102.5	67.7	24.9	6.7	0.00	0.00	0.00	0.00
1/2h	--	--	--	--	37.8	23.1	--	--
h	86.9	57.6	22.5	6.3	52.6	32.0	9.9	1.96
2h	59.6	42.1	18.6	5.7	48.3	31.7	11.6	2.68
3h	39.6	30.2	15.0	5.10	35.3	25.4	10.9	2.86
4h	27.1	22.0	12.2	4.54	25.7	19.6	9.6	2.86

TABLE E-1

STRESSES BENEACH THE CENTER OF A UNIFORMLY LOADED CIRCULAR AREA, AT THE INTERFACES OF A THREE-LAYER SYSTEM, GIVEN AS PERCENTAGE OF THE APPLIED LOADING

$h_1/h_2 = 2$, $R/h_2 = 1$

E_2/E_3 \ E_1/E_2	5		10		20		50		100		500	
5	9.51	3.64	6.00	2.59	3.66	1.79	1.87	1.05	1.11	0.690	0.349	0.261
	72.70	15.30	93.90	10.20	113.00	6.44	136.00	3.30	151.00	1.90	187.00	0.513
	14.50	3.06	9.38	2.04	5.66	1.29	2.73	0.66	1.51	0.380	0.374	0.101
10	8.24	2.38	5.06	1.69	3.01	1.16	1.47	0.684	0.852	0.451	0.252	0.169
	79.30	18.70	103.00	12.30	124.00	7.68	148.00	3.85	164.00	2.21	203.00	0.586
	15.80	1.86	10.30	1.23	6.21	0.77	2.96	0.385	1.64	0.221	0.405	0.059
50	6.74	0.860	3.97	0.612	2.23	0.424	1.01	0.252	0.554	0.166		
	95.20	26.00	124.00	16.90	149.00	10.40	178.00	5.12	198.00	2.94		
	19.00	0.519	12.40	0.339	7.44	0.208	3.55	0.103	1.98	0.059		
100	6.43	0.552	3.75	0.397	2.08	0.277	0.921	0.163				
	102.00	29.00	133.00	18.90	161.00	11.60	193.00	5.75				
	20.40	0.290	13.30	0.189	8.04	0.118	3.85	0.058				

TABLE E-2

STRESSES BENEATH THE CENTER OF A UNIFORMLY LOADED CIRCULAR AREA, AT THE INTERFACES OF A THREE-LAYER SYSTEM, GIVEN AS PERCENTAGE OF THE APPLIED LOADING

$h_1/h_2 = 1$, $R/h_2 = 1$

E_2/E_3 \ E_1/E_2	5		10		20		50		100		500	
5	30.30	9.22	20.80	7.14	13.50	5.33	7.26	3.44	4.43	2.36	1.38	0.921
	162.00	37.80	229.00	28.10	300.00	19.70	390.00	11.40	457.00	7.10	594.00	2.11
	32.30	7.56	22.90	5.63	15.00	3.96	7.84	2.29	4.57	1.42	1.19	0.420
10	27.90	6.11	18.70	4.73	11.80	3.53	6.13	2.26	3.60	1.55	1.04	0.599
	173.00	47.10	250.00	35.00	330.00	24.40	431.00	13.90	502.00	8.55	645.00	2.46
	34.70	4.70	25.00	3.50	16.50	2.44	8.66	1.39	5.02	0.86	1.29	0.245
50	25.00	2.23	16.10	1.74	9.76	1.30	4.68	0.833	2.60	0.572		
	201.00	68.20	298.00	50.90	399.00	35.30	523.00	19.50	606.00	11.80		
	40.40	1.37	29.80	1.02	20.00	0.70	10.50	0.392	6.05	0.236		
100	24.30	1.42	15.60	1.11	9.35	0.839	4.40	0.540				
	213.00	75.10	319.00	57.80	428.00	39.80	563.00	22.00				
	42.60	0.76	31.80	0.57	21.40	0.400	11.30	0.22				

TABLE E-3

STRESSES BENEATH THE CENTER OF A UNIFORMLY LOADED CIRCULAR AREA, AT THE INTERFACES OF A THREE-LAYER SYSTEM, GIVEN AS PERCENTAGE OF THE APPLIED LOADING

$h_1/h_2 = 1/2, R/h_2 = 1$

E_2/E_3 \ E_1/E_2	5		10		20		50		100		500	
5	66.40	18.10	53.40	15.60	39.90	12.90	24.70	9.42	16.20	7.06	5.48	3.13
	215.00	72.80	366.00	62.00	561.00	49.80	868.00	34.00	1116.00	23.80	1687.00	8.60
	43.00	14.60	36.70	12.40	28.10	10.00	17.40	6.81	11.20	4.77	3.37	1.72
10	63.40	12.10	50.40	10.40	37.00	8.59	22.20	6.29	14.20	4.72	4.43	2.08
	223.00	91.70	396.00	78.00	615.00	62.80	963.00	42.90	1244.00	29.80	1866.00	10.50
	44.60	9.20	39.40	7.81	30.70	6.28	19.30	4.29	12.40	2.98	3.73	1.05
50	59.80	4.36	46.70	3.74	33.50	3.14	19.10	2.34	11.60	17.70		
	239.00	134.00	449.00	115.00	730.00	93.30	1180.00	63.90	1541.00	44.20		
	47.80	2.69	44.90	2.30	36.50	1.87	23.60	1.28	15.40	0.88		
100	59.10	2.77	46.00	2.37	32.80	2.00	18.50	1.51				
	244.00	152.00	469.00	130.00	776.00	106.00	1270.00	73.10				
	48.80	1.52	46.90	1.30	38.70	1.06	25.40	0.730				

TABLE E-4

STRESSES BENEATH THE CENTER OF A UNIFORMLY LOADED CIRCULAR AREA, AT THE INTERFACES OF A THREE-LAYER SYSTEM, GIVEN AS PERCENTAGE OF THE APPLIED LOADING

$h_1/h_2 = 1/4$, $R/h_2 = 1$

E_2/E_3 \ E_1/E_2	5		10		20		50		100		500	
5	94.70	26.50	90.70	24.80	82.10	22.80	64.20	19.40	49.00	16.30	20.80	9.19
	127.00	104.00	301.00	99.00	614.00	90.70	1273.00	75.20	1966.00	61.20	3991.00	30.10
	25.40	20.90	30.20	19.80	30.70	18.20	25.50	15.00	19.70	12.20	8.00	6.03
10	92.80	18.00	88.30	16.60	79.60	15.20	61.20	12.90	45.90	10.90	18.30	6.19
	112.00	134.00	308.00	125.00	657.00	115.00	1404.00	95.60	2195.00	77.90	4500.00	38.00
	22.60	13.40	30.60	12.50	33.00	11.50	28.10	9.56	21.90	7.77	9.00	3.82
50	70.80	6.52	85.50	5.91	76.40	5.38	57.60	4.63	42.20	3.97		
	14.20	197.00	303.00	185.00	725.00	169.00	1657.00	142.00	2668.00	117.00		
	22.60	3.94	30.20	3.69	36.40	3.40	33.10	2.85	26.60	2.33		
100	89.70	4.13	84.90	3.71	75.80	3.37	57.00	2.92				
	50.80	223.00	295.00	208.00	745.00	191.00	1745.00	161.00				
	10.20	2.23	29.40	2.08	37.40	1.91	34.90	1.61				

TABLE E-5

STRESSES BENEATH THE CENTER OF A UNIFORMLY LOADED CIRCULAR AREA, AT THE INTERFACES OF A THREE-LAYER SYSTEM, GIVEN AS PERCENTAGE OF THE APPLIED LOADING

$h_1/h_2 = 2$, $R/h_2 = 1/2$

E_2/E_3 \ E_1/E_2	5		10		20		50		100		500	
5	2.85	0.950	1.76	0.670	1.06	0.459	0.522	0.268	0.307	0.175	0.093	0.066
	21.50	4.09	27.20	2.70	32.40	1.69	38.20	0.853	42.10	0.492	50.80	0.131
	4.30	0.817	2.72	0.540	1.62	0.338	0.765	0.170	0.421	0.098	0.101	0.026
10	2.51	0.621	1.52	0.435	0.884	0.297	0.422	0.174	0.241	0.114	0.068	0.042
	23.10	4.96	29.40	3.24	35.00	2.01	41.20	0.999	45.20	0.570	54.90	0.149
	4.62	0.495	2.94	0.323	1.75	0.201	0.825	0.100	0.454	0.057	0.110	0.015
50	2.12	0.220	1.23	0.155	0.682	0.108	0.305	0.064	0.165	0.042		
	27.10	6.80	34.60	4.40	41.20	2.69	48.50	1.32	53.70	0.753		
	5.42	0.136	3.47	0.088	2.06	0.054	0.971	0.026	0.537	0.015		
100	2.02	0.140	1.17	0.101	0.644	0.070	0.281	0.041				
	28.70	7.56	37.00	4.90	44.10	2.99	52.30	1.47				
	5.74	0.076	3.70	0.049	2.21	0.030	1.05	0.015				

TABLE E-6

STRESSES BENEATH THE CENTER OF A UNIFORMLY LOADED CIRCULAR AREA, AT THE INTERFACES OF A THREE-LAYER SYSTEM, GIVEN AS PERCENTAGE OF THE APPLIED LOADING

$h_1/h_2 = 1$, $R/h_2 = 1/2$

E_2/E_3 \ E_1/E_2	5		10		20		50		100		500	
5	12.00	2.55	7.72	1.93	4.74	1.42	2.39	0.899	1.40	0.610	0.404	0.235
	66.10	10.90	87.10	7.89	107.00	5.43	132.00	3.07	149.00	1.89	184.00	0.550
	13.20	2.18	8.69	1.58	5.36	1.09	2.64	0.616	1.49	0.376	0.368	0.111
10	11.30	1.66	7.13	1.26	4.29	0.929	2.08	0.586	1.18	0.400	0.318	0.152
	69.10	13.30	92.30	9.68	115.00	6.64	142.00	3.71	160.00	2.26	197.00	0.637
	13.80	1.33	9.22	0.969	5.74	0.664	2.84	0.371	1.60	0.227	0.394	0.064
50	10.50	0.586	6.46	0.453	3.74	0.336	1.71	0.213	0.927	0.145		
	76.10	18.70	104.00	13.70	132.00	9.39	165.00	5.14	186.00	3.08		
	15.20	0.374	10.40	0.275	6.61	0.189	3.30	0.103	1.86	0.062		
100	10.30	0.370	6.32	0.287	3.64	0.215	1.64	0.137				
	79.00	21.10	109.00	15.40	140.00	10.60	175.00	5.75				
	15.80	0.210	10.90	0.154	6.99	0.106	3.50	0.057				

TABLE E-7

STRESSES BENEATH THE CENTER OF A UNIFORMLY LOADED CIRCULAR AREA, AT THE INTERFACES OF A THREE-LAYER SYSTEM, GIVEN AS PERCENTAGE OF THE APPLIED LOADING

$h_1/h_2 = 1/2$, $R/h_2 = 1/2$

E_2/E_3 \ E_1/E_2	5		10		20		50		100		500	
5	36.20	5.41	25.60	4.52	17.10	3.64	9.41	2.58	5.76	1.89	1.73	0.815
	144.00	23.20	204.00	19.00	270.00	14.70	363.00	9.69	433.00	6.63	583.00	2.31
	28.80	4.64	20.40	3.81	13.50	2.94	7.26	1.94	4.32	1.32	1.16	0.462
10	35.40	3.52	24.70	2.94	16.30	2.39	8.71	1.69	5.20	1.25	1.46	0.538
	147.00	28.40	211.00	23.30	284.00	18.20	388.00	12.00	465.00	8.18	627.00	2.79
	29.40	2.85	21.10	2.34	14.20	1.83	7.76	1.20	4.65	0.818	1.26	0.279
50	34.20	1.20	23.60	1.01	15.30	0.835	7.88	0.612	4.51	0.457		
	151.00	39.60	226.00	33.00	314.00	26.10	443.00	17.40	540.00	11.80		
	30.10	0.794	22.50	0.659	15.70	0.522	8.87	0.348	5.40	0.237		
100	33.90	0.748	23.40	0.633	15.10	0.526	7.72	0.390				
	152.00	44.10	230.00	36.80	325.00	29.40	466.00	19.70				
	30.30	0.441	23.00	0.369	16.30	0.294	9.32	0.197				

TABLE E-8

STRESSES BENEATH THE CENTER OF A UNIFORMLY LOADED CIRCULAR AREA, AT THE INTERFACES OF A THREE-LAYER SYSTEM, GIVEN AS PERCENTAGE OF THE APPLIED LOADING

$h_1/h_2 = 1/4$, $R/h_2 = 1/2$

E_2/E_3 \ E_1/E_2	5		10		20		50		100		500	
5	74.10	8.79	61.40	8.03	47.50	7.15	30.80	5.80	20.90	4.72	7.30	2.50
	189.00	38.00	312.00	34.70	476.00	30.50	747.00	23.80	984.00	18.60	1582.00	8.52
	37.90	7.61	31.30	6.95	23.80	6.10	15.00	4.77	9.87	3.72	3.17	1.71
10	73.40	5.70	60.60	5.17	46.60	4.60	29.80	3.76	19.90	3.08	6.61	1.65
	186.00	46.50	315.00	42.50	489.00	37.40	783.00	29.50	1045.00	23.10	1713.00	10.60
	37.10	4.65	31.50	4.25	24.50	3.74	15.60	2.95	10.50	2.31	3.43	1.06
50	72.40	1.90	59.60	1.71	45.60	1.52	28.70	1.28	18.80	1.07		
	175.00	63.90	314.00	58.40	508.00	51.90	850.00	41.70	1167.00	33.30		
	34.80	1.28	31.30	1.17	25.40	1.04	17.00	0.836	11.67	0.665		
100	72.40	1.17	59.40	1.04	45.40	0.934	28.50	0.791				
	170.00	70.70	311.00	64.50	513.00	57.50	872.00	46.60				
	34.00	0.707	31.20	0.645	25.70	0.575	17.40	0.466				

TABLE F1

INFLUENCE VALUES FOR STRESS AT INTERFACE
(Perfect Continuity at Interface)
Tensile Stresses Are Negative
Two-Layered System Flexible Pavement

E_1/E_2	h/R	Vertical Stress σ_z	Radial Stress σ_r	
			Layer 2	Layer 1
2000	1.000	0.0121	0.0092	-5.718
	1.111	0.0099	0.0075	-4.834
	1.250	0.0079	0.0059	-3.991
	1.429	0.0061	0.0045	-3.195
	1.667	0.0046	0.0034	-2.456
	2.000	0.0032	0.0023	-1.782
	2.500	0.0021	0.0015	-1.188
	3.333	0.0012	0.0009	-0.6928
	5.000	0.0005	0.0003	-0.3164
	10.000	0.0001	0.0001	-0.0805
400	1.000	0.0341	0.0222	-4.706
	1.111	0.0282	0.0181	-4.010
	1.250	0.0227	0.0143	-3.337
	1.429	0.0178	0.0010	-2.694
	1.667	0.0133	0.0080	-2.087
	2.000	0.0094	0.0056	-1.526
	2.500	0.0062	0.0036	-1.024
	3.333	0.0035	0.0020	-0.6000
	5.000	0.0016	0.0009	-0.2752
	10.000	0.0004	0.0002	-0.0702
200	1.000	0.0529	0.0323	-4.069
	1.111	0.0438	0.0261	-3.494
	1.250	0.0356	0.0208	-2.929
	1.429	0.0279	0.0159	-2.380
	1.667	0.0211	0.0117	-1.850
	2.000	0.0150	0.0081	-1.358
	2.500	0.0098	0.0052	-0.9133
	3.333	0.0056	0.0029	-0.5342
	5.000	0.0023	0.0011	-0.2459
	10.000	0.0006	0.0003	-0.0627
100	1.000	0.0809	0.0449	-3.52
	1.111	0.0676	0.0365	-3.04
	1.250	0.0552	0.0289	-2.57
	1.429	0.0436	0.0222	-2.10

(Continued)

TABLE F1 (Continued)

INFLUENCE VALUES FOR STRESS AT INTERFACE
(Perfect Continuity at Interface)
Tensile Stresses Are Negative
Two-Layered System Flexible Pavement

E_1/E_2	h/R	Vertical Stress σ_z	Radial Stress σ_r	
			Layer 2	Layer 1
	1.667	0.0330	0.0163	-1.64
	2.000	0.0237	0.0113	-1.22
	2.500	0.0156	0.0072	-0.82
	3.333	0.0090	0.0040	-0.49
	5.000	0.0041	0.0018	-0.23
	10.000	0.0010	0.0004	-0.06
20	1.000	0.2047	0.0856	-2.178
	1.111	0.1748	0.0698	-1.93
	1.250	0.1457	0.0551	-1.67
	1.429	0.1177	0.0420	-1.40
	1.667	0.0911	0.0306	-1.12
	2.000	0.0665	0.0210	-0.844
	2.500	0.0446	0.0133	-0.582
	3.333	0.0260	0.0073	-0.348
	5.000	0.0119	0.0032	-0.162
	10.000	0.0030	0.0008	-0.040
10	1.000	0.2916	0.1045	-1.579
	1.111	0.2523	0.0847	-1.424
	1.250	0.2129	0.0667	-1.249
	1.429	0.1741	0.0506	-1.061
	1.667	0.1364	0.0366	-0.862
	2.000	0.1006	0.0248	-0.657
	2.500	0.0681	0.0155	-0.458
	3.333	0.0401	0.0085	-0.276
	5.000	0.0185	0.0037	-0.130
	10.000	0.0047	0.0009	-0.033
3.33	1.000	0.4629	0.1227	-0.6710
	1.111	0.4108	0.0986	-0.6300
	1.250	0.3554	0.0765	-0.5743
	1.429	0.2976	0.0567	-0.5053
	1.667	0.2384	0.0397	-0.4240
	2.000	0.1796	0.0259	-0.3327
	2.500	0.1236	0.0154	-0.2370
	3.333	0.0739	0.0081	-0.1453
	5.000	0.0344	0.0033	-0.0693
	10.000	0.0088	0.0008	-0.0180

(Continued)

TABLE F1 (Continued)

INFLUENCE VALUES FOR STRESS AT INTERFACE
(Perfect Continuity at Interface)
Tensile Stresses Are Negative
Two-Layered System Flexible Pavement

E_1/E_2	h/R	Vertical Stress σ_z	Radial Stress σ_r	
			Layer 2	Layer 1
2	1.000	0.5469	0.1230	-0.3010
	1.111	0.4906	0.0979	-0.2948
	1.250	0.4297	0.0747	-0.2802
	1.429	0.3638	0.0542	-0.2554
	1.667	0.2948	0.0368	-0.2212
	2.000	0.2240	0.0230	-0.1780
	2.500	0.1557	0.0129	-0.1298
	3.333	0.0936	0.0062	-0.0812
	5.000	0.0439	0.0024	-0.0392
	10.000	0.0112	0.0006	-0.0100
1	1.000	0.646	0.116	
	1.250	0.524	0.067	
	1.500	0.424	0.040	
	1.750	0.346	0.025	
	2.000	0.284	0.016	
	2.500	0.200	0.008	
	3.000	0.146	0.004	
	4.000	0.087	0.001	
	5.000	0.057	0.001	

BIBLIOGRAPHY

I. Stress Distribution in Soil

1. Boussinesq, J., Application des Potentiels à l'Etude de l'Equilibre et du Mouvement des Solides Elastiques; Paris, 1885. (Gauthier - Villars.)

2. Gilboy, G., Influence Tables for Solution of Boussinesq Equation; Progress Report of Special Committee, Proc. Am. Soc. Civ. Engrs. Vol. 59 (1933) pp. 781.

3. Love, A. E. H., The Stress Produced in a Semi-Infinite Body by Pressure on Part of the Boundary, Phil. Trans. Roy. Soc., series A Vol. 228 (1928) pp. 377-420.

4. Steinbrenner, W., Tafeln zur Setzungsberechnung; Die Strasse Vol. 1 (1934).

5. Newmark, N. M., Influence Charts for Computation of Stresses in Elastic Foundations, Univ. of Illinois Eng. Exp. Sta. Bull. No. 338, Urbana, 1942.

6. Newmark, N. M., Influence Charts for Computation of Stresses in Elastic Foundations, Univ. of Illinois Eng. Exp. Sta. Bull. No. 338, Urbana, 1942.

7. Fergus and Miner, Distributed Loads on Elastic Foundation, Proc. Hwy. Res. Board, Vol. 34 (1955) pp. 582-597.

8. Waterways Experiment Station, Investigations of Pressures and Deflections for Flexible Pavements, Report No. 3, Theoretical Stresses Induced by Uniform Circular Loads, Vicksburg, Miss., 1953

9. Foster & Ahlvin (1954), Stresses and Deflections Induced by a Uniform Circular Load, Proc. Hwy. Res. Board, Vol. 33 (1954), pp. 467-470.

10. Griffith, J. H., The Pressures Under Substructures; Engineering and Contracting, Vol. 1 (1929), pp. 113-119.

11. Fröhlich, O. K., Druckverteilung in Baugrunde; Berlin, 1934, (J. Springer).

12. Ohde, J., Die Berechnung der Sohldruckverteilung unter Gründungskörpern, Der Bauingenieur, Vol. 23 (1942) H. 14/16 and 17/18.

13. Wolf, K., Ausbreitung der Kraft in der Halbebene und in Halbraum bei anisotropem Material, Zeitschift angew. Math. und Mech. Vol. 15 (1935) pp. 249-254.

14. Jelinek, R., Der Boden als querisotropes Medium; Abhandlungen über Bodenmechanik und Grundbau, Berlin 1948 (E. Schmidt) pp. 19-24.

15. Jelinek, R., Die Kraftausbreitung im verallgemeinerten ebenen Spannungszustand für querisotrope Böden; Abhandlungen über Bodenmechanik und Grundbau Berlin 1948 (E. Schmidt) pp. 24-27.

16. Jelinek, R., Die Kraftausbreitung im Halbraum für querisotrope Böden; Abhandlungen über Bodenmechanik und Grundbau Berlin 1948 (E. Schmidt) pp. 28-33.

17. Koning, H., Stress Distribution in a Homogeneous, Anisotropic, Elastic Semi-infinite Solid; Proceedings, Fourth Int. Conf. Soil Mech. and Found. Engrg. London, 1957, Vol. 1, pp. 335-338.

18. Westergaard, H. M., A Problem of Elasticity Suggested by a Problem in Soil Mechanics, Soft Material Reinforced by Numerous Strong Horizontal Sheets, Contribution to Mechanics of Solids, Stephen Timoshenko 60th Anniversary Volume, New York, 1938, (MacMillan).

19. Fadum, R. E., Influence Values for Vertical Stresses in a Semi-Infinite Solid due to Surface Loads, Harvard University, 1941.

20. Melan, E., Die Druckverteilung durch eine elastische Schicht, Beton and Eisen, Vol. 18, (1919) pp. 83-85.

21. Marguerre, K., Druckverteilung durch eine elastische Schicht auf starrer, rauher Unterlage, Ing. Archiv., Vol. 2, (1931) pp. 108-117.

22. Biot, M. A., Effect of Certain Discontinuities on the Pressure Distribution in a Loaded Soil, Physics Vol. 6 (1935), pp. 367-375.

23. Picketts, G., Stress Distribution in a Loaded Soil with Some Rigid Boundaries, Proceedings, Highway Research Board, Vol. 18, (1938) pp. 35-48.

24. Burmister, D. M., The Theory of Stresses and Displacements in Layered Systems and Application to the Design of Airport Runways, Proceedings, Highway Research Board, Vol. 23 (1943) pp. 126-148.

25. Burmister, D. M., The General Theory of Stresses and Displacements in Layered Systems, Journal of Applied Physics, Vol. 16, (1945) pp. 296-302.

26. Fox, L., Computation of Traffic Stresses in a Simple Road Structure, Road Research Laboratory (England), Road Research Paper No. 9, London, 1948, (H. M. Stationary Office), also, Proc. Sec. Inf. Conf. Soil Mech. and Found. Engg. Vol. II, pp. 236-246.

27. Hank and Scrivner, Some Numerical Solutions of Stresses in Two and Three Layered Systems, Proceedings Highway Research Board, Vol. 28, 1948, pp. 457-468.

28. Acum, W. E. A. and Fox, L., (1951) Computation of Load Stresses in a Three-Layer Elastic System, Geotechnique Vol. II, No. 4, pp. 293-300.

29. Burmister, D. M., Stress and Displacement Characteristics of a Two-Layer Rigid Base Soil System, Influence Diagrams and Practical Applications, Proceedings, Highway Research Board, Vol. 35, (1956) pp. 773-814.

II. Tests on Stress Distribution

30. Steiner, Handbuch der Ingenieurwissenschaften II Bd., Der Bruckenbau, p. 195, Leipzig, 1882, (W. Engelmann).

31. Strohschneider, O., Elastische Druckverteilung und Drüchüberschreitung in Schüttungen, Sitz. Berichte der K. K. Akad. Wiss. Wien, Vol. 121 (1912) p. 301.

32. Moyer, J. A., Distribution of Vertical Soil Pressure Eng. Record, Vol. 69 (1914) p. 608 and Vol. 71 (1915) p. 330.

33. Enger, M. L., High Unit Pressures Found in Experiments on Distribution of Vertical Loading through Sand; Eng. Record, Vol. 73 (1913) p. 106.

34. Goldbeck, A. T., Distribution of Pressures through Earth Fills, Proc. ASTM. Vol. 17 (1917) p. 640.

35. Kögler, F. & Scheidig, A., Druckverteilung im Baugrunde, Bautechnik Vol. 5, (1927) p. 418, Vol. 6, (1928) p. 205, Vol. 7 (1929), p. 268.

36. Hugi, A., (1927) Untersuchungen über die Druckverteilung im örtlich belasteten Sand, Dissertation, Technische Hochshule Zürich.

37. Gerber, E., (1929), Untersuchungen über die Druckverteilung im örtlich belasteten Sand, Dissertation , Technische Hochschule Zürich.

38. Fischer, Ch., A Method of Representing the Distribution of Stress in Ground, Proc. First Int. Conf. Soil Mech. and Found. Engrg, Harvard University, Cambridge, Mass. (1936) Vol. II., p. 144.

39. Press, H., Der Boden als Baugrund, Berlin 1940 (W. Ernst & Sohn).

40. Corps of Engineers, Sacramento District, Report on Stockton Runway Test Section, Sacramento, Calif., 1942.

41. Corps of Engineers, Little Rock District, Report on Barksdale Field Service Behavior Tests, Little Rock, Ark., 1944.

42. Waterways Experiment Station, Flexible Pavement Tests, Marietta, Ga., Appendix to Certain Requirements for Flexible Pavement Design for B-29 Planes. Vicksburg, Miss., 1945.

43. Waterways Experiment Station, Investigations of Pressures and Deflections for Flexible Pavements, Report No. 1, Homogeneous Clayey-Silt Test Section, Vicksburg, Miss., 1951.

44. Waterways Experiment Station, Investigations of Pressures and Deflections for Flexible Pavements, Report No. 4, Homogeneous Sand Test Section, Vicksburg, Miss., 1954.

III. Design Methods

45. Abercrombie, W. F., (1954), A System of Soil Classification Proceedings, Highway Research Board, Vol. 33, p. 509.

46. Abercrombie, W. F., (1958), Flexible Pavement Design as Currently Practiced in Georgia, Bulletin 177, Highway Research Board.

47. Porter, O. J., The Preparation of Subgrades, Proc. Highway Research Board, Vol. 18, (1938) pp. 324-331.

48. American Society of Civil Engineers, Development of CBR Flexible Pavement Design Methods for Airfields, Transactions, Am. Soc. Civ. Engr. Vol. 115, (1950), pp. 453-589.

49. Boyd, K., Analysis of Wheel Load; Proceedings, Highway Research Board, Vol. 22, pp. 185-194.

50. U. S. Navy, Bureau of Yards and Docks, Procedure for Determination of Thickness of Flexible Type Pavements, Manual No. 1, Rev. June 1943.

51. McLeod, N. W., Airport Runway Evaluation in Canada, Highway Research Board, Research Reports No. 4B. (1947).

52. McLeod, N. W., A Canadian Investigation of Load Testing Applied to Pavement Design, ASTM Spec. Techn. Pub. No. 79, pp. 83-127, Philadelphia, 1947.

53. Worley, H. E., Triaxial Testing Methods Usable in Flexible Pavement Design, Proceedings, Highway Research Board, Vol. 23 (1943) pp. 109-126.

54. McDowell, C., Triaxial Tests in Analysis of Flexible Pavements, Highway Research Board Research Report No. 16B (1954).

55. McDowell, C., Wheel Load Stress Computations Related to the Texas Highway Department's Triaxial Method of Flexible Pavement Design, Highway Research Board Bulletin No. 114 (1955) pp. 1-20.

56. Waterways Experiment Station: The CBR Test as Applied to the Design of Flexible Pavements for Airports, Technical Memorandum No. 213-1, Vicksburg, Miss., 1945.

57. Glossop, R., and Golder, H. Q., Construction of Pavements on a Clay Foundation Soil, Institution of Civil Engineers, London, Road Paper No. 15 (1944).

58. Golder, H. Q., Relationship of Runway Thickness and Under-carriage Design to the Properties of the Subgrade Soil; Institution of Civil Engineers, London, Airport Paper No. 4 (1947).

59. McLeod, N. W., An Ultimate Strength Approach to Flexible Pavement Design, Proceedings of the Association of Asphalt Paving Technologists Vol. 23 (1954) pp. 119-236.

IV. General References

60. Caquot A., & Kérisel J., Traité de Mécanique des Sols, Paris 1956 (Gauthier-Villars) Ch. VI, XIX.

61. Krynine, D. P., Soil Mechanics, New York 1941 (McGraw-Hill) Ch. IV.

62. Lambe, W., Soil Testing for Engineers, New York, 1951 (J. Wiley & Sons).

63. Reiner, M., (editor), Building Materials, Ch. IX, Road Asphalt (by C. vander Poel), Amsterdam 1954 (North Holland Publ. Co.)

64. Road Research Laboratory D.S.I.R., Soil Mechanics for Road Engineers, London 1952 (H. M. Stationery Office), Ch. 20.

65. Sowers, G. B. and Sowers, G. F., Introductory Soil Mechanics and Foundations, New York 1951 (Macmillan).

66. Sowers, G. F., Laboratory Manual for Soil Testing, Atlanta 1955, (Georgia Institute of Technology).

67. Terzaghi, K., Theoretical Soil Mechanics, New York 1943 (J. Wiley & Sons) Ch. XVII, XVIII.

68. Timoshenko, S. P., Theory of Elasticity, New York 1934, (McGraw-Hill) Ch. III, XI.

ANNUAL REPORT NO. 2

PROJECT NO. B-133
HPS-1(53)

THE STUDY OF STRESSES IN A FLEXIBLE PAVEMENT SYSTEM

By

GEORGE F. SOWERS and ALEKSANDAR B. VESIĆ

Contract with
THE STATE HIGHWAY DEPARTMENT OF GEORGIA
in cooperation with
THE BUREAU OF PUBLIC ROADS

MARCH 1, 1959 through JULY 1, 1960

Engineering Experiment Station
Georgia Institute of Technology
Atlanta, Georgia

ENGINEERING ESPERIMENT STATION
of the Georgia Institute of Technology
Atlanta, Georgia

ANNUAL REPORT NO. 2

PROJECT NO. B-133
HPS-1(53)

THE STUDY OF STRESSES IN A FLEXIBLE PAVEMENT SYSTEM

By

GEORGE F. SOWERS and ALEKSANDAR B. VESIĆ

Contract with
THE STATE HIGHWAY DEPARTMENT OF GEORGIA
in Cooperation with
THE BUREAU OF PUBLIC ROADS

MARCH 1, 1959 through JULY 1, 1960

TABLE OF CONTENTS

This report contains 61 pages.

LIST OF FIGURES

LIST OF FIGURES (Continued)

LIST OF TABLES

CHAPTER I

INTRODUCTION

1. Scope of the Project

The rational design of any structural system, including pavements, must commence with the stresses. However, little is known about the stresses developed in the soil by loads of wheeled vehicles supported by pavements. It is the objective of this research to investigate the stresses produced in the subgrade beneath a flexible pavement by heavy loads such as trucks. This includes a study of the stress propagation, a comparison of the relative load-spreading qualities of different pavements, and the formulation of a method for predicting the stresses from the loads and the physical properties of the pavement system.

The problem has been attacked from two sides: measurement of actual stresses produced by wheels in a full-scale model of a pavement-base-subgrade system, and theoretical computation of stresses produced in various forms of elastic masses, including homogeneous or layered and isotropic and anisotropic. The measured stresses are compared with those computed from theory, using the physical properties of the pavement system as measured by both laboratory and in-place tests. From the comparison it is possible to evaluate the validity of the theories and to devise the modifications and corrections that are required to translate the theoretical analyses into actual practice.

2. Summary of First Year's Work

The first year's work was reported in Annual Report No. 1. It included three phases. The first phase was an intensive review of existing methods of analyzing stresses in large masses similar to soils acted on by wheel loads. This phase was completed and presented in detail.

The second phase was the design and construction of a full-scale model consisting of pavement subgrade and truck wheels, that permitted the placing of loads and the measurement of stresses under controlled conditions. This included the design and construction of loading and measuring instruments, and their calibration under field conditions. This work was largely completed although some changes and improvements have continued throughout the second year's work.

The third phase was the measurement of stresses in a flexible pavement system consisting of a 3-inch-thick asphaltic surface, an 8-inch-thick sandy (topsoil) base course, and a micaceous, sandy-silt subgrade. Such pavements are widely used throughout Georgia. The test results indicated that the topsoil base course was no more efficient in spreading the wheel load than the soil beneath, and that the theoretical analyses of stress based on a semi-infinite homogeneous, isotropic elastic medium were a satisfactory representation of the stresses produced in the pavement system.

3. Summary of Second Year's Work

The second year's work, herein reported, includes two phases: load-stress measurements on three more pavement systems, and laboratory tests on the physical properties of soils and aggregates that comprised all four pavement systems.

The pavements tested employed the same surface and subgrade as previously, but base courses of soil-bound macadam, a soil-cement macadam, and a sand-asphalt. The results indicate that the soil-bound macadam and the sand-asphalt are no more effective in spreading the load than a homogeneous soil. The soil-cement, however, was much more efficient, and the stresses in the subgrade were appreciably lower than when the other bases were employed. Deflections were measured in some tests but are not discussed in this report.

The physical tests included compaction, triaxial compression or shear, consolidation, and routine identification and classification. Field tests included plate load tests on the pavement, base, and subgrade, and the California bearing ratio.

The equipment, methods, and results will be discussed in the following chapters.

CHAPTER II

LABORATORY TESTS OF SOIL AND BASE MATERIALS

1. Classification and Identification

Classification and identification tests were made on all the soil and aggregate materials. The standard ASTM procedures were used for grain size, liquid limit, plastic limit, and specific gravity of solids, with only minor variations to suit the peculiarities of the materials. All were then examined microscopically to determine the minerals present and the particle shapes of the fraction coarser than the No. 200 sieve. The detailed results of tests on the subgrade and topsoil were given in the first Annual Report, and those on the macadam stone and sand in the Appendix of the present report. They are summarized in Table I.

Grain size curves of subgrade, topsoil and sand for sand-asphalt base are shown in Figure 1. Strength and deformation characteristics of all the materials are given in Table II.

2. Compaction Tests

Standard compaction tests were made of the sand-asphalt base, using the 4-inch-diameter compaction mold and the procedure specified by ASTM D698-58T Method C. The soil-bound macadam and the soil-cement base contained particles too large for the ordinary compaction molds, and so special large molds were designed to handle them.

Three molds were designed as shown in Figure 2, with 4-, 6-, and 8-inch diameters and 8-, 12-, and 16-inch heights respectively. The mold cylinders were made in three pieces to permit their removal without damage to the compacted samples. These molds were constructed out of School of Civil Engineering funds in the laboratory shops.

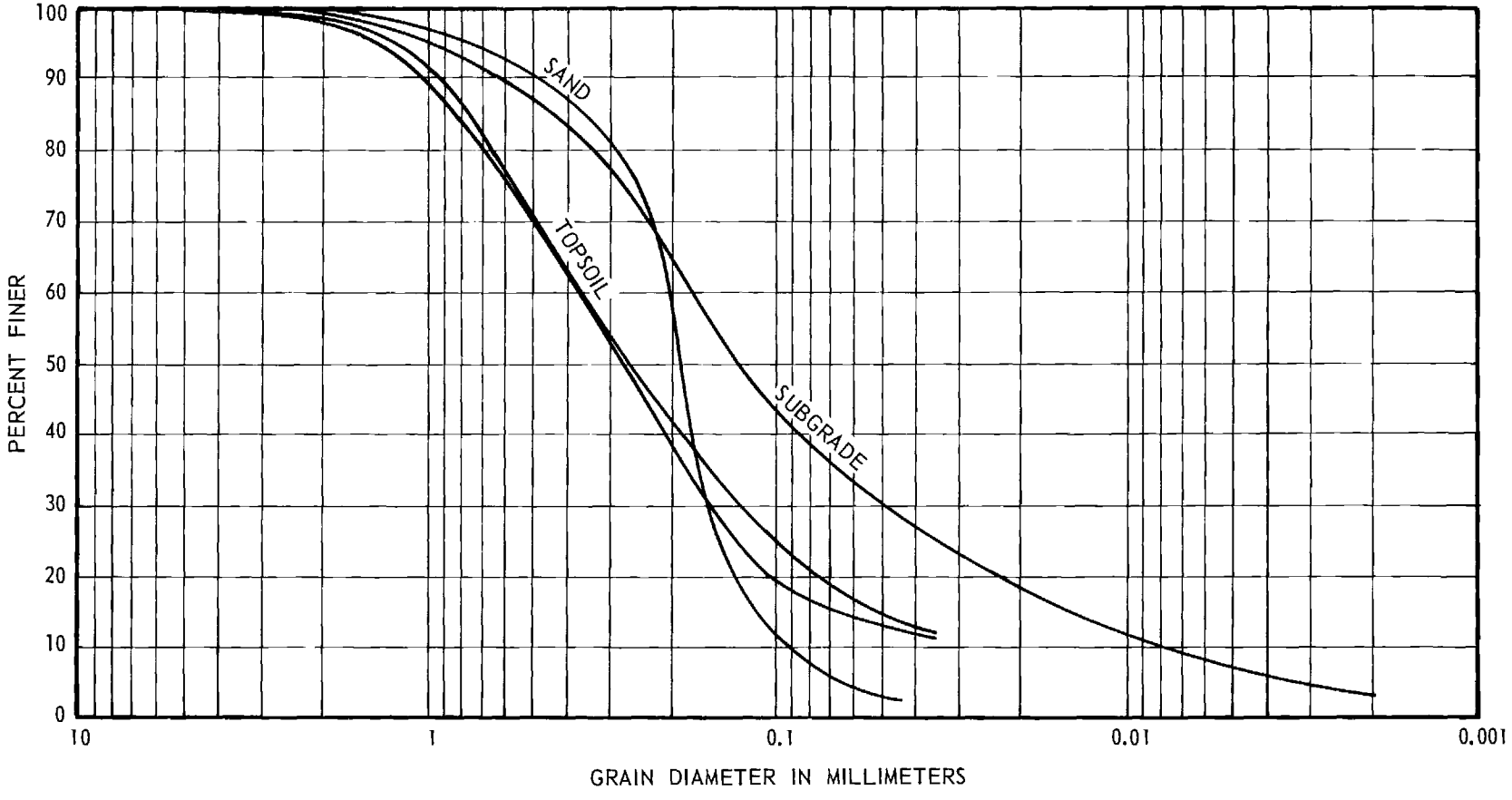

Figure 1. Grain-Size Curves.

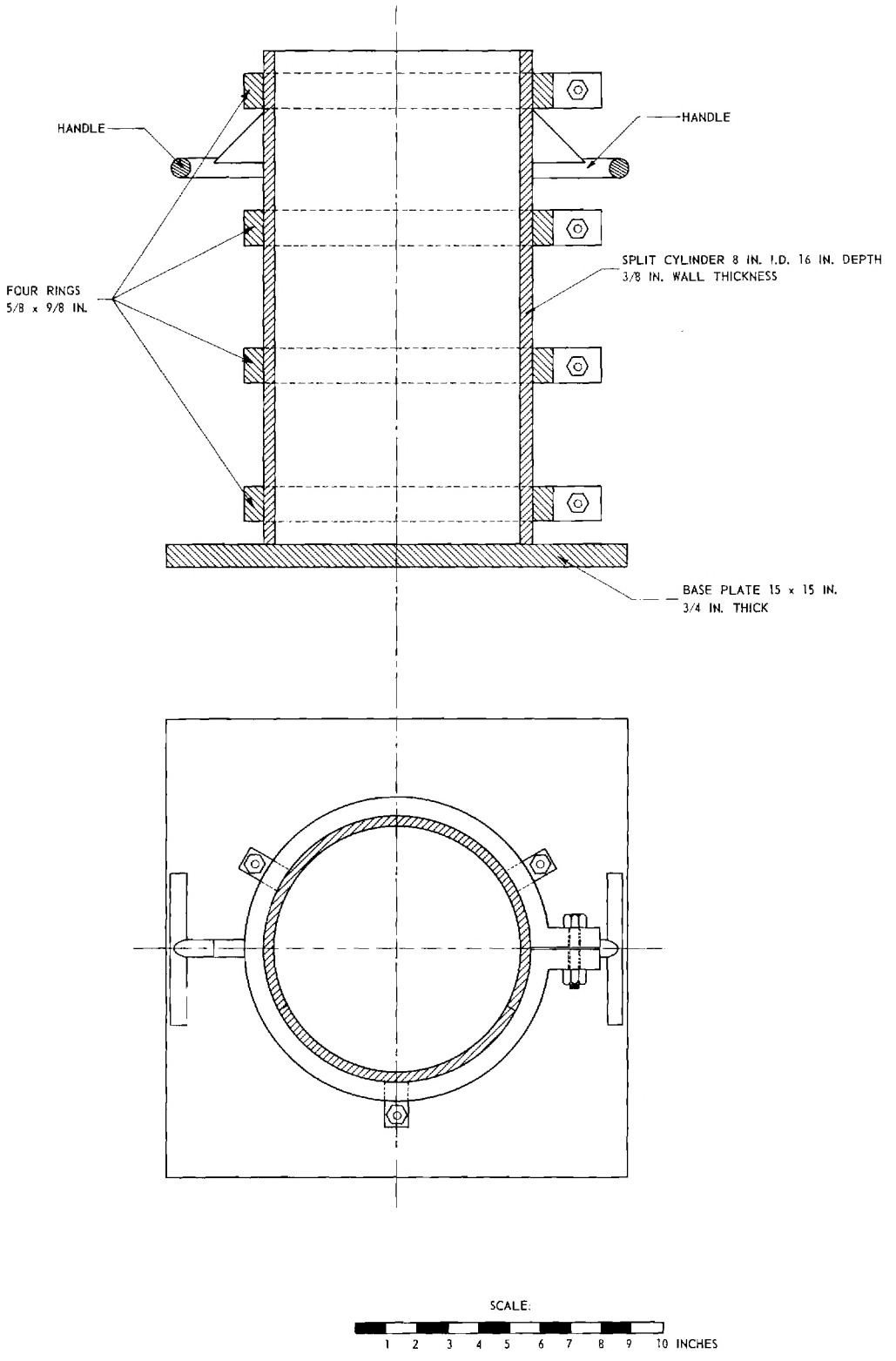

Figure 2. Large Compaction Mold (Diameter: 4, 6, and 8 inches).

TABLE I

SUMMARY OF CHARACTERISTICS OF SUBGRADE AND BASE MATERIALS

Material	Detailed Description	Liquid Limit (%)	Plasticity Index (%)	Passing No. 200 (%)	Maximum Density (lb/ft³)	Class
Subgrade	Micaceous fine sandy silt	45.0	8	36-40	94.5††	A-5
Topsoil base	Silty, well-graded sand	14.5	0	12-16	128.0†	A-1
Soil-bound macadam base	Angular to sub-angular, granite gneiss, sizes 4 6 7† plus 40 per cent topsoil (above)			0		
Soil-cement base	4 per cent by weight. Type 1 portland cement plus 96 per cent soil-bound macadam (above)			--		--
Sand-asphalt base	Uniform subangular quartz sand with traces of silt, plus 5 per cent RC-3 cutback	--	--	0		A-3†††

† ASTM D448.

†† ASTM D698-58T (Method C).

††† Soil alone.

The materials were compacted in the molds with the standard compaction hammers that are 2 inches in diameter, weigh 5.5 lb., and fall 12 inches. The soils were compacted in layers the same thickness as in the standard test, and with the number of hammer blows required to give the same compaction energy per cubic foot of soil as in the standard test.

3. Preparation of Samples

Cylindrical samples of each material were prepared at the same density as employed in the full-scale model tests, using 4-inch-diameter by 8-inch-height

specimens for the subgrade, topsoil base, and sand-asphalt base; and 8-inch-diameter by 16-inch-height specimens for the soil-bound macadam and the soil-cement bases. These were cured the same length of time as in the full-scale model and then tested for strength and elasticity. Also, undisturbed samples of subgrade, topsoil and sand-asphalt base were extracted from the model after the loading tests.

4. Triaxial Testing

Triaxial compression tests were made on the cylindrical specimens to determine their shear strength parameters and modulus of elasticity characteristics. A new triaxial chamber (Figure 3) was designed for these tests to accommodate the large specimens. It has interchangeable bases on top caps 4, 6, and 8 inches in diameter, and has bushings of different heights so that all three specimen sizes can be tested in the same cell. The cell bases are of wrought aluminum, with stainless steel fittings. The load is applied through a high strength, stainless steel piston supported by linear ball bearings (ball bushings to minimize piston friction). The piston is sealed with an O-ring.

The specimens were tested in undrained (quick) loading, using controlled strain. All were tested at a strain rate of 0.02 inch per minute until failure occurred. The sand-asphalt base was also tested at a slower rate of 0.01 inch per minute to determine if creep had any effect on the shear properties. Axial deformations were measured throughout each test so that stress-strain curves could be plotted. No attempts were made to measure lateral strains. The effect of bulging was included by assuming that the average sample cross-sectional area was equal to $\frac{A}{1-\epsilon}$ where A is the original area and ϵ the strain.

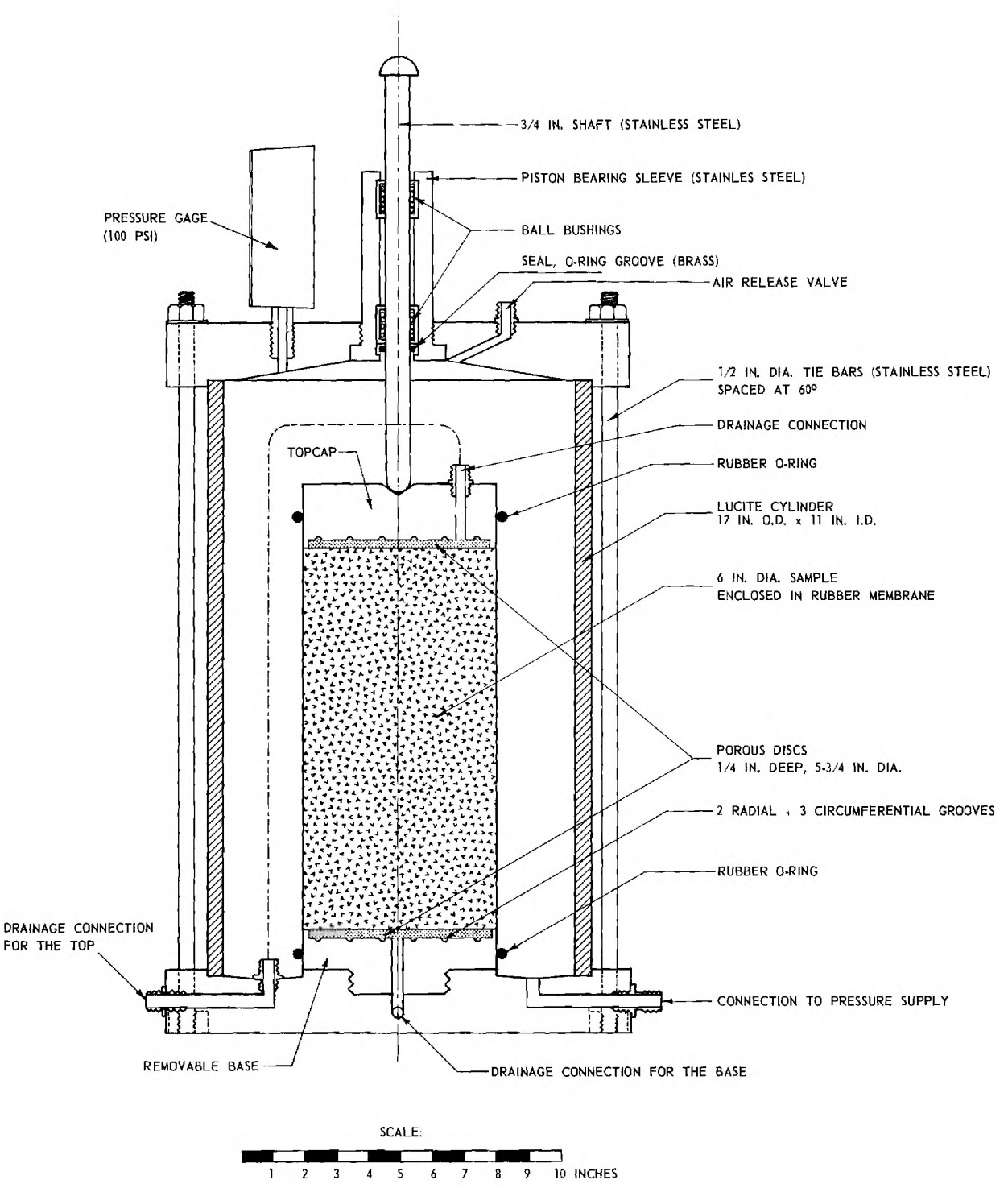

Figure 3. Large Triaxial Cell Sample Diameter (4, 6, and 8 inches).

CHAPTER III

LOAD TESTS ON PAVEMENTS

1. Systems Tested

Load tests were made on full scale pavements with the following dimensions:

Surface Course - 3-inch asphaltic concrete.

Base Course - 8-inch-thick, compacted to 100 per cent of maximum.

Subgrade - Top 37-inch micaceous sandy silt compacted to 95 per cent or more of maximum.

Botton 36-inch micaceous sandy silt. Compaction to approximately 90 per cent of maximum.

Three different base courses were employed:

1. Soil-bound macadam - 40 per cent topsoil plus 60 per cent 4, 6, 7 crushed stone aggregate.
2. Soil cement - soil-bound macadam plus 4 per cent cement by weight.
3. Sand-asphalt - natural sand plus 5 per cent RC-3 cutback asphalt by weight.

All three bases are currently employed in road construction in Georgia, and all three met the appropriate Georgia State Highway Department specifications.

2. Wheel Load Tests

Load tests were made employing truck tires, using essentially the same equipment, instrumentation, and procedure as outlined in Chapters 3 and 4 of Annual Report No. 1. A few minor changes were made.

The depths and locations of the test cells were changed to secure better definition of the stresses, and the tests of dual tandem tires omitted because the stresses were found to be essentially the same as those for duals. Tests of the single tire loaded to 13,500 lb. were omitted in some cases since this

represents an excessive overload of the tire (where maximum rated load is 9,000 lb.) which produced severe rutting of the pavement.

Deflections of the surface were measured in some tests during loading, and the residual deflections were measured on the previously loaded cross section after the tire was removed. The measurements were made with micrometer dial gauges mounted on cross arms supported by the walls of the test pits. These data will be presented in the final report.

3. In-Place Tests of Soil and Pavement

Two types of in-place tests were made on the pavements: California Bearing Ratio (CBR) and plate load tests. The CBR tests were conducted in the upper surfaces of the subgrade and base courses, using standard procedures developed by the Corps of Engineers.

Plate load tests were made on the upper surfaces of the subgrade and all base courses and on the surface course of all but the sand-asphalt base pavement. The plate used (Figure 4) is circular, 18 inches in diameter, and reinforced so that its deflection would be negligible. It was loaded in increments, using the calibrated hydraulic jack. A ball and socket joint permitted the plate to tilt as it deflected. Settlement of the plate was measured by micrometer dial gauges mounted on beams supported by the pit walls. A few tests were also made with a 24-inch square plate.

The temperatures of the pavement system were measured during all wheel and plate load tests. In most of the tests the pavement temperatures were within the range 75° to 85° F. Tests of the soil cement base system were made during colder weather, with the temperature range 50° to 60° F.

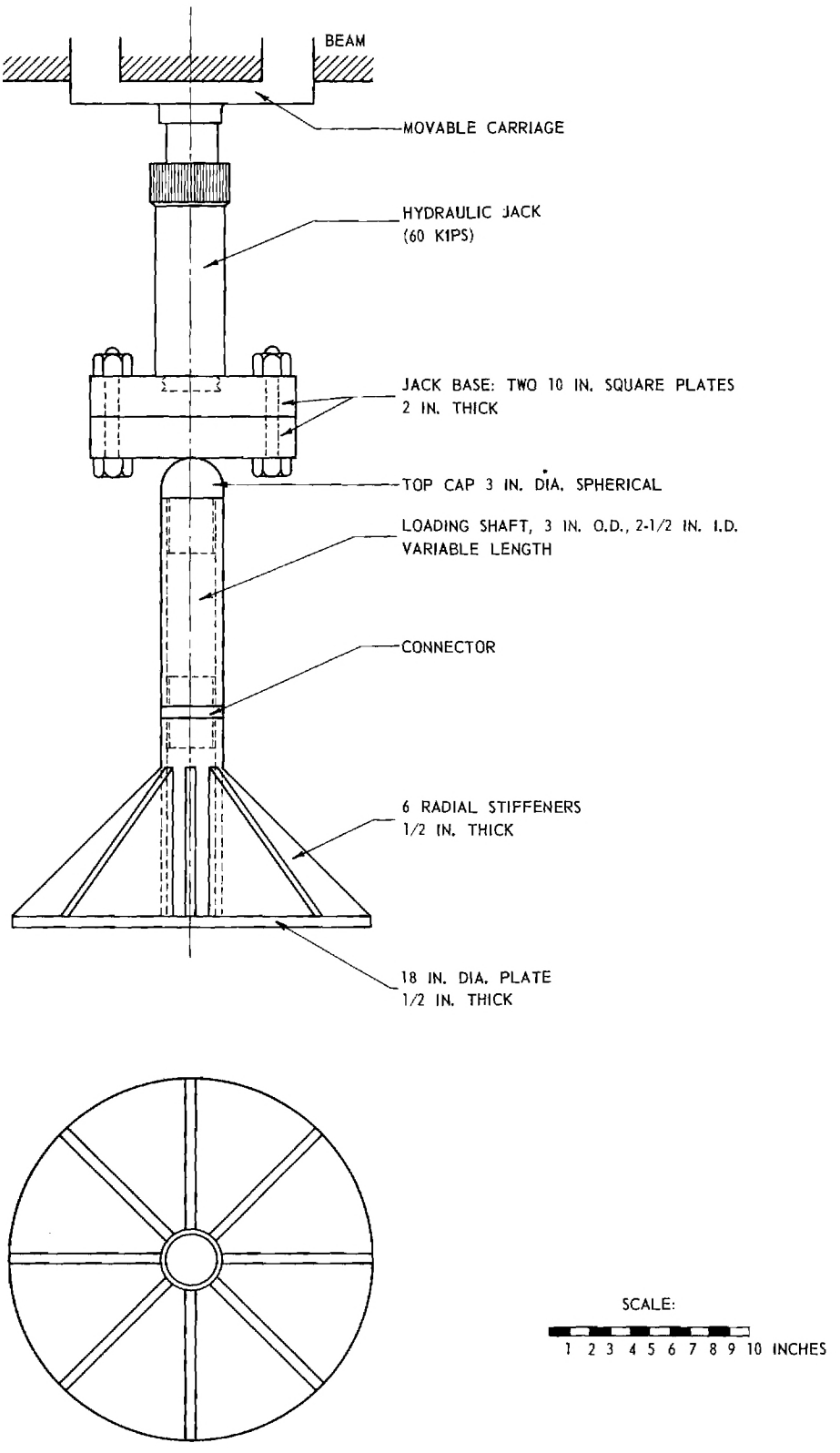

Figure 4. Plate Load Test Rig.

CHAPTER IV

TEST RESULTS

1. Identification and Description of Data

The detailed triaxial tests results are presented in graphical form in Figures 5-11 as well as in Table I. The triaxial compression data are expressed three ways: Stress-axial strain curves show the loading characteristics for individual specimens (Figures 5b, 6b, 7b, 8b, and 9b). Mohr diagrams of the failure stresses for each different material show the strength parameters of apparent cohesion, c', and angle of shearing resistance φ' (Figures 5a, 6a, 7a, 8a, and 9a). Modulus of elasticity curves, derived from the tangent to the initial segment of each stress-strain show the initial modulus of elasticity as a function of confining pressure, (Figure 10a,b). The relative rigidity of different base materials in respect to the subgrade is seen from Figure 11, which presents ratio of moduli E of different bases and of the subgrade as a function of lateral confining pressure.

The CBR results are given as stress-strain curves with the final CBR number computed from the load required for a deformation of 0.1 or 0.2 inch (Figures 12-15). The initial or tangent modulus of elasticity from the CBR loading is also given in Table II.

The plate load tests are presented as load-deflection curves (Figure 16). The tangent modulus of elasticity for each curve was computed and is shown in Table II. These computations were made under the assumption that the pavement system consists of two layers of different rigidities and that the two-layer theory is valid.

The wheel load tests are presented in Figures 17-34. They show the normal component of stresses on horizontal planes σ_z in the soil as measured by the pressure cells as functions of the horizontal distance from the center of load.

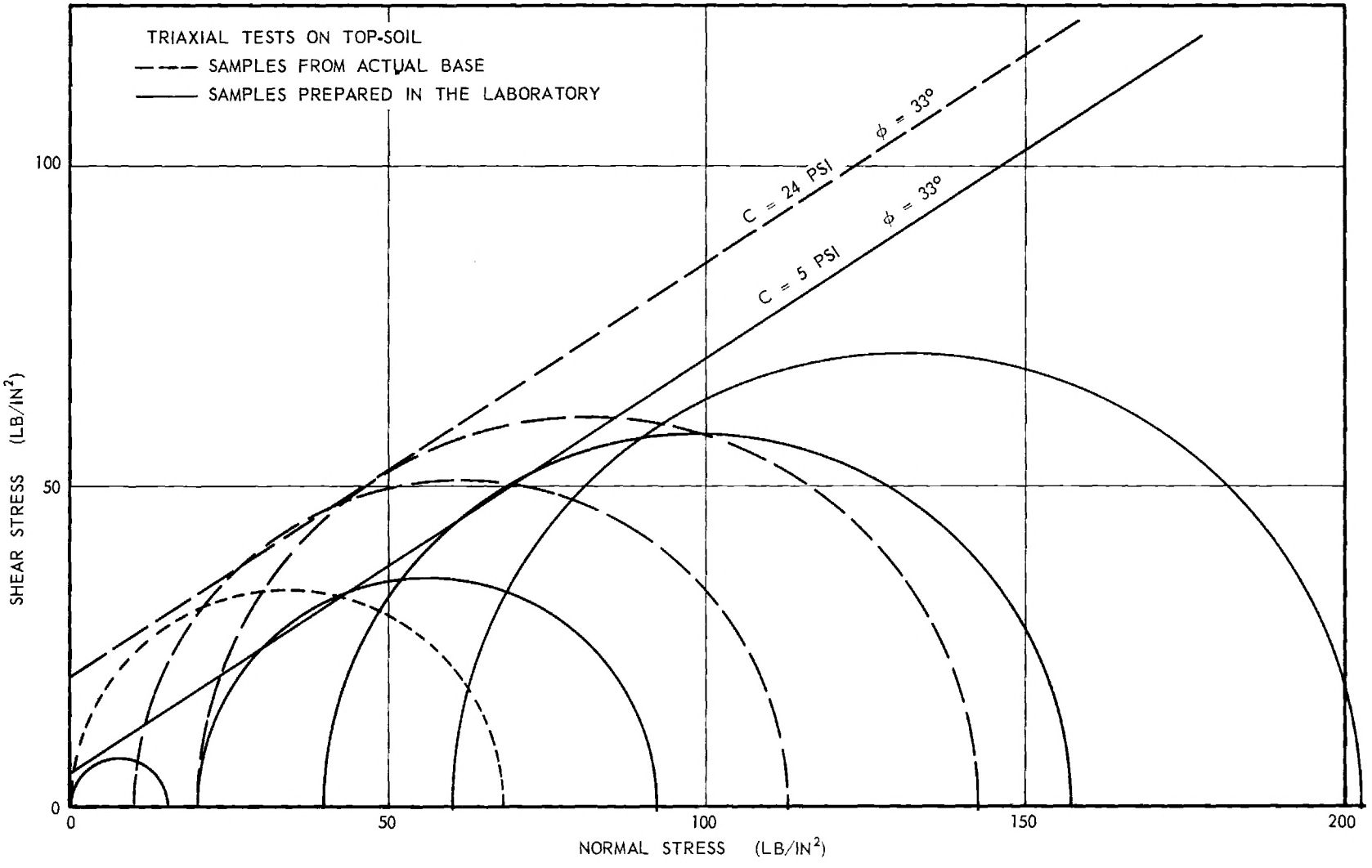

Figure 5a. Triaxial Test Results: Topsoil.

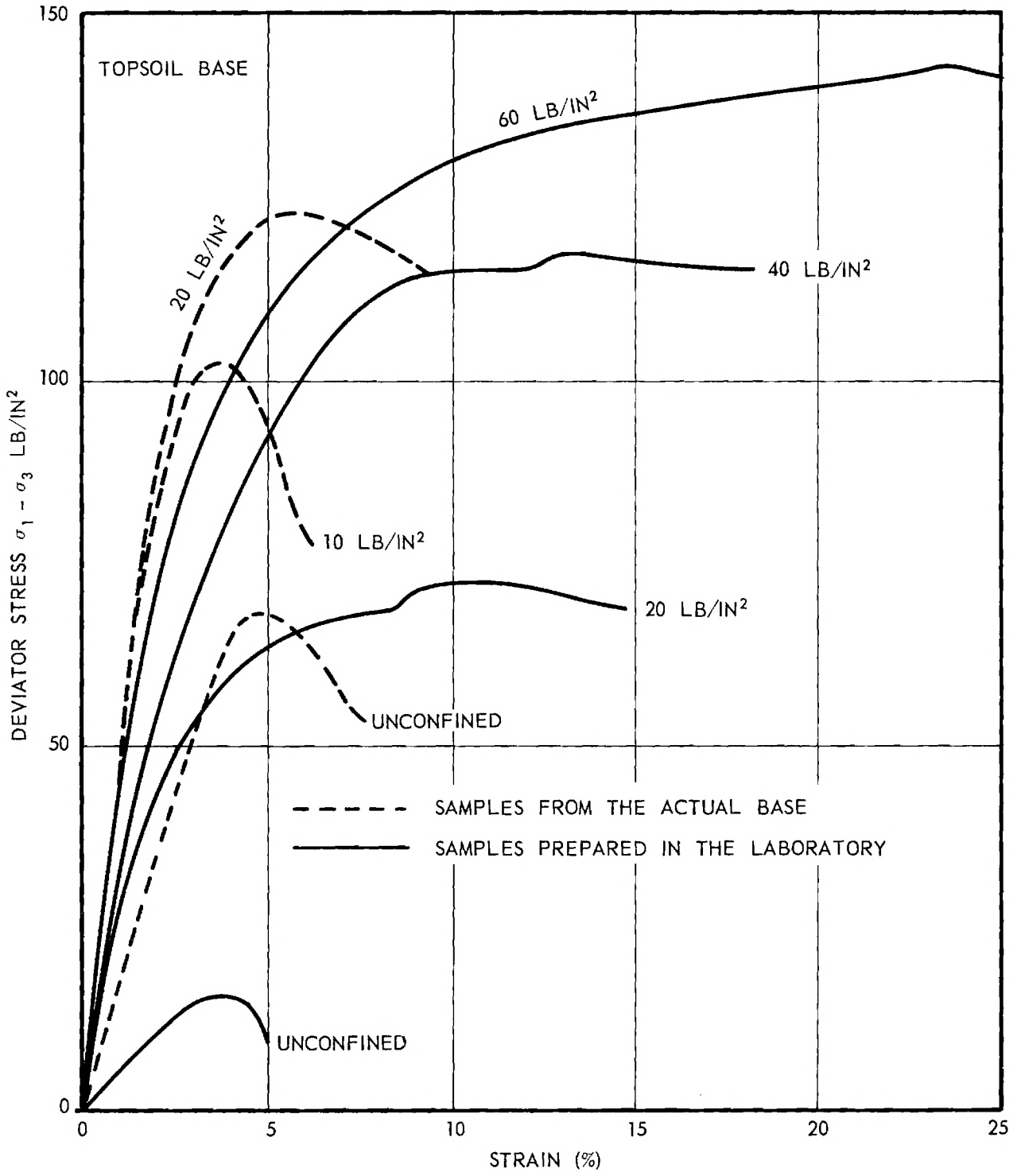

Figure 5b. Triaxial Test Results: Topsoil.

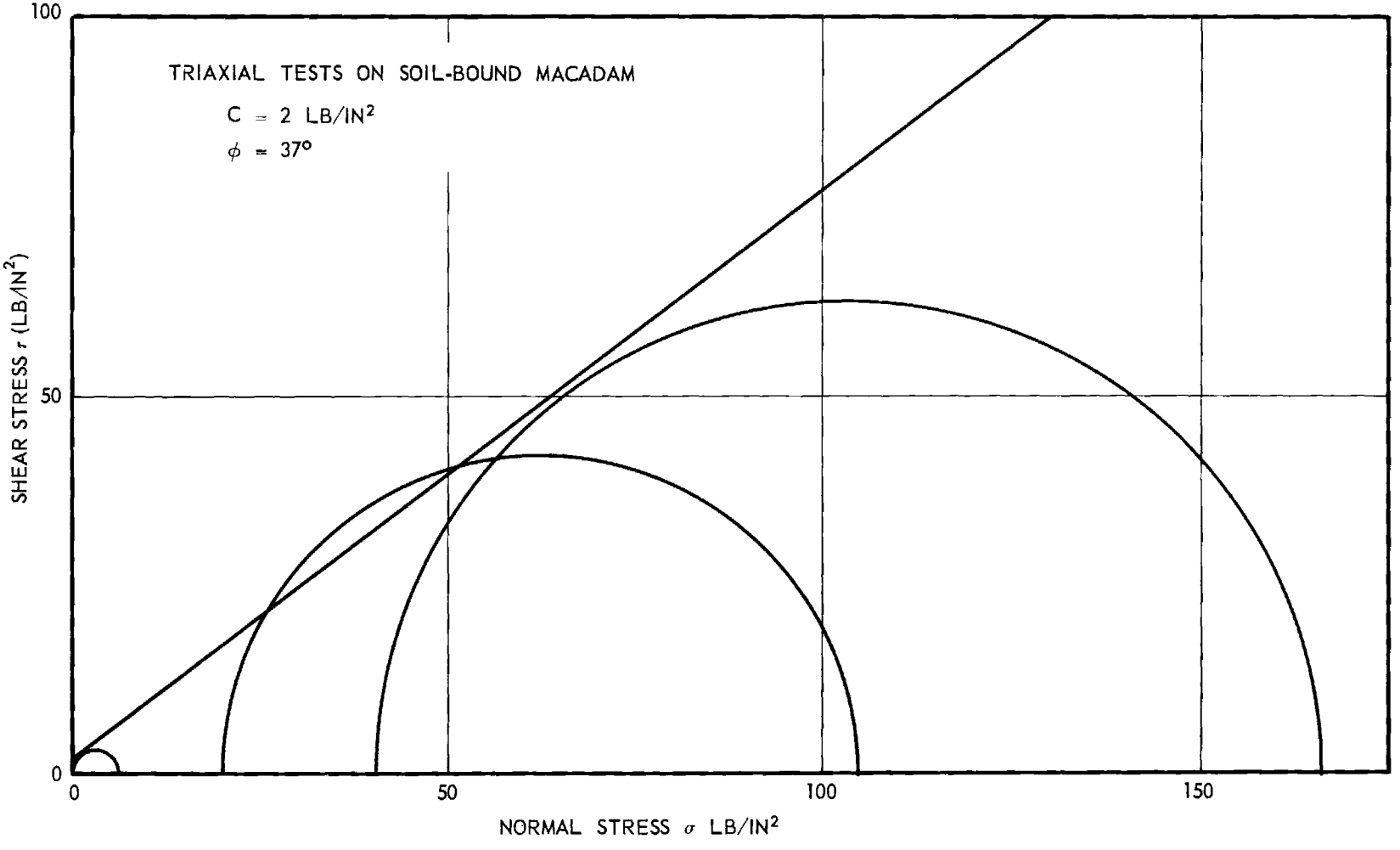

Figure 6a. Triaxial Test Results: Soil-Bound Macadam.

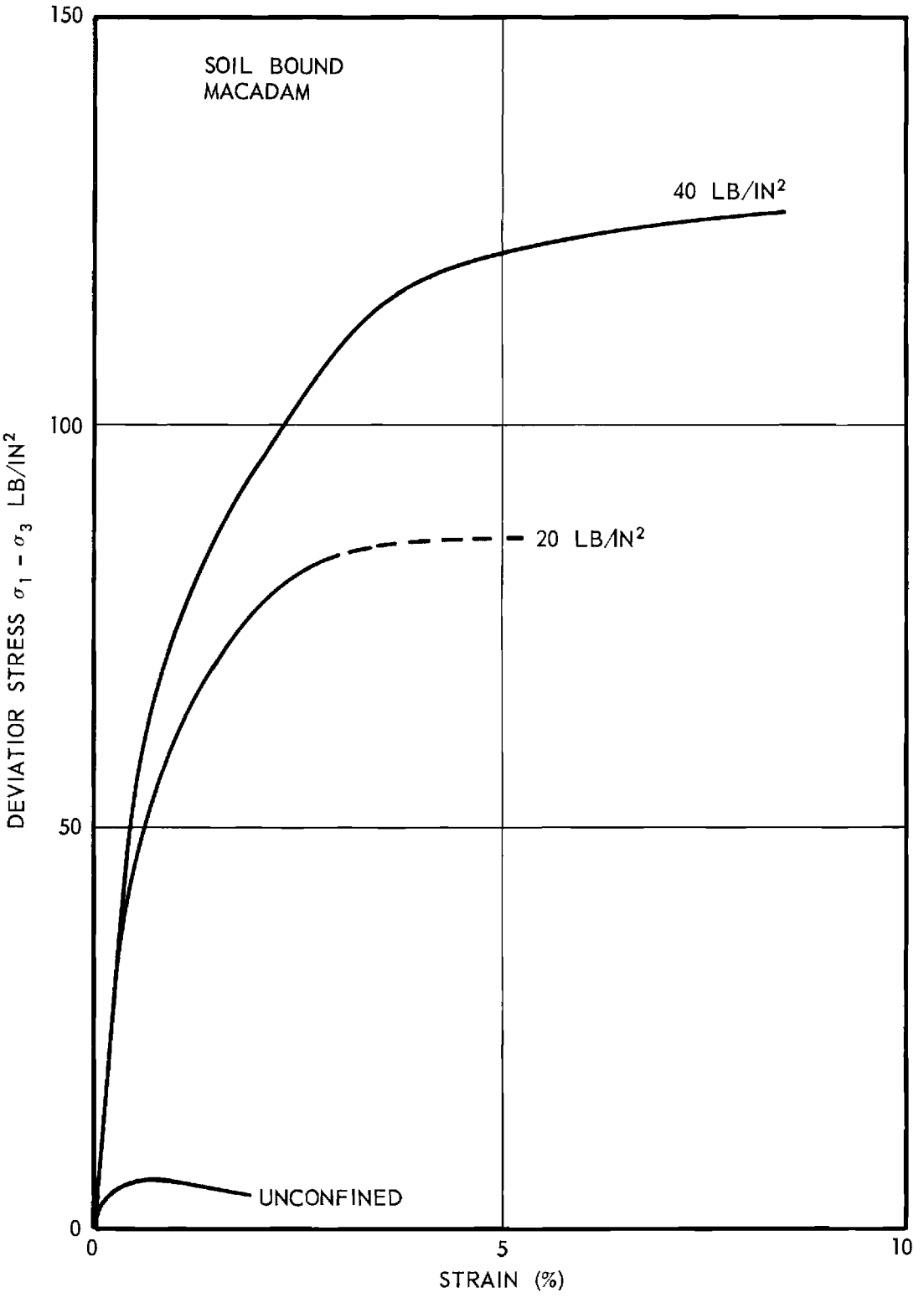

Figure 6b. Triaxial Test Results: Soil-Bound Macadam.

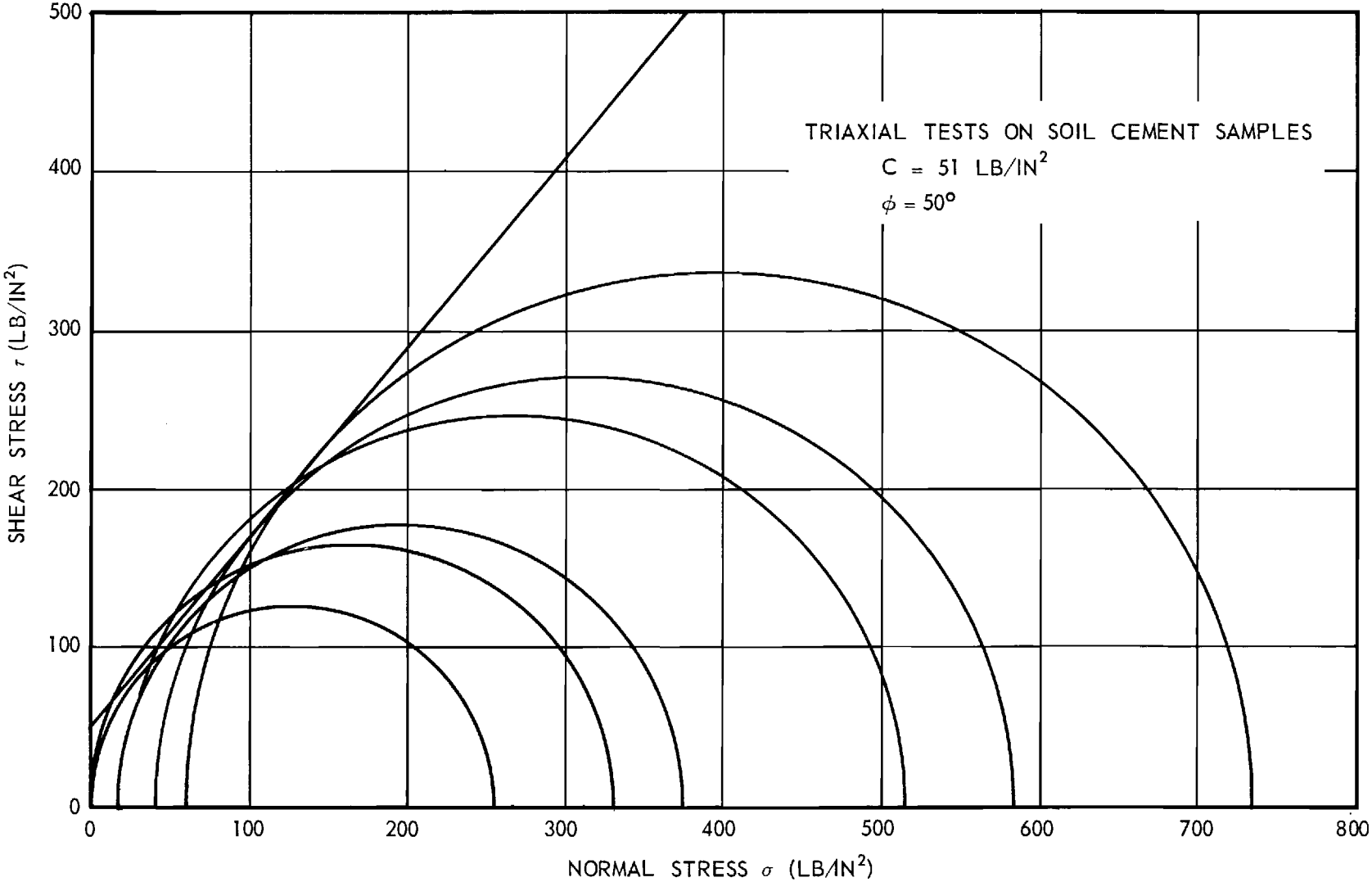

Figure 7a. Triaxial Test Results: Soil-Cement.

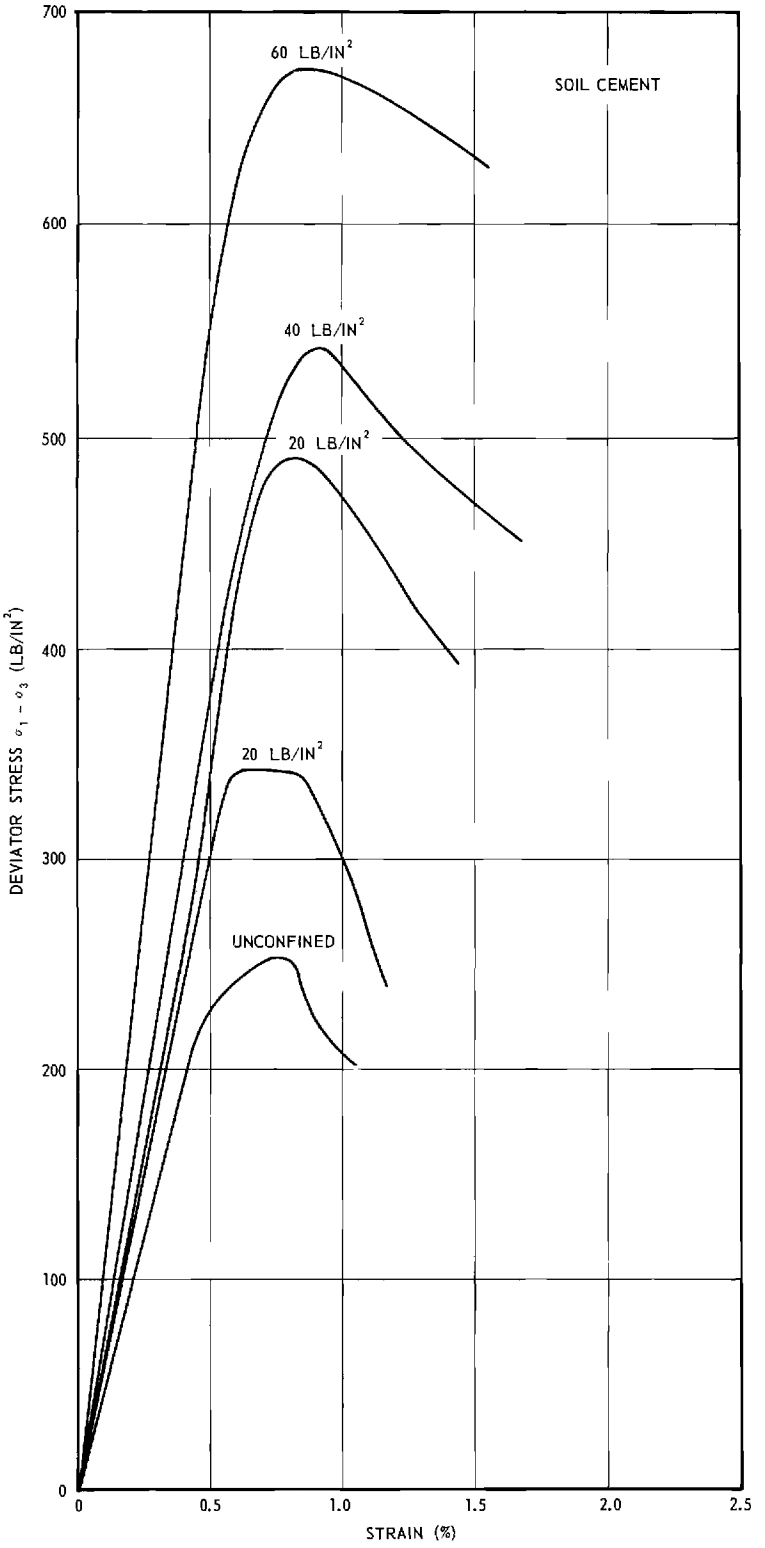

Figure 7b. Triaxial Test Results: Soil-Cement.

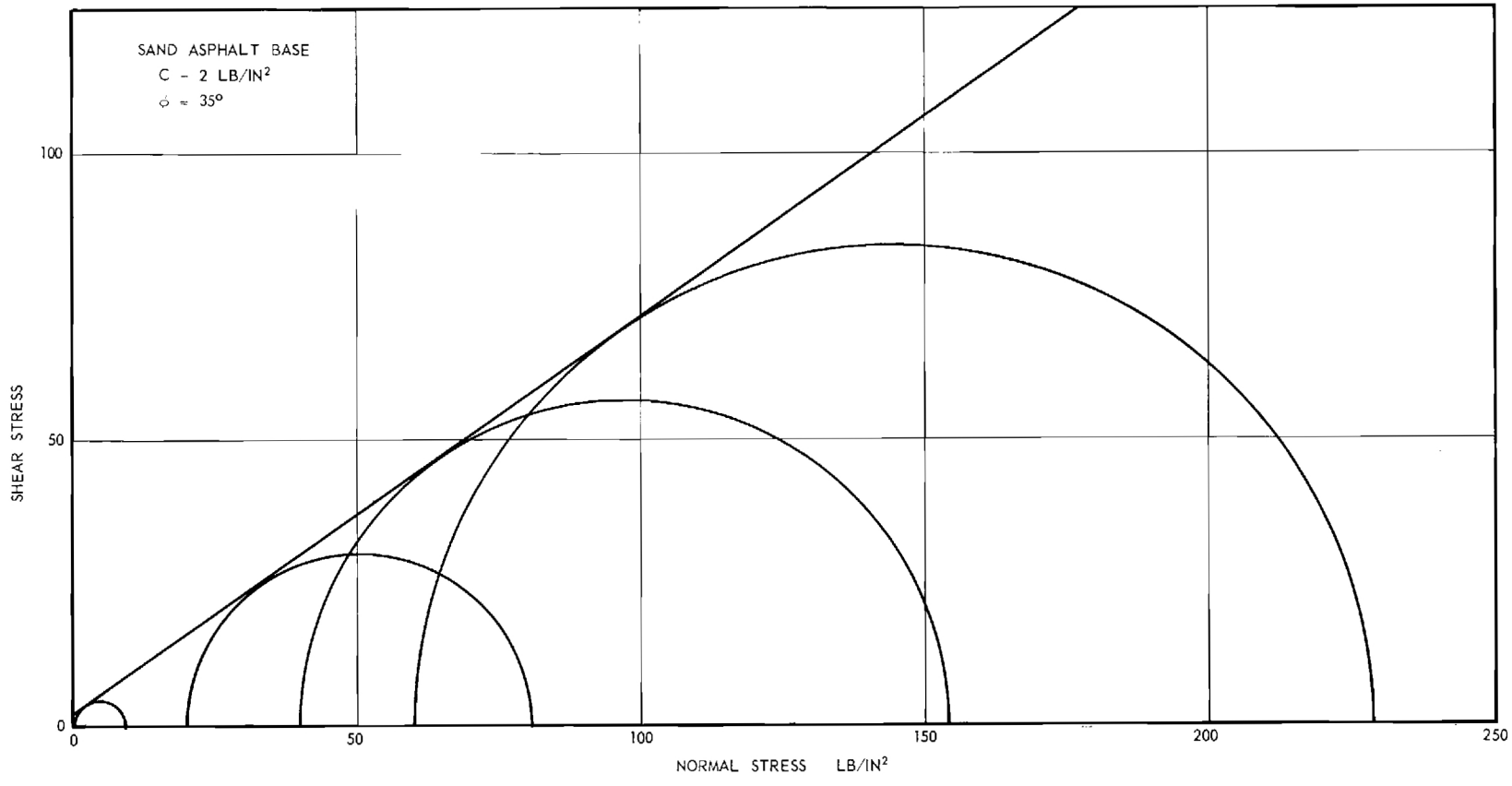

Figure 8a. Triaxial Test Results: Sand-Asphalt; Loading Rate 0.02 in./min.

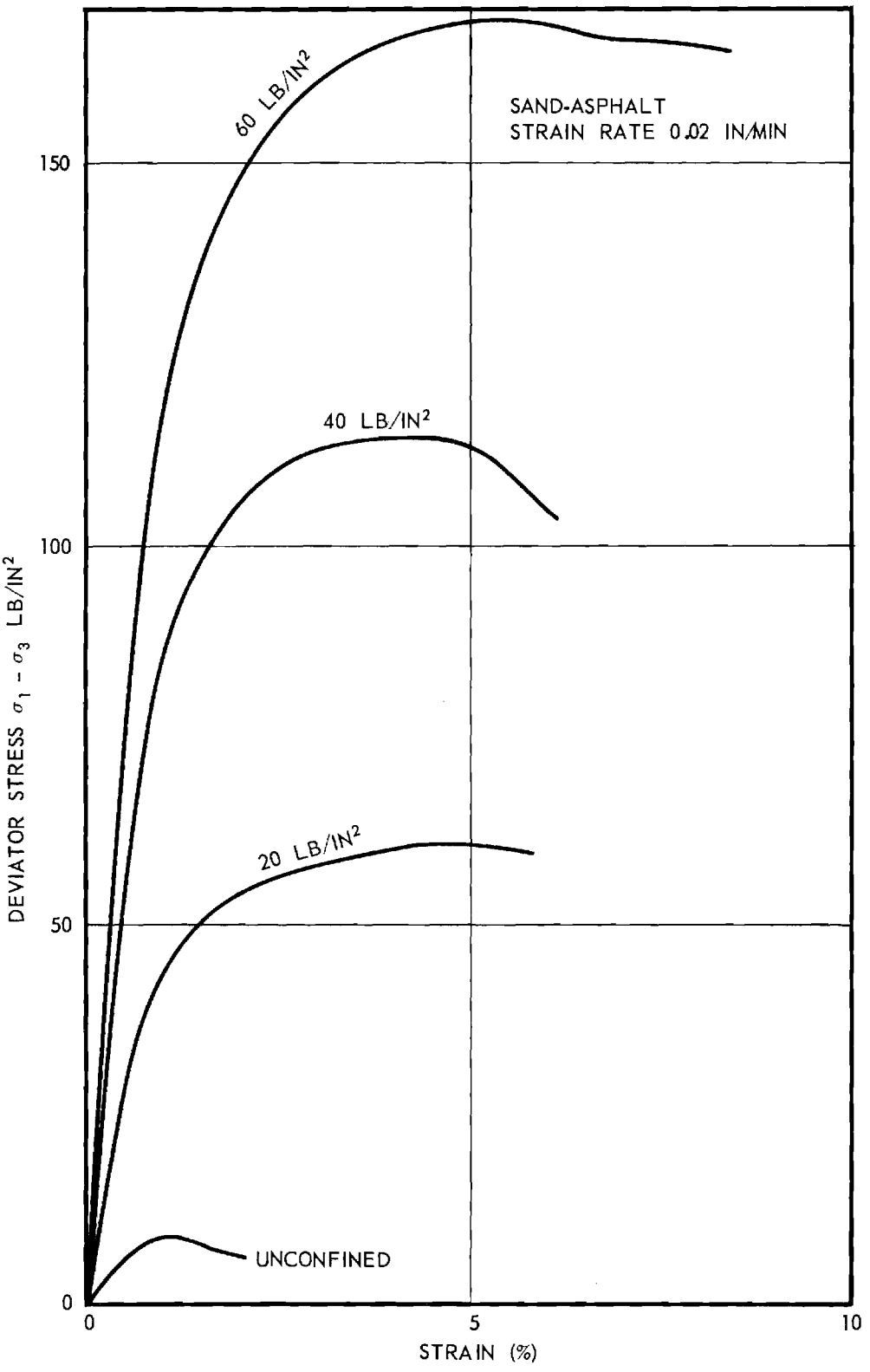

Figure 8b. Triaxial Test Results: Sand-Asphalt; Loading Rate 0.02 in./min.

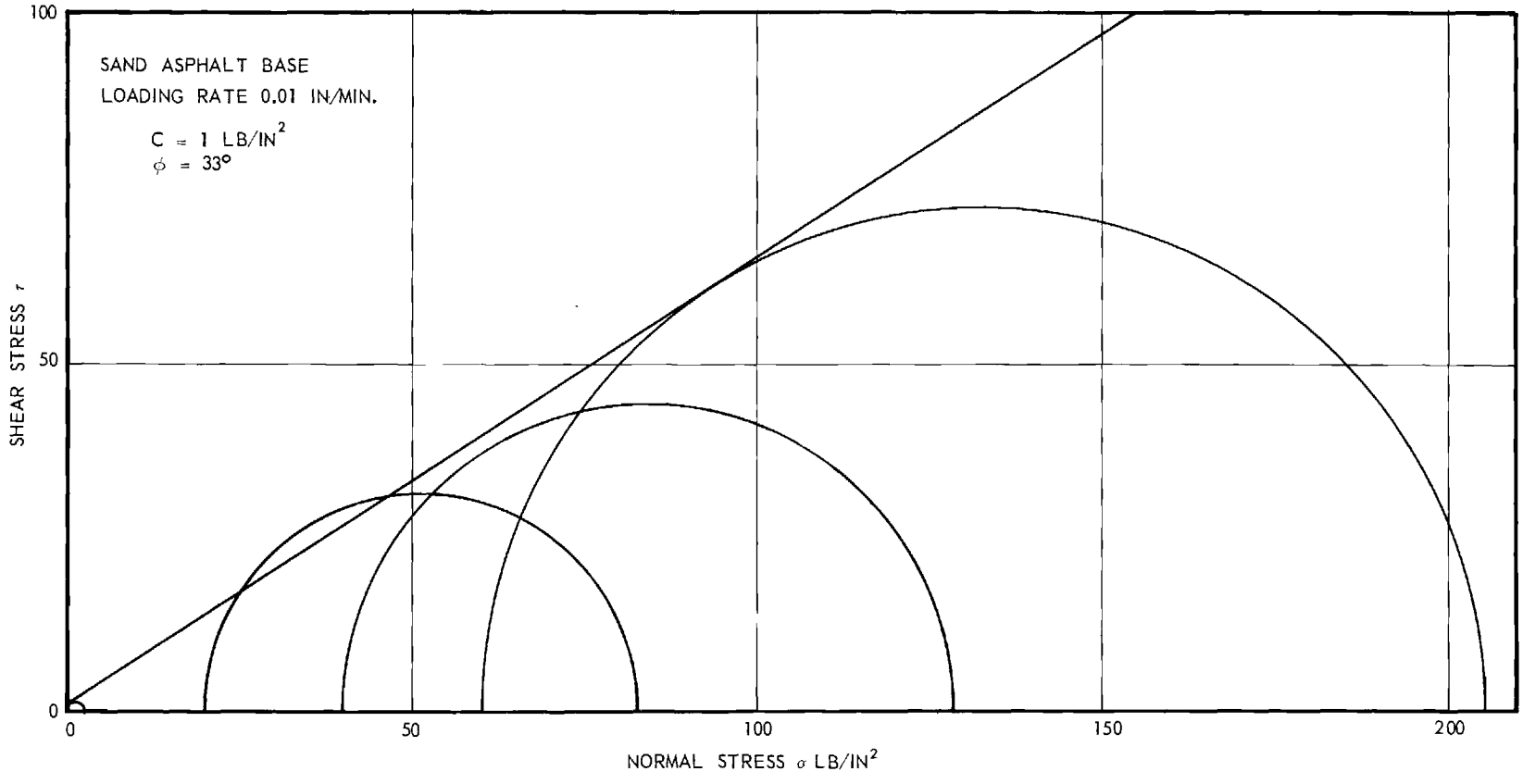

Figure 8c. Triaxial Test Results: Sand-Asphalt; Loading Rate 0.01 in./min.

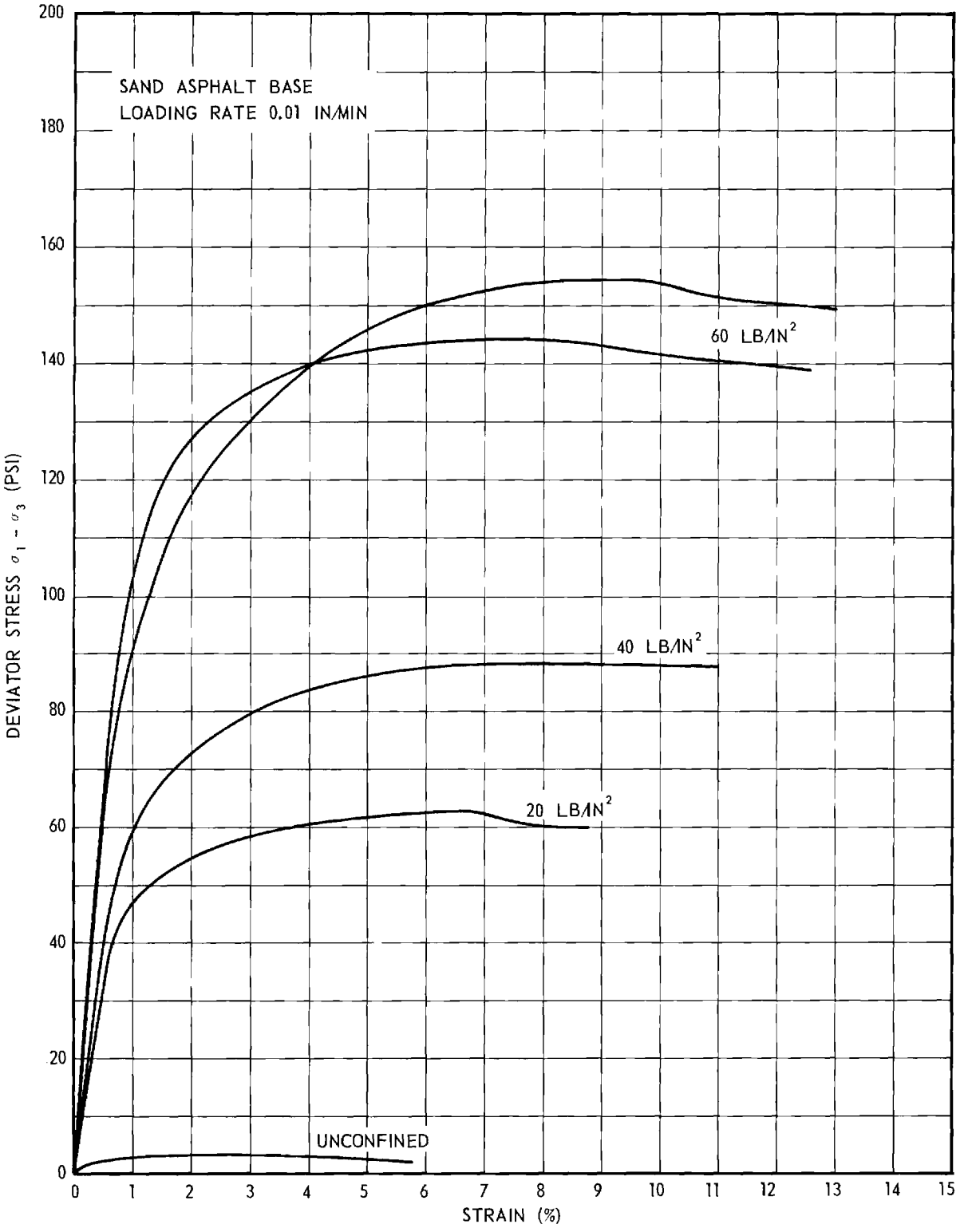

Figure 8d. Triaxial Test Results: Sand-Asphalt; Loading Rate 0.01 in./min.

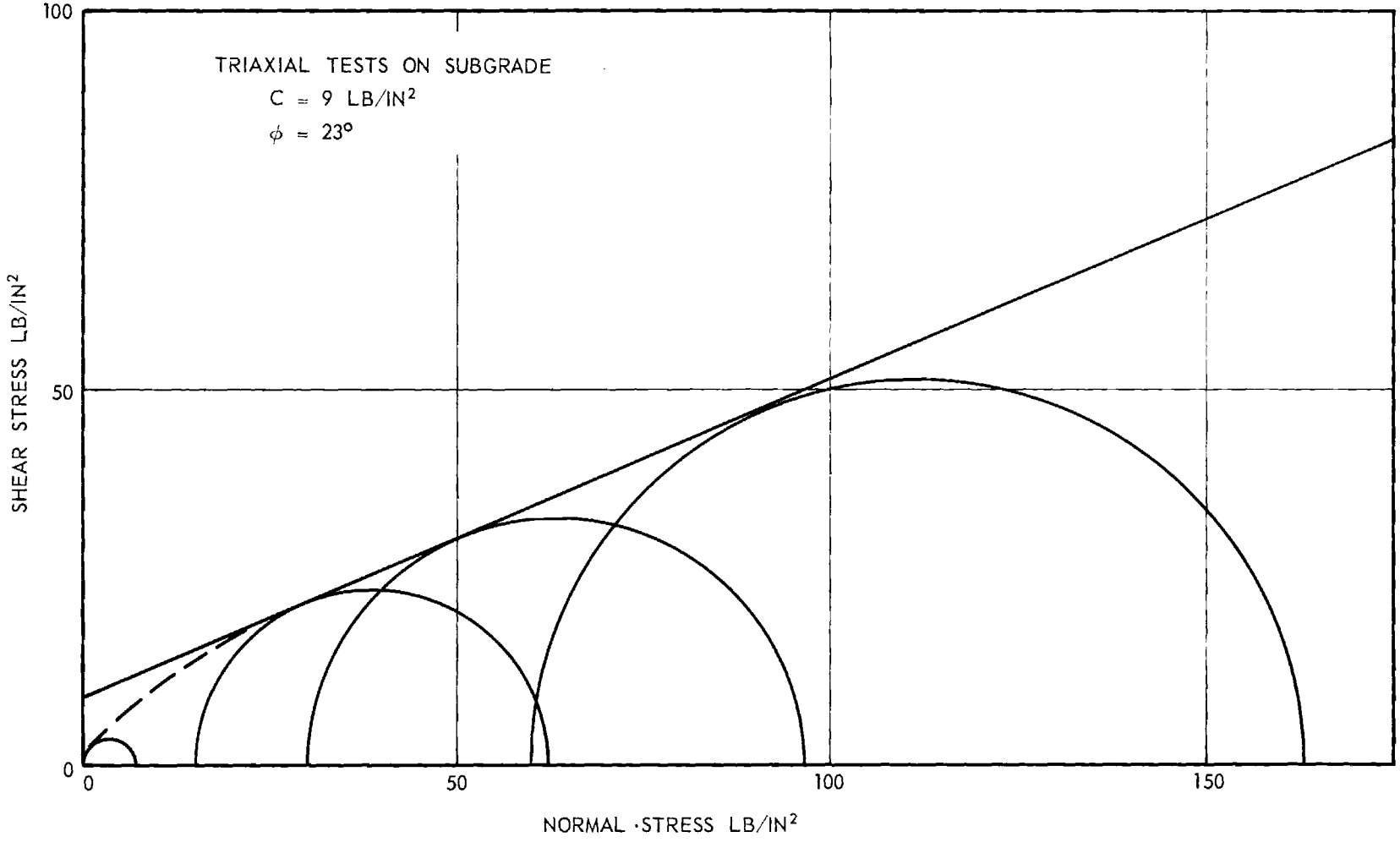

Figure 9a. Triaxial Test Results: Subgrade.

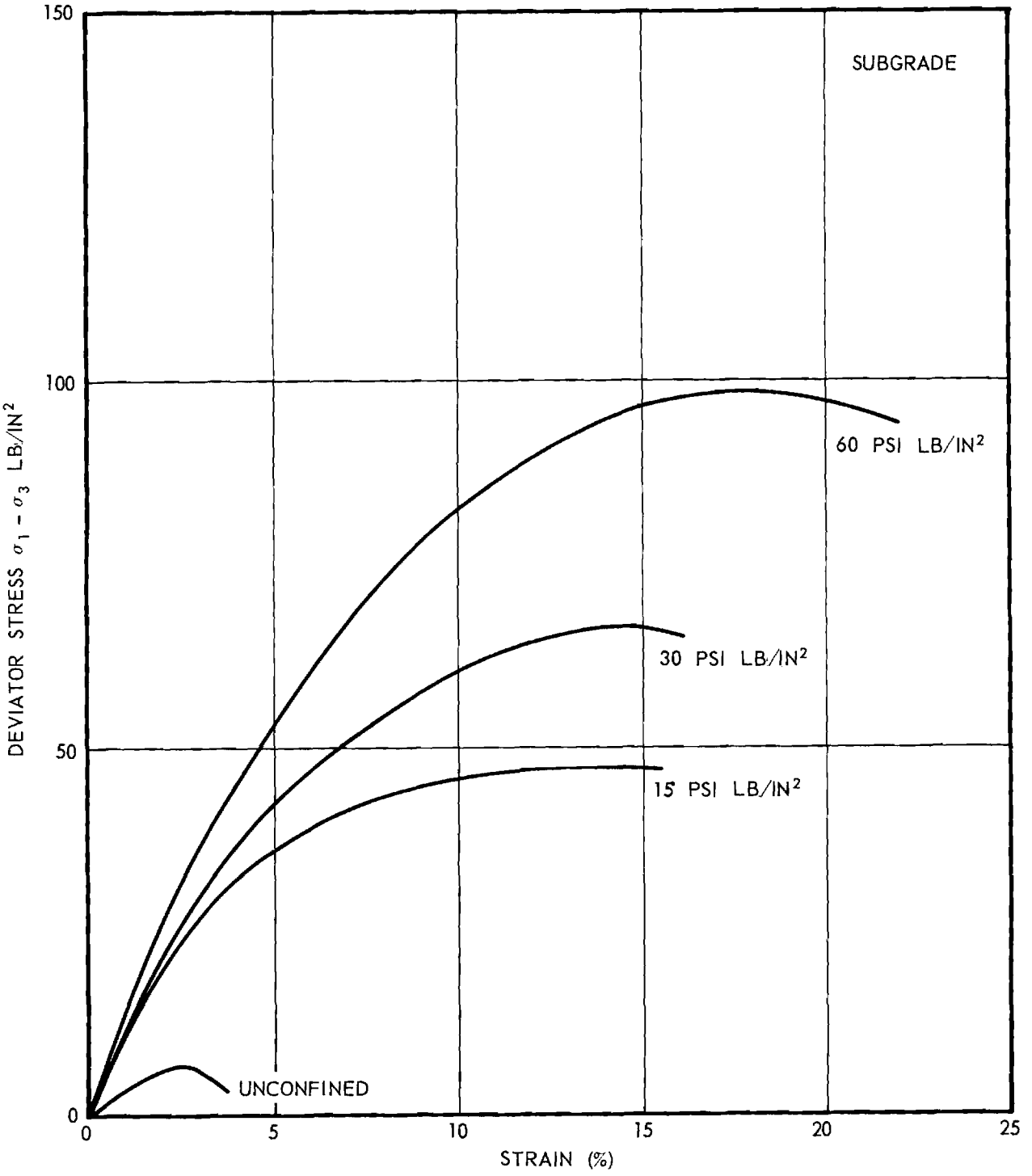

Figure 9b. Triaxial Test Results: Subgrade.

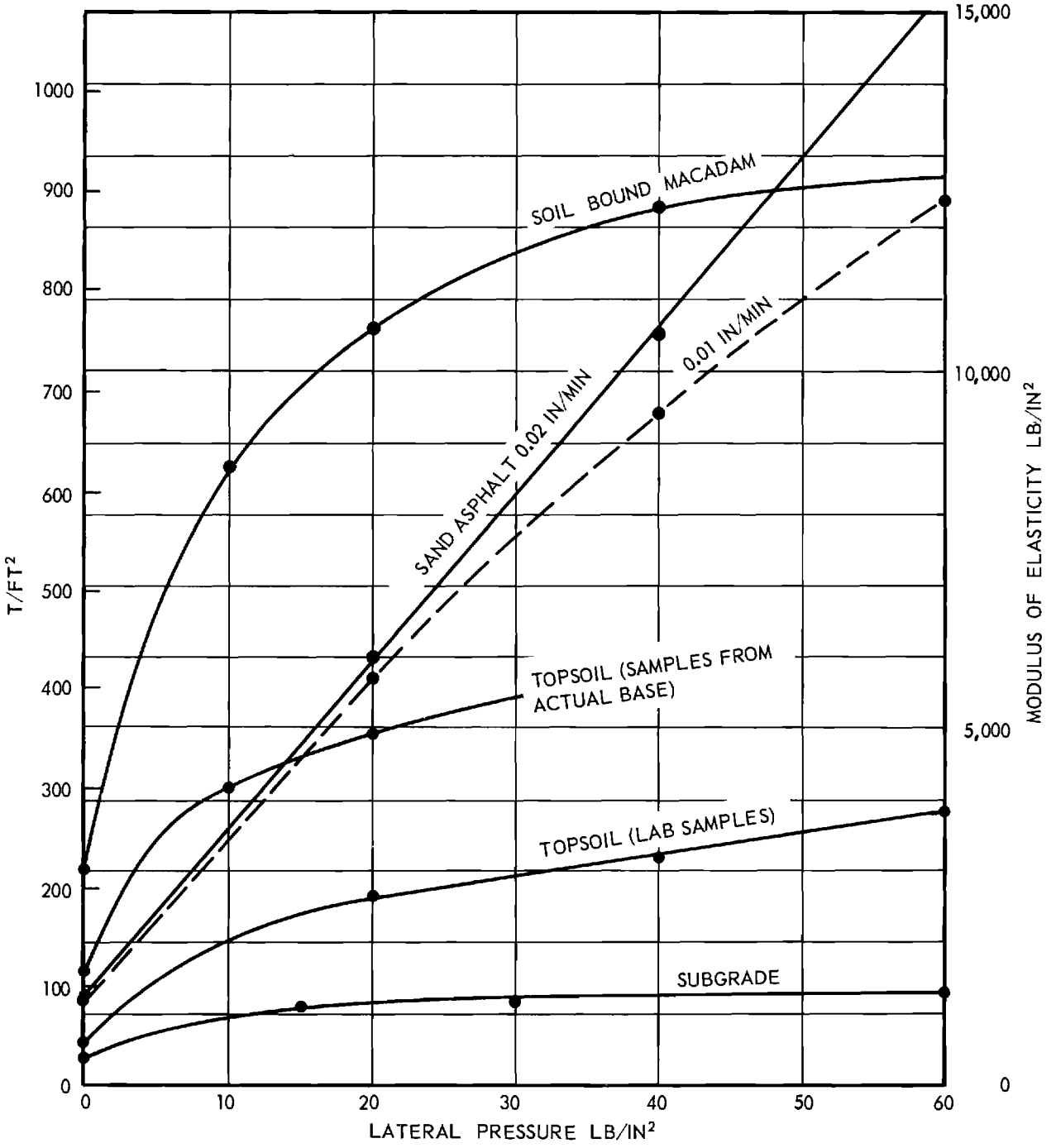

Figure 10a. Modulus of Elasticity E of Base and Subgrade Material, Obtained by Triaxial Tests at Different Lateral Confining Pressures.

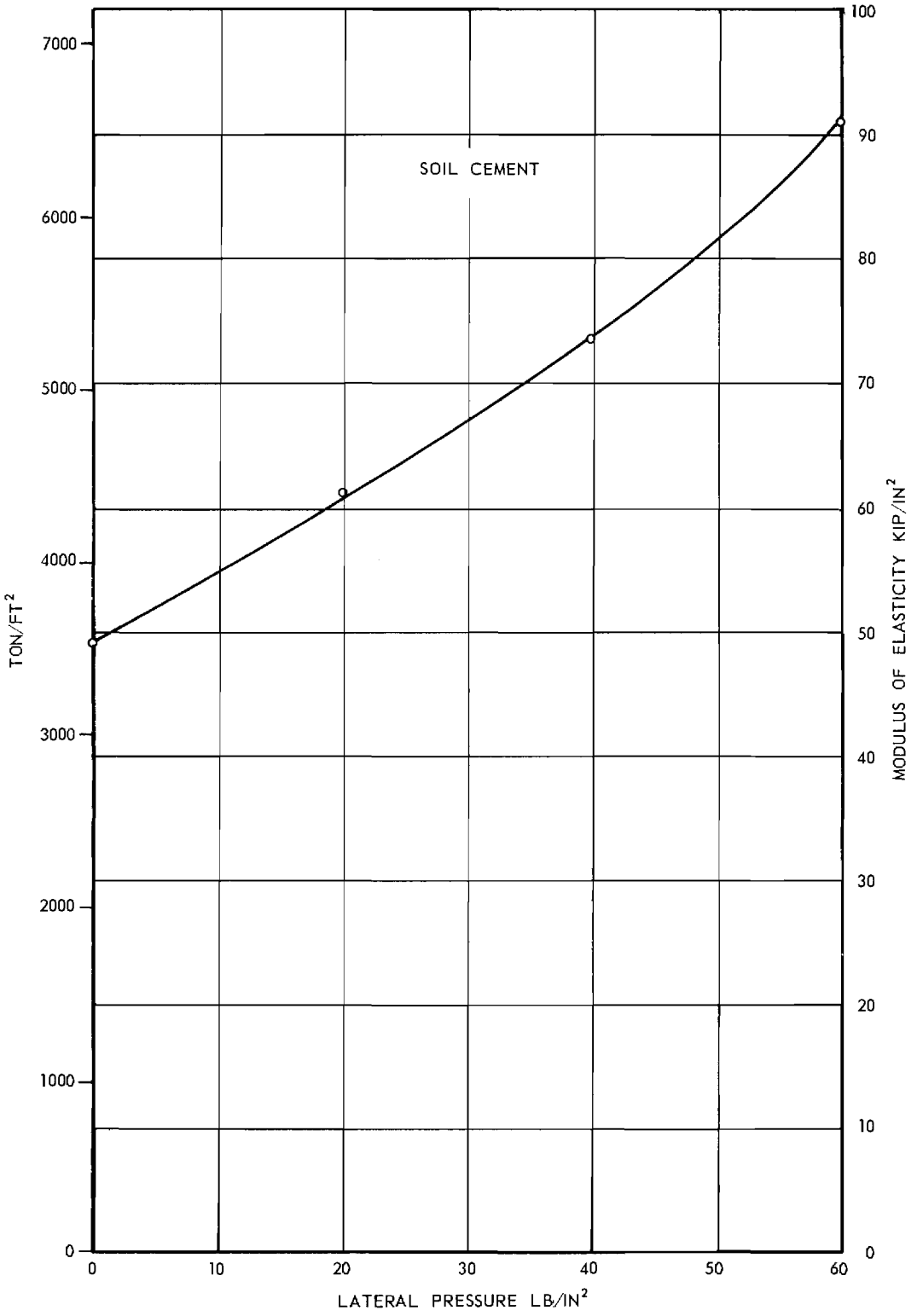

Figure 10b. Modulus of Elasticity E of Base and Subgrade Material, Obtained by Triaxial Tests at Different Lateral Confining Pressures.

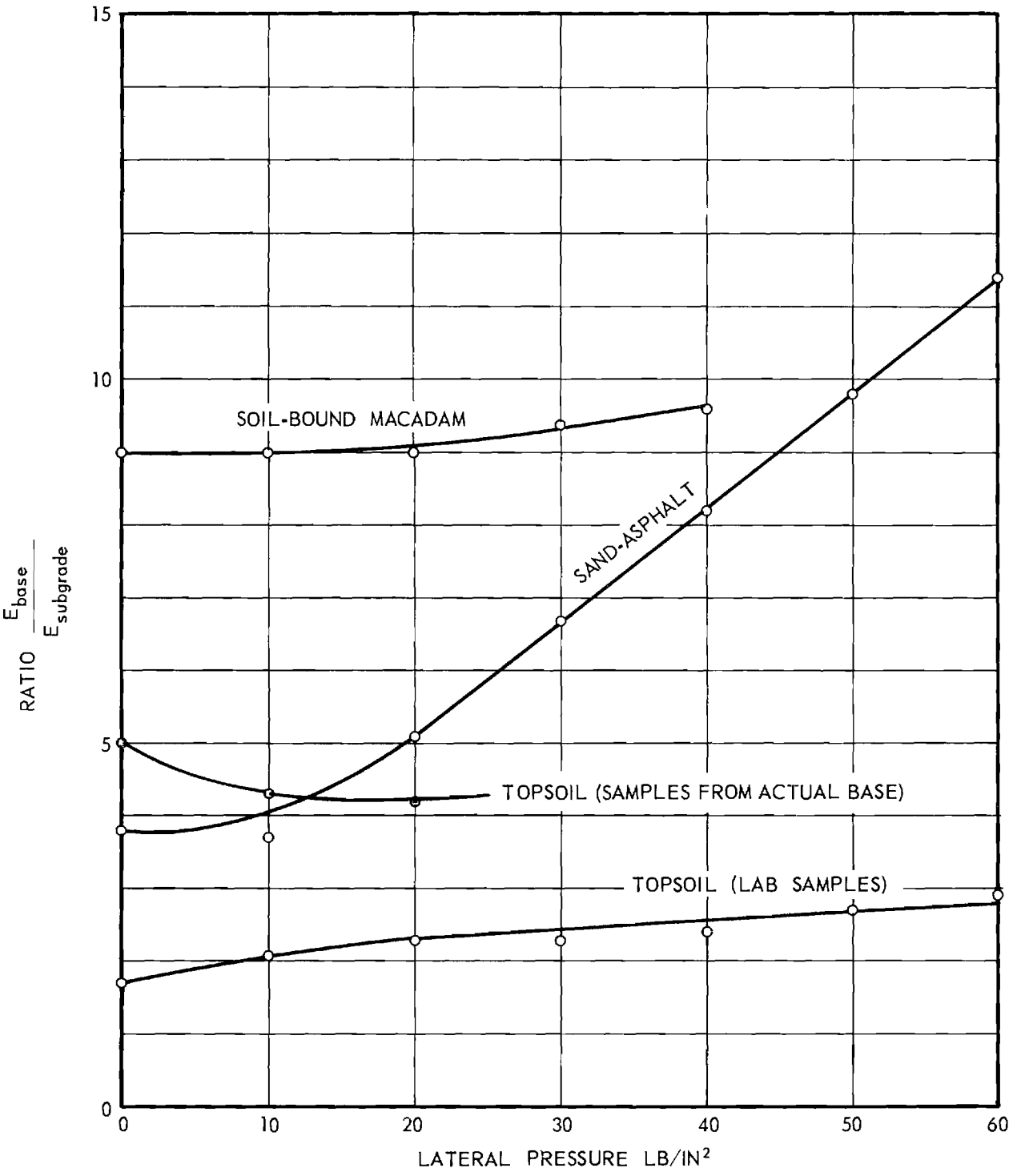

Figure 11a. Ratio of Moduli E of Base and Subgrade Materials at Different Lateral Confining Pressures.

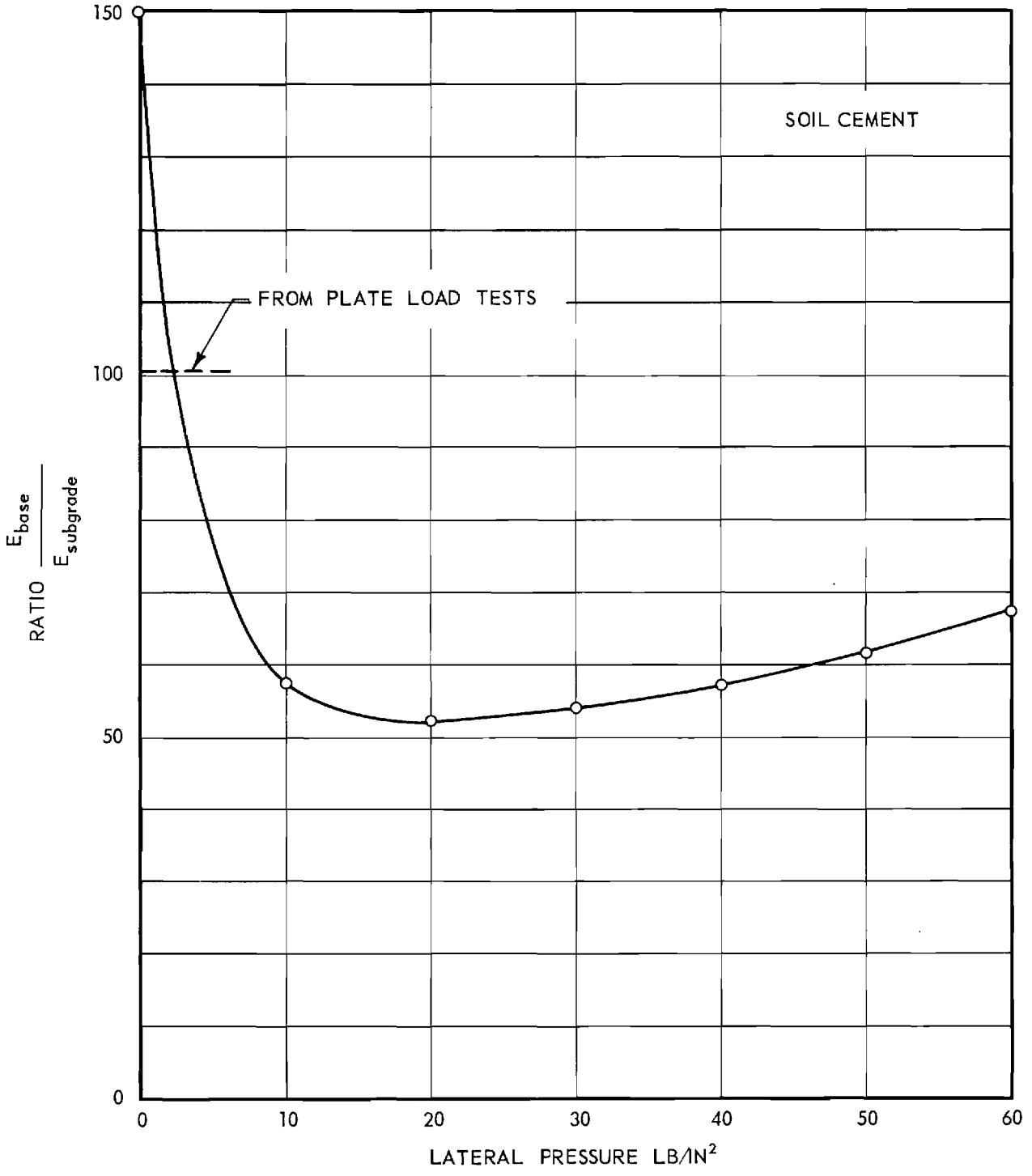

Figure 11b. Ratio of Moduli E of Base and Subgrade Materials at Different Lateral Confining Pressures.

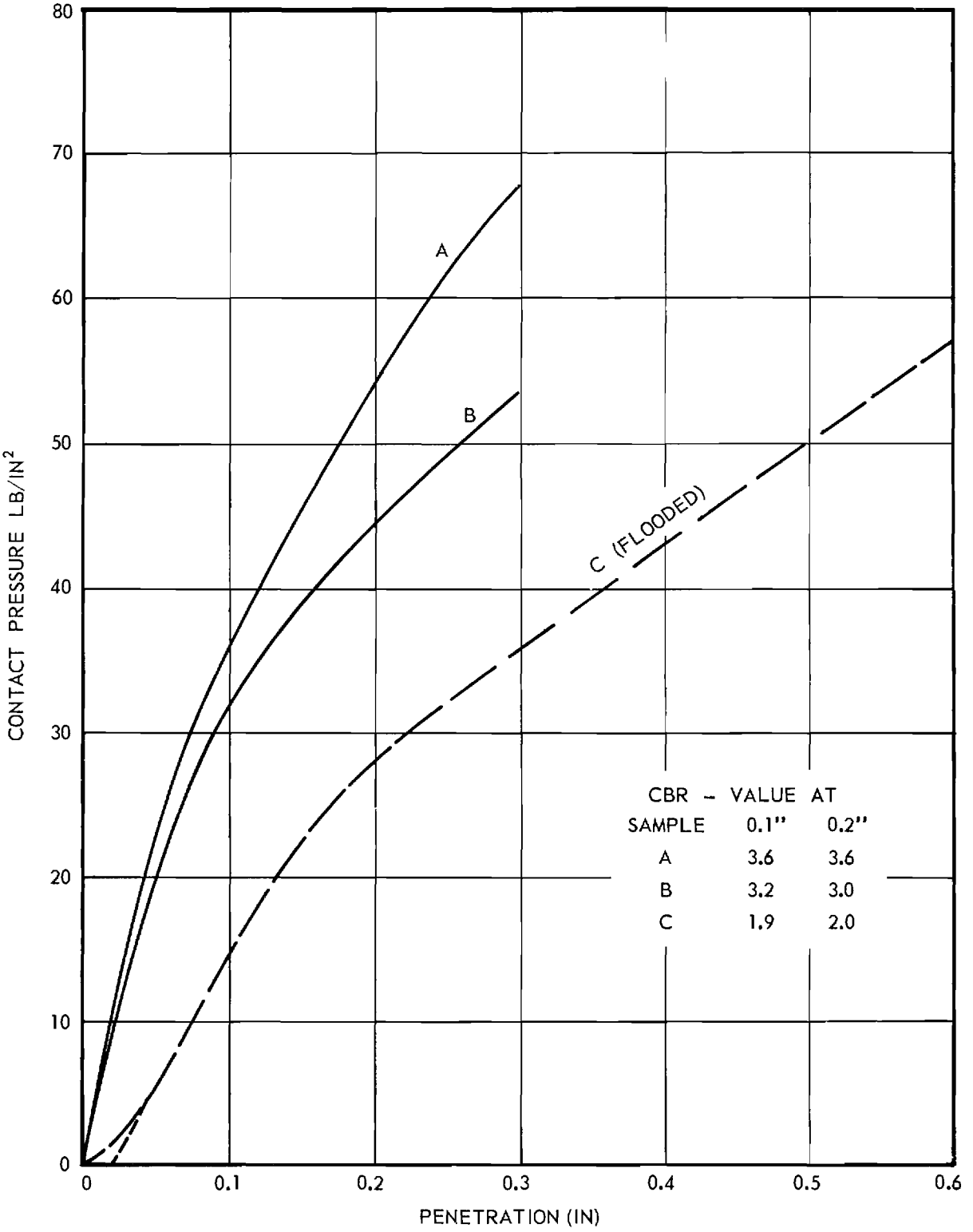

Figure 12. CBR-Test Results: Subgrade.

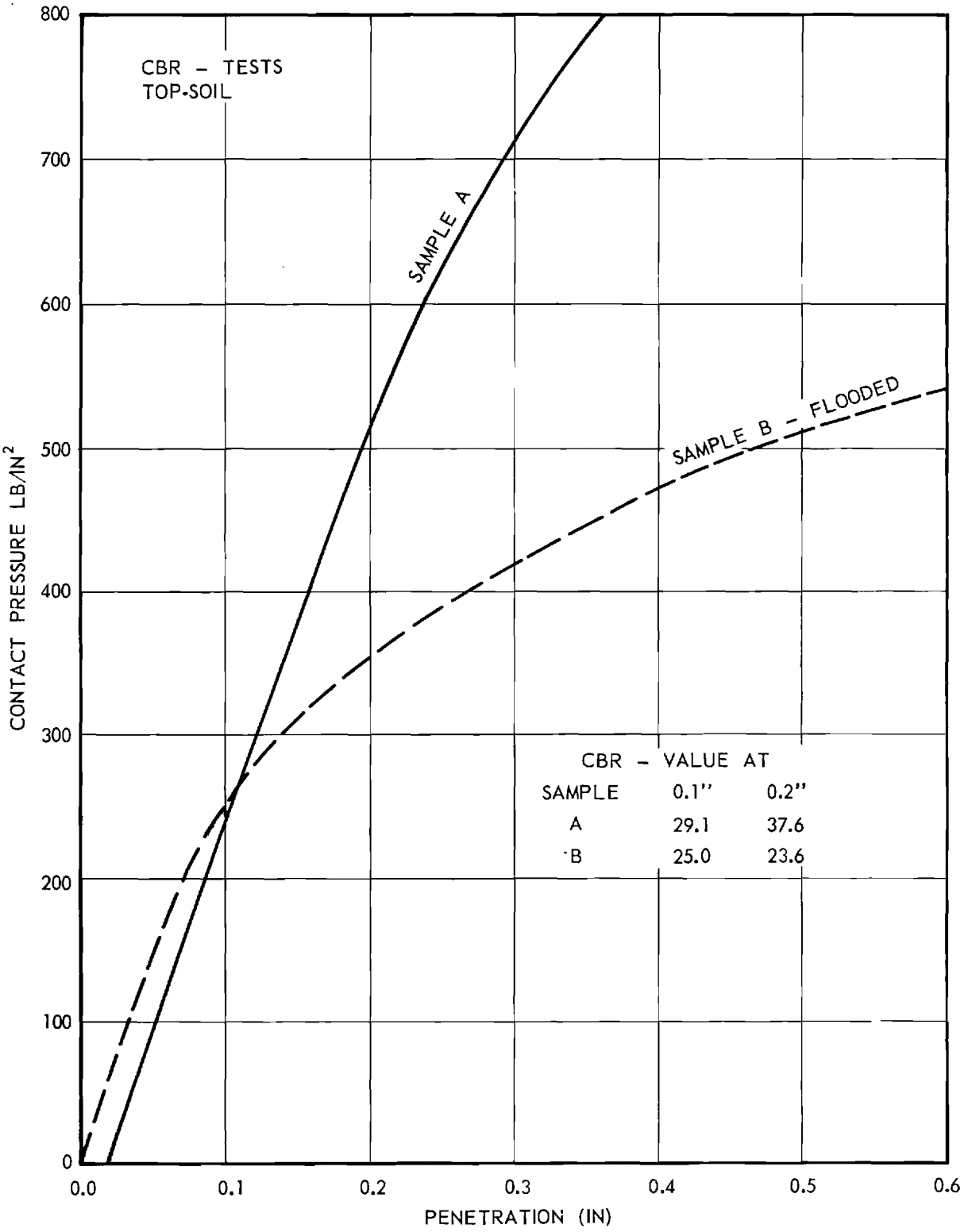

Figure 13. CBR-Test Results: Topsoil.

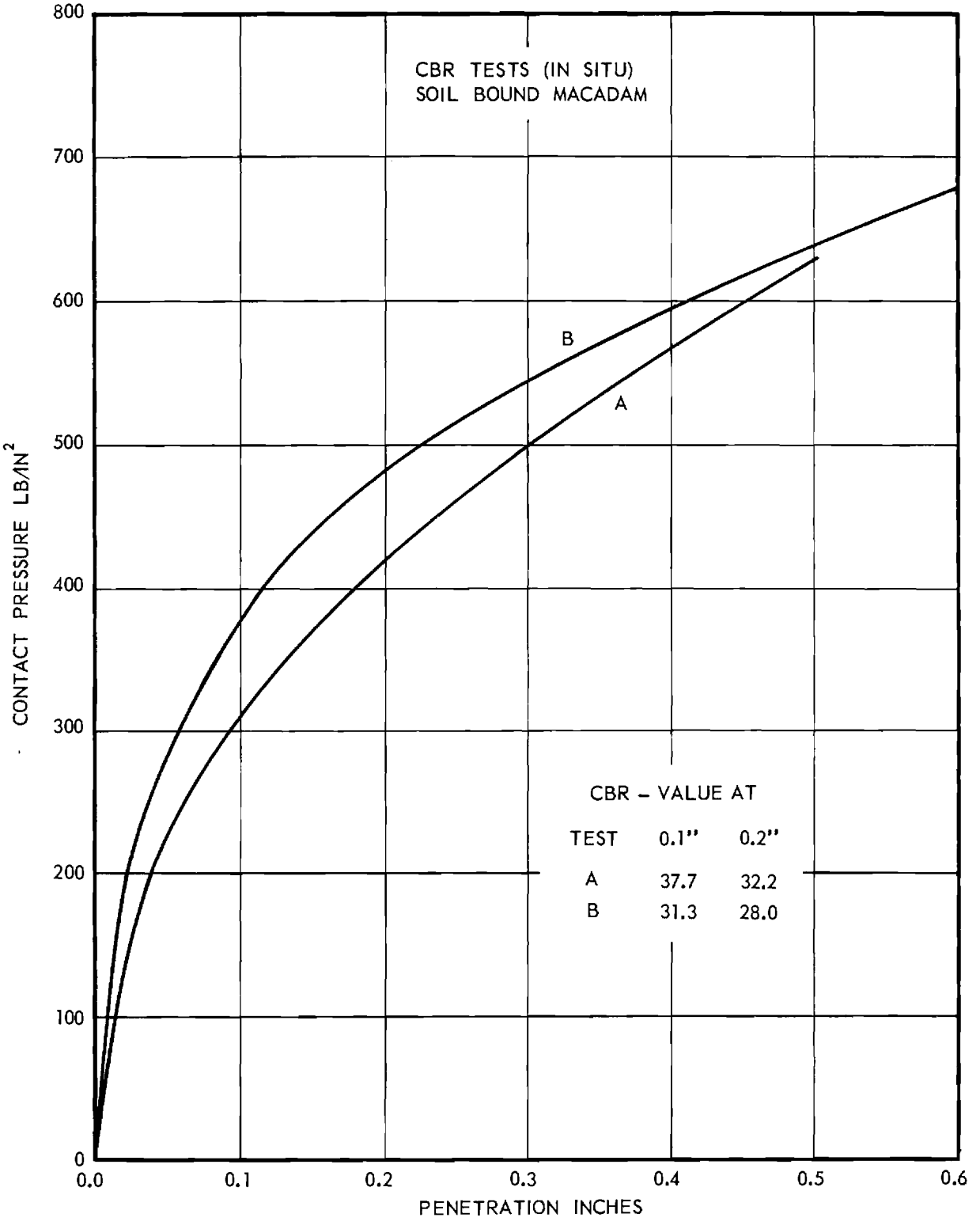

Figure 14. CBR-Test Results: Soil-Bound Macadam.

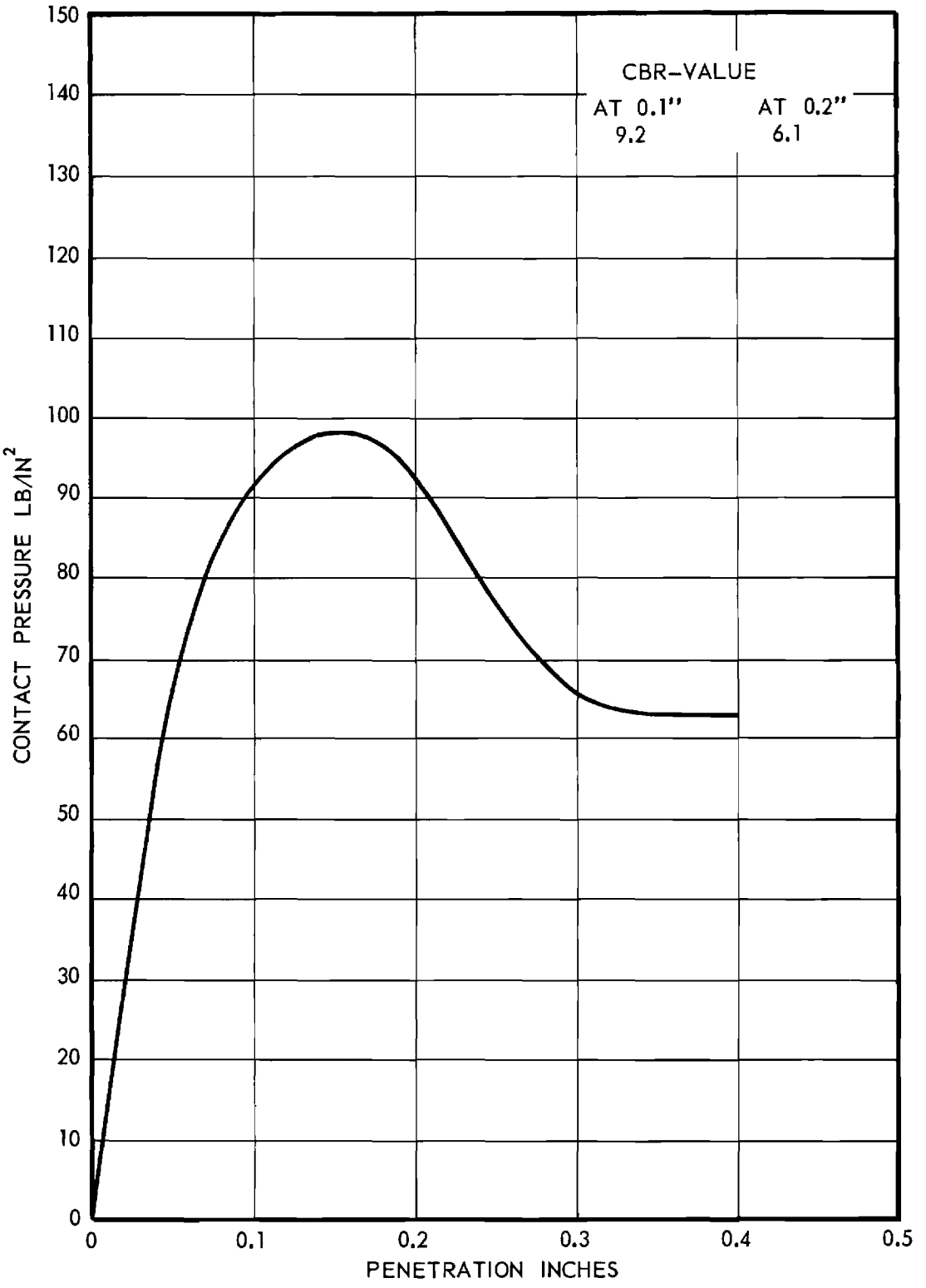

Figure 15. CBR-Test Results: Sand-Asphalt.

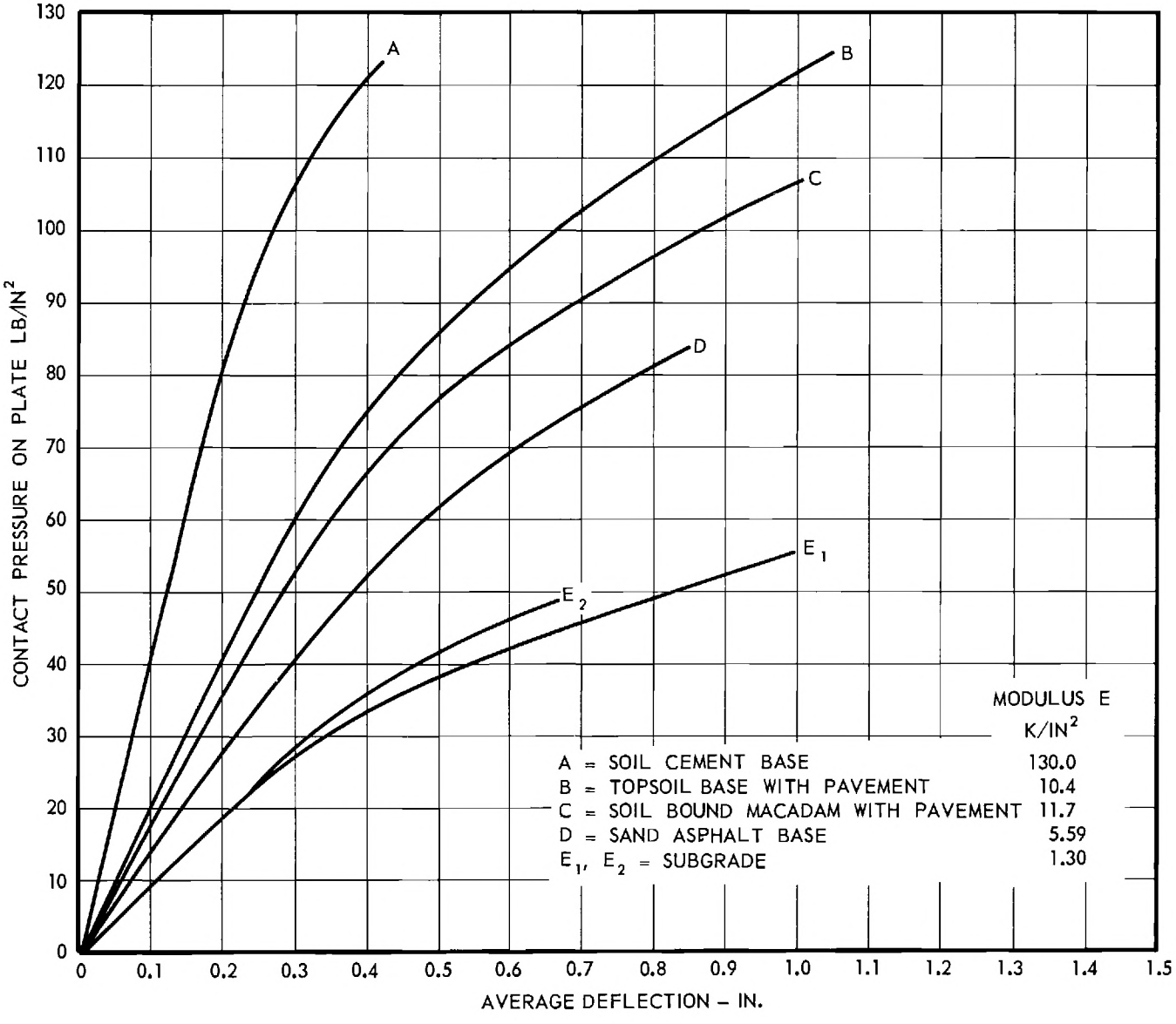

Figure 16. Plate Load Test Results.

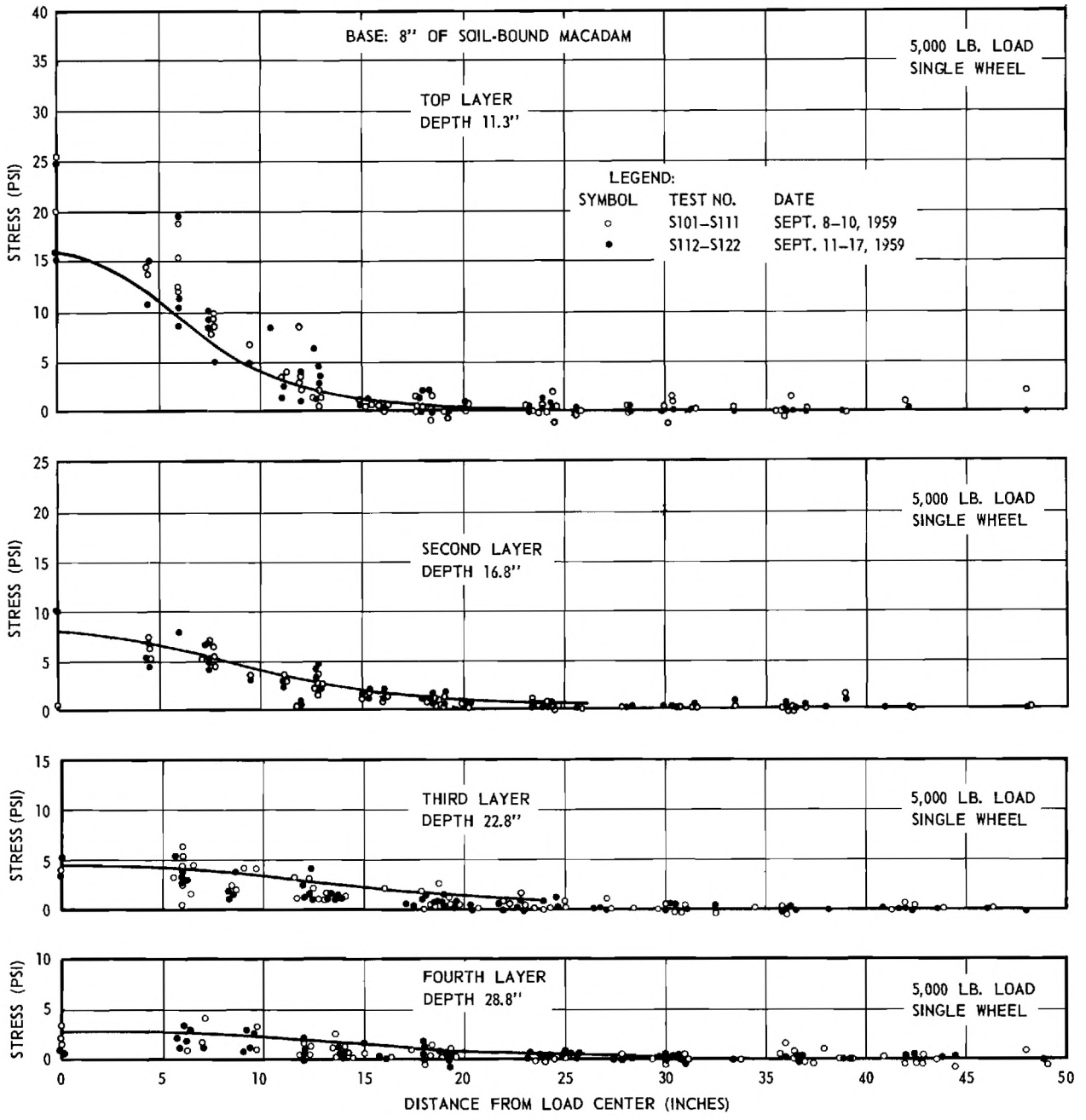

Figure 17. Measured Stresses: Single Load 5,000-lb Soil-Bound Macadam Base.

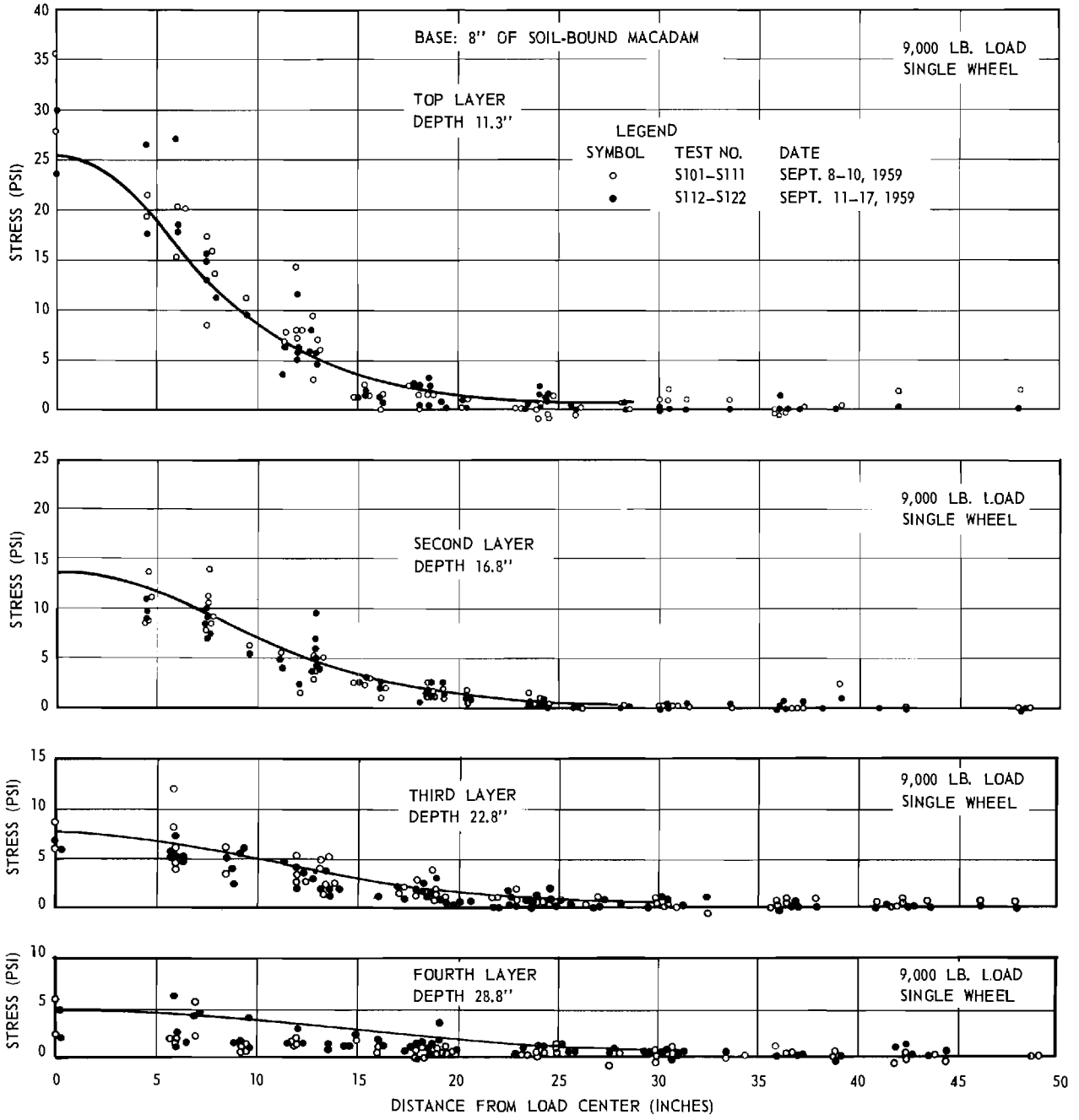

Figure 18. Measured Stresses: Single Load 9,000-lb Soil-Bound Macadam Base.

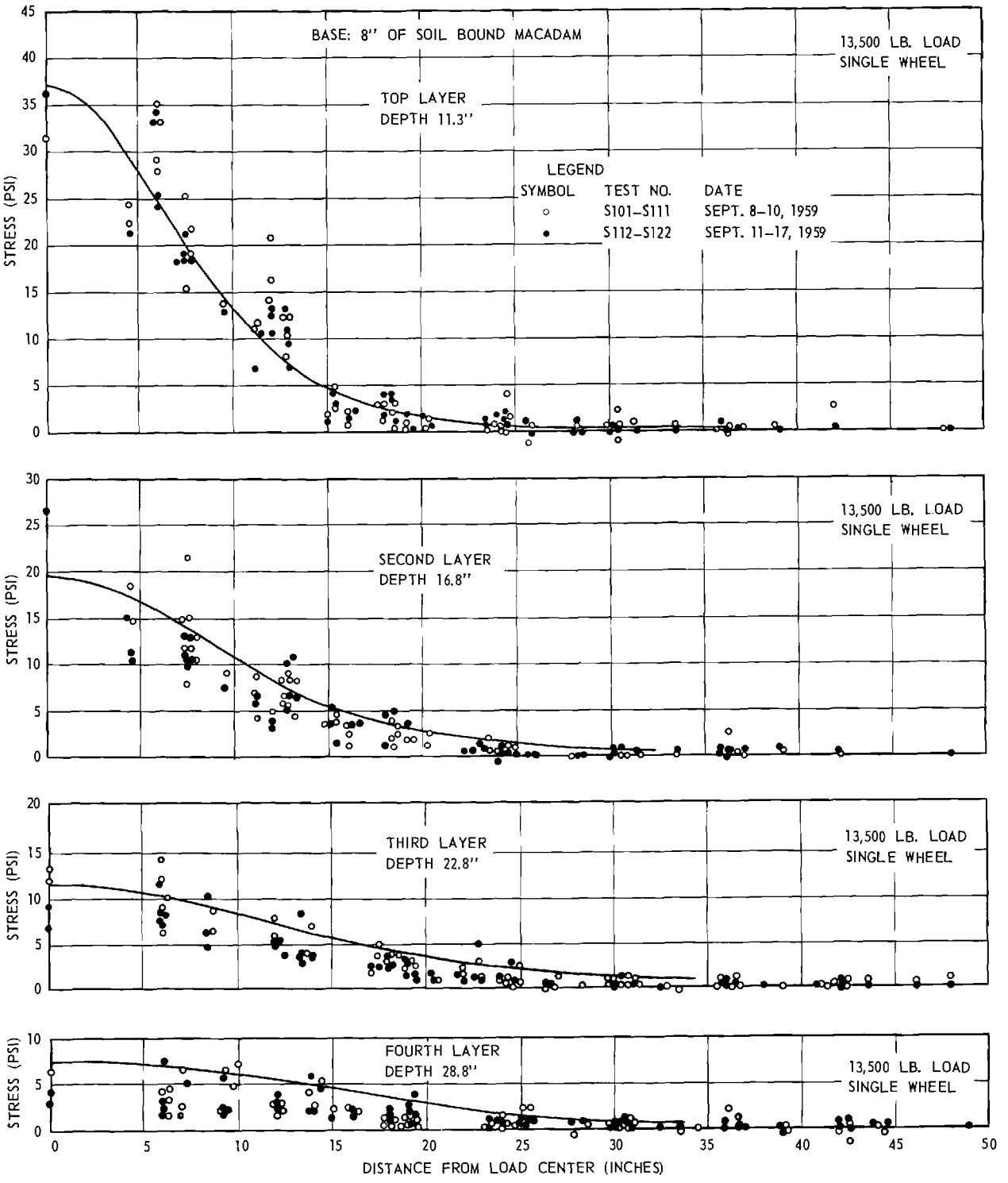

Figure 19. Measured Stresses: Single Load 13,500-lb Soil-Bound Macadam Base.

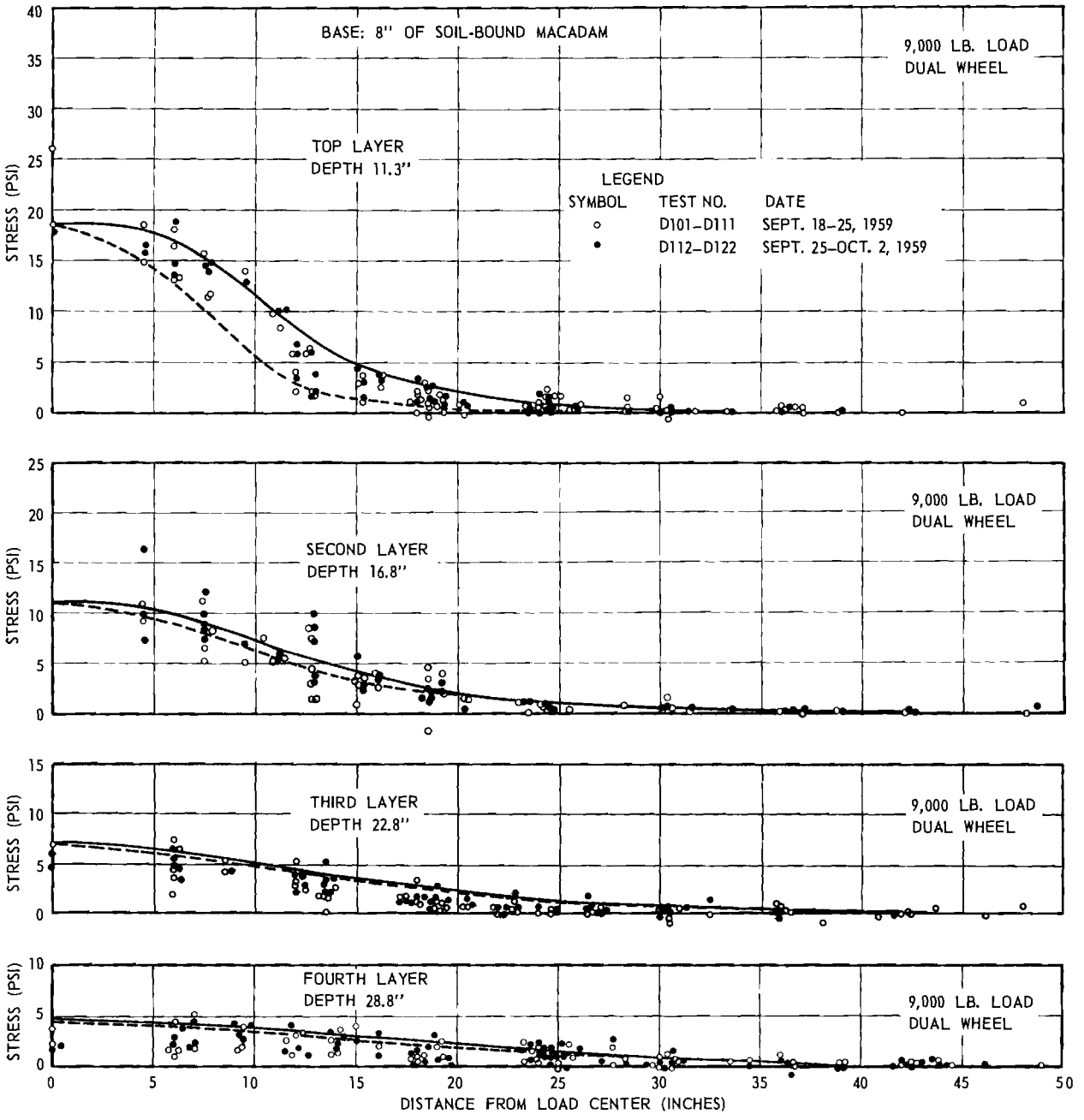

Figure 20. Measured Stresses: Dual Load 9,000-lb Soil-Bound Macadam Base.

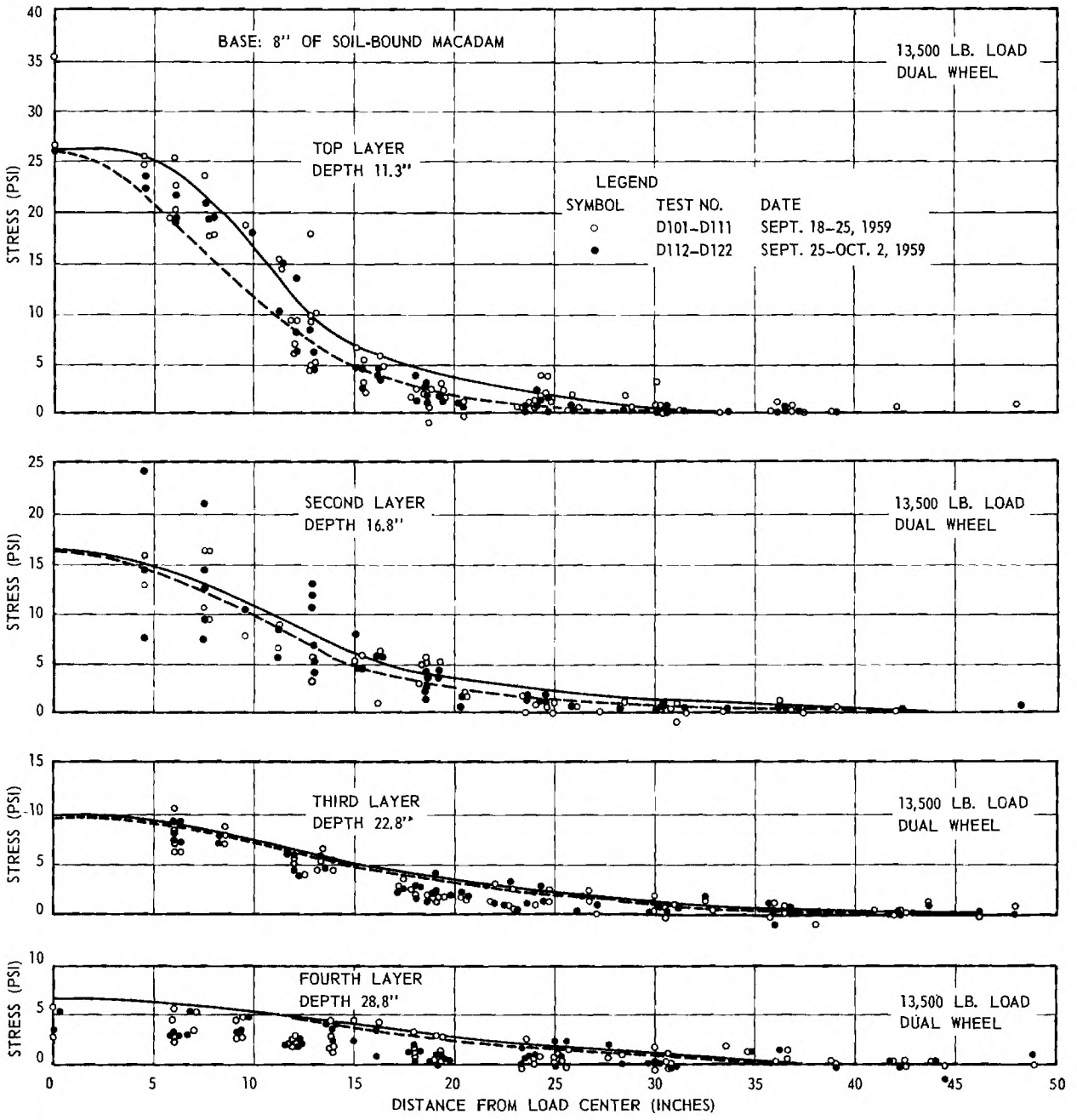

Figure 21. Measured Stresses: Dual Load 13,500-lb Soil-Bound Macadam Base.

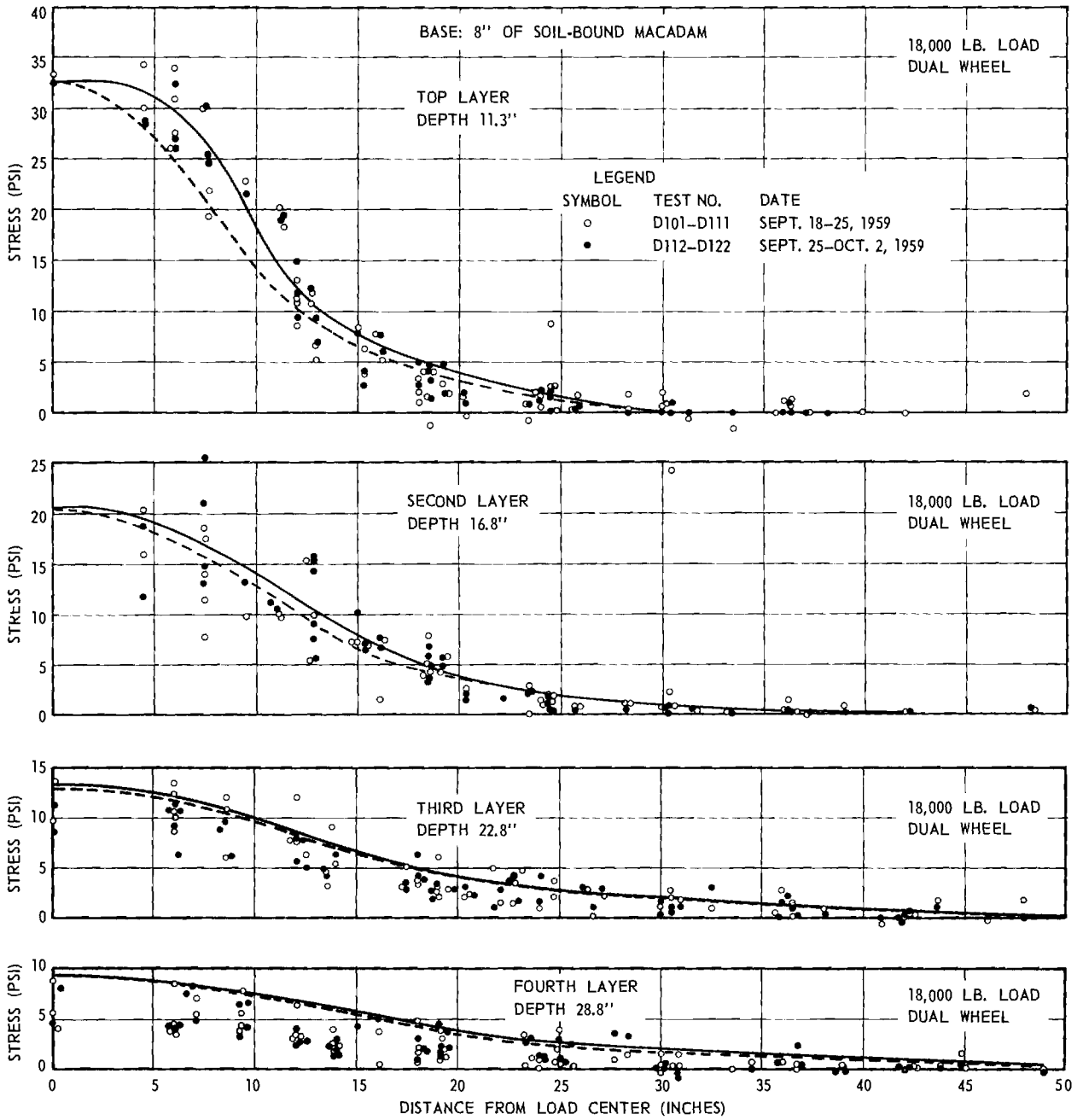

Figure 22. Measured Stresses: Dual Load 18,000-lb Soil-Bound Macadam Base.

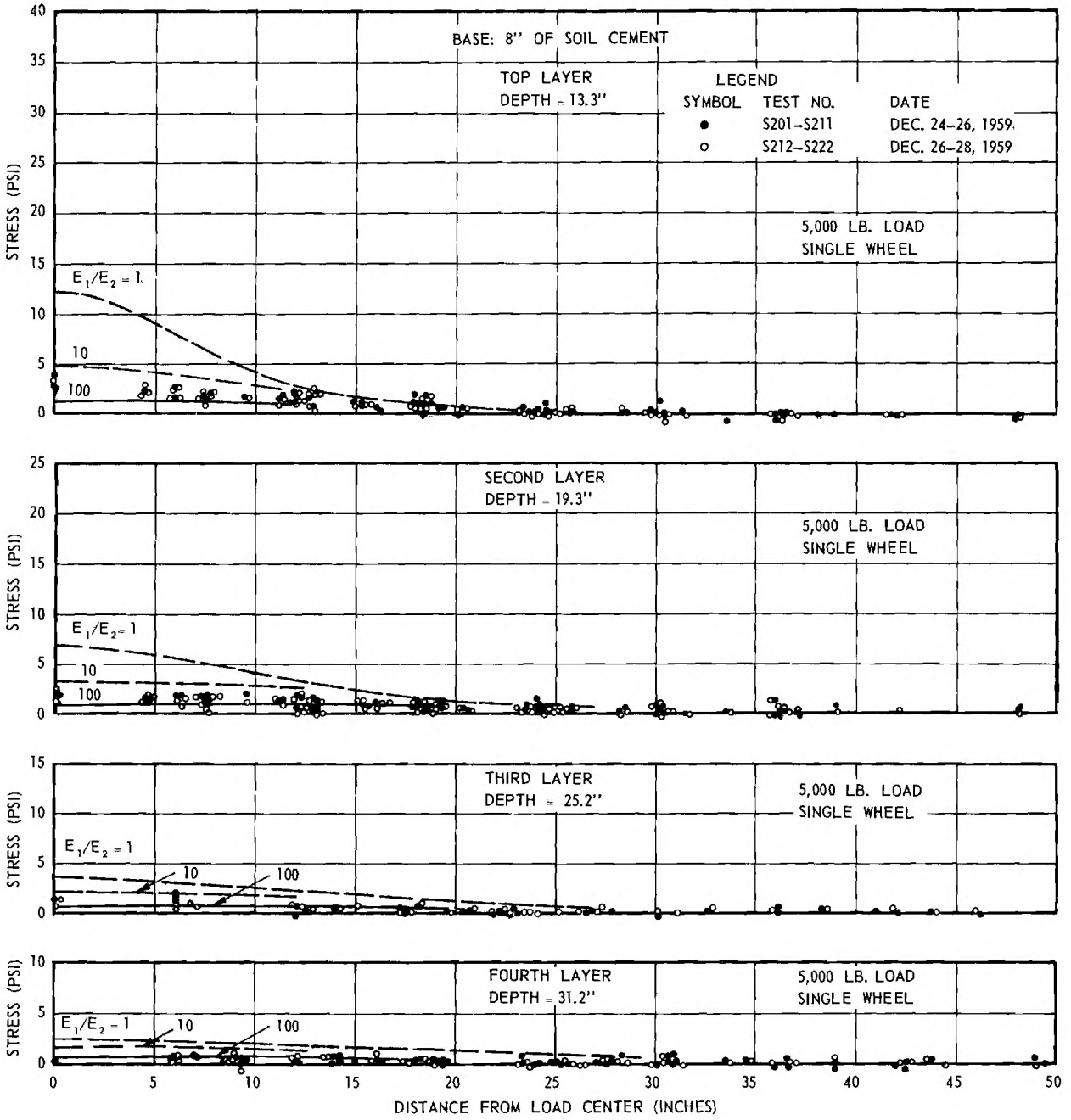

Figure 23. Measured Stresses: Single Load 5,000-lb Soil-Cement Base.

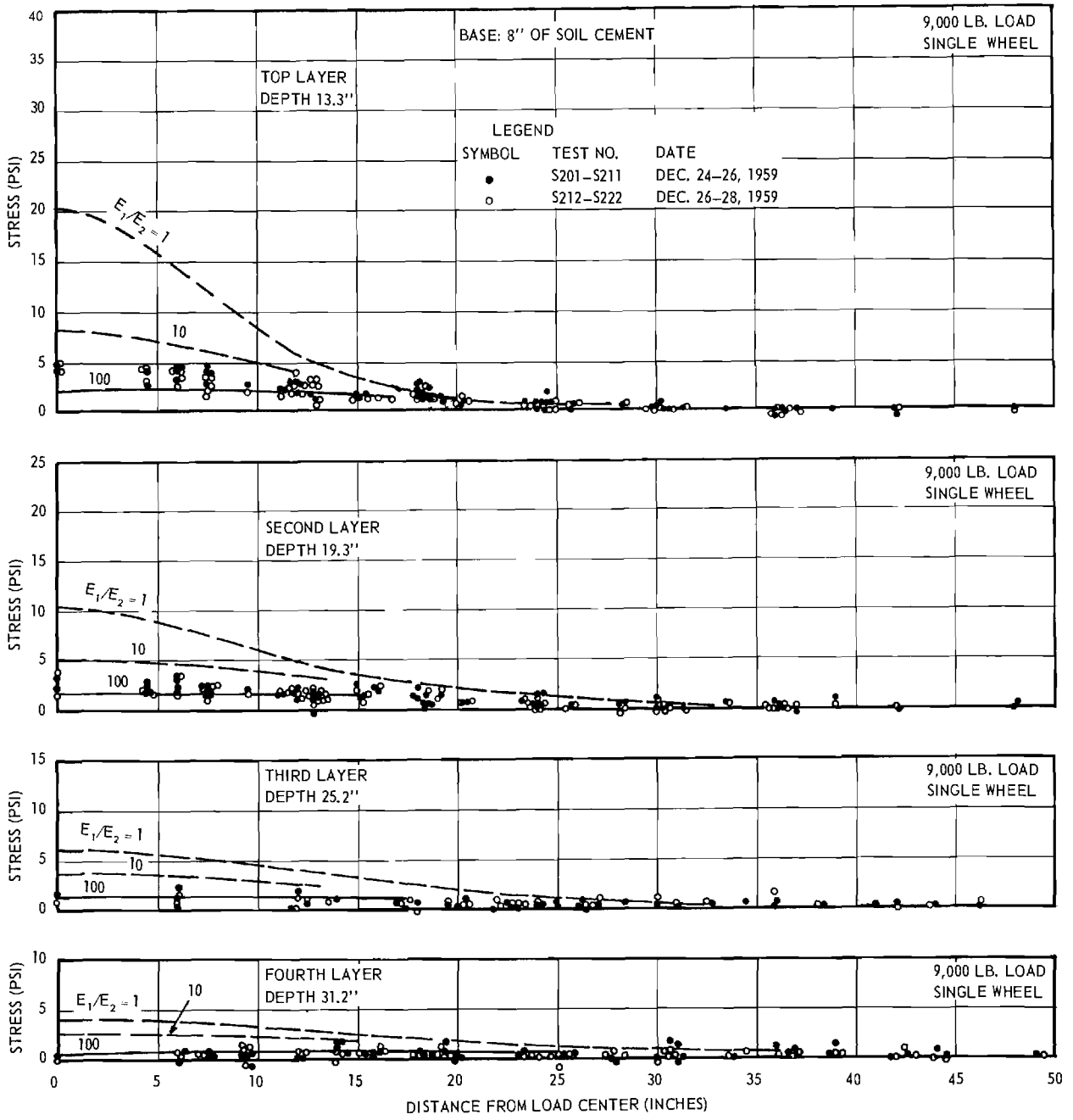

Figure 24. Measured Stresses: Single Load 9,000-lb Soil-Cement Base.

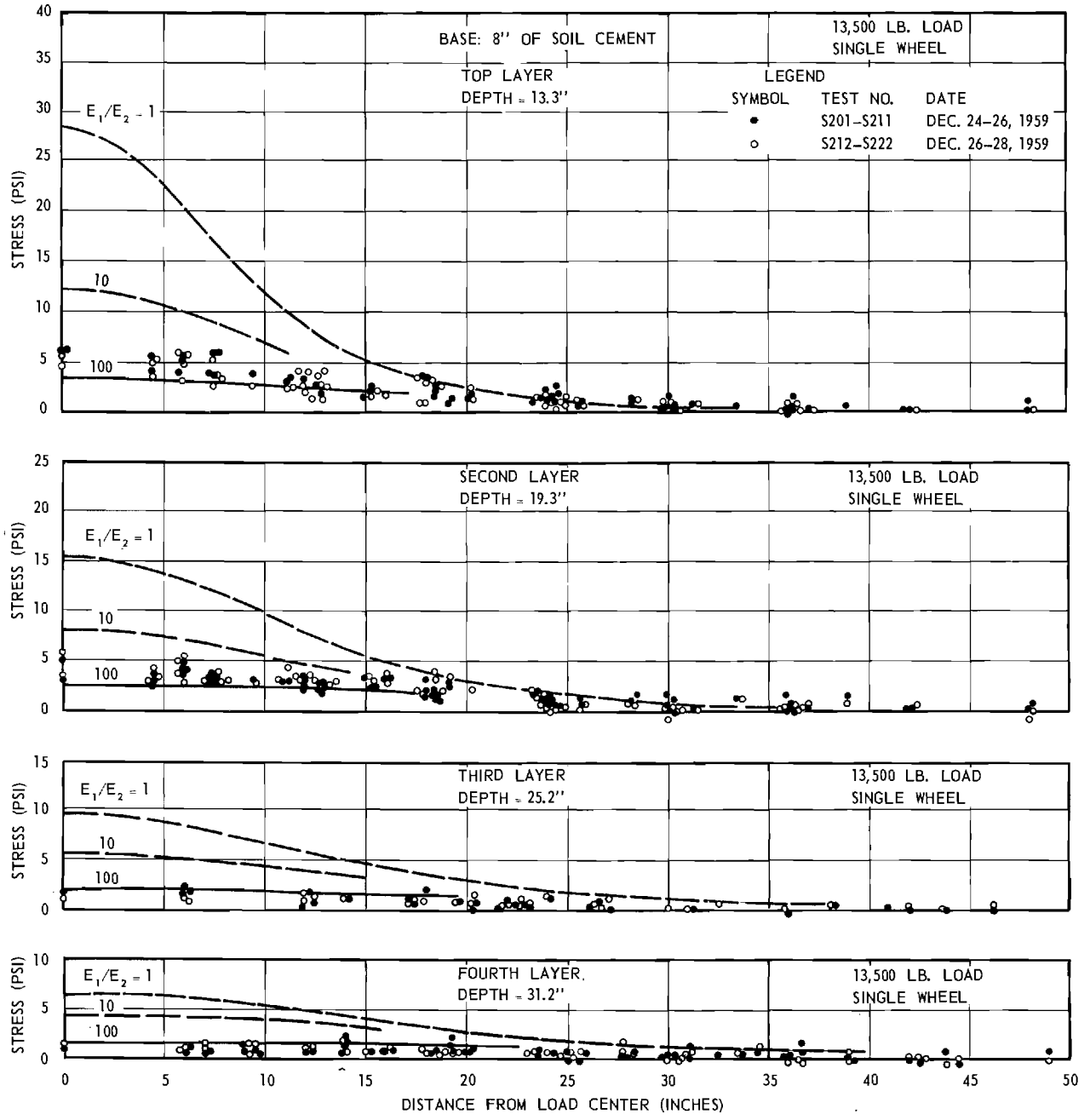

Figure 25. Measured Stresses: Single Load 13,500-lb Soil-Cement Base.

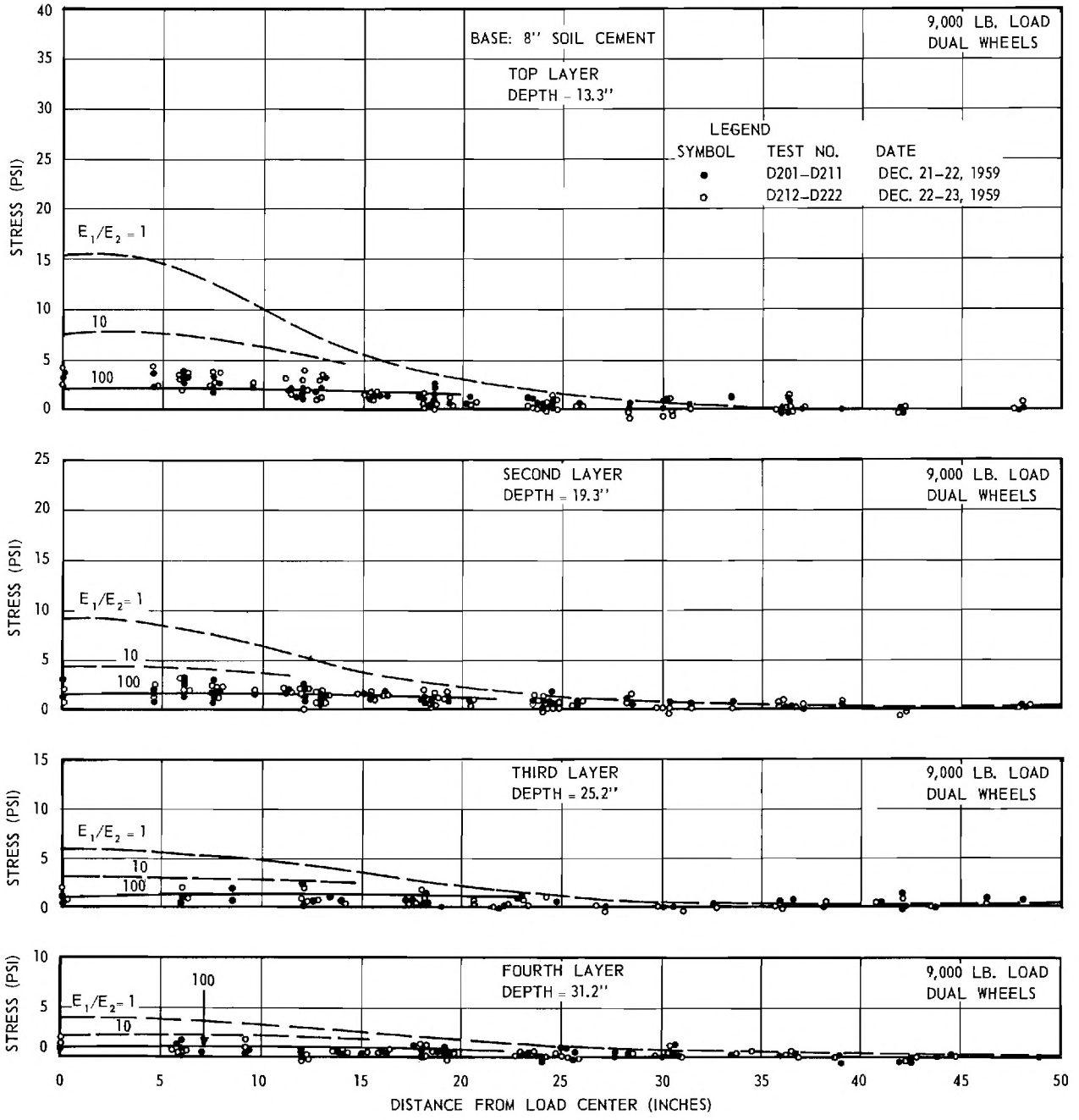

Figure 26. Measured Stresses: Dual Load 9,000-lb Soil-Cement Base.

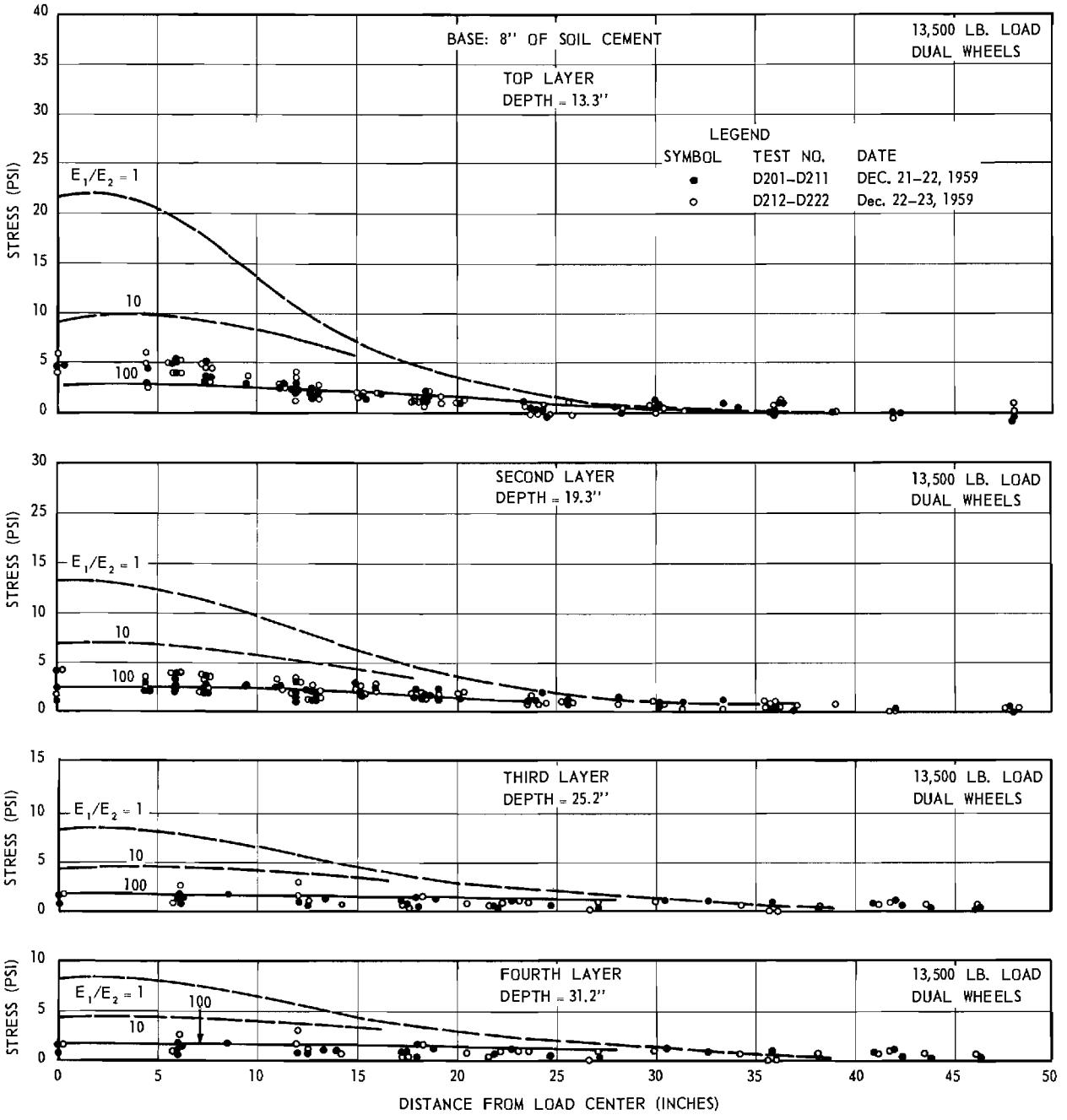

Figure 27. Measured Stresses: Dual Load 13,500-lb Soil-Cement Base.

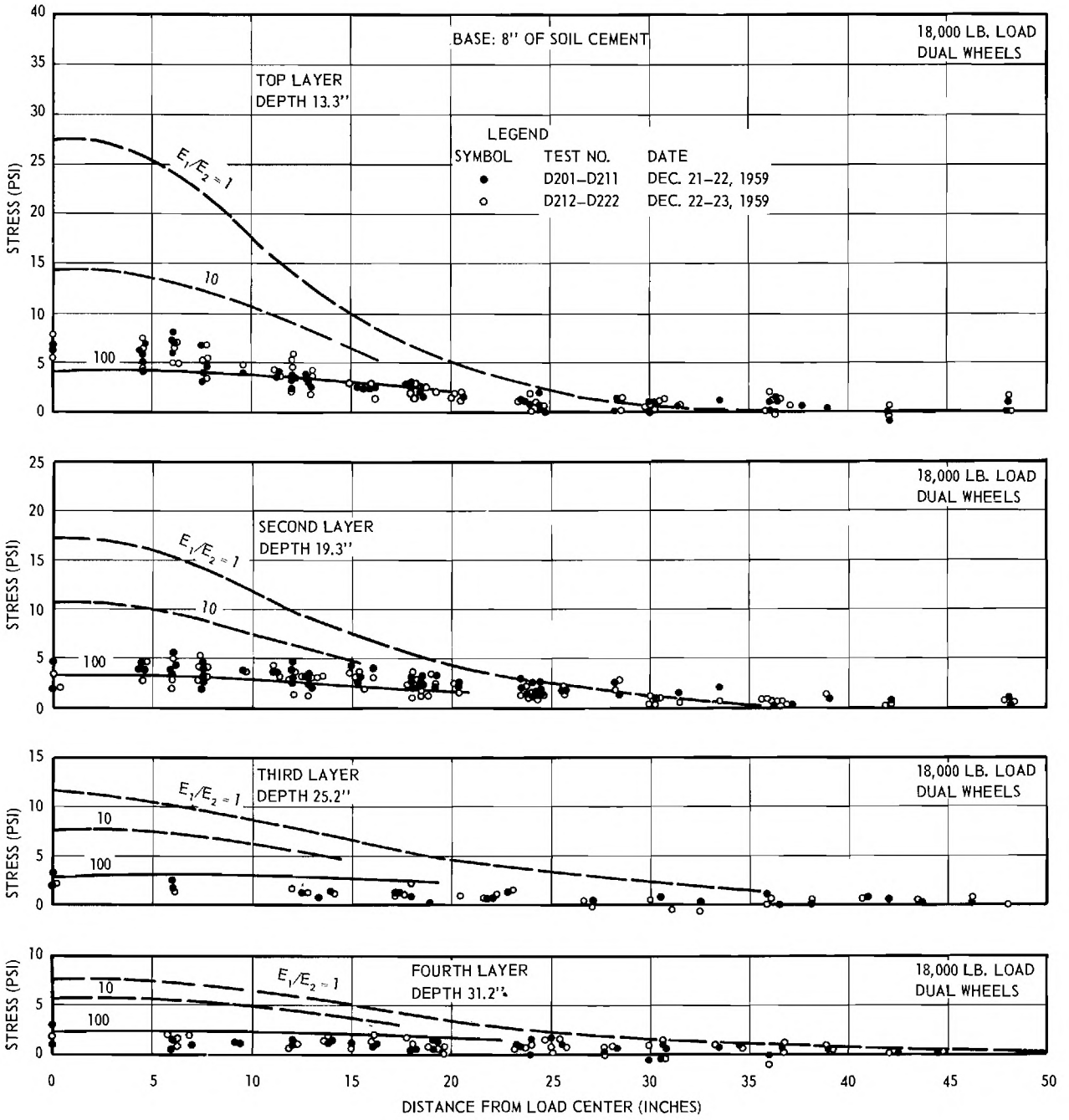

Figure 28. Measured Stresses: Dual Load 18,000-lb Soil-Cement Base.

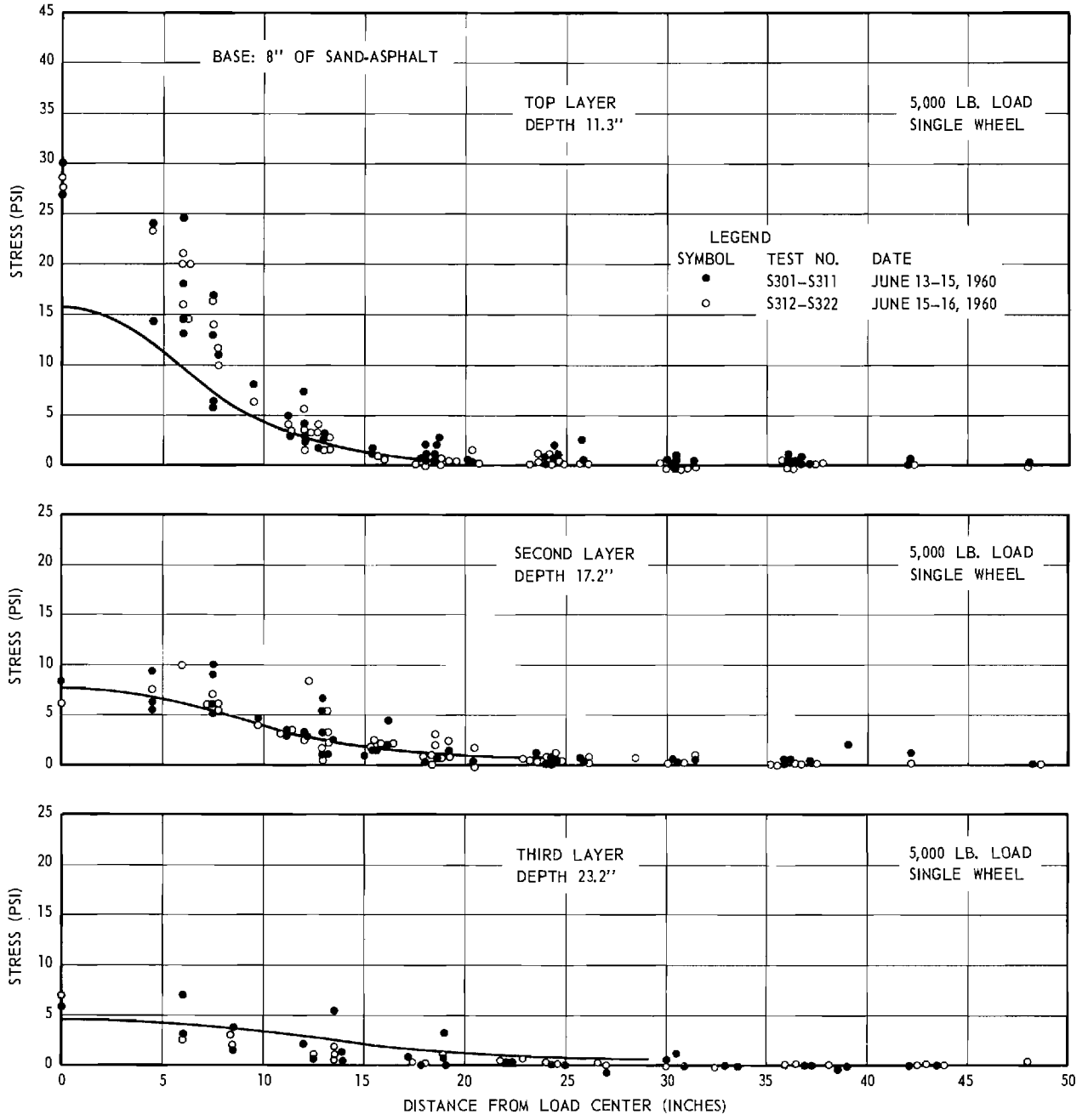

Figure 29. Measured Stresses: Single Load 5,000-lb Sand-Asphalt Base.

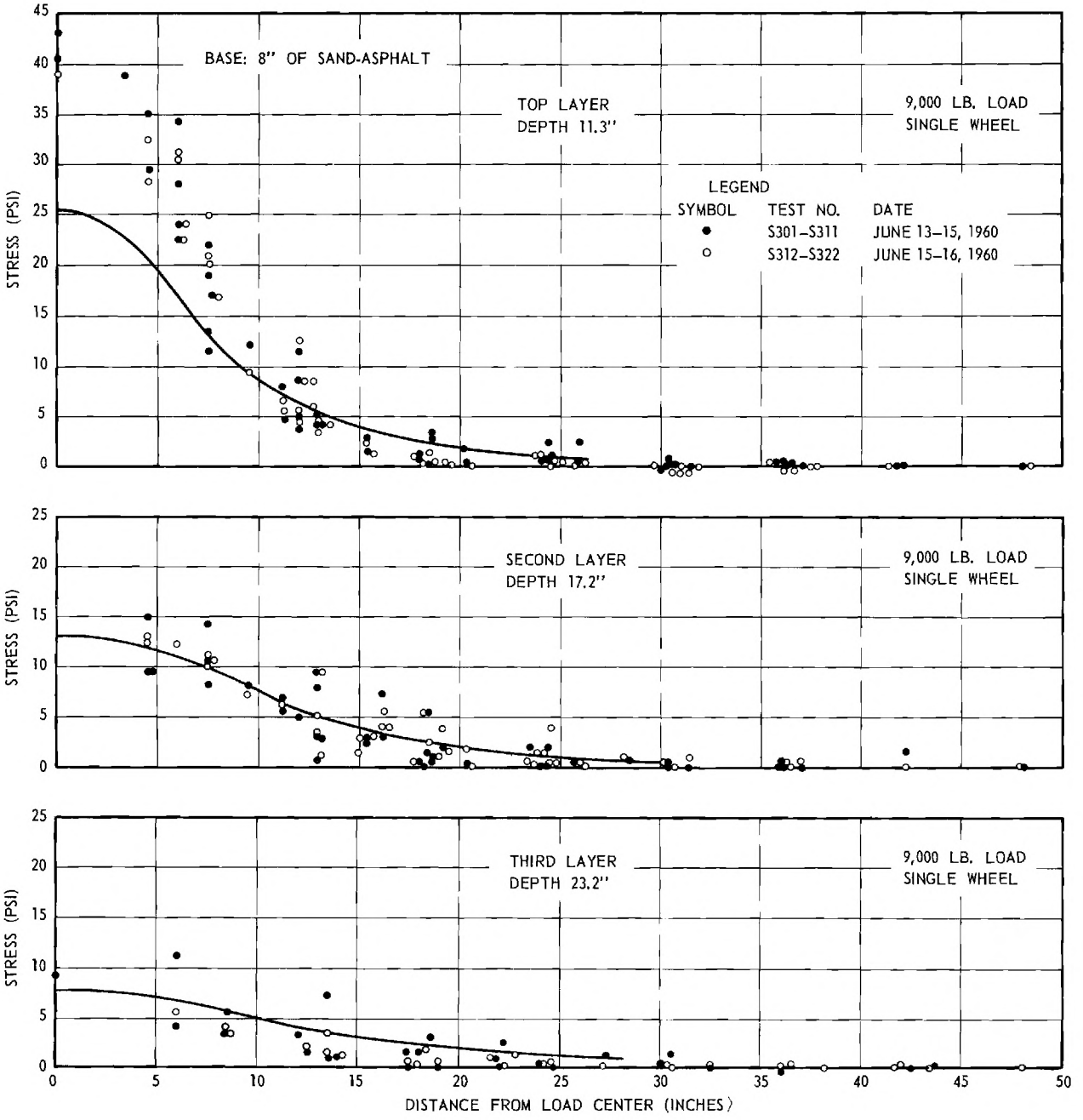

Figure 30. Measured Stresses: Single Load 9,000-lb Sand-Asphalt Base.

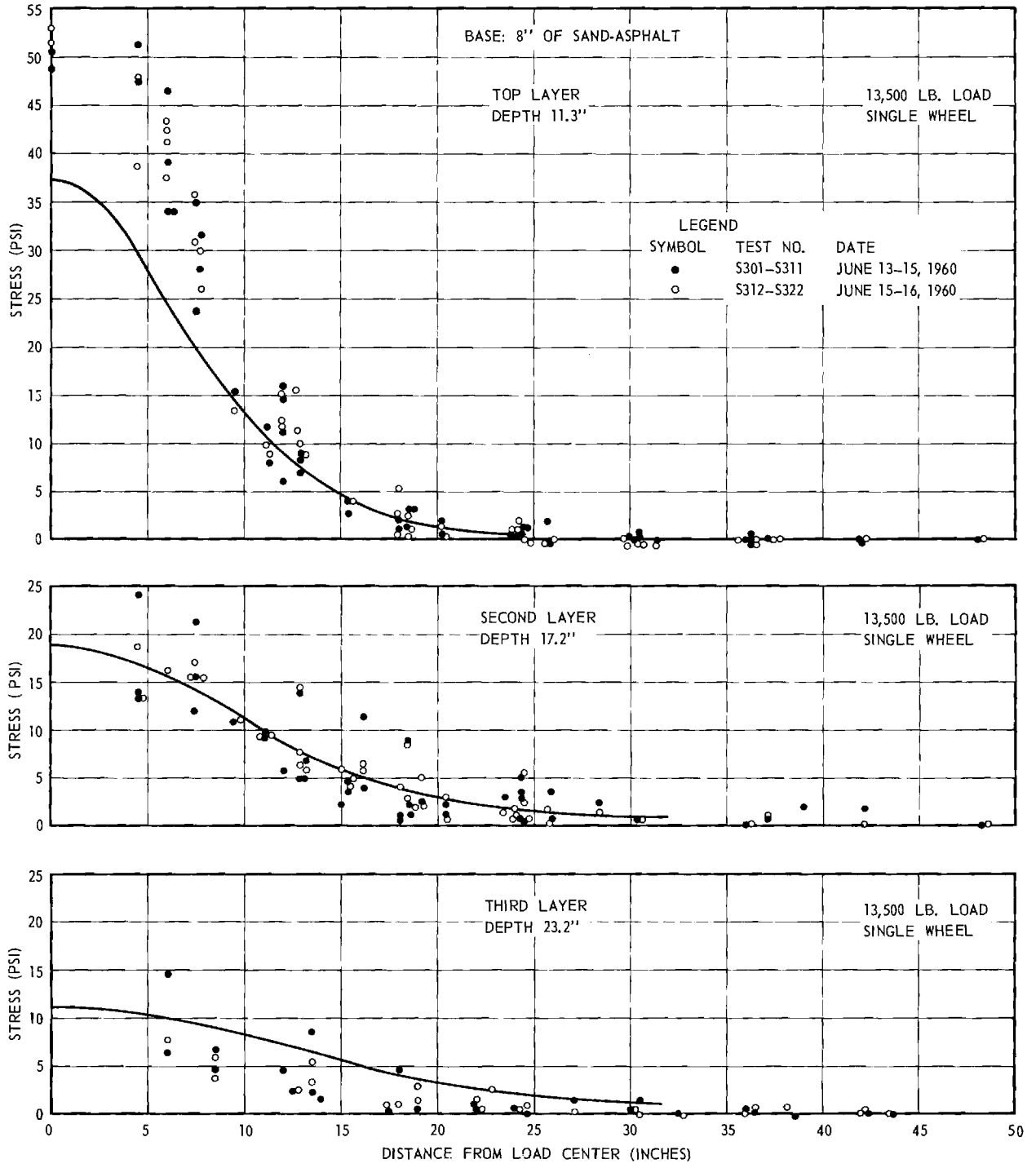

Figure 31. Measured Stresses: Single Load 13,500-lb Sand-Asphalt Base.

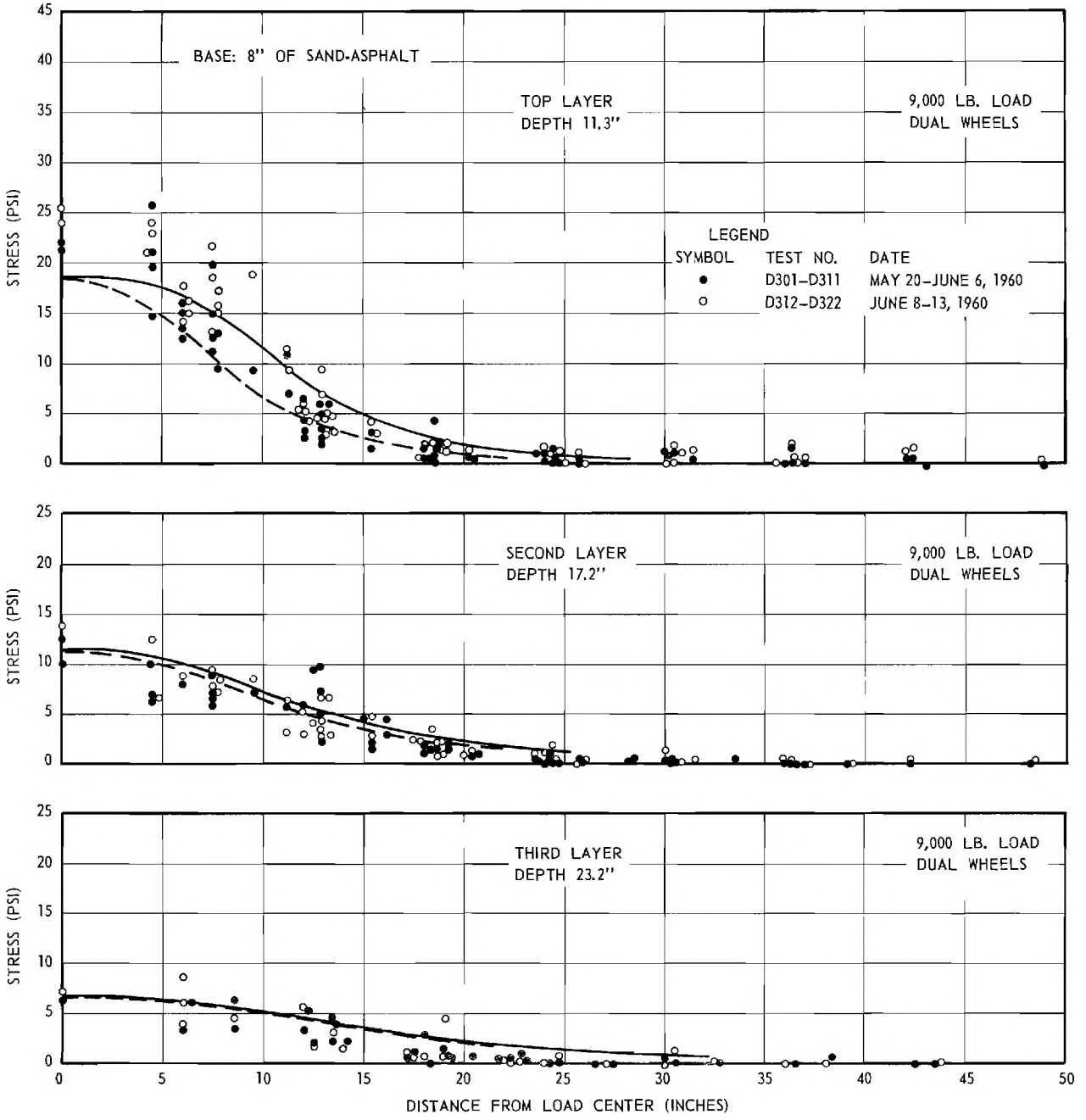

Figure 32. Measured Stresses: Dual Load 9,000-lb Sand-Asphalt Base.

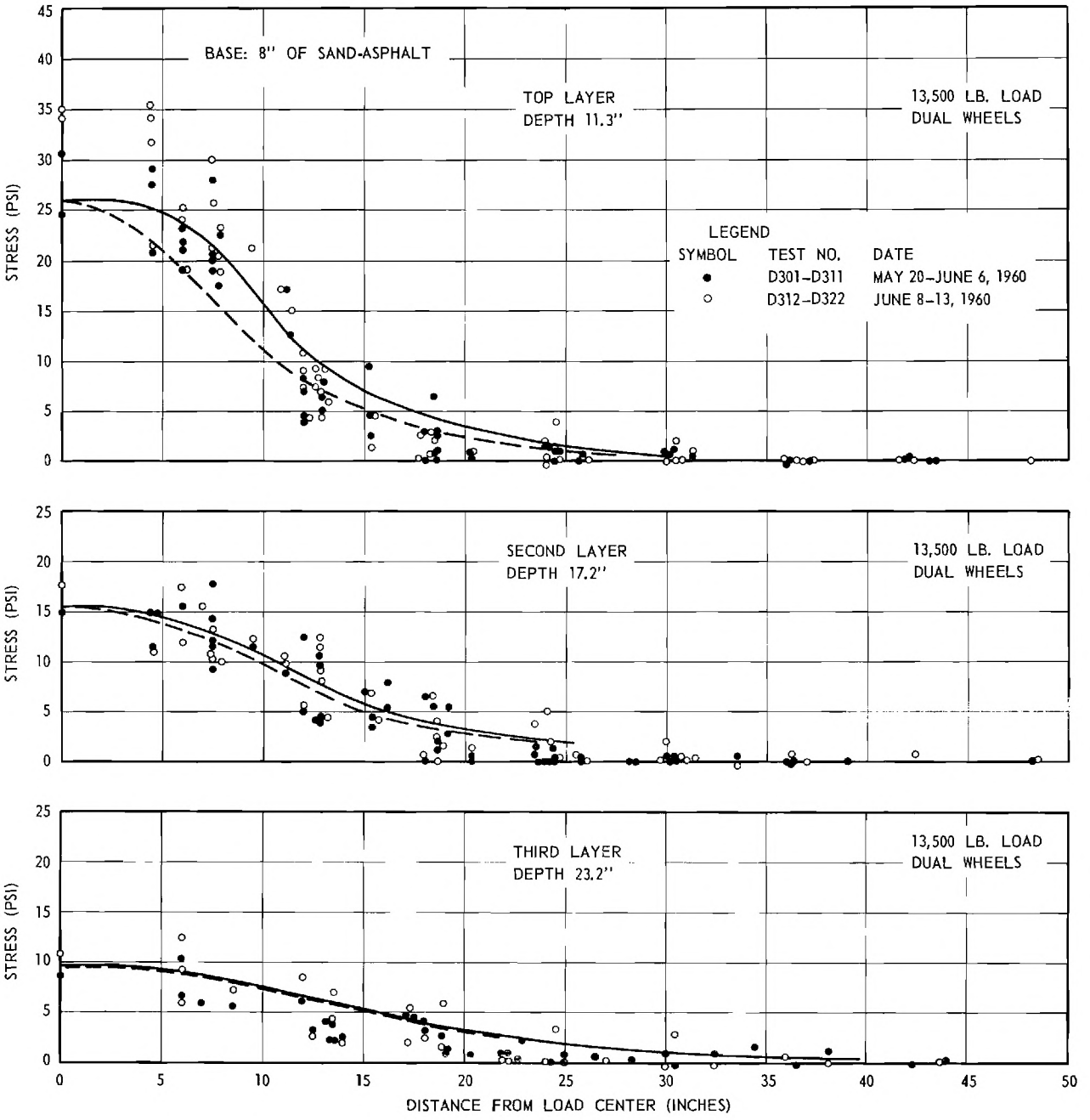

Figure 33. Measured Stresses: Dual Load 13,500-lb Sand-Asphalt Base.

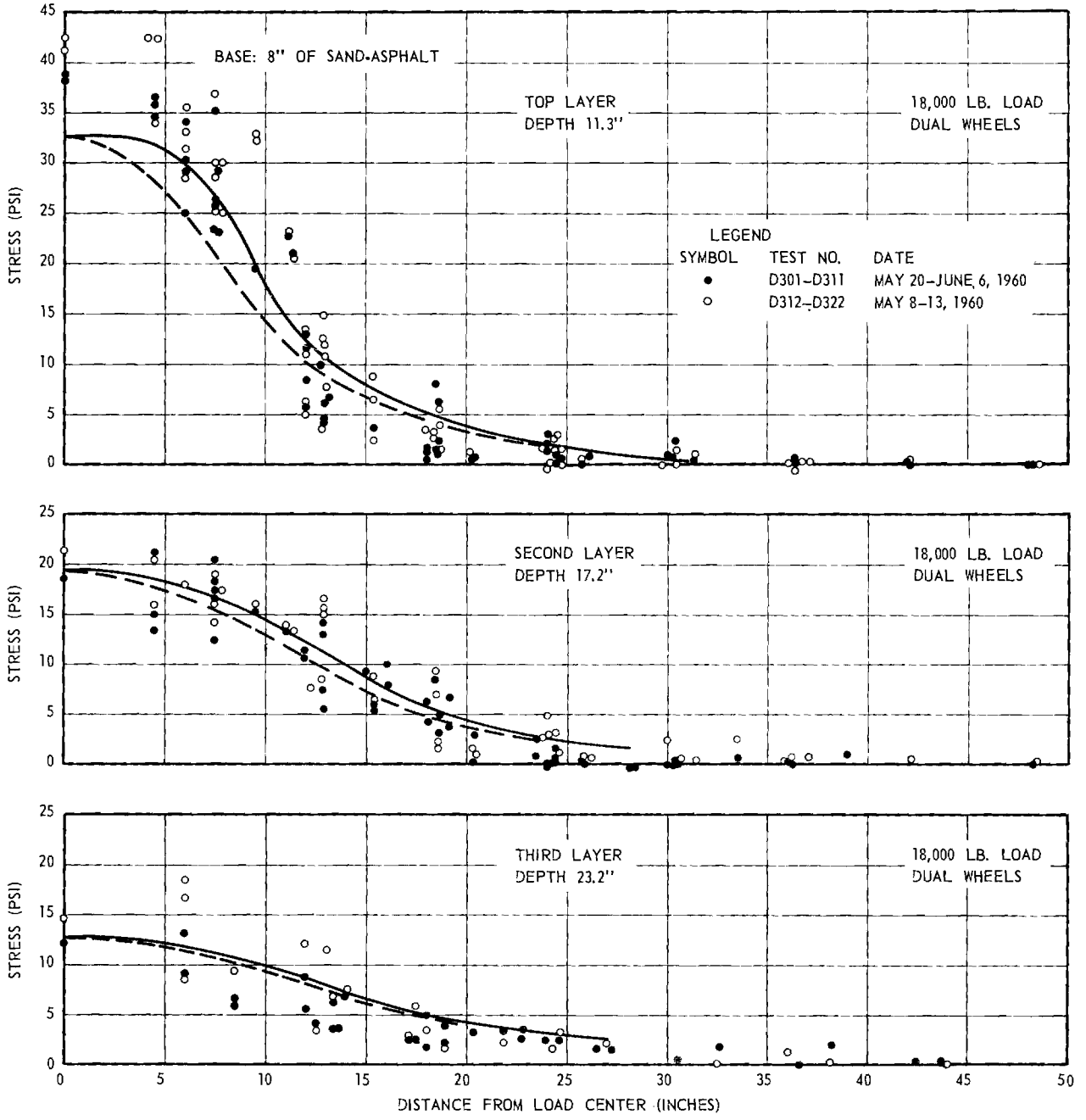

Figure 34. Measured Stresses: Dual Load 18,000-lb Sand-Asphalt Base.

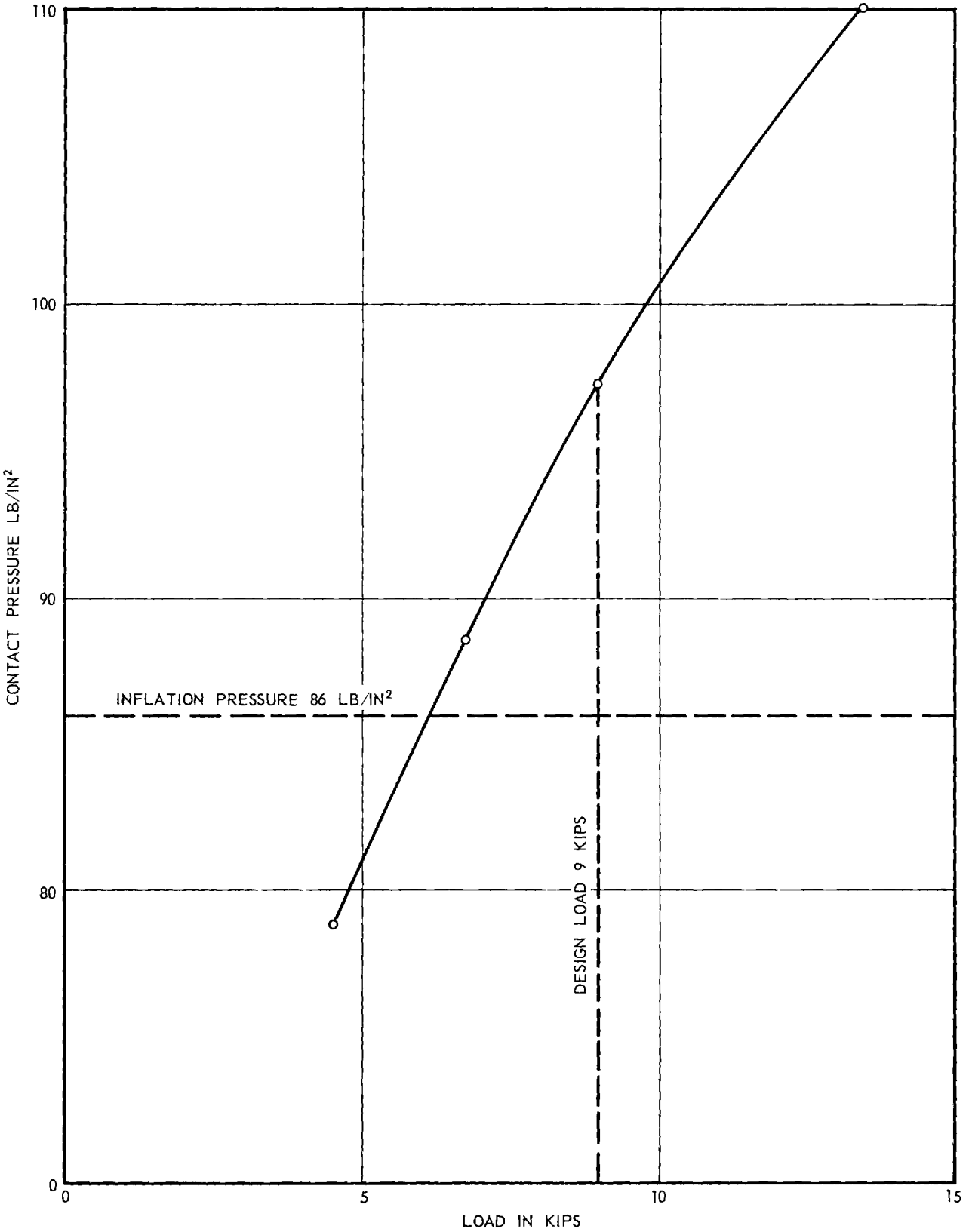

Figure 35. Variation of Average Contact Pressure of a Tire as a Function of Tire Load.

Material	Dry Unit Weight (lb/ft3)	Water Content (%)	Strength Characteristics c' (lb/in.2)	Strength Characteristics φ (Degrees)	Deformation Characteristics: Modulus of Elasticity in lb/in.2 (First no.) Strain at Failure in % (Second no.) from Triaxial Tests at Confining Pressures of: 0 lb/in.2	20 lb/in.2	40 lb/in.2	60 lb/in.2	Modulus of Elasticity from Plate Load Tests (lb/in.2)	Tangent Modulus from CBR-Tests (lb/in.2) and CBR-Value *
Subgrade	79.1	26.8	9.0	23	328 2.5	1,104† 13.7	1,160†† 14.3	1,346 17.6	1,300	691 3.4
Topsoil samples from the actual base	121.2	10.2	20.2	33	1,640 4.9	4,910 6.3	4,800 8.2	--	10,400†††	4,400 29.1
Topsoil samples prepared in the laboratory	123.0	10.6	5.1	33	545 3.8	2,700 10.4	3,140 13.2	3,970 23.9	--	--
Soil-bound macadam	131.1	3.9	2.5	37	2,940 0.6	10,520 2.9	12,360 8.2	--	11,200†††	12,660 34.5
Soil cement	134.5	3.5	51.3	50	49,400 0.8	61,500 0.7	74,000 0.9	91,000 0.9	130,000	--
Sand asphalt: loading rate 0.02 in./min.	103.4	8.5	2.2	35	1,245 1.4	5,970 4.8	10,520 4.4	15,380 5.9	5,590	2,370 9.2
Sand asphalt: loading rate 0.01 in./min.	105.2	8.8	1.0	33	1,080 2.9	5,670 6.2	9,450 8.2	12,350	5,590	2,370 9.2

† At 15 lb/in.2

†† At 30 lb/in.2

††† With 3 inches of pavement above.

* No surcharge.

Four graphs are given on each figure, each representing a different depth below the pavement surface.

The theoretical stress distribution for each depth is shown by continuous curves on each graph. The theoretical calculation is based on a rectangular loaded area, as found in the tire print tests (p. 16 of Annual Report No. 1), and uniform contact pressure computed from the tire print areas (Figure 16, Annual Report No. 1 see also Figure 35 of this report). A single curve is given for stress distribution beneath the single tire. Two curves are shown for the dual and dual-tandem arrangements: the dashed line represents stresses on a cross section midway between the tires and perpendicular to the axle, and the solid line represents stresses on a cross section parallel to the axles. The difference between the curves is significant only at the shallowest depth. It should be noted that the difference between the maximum stresses, parallel and perpendicular to the axle, is less than 5 per cent.

The theoretical stresses for all the bases were computed using the theory of a semi-infinite homogeneous isotropic elastic solid (Boussinesq). The theoretical stresses for the soil cement base were also computed assuming circular loaded areas and using the theory for a system consisting of two homogeneous, isotropic, elastic layers of infinite lateral extent, the upper of finite thickness with a modulus of elasticity of E_1, and the lower of infinite thickness with a modulus of elasticity of E_2, and a rough interface between the two layers. Stress curves for ratios of E_1/E_2 of 1, 10 and 100 are shown on the stress charts for the soil cement base. (Only the curves computed for the cross section perpendicular to the axles are shown for the dual loading on the soil-cement base.)

2. Strength of Materials

The results of quick triaxial tests are shown in Figures 5-9, as well as in

Table I. The Mohr envelope of the soil subgrade is slightly curved, with low strengths and very low confining pressures, a rapid increase in strength with increased confinement, and finally a slower rate of strength increase with still higher confining pressures. Such an envelope implies little or no tensile strength The soil-bound macadam and the sand-asphalt have nearly straight Mohr envelopes with little cohesion and tensile strength, but considerable internal friction. The soil-cement Mohr envelope has significant strength at zero confining pressure and its shape implies appreciable tensile strength.

The sand-asphalt envelopes show a strength difference with differences in the rate of loading: the slower the rate, the less the strength. Similar differences have been noted from changes in temperature in asphaltic mixtures: the higher the temperature, the lower the strength (1).

3. Elasticity of Materials

The modulus of elasticity curves (Figure 10) all show an increase in the modulus of elasticity with increasing confining pressure.

The curve shapes indicate for sand-asphalt a continuing, nearly linear increase with increasing confinement; while for other materials the moduli E increase rapidly at low confining pressures and then level and approach a constant at higher confining pressures. (The constant E is a basic assumption of the theories of stress distribution for a homogeneous, elastic, isotropic solid.) The ratio of the modulus of elasticity of the base to the subgrade (Figure 11) is also very revealing: for the topsoil and soil-bound macadam bases the ratios are nearly constant, regardless of the confining pressure. For the sand-asphalt, however, the ratio increases rapidly with increasing confinement.

4. Pavement System Stresses

The measured stresses in the subgrade (Figures 17-34), show appreciable

scatter. Such scatter is to be expected because each point plotted represents a single stress reading rather than the average of several. Erratic readings, which appeared to be caused by malfunctioning of the pressure cells, were included, unless there was direct evidence that the cell was faulty, so that the real variations of stress within the soil mass could be observed. It is the writers' opinion that these variations are the combined result of differences in soil characteristics and the way in which the load is applied, and represent the range in stress variations to be expected when computing stresses from surface loads. Averaging the individual readings for each test run as was done in the Waterways Experiment Station tests (3), (4) will produce less scatter but will somewhat obscure the meaning of the results.

The results of the tests on the soil-bound macadam base indicate a stress distribution in the soil that approximates the theoretical distribution in a homogeneous, isotropic, elastic medium (Boussinesq). This indicates that the soil-bound macadam is no more effective in spreading the wheel loads than is a homogeneous soil. Similar results were obtained for the topsoil base, reported in Annual Report No. 1.

The ratio of the modulus of elasticity of the soil-bound macadam to that of the subgrade (Figure 11) as shown by the triaxial tests was 9, and by the plate load tests 8.6. The corresponding ratios for the topsoil base were respectively 4.8 and 8.0. If those ratios of elastic moduli are used to compute the stresses by the two layer elastic theories, the theoretical stresses are found to be appreciably less than those measured. The lack of validity of the three-layer theory can be explained by the lack of tensile strength in the upper or base course layer. In a two-layered system with a more rigid material on top and with a rough interface, tensile stresses develop at the bottom of the upper layer. In order

for the theory to be valid, the layer must remain intact in spite of tension; therefore, the theory requires that the upper layer have sufficient tensile strength to resist these stresses. The Mohr diagrams (Figures 5 and 6), however, indicate little cohesion and negligible tensile strength. Therefore, it should be expected that the two-layer theory would be invalid.† This conclusion supports to some extent the practice of neglecting any effect of base course rigidity in design of flexible pavements by the CBR method. By the same token it casts some doubt on the methods of pavement design based on the two-layer theory.

The stresses beneath the soil cement base (Figures 23-28) are considerably lower than those computed by the homogeneous, isotropic elastic theory. They indicate that the soil cement is much more effective in spreading stresses than any other of the bases tested.

The ratio of the modulus of elasticity of the base to that of the subgrade as found by the plate load tests was approximately 100. The triaxial test results indicate a ratio between 150 and 60 at low confining pressures and a ratio of 60 at high confining pressures. The theoretical stress distribution for such an elasticity ratio closely approximates the measured stresses. Therefore it appears that in this case the two-layer theory is reasonably valid. The explanation is again found in strength characteristics of the material. The Mohr envelope for soil-cement samples (Figure 7) indicates a cohesion of more than 50 lb/in.^{2} (3.50 ton/ft) and considerable tensile strength. There is some question in the writer's minds regarding the performance of the tensile strength and the high

†It is interesting to note here that this finding fully supports the results of of a theoretical investigation by Ruckli[2] in a two-layer system with the upper layer lacking tensile strength. He found for a single load, a modulus of elasticity ratio $E_1/E_2 = 10$ and at a depth of 12 inches a stress concentration factor of $\nu = 2.82$ (compared to $\nu = 3$ for homogeneous soil).

efficiency of load spreading shown by the soil cement. It is possible that the material will crack under repeated loading or severe temperature fluctuations and lose its tensile strength. The effect of repeated loads will be determined in a subsequent test.

The results of tests on the sand-asphalt (Figures 29-34) show stresses that are higher than those obtained by the Boussinesq theory for homogeneous and isotropic materials. However, the modulus of elasticity ratio (Figure 10) as indicated by triaxial tests is greater than 4, and at high confining pressures exceeds 10 (plate load tests indicate a value of 4.3). Therefore a spreading rather than a concentration of stresses should be expected if the multilayer theory were applicable in this case. The relatively high stresses found are explained by the combined effect of lack of tensile strength and of linear increase with confining pressure of the modulus of elasticity of the base material. Theoretical investigations of stress distribution in a homogeneous semi-infinite mass having an elasticity modulus linearly increasing with depth (5) show concentration of stresses immediately beneath the loaded area as compared to those in the homogeneous material. Expressed in terms of Griffith-Fröhlich concentration factor, the theoretical investigation indicates a $\nu \backsimeq 4$ value for such masses. Our experimental results correspond approximately to a concentration factor ν of 4, which is also a value that many investigators have found experimentally on homogeneous sand subgrades.

CHAPTER V

PREVIEW OF FINAL PHASE OF PROJECT

The second year's work completed the evaluation of the four basic base courses now in use by the Georgia State Highway Department. It showed the relative value of these materials and demonstrated the conditions under which the stresses in the subgrade could be computed analytically.

The final phase will be concerned with the effect of variations in the base and pavement design, an evaluation of the pavement deflections, and a development of curves of thickness-load-stress for use in pavement design.

The variations to be tested include:

a. the effect of an asphaltic concrete overlay,

b. the effect of a different soil-cement base thickness,

c. the change in stresses due to repeated loading of the soil cement, and

d. the effect of inundating the subgrade.

Also, it would be desirable to repeat some of the performed tests using some more rigid subgrades.

Prepared and submitted by:

George F. Sowers,
Project Director

Aleksandar B. Vesić
Research Associate

Approved by:

Thomas W. Jackson, Chief
Mechanical Sciences Division

Released by for J. E. Boyd, Director
Engineering Experiment Station

REFERENCES

(1) Cox, B. E., Effect of Temperature on Stability of an Asphaltic Mixture, M. S. Thesis, Georgia Institute of Technology, 1960.

(2) Ruckli, R., On Pavement Bearing Capacity. Discussion, Trans. ASCE Vol. 116, 1951.

(3) Waterways Experiment Station, Investigation of Pressures and Deflections for Flexible Pavements, Report No. 1, Homogeneous Clayey Silt Test Section, Vicksburg, Miss., 1951.

(4) Waterways Experiment Station, Investigations of Pressures and Deflections for Flexible Pavements, Report No. 4, Homogeneous Sand Test Section, Vicksburg, Miss., 1954.

(5) Buisman, K. S., Druckverdeeling in bouwgrond in verband met ongelijke samendruckbaarheid en vertikale richting, De Ingenieur, No. 37, 1932.

FINAL REPORT

PROJECT NO. B-133

THE STUDY OF STRESSES IN A FLEXIBLE PAVEMENT SYSTEM

By

GEORGE F. SOWERS and ALEKSANDAR B. VESIĆ

Contract with
THE STATE HIGHWAY DEPARTMENT OF GEORGIA
in Cooperation with
THE BUREAU OF PUBLIC ROADS

JULY 1, 1960 through DECEMBER 31, 1960

Engineering Experiment Station
Georgia Institute of Technology
Atlanta, Georgia

ENGINEERING EXPERIMENT STATION
of the Georgia Institute of Technology
Atlanta, Georgia

FINAL REPORT

PROJECT NO. B-133

THE STUDY OF STRESSES IN A FLEXIBLE PAVEMENT SYSTEM

By

GEORGE F. SOWERS and ALEKSANDAR B. VESIĆ

Contract with
THE STATE HIGHWAY DEPARTMENT OF GEORGIA
in Cooperation with
THE BUREAU OF PUBLIC ROADS

JULY 1, 1960 through DECEMBER 31, 1960

TABLE OF CONTENTS

This report contains 55 pages.

LIST OF FIGURES

LIST OF FIGURES (Continued)

CHAPTER I

INTRODUCTION

1. Scope of the Project

The rational design of any structural system, including pavements, requires a knowledge of the stresses induced by the imposed loads. However, little information has been available regarding the stresses developed in the underlying soils by wheeled vehicles supported by pavements. It is the object of this research to investigate the stresses produced in soil subgrades by wheel loads, such as truck tires, or flexible pavements.

The problem has been attacked from two sides: theoretical computation of stresses in various idealized representations of soil, such as homogeneous or layered, isotropic or anisotropic elastic masses, and the measurement of actual stresses produced by static wheel loads on full scale model pavement-subgrade systems. The theoretical stresses, computed from the physical properties of the materials as measured by laboratory tests, are compared with the observed stresses to test the validity of the theories. This will lead to development of modifications, corrections or simplifications in the theories which are necessary to translate the analyses into realistic design tools.

2. Summary of First Two Year's Work

The work of the first two years was reported in Annual Reports 1 and 2. The first phase was an intensive review of existing methods of analyzing stresses in large masses similar to soil subgrades acted upon by wheel loads. This phase was completed and reported in detail in Annual Report 1. The second phase was the design and construction of a full scale model consisting of a pavement, subgrade, and truck wheels that permitted imposing loads and measuring stresses in the soil under controlled conditions. This work was also

completed and reported in Annual Report 1 (although minor modifications and improvements have continued throughout the work).

The third phase consisted of measurements of stresses in a flexible pavement system consisting of a 3-inch-asphaltic concrete surface, a base course, and a micaceous sandy silt subgrade. Four different base courses were used: sandy (topsoil), soil-bound Macadam, soil-cement Macadam, and sand asphalt. The test conditions are summarized in Table I. The results of the topsoil base pavement tests were given in Annual Report 1; the results of the tests on other bases were given in Annual Report 2.

The fourth phase consisted of laboratory tests on the physical properties of the soils and aggregates that were employed in all four pavement systems. The results of all these tests (except the shear tests on the asphaltic concrete) were presented in Annual Report 2.

The tests on the pavement systems employing topsoil and soil-bound Macadam base courses showed that the stresses in the subgrade from static wheel loads on the surface were essentially the same as those which are computed by the Boussinesq theory. The layered pavement-subgrade system with a base course 5 times (topsoil) to 10 times (soil-bound Macadam) more rigid than the subgrade distributed the stresses like a homogeneous isotropic mass. Thus it must be concluded that the more rigid fragmental bases are no more effective as load spreading media than elastic soils such as the subgrade itself.

The tests on the pavement system employing a soil cement base showed that the stresses in the subgrade produced by wheel loads in the surface were considerably less than those computed by the Boussinesq theory and were comparable to those computed by the elastic layer theory (assuming the asphaltic

TABLE I

Test Conditions

Test Series	Surface Course - (Plant Mix Asphaltic Concrete) Thickness	Base Course Composition	Base Course Thickness	Loading Wheel	Loading Total Load, Kips
I	3	Topsoil I	8 in.	Single	5, 9, 13.5
				Dual	5, 9, 13.5, 18
II	3	Soil bound Macadam	8	Single	5, 9, 13.5
				Dual	9, 13.5, 18
III	3	Soil cement Macadam	8	Single	5, 9, 13.5
				Dual	9, 13.5, 18
IV-1	3	Sand Asphalt	8	Single	5, 9, 13.5
				Dual	9, 13.5, 18
IV-2	6 (3" overlay)	Sand Asphalt	8	Single	5, 9, 13.5
				Dual	9, 13.5, 18
V-1	3	Topsoil II	8	Dual	9, 13.5, 18
V-2	6.5	Topsoil II	8	Single	8.5, 12.5, 17
				Dual	9, 13.5, 18
VI-1	3	Soil cement Macadam	6	Single	5, 9, 13.5
				Dual	9, 13.5, 18
VI-R	3	Soil cement Macadam		Single	13.5 (1000 cycles)
VI-2	6.5	Soil cement Macadam		Single	5, 9, 13.5
				Dual	9, 13.5, 18
VI-F	6.5	Soil cement Macadam*		Dual	9, 13.5, 18

*Subgrade and base inundated.

surface to be as rigid as the soil cement). The stresses in the subgrade beneath the 8 inch soil cement base were one third to one fourth of those at the same depth beneath the topsoil and soil-bound Macadam bases. The difference in the behaviour between the soil cement base and the topsoil and soil-bound Macadam bases is in the ability of the former to resist tension. Tensile stresses are set up in the more rigid layers in an elastic layered system; therefore, a stress analysis for a layered system is applicable only to rigid layers which can support tension. The fragmental topsoil and soil-bound Macadam bases cannot; the soil cement can.

The test on the pavement system employing the sand-asphalt base showed that the stresses in the subgrade just under the base were somewhat higher than those computed by the Boussinesq theory. The difference can be attributed to the increase in rigidity in sands with increased confining pressure -- a phenomenon which brings on a concentration of stresses beneath the center of the load. For the lightly loaded (5000 lb) single wheels, the stress was 1.75 times the Boussinesq while for the heavily loaded dual wheels (18,000 lb) the maximum stress was 1.25 the Boussinesq. Deeper in the subgrade, however, the stresses approximated those computed by the Boussinesq theory.

3. Summary of Complementary Phase

The final phase of the pavement stress studies is herein reported. It consisted of measurements of stresses on the same or similar pavement systems as employed in Phase 3 but with an asphaltic concrete overlay. In addition, tests were made of certain variations of the pavement system with a soil cement base.

The topsoil base material was somewhat different than in Phase 3 and so the earlier test was repeated with a 3-inch surface. The results were nearly

identical to those in Phase 3. The tests with a 3-inch asphaltic overlay showed that the stresses in the subgrade were slightly higher than those computed by the Boussinesq theory. The difference was small, however. In other words, three inches of overlay are nearly as effective in spreading the wheel load as three inches of topsoil base. The original sand-asphalt-base pavement was tested with a three inch overlay. This overlay, too, was found to be as effective as additional sand-asphalt base of the same thickness.

The tests of a pavement employing soil cement were repeated with a 6-inch thick base rather than the 8-inch base used in Phase 3. The results indicate that the stresses are a fraction - a little less than one half - of those computed by the Boussinesq theory. As with the 8-inch base thickness, the layered theory appears applicable, although possibly not so rigorously. The stresses with a 3-1/2 inch thick asphaltic concrete overlay were appreciably less than without it. The reduction was equivalent to that produced by a topsoil base of equivalent thickness.

The pavement with the soil-cement base was subjected to repeated loading with a 13,500 lb single tire. After 1000 cycles of loading and unloading the stresses produced in the subgrade were the same, which indicates no loss of load spreading ability by the soil cement with even this gross repeated overload.

Finally the subgrade beneath the soil cement pavement was inundated. The stresses in the subgrade produced by wheel loads were not changed.

CHAPTER II

TESTS OF MATERIALS

1. Laboratory Tests

The sand asphalt in the overlay testing was the same as that employed in Phase 3 which was previously reported. No further tests were conducted in the laboratory on this material.

The topsoil used in Phase 3 was consumed in the later soil cement tests, and the borrow pit from which it was obtained was no longer available. A new topsoil was obtained from the same area. Laboratory identification tests made on this material show that the new topsoil is similar to the original material. Its compacted maximum density, however, was somewhat lower.

The soil cement employed the same aggregate as in Phase 3, previously reported, and the new topsoil. Because the materials were similar, no further tests of the properties of the soil cement were conducted.

Cores were made from the asphaltic concrete surface and overlay courses of test IV-2 (the sand asphalt). This surface was from the same source as the others and constructed in the same way. A mean density of 131 lb per cu ft was found for the cores. The greatest variation from the mean was only 1 pcf, in spite of the fact some cores were cut from the wheel tracks and others from areas where the wheel had not touched.

The 4 inch diameter cores were stacked together to form cylindrical specimens which were tested in triaxial compression. The results are given in Fig. 1. The stress-strain curves are similar to those for the sand asphalt, with a marked increase in the modulus of elasticity with an increase in confining pressure. The tests made at an elevated temperature show less strength and rigidity than those at ordinary temperatures, as might be expected. The surface

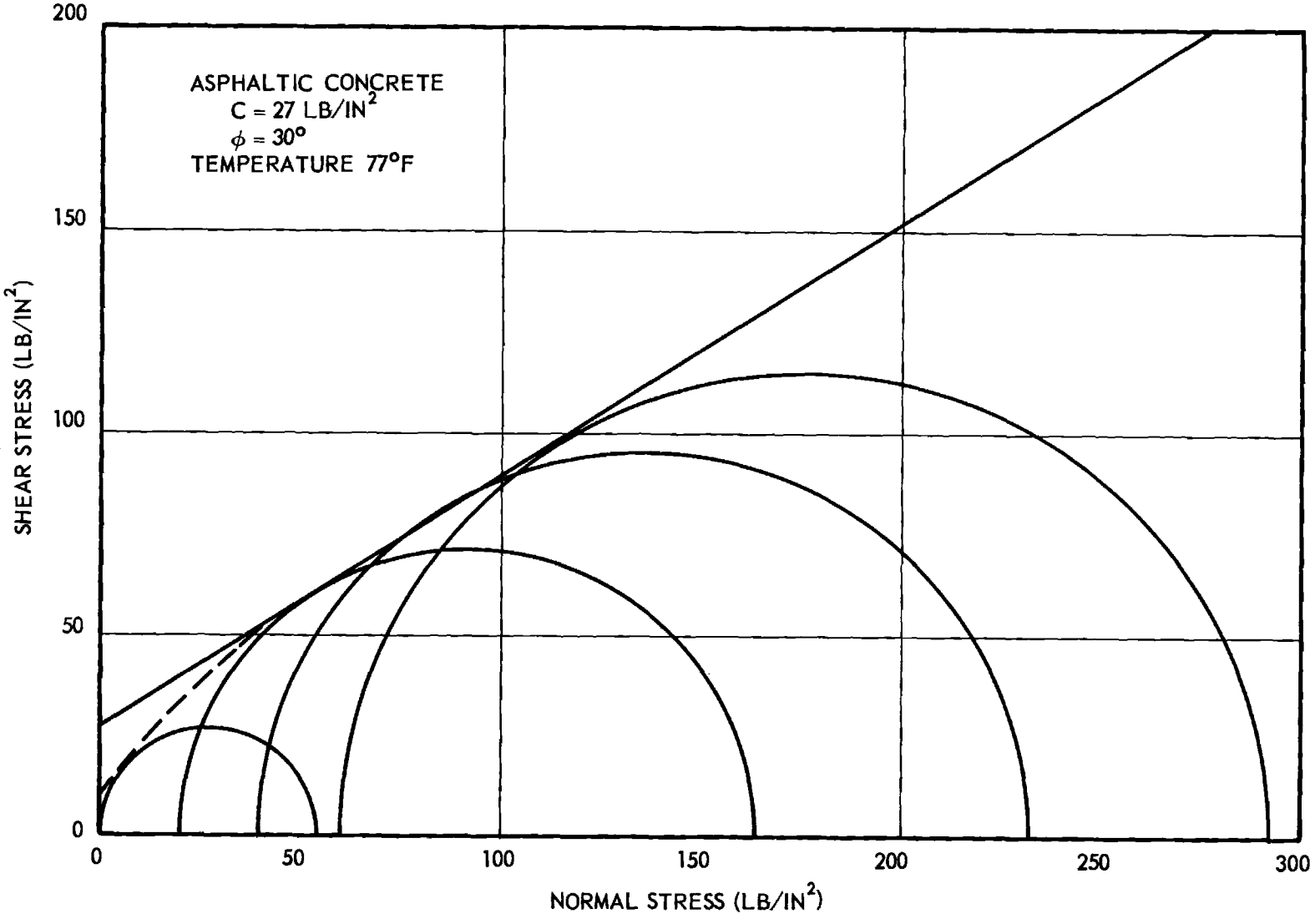

Figure 1a. Triaxial Test Results: Asphaltic Concrete.

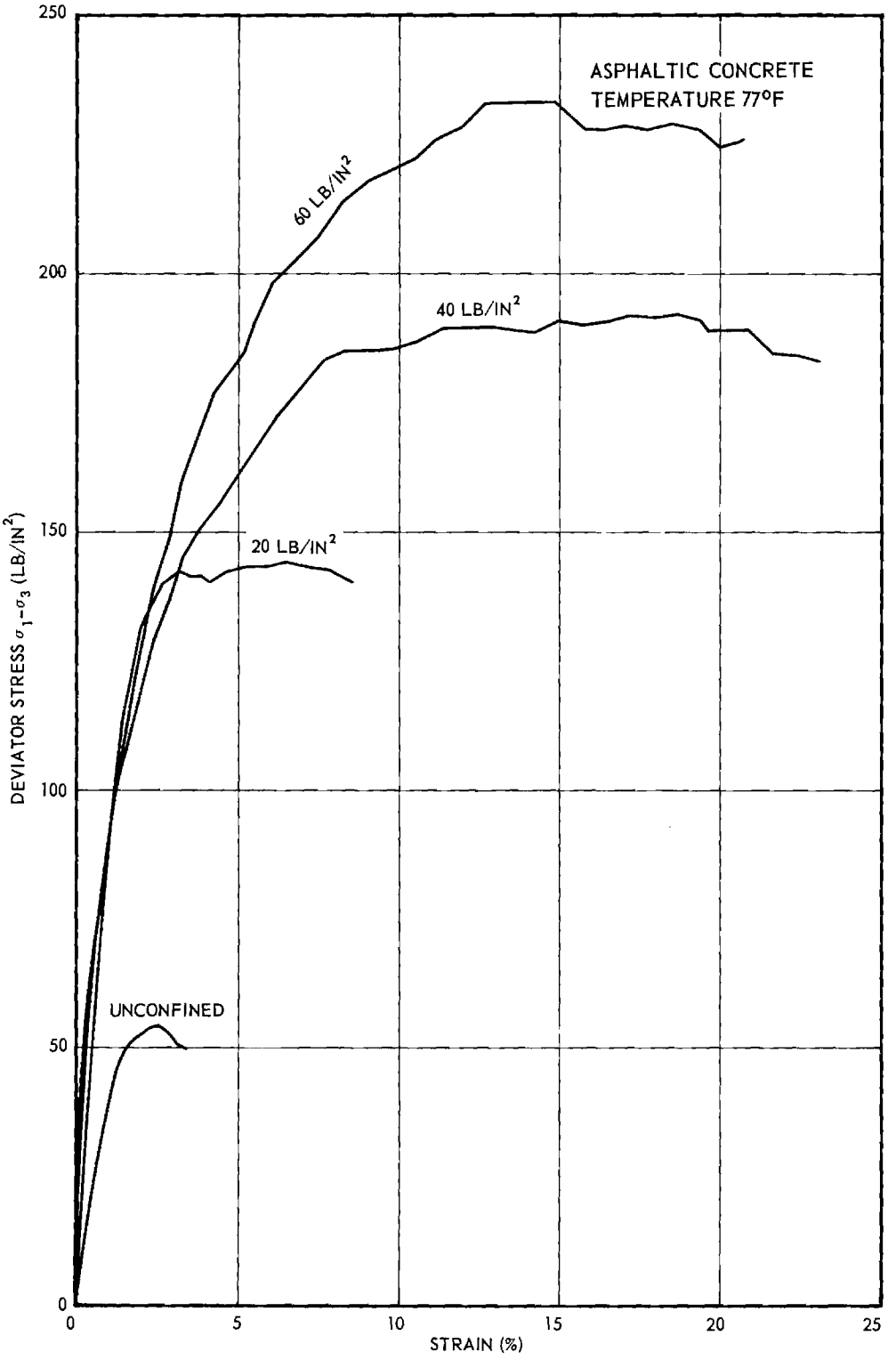

Figure 1b. Triaxial Test Results: Asphaltic Concrete.

density, strength and rigidity are considerably higher than was expected for an asphaltic concrete compacted with a small engine-powered tamper, and are nearly as great as for well-constructed, thoroughly rolled pavements.

California Bearing Ratio (CBR) tests were made on samples of the subgrade, Topsoil II, and the sand-asphalt base prepared in the laboratory. These were conducted with a surcharge loading equivalent to the weight of the pavement above. The results are given in Figs. 2 to 4.

2. In Place Tests

In-place tests were conducted on the sand-asphalt-base pavement and the new topsoil-base pavement using the same procedures as described in Annual Report 2. The results are given in Fig. 5.

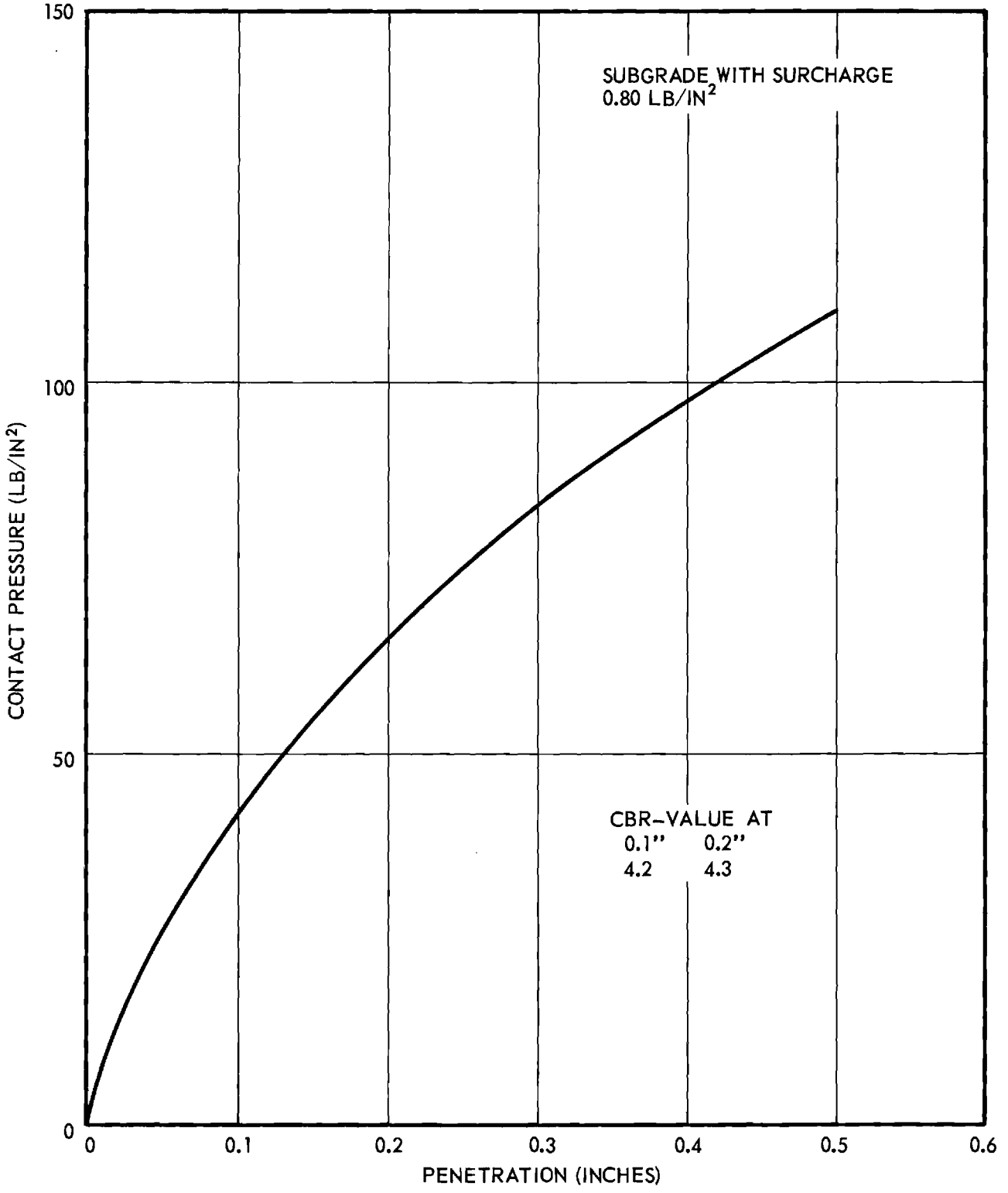

Figure 2. CBR-Test Results: Subgrade (with surcharge).

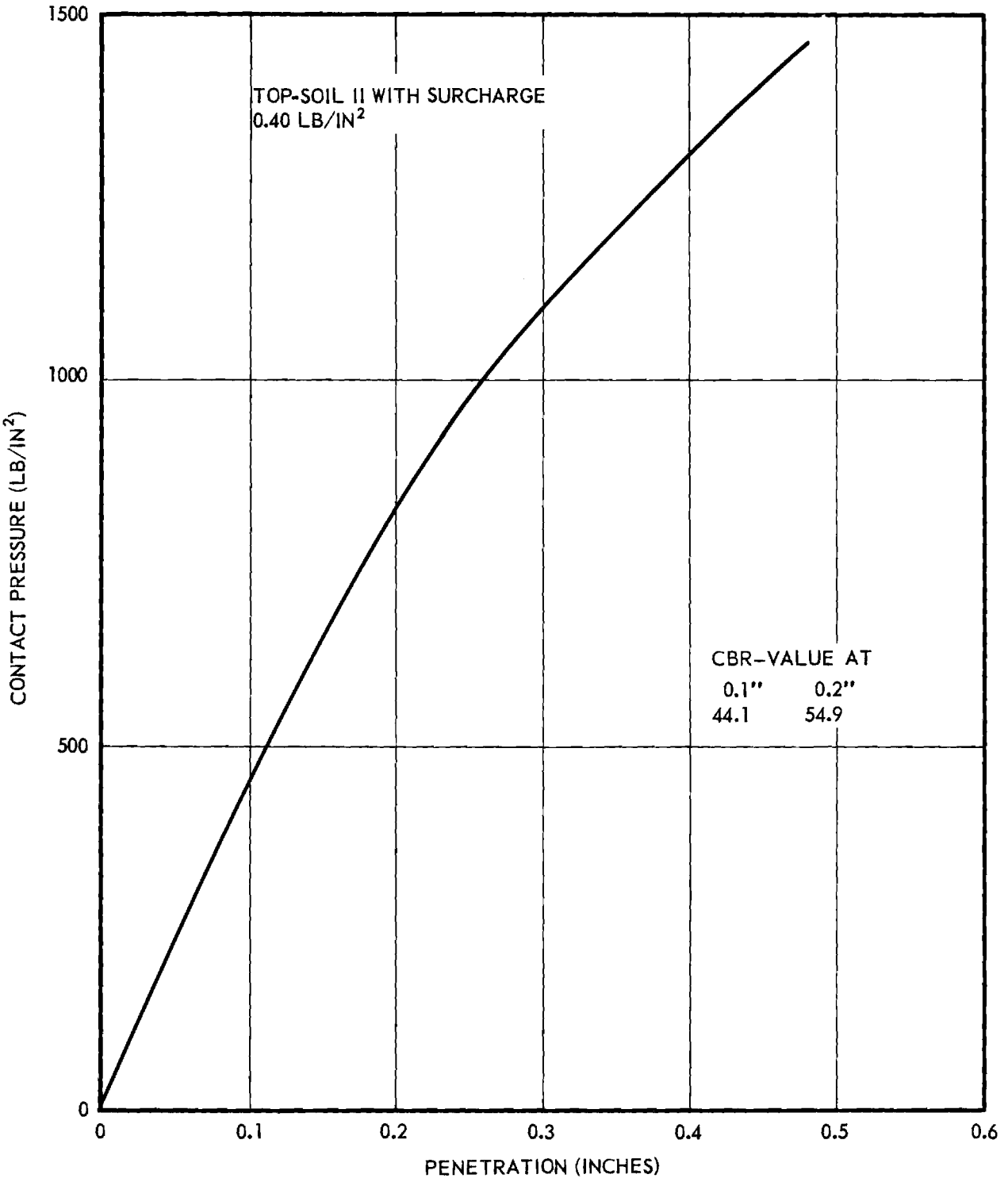

Figure 3. CBR-Test Results: Top-Soil II (with surcharge).

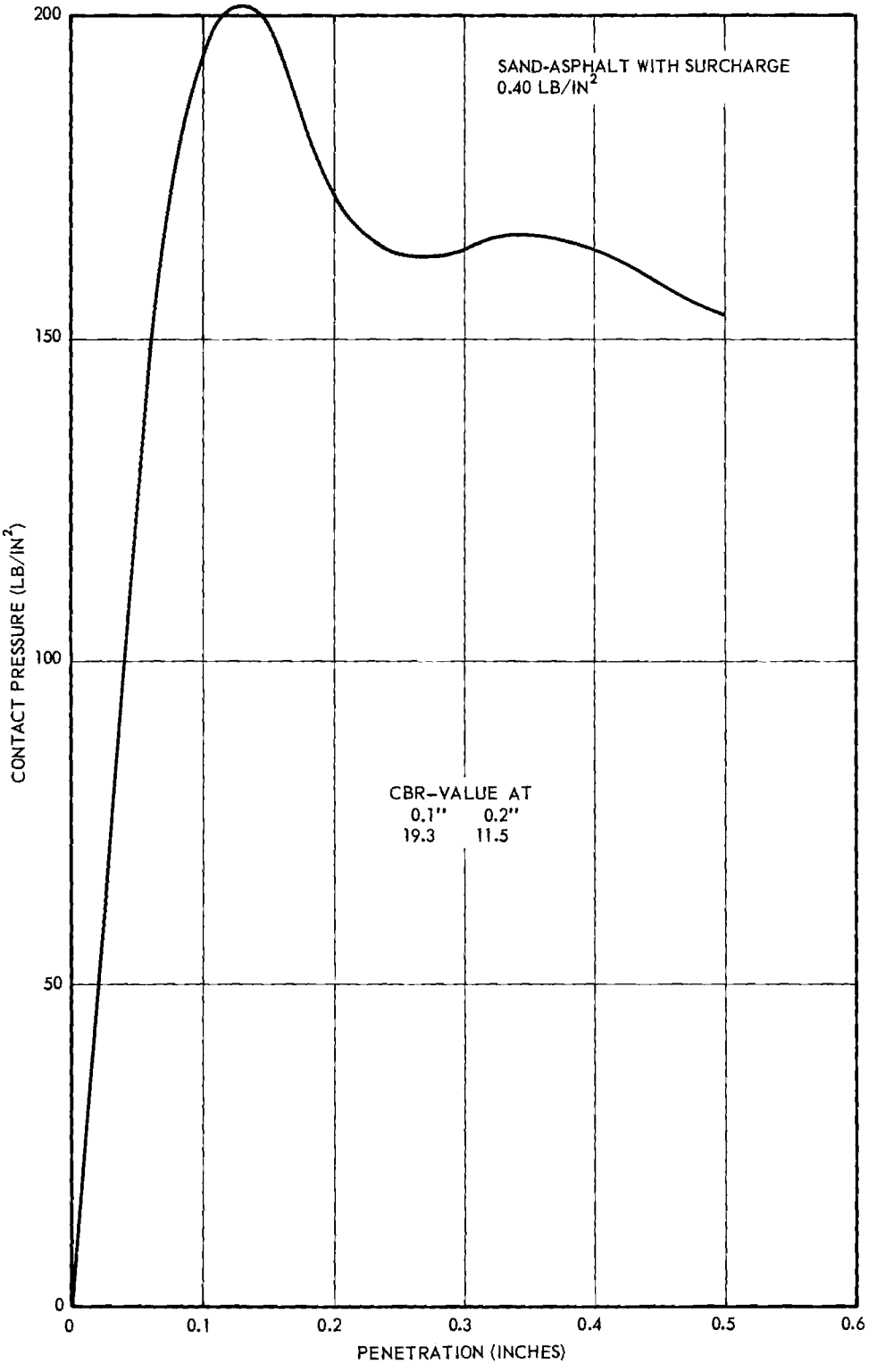

Figure 4. CBR-Test Results: Sand-Asphalt (with surcharge).

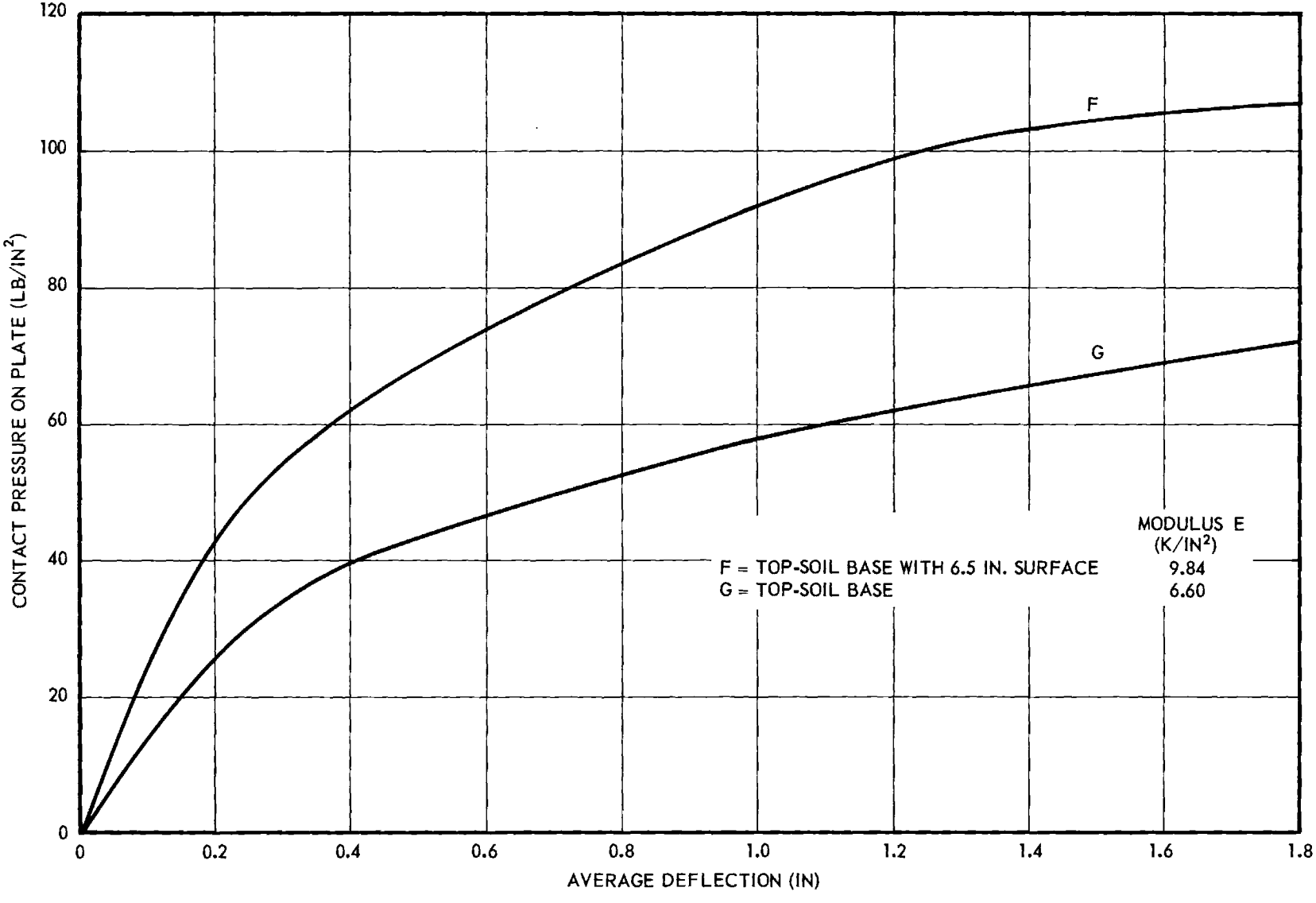

Figure 5. Plate Load Test Results: Top-Soil II.

CHAPTER III

PAVEMENT TESTS AND RESULTS

1. Pavement Systems Tested

The subgrade was the same micaceous sandy silt employed previously. The uppermost 37 inches was compacted to 95 per cent or more of the maximum density as given by ASTM D698-58T Method C; the remainder was compacted to 90 per cent.

Table I (below the solid line) lists the pavement systems tested in this program. The sand-asphalt base topsoil base systems are currently employed in road construction in Georgia and meet the Georgia State Highway Department specifications. The six inch thick soil cement base is not standard, but the construction of it followed current Georgia specifications. All were compacted to 100 per cent of the maximum density as given by ASTM D698-58T Method C.

2. Wheel Load Tests

Load tests were made on the pavement surface using single and dual tires, using the equipment instrumentation and procedure outlined in Chapters 3 and 4 of Annual Report 1. The depths and locations of the pressure measuring cells were changed slightly from those described in Report 1 in order to secure a better definition of stresses in the critical zone. These can be obtained from the individual graphs of test results.

The wheel load test data are presented in Figs. 6 to 36. They show the increase in the vertical normal stress in a horizontal plane, σ_z, in the soil, as measured by the pressure cells, as a function of the horizontal distance from the center of the load. Four graphs are given on each figure, each representing a different depth below the surface.

The theoretical stress distribution for each depth is shown by the curves on each graph. These are based on circular or rectangular loaded areas (p. 16,

Annual Report 1) and a uniform tire contact pressure computed from the contact area (Fig. 16 Annual Report 1 and Fig. 35 Annual Report 2). A single curve is given for the single tire. Two curves are given for the dual; the dashed curve represents stresses on a cross section midway between the tires and perpendicular to the axle; the solid curve represents stresses on a cross section parallel to and directly below the axles. The difference between the two curves is significant only immediately beneath the base course; and the greatest difference between the maximum stress in both directions is less than 5 per cent.

The theoretical stresses for all the bases were computed using the theory of a semi-infinite, homogeneous, isotropic elastic solid (Boussinesq). The theoretical stresses for the soil cement base were also computed assuming circular loaded areas and using the theory for a system consisting of two homogeneous, isotropic, elastic layers of infinite lateral extent, the upper of finite thickness with a modulus of elasticity of E_1, and the lower of infinite thickness with a modulus of elasticity of E_2, and a rough interface between the two layers. Stress curves for ratios of E_1/E_2 of 1, 10 and 100 are shown on the stress charts for the soil cement base. (Only the curves computed for the cross section perpendicular to the axles are shown for the dual loading on the soil-cement base.) The curves for the ratio $E_1/E_2 = 1$ are the same as those computed by the Boussinesq theory.

The measured stresses in the subgrade show appreciable scatter. Such scatter is to be expected because each point plotted represents a single stress reading rather than the average of several. Erratic readings, which appeared to be caused by malfunctioning of the pressure cells, were included unless there was specific evidence that the cell was faulty, so that the real variations of stress within the soil mass could be observed. It is the writers' opinion that

these variations are the combined result of differences in soil density, moisture, and rigidity and the way in which the load is applied. They represent the real range in stress variations to be expected in a subgrade rather than the fictitious but prettier results of averaging. Averaging the individual readings for each test run as was done in the Waterways Experiment Station work and similar tests elsewhere will produce less scatter but will somewhat obscure the meaning of the data.

3. Sand Asphalt Base With Overlay

The stresses in the subgrade beneath the overlaid pavement system employing the sand-asphalt subgrade are given in Figs. 6 to 11. The subgrade stresses for the same pavement system without the overlay are given in Figs. 29 to 34 of Annual Report 2. The overlay was 3 inches thick and of asphaltic concrete, making the total asphaltic surface six inches thick. No attempt was made to develop bond between the two surfaces, other than thorough sweeping, but the cored samples did not separate easily along the joint.

The stresses in the subgrade with the overlay are substantially lower than those without. They are 20 to 50 per cent higher than the theoretical stresses as computed by the Boussinesq theory for semi-infinite homogeneous, isotropic elastic solids. A similar excess (and slightly greater excess for the single tires) over the Boussinesq was observed in the same system without the overlay. This was explained in Annual Report 2 by the stress concentration produced in materials whose modulus of elasticity increases with increased confining pressure. Therefore, a similar excess was to be expected in the overlay system. The smaller degree of excess for the single tires with the overlay can be explained by the fact that the sand asphalt base without overlay (8 inch base + 3 inch surface)

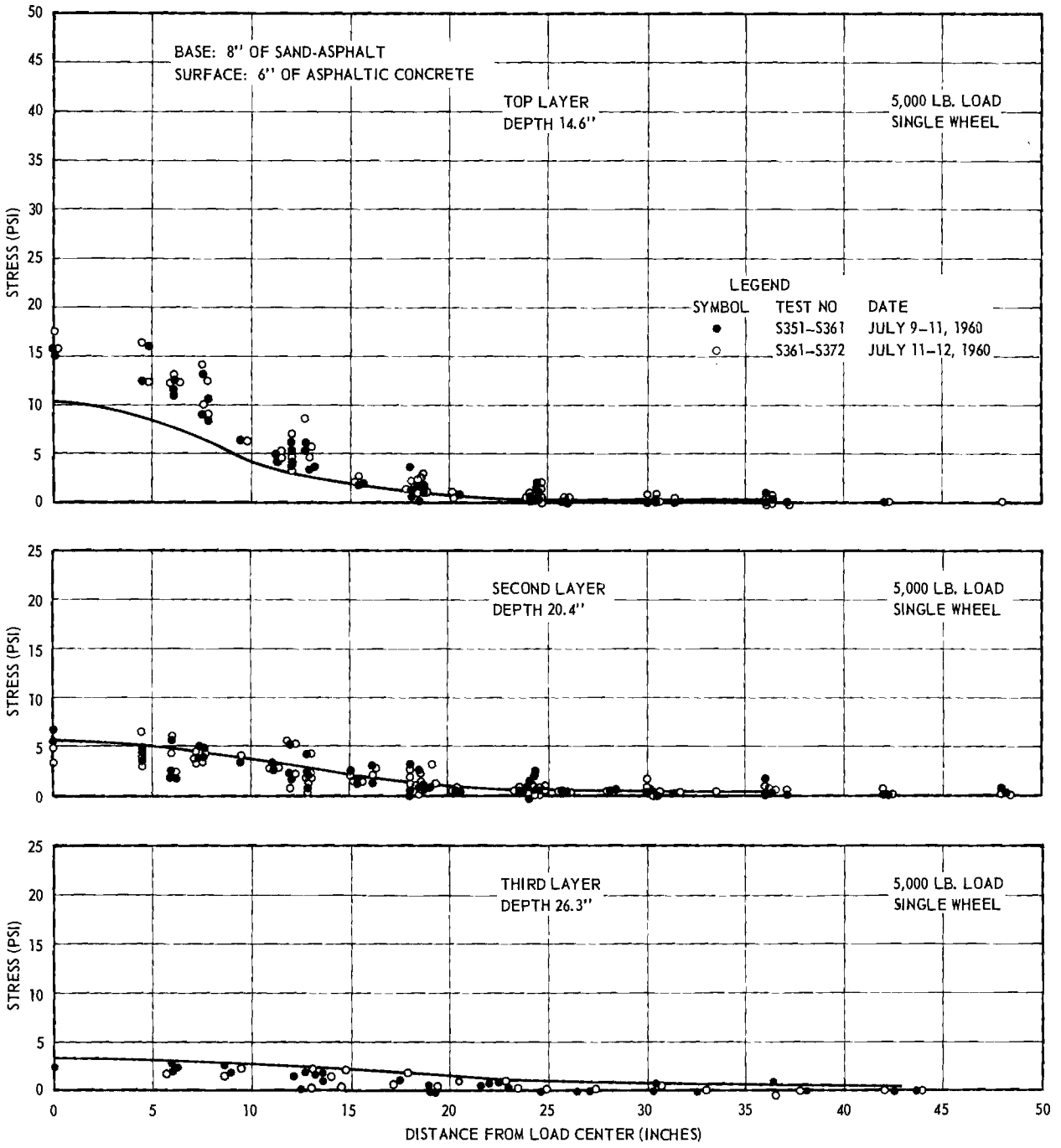

Figure 6. Measured Stresses: Single Load 5,000-lb Sand-Asphalt Base with Overlay.

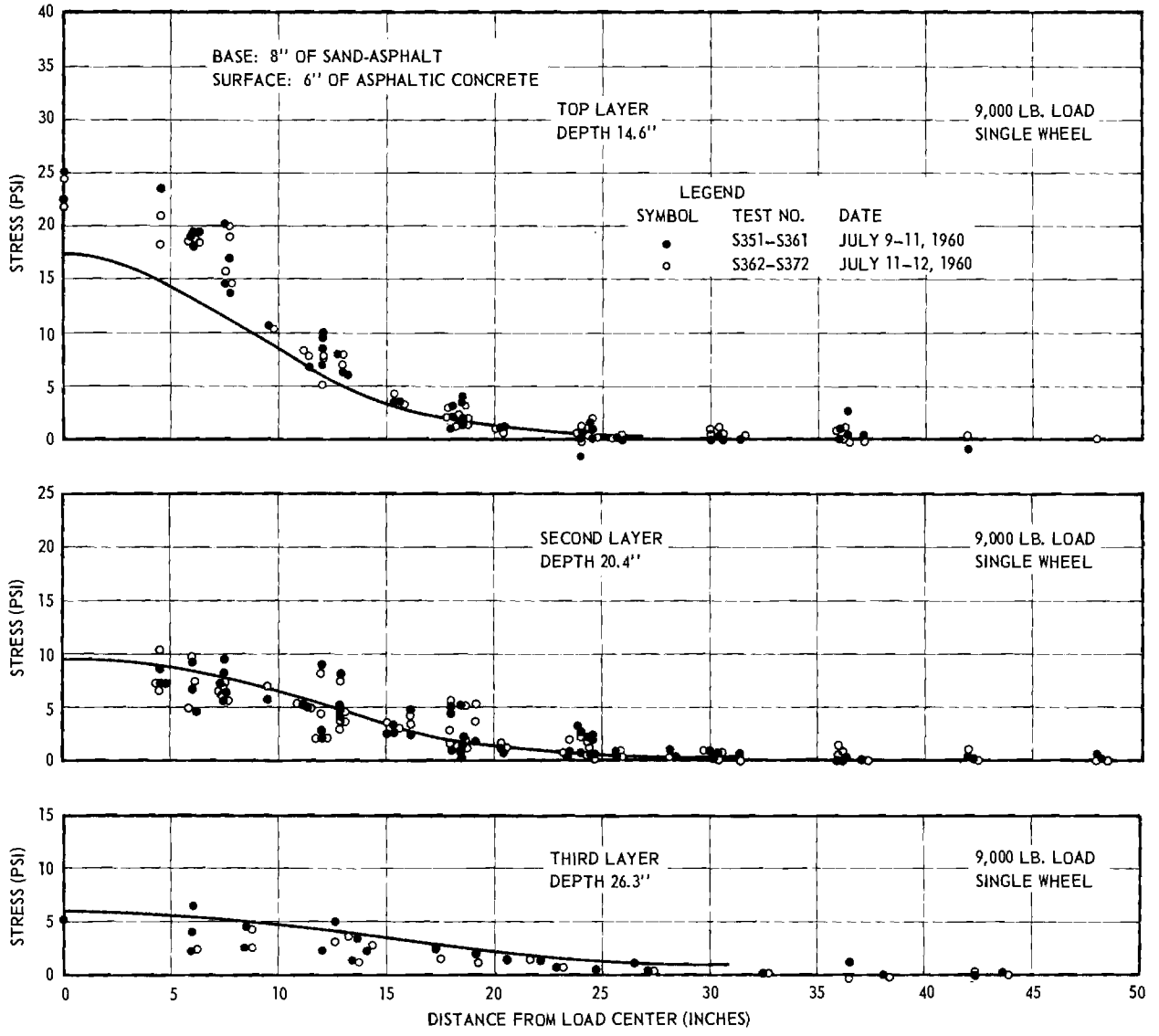

Figure 7. Measured Stresses: Single Load 9,000-lb Sand-Asphalt Base with Overlay.

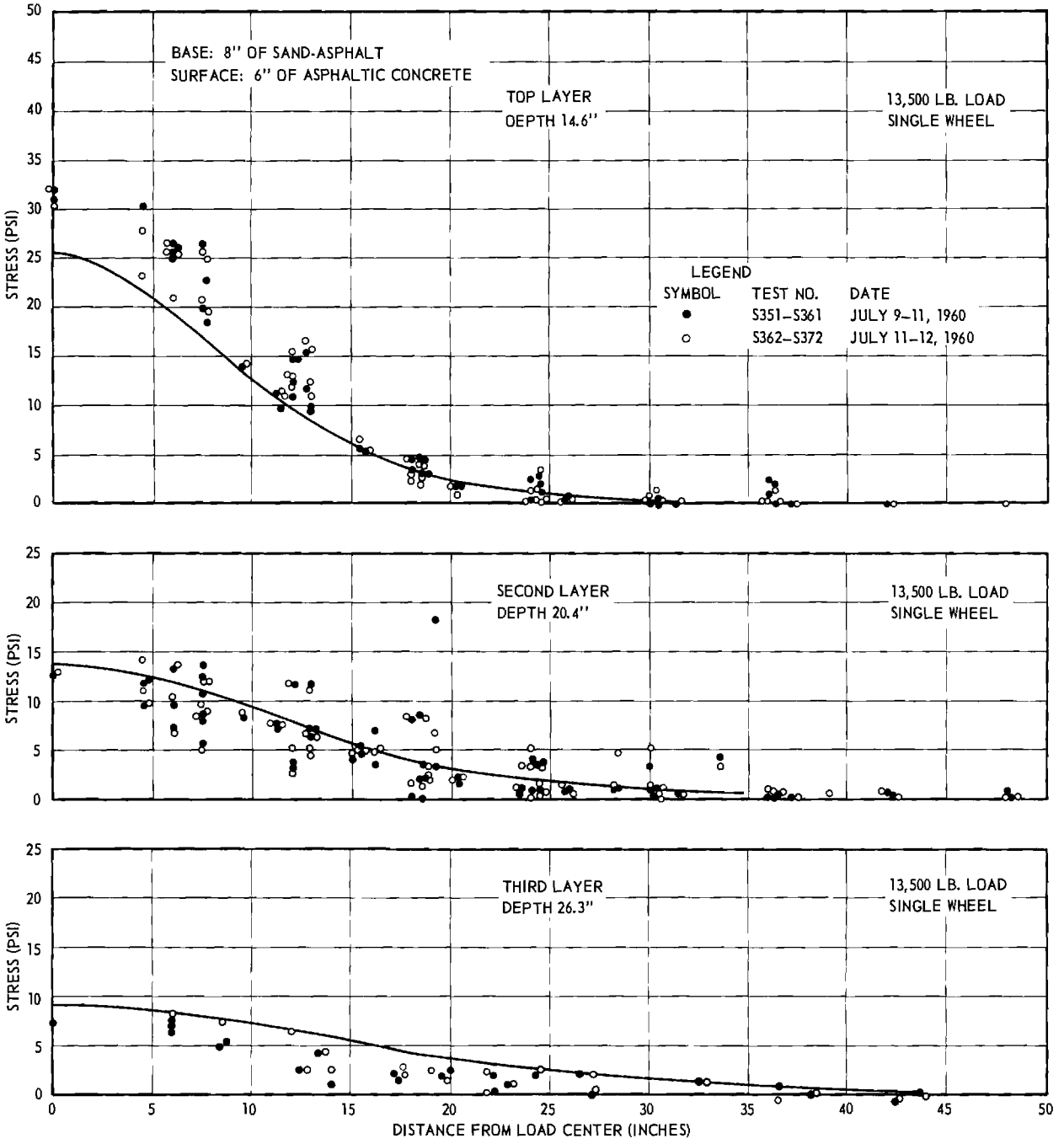

Figure 8. Measured Stresses: Single Load 13,500-lb Sand-Asphalt Base with Overlay

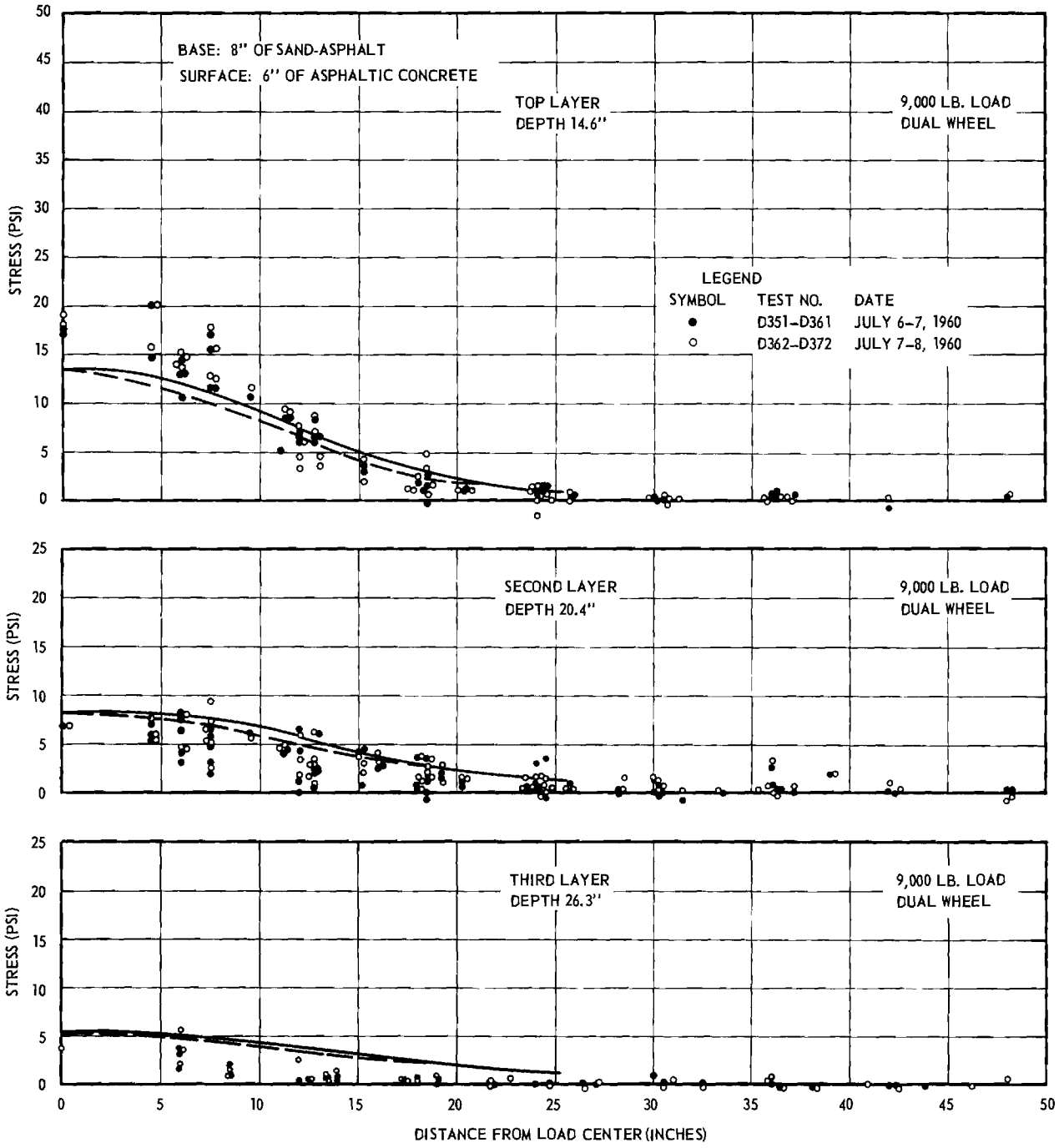

Figure 9. Measured Stresses: Dual Load 9,000-lb Sand-Asphalt Base with Overlay.

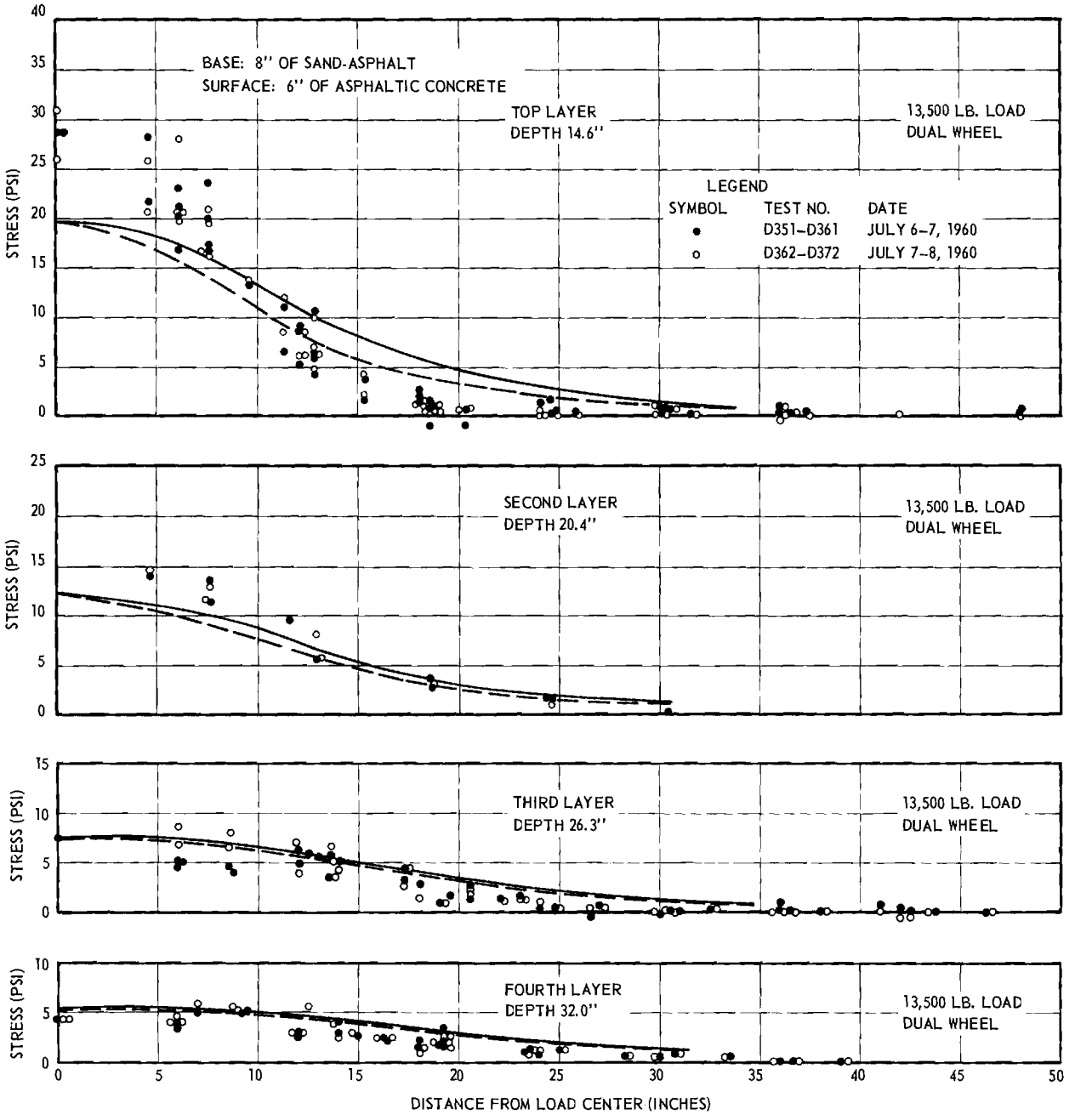

Figure 10. Measured Stresses: Dual Load 13,500-lb Sand-Asphalt Base with Overlay.

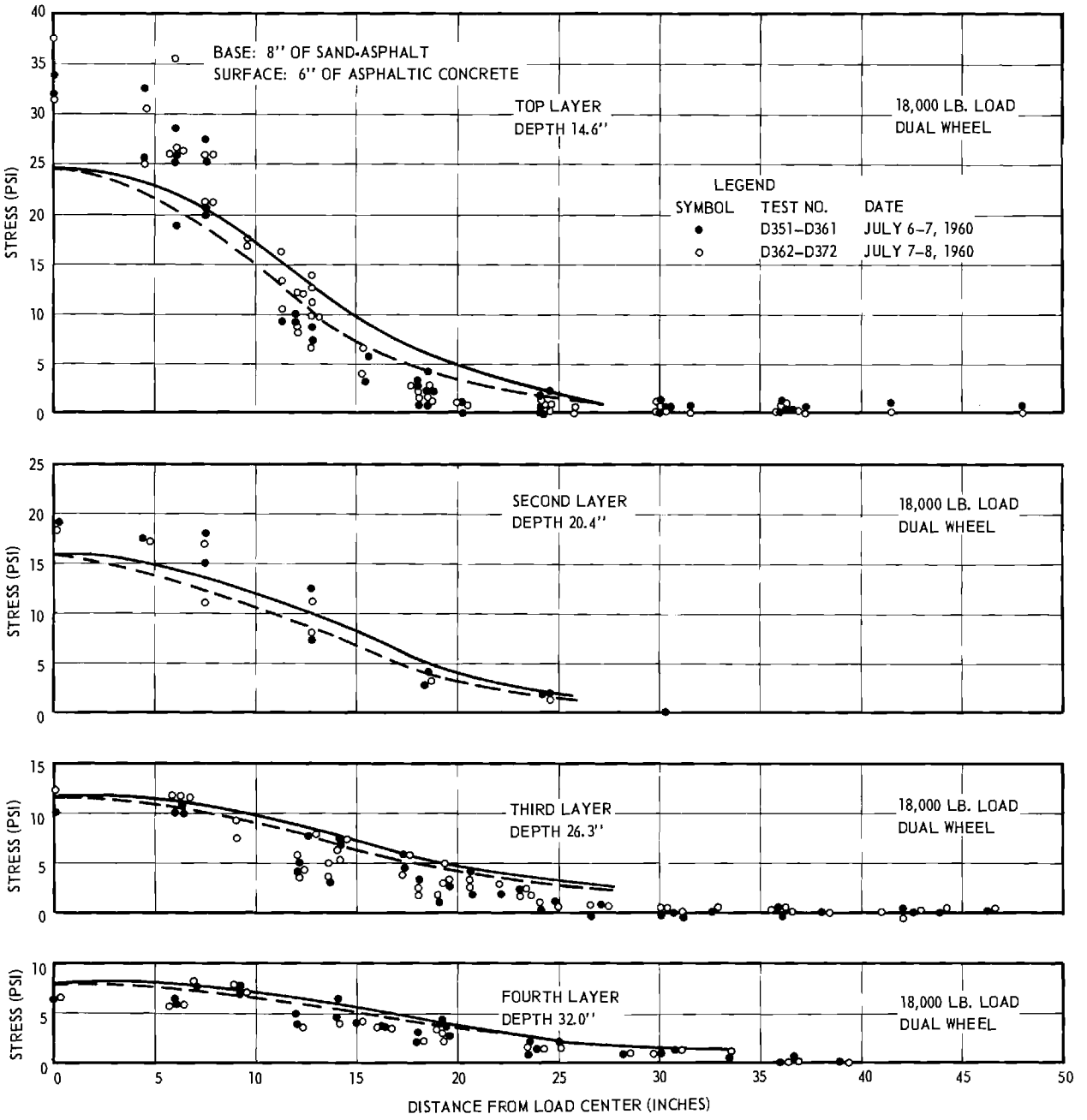

Figure 11. Measured Stresses: Dual Load 18,000-lb Sand-Asphalt Base with Overlay.

comprises 73 per cent of the total pavement thickness while with the 3 inch overlay the sand-asphalt is 57 per cent of the total.

The stress reduction produced by the 3-inch overlay is slightly less than that produced by an equal thickness of a homogeneous, isotropic elastic soil. This also is to be expected because the asphaltic overlay more nearly resembles the sand asphalt base in its elastic properties than it does a homogeneous isotropic elastic soil.

4. Topsoil Base Without Overlay

Because a different topsoil base was necessary in the overlay tests than was used in the original tests without overlay, the new topsoil-base pavement was tested first without overlay. The results are given in Figs. 12 to 14. The stresses immediately under the base and directly under the tire are slightly greater in the subgrade than those computed by the Boussinesq; the remainder are approximately equal to the Boussinesq. The pavement system composed of layers, each with a different modulus of elasticity, distributed the wheel load in approximately the same way as a homogeneous isotropic elastic solid.

5. Topsoil Base With Overlay

A 3-1/2-inch thick hot mix asphaltic concrete overlay, identical with the first 3-inch surface, was constructed over the topsoil-base pavement system. The stresses in the subgrade produced by wheel loads on the new surface are given in Figs. 15 to 20. They are substantially less than those found at the same points in the subgrade without the overlay.

The stress distribution in general follows the Boussinesq but the maximum stress is slightly higher. In other words the 3-inch overlay is not quite as effective in spreading the stress as would be on equal thickness of a homogeneous soil (or the topsoil base). This is not unexpected, because the modulus

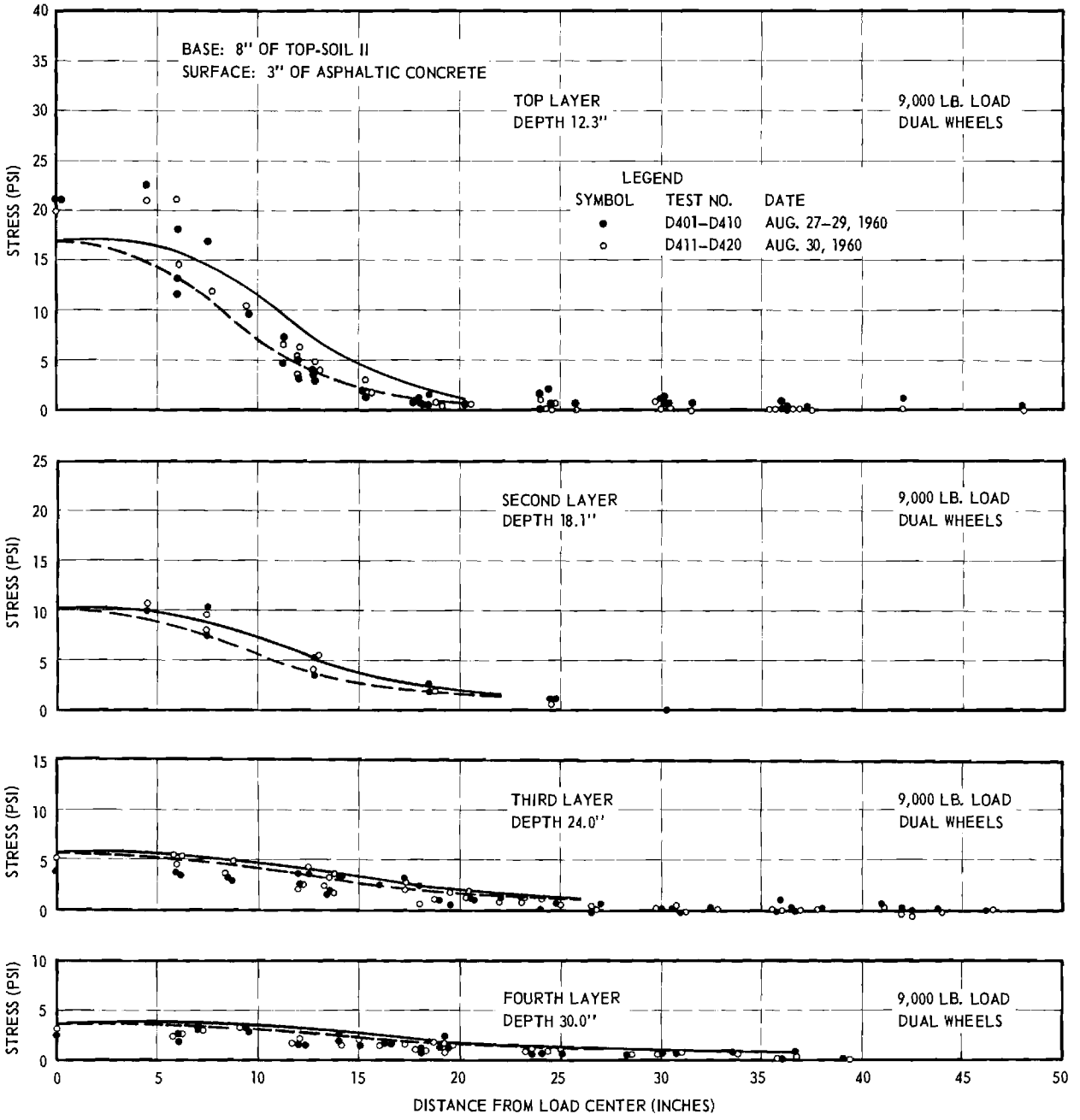

Figure 12. Measured Stresses: Dual Load 9,000-lb Top-Soil II Base.

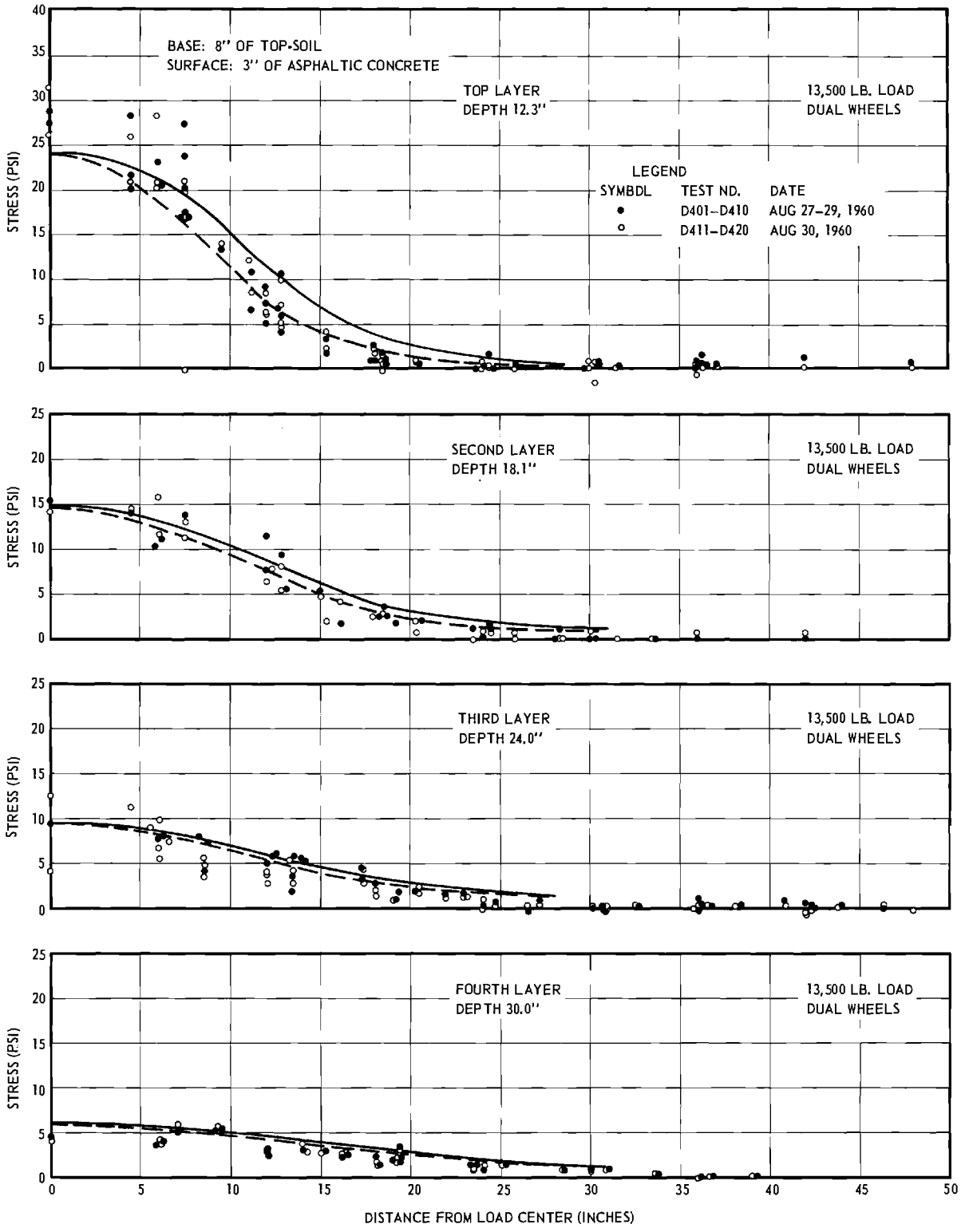

Figure 13. Measured Stresses: Dual Load 13,500-lb Top-Soil II Base.

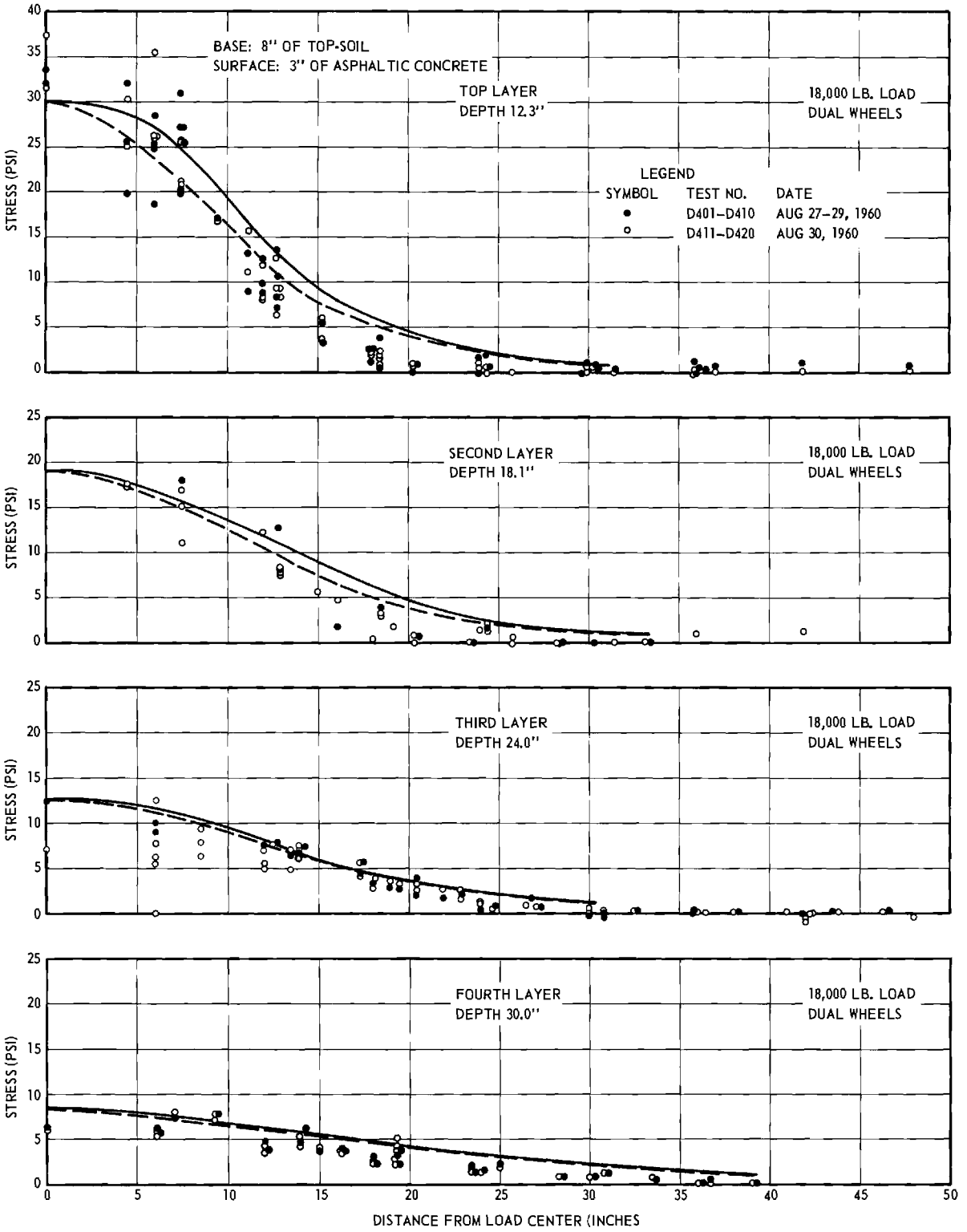

Figure 14. Measured Stresses: Dual Load 18,000-lb Top-Soil II Base.

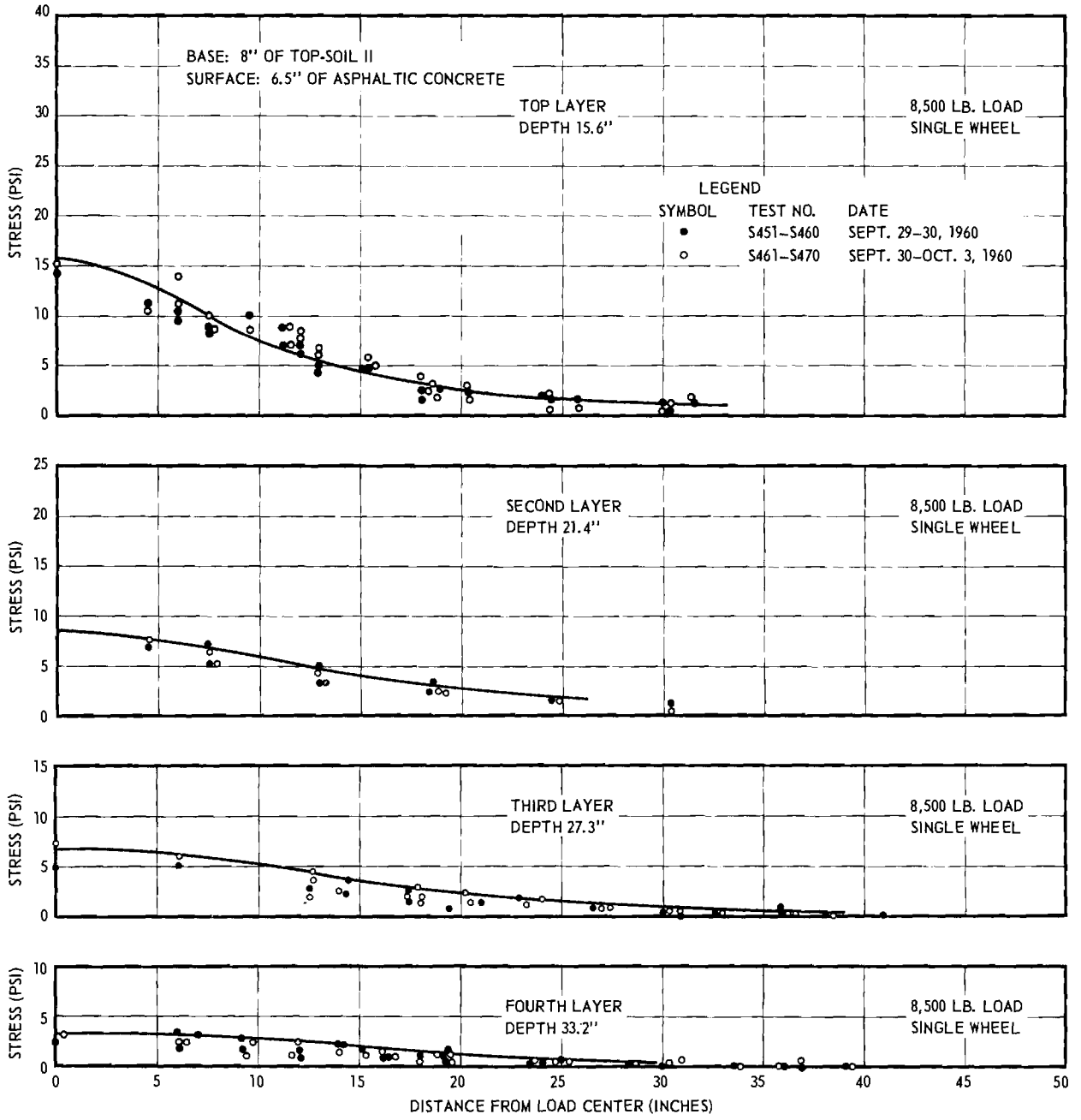

Figure 15. Measured Stresses: Single Load 8,500-lb Top-Soil II Base with Overlay.

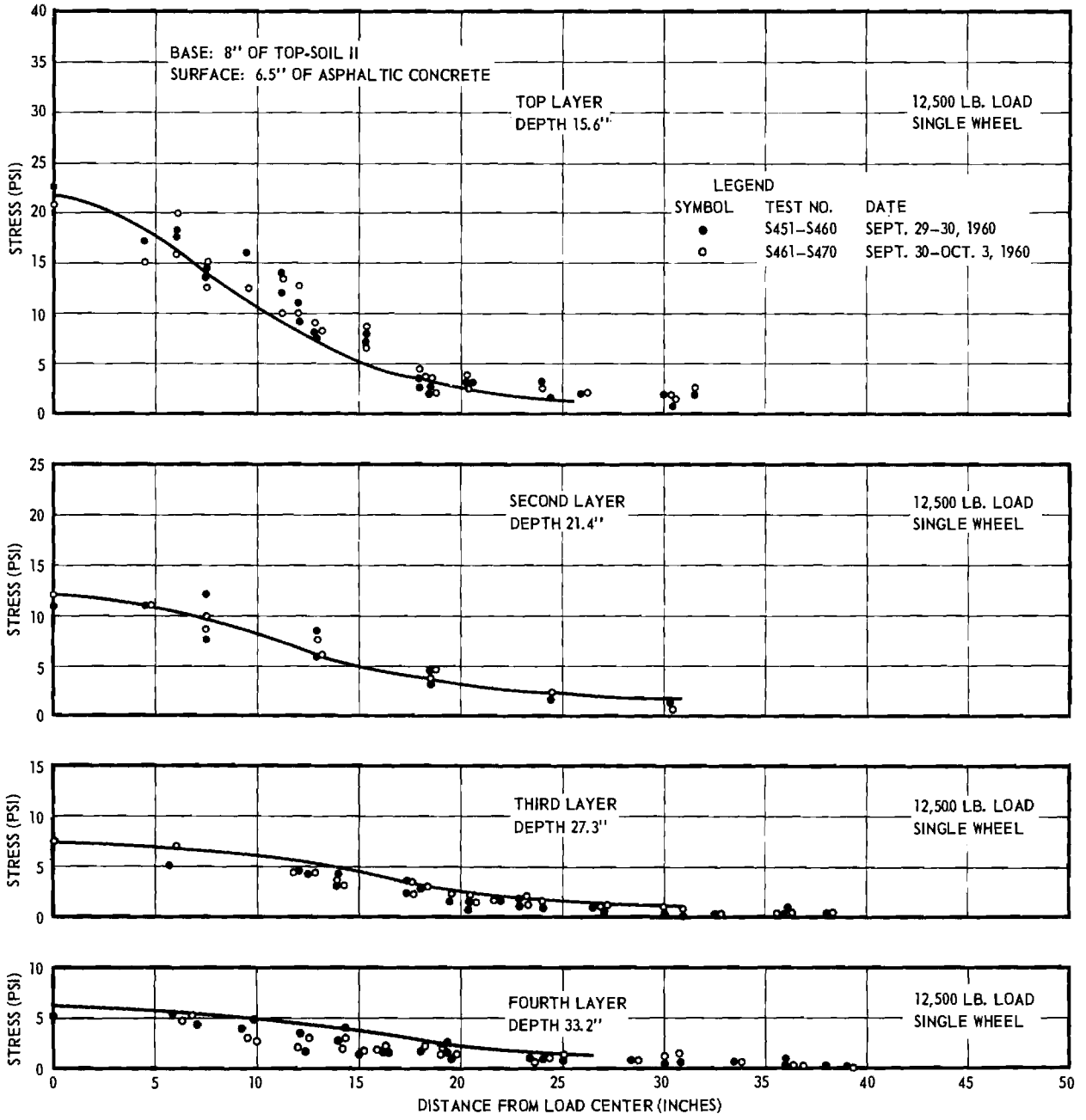

Figure 16. Measured Stresses: Single Load 12,500-lb Top-Soil II Base with Overlay.

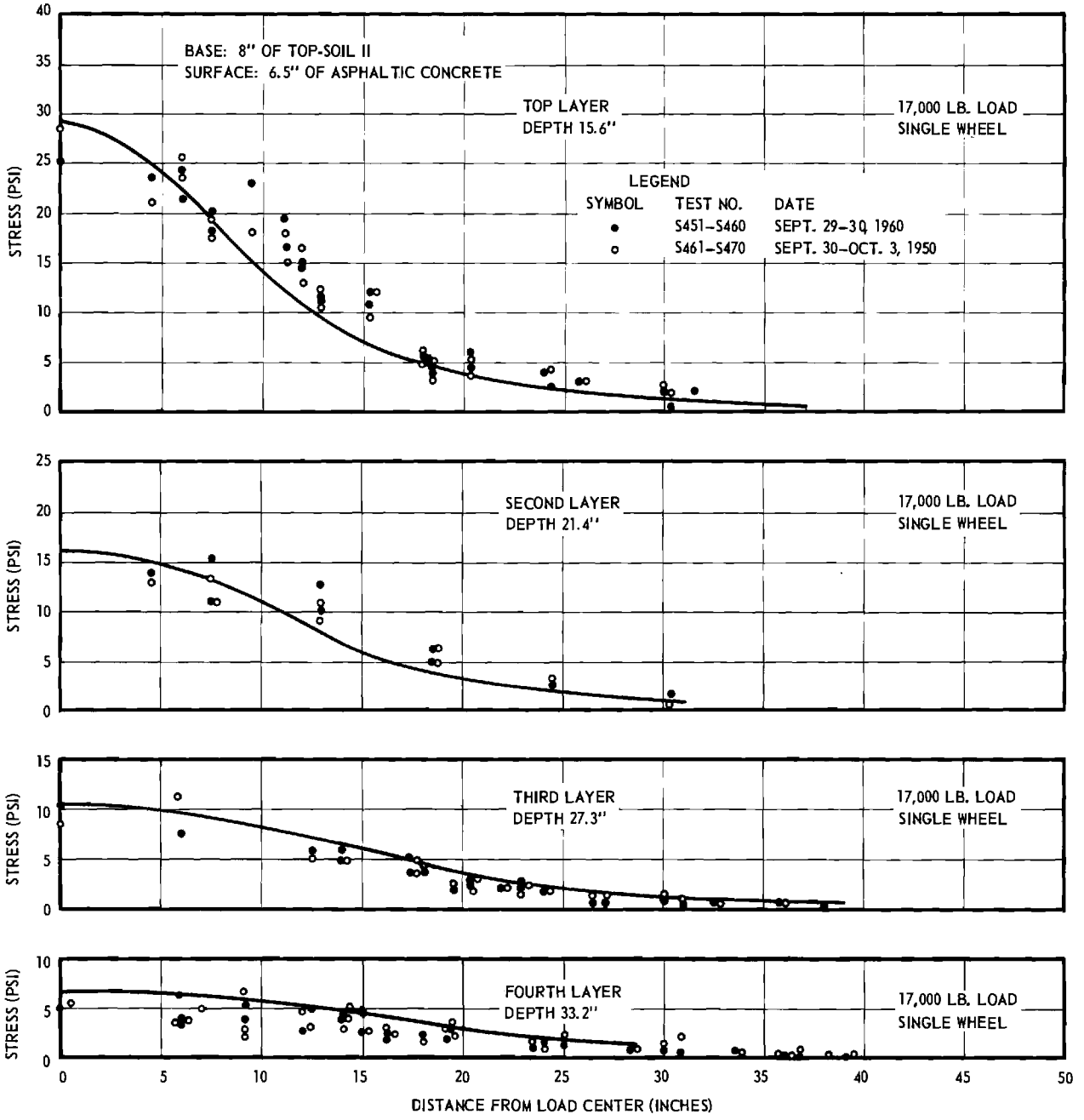

Figure 17. Measured Stresses: Single Load 17,000-lb Top-Soil II Base with Overlay.

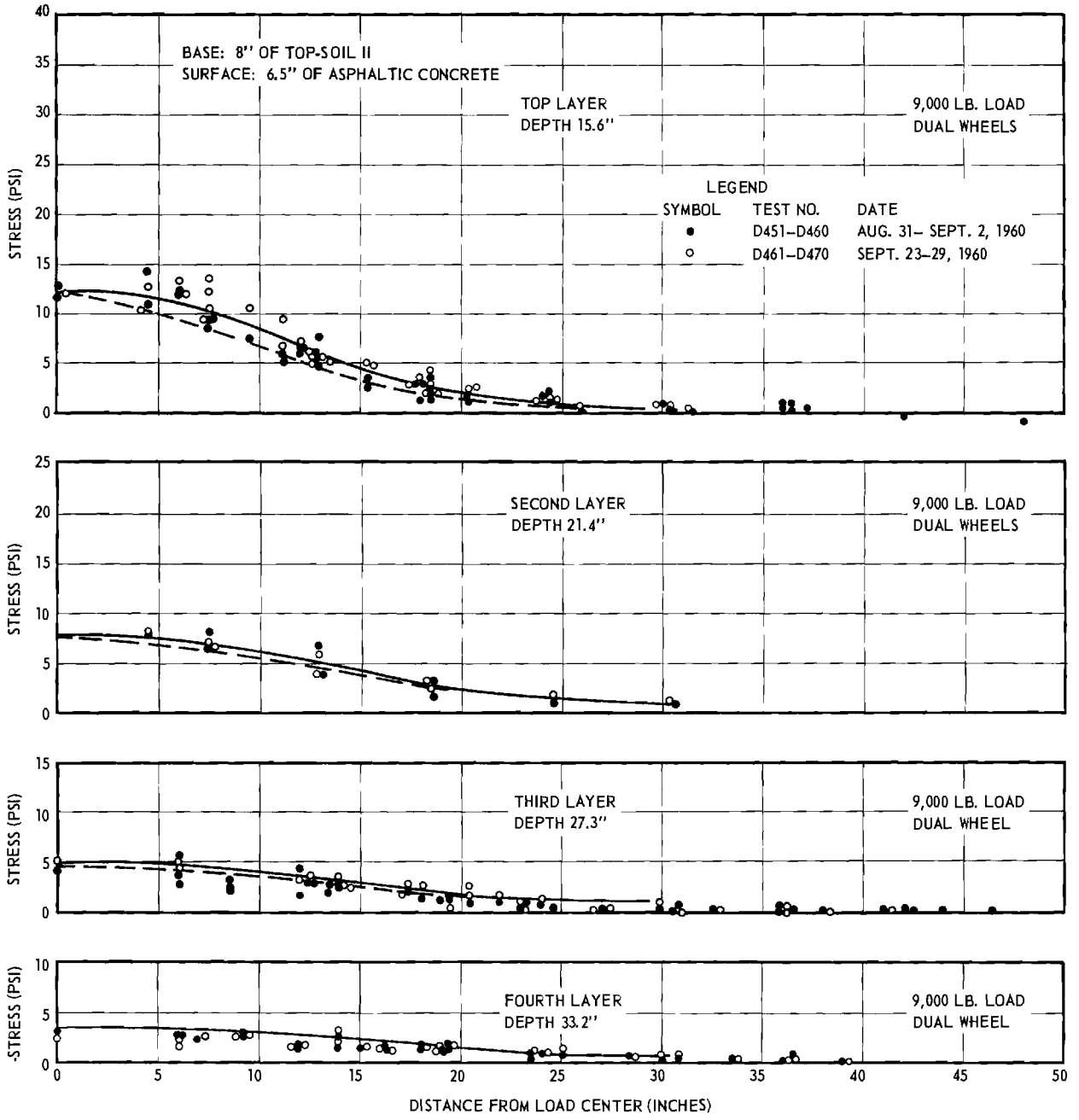

Figure 18. Measured Stresses: Dual Load 9,000-lb Top-Soil II Base with Overlay.

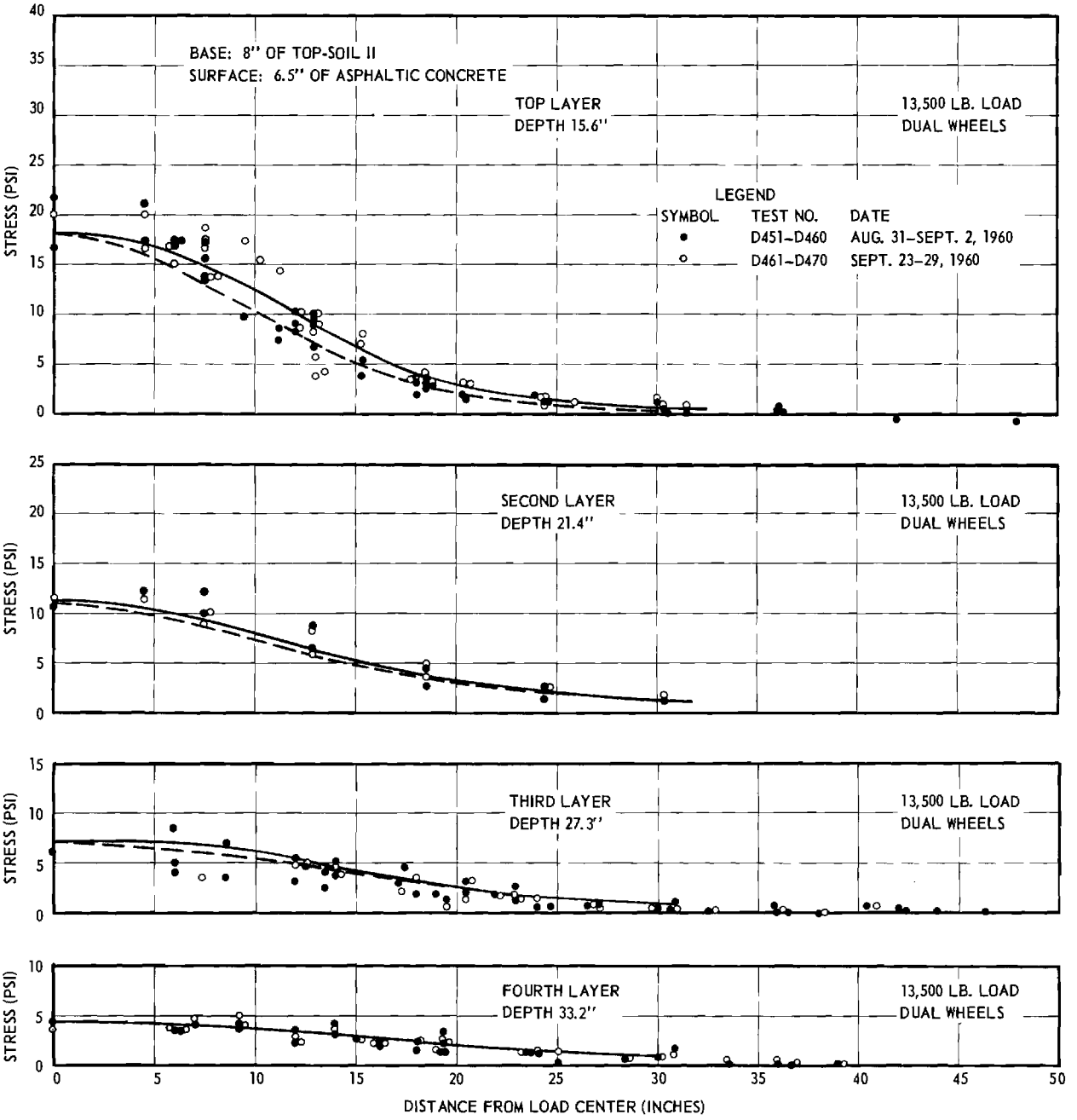

Figure 19. Measured Stresses: Dual Load 13,500-lb Top-Soil II Base with Overlay.

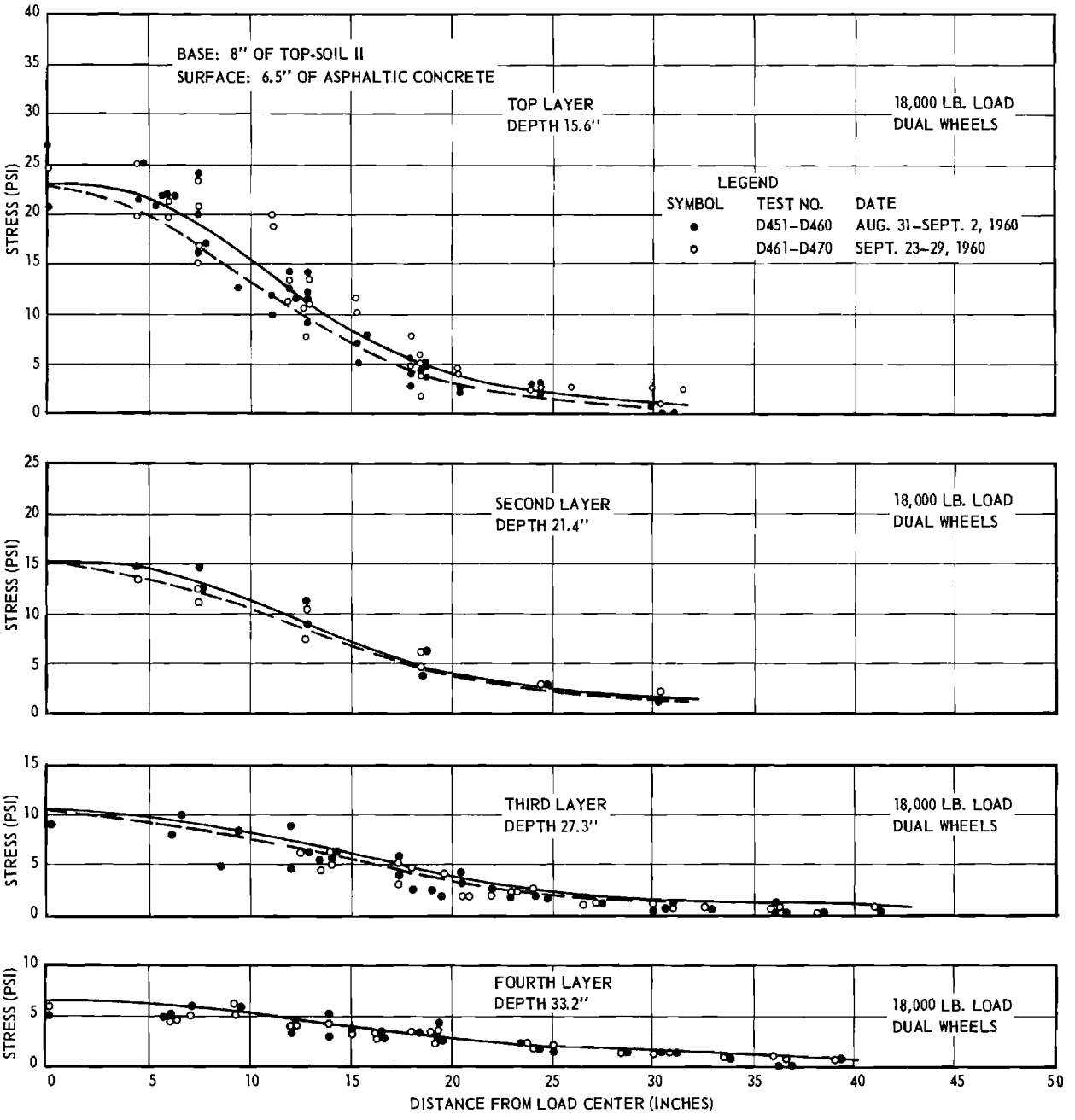

Figure 20. Measured Stresses: Dual Load 18,000-lb Top-Soil II Base with Overlay.

of elasticity of the surface course increases somewhat with increased confining pressure. This leads to stress concentrations similar to those observed in the sand-asphalt. However, it must be concluded that overlaying an existing pavement is a very effective way of reducing stresses in the soil subgrade.

6. Soil Cement Without Overlay

Since it was necessary to construct a new soil-cement pavement for the overlay tests it was decided to check the effectiveness of a 6 inch thick base rather than the 8 inch previously tested. Therefore, it was necessary to make new tests of the pavement system without the overlay to serve as a basis for direct comparison. The new pavement was constructed in the same way as the original one except for the 6-inch base thickness. The same mixture of 40 per cent topsoil and 60 per cent 467 stone plus 4 per cent (of the total dry weight) of Type 1 portland cement was employed.

The test results are given in Figs. 21 to 26. The stresses in the subgrade immediately beneath the pavement are considerably less than those observed beneath the other base courses and are about one half of those found at the same depth beneath the topsoil or soil-bound Macadam bases. These results are similar to those of the tests on the pavement employing the 8 inch soil cement base, but of course the degree of the stress reduction in this case is less because of the thinner base.

Computations were made of the stresses in the pavement using the two layer theory, as described in Annual Report 1, p. 13 - 15. In these theoretical analyses it was assumed that the soil cement base and the asphaltic surface were one homogeneous layer having the elastic properties of the soil cement. This, admittedly is not strictly correct, because the asphaltic concrete is not as rigid as the soil cement and it certainly does not have the same ability

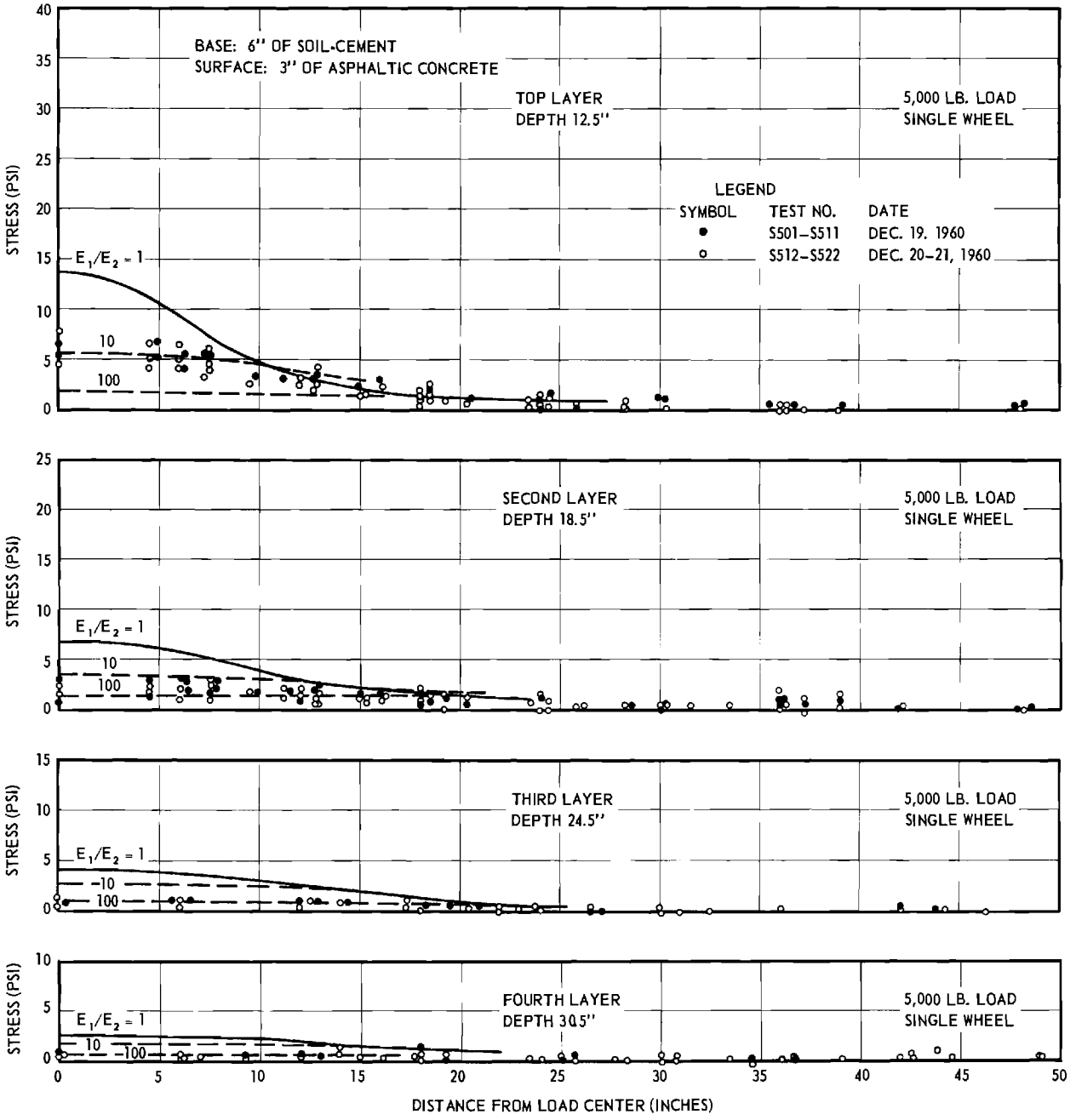

Figure 21. Measured Stresses: Single Load 5,000-lb 6" Soil-Cement Base.

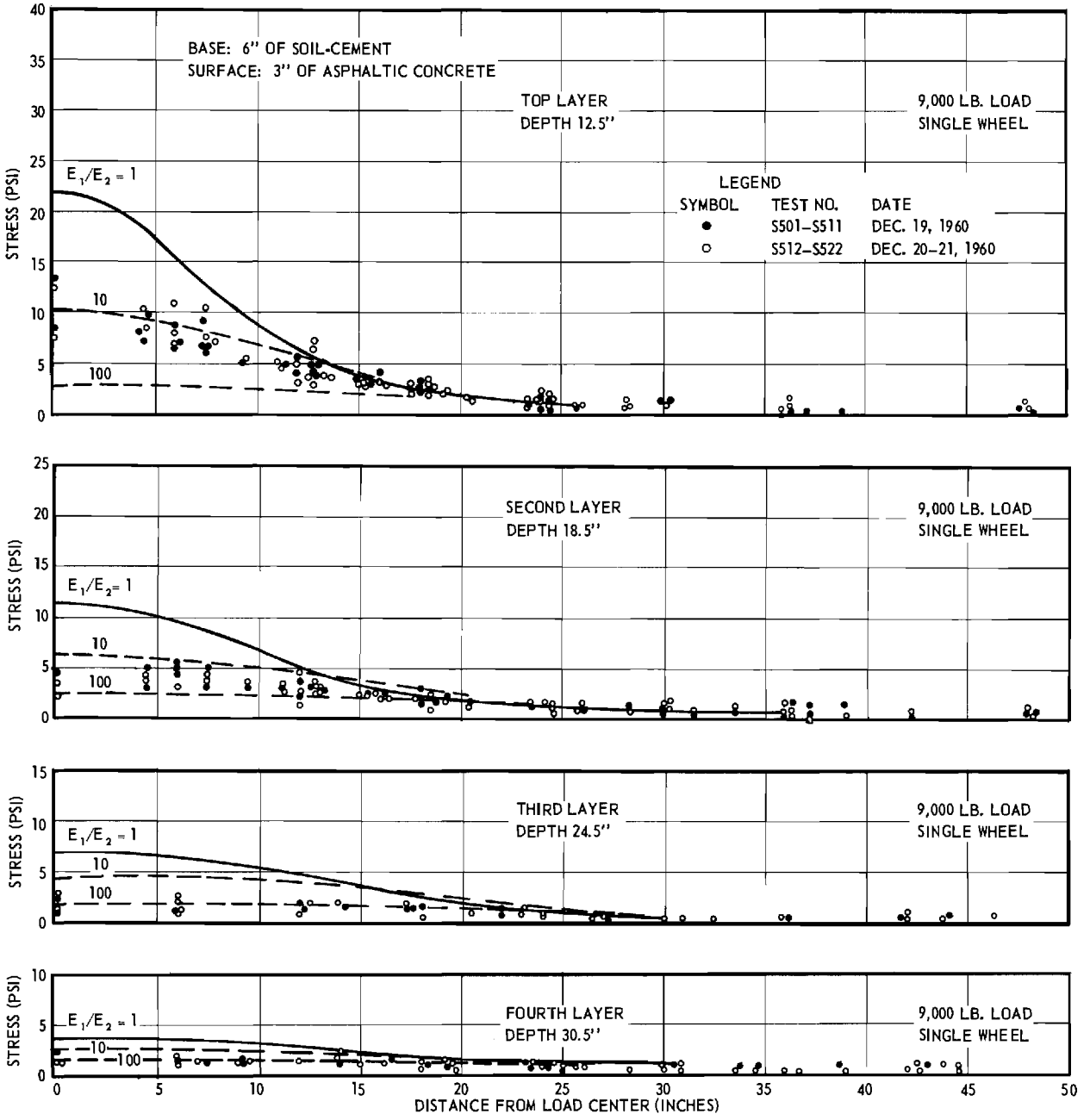

Figure 22. Measured Stresses: Single Load 9,000-lb 6" Soil-Cement Base.

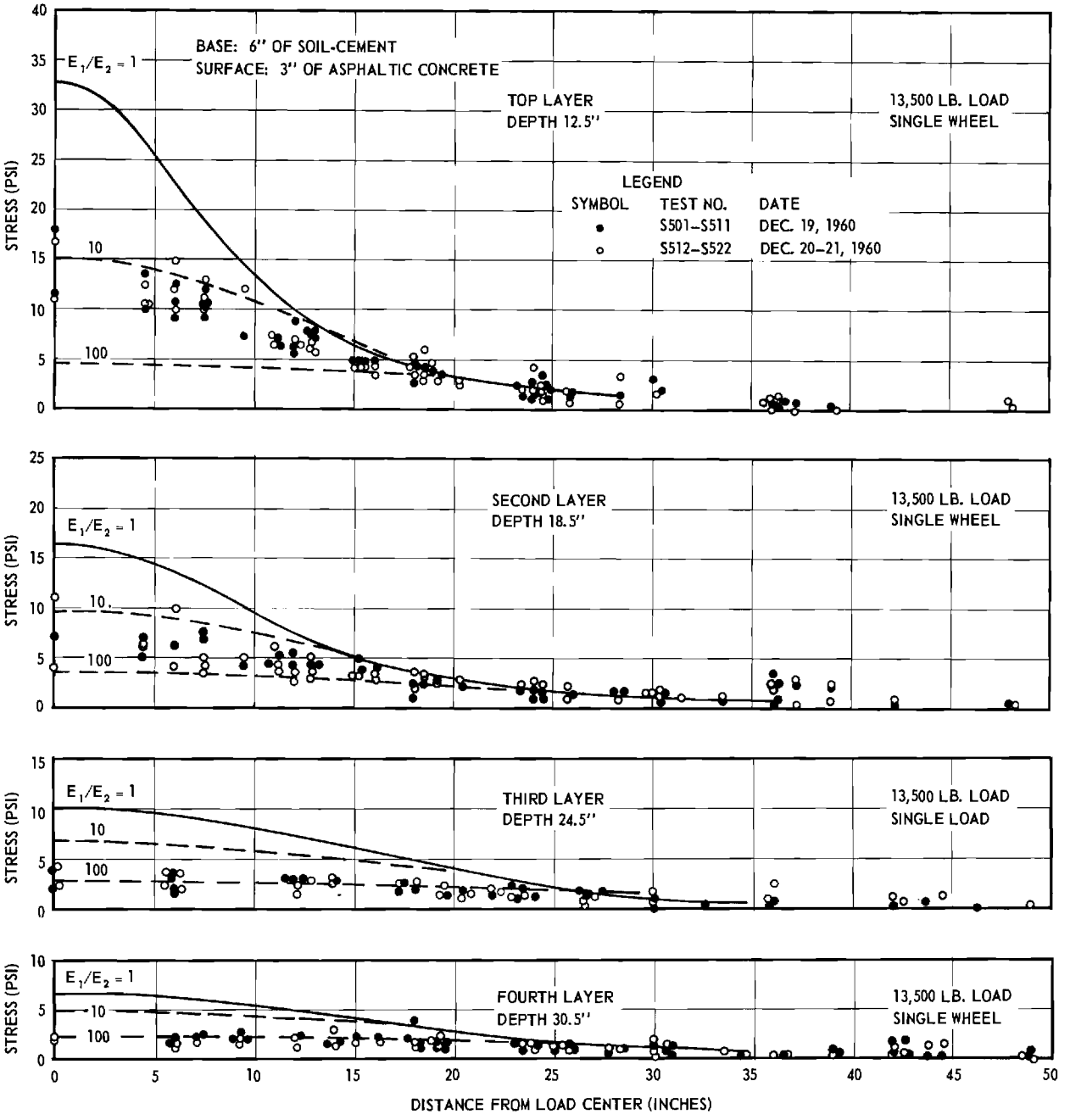

Figure 23. Measured Stresses: Single Load 13,500-lb 6" Soil-Cement Base.

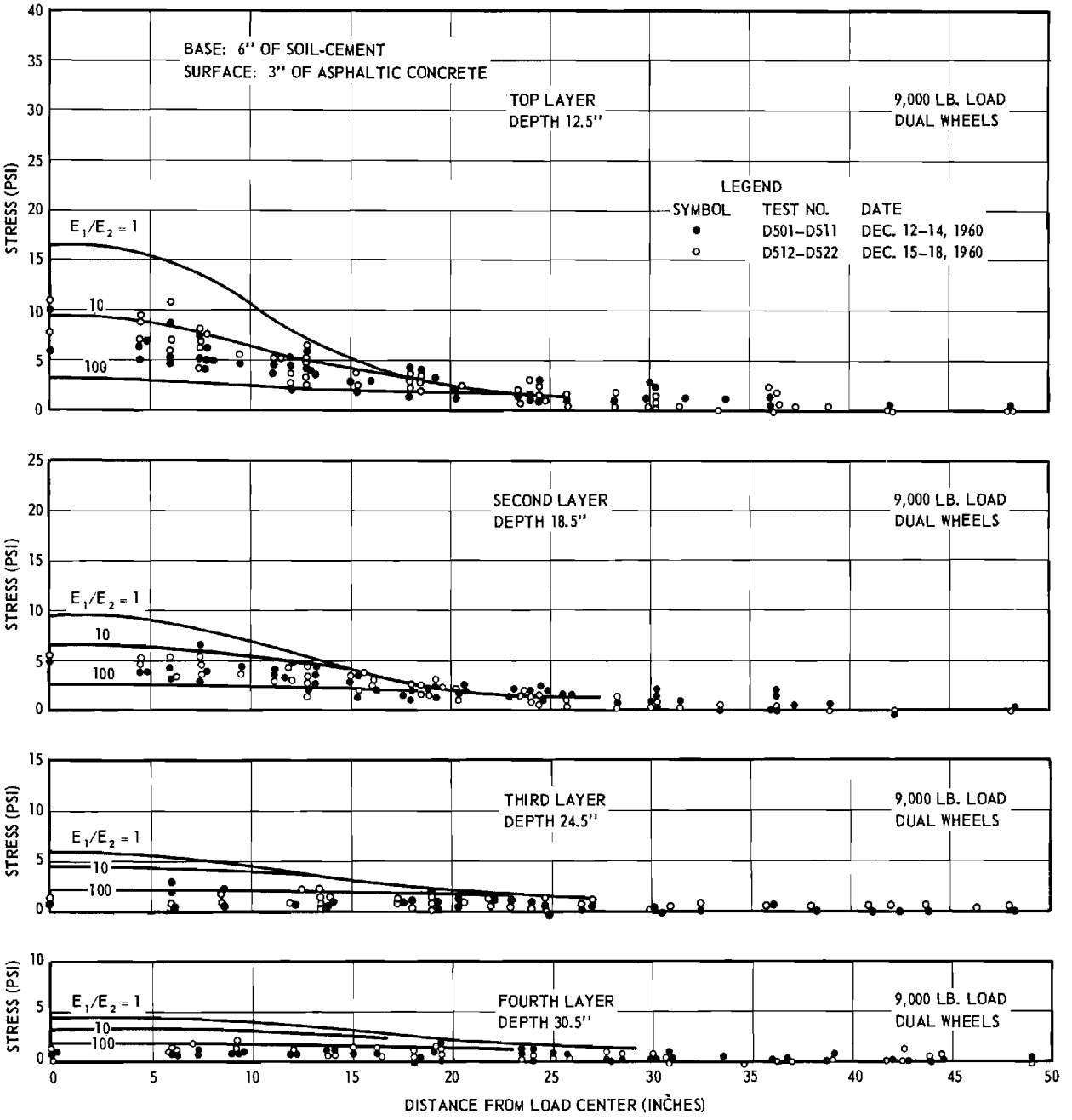

Figure 24. Measured Stresses: Dual Load 9,000-lb 6" Soil-Cement Base.

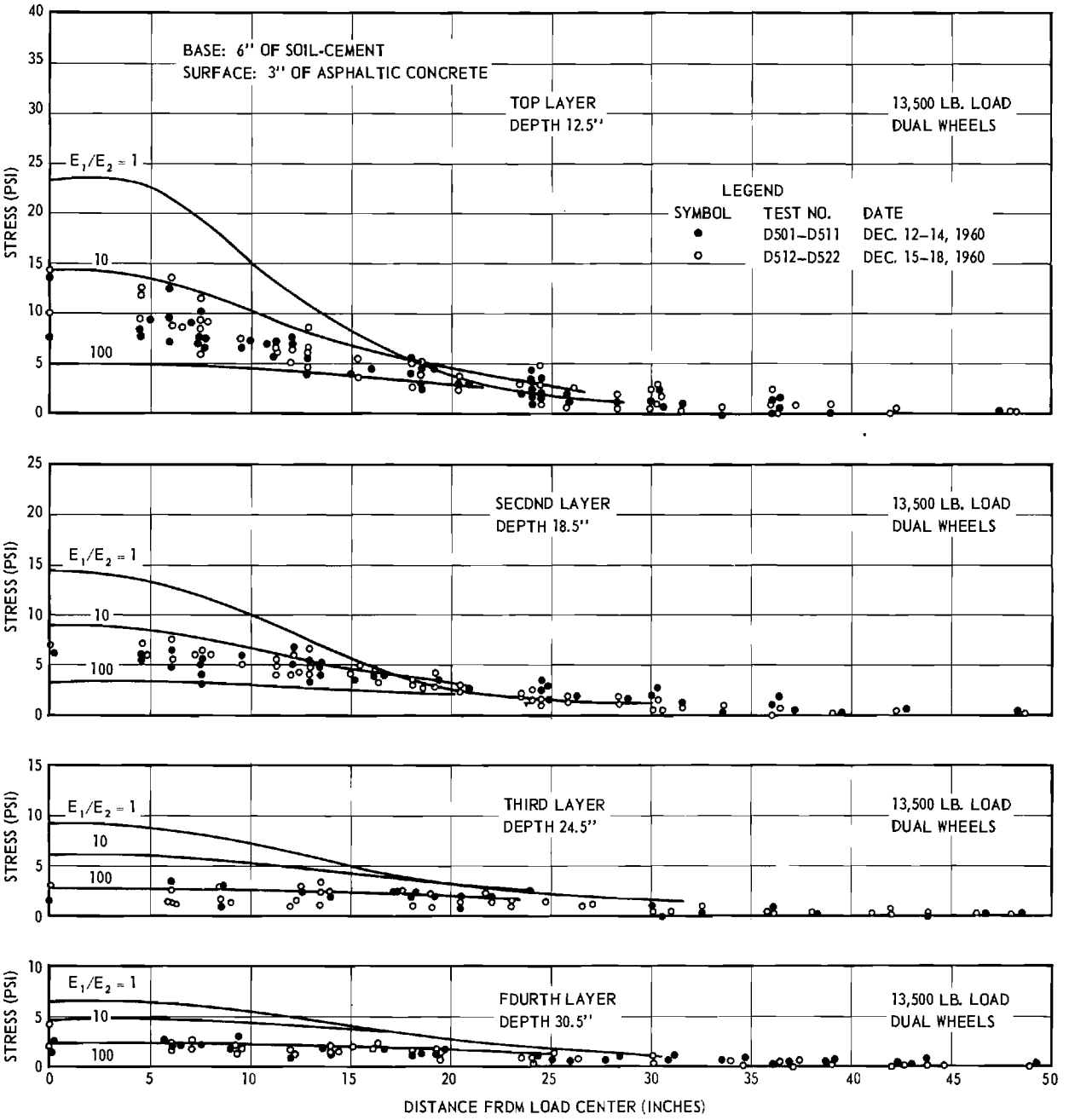

Figure 25. Measured Stresses: Dual Load 13,500-lb 6" Soil-Cement Base.

to resist tension as the soil cement. However, the soil cement is in the lower part of this combined layer where the greatest tensile stresses develop while the asphaltic surface is in the compression zone (immediately below the wheel) so at least a part of the theoretical objections to the use of a single layer to represent the surface and base is answered. The theoretical curves for a ratio of elastic moduli, $\frac{E_1}{E_2}$ (upper layer to lower layer) of 10 and 100 are plotted. (The curves for the ratio of elastic moduli of 1 are the same as the Boussinesq stress distribution.)

A comparison of the observed stresses with the theoretical shows that immediately beneath the base the points lie between the curves $\frac{E_1}{E_2} = 10$ and $\frac{E_1}{E_2} = 100$, but closer to $\frac{E_1}{E_2} = 10$. The tests of the 8 inch thick base system found stresses in the same range but closer to $\frac{E_1}{E_2} = 100$. The ratio of elastic moduli measured by laboratory tests on the base and subgrade, and by plate load tests of both (see Annual Report 2) was of the order of magnitude of 100. The tests of the 8 inch-base fit this ratio reasonably well in spite of the simplification employed in analysis of considering the less rigid surface and the more rigid base as one. With the 6-inch base, the error was greater because the less rigid surface is a greater percentage of the whole; and this confirmed by the observed stresses. In fact if a weighted average of the elasticities of the surface and base is used in the theoretical computations, the results are not greatly different than the observed stresses.

7. Soil Cement With Repeated Load

The 6 inch soil cement base with the 3 inch asphaltic surface was subjected to repeated loading and unloading to determine the effect of fatigue or progressive failure from overloading on its ability to spread a load. A single wheel load of 13,500 lb (axle load of 27,000 lb) was selected because it induces

a relatively high stress in the surface but a lower stress in the subgrade than the 18,000 lb dual tire arrangement with its 9,000 lb load on each tire. In this way the effect of any progressive cracking in the base could be observed without the risk of obscuring it with progressive failure of the subgrade.

The loading and unloading was conducted with the wheel in one position so as to concentrate the stress repetition. Whether this is more or less severe on the pavement than the repeated stress induced by moving wheels has not been established by any tests. The moving wheel would tend to exaggerate any stress reversals produced by the unloading, but on the other hand any two successive load repetitions would not re-stress exactly the same point to the same degree. In our opinion the fixed position repetition is at least as severe as that induced by moving loads.

The load - unload cycle occupied about 20 seconds: loading, 16 seconds and unloading 4 seconds. This is probably more severe than the loading imposed by a moving truck because greater time is allowed for soil consolidation, creep and plastic flow.

The regular load - load sequence was interrupted after progressively larger numbers of repetition's to measure the stresses: 1, 10, 100, 300, 1000, and 3000 cycles. The stress was measured before loading (after an interval of 30 min from the previous cycle) during the load application, and 30 seconds and 30 minutes after the load was released. Following the stress measurement cycle, the regular 20 second cycles of load-unload were resumed.

There was a slight progressive increase in the zero reading of some of the pressure cells as measured 30 minutes after the release in the load. Possibly this represents a build up of residual stress in the subgrade due to repeated loading. Such a build up was observed by Whitaker at the Road Research Laboratory

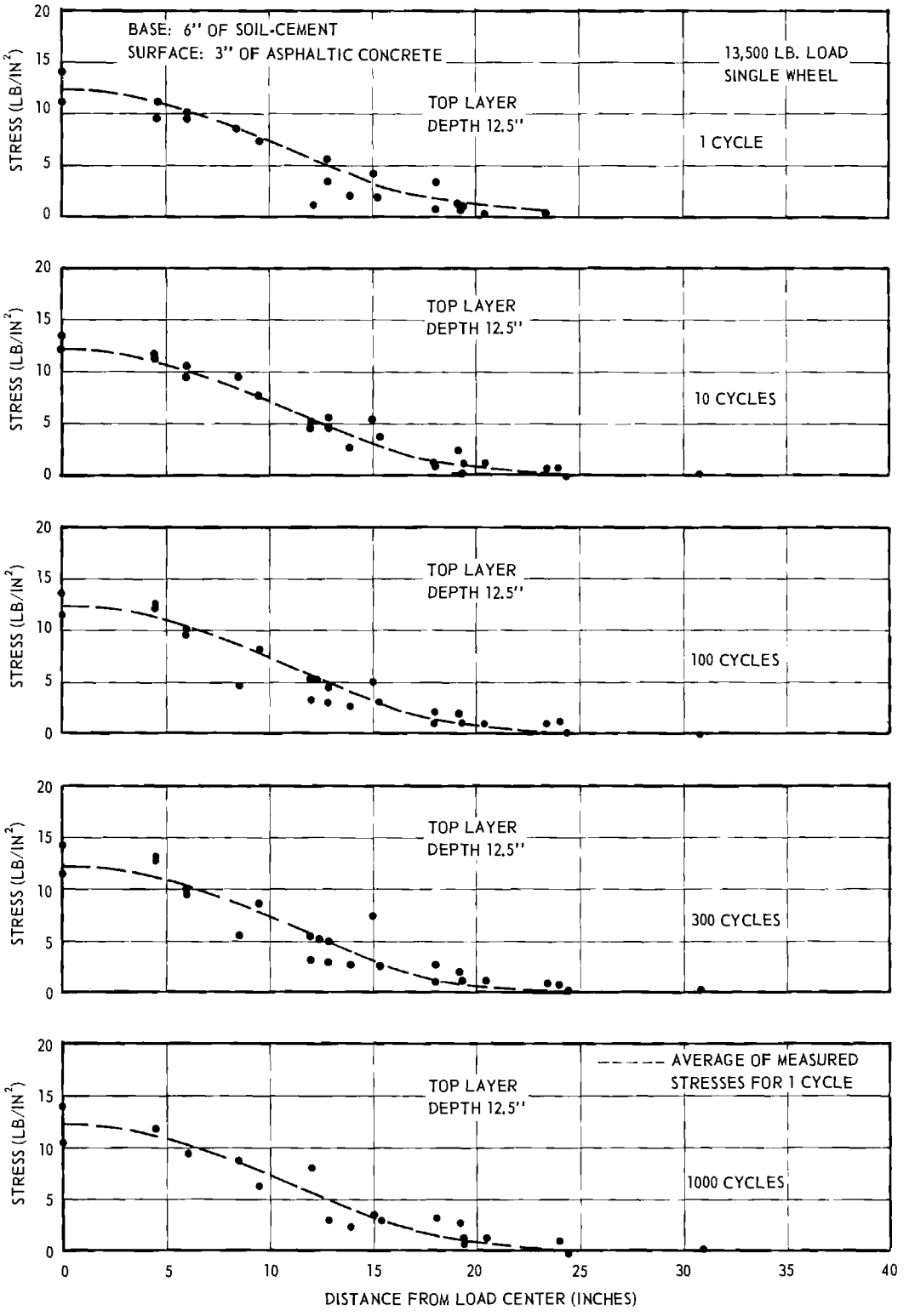

Figure 27. Measured Stresses: Repeated Single Load 13,500-lb 6" Soil-Cement Base.

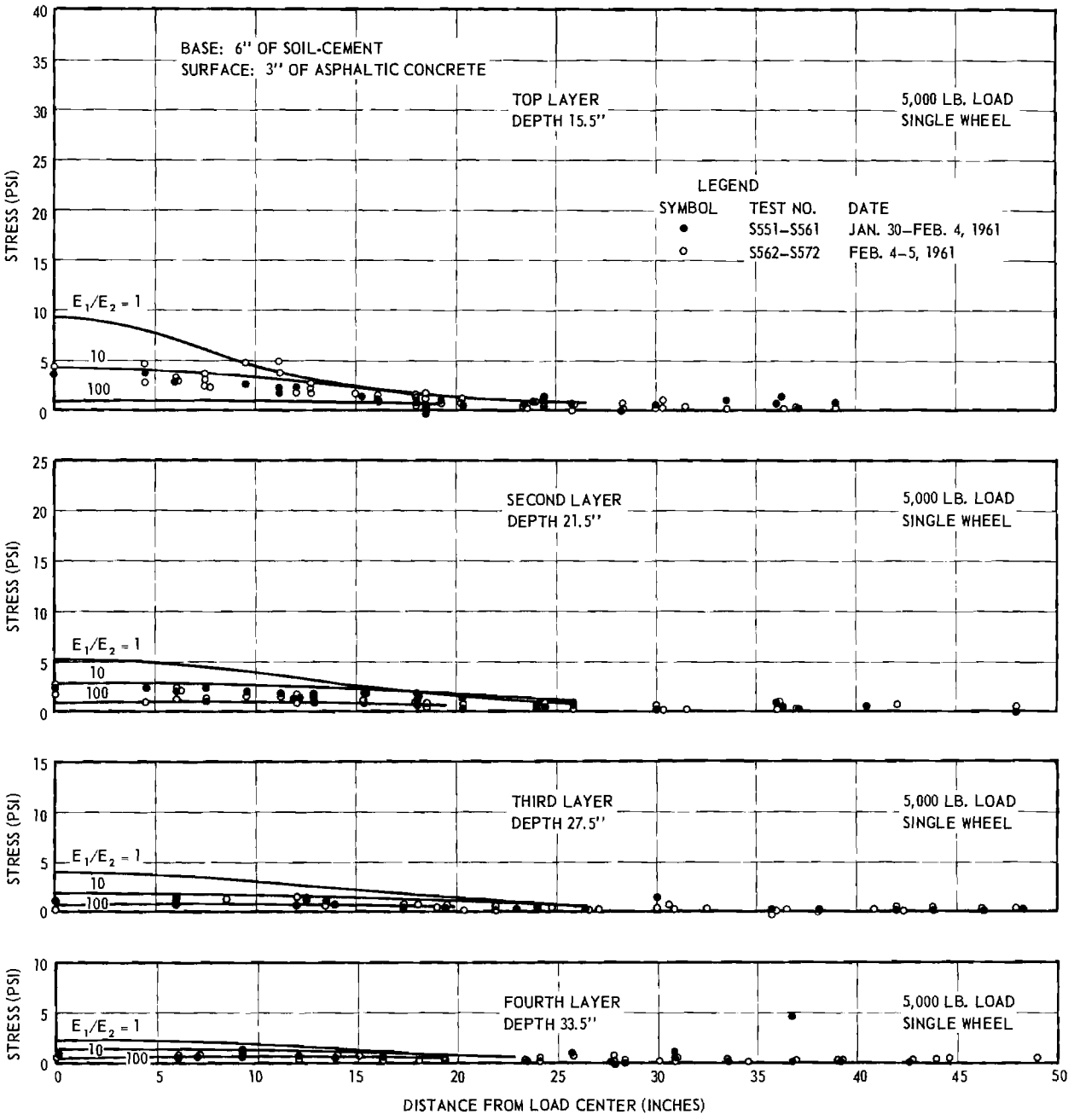

Figure 28. Measured Stresses: Single Load 5,000-lb 6" Soil-Cement Base with Overlay.

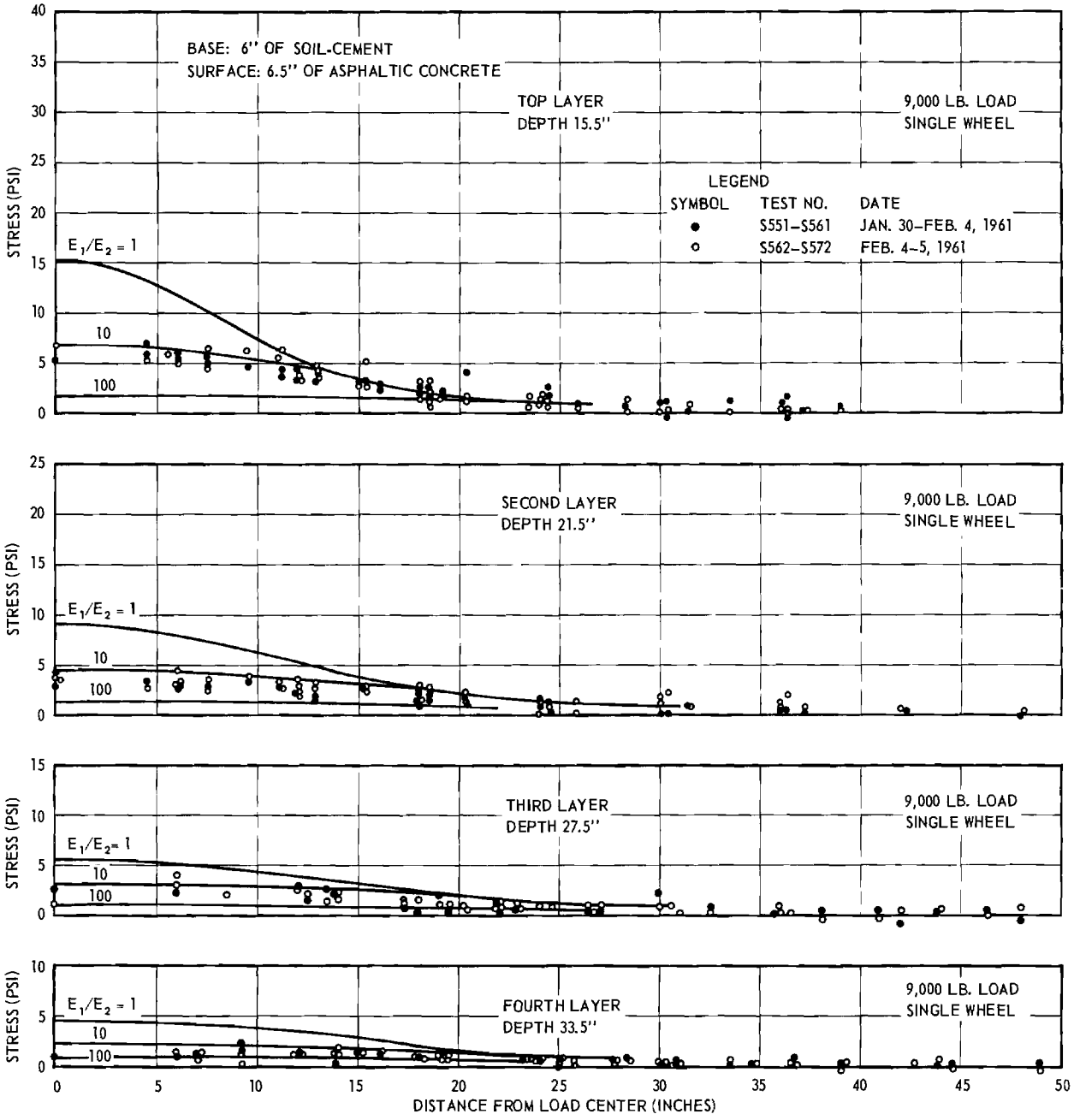

Figure 29. Measured Stresses: Single Load 9,000-lb 6" Soil-Cement Base with Overlay.

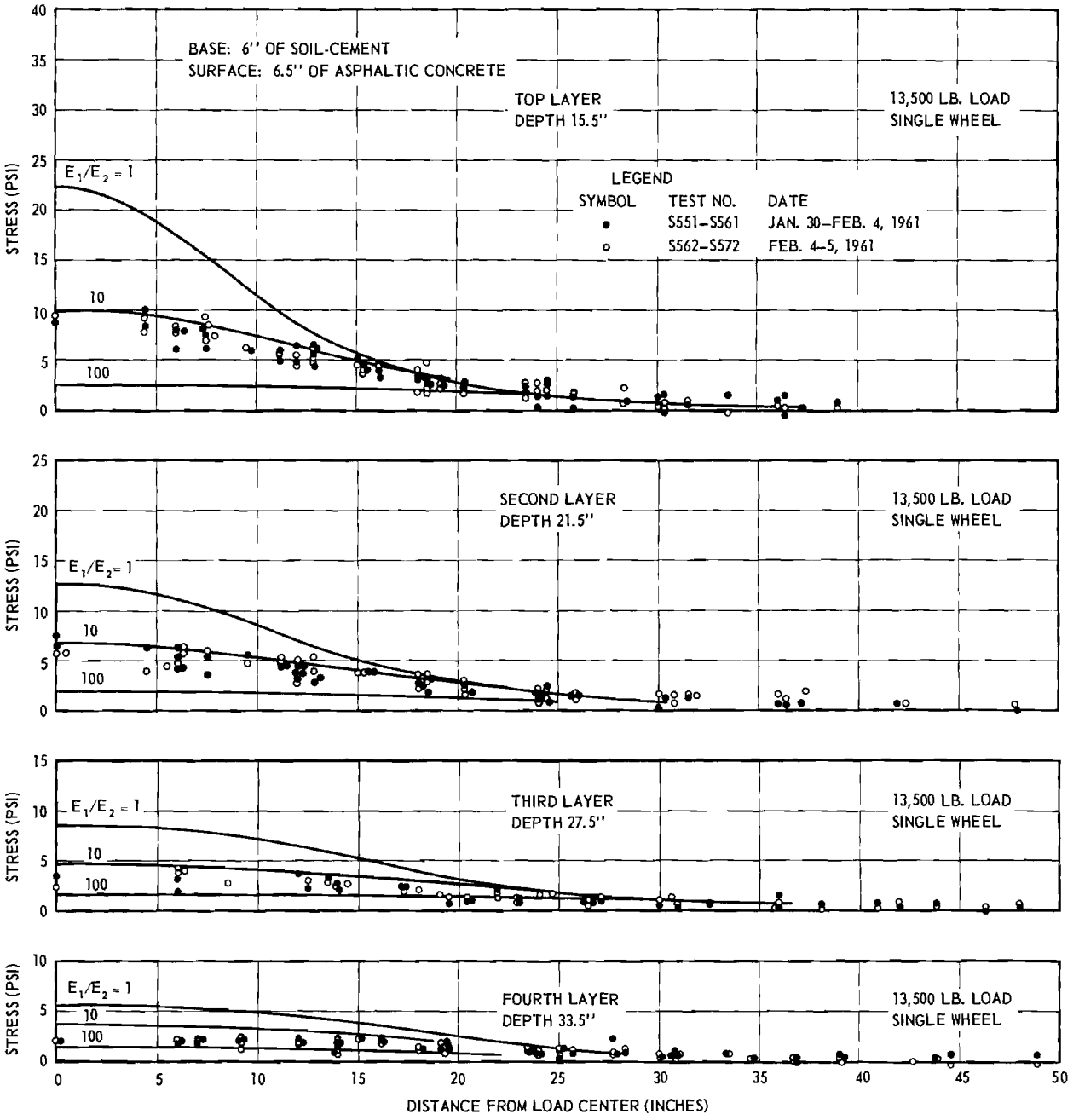

Figure 30. Measured Stresses: Single Load 13,500-lb 6" Soil-Cement Base with Overlay.

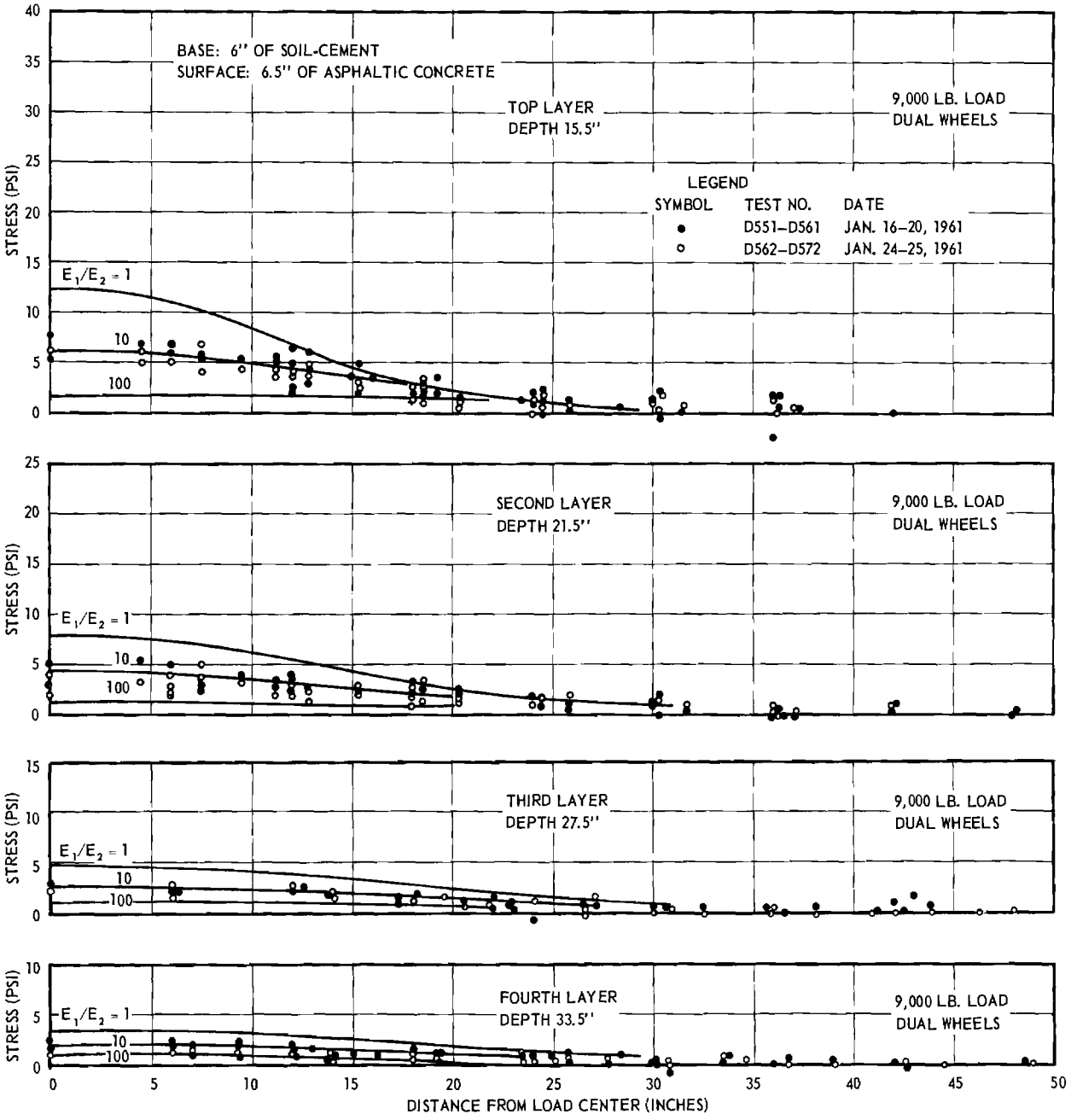

Figure 31. Measured Stresses: Dual Load 9,000-lb 6" Soil-Cement Base with Overlay.

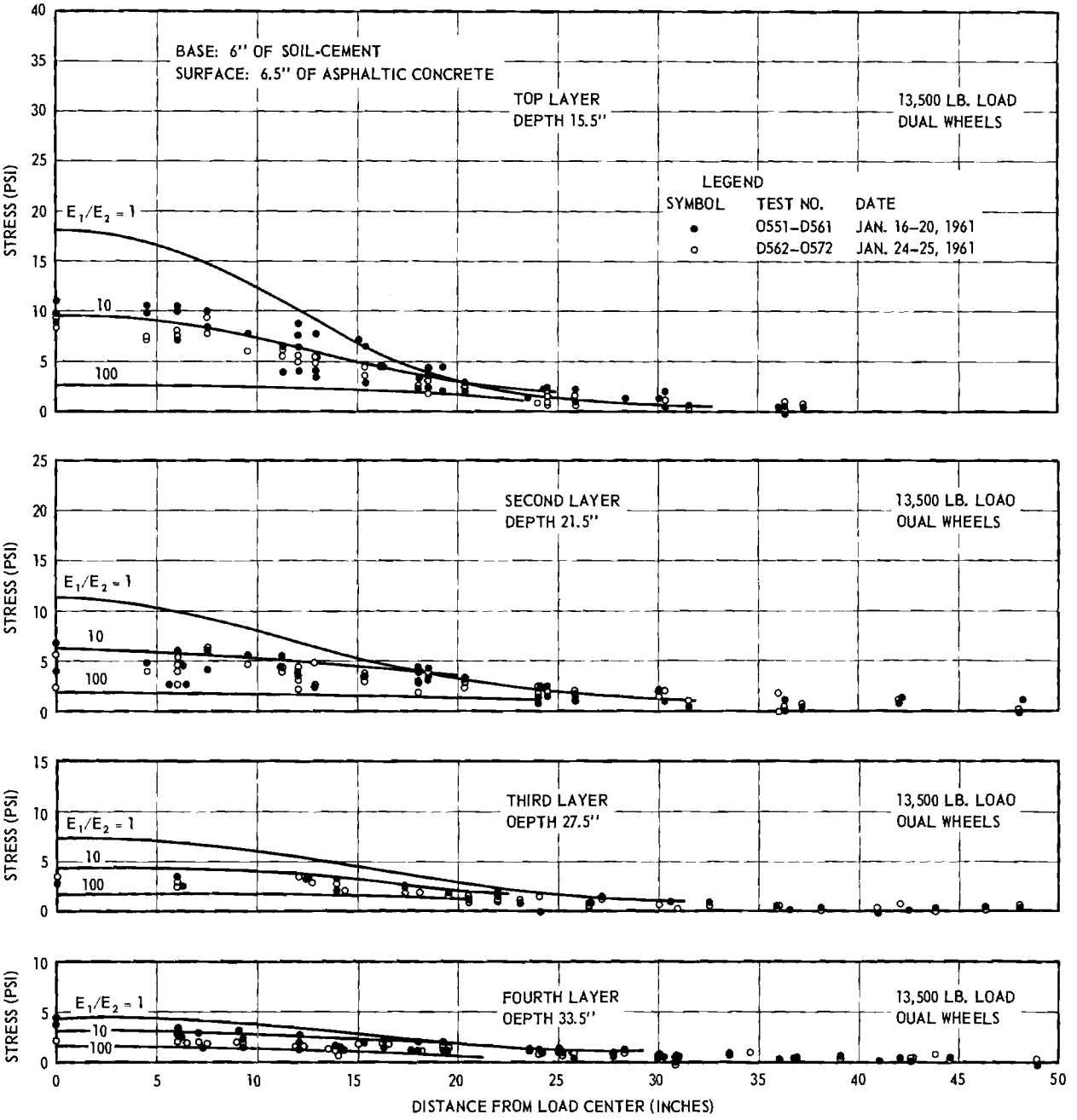

Figure 32. Measured Stresses: Dual Load 13,500-lb 6" Soil-Cement Base with Overlay.

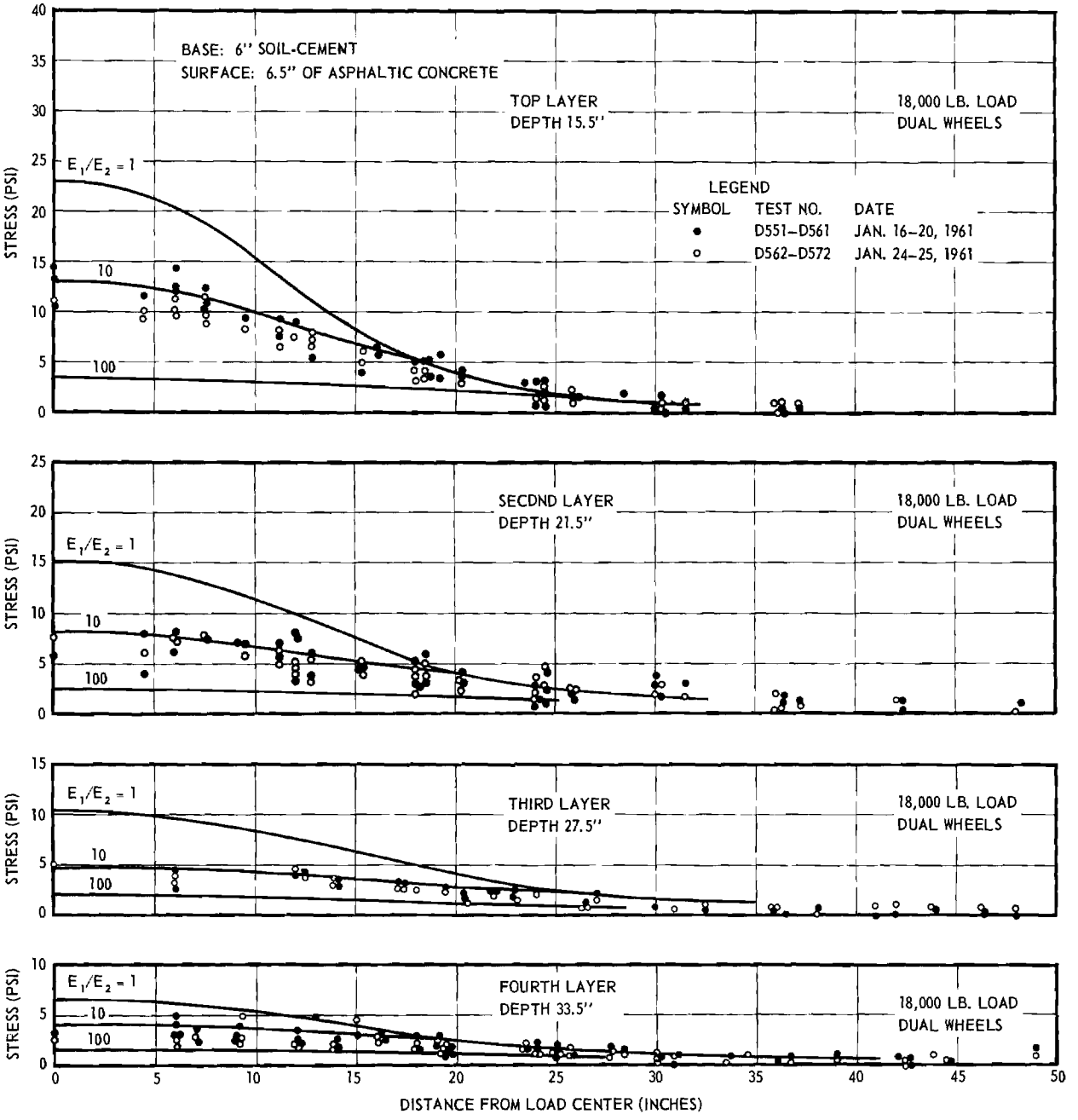

Figure 33. Measured Stresses: Dual Load 18,000-lb 6" Soil-Cement Base with Overlay.

the topsoil base pavement system, Figs. 15 to 20. They are from 20 per cent to 35 per cent less than the stresses at the same points without the overlay. As in the other tests the three inch thick overlay is nearly as effective in reducing subgrade stresses as an equal thickness of topsoil or soil bound Macadam base or of well compacted subgrade.

Computations were made of the stresses using the two layer theory (Annual Report 1, p. 13 - 15). As in the other soil-cement computations it was assumed that the asphaltic surface (and overlay) had the same elastic properties as the soil cement base. In this case the error involved in the simplifying assumption can be expected to be appreciable because the less rigid asphaltic surface is 52 per cent of the total thickness.

The observed stresses lie close to the theoretical curve computed for an elasticity ratio, $E_1/E_2 = 10$. They correspond to a lower theoretical elasticity ratio than do the observed stresses without the overlay. This should be expected because of the greater proportion of less rigid surface course in the total pavement.

9. Soil Cement With Inundated Subgrade

The stress measurements for the entire program had been made in a subgrade whose moisture content was comparable to the optimum. However, in actual practice subgrades sometimes are inundated. Since the effect of inundation on the stress propagation had not been investigated a final test was conducted to determine if it could have an appreciable effect on the stress distribution.

Six holes were cut in the 6-1/2 inch thick surface (including the 3 inch overlay) and in the 6 inch base. Wells were drilled through the entire 7 ft depth of subgrade and into the pea gravel layer previously placed in the pit bottom. These were then kept full of water to supply water to the subgrade and base.

The soil moisture was measured at intervals in other holes between the six inflow wells. Within a week the moisture had increased and had reached a new constant value. The original subgrade had a degree of saturation between 65 and 87 per cent. After inundation the saturation ranged from 94 to 99 per cent or an average of 96.5 per cent. Although this is not complete saturation it appears to be the limit the subgrade will absorb under field conditions because of air trapped in the voids.

The tests were conducted with the dual wheels and up to 18,000 lb total load. This is equivalent to a maximum axle load of 36,000 lb which is considerably greater than that now permitted on Georgia Highways. The results are shown on Figs. 34 to 36. They show no appreciable change from the stresses observed with the same pavement system without inundation of the subgrade. This is not surprising. The stress propagation through a homogeneous isotropic elastic material is independent of the modulus of elasticity. The stress propagation through a layered system is dependent on the elasticity ratio E_1/E_2, but is not proportional to it. Large changes in either E_1 or E_2 produce relatively small changes in the stresses. Therefore, the modest change in the subgrade elasticity produced by inundation produced no measurable change in the subgrade stresses.

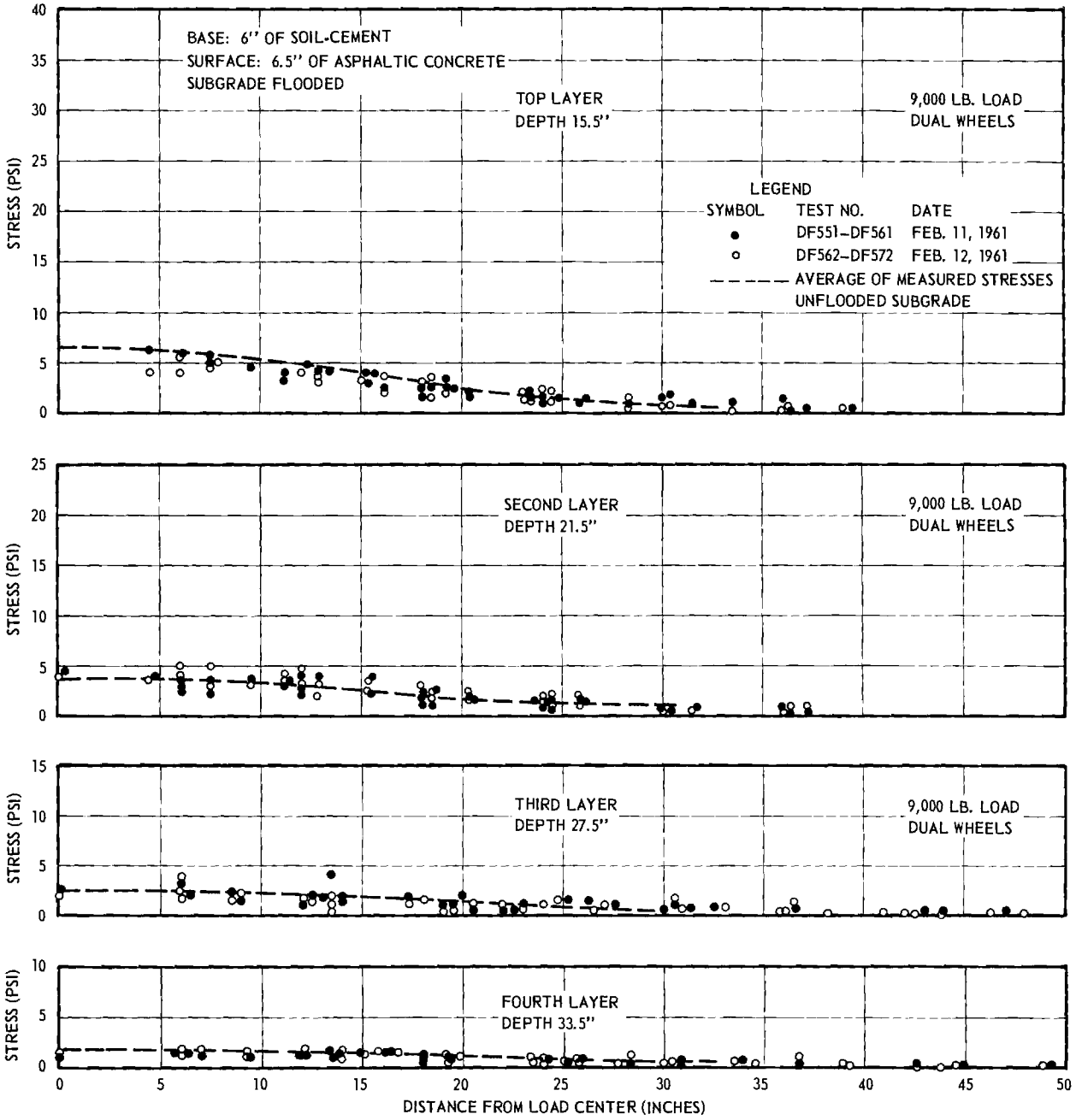

Figure 34. Measured Stresses: Dual Load 9,000-lb 6" Soil-Cement Base with Overlay, Subgrade Flooded.

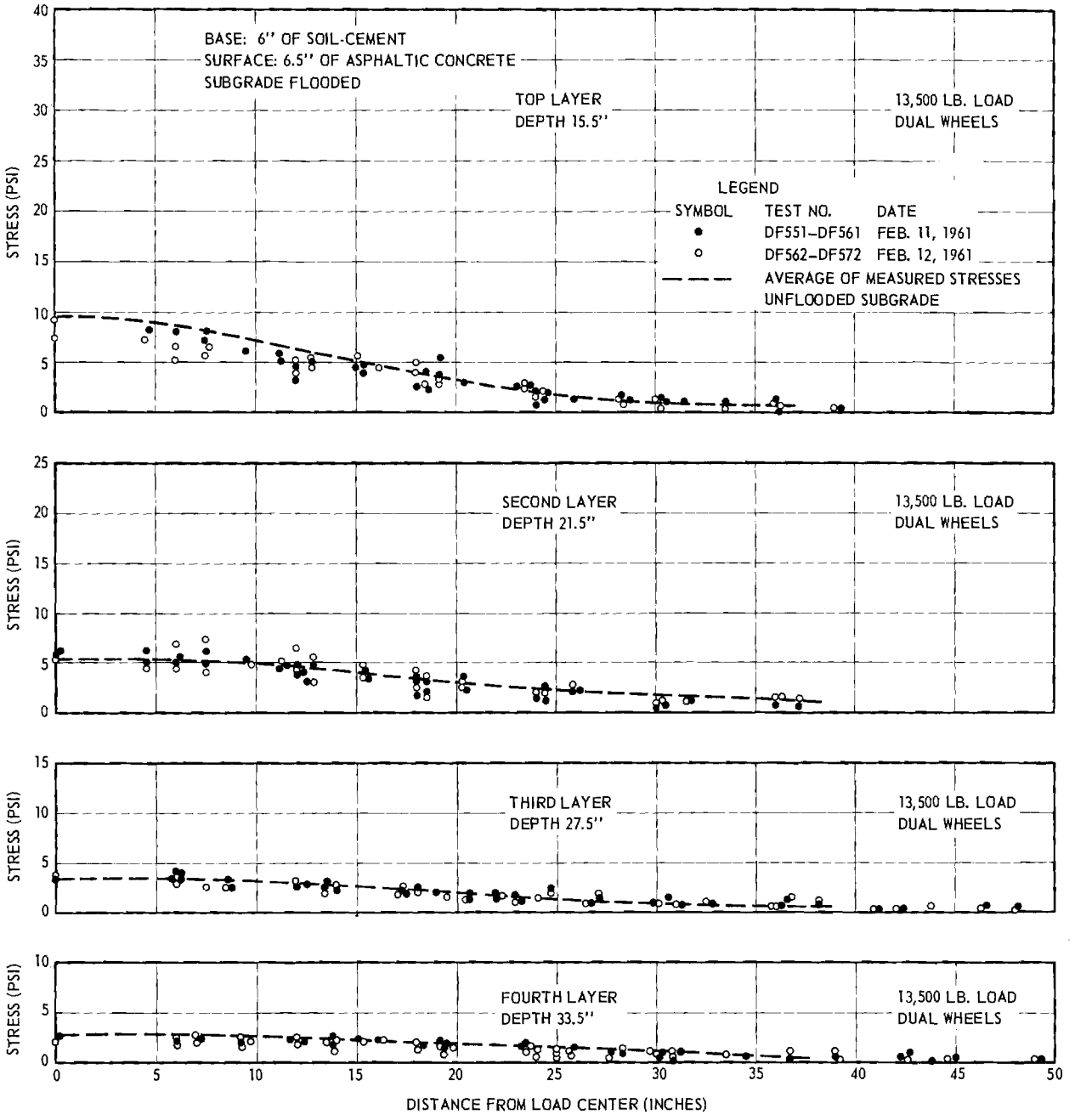

Figure 35. Measured Stresses: Dual Load 13,500-lb 6" Soil-Cement Base with Overlay, Subgrade Flooded.

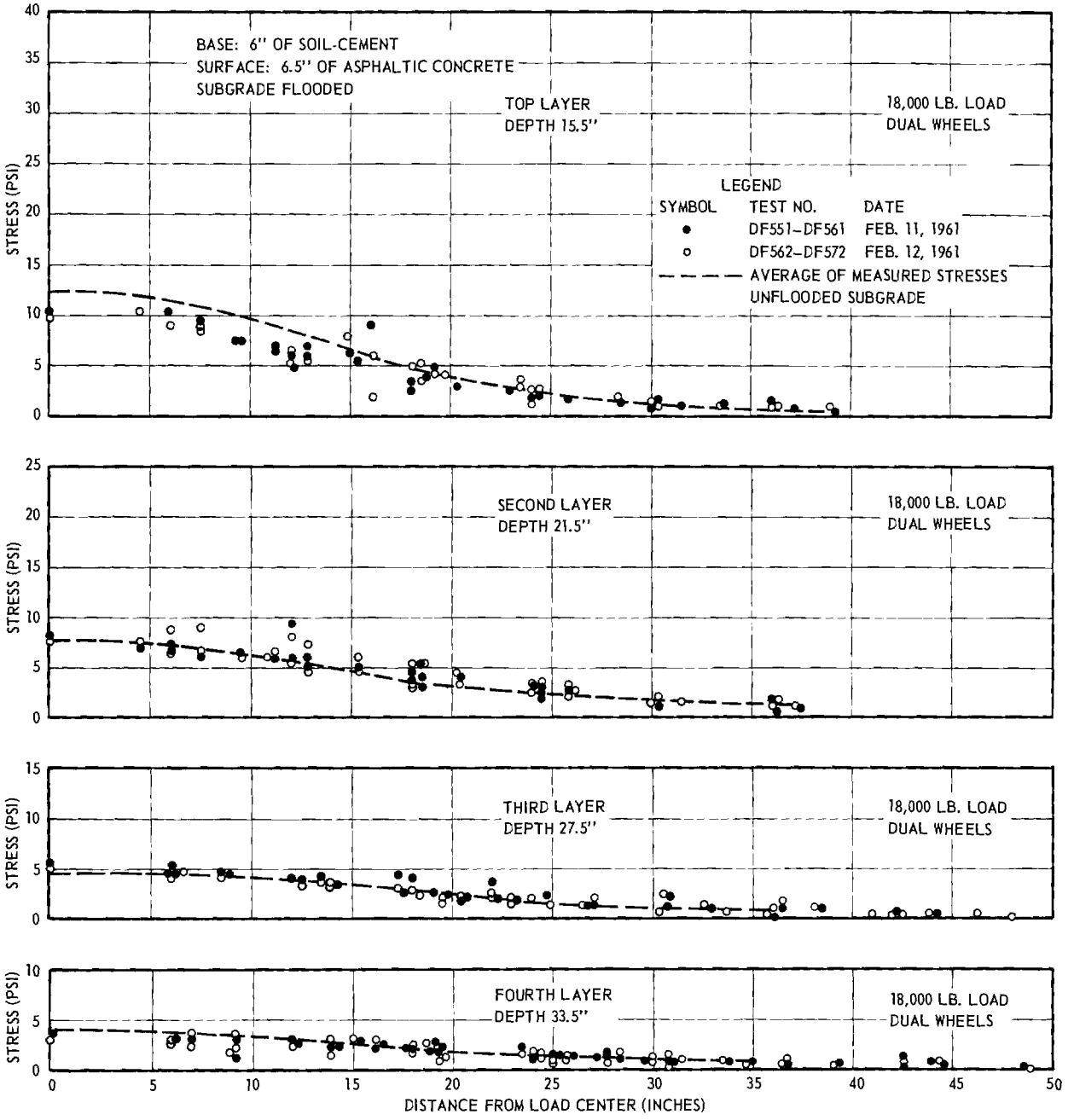

Figure 36. Measured Stresses: Dual Load 18,000-lb 6" Soil-Cement Base with Overlay, Subgrade Flooded.

CHAPTER IV

PREVIEW OF THE NEXT PHASE OF THE WORK

The work finished to date completed the pavement and overlay evaluations previously programed and the project as originally conceived. A question arose, however, regarding the sand asphalt tests which were made on the micaceous elastic subgrade effects. Therefore, a supplementary test was requested to evaluate the load spreading ability of a sand asphalt base over a well compacted (and more rigid) sand subgrade.

The major part of the continuing work will be the adaptation of the test results to design. This will proceed in two directions. First, the pavement design criteria developed in the AASHO tests will be analyzed in terms of stress spread into the subgrade. These will then be corrected by the project test results for the stress spreading characteristics of the Georgia pavement systems. From this a corrected AASHO design formula can be developed which will conform to Georgia conditions.

Second, typical pavement failures in Georgia will be analyzed. Data on traffic and weather will be secured and samples of the pavement components will be tested. These will be analyzed in terms of subgrade stress and behavior of the pavement components under stress. From these data it is hoped to develop a criteria for flexible pavement design that will fit Georgia materials and road conditions.

Approved by:

Thomas W. Jackson, Chief
Mechanical Sciences Division

Released by:

J. E. Boyd, Director
Engineering Experiment Station

Prepared and submitted by:

George F. Sowers
Project Director

Aleksandar B. Vesić
Research Associate